

Applied Mathematics and Mechanics
Volume 2

JETS, WAKES, AND CAVITIES

APPLIED MATHEMATICS AND MECHANICS

A Series of Monographs Prepared Under the Auspices of
the Applied Physics Laboratory, Johns Hopkins University

EDITOR-IN-CHIEF

F. N. FRENKIEL

Applied Physics Laboratory,

The Johns Hopkins University, Silver Spring, Maryland

ADVISORY EDITORIAL BOARD

RICHARD COURANT

A. M. KUETHE

W. R. SEARS

JOHN VON NEUMANN

Volume 1

K. OSWATITSCH: GAS DYNAMICS

ENGLISH VERSION BY G. KUERTI

Volume 2

G. BIRKHOFF and E. H. ZARANTONELLO: JETS, WAKES, AND CAVITIES

Volume 3

R. VON MISES: THEORY OF COMPRESSIBLE FLUID FLOW

REVISED AND COMPLETED BY HILDA GEIRINGER AND G. S. S. LUDFORD

ACADEMIC PRESS INC • PUBLISHERS • NEW YORK

JETS, WAKES, AND CAVITIES

GARRETT BIRKHOFF

*Harvard University
Cambridge, Massachusetts*

E. H. ZARANTONELLO

*Universidad Nacional de Cuyo
Mendoza, Argentina*



1957

ACADEMIC PRESS INC • PUBLISHERS • NEW YORK

EDITING SUPPORTED BY THE BUREAU OF ORDNANCE, U. S. NAVY, UNDER
CONTRACT NORD 7386.

Copyright©, 1957
by
ACADEMIC PRESS INC.
111 Fifth Avenue
New York 3, N. Y.
All Rights Reserved

NO PART OF THIS BOOK MAY BE REPRODUCED
IN ANY FORM, BY PHOTOSTAT, MICROFILM, OR ANY
OTHER MEANS, WITHOUT WRITTEN PERMISSION
FROM THE PUBLISHERS. REPRODUCTION IN WHOLE
OR IN PART IS PERMITTED FOR ANY PURPOSE OF
THE UNITED STATES GOVERNMENT.

Library of Congress Catalog Card Number: 56-8681

PRINTED IN THE UNITED STATES OF AMERICA

PREFACE

The present volume is intended to report systematically the most important findings of nearly 100 years of ingenious research in a fascinating and complex field. Jets, wakes, and cavities have been studied throughout this period, for many reasons, by "applied" mathematicians, "pure" mathematicians, engineers, and physicists. Yet, no thorough and well-rounded treatment of the subject as a whole seems to be available.*

Classical applied mathematicians have treated in detail many special flows, often omitting to describe the experimental conditions under which their formulas are applicable. Pure mathematicians have stressed general aspects of "ideal" fluid theory, such as questions of existence and uniqueness, almost exclusively. Specialists in modern fluid dynamics, guided by intuition and fragmentary reasoning, have found various relationships of great importance for engineering applications, but have not integrated their formulas into a systematic theory of "real" flows. Finally, physicists have established many striking effects under controlled laboratory conditions, whose significance under ordinary circumstances is not clear.

Our book attempts to bring together into a coordinated whole the work of these various groups of specialists. We have tried to overlook no really important ideas, and at least to include an appropriate reference to every significant paper published prior to 1955.

In spite of our efforts at coordination, the presentation retains much of the heterogeneous character of its original sources. Thus Chapters II, III, and V emphasize the formal treatment of special flows, while Chapters IV, VI, and VII deal mainly with general qualitative conclusions. On the other hand, Chapters XII–XIV center around intuitive momentum and similarity considerations. Finally, in Chapter XV, surprising physical complications are reported.

Our book draws on the resources of pure and applied mathematics, and on experimental physics, and it sheds light on numerous problems of hydraulics and aeronautics. Therefore, it will perhaps have the greatest interest for readers whose scientific curiosity spans all the fields just mentioned. However, we hope that others will also find it a useful and stimulating reference in connection with many special questions.

The need for a book such as this one has been intensified by the basic

* Ref. [64a] gives a systematic discussion of jets; some attempt at completeness is also made in refs. [16], [19], and [32]–[33],

advances of the past fifteen years. Since 1940, numerical methods have been revolutionized (Chapter IX), a significant theory of axially symmetric jets and cavities has been created for the first time (Chapter X), while the fundamental facts about vortex trails (Chapter XIII) and turbulent jets and wakes (Chapter XIV) have been reinterpreted in the light of new concepts.

Besides recalling well-known facts and summarizing these major recent advances, this book also includes various minor results of our own which are here published for the first time.

The book owes much to many individuals and institutions. First, we wish to thank the Office of Naval Research, whose generous support made it possible. We want to pay especial tribute to Dr. Mina Rees, for her personal encouragement. Thanks are also due to Harvard University and the University of Maryland, under whose auspices the book was written.

We are grateful to James Serrin, J. Kampé de Fériet, J. Kravtchenko, Arthur Read, and A. H. Armstrong, among others, for valuable criticisms of various parts of our manuscript. We thank Douglas Hartree for helpful discussions of the numerical methods used. Finally, we wish to express our appreciation to Eleanor Lawry, David Young, Richard Varga, Samuel Kneale, and James Hansen, for valuable assistance with calculations, and to Ellen Burns and Laura Schlesinger for their expert typing.

G. BIRKHOFF

E. H. ZARANTONELLO

CONTENTS

Preface	v
List of Reference Abbreviations	xiv
I. Background and Prospectus	
1. Examples of jets	1
2. Wakes and cavities	4
3. Plan of book	6
4. Dimensionless ratios	8
5. Real wakes	9
6. Kinds of cavitation	9
7. Parallel flow models	11
8. Euler flows	12
9. Free streamlines	13
10. Conservation laws and jets	14
11. Applications to cavities	17
12. Ideal plane flows	19
13. General theorems	20
14. Applications	21
15. Effective computation; generalizations	22
16. Viscosity and turbulence	22
17. Other physical variables	23
II. Circular Sector Hodographs	
1. Introduction	25
2. Cavity behind plate	27
3. Detailed formulas	29
4. Cavity behind wedge	30
5. Jet from funnel	32
6. Jet against plate	35
7. Réthy flows	37
8. Applications; superposition principle	39
9. Partial fractions	40
10. Beta functions	41
III. Simple Flows Past Wedges	
1. Introduction	43
2. Simple flows; reflection principle	44
3. <i>W</i> -diagrams of "simple" flows	45
4. Impinging jets	47

5. Divided jets.....	50
6. Physical applications ..	52
7. Simple flows past wedges ..	55
8. Reentrant jets.....	56
9. Geometrical classification of simple flows.....	59
10. Flows with circular sector hodograph.....	60
11. Other examples.....	62

IV. General Theory

1. Singularities of $W(T)$	64
2. Reflection principle.....	65
3. Asymptotic geometry of free streamlines.....	68
4. Momentum equations ..	71
5. Drag and lift.....	73
6. Moment.....	75
7. Separation curvature ..	76
8. Inflections of free boundaries ..	81
9. Free stream surfaces.....	83
10. Variational principle.....	85
11. Extension to infinite stream ..	87
12. Lavrentieff's theorem.....	90
13. Under-over theorem.....	92
14. Uniqueness theorem.....	94
15. Minimum cavity drag ..	97

V. Multiple Plates

1. Parametric rectangle.....	98
2. Case of m plates.....	99
3. Annular sector hodograph ..	100
4. Method of reflection.....	102
5. Impinging jets from nozzles, I ..	105
6. Perpendicular plates.....	107
7. Position integral	108
8. U-shaped obstacles ..	111
9. Riabouchinsky flows ..	115
10. Impinging jets from nozzles, II.....	118
11. General formulas.....	120
12. Plate in jet from nozzle ..	122
13. Interior sources and vortices.....	124
14. Cusped cavities.....	126
15. Hollow vortices ..	128

VI. Curved Obstacles

1. Semicircular parametrization	130
2. The function $\Omega(t)$	132
3. Geometrical interpretations.....	133

4. Basic integral equations	135
5. Symmetric cavities	137
6. Brillouin-Villat separation condition	139
7. Asymmetric case: parameter problem	140
8. Analogs of Réthy flows	142
9. Physical applications	143
10. Cusped cavities	145
11. Reentrant jets	146
12. Riabouchinsky flows	147
13. Cascades of airfoils	148
14. Other examples	150

VII. Existence and Uniqueness

1. Historical introduction	153
2. Nearly flat obstacles	154
3. Leray's use of fixpoint theory	157
4. Parameter problem	160
5. Jacob's Lemma	162
6. Convex obstacles	167
7. Method of continuity	171
8. Weinstein's function	173
9. Uniqueness	175
10. Variational method; symmetrization	177
11. The minimizing profile	181

VIII. Compressibility and Gravity

1. Hodograph equations	185
2. Chaplygin equation of state	187
3. Flows past wedges	189
4. Curved obstacles	190
5. Polytropic equation of state	191
6. General equation of state	193
7. Integral equations	196
8. Supersonic jets	197
9. Ultra-fast jets	199
10. Potential flows with gravity	200
11. Integral equation method	202

IX. Effective Computation

1. General remarks	205
2. Cavity behind a plate	206
3. Jet from a slot	207
4. Incomplete beta functions	208

5. Parameter problem...	210
6. Isobars and isoclines.	211
7. Related methods.....	213
8. Curved barriers.....	215
9. Theoretical discussion.	217
10. Other methods.....	219

X. Axially Symmetric Flows

1. Typical problems..	221
2. Potential theory...	222
3. Axial source distributions	224
4. Source and vortex rings...	225
5. Integral equation approaches..	226
6. Approximate methods.	228
7. Jets from conical orifices..	229
8. Impinging jets.....	230
9. Underwater cavities....	231
10. Swirling flows.....	233
11. Rising bubbles in tubes.	235

XI. Unsteady Potential Flows

1. Vapor-filled spherical bubbles....	236
2. Cavitation in a variable pressure field ...	237
3. Gas-filled cavities.....	239
4. Transient cavities behind missiles.....	240
5. Bubble migration; laws of Bjerknes...	241
6. Cavity induced mass....	243
7. Globule acceleration.....	245
8. Impact forces.....	246
9. Impact of cones and wedges.....	248
10. Constant acceleration coefficient.....	248
11. Stability of plane interface.....	251
12. Taylor instability.....	252
13. Spherical and cylindrical bubbles.	253
14. Helmholtz instability.....	254
15. Stability of capillary jets.....	255
16. Stability of other configurations.....	256

XII. Steady Viscous Wakes and Jets

1. Boundary value problem....	258
2. Critical discussion.....	259
3. Wakes in creeping flow...	261
4. Flow separation.....	262

5. Asymptotic wake structure	264
6. Wake momentum	265
7. Oseen equations	266
8. Boundary layer approximation	267
9. Momentum theorem	268
10. Similarity hypothesis	270
11. Creeping jets	272
12. Inertial effects	274
13. Schlichting's model	274
14. Laminar plane jets	276
15. Exact self-similarity	278

XIII. Periodic Wakes

1. Basic facts	280
2. Karman model	282
3. Shedding of vorticity	283
4. Vorticity and wake momentum	285
5. Vorticity and drag	286
6. Invariance theorem	287
7. Karman's stability argument	289
8. Strouhal number	290
9. Miscellaneous effects	292
10. Plate at zero incidence	293
11. Axially symmetric periodic wakes	293
12. Periodic jets; edge tones	294
13. Bird tones	296

XIV. Turbulent Wakes and Jets

1. General remarks	298
2. Flow separation	299
3. Base underpressure	300
4. Wake structure	301
5. Wake turbulence	302
6. Mixing length concept	304
7. Asymptotic wake behavior	305
8. Wakes with hydrodynamical self-propulsion	307
9. Mixing zone	309
10. Structure of jets	309
11. Mixing length "theories"	310
12. Further literature	312

XV. Miscellaneous Experimental Facts

1. General discussion	314
2. Bubbling and boiling	314
3. Tensile strength of liquids	315

4. Bubble dynamics...	317
5. Acoustic cavitation.	320
6. Cavitation damage	320
7. Propeller cavitation	323
8. Scale effects in water entry.	325
9. Bubble entrainment...	326
10. Jet persistence ...	328
11. Atomization of jets.	329
12. Other jet configurations.	330
Bibliography	332
Plates I-II	337
Index	351

REFERENCE ABBREVIATIONS

ARC RM	= Aeronautical Research Council, Reports and Memoranda (Great Britain)
CAHI	= Central Aerodynamic and Hydrodynamic Institute (USSR)
DTMB	= David Taylor Model Basin (USA)
NACA	= National Advisory Committee for Aeronautics (USA)
Navord	= Naval Ordnance (USA)
NOL	= Naval Ordnance Laboratory (USA)
QJMAM	= Quarterly Journal of Mechanics and Applied Mathematics
UCLA	= University of California at Los Angeles
ZaMM	= Zeitschrift für angewandte Mathematik und Mechanik.

CHAPTER I

BACKGROUND AND PROSPECTUS

1. Examples of jets. By a *jet* is meant a stream of material which travels for many diameters in a nearly constant direction. To produce such a jet, it suffices to make a hole or insert a tube into a reservoir, whose local pressure is higher than the surrounding pressure.

Jets have been used since earliest times. Thus Greenhill [33] refers to a Roman law governing the discharge rate from orifices supplying public water. Jets from fountains, faucets, and fire hose nozzles are familiar to all (see Fig. 1); their behavior has been systematically studied by scientists since Renaissance times, at least.

More recently, the atomization of jets in carburetors has been carefully studied (see Ch. XV, §§10–12), in connection with gasoline engine design. Again, metal jets from lined hollow charges, designed in World War II for use in anti-tank weapons¹, now find wide application in drilling for petroleum. Still more recently, liquid jets have been used to make subcutaneous injections under the trade name of “Hypospray”, and jets of abrasive particles to drill holes in teeth².

The preceding examples referred to liquid (or solid) jets in air. Gas jets in air, and water jets in water, are of equal importance.

For over a century, the behavior of heating (and illuminating) gas jets in air has also been studied. Likewise, jet pumps have fulfilled a useful purpose since their invention by James Thomson³ in 1852. Jet propulsion of boats has also been given careful study, while the spectacular recent development of jet propulsion for aircraft is familiar to all⁴. Very recently

¹ G. Birkhoff, D. P. MacDougall, E. M. Pugh, and G. I. Taylor, *Explosives with lined cavities*, J. Appl. Phys. 19 (1948), 563–82.

² R. B. Black, J. Am. Dental Assn. 41 (1950), 701–10; B. Dunne, B. Cassen and H. Gass, UCLA Rep. UCLA 212 (1952).

³ “Papers in physics and engineering”, pp. 26–35; A. H. Gibson, “Hydraulics and its applications”, 4th ed., Art. 213; A. Stodola-L. C. Loewenstein, “Steam and gas turbines”, New York, 1945, Arts. 152, 154; J. E. Gosline and M. P. O’Brien, “The water jet pump”, Univ. of Calif. Press, 1934.

⁴ For marine jet propulsion, see C. B. Brin, Trans. Inst. Nav. Arch. 12 (1871), 128–49; Gibson, op. cit., Arts. 136–7. Aircraft jet propulsion is being thoroughly treated in the 12-volume Princeton University Press Series, “High speed aerodynamics and jet propulsion”; see also J. G. Keenan, “Gas turbines and jet propulsion”, Oxford Press, 1946, Ch. XII.

I. BACKGROUND AND PROSPECTUS

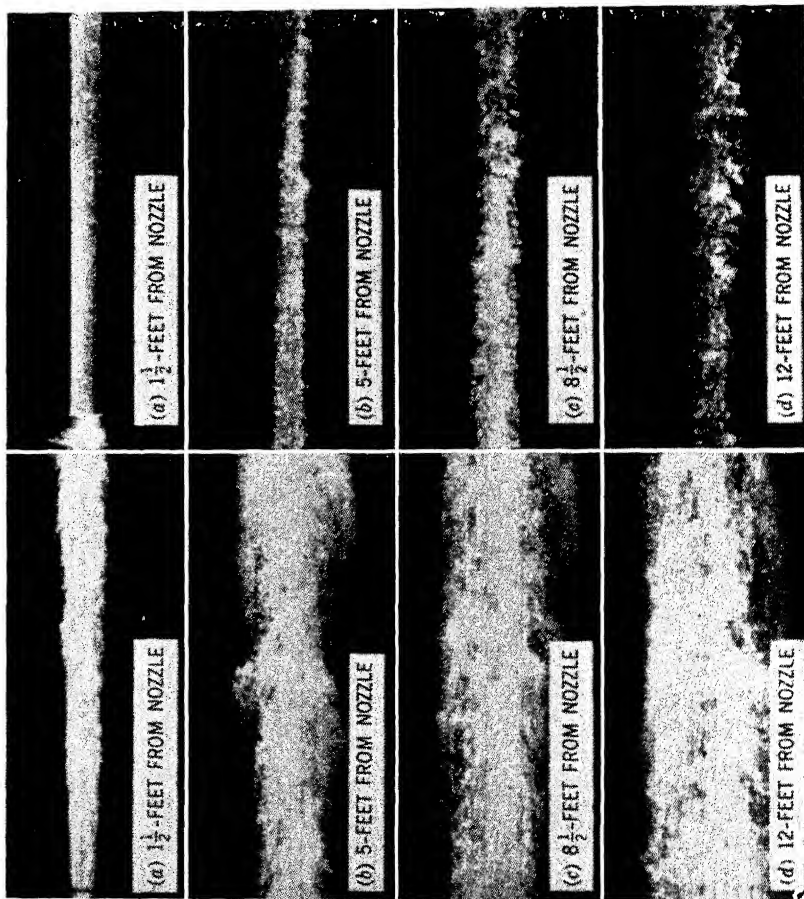
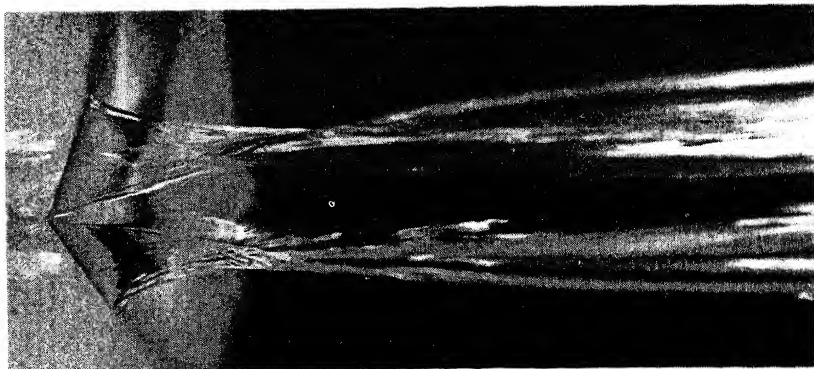




Fig. 1 (upper half). Jets from fire nozzles and square orifice. (Courtesy Iowa Institute of Hydraulics). (lower half). Divided plane jet between parallel glass plates. (Gordon McKay Laboratory, Harvard University)

meteorologists have also become aware of "jet streams" of air in the stratosphere, travelling 100–300 miles per hour⁵.

2. Wakes and cavities. It is easily observed that, if an obstacle or barrier is held stationary in a moving stream, the flow usually *separates* from the obstacle along so-called separating streamlines. The fluid between these streamlines constitutes the wake; it is usually relatively peaceful ("dead water") just behind the obstacle.

Relative to the fluid, the wake presents a very different appearance. In this case, it consists of a train of eddies extending far behind the solid, as in the familiar case of the wake behind a rowboat.

Fig. 2 reproduces photographs by O. Flachsbart^{5a} of the wake behind a flat plate at Reynolds numbers $R = 820$ –1,750. Note the development of turbulence, a few plate diameters behind the plate.

In any case, wakes are important because they represent the main source of real fluid resistance or *drag*. As is well known, no resistance would normally^{5b} occur in a non-viscous fluid at subsonic velocities, if it were not for flow separation and the attendant wake.

Wakes also play a role in other practical problems, as in the settling of smoke on the topdecks of steamers⁶, and in the design of shields to screen navigators from the wind.

In the case of high-speed motion through a liquid, the wake becomes gaseous; such a wake is called a *cavity*. Thus if a sphere is dropped into water at speeds of 25 f/s or more, an air-filled cavity is formed (see Figs. 3a–3b of Ch. XV). Again, if an obstacle is held in a stream of water moving at 100 f/s or more under atmospheric pressure, or at lower speeds under reduced pressure, a vapor-filled cavity is formed, like the one shown in Fig. 3.

Air-filled cavities were first studied around 1900 by Worthington [90], out of scientific curiosity. At about the same time, engineers became aware of the serious problems caused by vapor-filled cavity bubbles in marine propellers and hydraulic turbines; this had been anticipated in 1754 by Euler⁷. Some references to the enormous literature concerning these subjects will be found in Ch. XV, §§4–7.

⁵ Gen. elec. review 56 (1953), 42–7.

^{5a} ZaMM 15 (1935), 32–7, Abb. 7a–7f. For R, see (5).

^{5b} [4, Ch. I, §6]. In the case of airfoils of finite span with sharp trailing edges, "induced drag" provides an exception [31, §12].

⁶ See J. Valensi and L. Guillonde, Bull. Assn. Tech. Marit. Aero. 47 (1948), 180–2; F. W. Lanchester, *Aerodynamics*, 4th ed., London, 1908, p. 41. For wakes and resistance, see *ibid.*, §30 and pp. 129–37. For the wake of a jet, see Sir Geoffrey Taylor, *Riabouchinsky Anniv. Vol.*, 313–7.

⁷ L. Euler, Hist. de l'Academie Royale Berlin 10 (1754), 227–95; for a graphic modern exposition, see R. T. Knapp, Trans. Inst. Mech. Eng. London A166 (1952), 150–63.

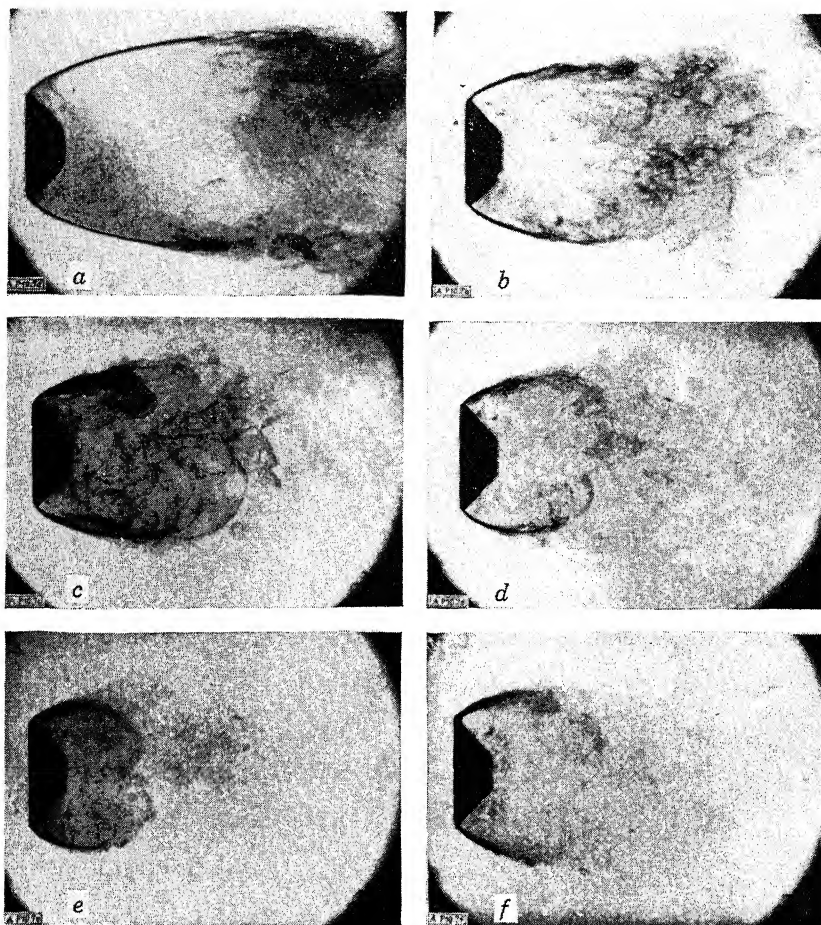


Fig. 2. Wake behind flat plate.

During World War I, Rayleigh [65, vol. 6, p. 504] analyzed the oscillating cavities formed in underwater explosions. However, the intensive scientific study of underwater explosions was really initiated in World War II (see [17]).

This cataclysmic event also gave a great practical importance to Worthington's studies, because of their relation to the entry into water of air-launched missiles (see [4, Ch. II], [30] and [59b]). At the same time, it became realized⁸ that the initiation of explosions by percussion was really due to the adiabatic heating of small internal cavities. Still more recently, it has

⁸ F. P. Bowden and A. D. Yoffe, *The initiation and growth of explosions in liquids and solids*, Cambridge Univ. Press, 1952, §§3.1-3.2, §4.1.

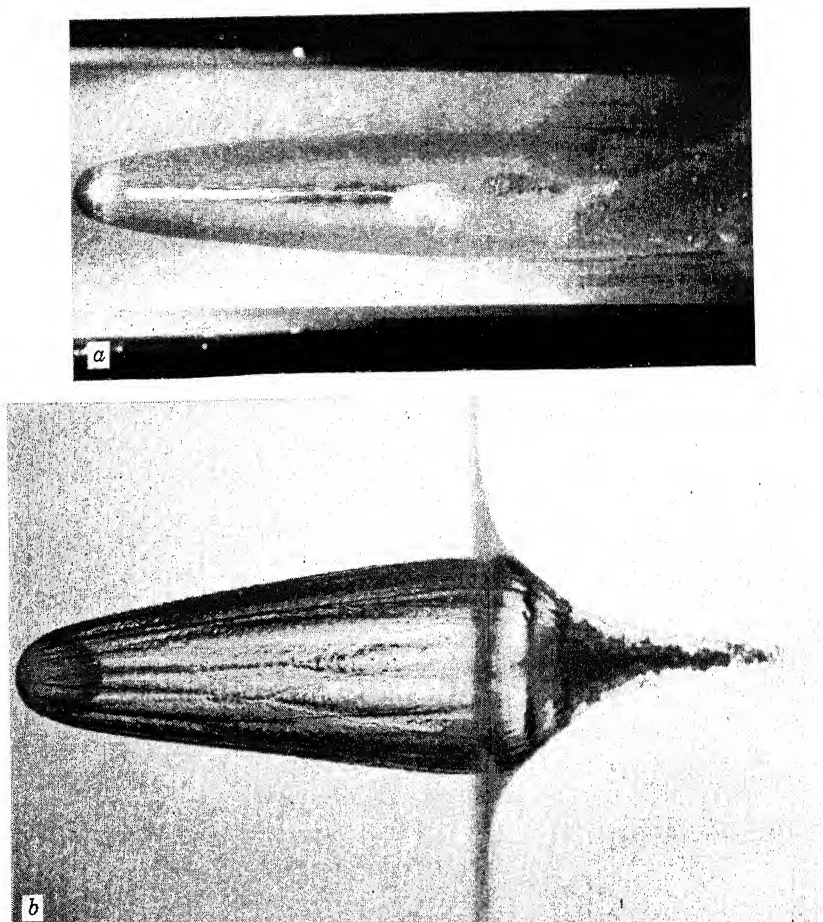


Fig. 3 (top). Cavity behind hemisphere in free jet. (Courtesy St. Anthony Falls Hydraulic Laboratory). (bottom). Cavity behind sphere dropped in water. (Courtesy Naval Ordnance Laboratory)

been found that cavities play an important role in the homogenation of milk⁹.

There are innumerable other practical questions involving the behavior of jets, wakes, and cavities, some of which will be mentioned from time to time below.

3. Plan of book. The present monograph is devoted to the quantitative scientific analysis of jets, wakes and cavities. Where possible, an attempt

⁹ C. C. Loo et al., J. Dairy Sci. 33 (1950), 692-702.

is made to predict their behavior by solving an appropriate *boundary value problem* involving the partial differential equations of fluid motion.

In the case of liquid jets in air, and of cavity flow, this program can be carried through successfully, at least in simple cases, *if* the flow is rapid enough for gravity to be negligible and for viscosity effects to be confined to the boundary layer. In these cases, Euler's partial differential equations for non-viscous flow (§8) are approximately applicable, and one can use the *free boundary* condition of *constant pressure on the liquid-gas interface* to locate the flow boundary, where it is not constrained by a solid wall. Thus, in the case of liquid jets in air, we will use potential theory (§8), and assume

$$(1a) \quad p = p_{\text{atm}} \text{ (atmospheric pressure) on the free boundary,}$$

In the case of vapor-filled "true" cavities, the conditions

$$(1b) \quad p = p_v \text{ (vapor pressure) on the cavity wall,}$$

$$p \geq p_v \text{ inside the liquid,}$$

provide a fair approximation to the true facts [1].

However, the cases of wakes, of gas jets in a gas of nearly equal density, and of liquid jets in a liquid, cannot be treated even approximately in this way—in spite of the enormous mathematical literature suggesting the contrary. Presumably, the flow is determined by the Navier-Stokes equations of Ch. XII, §1. But the complicated experimental phenomena summarized in §§13–15 should make the difficulties of rational prediction apparent.

Recognizing the preceding facts, we have treated first (in Chs. II–XI) the applications of Euler's differential equations to flows with free boundaries—i.e., to liquid flows bounded by a liquid-gas interface. The major portion of the book has been devoted to these applications, not because of their greater practical importance, but because more could be said about them theoretically.

In Chs. XII–XIV, we have turned our attention to the cases of laminar viscous, periodic, and turbulent jets and wakes. Here exact results are exceedingly rare, and a quasi-empirical approach has therefore been adopted.

Finally, in Ch. XV, we have summarized many important limitations on the deductions made in Chs. II–XI, due to neglect of surface tension, dissolved gas, and other physical variables. This discussion is almost entirely empirical.

Before launching into the detailed consideration of special cases, we will however briefly discuss some simple ideas which underlie the whole subject. To these simple ideas, then, the present chapter will be devoted.

4. Dimensionless ratios. As in all branches of mechanics, various dimensionless ratios play an important role in the theory of jets, wakes and cavities.

Perhaps the most important such ratio is the density-ratio

$$(2) \quad \rho'/\rho$$

between two components of a flow (e.g., of a liquid jet in air, or of a cavity flow). Intuitively, one easily guesses that if

$$(2^*) \quad \rho'/\rho \ll 1,$$

then the fluid of density ρ' can be ignored. Indeed, it is this condition, which was apparently first formulated explicitly by Betz and Petersohn [2], which underlies the relative success of potential theory in predicting the behavior of liquid jets in air and of cavities.

Next most important is the Thoma *cavitation number*

$$(3) \quad Q = (p_f - p_v)/\frac{1}{2}\rho v^2.$$

In (3), p_f denotes the ambient (free stream) pressure, ρ the density, and v the free stream velocity. Closely related to Q is the local *underpressure coefficient* $-C_p$, defined as the function

$$(4) \quad -C_p = (p_f - p)/\frac{1}{2}\rho v^2.$$

The underpressure coefficient is closely related to the cavitation number. Thus, inside vapor-filled cavities satisfying (1b), the local underpressure coefficient is the Thoma cavitation number. By analogy, we define the cavitation number of a cavity flow in general as

$$(3a) \quad Q = (p_f - p_c)/\frac{1}{2}\rho v^2,$$

where p_c is the pressure in the cavity just behind the obstacle.

In the case of wakes, the pressure just behind an obstacle is ordinarily nearly a constant p_B , the "base pressure". In this case, we shall let

$$(3b) \quad Q = (p_f - p_B)/\frac{1}{2}\rho v^2.$$

denote similarly the *wake* underpressure coefficient; typical values of Q are given in Ch. XIV, §3. (Note that, in the case of hypersonic flow, the wake pressure is nearly zero, and so the behavior of the wake closely resembles that of a cavity.)

Besides Q , the traditional *Reynolds number*

$$(5) \quad R = \rho v d / \mu = v d / \nu,$$

and the *Froude number*

$$(6) \quad F = v^2 / g d$$

play a basic role in the understanding of jets, wakes, and cavities. Here d is a typical linear dimension (e.g., a diameter), μ is the viscosity, $\nu = \mu/\rho$ the kinematic viscosity, and g the acceleration of gravity. As usual [4, Ch. III], $1/R$ and $1/F$ express the *relative* importance of viscosity and gravity, respectively.

Finally, we shall find it convenient to adopt the usual notation for drag and lift coefficients,

$$(7) \quad C_D = D/\frac{1}{2}\rho v^2 A \quad \text{and} \quad C_L = L/\frac{1}{2}\rho v^2 A,$$

where D is the drag, L the cross-force or lift, and A the cross-section area of an obstacle placed in a flow.

In §13, we shall see that the dimensionless ratios defined above are significant theoretically as well as empirically.

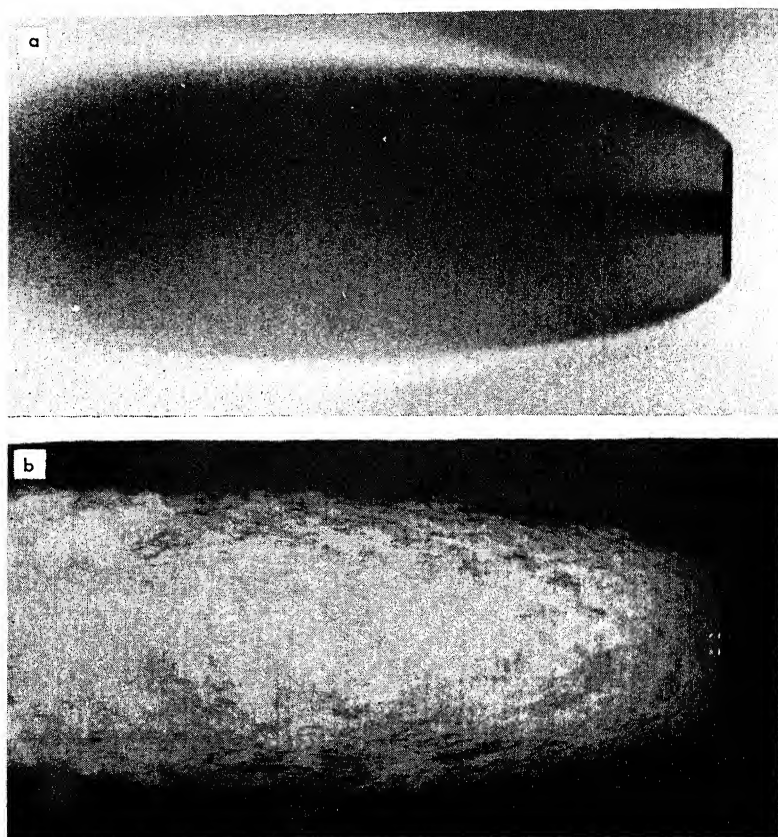
5. Real wakes. Real wakes provide a striking illustration of the importance of the Reynolds number R defined by (5). As $R = vd/\nu$ increases, the nature of the wake behind a circular cylinder, sphere, or other obstacle of diameter d , changes progressively through a quite well-defined sequence of metamorphoses, which may be described roughly as follows [31, p. 550]. (A more detailed discussion will be given in Chs. XII–XIV. Thus, Figs. 1 and 2a–2c of Ch. XII illustrate the sequence of changes pictorially.)

If $R < 0.1$, the streamlines have approximate fore-and-aft symmetry corresponding to “creeping flow”. In the interval $0.1 < R < 5$ (say), the streamlines open out behind the obstacle, destroying this symmetry. As R increases further (say, if $5 < R < 25$), two stationary vortices may form symmetrically behind the obstacle. In this range of R also, a well defined laminar “boundary layer” of concentrated vorticity along the body becomes apparent.

In the range $30 < R < 1500$, extreme diversity of flows is possible. Just behind a flat plate, a more or less fixed wake is typical, as shown in Fig. 2. In the case of a circular cylinder, the wake swings from side to side, and vortices of alternating sign are shed periodically, as in Fig. 1a of Ch. XIII. In the case of a disc, vortex loops are shed periodically.

As R increases further, the wake becomes increasingly turbulent, and periodicities harder to observe. Finally, in the range $R \simeq 10^5$ – 10^6 , the boundary layer itself becomes turbulent, flow separation is delayed, and the wake behind a streamlined body narrows markedly.

6. Kinds of cavitation. If we assume that cavitation occurs spontaneously when $p < p_v$, as in (1b), we get a rough idea of when to expect cavitation in steady flow. (Some notable exceptions to this assumption are described in Ch. XV, §§1–4.) Corresponding to this idea (cf. §8), the qualita-



Figs. 4a-4b. Photographs of the cavity behind a disc in a water tunnel. (Courtesy Naval Ordnance Laboratory)

tive nature of cavitating flow past an obstacle varies with the Thoma cavitation number Q defined by (3), roughly as follows (cf. [1], [23] or [48]).

The first sign of cavitation occurs when Q falls below some critical value Q_i , usually in the interval $0.35 < Q_i < 1.0$. The precise value of Q_i depends largely on the obstacle shape, but is also influenced by surface tension, air content, and viscosity (see Ch. XV, loc. cit.). When Q falls below Q_i , minute air or vapor filled cavities open up in the zone of negative pressure, collapsing noisily as soon as the flow has carried them back to a region of higher pressure. This type of flow is called *incipient cavitation*.

As Q decreases progressively, the cavitation bubbles become larger, and flow *separation* occurs in front of the zone of cavitation. For still smaller Q , the bubbles merge into a large envelope, which may be called "the cavity". Ordinary photographs of such cavities (see Fig. 4a) give them a

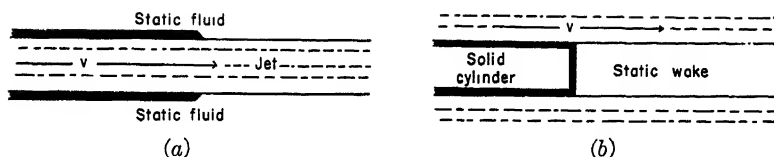


Fig. 5.

smooth, whitish appearance, because during the time of photographic exposure, the bubbles move many diameters (say 1" in 0.02 sec.). High-speed photographs¹⁰ (with exposure times of 10^{-4} secs.) reveal a foamy, turbulent wall in such cases (see Fig. 4b); the flows usually have a pronounced pressure gradient in the cavity. At still lower cavitation numbers (say, $Q = 0.10$), especially in the case of highly polished, sharp-edged obstacles in water tunnels having low turbulence and air content, a smooth, transparent, truly stationary cavity wall is apparent.

Various other types of cavitation are also possible; they will be described in Ch. XV. Besides "burbling cavitation" on the back side of propeller and turbine blades, there is "tip cavitation" spiralling off propeller tips, "vortex cavitation" near drowned jets, and "acoustic cavitation" stimulated by sound.

7. Parallel flow models. However, not all jets and cavities are so complicated. For example, liquid jets from faucets, and vertical cavity flows past long solids, can be approximately represented by the following two simple parallel flow models.

In the model for jets, the flow is assumed to have constant velocity v inside a straight circular cylinder of diameter $d = 2a$, while the surrounding medium is static, as in Fig. 5a. In the cavity model, the flow is uniform with velocity v outside the same cylinder. The cylinder is occupied by a semi-infinite solid in front, and by a cavity (or static wake filled with "dead water") behind, as in Fig. 5b.

In both models, each region of smooth flow is assumed bounded by a surface of discontinuity or *slipstream*¹¹, across which the velocity changes discontinuously. In a non-viscous fluid, such a slipstream would be in equilibrium, provided the pressure were continuous across the slipstream.

Actually, the flows of Figs. 5a-5b would satisfy the equations of motion exactly in any non-viscous, incompressible fluid of constant density ρ . This

¹⁰ Similarly, photographs with exposure times of 0.01 sec. or less gave the first clear picture of wake flow. See L. Ahlborn, "Über den mechanismus des hydrodynamischen Widerstandes", Hamburg, 1902. For jets, see [65, vol. 3, p. 444].

¹¹ The possibility of such a slipstream was conceived by Newton, "Principia Mathematica", Book II, Prop. 36, but his discussion is erroneous.

can be verified easily, by consulting the mathematical definition of such a fluid, given in §8. In this sense, as first observed by Helmholtz [35], these flows constitute possible models of a gas jet in a gas, and of a wake.

Instability. Unfortunately, the slipstreams are unstable¹². As will be shown in Ch. XI, §14, small perturbations in them grow exponentially. The rate of growth is roughly proportional to $\sqrt{\rho'/\rho}$, where ρ' is the smaller of the densities on the two sides of the slipstream. (Viscosity is relatively unimportant.)

Because of this instability, the models of Figs. 5a–5b represent real flows approximately only when (2*) is satisfied, or at the beginning of the jet or wake. Moreover, unless $\rho' = \rho$, the models fail because of gravity: the hydrostatic pressure can no longer be continuous across the slipstream, except in horizontal flow.

For these reasons, the preceding models correspond approximately to physical reality primarily when

$$(2^*) \quad \rho'/\rho \ll 1,$$

and

$$(7^*) \quad F \gg 1.$$

(Actually, $R \gg 1$ and $M \ll 1$ are also assumed.) The same limitations (2*) and (7*) apply ordinarily to the mathematical generalizations of the models of Figs. 5a–5b, with which Chs. II–X will be mainly concerned. (For some exceptions, see ftnt. 22 and Ch. II, ftnts. 4, 7, and 14.)

8. Euler flows. The generalizations of Chs. II–X are based on Euler's partial differential equations for incompressible, non-viscous flow, which are easily given. We assume that the vector velocity \mathbf{u} is a function of vector position \mathbf{x} and time t , which possesses continuous derivatives except perhaps on exceptional surfaces of discontinuity. Thus, in tensor notation,

$$(8) \quad u_i = u_i(x_1, x_2, x_3; t) \quad [i = 1, 2, 3].$$

A mathematically defined flow is called *volume-conserving* or *incompressible* if and only if it satisfies the identity

$$(9) \quad \text{Div } \mathbf{u} = \sum_{i=1}^3 \partial u_i / \partial x_i = 0, \quad \text{for all } \mathbf{x}, t.$$

At speeds up to 20 % of the speed of sound (e.g., up to 220 f/s in air and 950 f/s in water), real flows are nearly volume-conserving.

¹² This was recognized by Helmholtz [35, p. 222]; and earlier by G. Stokes, Trans. Camb. Phil. Soc. 8 (1843), p. 127.

Euler's *equations of motion* for a non-viscous, incompressible flow are

$$(10) \quad \rho \left\{ \frac{\partial u_i}{\partial t} + \sum_{k=1}^3 u_k \frac{\partial u_i}{\partial x_k} \right\} = - \frac{\partial p}{\partial x_i} + \rho g_i.$$

Here $\mathbf{g} = \mathbf{g}(\mathbf{x})$ is the vector gravity; ρ is the density and p the pressure.

A vector field (flow) $\mathbf{u}(\mathbf{x}; t)$ is called *irrotational* if it has a velocity potential $U(\mathbf{x}; t)$ whose gradient is $\mathbf{u}(\mathbf{x}; t)$, so that

$$(11) \quad u_i = \partial U / \partial x_i, \quad \text{or} \quad \mathbf{u} = \nabla U.$$

Such an irrotational flow is evidently volume-conserving if and only if

$$(12) \quad \nabla^2 U = \sum_{i=1}^3 \partial u_i / \partial x_i = \sum_{i=1}^3 \partial^2 U / \partial x_i^2 = 0.$$

It is easily verified that an irrotational volume-conserving flow satisfies (10), if and only if the associated pressure $p(\mathbf{x}; t)$ satisfies the *Bernoulli equation*

$$(13) \quad p + \frac{1}{2} \rho \nabla U \nabla U + \rho \partial U / \partial t + \rho G = p_0(t).$$

In (13), $G = G(\mathbf{x})$ is the gravitational potential, so that $\mathbf{g} = -\nabla G$. Such a flow, satisfying (11)–(13), will be called an *ideal* or *Euler flow*.

Conversely, it may be shown [50, Chs. I–III] that any non-viscous, incompressible fluid undergoes an Euler flow, if accelerated from rest or from any other irrotational initial condition.

9. Free streamlines. The Bernoulli equation (13) implies that the *velocity is constant on the boundary* of steady Euler flows like those of §7, under either of two hypotheses. (Note that $\partial U / \partial t = 0$ in any steady Euler flow.)

First, if the internal density ρ' is negligible, then the *pressure* along the slipstream is nearly constant, since the pressure in the internal medium is. Moreover this is true whether or not the low-density medium is at rest. Hence the boundary of the high-density fluid is at *constant pressure* p_c . Such a boundary is called a *free boundary*; boundaries between liquids and gases are typically of this kind.

Therefore, if \mathbf{g} is also negligible (i.e., if the Froude number v^2/gd is sufficiently large), and if the high-density flow is steady, then by (13)

$$\frac{1}{2} \rho \nabla U \nabla U = p_0(t) - \rho G_0 - p_c$$

is nearly constant on the bounding *free streamline*, at nearly constant pressure p_c .

Secondly, if $\rho' = \rho$, and the external fluid of density ρ' is static, then

continuity of pressure across the boundary gives (on the boundary)

$$\begin{aligned}\frac{1}{2}\rho\nabla U\nabla U &= p_0(t) - \rho G - p \\ &= p_0(t) - \rho G - [p_1(t) - \rho'G] = p_0(t) - p_1(t),\end{aligned}$$

where $p_1(t)$ is the constant in (13) for the static fluid. Hence the flow velocity along the bounding streamline of discontinuity (slipstream) is again constant, even though the pressure need not be.

Chs. II–X below will be concerned with the mathematical construction of steady Euler flows bounded by free streamlines, in the sense just defined. That is, they will be concerned with the construction of solutions $U(\mathbf{x})$ of the Laplace equation $\nabla^2 U = 0$, subject to the two boundary conditions

$$(14a) \quad \partial U / \partial n = 0 \text{ on the "fixed" boundary}$$

$$(14b) \quad |\nabla U| = \text{const. on the "free" boundary.}$$

In this sense, they will be concerned with finding analogs of the flows of Figs. 5a–5b, for jets from general orifices and cavities behind general barriers.

10. Conservation laws and jets. In general, the solution of the boundary value problem (12)–(14a)–(14b) just defined requires conformal mapping or potential theory. However, a few important results can be found by applying Bernoulli's equation and simple conservation laws. We shall now present briefly some such results, involving jets.

Torricelli's Theorem. For example, consider the jet from an orifice in a container, in which the water level is at a height h above the orifice. Then, by Bernoulli's equation (13), assuming the density ρ' outside the container to be negligible, so that the pressure is the atmospheric pressure p_a everywhere outside the container, the velocity $v = |\nabla U|$ on the (free) bounding streamline will satisfy

$$(14) \quad p_a + \frac{1}{2}\rho v^2 = p_a + \rho gh, \quad \text{or} \quad v = \sqrt{2gh}.$$

This is Torricelli's Theorem.

Borda tube. In general, the jet cross-section is less than the orifice cross-section by a factor C_c called the "coefficient of contraction". By momentum considerations, one can calculate C_c in one special case, as follows. Let¹³ a container with vertical walls be filled with a liquid of density ρ , into which is inserted, as in Fig. 6, a horizontal tube ("Borda mouthpiece") of cross-section area A ; let the pressure head at the level of the tube be p . We assume

¹³ See L. Prandtl and O. G. Tietjens, *Hydro- and aeromechanics*, New York, 1943, vol. 1, p. 242. The argument is due to J. Borda, *Mém. de l'Académie* (1766), p. 599. See James Thomson, *op. cit.* in fnnt. 3, pp. 91–6, for extensions.

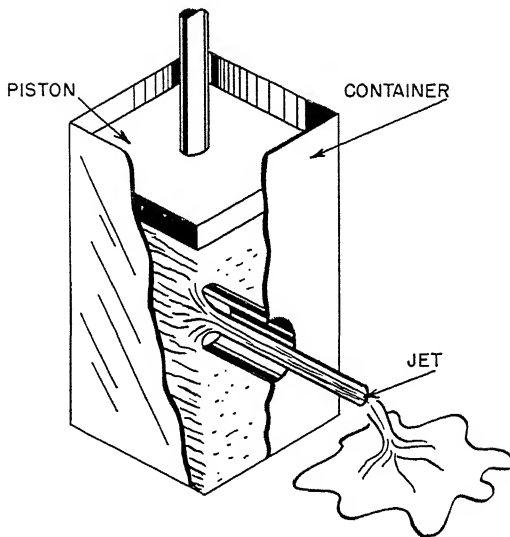


Fig. 6.

that the flow separates¹⁴ from the tube at its inner end, and that the jet from the tube tends asymptotically to a constant speed v ; this must be the constant “free streamline” velocity on the jet boundary. Let A^* be the asymptotic jet cross-section; then A^*/A is by definition the coefficient of contraction. We compute it as follows.

Per unit time, the volume efflux is vA^* ; the momentum efflux is $\rho v^2 A^*$; the kinetic energy efflux is $\frac{1}{2} \rho v^3 A^*$. The momentum supplied is however pA (pressure excess); the (potential) energy $p(vA^*)$. Hence $pA = \rho v^2 A^*$ and $p v A^* = \frac{1}{2} \rho v^3 A^*$. Dividing v times the first equation by the second, we get the result

$$(15) \quad \frac{A^*}{A} = \frac{1}{2}.$$

This argument is not restricted to plane flows, but is equally valid for a circular tube. (In Ch. II, §5, a complete description of the plane flow through a Borda tube is given.)

Jet Penetration. Again, let a homogeneous jet of density ρ_j and finite length λ impinge with velocity v_j on a fixed target of density ρ , as in Fig. 7a, so that the jet length diminishes at the rate $v_j - u$. Relative to an observer moving with the penetration velocity u , the phenomenon is stationary; the jet and target approach a common stagnation point with velocities $v_j - u$

¹⁴ This is the case of “free flow”; see A. H. Gibson, *Hydraulics, and its applications*, 4th ed., London, 1947, p. 122. “Full flow” can also occur.

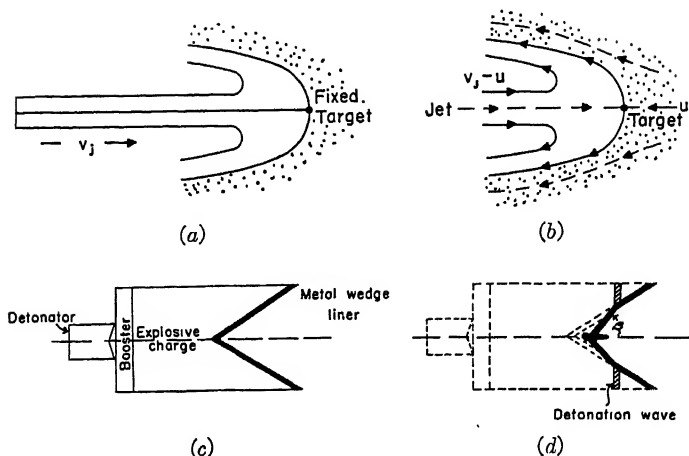


Fig. 7.

and u , as in Fig. 7b. Hence Bernoulli's theorem applies in both media; equating pressures at the stagnation point, we have $\frac{1}{2}\rho_j(v_j - u)^2 = \frac{1}{2}\rho u^2$. Applying this equation to the ratio of the rate u of penetration to the rate $v_j - u$ at which the jet is "eaten up", we get the fundamental equation¹⁵

$$(16) \quad \frac{\text{depth of penetration}}{\text{length of jet}} = \sqrt{\frac{\rho_j}{\rho}}.$$

This is quite well confirmed experimentally for shaped charges¹⁴, but would be of doubtful applicability to hypospray or dental drilling (§1).

Lined hollow charges. A final application is to lined hollow charges (cf. §1) having conical or wedge-shaped cavities¹⁶, as in Fig. 7c. When collapsed by a detonation wave, as in Fig. 7d, split microsecond X-ray shadowgrams reveal that the collapsed wall reforms in front of the moving collapse point J as a thin "jet", and behind J as a thicker "slug".

A rough explanation of the observed facts can be deduced from the following simplifying assumptions: (i) an impulsive velocity v_0 is imparted to the walls by the pressure of the passing detonation wave, after which pressure variations can be neglected, (ii) the process is nearly stationary, as viewed by an observer moving with the collapse point J . We let 2β denote the angle between the collapsing walls, and note that the direction

¹⁵ Discovered by R. Hill, N. F. Mott, and D. C. Pack in England, during World War II.

¹⁶ For further details, see G. Birkhoff, D. P. MacDougall, E. M. Pugh, and Sir Geoffrey Taylor, *J. Appl. Phys.* 19 (1948), 563-82, from which the exposition below is adapted. The extension to nonstationary conditions has been treated by E. M. Pugh, R. J. Eichelberger and N. Rostoker, *J. Appl. Phys.* 23 (1952), 532-42. See also R. J. Eichelberger, *ibid.* 26 (1955), 398-402 and 27 (1956), 63-8.

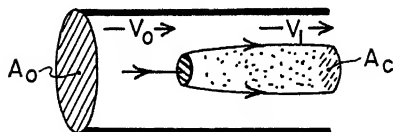


Fig. 8.

of motion will nearly bisect the angle $\beta - \alpha$ between the normal to the original liner surface, and the normal to the collapsing liner surface.

If m denotes the rate at which the liner mass is collapsed, and m_j the rate at which jet mass is created, slug mass will increase at the rate $m_s = m - m_j$, by mass conservation. Further, by (i)–(ii), Bernoulli's equation (§9) is applicable, and so all exposed surfaces have the same "free boundary" velocity v_2 . Thus the jet and slug lengthen at exactly the same rate during collapse. Hence the momentum equation has the simple form

$$mv_2 \cos \beta + m_s v_2 = m_j v_2.$$

Combining with $m_j + m_s = m$, and solving, we get

$$(17) \quad m_j/m = (1 - \cos \beta)/2, \quad m_s/m = (1 + \cos \beta)/2.$$

The velocity with which J is moving can be computed by trigonometry; it is $v_1 = v_0 \cos \frac{1}{2}(\beta - \alpha)/\sin \beta$. From this, the jet and slug velocities $v_1 + v_2$ and $v_1 - v_2$ are easily found.

Some limitations on the validity of this rough theory, due to compressibility, will be discussed in Ch. VIII, §9. A complete description of the velocity field in the two-dimensional case (of wedge-shaped cavities) will be given in Ch. III, §4. If the flow is reversed, one gets a theory of the conical sheets formed by two impinging coaxial jets.

11. Applications to cavities. Similar elementary methods can be used to deduce valuable information about cavities, subject to the approximations already described in §5.

Blocking constant. As a first example, we shall derive the *blocking constant* for steady cavity flow in a water tunnel (Fig. 8). We suppose¹⁷ an incompressible, non-viscous liquid, and a stationary liquid-gas interface, with negligible turbulence. Further, we suppose a uniform upstream flow with velocity v_0 , and a uniform free downstream velocity v_1 as the cavity approaches its maximum cross-section A_c , in a tunnel of cross-section A_0 . The rate of increase of liquid momentum per unit time is clearly $\rho v_1^2 A_1 - \rho v_0^2 A_0$, where $A_1 = A_0 - A_c$. The total thrust on a long section of liquid is

¹⁷ The discussion given is quoted verbatim from [6, Part I, §2]. It is assumed that gravity is negligible.

$(p_0 - p_v)A_0 = D$, where p_0 is the upstream pressure in the free stream, p_v is the cavity (vapor) pressure, and D is the drag. Hence

$$\rho v_1^2 A_1 - \rho v_0^2 A_0 = (p_0 - p_v)A_0 = D.$$

But by Bernoulli's equation, $p_0 + \rho v_0^2/2 = p_v + \rho v_1^2/2$; by conservation of volume, $v_1 A_1 = v_0 A_0$. Substituting

$$(18) \quad D = \rho A_0 (\frac{1}{2} v_1^2 - v_0^2) + (v_0 - v_1) v_0 = \frac{1}{2} \rho A_0 (v_1 - v_0)^2.$$

By Bernoulli's equation again, and (3),

$$(18') \quad Q = (v_1/v_0)^2 - 1, \quad \text{or} \quad (1 + Q)^{\frac{1}{2}} = v_1/v_0.$$

Hence if we define the *drag coefficient*, as is usual, in terms of the obstacle cross-section A and the *upstream* velocity $v_0 = v_f$, so that

$$C_D = 2D/\rho v_0^2 A = (v_1/v_0 - 1)^2 A_0/A,$$

we have the exact relation

$$(19) \quad C_D = [(1 + Q)^{\frac{1}{2}} - 1]^2 A_0/A \leq Q^2 A_0/4A.$$

Hence Q cannot drop below the *blocking constant*, Q_{\min} , defined by

$$(19') \quad Q \geq Q_{\min} = 2(C_D)^{\frac{1}{2}}(A/A_0)^{\frac{1}{2}}.$$

Since C_D ordinarily varies between .0625 and 1.00, we have in practice $(A/A_0)^{\frac{1}{2}}/2 \leq Q_{\min} \leq 2(A/A_0)^{\frac{1}{2}}$. Thus, to achieve $Q = .05$, we must have A_0/A about 400, at least. Since this is not practical, we conclude [6] that *free jet* is preferable to a closed water tunnel, for studies of cavitation if $Q < 0.1$.

Drag and Q. By assuming that the pressure variation is independent of Q , up to a scale factor, we also get the very useful approximate formula¹⁸

$$(20) \quad C_D(Q) = (1 + Q)C_D(0).$$

For, by Bernoulli's equation, the overpressure coefficient C_p varies from 1 at the stagnation point to $-Q$ in the cavity.

With the interpretation (3b), formula (20) is also very useful for wakes. Thus, it relates the mathematical $C_D(0)$ deduced theoretically for $Q = 0$ with the actual C_D . More generally, the formula

$$(20') \quad 1 - C_p(Q) = (1 + Q)(1 - C_p(0))$$

is also approximately applicable.

Cavity size. A similar approximate argument gives a fairly reliable idea of cavity size. This size is very important in wound ballistics, because the

¹⁸ Formula (20) is implicit in [1]. For further discussion, see [67a], [6], and [23, 138].

wounding power of high-speed bullets is often due more to the large transient cavity which they make, then to their perforating power¹⁹.

Underlying the argument is the idea that the flow around the closed cavity behind a high-speed missile is largely *radial*. Specifically, one supposes that the drag $D = \frac{1}{2}\rho v^2 AC_D$ (cf. (7)) is imparted to the water as kinetic energy, per unit length of travel. Assuming further that almost all this kinetic energy is converted to potential energy (work of cavity expansion) at the maximum cavity cross-section A_m , we get $\frac{1}{2}\rho v^2 AC_D = (p_f - p_c)A_m$, or²⁰

$$(21) \quad Q \simeq C_D A / A_m.$$

Similarly, in an open cavity extending to the water surface, it may be assumed that the work is done against hydrostatic pressure ρgy at depth y . This gives the approximate formula

$$(21') \quad A_m(y) \simeq D / \rho gy, \quad \text{or} \quad A_m / A = C_D v^2 / 2gy.$$

This inexact analysis will be pushed further in Ch. X, §6.

12. Ideal plane flows. To determine complete ideal (Euler) flows satisfying (12)–(14a)–(14b), more advanced methods are needed. The simplest case is that of ideal *plane* flows. Chs. II–VII are largely devoted to this case, which is the only case in which an extensive exact theory exists.

In plane flows, position in the physical plane may be represented by a single complex coordinate $z = x + iy$. The complex conjugate of the vector velocity may be denoted by $\bar{\zeta} = \bar{\xi} + i\bar{\eta}$, so that $\xi = u_1$ and $\eta = -u_2$. If the *complex potential* W is defined as $U + iV$, where U is the velocity potential and V the stream function, then it is a classic result [50, Ch. IV] for ideal plane flows that $W(z)$ is a complex analytic function, where

$$(22) \quad dW/dz = \bar{\zeta}, \quad \text{so that} \quad z = \int \bar{\zeta}^{-1} dW.$$

Hence conditions (14a)–(14b) reduce to

$$(22a) \quad V = \text{const. on the "fixed" boundary,}$$

$$(22b) \quad |\bar{\zeta}| = |dW/dz| = \text{const. on the "free" boundary.}$$

In certain cases of straight or polygonal fixed boundaries, ideal plane flows satisfying (22)–(22a)–(22b) can be found by *conformal mapping*, and the resulting flows expressed in closed form. Chs. II, III, and V will be

¹⁹ C. Cranz, "Handbook of Ballistics", vol. 1, §74, London, 1921.

²⁰ Formula (20) was developed in 1945 independently by H. Reichardt [67a] and L. H. Loomis. It predicts Q about 25% less than more exact theories (Ch. V, §9). Formula (21') was derived in 1944 by J. H. McMillen.

devoted to the exploitation of this technique, first applied in 1868–9 by Helmholtz [35] and Kirchhoff [47].

The case of curved fixed boundaries is much deeper theoretically, and is treated in Ch. VI. Although many of the basic ideas were discovered in 1907 by Levi-Civita [54], it was not until 1930 or so that the theory was completed by satisfactory existence and uniqueness theorems. These are proved in Ch. VII, whose §1 gives a brief historical discussion.

13. General theorems. Although most of Chs. II–XI will be concerned with those special configurations for which complete flows can be explicitly constructed, it is important to be aware of some general properties of (ideal) flows with free boundaries. We begin with an observation due to Kirchhoff²¹.

THEOREM 1. In any flow satisfying (12)–(13), the minimum pressure is assumed on the boundary.

Proof. Taking the Laplacian of (13), and noting that $\nabla^2 G = 0$ [44, p. 124], one gets after some calculation

$$0 = \nabla^2 p + \frac{1}{2} \rho \nabla^2 (\nabla U \nabla U) = \nabla^2 p + \rho \sum \nabla u_i \cdot \nabla u_i.$$

But clearly $\nabla u_i \cdot \nabla u_i \geq 0$; hence [44, p. 316] the pressure is *superharmonic*, and assumes its minimum value on the boundary.

It follows that, assuming (1b), cavitation in irrotational flow (but not vortex cavitation) must begin on the boundary.

Next, we give a general kinematic principle due to M. Brillouin [10].

THEOREM 2 (Brillouin's Principle). In steady irrotational flow, streamlines curve in the direction of increasing velocity.

Proof. The acceleration components of fluid particles satisfy, by definition

$$a_i = \sum u_k \frac{\partial u_i}{\partial x_k} = \sum u_k \frac{\partial u_k}{\partial x_i} = \frac{\partial}{\partial x_i} \left(\frac{1}{2} \sum u_k^2 \right) = v \frac{\partial v}{\partial x_i},$$

if $v = (\sum u_k^2)^{\frac{1}{2}}$ denotes the flow speed. The acceleration is consequently parallel to the velocity gradient ∇v .

The preceding theorems assumed that the flow was irrotational; we next state a result on dynamic similitude in which this is not assumed, but gravity is neglected.

THEOREM 3. Let Φ be an incompressible steady flow of a non-viscous flow with a free boundary. Then, for any real constants $\alpha, \beta, \gamma > 0$, and δ , the transformation $\mathbf{x}' = \alpha \mathbf{x}$, $\mathbf{u}' = \beta \mathbf{u}$, $\rho' = \gamma \rho$, and $p' = (\beta^2 \gamma) p + \delta$ defines a steady flow Φ' also satisfying Euler's equations.

²¹ *Vorlesungen über Mechanik*, 1876, p. 186; see also G. Bouligand, *J. de Math.*, 6 (1927), p. 427, or [4, p. 61].

The proof is immediate from (9)–(10), if \mathbf{g} and $\partial/\partial t$ are neglected [4, Ch. IV, §16]. The transformation carries free boundaries into free boundaries, and makes $U' = \alpha\beta U$ with Euler flows. It preserves all dimensionless coefficients such as C_D , the Q of (3a), etc.

COROLLARY. In determining an Euler flow with free boundaries, we can assume $\rho = \nu_f = 1$ and (say) $d = \pi$, without loss of generality.

Many other general results will be derived in Chs. IV and VII below.

14. Applications. The general theorems of §13 have some very important applications, which we shall now state as corollaries. These applications refer to steady ideal plane and axially symmetric flows, with gravity neglected.

COROLLARY 1. If (1b) holds, then $Q \geq 0$ and cavities must be convex.

Proof. Since (1b) implies $p_f \geq p_v$, $Q \geq 0$ is obvious. Again, since Du/Dt (the fluid acceleration) is $-\nabla p/\rho$, accelerations must be towards the cavity, if the pressure there is a minimum.

The preceding result, like Thm. 1, accords well with physical observation.

COROLLARY 2. With a finite cavity, the velocity on the cavity wall is a constant, and so a stagnation point is impossible.

Proof. By Bernoulli's Thm. along a streamline [61, p. 7], constant cavity pressure implies constant velocity. (As in Cor. 1, the flow need not be assumed irrotational.)

COROLLARY 3. A finite cavity, along whose wall the sense of velocity changes, must be cusped and with $Q \leq 0$.

(For such cusped cavities, see Ch. V, §14 and Ch. VI, §10. Using the Strict Maximum Principle of Ch. IV, §9, $Q < 0$ can be proved.)

COROLLARY 4. If (1b) holds, the cavity behind a simple barrier must have infinite length and satisfy $Q = 0$.

Corollary 4 creates a fundamental theoretical difficulty, since $Q > 0$ for real cavities (and wakes). This difficulty can be resolved by introducing fictitious barriers or reentrant jets at the rear end of the cavity (cf. Ch. II, §8, Ch. III, §8, and Ch. V, §9). This was first shown for wakes in 1920 by Riabouchinsky ([69], [70]), and the idea extended in 1932 to cavities by Weinig [46, pp. 294–300].

In the case of curved solid obstacles, there is a second, less serious difficulty, ignored by Levi-Civita, and first pointed out in 1911 by M. Brillouin [10]. Namely, the *separation point is variable*, even in the case of an infinite cavity. (In the case of a flat plate, separation must occur at the sharp ends, if infinite velocities and hence cavitation are to be avoided. —This was already remarked by Helmholtz [35], in 1868.)

To determine this separation point, an ingenious mathematical argument is required (Ch. VI, §6), whose physical justification through condition

(1b) was only pointed out recently [4, Ch. II, §5]. For a wide class of two-dimensional solid obstacles, including circular cylinders, the following conditions are equivalent: (i) separation is as far forward as possible, (ii) the pressure is minimized on the cavity wall, (iii) the cavity is convex, (iv) the cavity curvature at the separation point is finite.

15. Effective computation; generalizations. For the mathematician, the theory of ideal plane flows in Chs. VI–VII, and its implementation by *effective* computational procedures in Ch. IX, are the climax of the book. They represent the complete solution of a difficult boundary value problem in potential theory, which has interested mathematicians for nearly a century.

The last step, that of providing effective computational procedures, would hardly be practical if it were not for the recent development of high-speed computing machines. We have regarded this last step as of great importance, and have accordingly devoted an entire chapter to it (Ch. IX).

However, success in solving this problem leaves little room for complacency. The problem of ideal plane flows neglects effects of compressibility, gravity and viscosity. Moreover it ignores the (“Helmholtz”) instability of slipstreams, and turbulence. The remainder of the book discusses attempts to take the preceding neglected factors into account, and to obtain three-dimensional flows with free boundaries.

First, straightforward generalizations of complex variable methods are considered. Thus, in Ch. VIII, compressible plane flows without gravity (or viscosity) are analyzed, and incompressible plane flows with gravity. Especially for the former, the theory of Chaplygin [13] and his successors is still reasonably general and satisfactory.

In Ch. X, steady axially symmetric Euler flows with free boundaries are considered. Although no exact analytical formulas and few precise numerical results are available, many approximate facts are known in special cases. Moreover direct numerical methods are being developed, which promise to solve this problem before long.

The discussion of unsteady (i.e., time-dependent) potential flows in Ch. XI has a quite different flavor. Although the flows treated are very important for applications, specific results are mostly limited to simple symmetric (e.g., cylindrical and spherical cavity) free boundary configurations, and perturbations thereof, which can be handled by the method of separation of variables. The only exceptions are impulsive and self-similar flows, in which the time variable can be eliminated in other ways.

16. Viscosity and turbulence. Our understanding of the effects of viscosity and turbulence on jets and wakes is even more meager. Therefore,

a quasi-empirical approach has been adopted in Chs. XII–XIV, which are concerned with these effects.

This approach contrasts sharply with that adopted in Chs. II–XI, which mainly concern honest solutions of honest boundary value problems of potential theory. In the case of the non-linear Navier-Stokes equations, which presumably govern viscous and turbulent jets and wakes, no exact solutions relevant to the problem are known, except for “creeping” flows with $R \ll 1$.

In Chs. XII and XIV, what theory there is involves little more than interpretations of momentum conservation (which is much more complex than the non-viscous case would suggest), combined with similarity assumptions about the asymptotic behavior. Moreover even this meager theory will not always stand the test of critical inspection; this is especially true of “mixing length” concepts, in spite of the vogue which they have enjoyed.

The reliance on empiricism is even greater in Ch. XIII, dealing with the fascinating periodic manifestations which occur (cf. §5) at Reynolds numbers intermediate between those typical of laminar viscous jets and wakes (Ch. XII), and those typical of turbulent jets and wakes (Ch. XIV).

However unpalatable the discussion of Chs. XII–XIV may be to the mathematician, it comprises an important body of scientific fact and interpretation. In the important cases of liquid jets entering liquids, of gas jets entering gases, and of real wakes, it represents the best scientific understanding at the present time. The potential-theoretic models of Chs. II–X are too erroneous, in spite of occasional exceptions²². We hope that those who find the analysis of Chs. XII–XIV unpalatable, will try to improve on it!

17. Other physical variables. As in most other branches of continuum mechanics, even the problems which are too complicated to solve mathematically, are greatly oversimplified physically. To complete our realistic appraisal of the theory of jets, wakes, and cavities, we have concluded (in Ch. XV) by describing some important empirical facts involving physical variables which were ignored entirely in Chs. II–XIV.

Some of these variables are listed in Ch. XV, §1. The point which we wish to make now is, that the phenomena of real jets, wakes and cavities are exceedingly involved. The successful mathematical treatment of one simplified model should be regarded as an encouragement to progress to the next, more realistic model.

If this view is kept in mind, the arrangement of material in this book should appear quite logical, in spite of its heterogeneity. Successively more

²² Such as their success in predicting approximately the discharge coefficients of jets from orifices. See Ch. II, fnnts. 4, 7, and 14.

complicated situations, or mathematical approximations thereto, are treated in detail. At each stage of complication, we try to give a picture of what is known, organized as rationally as possible. As the complication increases, we pass gradually from theories which have been known for some time, to ideas which have been developed recently, then to theories which are highly fragmentary and incomplete, and finally to the simple narration of experimental facts, whose quantitative explanation is still shrouded in mystery.

Following this plan, we now turn our attention to the simplest mathematical models of jets and cavities, after the parallel flow models of §7. Until we get to Ch. VIII, we shall be considering exclusively ideal (irrotational, non-viscous) steady flows bounded by fixed and free streamlines, moving under the influence of inertia alone. We shall imagine these as describing the behavior of liquid jets in air, and of cavities behind obstacles in high-speed flows, and forget (temporarily) that the real flows are also influenced by gravity, surface tension, and viscosity.

CHAPTER II

CIRCULAR SECTOR HODOGRAPHS

1. Introduction. We recall from Ch. I, §12 that the mathematical theory of ideal plane flows involves three complex quantities: the position $z = x + iy$, the complex potential $W = U + iV$, and the conjugate $\zeta = \xi + i\eta$ of the complex velocity $\zeta^* = \xi - i\eta$. We also recall that

$$(1) \quad dW/dz = \zeta, \quad \text{whence} \quad z = \int \zeta^{-1} dW.$$

The *hodograph* of such a flow is simply the locus of the values of ζ .

In Chapters II, III, and V, we shall consider flows bounded by flat plates and free streamlines. In such cases, the hodograph boundary will consist of radial segments and circular arcs, centered at $\zeta = 0$. For, ζ has constant direction along any plate, and constant magnitude on any free streamline.

In Chapters II–III, we shall consider flows bounded by a single plate or wedge (which may, however, pass “through” a point at infinity), and a single free streamline. Typical examples of such flows are provided by the cavity behind a symmetric wedge (Fig. 1a), and the jet from a funnel (Fig. 1b). If we assume that there is at most one stagnation point, it follows that flow boundary is mapped onto the boundary of a circular sector in the hodograph plane. By Ch. I, §13, we can assume that this sector is (after a change of units and coordinate axes)

$$(2) \quad \Gamma: 0 \leq |\zeta| \leq 1 \quad 0 \leq \arg \zeta \leq \pi/n,$$

for some positive n , as in Fig. 1c. We shall suppose this normalization in all our formulas.

In fact, we shall assume in Ch. II that (i) *the hodograph is simply covered* (i.e., given ζ inside Γ , there is just one point z where the velocity is ζ^*). Defining the *W-diagram* of an Euler flow as the locus of all $W(z)$, we shall also make the customary assumption (ii) *the W-diagram is simply connected and simply covered*. In such cases, the flow can be determined using “elementary” conformal transformations, by the following technique.

In outline, the conformal mapping involved goes as follows. The function $t = \zeta^n$ maps Γ onto a semi-circle, which in turn is mapped by $\tilde{T} = -\frac{1}{2}(t + t^{-1})$ onto the upper half-plane

$$(2') \quad \Delta: \operatorname{Im}\{\tilde{T}\} \geq 0.$$

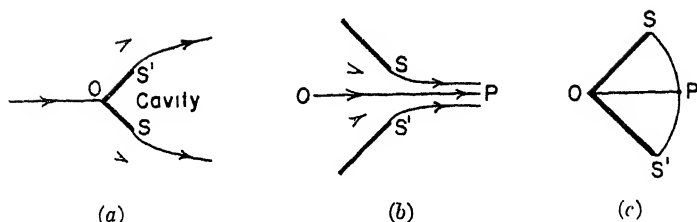


FIG. 1.

Again, it is clear that for any real a, b, c, d with $ad > bc$, $T' = (a\bar{T} + b)/(c\bar{T} + d)$ is a "schlicht", (i.e., one-one conformal) map of Δ onto itself. These facts are easily proved by elementary methods.

The Fundamental Uniqueness Theorem of Conformal Mapping¹ states that these are the *only* schlicht maps of Δ onto itself. There follows immediately

THEOREM 1. The most general schlicht map of Γ onto Δ is

$$(3) \quad T = \frac{a(\xi^{2n} + 1) + 2b\xi^n}{c(\xi^{2n} + 1) + 2d\xi^n},$$

where a, b, c, d are real and $ad < bc$.

We next note that any complete flow is bounded by streamlines, so that its W -diagram is bounded by cuts parallel to the real axis. It is thus a special case of the theory of Schwarz-Christoffel transformations [44, p. 370] that

THEOREM 2. If the W -diagram of a complete flow is simply connected, then there is a schlicht map which maps Δ onto the W -diagram, of the form

$$(4) \quad dW = f(T) dT = C \frac{\Pi(T - A_i)}{\Pi(T - B_k)} dT,$$

where the A_i, B_k are real, so that $f(T)$ is a rational function with real coefficients.

For example, in the case of a cavity behind a wedge, the W -diagram is a cut infinite plane; hence $W = T^2$ and $f(T) = 2T$, for a suitable determination of the constants a, b, c, d in (3). In the case of the jet from a funnel, the W -diagram is an infinite strip and $W = k \ln T$, whence $f(T) = k/T$. Another case is treated in Lemma 1 of §6. Note that, in all cases, W involves an arbitrary additive constant without physical meaning.

COROLLARY. Under the preceding hypotheses, z is the integral of a rational function of ξ^n and $\bar{\xi}$.

¹ [3, vol. 1, p. 61]. The proof is not so easy.

For T is a rational function (3) of ζ^n , and

$$(5) \quad z = \int \zeta^{-1} f(T) dT.$$

A general technique for integrating $z(\zeta)$ in closed form, when n is a rational number, will be given in §9. Special cases will be discussed in §§2-8. The physical significance of each case will be first briefly described; this description will be followed by the details of the calculations involved. We hope that by presenting these details (which are surprisingly troublesome in practice), we will save interested readers much time.

2. Cavity behind plate. We first consider the theoretical cavity behind a horizontal plate making an angle α with an infinite stream. Plates 1-3 show the cases $\alpha = 90^\circ$, $\alpha = 45^\circ$, $\alpha = 15^\circ$. Note that, when $\alpha = 15^\circ$, the dividing point is very near the leading edge, and that the nearby free streamline curves very sharply back so as to follow the main stream.

This model, originally designed to explain wake resistance², underestimates the actual fluid pressure by a factor $(1 + Q)$ of about two, when $\alpha > 15^\circ$ (the "stalling angle" where flow separates). Here $Q = (p_f - p_b)/\frac{1}{2}\rho v_f^2$ is the "wake underpressure coefficient" [p_f = free stream pressure, p_b = wake pressure, v_f = free stream velocity], as in Ch. I. At angles $\alpha < 15^\circ$, it underestimates the "lift" of an actual airfoil by still larger factors.

However, apart from its importance for cavity theory at $Q = 0$, and its historical importance, the model gives a fair idea of wake shape (see Plate 11). The theoretical stagnation point and the center of pressure, plotted in Fig. 2, also agree with observation. Finally, the model gives a good idea when $\alpha > 15^\circ$ of the pressure distribution along a flat plate, when corrected by the formula (see Ch. I, (20'))

$$(6) \quad (C_p)_{\text{obs}} = (1 + Q)(C_p)_{\text{theory}}.$$

The comparison is shown in Fig. 3.

The hodograph is the semicircle Γ of (2), with $n = 1$ since the flow is horizontal (ζ real) on the horizontal plate. Hence, Theorems 1-2 apply; moreover $W = T^2$, as in §1, for a suitable choice of the constants in (3). To determine these, note that $\zeta = 0$ when $T = 0$ at the dividing point. Hence $a = 0$ in (3), and so $bc > 0$. Dividing numerator and denominator of (3) through by c , we get

$$(7) \quad T = 2k\zeta/(\zeta^2 - 2C\zeta + 1), \quad k > 0 \quad \text{and} \quad C \text{ real.}$$

² See Kirchhoff [47]. Rayleigh [65, vol I, p. 287, and vol. III, p. 491] made the first quantitative comparison with experimental data; the most thorough comparison is due to Fage and Johansen [24].

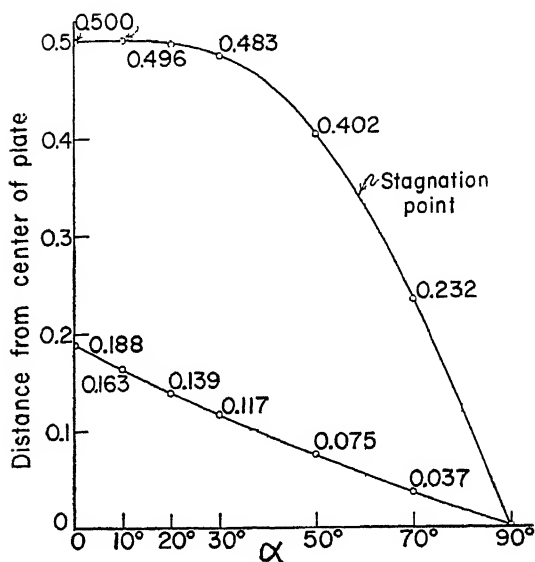


FIG. 2.

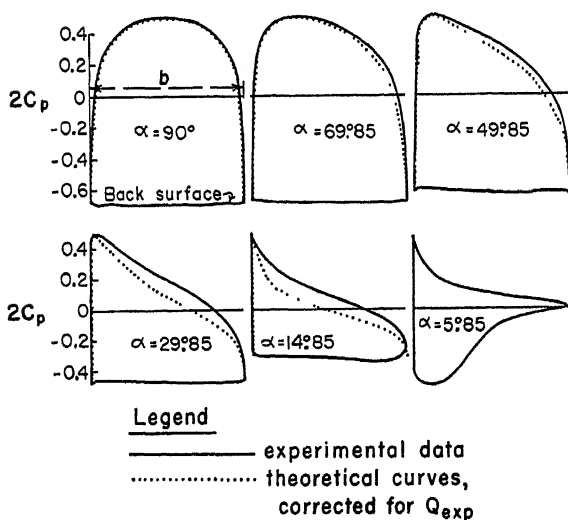


FIG. 3.

By similitude (Ch. I, §13), we can assume $2k = 1$ in computing dimensionless quantities. This choice gives, setting $W = T^2$ in (1) and using (7),

$$(7') \quad z = \int \frac{dW}{\xi} = \frac{W}{\xi} + \int \frac{W d\xi}{\xi^2} = \frac{T^2}{\xi} + \int \frac{d\xi}{(\xi^2 - 2C\xi + 1)^2},$$

after integration by parts. At infinity, $\zeta = e^{-i\alpha}$ and $W = \infty$; hence $C = \cos \alpha$. Integrating (7') by partial fractions in the complex domain, we get

$$(8) \quad z = \frac{\zeta}{(\zeta^2 - 2C\zeta + 1)^2} + \frac{1}{2S^2} \left\{ \frac{\zeta - C}{(\zeta^2 - 2C\zeta + 1)} - \frac{i}{2S} \operatorname{Ln} \frac{\zeta - e^{i\alpha}}{\zeta - e^{-i\alpha}} \right\},$$

where $S = \sin \alpha$. In summary, *the most general ideal cavity flow past a plate is similar to one satisfying (7)–(8), with $2k = 1$.*

3. Detailed formulas. There is an extensive technique for manipulating “elementary” complex formulas like (7)–(8), so as to get simple explicit expressions for real quantities of physical interest. We shall now give some indications of this technique.

On the plate, ζ is real; setting $\tau = \zeta - C$ so that $\zeta^2 - 2C\zeta + 1 = \tau^2 + S^2$, one can integrate (7') in real form [21, formula (120.2)] to get

$$(9) \quad z(\zeta) = \frac{\zeta}{(\tau^2 + S^2)^2} + \frac{1}{2S^2} \left\{ \frac{\tau}{\tau^2 + S^2} + \frac{1}{S} \arctan \frac{\tau}{S} \right\} + \frac{\pi}{4S^3}.$$

The constant $\pi/4S^3$ of integration is chosen to make (9) consistent with (8).

From (9), the plate width is found to be

$$(10) \quad b = z(1) - z(-1) = S^{-4} + \pi/(4S^3),$$

for our choice $2k = 1$ of dimensions in (7); the pressure coefficient $C_p = (1 - |\zeta|^2)/2$ is also easily found as a function of z/b , which permits one to compute the theoretical curves in Fig. 3. The position of the stagnation point is given by

$$z(1) - z(0) = \frac{1}{2S^3} \left[\frac{S}{1 - C} + SC + \frac{\pi - \alpha}{2} \right].$$

Again, since ζ is real, $|\zeta^2| = \zeta^2$ on the plate; hence the total force F on the plate is, by the Bernoulli equation

$$(11) \quad F = \frac{1}{2} i\rho \int (1 - \zeta^2) dz = \frac{1}{2} i\rho \int (\zeta^{-1} - \zeta) dW$$

taken along the plate in the sense of increasing z . (The pressure behind the plate corresponds to the assumed free streamline velocity $\zeta = 1$.) This can be easily integrated by standard formulas [21, p. 26], setting $\frac{1}{2} dW = T dT$ in (11) and using (7). One gets

$$(11a) \quad F = -i\rho\pi/4S^3,$$

whence by (10)

$$(11b) \quad C_D = \frac{2D}{\rho b} = \frac{2\pi S^2}{4 + \pi S} \quad \text{and} \quad C_L = \frac{2\pi SC}{4 + \pi S}.$$

Formulas (11b), being dimensionless, are applicable to any ideal cavity flow past a plate (see Ch. I, §13). The predicted drag is thus a maximum $C_D = 0.88$ when $\alpha = 90^\circ$, and the lift a maximum when $\alpha \simeq 37^\circ 30'$.

To compute the moment by "elementary" methods, one should (following Rayleigh) introduce bipolar coordinates, say by the complex substitution

$$(12) \quad e^{i(\omega+\alpha)} = (\zeta - e^{i\alpha})/(\zeta - e^{-i\alpha}).$$

Integrating trigonometric functions of ω , the moment about the center of the plate may be then found [50, §77] as

$$(13) \quad M = -3\pi\rho C/64S^7,$$

so that the center of pressure is at a distance

$$(13') \quad \bar{x} = 3C/16S^4 = 3Cb/4(4 + \pi S),$$

from the center of the plate. However, both (11a) and (13) are more efficiently derived from the less elementary asymptotic formulas of Ch. IV, §§5, 6.

Bipolar coordinates can also be used to give simple real parametric equations for the free streamlines. Let $\sigma = \text{Im}\{\omega\}$, so that $\sigma = \text{Ln} |\sin \frac{1}{2}(\phi + \alpha)/\sin \frac{1}{2}(\phi - \alpha)|$ where $-\phi = \arg \zeta$ is the velocity direction, and let $K = (2\alpha S + 3C)/8S^4$. Then, on the respective streamlines,

$$(14) \quad x = K + (C \cosh 2\sigma - 4 \cosh \sigma)/8S^4, \quad -y = (\sinh 2\sigma - 2\sigma)/8S^3,$$

$$(14') \quad x = K + (C \cosh 2\sigma + 4 \cosh \sigma - 4\pi S)/8S^4,$$

$$-y = (\sinh 2\sigma + 2\sigma)/8S^3.$$

We know of no simple real formula for the other streamlines—not even for the dividing streamline. The interior streamlines in Plates 1–3 were computed by methods described in Ch. IX, §2.

Neither do we know any formula expressing the time required for a particle to get from one point to another along an interior streamline, in this or any other case.

4. Cavity behind wedge. The extension of the results of §§2–3 to the case $n \neq 1$ of wedges illustrates several interesting theoretical points. Assuming a circular sector hodograph, one can repeat the argument leading to (7), to deduce $W = T^2$ and the relation

$$(15) \quad T = 2k\zeta^n/(\zeta^{2n} - 2C\zeta^n + 1); \quad k > 0, \quad C \text{ real.}$$

If n is rational, one can integrate $dz = 2\zeta^{-1}T dT$ to get $z(\zeta)$, etc., by general methods (§9); for irrational n , numerical integration (Ch. IX, §7) can be used.

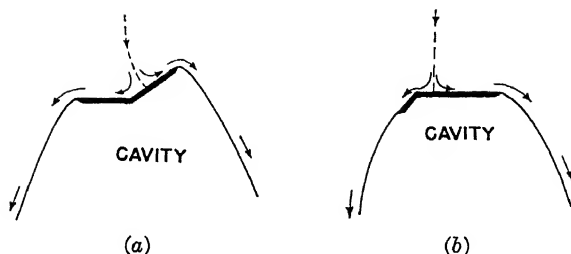


FIG. 4.

For a symmetric wedge, Bobyleff³ noted that since $C = 0$, (15) yields simply

$$(15') \quad dz = \frac{2n(\zeta^{4n-2} - \zeta^{2n-2})}{(\zeta^{2n} + 1)^3} d\zeta.$$

One such flow is shown in Plate 4.

If $u = \zeta^{2n}$ is taken as the variable of integration, the plate length l can easily be expressed in terms of the logarithmic derivative $\psi(x) = \Gamma'(x)/\Gamma(x)$ of the Γ -function by the formula [61, p. 310]

$$l = \frac{1}{8n} + \frac{1}{8n^2} + \frac{1}{16n^3} \left[\psi\left(1 - \frac{1}{4n}\right) - \psi\left(\frac{1}{2} - \frac{1}{4n}\right) \right].$$

The drag coefficient can also be⁴ plotted against the wedge angle $\beta = 2\pi/n$.

But the most interesting thing is the *theoretical insufficiency* of the preceding methods to cover the general asymmetric case. Thus, for each angle of inclination α , only one ratio of lengths for the two sides of the wedge is compatible with a simply covered circular sector hodograph. For other wedge dimensions, the simplest ideal cavity flow will not divide at the wedge vertex. In the case of an obtuse wedge (Fig. 4a), this will lead to a notched circular sector hodograph; with an acute wedge (Fig. 4b), infinite velocities will occur at the vertex. To avoid infinite velocities⁵, other free streamline configurations may be devised (Ch. V, §6, Fig. 10); in any case, more advanced techniques are needed.

Indeed, even the ideal cavity flow past a flat plate is not as inevitable as

³ Bobyleff, Beibl. Ann. phys. chemie 6 (1882), p. 163; see also J. Russ. Phys.-Chem. Soc. Petersburg 13 (1881), p. 63; G. H. Bryan and R. Jones, Proc. Roy. Soc. A91 (1915), 354-370. We set $2k = 1$ as in (7).

⁴ See also W. B. Morton, Phil. Mag. 48 (1924), 464-76; for experiments and facts, consult E. Brun, M. Plan and M. Vasseur, J. Rech. Centre Nat. Rech. Sci. No. 4-5 (1948), 17-25.

⁵ These occur when the fluid goes around the edges; for a flow past a plate with infinite velocity, see C. Schmieden, Luft. Forsch. 17 (1940) No. 2, p. 37. See also M. Kataoka, Proc. second Jap. nat. congr. appl. mech., 239-43.

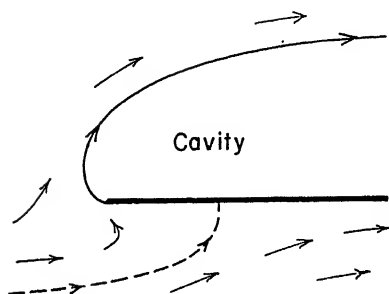


FIG. 5.

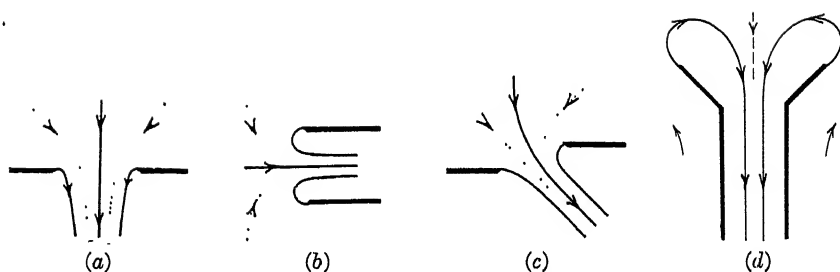


FIG. 6.

might be supposed. An alternative type is sketched in Ch. V, §2, Fig. 3. A further peculiar alternative to the uniform flow past a flat plate held parallel to a stream is obtained by letting $\alpha \downarrow 0$ in §2, but varying the plate location and dimensions so that the stagnation point and leading edge are held fixed at $z = 0$, $z = 1$, respectively. The resulting flow is sketched in Fig. 5; it is defined by the formula

$$(16) \quad z = \frac{16}{17} \left[\frac{3\zeta}{(1-\zeta)^4} + \frac{1}{(1-\zeta)^3} - 1 \right].$$

Actually, the determination of *all* flows with free streamlines past a flat plate is extremely involved⁶.

5. Jet from funnel. One of the simplest flows with free streamlines is provided by the jet from a funnel, as illustrated in Plates 5, 6. Diagrams sketching such flows are shown in Figs. 6a–6c. The mathematical treatment was first given by Helmholtz [35, p. 225]; see also [32, p. 31]. Contraction coefficients for liquid jets are predicted quite accurately by the theory⁷ as

⁶ There are nine cases; see [91].

⁷ [62]; [59a]; J. S. McNown and E.-Y. Hsu, Proc. first Midwest conf. fluid dyn. U.S.A. (1950), 143–55.

TABLE I. Jet from symmetric funnel, half-angle β

$\beta = \pi/n$	22.5°	45°	67.5°	90°	112.5°	135°	157.5°	180°
C_c (theory)	.855	.745	.666	.611	.568	.537	.516	.500
C_c (exper.)	.882	.753	.684	.632	.606	.577	.546	.541

TABLE II. Geometrical parameters for jet from slot

α	0°	18.4°	37.0°	56.2°	76.7°	91.8°	180°
C_c	.611	.609	.602	.588	.562	.532	0
γ	90°	75°	60°	45°	30°	20°	0°

shown in Table I. Table I is based on calculations by von Mises [62, p. 472] and data of Weisbach corrected for gravity by Zeuner [25, p. 351].

In this case, the W -diagram is evidently an infinite strip, with a stagnation point at $W = -\infty$. By proper choice of units, this reduces to $0 \leq V \leq \pi$. Hence the variable W , defined by

$$(17) \quad T = e^W, \quad \text{or} \quad W = \text{Ln } T,$$

simply covers the half-plane. If the hodograph is a circular sector, which seems very plausible, we will therefore have (17) and (3). Also, the stagnation point at $W = -\infty$, $T = 0$, makes $a = 0$ in (3). Finally, since a translation $W \rightarrow W + k$, which corresponds to $T \rightarrow e^k T$, has no physical meaning (Ch. I, §3), we can suppose $b = c = 1$ without loss of generality. Hence (3) reduces to (15), with $2k = 1$. Combining with (17), we get

$$(18) \quad \begin{aligned} W &= n \ln \zeta - \ln (\zeta^{2n} - 2C\zeta^n + 1) \\ &= n \ln \zeta - \ln (\zeta^n - e^{in\alpha}) - \ln (\zeta^n - e^{-in\alpha}). \end{aligned}$$

Here $C = \cos n\alpha$, $S = \sin n\alpha$, as in §§2-4, where $-\alpha$ is the direction of the jet at infinity.

In the case $n = 1$ of the *jet from a slot* (illustrated by Plate 7), one can easily integrate $dz = \zeta^{-1} dW$ in closed form, getting

$$(19a) \quad z = -\frac{1}{\zeta} + C(\ln \zeta + W) + iS \text{Ln} \frac{\zeta - e^{i\alpha}}{\zeta - e^{-i\alpha}}.$$

In Table II, we have tabulated the contraction coefficient⁸ C_c , and the angle γ between the slot walls and the line joining the slot edges, as functions of

⁸ Defined as the ratio of the asymptotic width of the jet to the distance between the plate edges.

α , for $0 < \alpha \leq 90^\circ$. The latter is $\pi/(2 + \pi) = 0.611$ if $\alpha = 90^\circ$; in this case, the free boundary is a tractrix. In general, the free boundaries may be expressed parametrically as follows. On the left free streamline, where $\zeta = e^{i\phi}$ [$0 < \phi < \alpha$],

$$(19b) \quad \begin{aligned} z = & -\cos \phi + i \sin \phi + iC\phi - C \ln [2(\cos \phi - \cos \alpha)] \\ & - S(\alpha + \pi) + \frac{1}{2}iS \ln \frac{1 - \cos(\phi - \alpha)}{1 - \cos(\phi + \alpha)}. \end{aligned}$$

Similarly, on the right-hand free streamline, where $\alpha < \phi < \pi$,

$$(19c) \quad \begin{aligned} z = & -\cos \phi + i \sin \phi + iC(\phi + \pi) - C \ln [2(\cos \phi - \cos \alpha)] \\ & - S\alpha + \frac{1}{2}iS \ln \frac{1 - \cos(\phi - \alpha)}{1 - \cos(\phi + \alpha)}. \end{aligned}$$

The most interesting case is the *symmetric* case⁹. In this case, half the flow again represents the jet from a funnel, of which one side (the axis of symmetry) extends to infinity. With the preceding choice of coordinate axes, the axis of symmetry makes an angle $\alpha = \beta/2 = \pi/2n$ with the horizontal, so that $C = 0$ and $S = 1$ in (18). Consequently, we have

$$(18a) \quad W = n \ln \zeta - \ln(\zeta^{2n} + 1)$$

$$(18b) \quad z = \int \zeta^{-1} dW = -\frac{n}{\zeta} - 2n \int \frac{\zeta^{2n-2} d\zeta}{\zeta^{2n} + 1},$$

from which the mouth opening h of the funnel is easily computed in terms of the logarithmic derivative $\psi(x) = \Gamma'(x)/\Gamma(x)$ of the Γ -function,

$$h = \sin \frac{\pi}{2n} \left\{ 2n + \psi \left(1 - \frac{1}{4n} \right) - \psi \left(\frac{1}{2} - \frac{1}{4n} \right) \right\}.$$

A particularly interesting case is that of a Borda mouthpiece, when $n = \frac{1}{2}$ (see Ch. I, §10). In this case, the free streamline is given explicitly [50, p. 98] by

$$(18c) \quad x = 2 \sin^2(\theta/2) - 2 \log \sec(\theta/2), \quad y = \theta - \sin \theta,$$

and the contraction coefficient $C_c = 0.5$ (cf. Ch. I, §10).

The idea, that $0.5 \leq C_c \leq 1.0$ always, has been very useful in hydraulics. For convergent orifices, this follows from the results above, combined with the Comparison Theorem of Ch. IV, §13. However, as shown by Levi-Civita^{9a}, it need not hold in the case of convergent-divergent orifices, like that of Fig. 6d.

⁹ [32, §18]; also J. Smetana, *La Houille Blanche* 3 (1948), 41-53, and H. W. Hahne-mann, *Forsch. Geb. Ing.* 18 (1952), 45-55.

^{9a} Atti R. Ist. Veneto Sci. Let. 64 (1905), 1465-72; see also U. Cisotti, *ibid.* 74 (1914), 1499-1509; also Ch. I, §10. The flow of Fig. 6d can be expressed in closed form, using the method of Ch. III, §7.

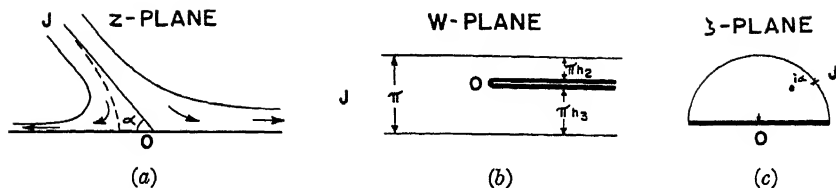


FIG. 7.

6. Jet against plate. The case of a jet impinging on an infinite plate¹⁰ (Fig. 7a) gives a more complicated W -diagram (Fig. 7b); the hodograph is semicircular (Fig. 7c). We normalize to the case that the plate is horizontal, while the jet has thickness π .

LEMMA 1. If the dividing point is mapped on $T = 0$, then the W -diagram corresponds to the half T -plane by

$$(20) \quad W = -\ln(T - T_1) + h_2 \ln(T - T_2) + h_3 \ln(T - T_3),$$

where T_1, T_2, T_3 correspond to the points at infinity on the impinging jet and its two branches respectively, and $h_2 + h_3 = 1$.

Proof. By the general theory of Schwarz-Christoffel transformations, we can set $f(T) = T/(T - T_1)(T - T_2)(T - T_3)$ in (4). Using partial fractions¹¹, we can hence write $f(T) = \sum h_i/(T - T_i)$ for suitable constants h_1, h_2, h_3 . Integrating (4), we get $W = \sum h_i \ln(T - T_i)$, where the πh_i are the jumps in V at the T_i . By our normalization, $h_1 = -1$; by conservation of mass ("uniformity" in the sense of complex variable theory), $h_2 + h_3 = 1$.

By a little closer attention, we can get entirely specific formulas. If we set

$$(21a) \quad T = 2\zeta/(\zeta^2 + 1),$$

the hodograph is mapped onto the half-plane Δ by Theorem 1, with $n = b = c = 1, a = d = 0$; also, at the dividing point $\zeta = 0$, whence $T = 0$ and the conditions of Lemma 1 hold.

Substituting $\zeta = e^{i\alpha}, \zeta = 1, \zeta = -1$ in (21a), we deduce $T_1 = 2e^{i\alpha}/(e^{2i\alpha} + 1), T_2 = 1, T_3 = -1$. Also, by conservation of horizontal momentum, $h_2 - h_3 = C$, where $C = \cos \alpha, \alpha$ being the angle made with the x -axis by the impinging jet. Combining with $h_2 + h_3 = 1$, we get

$$(21b) \quad 2h_2 = 1 + C \quad \text{and} \quad 2h_3 = 1 - C.$$

¹⁰ W. Schach, *Ing. Archiv* 5 (1934), 245-65, and 6 (1935), 51-8, has discussed this flow in detail, with numerical results, from the hydraulic point of view. See also [32, pp. 11-12] and [61, pp. 279-87].

¹¹ See G. Birkhoff and S. MacLane, *A survey of modern algebra*, New York, Macmillan, rev. ed., 1953, p. 84.

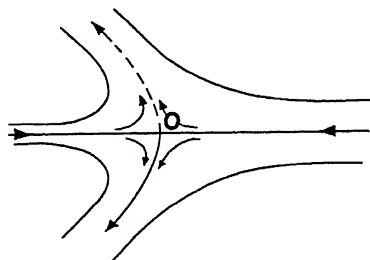


FIG. 8.

Substituting $f(T) = \sum h_i/(T - T_i)$ in (5), and integrating, we get

$$(21c) \quad z = z_0 + C \ln (\zeta^2 - 2C\zeta + 1) - iS \ln \frac{\zeta - e^{i\alpha}}{\zeta - e^{-i\alpha}} \\ - (1 + C) \ln (\zeta - 1) + (1 - C) \ln (\zeta + 1).$$

The corresponding equation for the free streamlines $\zeta = e^{i\phi}$ is

$$(21d) \quad z = z_1 + C \ln \left| \frac{C - \cos \phi}{\sin \phi} \right| + \ln \cot \frac{1}{2}\phi \\ + \frac{1}{2}iS \ln \left\{ \frac{1 - \cos (\phi + \alpha)}{1 - \cos (\phi - \alpha)} \right\},$$

where

$$z_1 = \begin{cases} (1 + C)\frac{1}{2}\pi i + S(\pi - \alpha) & \text{if } \phi < \alpha \\ (1 - C)\frac{1}{2}\pi i - S\alpha & \text{if } \phi > \alpha \end{cases}.$$

If we reflect the flow so obtained in the plate, we get a complete description of the ideal flow due to two *symmetrically impinging jets* (Fig. 8). Impinging jets are discussed in Ch. III, §§3-5.

An interesting limiting case is obtained if α is allowed to tend to π , h_3 being held fixed while h_1, h_2 are allowed to become infinite (see Plate 8). Relative to an observer having the velocity of the stream, this appears as the formation of a jet by a collapsing cavity¹². If velocities are reversed, it appears as the *penetration of a stationary fluid target by a two-dimensional jet of equal density*.

The flow is given by the mathematical formula

$$(22) \quad z = \frac{-2}{(\zeta + 1)^2} - \frac{2}{(\zeta - 1)} + \ln \frac{\zeta + 1}{\zeta - 1} + \text{const.}$$

¹² See G. Birkhoff and T. E. Caywood, J. appl. phys. 20 (1949), p. 650; [4, Ch. II, §13]. A very brief description is given in [32, p. 49], without physical interpretation. See also Ch. I, §10.

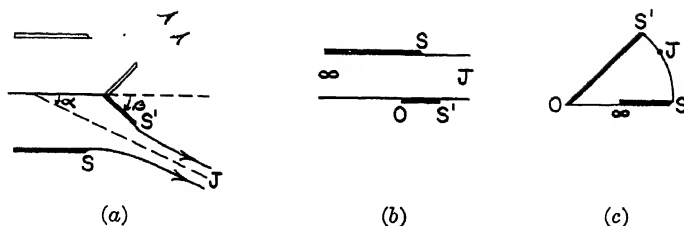


FIG. 9.

The discussion of §1 makes it natural to try to treat jets against infinite wedges by generalizing (21a) to $T = 2\zeta^n/(\zeta^{2n} + 1)$. However, except in the symmetric case, one does not get a circular sector hodograph (cf. the end of §4). The symmetric case is more easily treated by considering half the flow, whose W -diagram is an infinite strip. We shall now consider this class of flows.

7. Réthy flows. Consider half the flow past a wedge held symmetrically in the jet from a nozzle (Fig. 9a). Its W -diagram is an infinite strip (Fig. 9b); its hodograph (as we assume) a circular sector (Fig. 9c), subtending the wedge semi-angle $\gamma = \pi/n$. Such a flow may be called a "Réthy" flow.

If we normalize so that the W -diagram has width π , and the free stream-line velocity is one, we can set $W = \ln T$, as in (17), where T is given¹³ by (3). This gives

$$W = \ln [a(\zeta^{2n} + 1) + 2b\zeta^n] - \ln [c(\zeta^{2n} + 1) + 2d\zeta^n].$$

Now if $v < 1$ is the velocity in the nozzle, and $e^{-i\alpha}$ that in the impinging jet, then $\zeta = v$ when $W = -\infty$ and $T = e^W = 0$, while $\zeta = e^{i\alpha}$ when $W = T = \infty$. Thus, neglecting additive constants, we have

$$\begin{aligned} (23) \quad W &= \ln [(\zeta^n - e^{in\alpha})(\zeta^n - e^{-in\alpha})] - \ln [(\zeta^n - v^n)(\zeta^n - v^{-n})] \\ &= \ln [\zeta^{2n} - 2C\zeta^n + 1] - \ln [\zeta^{2n} - (v^n + v^{-n}) + 1], \end{aligned}$$

where $C = \cos n\alpha$. Writing $z = \int \zeta^{-1} dW$, we thus get

$$(24) \quad z = 2n \int \frac{\zeta^{2n-2} - C\zeta^{n-2}}{\zeta^{2n} - 2C\zeta^n + 1} d\zeta - 2n \int \frac{\zeta^{2n-2} - D\zeta^{n-2}}{\zeta^{2n} - 2D\zeta^n + 1} d\zeta,$$

where $D = \frac{1}{2}(v^n + v^{-n}) > 1$ and $C < 1$.

¹³ The treatment outlined here was first suggested by M. Réthy [68] in 1881. For the important extension by von Mises [62], see §9. See also [58] and V. Valcovici, *Inaugural dissertation*, Univ. of Gött. (1913); T. T. Siao and P. G. Hubbard [59a, 33-44] give graphs of the effect of jet thickness on jet deflection for several wedge angles. See also D. W. Apell and E. M. Laursen [59a, 21-32]. The limiting case of an infinite wedge is treated by H. H. Ambrose [59a, 73-80].

Nomograms are given in Plates 9a, 9b, expressing the relative jet deflection α/γ and the ratio v of upstream to downstream velocity in terms of the wedge length and position, for 15° , 30° , 45° , 60° , and 90° wedge semi-angles γ . The deflection of a free jet and the contraction of a stream in a channel by a symmetric wedge are shown in Plate 10.

Special cases of this will be discussed in §8; the formal integration of (24) for general rational n will be treated in §9. For the present, we note only some interesting extensions by symmetry, besides that to a wedge in the jet from a nozzle depicted in Fig. 9a.

In the limiting case $\alpha = 0$, when the straight wall becomes *infinite*, we can obtain half the jet from an angular mouthpiece (Fig. 10a), as well as a wedge in a channel [14]. Iterating the reflection, we get the jets formed by an infinite series of symmetric equally spaced wedges.

In the limiting case when the bent wall extends to infinity in both directions (Fig. 10b), we can reflect in both straight sections of the wall. If $n = 2m$ is an even integer, one can iterate so as to make the stagnation point an *interior stagnation point*, as in the case of impinging jets, already discussed in §6. An especially simple case occurs when the straight wall vanishes ($v = 1$), ($C = -1$) corresponding to

$$(23') \quad W = 2 \ln \left(\frac{\zeta^n - 1}{\zeta^n + 1} \right)$$

$$(24') \quad z = 4n \int \frac{\zeta^{n-2}}{\zeta^{2n} - 1} d\zeta,$$

and representing a free stream flowing in an angle [32, §21]. The ratio of the maximum width to the final width expresses the thickening of the jet, and is found to be

$$\frac{4n}{\pi} \left| \int_0^i \frac{\zeta^{n-2}}{\zeta^{2n} - 1} d\zeta \right| = \frac{1}{\pi} \left[\psi \left(\frac{3}{4} - \frac{1}{4n} \right) - \psi \left(\frac{1}{4} - \frac{1}{4n} \right) \right].$$

The case $n = 6$ is shown in Fig. 10c; it is a curious fact that (theoretically, in an ideal fluid) the flow in any one of the six branches could be reversed; the equations of motion would still be satisfied!

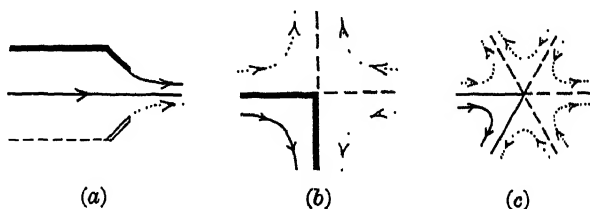


FIG. 10.

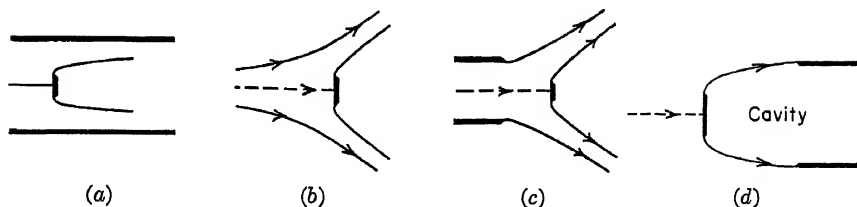


FIG. 11.

8. Applications; superposition principle. Of especial interest for applications is the case $n = 2$, which has been discussed in great detail by Réthy and others^{13, 14}.

Thus, consider half of the cavity flow past a plate of half-width b , held perpendicularly in the middle of a *closed channel* of width π/v (Fig. 11a). One can easily integrate (24) in closed form, getting

$$(25a) \quad z = f_1(\zeta) = 4 \tanh^{-1} \zeta - 2v \tanh^{-1} v\zeta - \frac{2}{v} \tanh^{-1} \frac{\zeta}{v},$$

$$(26a) \quad b = \frac{v-1}{v} [(2+2v) \tan^{-1} v - \pi],$$

where v is the asymptotic upstream velocity. The drag coefficient based on the (downstream) free streamline velocity is $C_D = \pi(1 - v^2)/bv$; that based on the upstream velocity is C_D/v^2 . Using (26a), one can show [6] that *the wall correction for cavity C_D is small if it is based on the free streamline velocity, but very large if based on the upstream velocity.* For example, in a channel of half-width $a = 6b$, the correction is 1 %, as against 150 % if the upstream velocity is used.

Similarly, if the plate (of half-width b') is in a *free jet* of width π (Fig. 11b), we have

$$(25b) \quad z = f_2(\zeta) = 2 \ln(1 + \zeta) - 2 \ln(1 - \zeta) - e^{i\alpha} \ln \frac{1 + e^{i\alpha}\zeta}{1 - e^{i\alpha}\zeta} - e^{-i\alpha} \ln \frac{1 + e^{-i\alpha}\zeta}{1 - e^{-i\alpha}\zeta},$$

$$(26b) \quad b' = \pi(1 - \cos \alpha) - 2 \sin \alpha \log \tan(\pi/4 - \alpha/2),$$

where α is the asymptotic jet angle. In this case, the wall correction for C_D is about that for a closed channel of the same width, when the latter is based on the free streamline velocity.

¹⁴ See [62]; [6]; F. Kretzschmer, VDI Forschungsheft 381 (1936); M. I. Gurevich, Izv. Akad. Nauk SSSR Otd. tekhn. Nauk 4 (1946), 487-98. Formulas (25a)-(26a) apply approximately to valve wakes also [22], provided the clearance is small enough for the channel wall to stabilize the flow; B. Gentilini, La houille blanche 2 (1947), 145-9.

In the case of a plate in the *jet from a nozzle* (Fig. 11c), W has a source at $\zeta = v$ and a sink at $\zeta = e^{i\alpha}$ in the hodograph plane. In the closed channel case, the source is at $\zeta = v$, and the sink at $\xi = 1$. For a plate in a free jet, the source is at $\xi = 1$ and the sink at $\zeta = e^{i\alpha}$. Since $z = \int \zeta^{-1} dW$ is linear in $W(\zeta)$, it follows that any cavity flow past a plate held symmetrically in a bounded jet is a superposition

$$(25c) \quad z = f_1(\zeta) + f_2(\zeta)$$

of flows past a plate in a closed channel and past a plate in a free jet.

The preceding construction is a special case of the following

Superposition Principle. Let $z = f_1(\zeta)$ and $z = f_2(\zeta)$ be two ideal plane flows having a given hodograph. Then any real linear combination

$$(27) \quad z = a_1 f_1(\zeta) + a_2 f_2(\zeta) \quad [a_1, a_2 \text{ real}]$$

describes an ideal plane flow having the same hodograph.

For, since V_1 and V_2 are piecewise constant on the boundary, $\text{Im}\{a_1 W_1 + a_2 W_2\} = a_1 V_1 + a_2 V_2$ has the same property; hence the superposition (27) is bounded by streamlines.

The Superposition Principle is often useful for flows with circular sector hodographs. However, the superpositions may be self-overlapping in the large, or lack physical interest for other reasons.

Cavity with underpressure. The case of a source at $\zeta = v$ and equal sink at $\zeta = v_1$ ($0 < v \leq v_1 < 1$) has also been studied recently^{14a}. The limiting case $v = v_1$ of an infinite stream provides the simplest model for cavity flow with positive cavitation number, $Q > 0$. It represents half of an ideal flow past a plate, followed by a cavity whose boundary terminates in (non-free) parallel streamlines, as in Fig. 11d. The half-flow is determined by the formulas

$$W = 2\zeta^2/(\zeta^4 - 2K\zeta^2 + 1), \quad K = (v^2 + v^{-2})/2,$$

as can be seen from the fact that $-(\zeta^2 + \zeta^{-2})/2$ maps the hodograph on the upper half T -plane.

9. Partial fractions. We shall now consider expressions of $z(\zeta)$ in closed form, for flows with circular sector hodographs whose W -diagrams are simply connected and simply covered.

Von Mises [62] first observed¹⁵ that the method of §8 could be applied

^{14a} A. Roshko, NACA TN 3168 (1954); [23a]; M. S. Plesset and B. Perry, *Riabouchinsky Jubilee Volume* (1954), 251-62.

¹⁵ The theoretical discussion is reproduced, as an Appendix, in the German edition of [50], and in Frank-von Mises, *Differentialgleichungen der Physik*, vol. 2, Ch. XI, §2.

to all Réthy flows with rational $n = r/s$ (r, s integers). Indeed, we have immediately from (23)

$$(28) \quad dz = \zeta^{-1} dW = \left[\frac{\zeta^{n-2}}{\zeta^n - e^{in\alpha}} + \frac{\zeta^{n-2}}{\zeta^n - e^{-in\alpha}} - \frac{\zeta^{n-2}}{\zeta^n - v^n} - \frac{\zeta^{n-2}}{\zeta^n - v^{-n}} \right] n d\zeta.$$

We infer directly

$$(29) \quad z = I_n(\zeta, e^{i\alpha}) + I_n(\zeta, e^{-i\alpha}) - I_n(\zeta, v) - I_n(\zeta, v^{-1}),$$

where the complex functions I_n are defined by

$$(29') \quad I_n(\zeta, \zeta_1) = n \int_0^{\zeta} \frac{\zeta^{n-2}}{\zeta^n - \zeta_1^n} d\zeta.$$

If $n = r/s$ is rational (r, s integers), and we introduce the parameter $u = \zeta^{1/s} = t^{1/r}$, we have

$$I_{r/s}(\zeta, \zeta_1) = r \int_0^{\sqrt[s]{\zeta}} \frac{u^{r-s-1}}{u^r - u_1^r} du \quad [u_1 = \zeta_1^{1/s}].$$

Since $n > 1$, $r > s$; hence $r \geq s + 1$, and the integrand is finite at $u = 0$. Further, by the partial fraction decomposition

$$(30) \quad \frac{u^{r-s-1}}{u^r - u_1^r} = \frac{1}{r} \sum_{k=0}^{r-1} \frac{u_1^{-s} e^{-2\pi i ks/r}}{u - u_1 e^{2\pi i k/r}},$$

$$I_{r/s}(\zeta, \zeta_1) = u_1^{-s} \sum_{k=0}^{r-1} e^{-2\pi i ks/r} \text{Ln} [1 - u/(u_1 e^{2\pi i k/r})].$$

This expresses $z(\zeta)$ in terms of *elementary* complex functions.

10. Beta functions. Each function $I_n(\zeta, \zeta_1)$ of §9 can also be written as an *incomplete beta function*

$$(31) \quad B_\beta(\tau) = B(\beta, 0; \tau) = \int_0^\tau \tau^{\beta-1} (1 - \tau)^{-1} d\tau \quad [\beta = (n - 1)/n].$$

In fact, writing $\zeta = \zeta_1 \tau^{1/n}$, we get

$$(32) \quad I_n(\zeta, \zeta_1) = -\zeta_1^{-1} B_\beta(\zeta^n/\zeta_1^n).$$

Conversely, if $n = r/s$ is rational, then $B(1 - s/r, 0; \tau)$ can be expressed by (30) and (32) in terms of elementary functions.

Using beta functions, we get the following generalization of von Mises' result.

THEOREM 3. If the W -diagram of a flow is simply covered and simply connected, and the hodograph is the circular sector (2), then $z(\zeta)$ is ζ times a rational function of $\zeta^n = t$, plus complex constants c_i times incomplete beta functions $B_\beta(t/t_i)$, where $\beta = (n - 1)/n$.

Proof (cf. [6, §§5-6]). Since $T = [a(t^2 + 1) + 2bt]/[c(t^2 + 1) + 2dt]$ and $dW/dT = f(T)$ are rational functions,

$$dW = (dW/dT)(dT/dt) dt = r(t) dt,$$

where $r(t)$ is a (real) rational function. But any rational function can be written as a complex linear combination of partial fractions $(t - t_i)^m$, by a classic theorem of algebra. (In our case, $m \leq 3$ by Cor. 1 of Theorem 4, Ch. III.) It follows that

$$(33) \quad z = \int \frac{dW}{\zeta} = \sum_i c_i \int \frac{t^{-1/n}}{(t - t_i)^m} dt,$$

where $m = m(i)$ is a positive integer. But for any i , either $t_i = 0$, and the integral is ζ times a negative integral power of t , or the integral is a complex constant times $B_\beta(t/t_i)$. Setting $\tau = t/t_i$, and using the reduction formula

$$\int \frac{\tau^{-1/n}}{(1 - \tau)^m} d\tau = \frac{1}{m-1} \frac{\tau^{-1/n}}{(1 - \tau)^{m-1}} + \frac{1}{n(m-1)} \int \frac{\tau^{-1/n}}{\tau(1 - \tau)^{m-1}} d\tau,$$

and decomposing the last integral by partial fractions, we can reduce by induction to the case $m = 1$, in which the result is immediate (cf. (29), (32)). This completes the proof.

Effective calculation based on the preceding formulas will be discussed in Ch. IX, §4.

CHAPTER III

SIMPLE FLOWS PAST WEDGES

1. Introduction. In Ch. II, various flows involving plates and wedges were found by guessing the hodograph and W -diagram, and then finding an elementary conformal transformation of one onto the other. We shall now replace this intuitive procedure by more rigorous arguments, based on the Schwarz Reflection Principle and related results of complex variable theory.

These deeper results will free us from special hypotheses (e.g., of being simply covered, cf. Ch. II, §1) about the hodograph and the W -diagram. Instead, we shall make assumptions about behavior in the *physical* plane. Specifically, we shall first assume only that we are dealing with an ideal (Euler) "simple flow" (§2), which is simply connected in the physical plane. From this assumption, it will follow that $dW/dT = R(T)$ is a real rational function (Theorems 1-2).

The preceding result, and the considerations mentioned above, will prove essential for the later work of Chs. IV-VII. In the present chapter, we shall apply them primarily to simple flows past generalized "wedges"—i.e., to flows whose boundary is in turn (i) horizontal, (ii) at a constant angle $\beta = \pi/n$ with the horizontal, and (iii) free. In this case, using the Reflection Principle again, one can prove (Theorem 3) that the flow can be mapped onto the unit semicircle Γ in the t -plane, so that $\zeta t^{-1/n} = r(t)$ is a rational function of t .

Just as in Ch. II, one can then relate T and t by the relation $T = -(t + t^{-1})/2$. This will give

$$(1) \quad z = \int \zeta^{-1} dW = \int t^{-1/n} [R_1(t)/r(t)] dt,$$

where $R_1(t) = (1 - t^2)R(T)/2t^2$ is rational. Hence the method requires a single numerical quadrature.

The special case of a circular sector hodograph corresponds to $r(t) = 1$. As a by-product of our deeper analysis, we shall enumerate in §10 *all* geometrical types of flow having a circular sector hodograph and stable free boundaries. Part of this classification theory will be applicable to simple flows in general (see formula (30)), and will be used extensively in Ch. V.

2. Simple flows; reflection principle. First, the concept of a "simple flow" will be given a precise technical definition¹.

DEFINITION. A complex velocity field $\zeta(z)$, defined on an open domain R with closure \bar{R} , will be called a "simple flow" if and only if (i) R is locally simply covered, (ii) R is simply connected, (iii) $\zeta(z)$ is bounded and continuous in \bar{R} and analytic in R , (iv) the boundary $\bar{R} - R$ of R consists of a finite number of rectifiable streamlines turning through a finite total angle.

Remark 1. The "complex potential" $W = \int \zeta dz$ of any flow satisfying (iii) is clearly defined and continuous on \bar{R} , analytic in R , and bounded except where z becomes infinite. By a "streamline", we mean a curve along which $V = \text{Im}\{W\}$ is constant. By a "rectifiable" curve, we mean one such that the segment joining any two points has finite total length.

Remark 2. The angle through which a curve turns is the l.u.b. of the sums of the magnitudes of the changes in direction of approximating polygons; since such sums increase under subdivision, it is also their limit. Equiangular spirals turn through an infinite total angle (see Ch. IV, §1).

LEMMA 1. There is a schlicht function $z(T)$ mapping the upper half T -plane conformally and one-one onto any "simple" flow; moreover $\zeta(T)$ and $W(T)$ are complex analytic functions.

Proof. The first statement is an immediate consequence of the fundamental theorem of conformal mapping [2, vol. 2, p. 6]; the analyticity of $\zeta(T) = \zeta(z(T))$ and $W(T)$ are corollaries.

Many important properties of simple flows can be proved by applying the Schwarz Reflection Principle [3, vol. 1, p. 225], which we will now state without proof.

Reflection Principle. Let $f(t)$ be an analytic complex function, regular and single-valued inside a domain D partially bounded (as in Fig. 1) by a segment \overline{AB} of the real axis, and tending continuously to real values on \overline{AB} . Then the relation $f(t^*) = \overline{f^*(t)}$ continues $f(t)$ analytically across \overline{AB} to the mirror image D^* of D , so that $f(t)$ is analytic in the domain $D \cup D^* \cup \overline{AB}$.

Many useful corollaries of this principle can be proved by elementary conformal transformations.

COROLLARY 1. Let $f(t)$ be analytic and single-valued in a domain D partially bounded by an arc \widehat{AB} of a circle of radius r with center $t = 0$,

¹ This definition, and the rigorous discussion of its consequences, are new—though all the methods used will be found scattered through the literature. The hypotheses can be weakened considerably (cf. Ch. IV, §1, and Ch. VI, §3). Thus, in the Reflection Principle, only the continuous vanishing of $\text{Im}\{f(t)\}$ or $\text{Re}\{f(t)\}$ need be assumed [18, vol. II, p. 247].

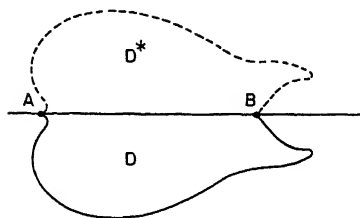


FIG. 1.

except for a finite number of zeros and poles. Let also $f(t)$ be continuous on the closed domain \bar{D} , except at poles, and map \widehat{AB} onto an arc of a circle of radius R and center 0. Then the relation $f(r^2/t^*) = R^2/f^*(t)$ continues $f(t)$ analytically to the reflected image of D under inversion in the circle $|t| = r$, interchanging zeros and poles.

3. W -diagrams of "simple" flows. Using the ideas of §2, it is not hard to give a complete *local* classification of the singularities of $W(T)$ in Lemma 1.

THEOREM 1. Near any singularity $T = T_0$ in the finite T -plane, W can be written

$$(2) \quad W = c(T - T_0)^{-2} + d(T - T_0)^{-1} + h \ln(T - T_0) + r(T),$$

where T_0 , h , c and d are real and $r(T)$ is regular (i.e., a convergent power series in $(T - T_0)$).

Proof. By Remark 1, any such singularity T_0 must be on the boundary—i.e., T_0 must be real. Since the boundary consists of streamlines, V is *piecewise constant* on it. Hence, for suitable constants V_0 and πh (the jump in V across T_0 on the boundary), we have

$$(3) \quad W = h \ln(T - T_0) + V_0 + W_1(T),$$

where $W_1(T)$ is real near T_0 when T is real. By Remark 1, $W(T)$ and $W_1(T)$ are bounded and continuous except at a finite number of points; hence T_0 is an *isolated* singularity. The Reflection Principle then shows that $W_1(T)$ can be extended to a single-valued analytic function, defined in an entire neighborhood of T_0 . It remains to discuss the singularity in $W_1(T)$ at T_0 .

We shall show in Ch. IV, §1, that an essential singularity is impossible. Therefore $W_1(T)$ has a pole at $T = T_0$. We must now determine the limitation on its order n . But if $n > 2$, then, since $\zeta \neq \infty$ and $dz = \zeta^{-1} dW$, the image in the z -plane of the sector $0 < \arg(T - T_0) < \pi$ in the T -plane will subtend an angle $n\pi > 2\pi$. Therefore the z -plane will be multiply covered, even *locally*, contrary to assumption.

DEFINITION. If $\zeta \neq 0$, a neighborhood of a point at infinity in the z -plane corresponding to $T = T_0$ will be called an *infinite stream*, an *ocean* or *jet* according as the first non-zero coefficient in (2) is c , d or h . (If the boundary is not a free streamline, we use the word *tube* instead of jet.)

Remark 3. The cases are easily distinguished in the physical plane, since the flow at infinity subtends an angle 2π , an angle π , or fills a strip of thickness $|h\pi/\zeta|$ in the three cases. The case $\zeta = 0$ of stagnation points at infinity requires a more elaborate discussion (see §9 below).

In other applications, it is convenient to map "simple" flows on various domains B in the t -plane (parameter-plane). For such applications, the following corollary is useful.

COROLLARY. Let t_0 be any point on the boundary of a domain B , where the boundary curve is analytic. Then Theorem 1 holds, with t replacing T .

For [3, vol. 2, p. 34] there is a local analytic map of the upper half-plane onto the interior of B .

The *global* behavior of W can be deduced very easily from Theorem 1. Of course, its form can often be guessed even more easily.

THEOREM 2. The complex potential of any "simple" flow has the *additive* decomposition

$$(4) \quad W = \sum_{k=1}^n \left[\frac{c_k}{(T - T_k)^2} + \frac{d_k}{T - T_k} + h_k \ln (T - T_k) \right] + cT^2 + dT.$$

Its derivative has the *multiplicative* decomposition

$$(5) \quad \frac{dW}{dT} = R(T) = C \prod_i (T - A_i)(T - A_i^*) \prod_j (T - B_j) / \prod_k (T - T_k).$$

All coefficients in (4) are real; so are all B_j in (5).

Proof. First we consider the case where $T = \infty$ is mapped onto a point where W is finite. Then, by Theorem 1, summing over all local singularities, the difference $h(T)$ between the two sides of (4) (with $c = d = 0$) is analytic and single-valued, real on the real axis, and without singularities in the (closed) upper half-plane. By the Schwarz Reflection Principle, $h(T)$ can be continued to a function regular in the whole finite T -plane. Moreover, $W(\infty)$ being finite, $h(T)$ is also bounded. Hence, by Liouville's Theorem [3, vol. 1, p. 153], $h(t)$ will be a constant. Since W is defined only up to an additive constant, (4) is proved, with $c = d = 0$. If W has a singularity at $T = \infty$, we can transform the upper half T -plane into itself by an inversion, use the result just obtained for finite $W(\infty)$, and then transform back to the original T . This yields the extra terms $cT^2 + dT$ by inversion from a finite singularity (2). Finally, differentiating (4), we get a real rational function with common denominator $\Pi(T - T_k)$ (some factors may be repeated). Factoring the real polynomial numerator into linear factors, we get (5).

Remark 4. Though (4) looks complicated, all cases may be obtained by passage to the limit from the simple general formula $W = \sum h_k \ln (T - T_k)$. "Oceans" may be regarded as a limiting case of two coalescing jets, and "infinite streams" of three.

Remark 5. Just as the T_k can be identified with infinite streams, oceans, or jets, according as the first non-vanishing coefficient in the corresponding expression (2) is c , d or h , so the A_i and B_j have simple physical interpretations. Since $\zeta = (dW/dT)/(dz/dT)$, and $dz/dT \neq 0$ in the interior, complex zeros A_i correspond to *interior stagnation points*, where $\zeta = 0$. Again, at a *dividing point* on the boundary, where the flow changes direction, the W -diagram must cover an angle 2π at least, so that $dW/dT = 0$ (and conversely). Hence *real zeros* B_j correspond to *dividing points* (either stagnation points or cusps).

Remark 6. Cases, such as reentrant jets (§8), where the flow covers the complete exterior of some sufficiently large circle, can also be dealt with by a slight modification of Theorem 2. The point $z = \infty$ must then be regarded as an interior isolated singularity T_∞ of the flow. Since the correspondence $T \rightleftharpoons z$ is schlicht, we can write $z = c/(T - T_\infty) + \dots$, and so dz/dT has a pole of the second order at $T = T_\infty$. Hence, ζ being bounded, $dW/dT = \zeta dz/dT$ has a second-order pole at most. Therefore dW/dT has a second-order pole at T_∞ , and another (by reflection) at T_∞^* . This means that (4) must in general be supplemented by an expression of the form

$$(4') \quad d/(T - T_k) + d^*/(T - T_k^*) + h \ln (T - T_k) + h^* \ln (T - T_k^*).$$

In the multiplicative form (5), there is a corresponding extra factor $(T - T_k)^2(T - T_k^*)^2$ in the denominator.

Remark 7. Various simplifications in (4)-(4') are possible in the case of a stagnation point $\zeta = 0$ at infinity; this case is discussed in §9.

4. Impinging jets. Consider now the flow defined by two impinging jets² J_1, J_3 , and two outgoing jets J_2, J_4 (Fig. 2a). We let α_k denote the clockwise angle from the x -axis to J_k , and πh_k the time rate of influx of area (mass) of J_k . By conservation of mass, clearly

$$(6) \quad h_1 + h_2 + h_3 + h_4 = 0.$$

We assume that all four free streamline velocities are the same, which is the only possibility if the jets have infinite length, provided we assume continuity at infinity. (For a more general proof, see the end of Ch. IV,

² Due to W. Voigt, Gött. Nachr. (1885), 285-305. See also U. Cisotti, Annali di mat. 23 (1914), 285-340; T. Boggio, Atti accad. sci. Torino 50 (1915), 1103-19; M. Caldonazzo, Annali di mat. pura appl. Milano 26 (1916), 38-75, Rend. R. Inst. Lombardo 52 (1919), 149; [61, §§11.42-11.43]. For the *symmetric* case $\alpha_1 = 0, \alpha_2 = \pi, \alpha_4 = -\alpha_3$, see Ch. II, §6.

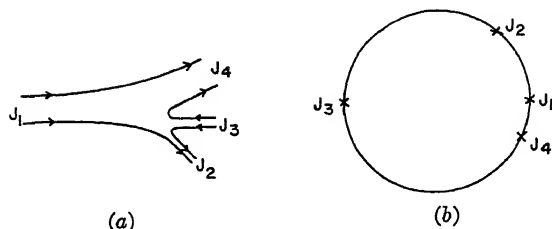


FIG. 2.

§1.) Hence the boundary of the *hodograph* is a *circle*. By proper choice of unit, it becomes the unit circle, so that $|\pi h_k|$ is the asymptotic jet width of J_k . Actually, the hodograph is a simply covered circle, as we shall prove below.

We first map the flow onto the unit circle Γ , and note that the complex potential has logarithmic singularities at J_1, J_2, J_3, J_4 (Fig. 2b), and is regular elsewhere because Schwarz *reflection of these singularities in Γ does not produce new singularities*. Thus we write³ (see the Cor. of Thm. 1)

$$(7) \quad W = f(t) = \sum_{k=1}^4 h_k \ln(t - t_k), \quad t_k = e^{i\alpha_k}.$$

LEMMA 1. The hodograph is a circle, and we can assume $t = \zeta$ in (7).

Proof. By inspection of Fig. 2a, $\arg \zeta$ changes by 2π around the boundary of the flow. Since $\zeta(z)$ is bounded and analytic inside the flow, the change equals $2\pi n_s$, where n_s is the number of interior stagnation points (multiplicity being counted) where $\zeta = 0$. Hence $n_s = 1$. (This calculation is generalized in §9.) Putting the stagnation point at $t = 0$, we make $\ln |\zeta/t|$ harmonic and bounded in Γ , and identically zero on the boundary. It follows that it vanishes identically, whence $\zeta = e^{i\psi}t$; rotating, we get $\zeta = t$.

LEMMA 2. We have the identity

$$(6') \quad \sum_{k=1}^4 \frac{h_k}{\zeta_k} = 0, \quad \text{or} \quad \sum_{k=1}^4 C_k h_k = \sum_{k=1}^4 S_k h_k = 0,$$

where $C_k = \cos \alpha_k$, $S_k = \sin \alpha_k$, and $\zeta_k = C_k + iS_k$.

Proof. Formula (6') is equivalent to the conservation of momentum. Alternatively, we can prove it analytically. By (7), we can write

$z = \int \zeta^{-1} dW$ as

$$z = \sum_{k=1}^4 \frac{h_k}{\zeta_k} \ln(\zeta - \zeta_k) - \sum_{k=1}^4 \frac{h_k}{\zeta_k} \ln \zeta.$$

But since $z(t) = z(\zeta)$ is single-valued near $\zeta = 0$, (6') follows.

³ Since $W - f(t) = g(t)$ is real on $|t| = 1$, $g(1/t^*) = g^*(t)$ defines a function which is bounded in the whole plane, and hence constant.

If z_0 is the stagnation point, we thus have

$$(8) \quad z = z_0 + \sum_{k=1}^4 \frac{h_k}{\zeta_k} \ln \left(1 - \frac{\zeta}{\zeta_k} \right), \quad \left[\frac{1}{\zeta_k} = C_k - iS_k \right].$$

Conversely, if (6)–(6') hold, and if the jets do not recross, then (8) defines an admissible flow corresponding to impinging jets. Clearly z_0 is arbitrary.

Indeterminacy. The axis or *midline* of the jet J_k may be defined as the straight line which is asymptotic at infinity to the curve given in terms of a real parameter r by

$$(9) \quad z(r\zeta_k) = \frac{h_k}{\zeta_k} \ln(1-r) + z_0 + \sum_{j \neq k} \frac{h_j}{\zeta_j} \ln \left(1 - \frac{\zeta_k}{\zeta_j} \right) + o(1-r).$$

The midline is parallel to ζ_k^* (i.e., $\zeta_k^{-1}h_k$), so that its Cartesian equation is $S_kx + C_ky + m_k = 0$, where m_k is the moment, about $z = 0$, of the unit vector $\zeta_k^* = C_k - iS_k$, acting along the midline. This is $-S_kx - C_ky = -Im\{\zeta_k z\}$, where $z = x + iy$ is any point of the midline. Hence, by (9), passing to the limit

$$(9') \quad m_k = -I \left\{ \zeta_k z_0 + \sum_{j \neq k} h_j \frac{\zeta_k}{\zeta_j} \ln \left(1 - \frac{\zeta_k}{\zeta_j} \right) \right\}.$$

Physically, it is natural to suppose that if the incoming jets J_1 and J_3 are given (i.e., that $h_1, h_3, \alpha_1, \alpha_3$ and the midlines of J_1 and J_3 are given), then the resulting flow is determined. However, it can be shown that, contrary to expectation, the resulting flow is in fact *indeterminate, except in the case $\alpha_3 = \alpha_1 + \pi$ of parallel impinging jets!*

Indeed, except in this case, (6)–(6') and (9') with $k = 1, 3$ give five equations between the six unknowns $h_2, h_4, \alpha_2, \alpha_4, x_0, y_0$ ($z_0 = x_0 + iy_0$). These have a one-parameter family of solutions, which may easily be obtained graphically.

The physical significance of this indeterminacy is hard to grasp; all flows are in equilibrium. It is not clear what is the condition, if any, for the *stable* equilibrium of non-parallel impinging jets. It may be that all stationary configurations are unstable⁴.

In the case of *parallel* jets, we can use the same graphical construction as before, but since $\zeta_1 + \zeta_3 = 0$, summing (9') with $k = 1, 3$, we get an additional equation between $h_2, h_4, \zeta_2, \zeta_4$, which involves the moment $m_1 + m_3$ of the couple defined by ζ_1, ζ_3 acting along their respective midlines. Hence this case is determinate, up to a translation.

⁴ A. Palatini, Atti Ist. Veneto Sci. 75 (1916), 451–3, has proposed the condition that the total energy of that portion of the fluid having velocity $|\zeta| < r$, as $r \rightarrow 1$, be a minimum. He has shown that this implies that the outgoing jets must be symmetric or parallel. See also Ch. XI, §15, on jet stability.

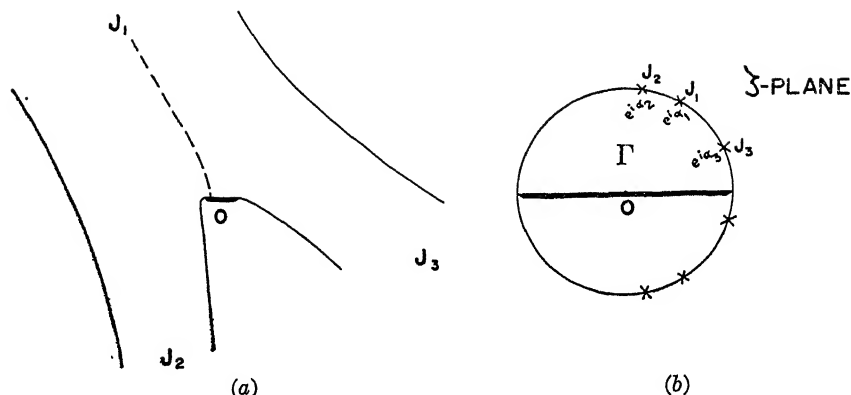


FIG. 3.

5. Divided jets. The case of a jet divided by a horizontal plate (Fig. 3a) can be treated very neatly by reflecting its singularities⁵, and using the topological results of §9. We map the flow on the unit semicircle Γ (Fig. 3b) in the t -plane so that the semicircumference corresponds to the free boundaries, the diameter to the plate, and $t = 0$ to the dividing point.

We first prove the easily guessed formula $\zeta = t$. In the notation of §9, $n_0 = 3$, while $n_1 = n_2 = 0$. Hence, by (30), $n_d = 1$ and $n_s = 0$; this is also intuitively obvious. It follows that ζ/t is bounded in Γ , real on the diameter, and of modulus unity on $|t| = 1$. Reflecting by (19) both in the diameter and in $|t| = 1$, we see that ζ/t is bounded everywhere. Hence, by Liouville's Theorem, ζ/t is a constant. Since ζ/t is real on the diameter, and of modulus unity, we thus have $\zeta = \pm t$. With the incoming jet in the upper half-plane, as in Fig. 3a, clearly $\zeta = t$.

We now consider $W(t) = W(\zeta)$ similarly. Reflection of the singularities in the real axis gives three conjugate logarithmic singularities of equal strength, at $e^{-i\alpha_1}$, $e^{-i\alpha_2}$, $e^{-i\alpha_3}$. Reflection in the *circular* part of Γ (or its mirror image) gives no new singularities (see Fig. 3b). Summing, we get

$$(10a) \quad W = \sum_{j=1}^3 h_j \ln (\zeta - e^{i\alpha_j})(\zeta - e^{-i\alpha_j}),$$

whence

$$z = \int \sum h_j \left[\frac{C_j - iS_j}{\zeta - e^{i\alpha_j}} + \frac{C_j + iS_j}{\zeta - e^{-i\alpha_j}} - \frac{2C_j}{\zeta} \right] d\zeta.$$

To keep z finite at $\zeta = 0$, clearly $\sum h_j C_j = 0$; this also corresponds to conservation of the x -component of momentum. Hence

⁵ Or by the methods of Ch. II. See [58], [32, pp. 6-10]. The generalization to wedges leads to the complications described in Ch. II, §4.

$$(10b) \quad z = z_0 - \sum_{j=1}^3 h_j \left\{ C_j \ln (\zeta^2 - 2C_j\zeta + 1) - iS_j \ln \frac{\zeta - e^{i\alpha_j}}{\zeta - e^{-i\alpha_j}} \right\}.$$

Again, since $\sum h_j C_j = 0$ and (by conservation of mass) $\sum h_j = 0$, we must have

$$(10c) \quad h_2 = \frac{C_3 - C_1}{C_2 - C_3} h_1, \quad h_3 = \frac{C_1 - C_2}{C_2 - C_3} h_1.$$

Hence, for given h_1 , α_1 , the divided jet depends on two independent parameters, as one would also expect physically.

Using the laws of conservation of momentum and of moment of momentum, we can also compute the thrust Y and the moment M on the plate, as

$$(11a) \quad Y = \rho \sum_{j=1}^3 h_j S_j$$

$$(11b) \quad M = \rho \sum_{i,j=1}^3 h_i h_j \{ S_i S_j (\frac{1}{2}\pi - \alpha_j) + \sin(\alpha_i + \alpha_j) \ln \sin \frac{1}{2}(\alpha_i + \alpha_j) \}.$$

On the plate, $\zeta = v$ is real, together with $i \ln (\zeta - e^{i\alpha_j}) / (\zeta - e^{-i\alpha_j}) = -2 \arctan [S_j / (v - C_j)]$; hence so is $z - z_0$. To put the *origin at the stagnation point*, we must set

$$z_0 = x_0 = -2 \sum_{j=1}^3 h_j S_j (\pi - \alpha_j).$$

If we do this, we will get the following symmetrical expression⁶ for x

$$(12) \quad x = - \sum_{j=1}^3 h_j F(\alpha_j; v),$$

where

$$F(\alpha_j, v) = 2S_j(\pi - \alpha_j) + C_j \ln (v^2 - 2C_j v + 1) - 2S_j \arctan [S_j / (v - C_j)].$$

In particular, the endpoints $x(-1) = x_1$ and $x(1) = x_2$ of the plate satisfy the equations

$$(13) \quad x_2 = - \sum_{j=1}^3 h_j [S_j(\pi - \alpha_j) + 2C_j \ln \sin \frac{1}{2}\alpha_j]$$

$$(13') \quad x_1 = - \sum_{j=1}^3 h_j [-S_j \alpha_j + 2C_j \ln \cos \frac{1}{2}\alpha_j],$$

⁶ See W. B. Morton, *Phil. Mag.* 48 (1924), 464-76, and W. B. Morton and E. J. Harvey, *Phil. Mag.* 31 (1916), 130-8.

while the plate width p satisfies

$$(14) \quad p = -\sum_{j=1}^3 h_j [\pi S_j + 2C_j \ln \tan \frac{1}{2}\alpha_j].$$

The equation of the free streamlines $\zeta = e^{i\phi}$ is

$$(15) \quad z = \text{const.} - \sum h_j \left\{ S_j(\pi - \alpha_j) + C_j \ln |\cos \phi - C_j| + \frac{1}{2} S_j \ln \frac{1 - \cos(\phi + \alpha_j)}{1 - \cos(\phi - \alpha_j)} \right\}.$$

6. Physical applications. The most obvious hydraulic application of the theory of divided jets is to predicting the flow, given the angle α_1 , plate width p , and the distance $q = S_1[x' - \frac{1}{2}(x_1 + x_2)]$ along the plate from the midline of the impinging jet to the midpoint of the plate. Here x' is readily calculated from the asymptotic equations of the free streamlines. To make this prediction, one must construct a nomogram.

Using a simple graphical construction due to Morton and Harvey⁶, we have plotted in Fig. 4, for the case $\alpha_1 = 60^\circ$, the contour lines $\alpha_2 = \text{const.}$ and $\alpha_3 = \text{const.}$ in the (p, q) -plane. Symmetric flows with $\alpha_1 = 90^\circ$ are covered in Ch. II, §8. The qualitative nature of the functions $\alpha_j(p, q; \alpha_1)$ is as one might expect physically.

Planing surfaces. However, the limiting case $\alpha_1 = \alpha_3$, in which one branch of the jet becomes infinitely thick, is more surprising. If rotated through α_1 clockwise, the flow can be imagined to represent a flat *planing surface*⁷ in an ocean of infinite depth (Fig. 5a).

In our previous coordinates, normalizing so that the outgoing jet has thickness $d = \pi$, W has a logarithmic singularity at $\zeta_I = e^{i\alpha_2}$, and a simple pole plus a logarithmic term at $\zeta_I = e^{i\alpha_1} = e^{i\alpha_3}$. That is

$$(16a) \quad W = \frac{\alpha_1}{T - T_I} + \ln \frac{T - T_I}{T - T_J} \quad [T = -\frac{1}{2}(\zeta + \zeta^{-1})].$$

Integrating $z = \int \zeta^{-1} dW$, and noting that the stagnation point is in the finite plane if and only if $\alpha_1 = \cos \alpha_1 - \cos \alpha_2$, we get

$$(16b) \quad z = \frac{2(C_1 - C_2)}{(\zeta - \zeta_I)(\zeta - \zeta_J)} + iS_2 \ln \frac{\zeta - \zeta_J}{\zeta - \zeta_J^*} + C_2 \ln \frac{(\zeta - \zeta_I)(\zeta - \zeta_I^*)}{(\zeta - \zeta_J)(\zeta - \zeta_J^*)} - i \frac{1 - C_1 C_2}{S_1} \ln \frac{\zeta - \zeta_I}{\zeta - \zeta_I^*}.$$

⁷ This case has been treated by A. Green, Proc. Camb. phil soc. 32 (1936), 67-85; see also [46, §12.3].

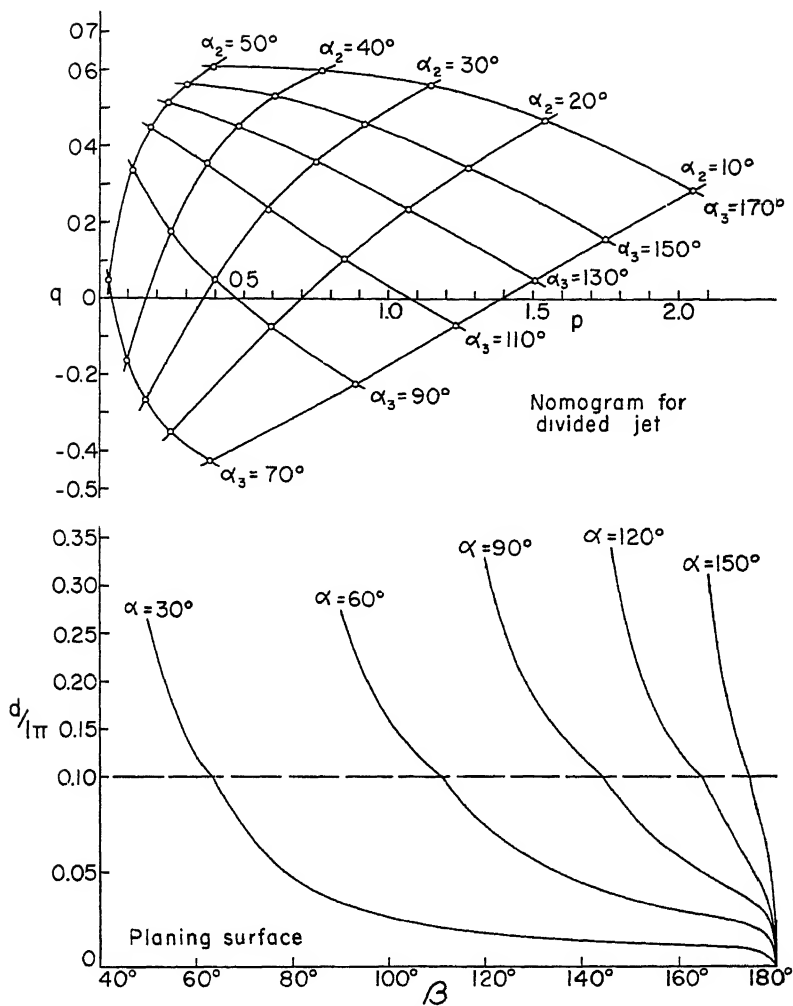


FIG. 4.

The width l of the plate is

$$(16c) \quad l = 2C_1(C_1 - C_2)/S_1^2 + \frac{\pi}{S_1} [1 - \cos(\alpha_1 - \alpha_2)] + 2C_2 \ln \frac{\tan \frac{1}{2}\alpha_1}{\tan \frac{1}{2}\alpha_2}.$$

We plot in Fig. 4, d/l as a function of α_2 , for several values of α_1 .

Calculating the imaginary part $Im\{ze^{i\alpha_1}\}$ of the (rotated) free surface $\{z = e^{i\phi}\}$ "at infinity", we get $S_1^{-1}(C_2 - C_1) \ln |2 \sin \frac{1}{2}(\phi - \alpha_1)|$. This shows that there is an *infinite depression*, relative to the free surface at infinity.

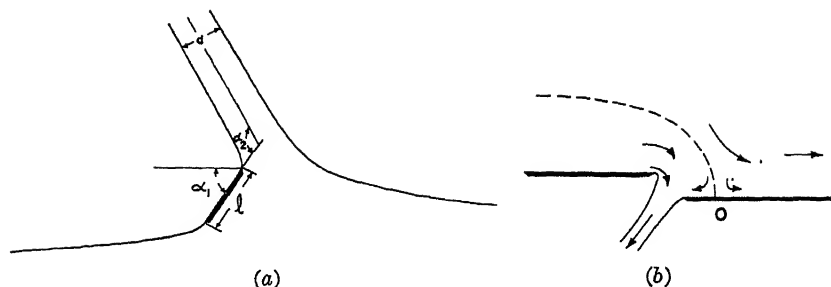


FIG. 5.

In order to interpret this result physically, one must consider the effect of *gravity*, which has been neglected in the preceding discussion. Suppose a plate of width l moving horizontally at speed v , with its bottom at a depth b below the surface, and making an angle α_1 with the horizontal. The preceding result indicates that, as v increases, the height of the wave piled up ahead of the plate will increase without limit in an "ocean" of infinite depth, being in equilibrium for sufficiently high speeds even if b is negative. A similar remark holds for the penetration of an ocean by a jet, which can be treated as a limiting form, in which two jets coalesce, of the impinging jet model of §4. —The case of an "ocean" of finite depth will be treated in Ch. V, §§6–7.

It is nevertheless interesting to compute the force F and the moment M , for the normalized case of a jet of thickness π . These formulas may apply to the case of high-speed motion, just as it may well be true that d/l satisfies (16c), so that the flow is determined by α_2 or d/l . We get, passing to the limit,

$$(17a) \quad F = \rho \pi i \left[\frac{1 - \cos(\alpha_1 - \alpha_2)}{\sin \alpha_1} \right].$$

From this, the drag and the lift can easily be computed.

The moment is most easily computed as the limit of the moment for the divided jet when the thicknesses of two of the jets tend to infinity. The moment with respect to the stagnation point is found to be

$$(17b) \quad M = \rho \pi i m \left\{ \frac{1}{2} f''(\alpha) \left[\frac{\cos \alpha - \cos \beta}{\sin \alpha} \right]^2 + f(\alpha) + f(\beta) - 2f\left(\frac{\alpha + \beta}{2}\right) + \frac{\cos \alpha - \cos \beta}{\sin \alpha} \left[f'(\alpha) - f'\left(\frac{\alpha + \beta}{2}\right) \right] \right\}.$$

where $f(\phi) = e^{2i\phi} \ln(1 - e^{2i\phi})$.

Suction slots. Another application is to the flow of an infinite stream along an interrupted wall⁸, or "suction slot" (see Fig. 5b). Formulas (16a)–(16b)

⁸ See F. Salzmänn, Escher Wyss News 8 (1935), No. 4/5, 95–102; E. J. Watson,

can also be applied to this case, if $\zeta_1 = v$ is the ratio of free stream velocity to free streamline (branch) velocity. The special case $v = 0$ has already been treated in Ch. II, §5.

7. Simple flows past wedges. We shall now describe in detail the rest of the general method outlined in §1. Only part of the method was needed in §§4-6, whose conclusions might also have been reached (though less rigorously) by the method of Ch. II. We first repeat (cf. §1) the definition of a simple flow past a wedge.

DEFINITION. A "simple flow past a wedge" is a "simple" flow (see §2) whose boundary is in turn (i) horizontal, (ii) at a constant angle $\beta = \pi/n$ with the horizontal, and (iii) free.

Any such flow can be mapped conformally onto the unit semicircle Γ in the t -plane, so that the free boundary (iii) goes into the arc $|t| = 1$, and the straight portions (i) and (ii) of the boundary go into $-1 < t < 0$ and $0 < t < 1$ on the real axis, respectively.

THEOREM 3. In any simple flow past a wedge,

$$(18) \quad \zeta = t^{1/n} r(t) = t^{1/n} \Pi \frac{(t - a_i)(t - a_i^*)(t - b_j)}{(a_i t - 1)(a_i^* t - 1)(b_j t - 1)}.$$

The a_i and b_j which represent points in the *finite* z -plane can be made to correspond to the A_i and B_j of (5), under

$$(18a) \quad A_i = -\frac{1}{2}(a_i + a_i^{-1}), \quad B_j = -\frac{1}{2}(b_j + b_j^{-1}).$$

Remarks. The case $\beta = 0$ of a flat plate corresponds to $n = \infty$, hence the factor $t^{1/n} = 1$ can be ignored in this case. If a *dividing* point on the plate is mapped on $t = 0$, (18) still has a factor t , as explained below. (If $n = 1$, it is convenient to map a stagnation point on $t = 0$, if one exists on the boundary.)

Proof. Clearly $\zeta/t^{1/n} = r(t)$ is real when t is real, satisfies $|r(t)| = 1$ when $|t| = 1$, and is bounded in and on Γ , except possibly at $t = 0$. By conformal mapping theory, $t^{1/n} dz/dt$ is non-zero at $t = 0$, while dW/dt is regular there by the Corollary of Theorem 1. Hence $(dW/dt)/(t^{1/n} dz/dt) = t^{-1/n} \zeta$ is bounded at $t = 0$ also. It follows, by a triple application of the Reflection Principle, that

$$(19) \quad r(t^*) = r^*(t), \quad r(1/t) = 1/r(t), \quad r(1/t^*) = 1/r(t^*)$$

defines a function analytic in the entire t -plane, except at those points with $|t| > 1$ which are images of stagnation points where $\zeta = 0$. These correspond to *poles* of $r(t)$, which is therefore a *rational function*. Specifically,

ARC RM 2177 (Feb. 1946), where some tables are given. Suction slots in finite channels are treated by R. von Mises [62, p. 473], and by J. S. McNown and E.-Y. Hsu, Proc. first Midwest conf. fluid dyn. U.S.A. (1951), 143-53.

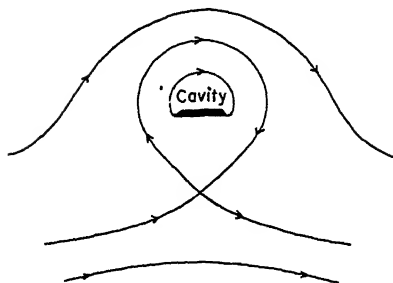


FIG. 6.

let a_i and b_j represent the zeros of ζ in the interior of Γ and on its boundary, respectively, multiple zeros being represented by repeated factors. Then the function

$$r_1(t) = r(t)/\Pi \frac{(t - a_i)(t - a_i^*)(t - b_j)}{(a_i t - 1)(a_i^* t - 1)(b_j t - 1)}$$

neither vanishes nor becomes infinite in Γ , and satisfies (19). Hence it is regular and bounded over the entire t -plane. Thus, by Liouville's Theorem [3, vol. 1, p. 153], it is a constant, namely a real constant of modulus one, that is, ± 1 .

The stagnation points in the finite z -plane, other than the wedge vertex at $t = 0$, are zeros of ζ whose multiplicity equals their multiplicity as dividing points. The same holds at the vertex, if the factor $t^{1/n}$ is taken out. Hence the a_i and b_j of (18) correspond to the A_i and B_j of (5) under (18a), if they represent points in the finite z -plane.

Remark. A flow having no stagnation point on the boundary is sketched in Fig. 6. It is one of the nine possible parallel flows past a plate⁹.

COROLLARY. For any simple flow past a wedge, $z(t)$ can be expressed explicitly in terms of incomplete beta functions. If $n = 1$, $z(t)$ is an elementary function.

Proof. By (18), $dz'/dt = \zeta^{-1}dW/dt$ equals $t^{-1/n}$ times a rational function of t . Expanding the latter into partial fractions, we can copy the arguments of Theorem 3 of Ch. II.

8. Reentrant jets. The method of reflection of §7 is well illustrated by the "reentrant jet" model which has been proposed¹⁰ for the cavity

⁹ See E. H. Zarantonello, *J. de math.* 33 (1954), 29-80. The case of pure circulation was treated by U. Cisotti, *Atti accad. Lincei* 13 (1931), 85-92.

¹⁰ See D. A. Efros, *Doklady URSS* 51 (1946), 267-70, and 60 (1948), 29-31; G. Kreisel, *Adm. Res. Lab. Rep. R1/H/36* (1946); D. Gilbarg and H. H. Rock, *NOL Memo. 8718* (1946); M. I. Gurevitch, *Izv. Akad. Nauk* (1947), 143-50 (DTMB Rep. 224); D. Gilbarg and J. Serrin, *J. math. phys. MIT* 29 (1950), 1-12; E. L. Arnoff, *NOTS Report 368* (1951) (Navord 1298).

behind a flat plate or other obstacle in an infinite stream (see Fig. 7a). In this model (cf. Ch. I, §13), the cavity is at a lower pressure than the free stream, so that $Q > 0$. The back of the cavity is supposed to end in a "reentrant jet" J , which disappears on another sheet of the "Riemann surface" representing the physical plane. Reentrant jets have been observed experimentally [30], though they appear to form intermittently and be unstable. At any rate, the model bears the closest resemblance of any known type of ideal flow to observed *finite cavities with* $Q > 0$.

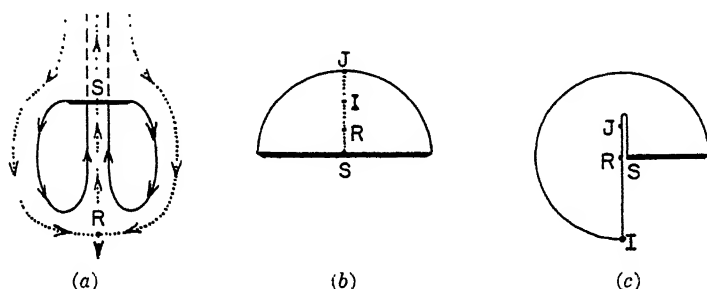


FIG. 7.

In the model, two stagnation points are assumed: one S on the obstacle, and another R inside the flow at the base of the jet, as in Fig. 7a. We shall consider first the case of symmetric cavity flows past a flat plate perpendicular to the stream¹¹. As in §3, we shall map the flow symmetrically onto the unit semicircle Γ of an abstract t -plane (see Fig. 7b), so that the plate goes into the real axis, and the free boundary into the circumference. This conformal mapping exists, is unique, and maps S , I , R , J into four points of the imaginary axis: $t_S = 0$, $t_I = ia$, $t_R = ib$, and $t_J = i$ ($0 < a < b < 1$). Since the point $t = t_I$ at infinity is interior to the flow, Remarks 5 and 6 after Theorem 2 apply, so that

$$(20) \quad \frac{dW}{dT} = \frac{C(T - T_R)(T - T_R^*)}{T(T - T_I)^2(T - T_I^*)^2} = C \frac{T^2 - T_R^2}{T(T^2 - T_I^2)^2},$$

where $T = -(t + t^{-1})/2$, so that $2T_R = i(b^{-1} - b)$, $-4T_R^2 = (b^{-1} - b)^2$, etc. From this, a routine calculation gives

$$(20') \quad \frac{dW}{dt} = C_1 t \frac{(t^2 + b^2)(t^2 + b^{-2})(t^2 - 1)}{(t^2 + a^2)^2(t^2 + a^{-2})^2(t^2 + 1)},$$

where $C_1 = -4C$ is a new real constant.

The conjugate velocity is, applying Theorem 3,

¹¹ Asymmetrical flows with and without circulation have been treated by Efros; plates in channels by Gurevitch; symmetric wedges by Arnoff, in the refs. above.

$$(21) \quad \zeta = \frac{t(t^2 + b^2)}{(b^2t^2 + 1)}, \quad \text{or} \quad \zeta^{-1} = \frac{b^2t^2 + 1}{t(t^2 + b^2)}.$$

Half the hodograph is sketched in Fig. 7c.

We are only interested in cases for which $z(t)$ is single-valued (without branch points in Γ). Inspecting $dz/dt = \zeta^{-1} dW/dt$, we see that $t = ia$ is the only possible branch point in Γ . For this not to be a branch point, writing $dz/dt = \phi(t)/(t - ia)^2$, it is necessary and sufficient that, $\phi'(ia) = 0$. With a little algebra, this reduces to

$$(22) \quad b^2 = (5a^2 + 1)/a^2(a^2 + 3),$$

leaving just *one* arbitrary parameter a .

The cavitation number Q is by definition

$$(23) \quad Q = (p_\infty - p_c)/\frac{1}{2}\rho v_\infty^2 = (1 - |\zeta_I|^2)/|\zeta_I|^2.$$

This can easily be found from (21) and (22) since,

$$(24) \quad \zeta_I = \zeta(ia) = -\frac{i}{4} \left(a^3 + 4a - \frac{1}{a} \right).$$

A plot of Q against a is shown in Plate 11; evidently, exactly one flow of the type postulated exists for each value of Q , $0 < Q \leq +\infty$. This agrees with the physical intuition that the cavity underpressure, the velocity at infinity, and the obstacle should determine the flow. The limiting case $Q = \infty$ is possible, and corresponds to

$$a = (\sqrt{5} - 2)^{\frac{1}{2}} = .485868 \dots;$$

it gives the penetrating jet of Ch. II, §6.

Substituting from (22) in (20')-(21), expanding dW/dt in partial fractions, and integrating, one gets to within a constant factor

$$(25) \quad z = \frac{2t\zeta_I^2}{a^2t^2 + 1} - \frac{2t}{t^2 + a^2} + 2\zeta_I\zeta_I' \ln \frac{1 - iat}{1 + iat} - 4\zeta_I' \arctan t,$$

where

$$(25') \quad \zeta_I' = \zeta'(ia) = (a^{-2} - a^2)/8.$$

Here the origin $z = 0$ is at the stagnation point S .

The width p of the plate is

$$(26) \quad z(-1) - z(1) = 4 \left[\frac{1 + \zeta_I^2}{1 + a^2} + 2|\zeta_I|\zeta_I' \arctan a + \frac{1}{2}\pi\zeta_I' \right],$$

and the thickness of the jet,

$$(27) \quad d = \frac{1}{4}\pi(a^{-2} - a^2).$$

An easy calculation shows that the two points on the free streamline where the velocity is real correspond to $t = e^{i\theta}$ with $\cos \theta = \pm(1 - b^2)$, and those where it is purely imaginary to $t = e^{i\phi}$, $\sin \phi = \frac{1}{2}(1 + b^2)$. Substituting in (25), we get immediately the formulas for the length l and width $2w$ of the cavity. Moreover, the stagnation point T is obtained by setting $t = ib$ in (25). In Plate 11, we have plotted $\text{Log}_{10} L$ and $2W/\sqrt{L}$ ($L = l/p$, $W = w/p$) as functions of Q , together with the drag coefficient C_D . This is easily computed since the drag D satisfies (Ch. IV, §5)

$$(28) \quad D = \frac{1}{2}i\rho \int_{-\infty}^{\infty} dz = 2\pi\rho\zeta'_T(1 + |\zeta_T|).$$

In Plate 11, we have also plotted the free streamlines for different values of the cavitation number Q , and fixed d . Obviously the limit case $Q = 0$ corresponds to the Kirchhoff-Rayleigh flow of Ch. II, §2.

The preceding treatment can be extended, as in §7, to a wedge with vertex angle $\beta = \pi/n$, but the first factor t in (21) must be replaced by $t^{1/n}$, and $z(t)$ is no longer an elementary function.

9. Geometrical classification of simple flows. It is interesting to make a *topological* classification of singularities, in terms of the streamline configuration. Consider the increment, around a contour B consisting of the flow boundary with small detours around stagnation and dividing points, in the multiple-valued function

$$(29) \quad \begin{aligned} n(z) &= \frac{1}{\pi} \arg dW = \frac{1}{\pi} \arg \zeta + \arg dz \\ &= \frac{1}{\pi} [\arg dW/dt + \arg dt], \end{aligned}$$

for any non-singular map $t = f(z)$ of the flow into an auxiliary t -plane (e.g., onto a circle or half-plane). This is an even or odd integer according as the flow is counterclockwise or clockwise. Further, it increases at infinity by one across a jet (source or sink, see Fig. 8a), by two across an "ocean"¹² (Fig. 8b), and by three around an infinite stream (Fig. 8c); these facts are easily verified analytically. At a simple *dividing* point (Fig. 8d), $n(t)$ decreases by one.

Clearly, $\arg dz$ increases by 2π around B ("simple" flows being simply connected), while $\oint d(\arg \zeta) = 2\pi n_s$, where n_s is the number of *interior*

¹² "Dipole", in the sense of logarithmic potential theory—or "simple pole" in the sense of complex variable theory; this is a bit confusing! In Figs. 9a-9d, the neighborhood of a *finite* point subtends an angle of 180° . Diagrams for other points can be obtained by conformal mapping.

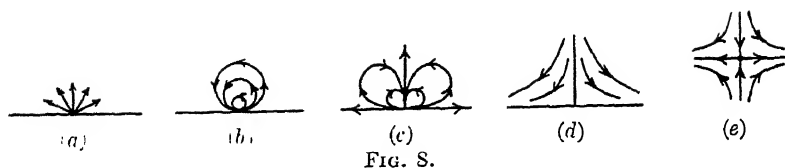


FIG. 8.

stagnation points (see Fig. 8e), counting multiplicity. Hence we have the following result

$$(30) \quad n_0 + 2n_1 + 3n_2 = 2 + n_d + 2n_s,$$

where n_0 is the number of jets and tubes, n_1 of "oceans", n_2 of "infinite streams", and n_d of dividing points on the boundary.

Remarks. Stagnation points at infinity ("stagnant tubes") should be counted on both sides of (30)—that is, as jets, oceans or "infinite streams" on the left side, and as stagnation points (dividing points) on the right. For instance, a jet from a slot (Ch. II, §5) issues from a "stagnant ocean", and one should put in (30): $n_0 = 1$, $n_1 = 1$, $n_2 = 0$, $n_d = 1$, $n_s = 0$. The general rules in such cases for substituting in (30) are complicated. "Interior" points at infinity (§3, Remark 6) give a contribution 4 to the left side of (30); thus, with the reentrant jet flow of §8, (30) becomes $4 + 1 + 0 + 0 = 2 + 1 + 2$.

With these qualifications, we have sketched a proof of

THEOREM 4. Equation (30) holds in any "simple" flow, provided n_d and n_s are counted according to their multiplicity.

For example, Fig. 10c of Ch. II depicts a double internal stagnation point ($n_s = 2$). Unless the plane is multiply covered at infinity, we also know $2n_1 + n_2 \leq 2$.

An enumeration of the various geometrical types of simple flows, in terms of the streamline configuration, can be based on formula (30). The idea is to consider successively larger integral values of $n_d + n_s$, and to enumerate and interpret for each $n_d + n_s$ the corresponding arrangements of n_0 , n_1 , and n_2 on the fixed and free boundaries (i), (ii), (iii). In the case of simple flows past wedges, each such type of flow is completely determined by this arrangement, up to a finite set of real parameters.

This idea will now be illustrated by enumerating every stable type of simple flow having a circular sector hodograph.

10. Flows with circular sector hodograph. In the case of a "simple" flow with a (simply covered) circular sector hodograph, (18) evidently reduces simply to

$$(31) \quad \zeta = t^{1/\alpha} = t^{\pi/\beta}, \quad \text{or} \quad \zeta^\alpha = t.$$

There is no interior stagnation point, and the velocity is a maximum on

the free boundary, which is therefore convex (Ch. I, §13). Hence¹³ the only possible dividing point is at $t = t = 0$. Choosing $T = -(t + t^{-1})/2$, this is at $T = \infty$, and (5) simplifies to

$$(32) \quad dW/dT = C \bigg/ \prod_{j=1}^N (T - T_j).$$

Now referring to (30), we get $n_0 + 2n_1 + 3n_2 \leq 3$. But $N \leq n_0 + 2n_1 + 3n_2$ by Remark 5 of §3, the inequality being due to possible poles in W (jets, etc.) at $T = \infty$. This proves

THEOREM 5. For any simple flow with circular sector hodograph, (31)–(32) hold with $N \leq 3$, and $T = -(t + t^{-1})/2$.

Next, we observe that by (30), $N = n_0 + 2n_1 + 3n_2 \geq 2$, unless there is a singularity at the vertex. Hence $N = 2$ or $N = 3$. Corresponding to $N = 2$, the only possibilities are $n_0 = 2$, $n_1 = n_2 = 0$, and $n_1 = 1$, $n_0 = n_2 = 0$. We shall explore these in turn.

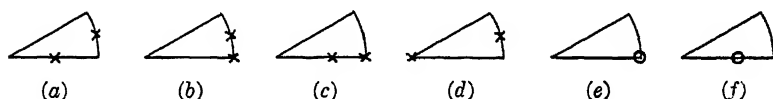


FIG. 9.

The case $n_0 = 2$ includes Rethy flows, with singularities located¹⁴ as in Fig. 9a, one on a fixed and the other on a free boundary, except in the limiting cases of half the flow past a wedge in a jet (Fig. 9b) or a channel (Fig. 9c). Fig. 9d corresponds to the jet from a funnel, and Fig. 9e (a circle represents a dipole), to half of the Bobyleff flow past a wedge. Another interesting case corresponds to Fig. 10a, and represents a pipe elbow (Fig. 10b) in which the pressure is constant around the bend, in ideal flow. This has some possible practical interest, as indicating a pipe elbow in which the flow should not separate.

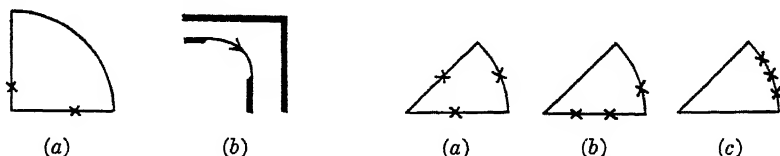


FIG. 10.

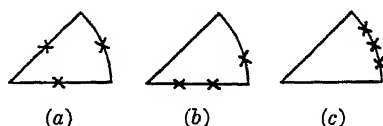


FIG. 11.

However, it should be noted that the flow on one free boundary ap-

¹³ Overlapping cusps and coalescing straight walls (360° wedges) are discarded; see Ch. IV, §7. For the present material, see also M. Miyadzu, Tech. Rep. Tohoku Imp. Univ. 10 (1932), 545–83.

¹⁴ A cross on the hodograph denotes a jet, a circle, an ocean, and a square or diamond denotes an infinite stream. Fig. 9f corresponds to the “streamline struts” treated by R. Gerber and J. S. McNown [59a, 14–20].

proaches a straight wall. If the curved free boundary were not held in by a solid wall, such a flow would obviously splash, and be unstable. It is not hard to show that Figs. 9a-9e give all types which satisfy the stability condition

(S) At every separation point, the flow is from the fixed to the free boundary.

Corresponding to $N = 3$, there are only three essentially different cases satisfying the stability condition (S) (Figs. 11a, 11b, 11c). Figs. 11a and 11b represent the flows given in Figs. 12a and 12b, respectively; Fig. 11c represents a jet divided by a finite wedge.

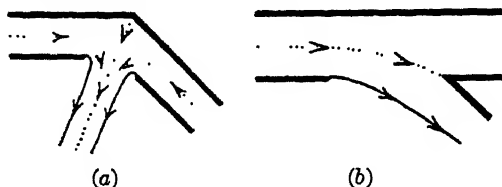


FIG. 12.

Limiting forms are obtained by either letting two or three singularities coalesce into one or by displacing one or more into a corner of the diagram. Thus for instance the diagrams in Figs. 13a and 13b correspond to the flows in Figs. 14a and 14b, respectively¹⁵, while Fig. 13c corresponds to a Bobyleff flow (Ch. II, §4).

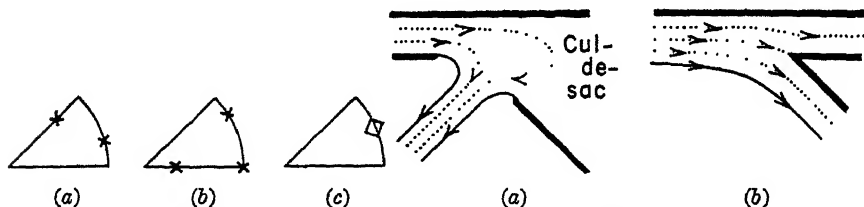


FIG. 13.

FIG. 14.

II. Other examples. A classification of other simple flows past wedges, based on Theorems 2-3 and equation (30), is also possible. In this classification, stagnation points must be located in the semicircle Γ . Vortices can be treated similarly. Thus, from a mathematical point of view, the enumeration of such flows is now a routine problem.

Many such flows are, however, of sufficient physical interest to make the details worth carrying through. For example, consider the deflection of a free jet by a "deviating vortex" (Fig. 15)—this describes the effect of a lifting surface on such a jet, to a first approximation¹⁶.

¹⁵ Flow 14b has been investigated by G. Banzi, *Annali di mat. pura appl.* Milano 28 (1919), 95-108.



FIG. 15.

We map the flow onto the unit circle of the parameter t -plane so that the vortex V goes into the origin, and the jets J_1 and J_2 onto the points $e^{i\alpha}$ and $e^{-i\alpha}$ of the boundary, respectively. If γ is the strength of the vortex, W has at $t = 0$ a logarithmic singularity with coefficients $i\gamma/2\pi$, and at the points $e^{i\alpha}$, $e^{-i\alpha}$ opposite logarithmic singularities with coefficients $\pm d/\pi$ (d is the asymptotic thickness of jets). By reflection in the unit circle, the vortex of $t = 0$ goes into an equal and opposite vortex at $t = \infty$, but no new singularity is generated by the jets. Thus

$$W = \frac{d}{\pi} \ln \frac{t - e^{i\alpha}}{t - e^{-i\alpha}} + \frac{i\gamma}{2\pi} \ln t.$$

From

$$\frac{dW}{dt} = 2i \frac{d}{\pi} \frac{\sin \alpha}{t^2 + 1 - 2t \cos \alpha} + \frac{i\gamma}{2\pi} \frac{1}{t} = \frac{i\gamma}{2\pi} \frac{(t - t_0)(t - t_0^{-1})}{t(t - e^{i\alpha})(t - e^{-i\alpha})}$$

it follows that there must be a new stagnation point at t_0 satisfying $t_0^2 - 2[\cos \alpha - (2d/\gamma) \sin \alpha] t_0 + 1 = 0$. Hence the velocity ζ has a zero at $t = t_0$, a pole at $t = 0$ and its modulus is 1 on $t = e^{i\alpha}$. By reflection in the unit circle the pole generates a zero, and the zero a pole at reflected points. Consequently

$$\zeta = \frac{1}{t} \frac{t - t_0}{1 - tt_0}.$$

Upon integration, one gets

$$z = \int \zeta^{-1} dW = -\frac{i\gamma}{2\pi} t_0 [t + (e^{i\alpha} - t_0^{-1})^2 \ln(1 - e^{-i\alpha}t) + (e^{-i\alpha} - t_0^{-1}) \ln(1 - e^{i\alpha}t)]$$

The deflection angle $\delta = \arg \zeta_j$ is given by

$$\delta = -\arctan \frac{\gamma}{4d} (1 - t_0 \cos \alpha).$$

Still other illustrations of the method of reflection could be given¹⁷.

¹⁶ The slightly more complicated case of a deviating vortex in the jet from a nozzle has been treated by N. Simmons, *Quar. J. math.* 10 (1939), 283-311. See also *Phil. Mag.* (7) 31 (1941), 81-102.

¹⁷ See for example P. W. Ketchum, *Quar. appl. math.* 1 (1943), 149-67; A. Masotti, *Acta Pont. Acad.*, (1933-34), 248-55; Y. Shibaoka, *J. Inst. Polytech. Osaka B3* (1952), 53-7.

CHAPTER IV

GENERAL THEORY

1. Singularities of $W(T)$. In Chs. II–III, we have determined many ideal plane flows bounded by wedge-like barriers and free streamlines. We now turn our attention to general properties of ideal flows with free streamlines past arbitrary obstacles, both in the plane (through §8) and in space (§§9–13). This discussion is independent of Chs. II–III, except for the concepts of a “simple” flow and of reflection treated in Ch. III, §§2–3.

We first complete the proof of Theorem 1 of Ch. III, by showing that $W(T)$ cannot have an essential singularity. This proof assumes only that (i) the flow domain R is locally simply covered, (ii) R is locally simply connected, and (iii) the velocity field $\zeta(z)$ is bounded and analytic in R . Thus it does not require that the flow be “simple” in the large (cf. Ch. III, §2, and the Remark at the end of Ch. VI, §3). By a “simple point” of a flow satisfying (i)–(iii), we mean a regular point or isolated singularity. We recall (Ch. III, §3) that every point of a “simple flow” is a “simple point”.

THEOREM 1. At a “simple” point on the boundary C of a flow, dW/dT is either regular or has a pole of order three at most.

Proof. By the fundamental theorem of conformal mapping, we can map the flow in a neighborhood of the simple point onto a semicircle with center $T = 0$ in the upper half T -plane, by a schlicht (one-one conformal) transformation, so that the boundary goes into the real diameter. Since $z(T)$ is schlicht, we know by Koebe’s distortion theorem [3, vol. 2, p. 77] that, locally,

$$(1) \quad A_0 |\eta| \leq |z'(T)| \leq A_1 |\eta|^{-3}, \quad [\eta = \text{Im } T, \quad 0 < A_0].$$

Hence, if A is an upper bound to the velocity near the simple point in question,

$$(1') \quad |dW/dT| = |\zeta z'(T)| \leq AA_1 |\eta|^{-3}.$$

Since dW/dT is real on the boundary, it can moreover be extended to the lower half-plane by reflection, so that (1') holds in a complete (circular) neighborhood of $T = 0$.

We now use the following slight generalization of a theorem of Polya and Stone¹

¹ G. Polya, *Jahr. Deutsche Math. Ver.* 40 (1931), p. 81; M. H. Stone, *J. Ind. Math. Soc.* 12 (1948), 1–7.

LEMMA. Let $h(T)$ be analytic and regular in a neighborhood of $T = 0$, the origin excepted, such that $|h(T)| \leq B|\eta|^{-N}$, where N is a non-negative integer. Then either $h(T)$ is regular, or it has a pole of order N at most at $T = 0$.

Proof. Since $|r^2 - T^2| \leq 2r|\eta|$ on the circle Γ_r : $T = re^{i\theta}$, and since by hypothesis $|h(T)| \leq B|\eta|^{-N}$,

$$(2) \quad I(r, k) = \frac{1}{2\pi i} \oint_{\Gamma_r} T^{k-1} \left(1 - \frac{T^2}{r^2}\right)^N h(T) dT = O(r^{k-N}).$$

If $k > N$, then $I(r, k) \rightarrow 0$ as $r \rightarrow 0$. On the other hand, by Cauchy's theorem, $I(r, k)$ is the residue of the integrand which, if $\sum_{-\infty}^{\infty} a_k T^k$ is the Laurent series of $h(T)$, is

$$(2') \quad \sum_{p=0}^N \binom{N}{p} (-1)^p a_{-(2p+k)} r^{-2p} = I(r, k).$$

By (2'), $I(r, k) \rightarrow 0$ implies in turn $a_{-(2N+k)} = 0, \dots, a_{-k} = 0$; by (2), this implies $a_{-k} = 0$ if $k > N$.

Combining this lemma with (1'), we have the proof of Theorem 1. Clearly, any finite point $T = T_0$ on the real axis could have been used instead of $T = 0$.

If a simple flow is mapped onto a semicircle in the t -plane, the mapping $T = -(t + t^{-1})/2$ shows that, again, essential singularities cannot occur. However, poles of order up to five can occur at the corner, since the transformation there is locally quadratic.

Theorem 1 has been proved without assuming the continuity of $\zeta(z)$. However, the classification of isolated singularities given in Ch. III, §3, is not complete unless conditions (i)–(iii) made in proving Theorem 1 are supplemented, by assuming either the continuity of $\zeta(z)$ or the boundedness of $\arg \zeta(z)$ (cf. Ch. VI, §3).

The same should be said about the asymptotic formulas of §§3–6 below.

Consider, for example, the flow defined by

$$(3) \quad \zeta = T^{-i\beta} \text{ and } T = W, \quad [\beta > 0].$$

This gives a flow between two equiangular spirals (Fig. 1), the first being a free streamline with velocity 1, and the second one with velocity $e^{\beta\pi}$. Conversely, it may be shown that this is the only way two free streamlines of different velocities can meet locally².

2. Reflection principle. Following an idea of Shiffman [77], we now apply the method of reflection (Ch. III, §2) directly to the physical plane. We consider a neighborhood of a fixed point z_0 on a free streamline C with free streamline velocity v ; we assume $\zeta(z)$ continuous. Since $\zeta(z)$ maps C

² E. H. Zarantonello, *J. de math.* 33 (1954), 29–80.

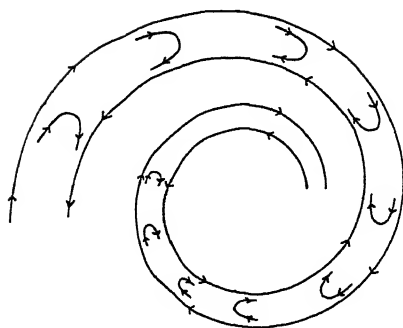


FIG. 1.

onto a circular arc, the formulas of Ch. III, §2 show that, under analytic reflection $z \rightarrow \bar{z}$ in C , we must have

$$(4a) \quad \bar{\zeta} = v^2/\zeta^*, \quad \overline{dW} = dW^*$$

at corresponding points. Consequently, we must have

$$\overline{dz} = \bar{\zeta}^{-1} \overline{dW} = v^{-2} \zeta^* dW^* = v^{-2} (\zeta^2 dz)^*.$$

We shall now show that such a reflection is always possible; it will of course make

$$(4b) \quad \bar{z} = z_0 + v^{-2} \left[\int_{z_0}^z \zeta^2 dz \right]^*, \quad \bar{W} = W - 2V_0,$$

where V_0 is the (constant) value of $\text{Im}\{W\}$ on C .

THEOREM 2. Any plane flow can be extended locally across a free streamline, by formulas (4a)–(4b).

Proof. In the W -plane, it is easy to show that $z(W)$ is single-valued, and that ζ^{-1} is continuous and satisfies the condition of Morera's Theorem [3, vol. I, p. 133], that $\oint \zeta^{-1} dW = 0$ around any closed curve. Hence ζ^{-1} , ζ , and $z = \int \zeta^{-1} dW$ are analytic functions of W . Since $dz/dW = \zeta^{-1} \neq 0$, $W(z)$ is also analytic [3, vol. I, p. 190], so that the flow is analytic in the physical plane.

COROLLARY 1. In any ideal plane flow³, free streamlines are analytic. For, since $W(z)$ is analytic, any interior curve $V = \text{const.}$ is analytic.

COROLLARY 2. The velocity fields of two flows having a common arc of a free streamline coincide up to a real factor.

For, under the hypotheses of Corollary 2, the ratio $\zeta(z)/\zeta_1(z)$ of the

³ P. Garabedian, H. Lewy and M. Schiffer [27] have proved that this result is also true for axially symmetric flows. It is not known whether or not a similar result holds for all space flows.

velocities is constant and real on a continuous arc; hence it must assume this value identically [3, vol. 1, p. 140].

THEOREM 3. Reflection carries streamlines into streamlines, isobars and isoclines into isobars and isoclines, free streamlines into free streamlines, polygonal walls into parallel polygonal walls, sources and vortices into sources and vortices at infinity. If the free streamline velocity is v , the force F on an obstacle is $i\rho v^2/2$ times the vector joining one end z_1 of the obstacle with its reflected image \bar{z}_1 .

Proof. The statements about streamlines, isobars, isoclines, free streamlines, and polygonal walls are obvious from (4a)–(4b); moreover, the flow direction $-\arg \zeta = \arg \zeta^* = -\arg \bar{\zeta}$ is unchanged by reflection. The facts about sources and vortices follow from the fact that the W -diagram is reflected by (4b), while $\zeta = \infty$ and $\zeta = 0$ are interchanged. Hence sources and vortices in the finite plane (where $\zeta = \infty$) go into corresponding points where $\zeta = 0$, which must be at infinity.

As regards the net force F , assuming a constant pressure on the rear of the obstacle, we have

$$F = \frac{i}{2} \rho \int_{z_1}^{z_2} [|\zeta|^2 - v^2] dz = \frac{i}{2} \rho \left[\int_{z_1}^{z_2} \zeta^* dW - v^2 \int_{z_1}^{z_2} dz \right],$$

by Bernoulli's theorem. But $\zeta^* = v^2 \bar{\zeta}^{-1}$, while $dW = dW^* = d\bar{W} = \zeta dz$ since dW is real along a streamline. Hence, by (4b),

$$(5) \quad F = \frac{i}{2} \rho v^2 \left[\int_{z_1}^{z_2} \bar{dz} - \int_{z_1}^{z_2} dz \right] = \frac{i}{2} \rho v^2 \int_{z_1}^{z_1^*} dz = \frac{i}{2} \rho v^2 (z_1 - \bar{z}_1).$$

This completes the proof.

Reflection ordinarily carries interior stagnation points into three-sheeted branch points; thus the reflection of a flow with an interior stagnation point will not usually be "simple."

One illustration of Theorems 2–3 is furnished by a jet in an angle; its reflection (Fig. 2a) is a jet going around an angle. An especially nice example is the swirl in a square (Fig. 2b); combined with its image, it gives the flow between two concentric squares⁴.

An interesting application of Corollary 2 above consists in finding the flow with a given free streamline C . This can be done by conformal mapping. To find the flow, determine the conformal mapping $z = f(T)$ of one side of C onto a half-plane and set

$$(6) \quad \begin{aligned} dW/dT &= [f'(T)f^*(T)]^{\frac{1}{2}} \\ \zeta(T) &= [f^*(T^*)/f'(T)]^{\frac{1}{2}}. \end{aligned}$$

⁴ The reflection of a jet from a funnel gives a jet from a wedge with a source at the vertex, as has been observed by F. Weinig, *Ing. Archiv* 11 (1940), 264–8. See also Ch. V, §15.

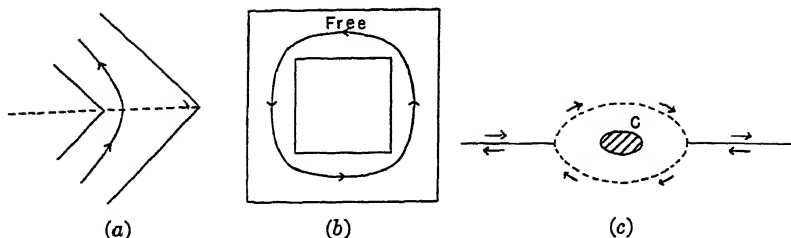


FIG. 2.

Thus, if C is an ellipse, one gets a flow which can be imagined as the hollow vortex generated by two opposite parallel streams flowing at each side of an interrupted wall (Fig. 2c).

3. Asymptotic geometry of free streamlines. Consider the portion of a flow bounded by two free streamlines extending to infinity, and a connected arc joining them. We wish to study the asymptotic or "local" behavior of the flow at infinity. We shall assume in §§3-8 that $v = 1$: the free streamline velocity is unity.

Clearly the domain described is simply connected, and can be mapped conformally onto the lower half T -plane, so that the point at infinity goes into $T = 0$. By Theorem 1, after integration, we get

$$(7) \quad W = h_{-2}T^{-2} + h_{-1}T^{-1} + h \ln T + h_0 + h_1T + \dots, \quad (\text{all } h_k \text{ real})$$

where h, h_{-1}, h_{-2} are not all zero. As in Ch. III, §3, we shall speak of a "jet", "ocean", or "infinite stream" according as the first non-zero coefficient in (7) is $h, h_{-1},$ or h_{-2} .

Formula (7) can be simplified by a more precise choice of parameter. Since the flow at infinity is bounded by free streamlines, $\zeta(0) \neq 0$ there, so that *all streamlines are asymptotically parallel at infinity* and the W -domain covers all points between two half-lines parallel to the real axis outside a sufficiently large circle (Figs. 3a-3c). Correspondingly, one of the following functions will map a whole neighborhood of infinity into the exterior of some circle in the lower half-plane (Fig. 3d):

$$(8a) \quad W = \frac{d}{\pi} \ln t \quad (\text{jet})$$

$$(8b) \quad W = t + \frac{d}{\pi} \ln t \quad (\text{ocean})$$

$$(8c) \quad W = t^2 + \frac{d}{\pi} \ln t \quad (\text{infinite stream}).$$

Here d is the jump in V between the two free streamlines; hence we may

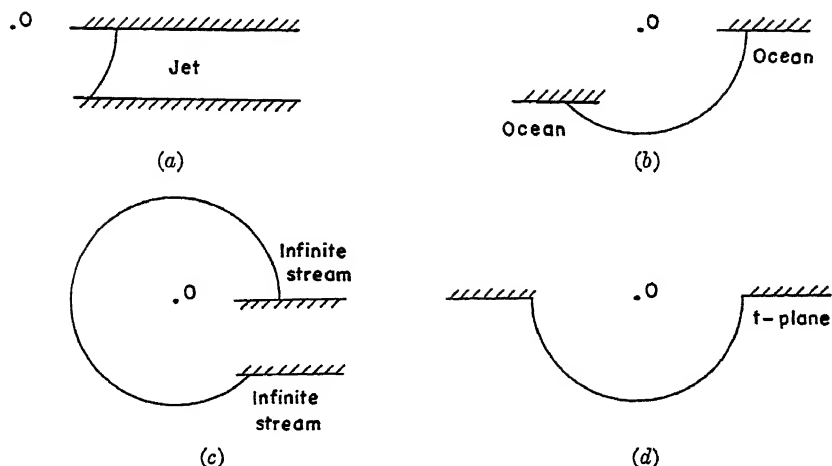


FIG. 3.

refer to t as the *intrinsic parameter*. Indeed, the images under (8a)–(8c) of a sufficiently large semicircle in the lower half t -plane are as in Figs. 3a–3c. Formulas (8a)–(8c) can also be obtained by making a substitution of the form

$$T = \phi(t) = a_{-1}t^{-1} + a_0 + a_1t + a_2t^2 + \dots \quad (\text{all } a_i \text{ real})$$

in (7).

By the Reflection Principle (Ch. III, §2), rotating the flow so that $\zeta(\infty) = 1$, we also have

$$(9) \quad \zeta = \exp i(\alpha t^{-1} + \beta t^{-2} + \gamma t^{-3} + \delta t^{-4} + \dots),$$

where $\alpha, \beta, \gamma, \dots$ are all real. Equations (8)–(9) determine the asymptotic behavior. Thus, since $-\arg \zeta = -\alpha t^{-1} - \beta t^{-2} - \dots$ is the tangent direction on the free streamlines, when t is real, the asymptotic convexity of the free streamlines is determined by the first non-zero coefficient of (9). If $\alpha > 0$, both free streamlines turn away from the flow, showing (by the Brillouin Principle of Ch. I, §13) that the velocity is asymptotically a local maximum on the free streamlines. If $\alpha = 0$ but $\beta \neq 0$, one free streamline bends toward the flow and the other away from it.

A clearer picture of the flow geometry is obtained by expanding for z ,

$$(10) \quad z = \int \zeta^{-1} dW = \int (1 - i\alpha t^{-1} - (\tfrac{1}{2}\alpha^2 + i\beta)t^{-2} + \dots) dW.$$

Thus, in the case of a *jet*, $t = e^{aW}$ [$a = h^{-1}$], and so

$$(11a) \quad z = z_0 + W + \frac{i\alpha}{a} e^{-aW} + \frac{\alpha^2 + 2i\beta}{4a} e^{-2aW} + \dots;$$

hence the jet tends exponentially to *parallel flow*, in a channel of diameter $d = h\pi$ (Fig. 4 and Plate 7). In the typical case of a jet from a contracting orifice, $\alpha > 0$, and a good picture can be had by considering $z = z_0 + W + (i\alpha/a)t^{-1}$, which contracts symmetrically along the lower and upper free streamlines $t > 0$ and $t < 0$, respectively.

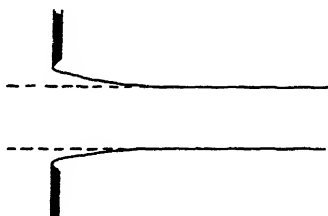


FIG. 4.

The case of an *ocean* is less simple. We have

$$\begin{aligned}
 (11b) \quad z &= \int (1 - i\alpha t^{-1} - (\tfrac{1}{2}\alpha^2 + i\beta)t^{-2} + \dots)(1 + at^{-1}) dt \\
 &= z_0 + W - i\alpha \ln t + [\tfrac{1}{2}\alpha^2 + i(a\alpha + \beta)]t^{-1} + \dots \\
 &= z_0 + W - i\alpha \ln W + O(W^{-1}).
 \end{aligned}$$

Thus, unless $\alpha = 0$, the ocean is infinitely depressed (or raised) at infinity, relative to the planing surface (Fig. 5); a special case of this paradox has already been discussed in Ch. III, §6. We shall show in §5 that a lift $L = \rho\pi\alpha$ is associated with this configuration. If $\alpha = 0$, then the depression is asymptotically finite, but (cf. §5) $L = 0$; this case is ordinarily incompatible with the Brillouin separation condition of Ch. I, §13. In any case, the difference in elevation of the "ocean" surface on the two sides of any fixed vertical axis, at equal distances from it, tends to the thickness of the jet diverted.

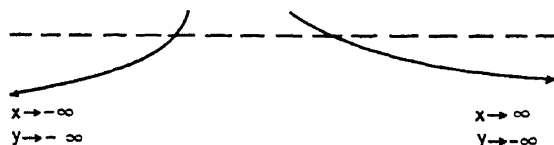


FIG. 5.

The case of an *infinite stream* is the most complicated. In the typical case $d = 0$ of the cavity behind an obstacle, clearly

$$\begin{aligned}
 (11c) \quad z &= \int [1 - i\alpha W^{-\frac{1}{2}} - (\tfrac{1}{2}\alpha^2 + i\beta)W^{-1} - \dots] dW \\
 &= z_0 + W - 2i\alpha \sqrt{W} - (\tfrac{1}{2}\alpha^2 + i\beta) \ln W + \dots
 \end{aligned}$$

Moreover (11c) holds even if $d \neq 0$, since then

$$t^{-1} \sim W^{-1}(1 + (d \ln W)/\pm \pi W + \dots).$$

Since the two boundaries of the cavity correspond to the two sides of the cut along the positive axis in the W -plane, and $\sqrt{W} = t$ has opposite signs along these, clearly⁵ the *cavity shape is essentially parabolic* if $\alpha > 0$ (Fig. 6a), its symmetry being skewed by $\beta \ln W$ if $\beta \neq 0$. In the z -plane, elementary calculations verify

$$(11d) \quad y - y_0 = \pm 2\alpha \sqrt{x} - \beta \ln x + O(1).$$

Clearly $\alpha < 0$ leads to a flow which is self-overlapping, which is physically impossible.

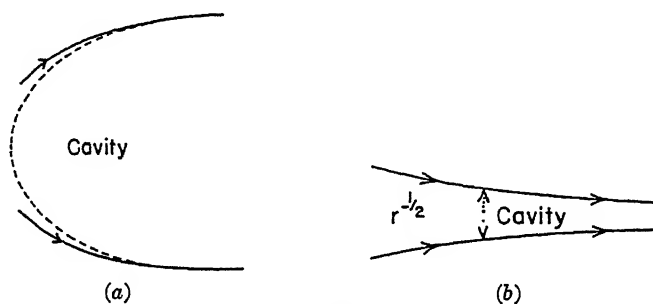


FIG. 6.

The case $\alpha = 0$ leads to a cavity of *finite width*, which will be asymptotically straight in the symmetric case $\beta = 0$, but which will ordinarily deviate logarithmically from a straight line in the asymmetric case. This will be shown in §5 to be the case of a *cavity of zero drag*⁶ (Fig. 6b).

More generally, it will be shown there that α and β measure the drag and lift, respectively, according to the formulas $D = \pi\rho\alpha^2$ and $L = \pi\rho\beta$.

4. Momentum equations. The rate of efflux of momentum across any oriented⁷ boundary element dz is, almost by definition (Ch. I, §12),

$$(12) \quad d\mathbf{M} = \rho \xi^* dV = \rho(\xi dV - i\eta dV).$$

Again, by Bernoulli's equation⁸

⁵ This result, and formula (17) for cavity drag, are essentially due to Levi-Civita [59].

⁶ Using the "dead water" wake interpretation of Ch. I, §7, von Mises (*Theory of flight*, p. 101) has suggested this as a possible model for flow outside the wake above the critical Reynolds number.

⁷ We adopt the convention that the interior is to the left of the boundary, corresponding to orienting the boundary in the counterclockwise sense.

⁸ Here and below, p_0 will denote the stagnation pressure, p_f the ambient (free streamline) pressure, and an asterisk the complex conjugate.

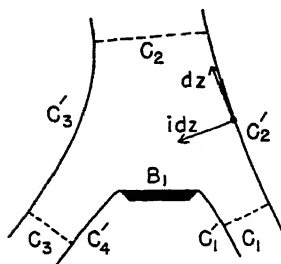


FIG. 7.

$$p = p_0 - \frac{1}{2}(\xi^2 + \eta^2) = p_0 - \frac{1}{2}\rho\zeta\zeta^*.$$

Since $i dz$ is the inward normal (see Fig. 7) and $\zeta = \xi + i\eta = dW/dz$, the vector pressure thrust of an element dz of boundary on the fluid is

$$(13) \quad \begin{aligned} d\mathbf{p} &= ip dz = ip_0 dz - \frac{1}{2}\rho i \zeta^* (dW/dz) dz \\ &= ip_0 dz - \frac{1}{2}\rho i (\xi - i\eta)(dU + i dV). \end{aligned}$$

Combining (12) and (13), we get

$$(14) \quad d\mathbf{M} - d\mathbf{p} = -ip_0 dz + \frac{1}{2}\rho i (\zeta dW)^*.$$

Similarly, if $d\mathbf{P} = i(p - p_f) dz$ denotes the relative pressure thrust, we have

$$(14') \quad d\mathbf{M} - d\mathbf{P} = i(p_f - p_0) dz + \frac{1}{2}\rho i (\zeta dW)^*.$$

But by Cauchy's Integral Theorem, $\oint dz = 0$ and $\oint (\zeta dW)^* = 0$; hence the contour integral of the right side of (14') vanishes, if taken around the boundary of any finite domain of the flow. That is, $\oint (d\mathbf{M} - d\mathbf{P}) = 0$.

(The corresponding formula $\oint d\mathbf{M} = \oint d\mathbf{p}$, obtained similarly from (14), expresses the ordinary momentum theorem of Ch. I, §10.)

We now wish to find an asymptotic analog of this equation, valid for *infinite* domains bounded by *free* streamlines C_i' at a given pressure p_f , and finite *fixed* barriers B_j [$i = 1, \dots, r'$, $j = 1, \dots, s$]. We assume the units so chosen that the free streamline velocity is one.

To do this, we apply the basic equation $\mathbf{M} - \mathbf{P} = 0$ to a finite domain bounded by the B_j , by portions of the free streamlines C_i' extending to a large distance, and by cuts C_k [$k = 1, \dots, r$] joining adjacent free streamlines, as in Fig. 7. Clearly, $d\mathbf{M} \equiv 0$ along any streamline, while $d\mathbf{P} \equiv 0$ along any free streamline. Now let $\mathbf{F}_j = \int_{B_j} d\mathbf{P}$ denote the total thrust (relative to the ambient pressure) exerted by the barrier B_j on the

moving fluid. Since $\oint (d\mathbf{M} - d\mathbf{P}) = 0$, clearly

$$(15) \quad -\mathbf{F} = -\sum_{j=1}^s \mathbf{F}_j = \sum_{k=1}^r \int_{C_k} (d\mathbf{M} - d\mathbf{P}) = \sum_{k=1}^r \mathbf{G}_k.$$

Our aim will be to evaluate the integrals \mathbf{G}_k . Since $\oint (d\mathbf{M} - d\mathbf{P}) = 0$ around a contour consisting of segments of two free streamlines and cuts joining them, and since $d\mathbf{M} - d\mathbf{P} = 0$ along the free streamlines, the \mathbf{G}_k are the same for all cuts joining the same two free streamlines. We shall now evaluate the \mathbf{G}_k asymptotically.

5. Drag and lift. The evaluation of \mathbf{G}_k across any *jet* is obvious. Because of the finite cross-section, and the exponential approach (11a) to uniform flow at the free streamline velocity v_f and the ambient pressure, \mathbf{G}_k is equal $\rho \zeta_k^* v_f d$, that is, to a vector of magnitude $\rho d v_f^2$, acting along the midline of the jet. Hence if a jet is divided by any barrier B whatever, and \mathbf{F} denotes the force exerted by the jet on the barrier, then

$$(15a) \quad -\mathbf{F} = \mathbf{G}_1 + \mathbf{G}_2 + \mathbf{G}_3,$$

where the \mathbf{G}_k are the rates of momentum efflux associated with the impinging jet and its two branches.

For an ocean or cavity, \mathbf{G}_k is given by (14'), since $p_f - p_0 = \rho/2$ if $v_f = 1$, as

$$(16) \quad \mathbf{G}_k = \frac{1}{2} \rho i \left\{ \int_{C_k} (\zeta dW)^* - \int_{C_k} dz \right\}.$$

We shall now evaluate this integral asymptotically, around a large semi-circle C_k in the lower half t -plane, with its center at the origin, and radius R . In this evaluation, it is convenient to observe that

$$\int_{C_k} [f(t) dt]^* = \int_{C_k^*} f^*(t) dt,$$

where $f^*(t)$ is the power series obtained from $f(t)$ by replacing each coefficient by its conjugate, and C_k^* is the semicircle conjugate to C_k , on which $\ln t$ decreases by $i\pi$.

In an infinite ocean, by (8b) and (9),

$$\begin{aligned} \int_{C_k} \zeta^* dW^* &= \int_{C_k^*} \left(1 - \frac{i\alpha}{t} + \dots\right) \left(1 + \frac{d}{\pi t}\right) dt \\ &= [t + (-i\alpha + d/\pi) \ln t + \text{const.} + o(1)]_{-R}^{+R} \\ &= 2R - \pi\alpha - id + o(1). \end{aligned}$$

Similarly, over C_k , $\int dz = \int \zeta^{-1} dW = 2R + \pi\alpha + id + o(1)$. Substituting in (16), we get

$$(15b) \quad \mathbf{G}_k = \frac{1}{2}\rho i(-2\pi\alpha - 2id) = \rho(d - i\pi\alpha).$$

Hence, for any "planing" barrier B on an infinite ocean, the rate at which the ocean supplies momentum, to the jet and barrier combined, has a *horizontal* component equal to the mass of jet peeled off per unit time, and a *vertical* component proportional to the logarithmic depression at infinity.

Since (16) is additive, we can say that the "drag" $D = \rho d$ comes from the "jet" term $(d/\pi) \ln t$ in (8b), while the "lift" $L = \pi\rho\alpha$ comes from the "pure ocean" term $W = t$.

We shall now compute the force due to the "pure cavity" term $W = t^2$ in (8c)—which is the only term in most applications. This gives, in an *infinite stream*

$$\begin{aligned} \int_{C_k} \zeta^* dW^* &= \int_{C_k} \left(1 + \frac{i\alpha}{t} - \frac{\alpha^2 - 2i\beta}{t^2} + \dots \right) 2t^* dt^* \\ &= [t^{*2} - 2i\alpha t^* - (\alpha^2 + 2i\beta) \ln t + o(1)]_{-R}^R \\ &= -4i\alpha R + i\alpha^2\pi - 2\beta\pi + o(1); \\ \int_{C_k} dz &= \int_{C_k} \zeta^{-1} dW = \int_{C_k} \left(1 - \frac{i\alpha}{t} - \frac{\alpha^2 + 2i\beta}{t^2} + \dots \right) 2t dt \\ &= [t^2 - 2i\alpha t - (\alpha^2 + 2i\beta) \ln t + o(1)]_{-R}^R \\ &= -4i\alpha R - i\alpha^2\pi + 2\beta\pi + o(1). \end{aligned}$$

Substituting again in (16), we get

$$(15c) \quad \mathbf{F} = -\mathbf{G} = \frac{1}{2}\rho i[-2i\alpha^2\pi + 4\beta\pi] = \rho\pi(\alpha^2 + 2i\beta).$$

Letting D denote (cavity) *drag* and L (cavity) *lift*, as usual, we get

THEOREM 4. In an infinite stream, the constants α , β of (11c)–(11d) satisfy

$$(17) \quad D = \pi\rho\alpha^2 \quad \text{and} \quad L = 2\pi\rho\beta,$$

in the case of unit free streamline velocity.

Substituting back in (11c)–(11d), we get

$$(17a) \quad z = z_0 + W - 2i \sqrt{\frac{D}{\rho\pi}} \sqrt{W} - \frac{D + iL}{2\rho\pi} \ln W + o(1/\sqrt{W}),$$

$$(17b) \quad y - y_0 = \pm 2 \sqrt{\frac{D}{\rho\pi}} \sqrt{x} + \frac{L}{2\rho\pi} \ln x + o(1/\sqrt{x}).$$

In this sense, the cavity width is determined by the drag, and its asymmetry by the lift. In the interesting case $D = 0$ of a symmetric cavity of zero drag (Fig. 6b), we thus have typically $y - y_0 = O(1/\sqrt{x})$.

Another interesting asymptotic formula applies to reentrant jet motion, both in the plane and axially symmetric jet case. It is⁹

$$(18) \quad C_D = 2[1 + Q + \sqrt{1 + Q}] A^*/A,$$

where A^* is the jet cross-section, and A is the obstacle cross-section.

6. Moment. The moment coefficient C_M can also be evaluated by a refinement of the preceding asymptotic considerations; indeed, this is apt to be the most practical way to evaluate C_M in specific problems. We now give the detailed formulas.

The *moment* about the origin of a complex vector $f = g + ih$, applied at the point z , is $xh - yg = \text{Im}\{fz^*\}$. Hence, by (12), the rate of efflux of *moment* of momentum across the boundary element dz is

$$(19) \quad dN = \rho \text{Im}\{\xi^* z^*\} dV.$$

Similarly for the moment dQ of the relative pressure thrust,

$$dQ = \text{Im}\{i(p_0 - p_f)z^* dz - \frac{1}{2}\rho i \xi^* z^* dW^*\},$$

whence

$$(20) \quad dN - dQ = (p_f - p_0) \text{Re}(z^* dz) + \frac{1}{2}\rho \text{Re}(z\xi^* dW)^*.$$

Integrating around the boundary of any finite domain (containing no sources, sinks, or other singularities), since

$$\oint \text{Re}(z^* dz) = \oint (xdx + y dy) = 0 = \oint z\xi^* dW,$$

we deduce the usual moment of momentum theorem $N = Q$.

We now wish to find an asymptotic analog of this equation, expressing the moment required to produce a given asymptotic flow at infinity. We do this just as in §5, getting finally

$$(21) \quad -N(\mathbf{F}) = \sum_{k=1}^r \int_{C_k} (dN - dQ) = \sum_{k=1}^r N(\mathbf{G}_k).$$

In other words (cf. (15)), the *moment* of the total hydrodynamic force exerted by the moving fluid on the barrier is the sum of certain integrals, which we shall now try to evaluate asymptotically.

The case of a *jet* is obvious; as already stated in §5, $N(\mathbf{G}_k)$ is the moment of a vector of magnitude $\rho v_f^2 d$, acting along the midline of the jet.

⁹ G. Birkhoff, Rev. Ciencias Lima 50 (1948), 105-16.

For polygonal obstacles, in cavity motion or planing on the ocean surface, it is often possible to evaluate $N(\mathbf{G}_k)$ as a limiting case of divided jets. But it is usually more convenient to substitute directly in the appropriate limit formula. We shall therefore evaluate $N(\mathbf{G}_k)$ for the case of an ocean or a cavity.

THEOREM 5. The moment of the pressure thrust about $z = 0$ is

$$(22) \quad N(\mathbf{G}_k) = \rho\pi \left[\beta + \frac{\alpha d}{\pi} - \frac{\pi}{2} \left(\frac{d^2}{\pi^2} + \alpha^2 \right) \right] + \text{Im}\{\mathbf{G}_k z_0^*\},$$

for an ocean, and (cf. (9))

$$(23) \quad N(\mathbf{G}_k) = \rho\pi[2\delta + 3\alpha^2\beta - \frac{1}{2}(\alpha^4 + 4\beta^2)\pi] + \text{Im}\{\mathbf{G}_k z_0^*\},$$

for an infinite stream¹⁰.

Proof. By (20), since $v_f = 1$, we have in all cases

$$(24) \quad \begin{aligned} N(\mathbf{G}_k) &= \frac{1}{2}\rho \text{Re} \left\{ \int_{C_k} z \zeta \, dW - \int_{C_k} z^* \, dz \right\} \\ &= \frac{1}{2}\rho \text{Re} \left\{ \int_{C_k} (z \zeta - z^* \zeta^{-1}) \, dW \right\}, \end{aligned}$$

for an ocean or a cavity. We shall now evaluate the integral (24) asymptotically in the t -plane, much as in §5. In this evaluation, we shall use the consequence of (21), that $N(\mathbf{G}_k)$ is *independent of the path of integration*, to simplify the calculations. Writing $t = Re^{i\phi}$, and letting C_k be the contour of integration $|t| = R$, we see that (24) must be independent of R . But we can expand (24) in a series in R , consisting of R^2 , R , 1, $\ln R$, R^{-1} , ... times definite integrals in ϕ , which are independent of R since ϕ varies from $-\pi$ to 0. Therefore, since the sum must be independent of R , all integrals are zero, except that of the constant term.

For an ocean, we have by (8b)–(9) and $z = \int \zeta^{-1} \, dW$,

$$\zeta^{-1} = 1 - i\alpha/t - (\alpha^2/2 + i\beta)/t^2 - (i\alpha^3/6 + \alpha\beta + i\gamma)/t^3 + \dots$$

$$\begin{aligned} z &= t + z_0 + (d/\pi - i\alpha) \ln t + (i\alpha d/\pi + \alpha^2/2 + i\beta)/t \\ &\quad + \frac{1}{2}[d(\alpha^2/2 + i\beta)/\pi + i\alpha^3/6 + \alpha\beta + i\gamma]/t^2 + \dots \end{aligned}$$

Substituting in (24), and retaining only integrals which do not involve R or $\ln R$ as a factor, one obtains (22). In a similar way, one proves (23).

7. Separation curvature. It is easily verified, in special cases, that the free streamline curvature is usually infinite at a separation point. We

¹⁰ Cf. [10, p. 197] and S. Brodetsky, Proc. roy. soc. 102 (1922), 361–72.

shall now give a general discussion of this question; without loss of generality, we can continue to assume that the free streamline velocity is one.

Consider any flow satisfying conditions (i)–(iii) of §1, and separating from a barrier S at a point A , as in Fig. 8a.¹¹ Take a subdomain D about

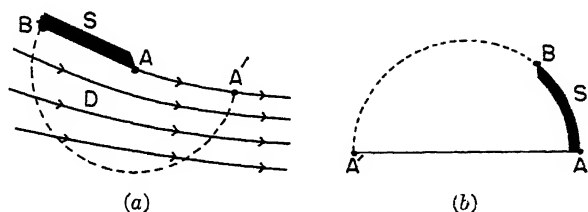


FIG. 8.

A and map it conformally onto the unit semicircle $\Gamma: |t| < 1, \text{Im } t > 0$, so that the separation point A goes into $t = 1$, the free boundary AA' into the real axis, and the barrier into the circumference (Fig. 8b). As a function of $T = -\frac{1}{2}(t + t^{-1})$, by Ch. III, Theorem 1, W is regular at the separation point $T = -1$, and so has an expansion of the form

$$(25) \quad W = W_0 + \sum_1^{\infty} \alpha_k (T + 1)^k, \quad \alpha_k \text{ real.}$$

Clearly, if A is not a dividing point, as in Fig. 8a, $\alpha_1 \neq 0$. Now consider the function $\omega(t)$, defined by

$$(25') \quad \omega = i \ln \zeta = \theta + i\tau.$$

On AA' , $\tau = \ln |\zeta| = 0$; hence the reflection principle applies (Ch. III, §2), and

$$(26) \quad \omega = b_1 t + b_2 t^2 + \dots, \quad \text{all } b_i \text{ real.}$$

the series being convergent for $|t| < 1$.

LEMMA 1. If $q = |\zeta|$ is the velocity, $a = q \, dq/ds$, the tangential fluid acceleration, and $\kappa = d\phi/ds$, the streamline curvature, then

$$(27) \quad d\omega/dW = -i \, d\zeta^{-1}/dz = \kappa/q + ia/q^2,$$

ds being measured in the flow direction.

Proof. Along a streamline $\zeta^{-1} = q^{-1}e^{i\phi}$, $d\zeta^{-1} = e^{i\phi} dq^{-1} + iq^{-1}e^{i\phi} d\phi$, while $dz = e^{i\phi} ds$, giving $d\zeta^{-1}/dz = dq^{-1}/ds + iq^{-1} d\phi/ds$.

It is a corollary that the points of zero curvature on a free streamline are isolated.

With the help of this lemma, we can now prove

THEOREM 6. If $\omega'(1) \neq 0$ exists as a continuous limit of $\omega'(t)$ as $t \rightarrow 1$ in Γ , then the curvature of AA' at A is infinite, towards the fluid or away

from it, according as $\omega' > 0$ or $\omega' < 0$. Correspondingly, the velocity along AB increases or decreases with infinite acceleration as the point A is approached¹¹.

Remark. The case $\omega'(1) \neq 0$ is sometimes called the case of "abrupt" separation. The case $\omega'(1) = 0$ of "smooth" separation will be treated in Thm. 7.

Proof. Along the free streamline (t real) (27) becomes $\kappa = d\omega/dW = \omega'(t) / \frac{dW}{dt}$. As $t \uparrow 1$, clearly $dW/dt = (\alpha_1 + 2\alpha_2(T+1) + \dots) \frac{1}{2} (t^{-2} - 1)$ tends to -0 if α_1 is negative as in Fig. 8a, and the first part of the theorem is proved. Along the obstacle ($t = e^{i\sigma}$), we get from (27) $a/q^3 = \operatorname{Im} \left\{ \omega'(t) / \frac{dW}{dt} \right\}$ and the second part follows by observing that if $\sigma \rightarrow 0$, then dW/dt tends to zero along negative imaginary values.

The further discussion of separation curvature is more technical¹². To obtain different results, various hypotheses about the obstacle smoothness are needed. All these hypotheses are fulfilled if we assume that AB is of class C''' , that is, that the tangential direction $\theta(s)$ has a continuous second derivative as a function of the arc-length.

We first show that, if the fixed boundary is smooth, the flow direction θ is continuous near the separation point.

LEMMA 2. If the obstacle tangential direction ϕ is a continuous function of the arc-length s , then the function $\theta(t)$ is continuous in a neighborhood of $t = 1$.

Proof. It follows from the hypothesis and known theorems of conformal mapping¹³ that $\arg (dz/dT)$ tends to the tangential direction ϕ when the fixed boundary is approached. Thus

$\theta(\sigma) = \arg \zeta^{-1}(e^{i\sigma}) = \arg (dz/dT) - \arg (dW/dT) = \phi(s(\sigma)) - \pi$, and since $\phi(s)$ and $s(\sigma)$ are continuous, $\theta(\sigma)$ is continuous in an interval $0 < \sigma < \sigma_0$. By reflection ($\theta(\sigma) = \theta(-\sigma)$), the continuity is extended also to the interval $-\sigma_0 < \sigma < 0$; moreover $\lim_{\sigma \rightarrow 0} \theta(\sigma)$ exists. But any harmonic function approaching the boundary values $\theta(\sigma)$ is given by the Poisson integral formula, and so is continuous near $t = 1$. Such a function being $\theta(t)$, the lemma is proved.

From the formula relating $\theta(\sigma)$ to the tangential direction, and observing that dW/dT has by (25) a change of sign or none according to whether $\alpha_1 = 0$ or $\alpha_1 \neq 0$ respectively, it follows:

COROLLARY. At the separation point, the curve consisting of the obstacle

¹¹ Cf. [85; 11]; A. H. Armstrong, Arm. Res. Est. Memo 22/53 (Great Britain), 1953.

¹² Cf. [52, 85, 49].

¹³ E. Lindelöf, C. R. 4th Scand. Math. Congr. (1916); also S. Warschawski, Math. Zeits. 35 (1932), p. 406.

and the free boundary has either a cusp or a continuous tangent depending on whether the separation point is or is not a dividing point.

The detailed discussion below applies only to the case $\alpha_1 \neq 0$ when the separation point is not a dividing point. It involves the following definition.

Definition. A function $f(x)$ is said to satisfy a Lipschitz condition of order ν ($0 < \nu \leq 1$) in a domain B , if there is a positive constant C , such that for any x_1, x_2 in B

$$(28) \quad |f(x_1) - f(x_2)| \leq C_\nu |x_1 - x_2|^\nu.$$

LEMMA 3. If $\phi(s)$ or its first or second derivative satisfies a Lipschitz condition, then the same holds for $\omega(t)$ (and hence for $\zeta(t)$) or its corresponding derivatives in a closed subdomain of Γ : $|\arg t| \leq \epsilon$, $1 - \epsilon \leq |t| \leq 1$.

Proof. Since the separation point is not a dividing point, the correspondence between the T - and z - domains, both boundaries having continuously turning tangents (cf. Lemma 2), satisfies (locally) a Lipschitz condition of order arbitrarily close to one¹⁴; that is,

$$|s_1 - s_2| < C_\nu |T_1 - T_2|^\nu, \quad 0 < \nu \leq 1.$$

Hence setting $t = e^{i\sigma}$ [$T = -\cos \sigma$],

$$(29) \quad |s(\sigma_1) - s(\sigma_2)| \leq C_\nu |\cos \sigma_1 - \cos \sigma_2|^\nu \leq C_\nu |\sigma_1 - \sigma_2|^\nu.$$

If $\theta(s)$ satisfies a Lipschitz condition, it follows that $\theta(\sigma) = \theta(s(\sigma))$ satisfies a Lipschitz condition for sufficiently small non-negative σ . By reflection ($\theta(\sigma) = \theta(-\sigma)$), the Lipschitz condition for $\theta(\sigma)$ is extended to a whole neighborhood of $\sigma = 0$.

We shall now appeal to the following result of analysis¹⁵ which we state in a local form:

Fatou-Privaloff Theorem. If the real part of an analytic function regular in the unit circle $|t| < 1$ satisfies a Lipschitz condition of order ν ($0 < \nu < 1$) on the boundary in the vicinity of a point P , then the function itself satisfies the same condition in some neighborhood of P ¹⁶.

Now, since $\theta(\sigma)$ satisfies a Lipschitz condition near $\sigma = 0$, it follows that $\omega(t)$, and so $\tau(\sigma)$, also do, near the same point. On AB , the relation $dz = \zeta^{-1} d\omega$ gives

$$(30) \quad ds/d\sigma = e^{-\tau(\sigma)} |dW/d\sigma|,$$

¹⁴ Cf. M. Lavrentieff, *Rec. math. Moscou* 36 (1929), 112-15; also C. Gattegno and A. Ostrowski, *Mem. Sci. Math.* 110 (1949), p. 35.

¹⁵ See for instance A. Zygmund, *Trigonometrical series*, New York, 1952, p. 156. The proof there can be made local.

¹⁶ That is, on that part of a neighborhood contained in $|t| \leq 1$.

which, since $|dW/d\sigma|$ is analytic and $\tau(\sigma)$ Lipschitzian, implies a Lipschitz condition for $ds/d\sigma$ near $\sigma = 0$ ($\sigma > 0$). Repeating the cycle of reasoning, and noticing that $\theta'(\sigma)$ is an odd function¹⁷ vanishing at $\sigma = 0$, this successively implies Lipschitz conditions for $\theta'(\sigma) = d\theta(\sigma)/d\sigma = d\theta/ds \cdot ds/d\sigma$, $\tau'(\sigma)$, $d^2s/d\sigma^2$ and

$$\theta''(\sigma) = d^2\theta/d\sigma^2 = \frac{d^2\theta}{ds^2} \left(\frac{ds}{d\sigma}\right)^2 + \frac{d\theta}{ds} \frac{d^2s}{d\sigma^2}.$$

if $d\theta/ds$ or $d^2\theta/ds^2$ satisfies a Lipschitz condition.

By a final appeal to the Fatou-Privaloff Theorem, it now follows that the analytic functions $i d\omega/d(\ln t)$, $-d^2\omega/d(\ln t)^2$, which take the boundary values $\theta'(\sigma) + i\tau'(\sigma)$ and $\theta''(\sigma) + i\tau''(\sigma)$ respectively, satisfy a Lipschitz condition of order ν near $t = 1$ and consequently so does $\omega''(t) = t^{-2}(d^2\omega/d(\ln t)^2 - d\omega/d(\ln t))$.

COROLLARY. The following expansions hold in the vicinity of $t = 1$:

$$(31) \quad \omega(t) = \omega(1) + (t-1)\omega'(1) + \frac{1}{2}(t-1)^2\omega''(1) \\ + (t-1)^2O((t-1)^\nu), \quad 0 < \nu < 1,$$

$$(32) \quad W(t) = \sum_{k=0}^{\infty} \alpha_k (T+1)^k, \quad T = -\frac{1}{2}(t + t^{-1}),$$

with all real coefficients and $\alpha_1 \neq 0$. Furthermore,

$$(33) \quad \zeta^{-1}(t) = \zeta^{-1}(1)[1 + i\omega'(1)(t-1) + \frac{1}{2}(-\omega'(1)^2 + i\omega''(1))(t-1)^2 \\ + (t-1)^2O(|t-1|^\nu)],$$

$$(34) \quad z(t) = z(1) + \zeta^{-1}(1)[- \frac{1}{2}\alpha_1(t-1)^2 + (\frac{1}{3}\alpha_1 - \frac{i}{3}\alpha_1\omega'(1))(t-1)^3 \\ + (t-1)^3O(|t-1|^\nu)],$$

$$(35) \quad d\zeta^{-1}/dz = i \left[\frac{\omega'(1)}{1-t} + \omega''(1) + O(|t-1|^\nu) \right] \\ \times \frac{-2t^2}{(1+t)(\alpha_1 + 2\alpha_2(T+1) + \dots)}.$$

With the help of these expansions, we can now study the case $\omega'(1) = 0$. From (35) we get, regardless of the mode of approach,

$$\lim_{t \rightarrow 1} d\zeta^{-1}/dz = -i\omega''(1)/\alpha_1.$$

¹⁷ Precisely the fact that in general the derivatives of odd order do not vanish at $\sigma = 0$ prevents one from applying without modifications this argument to higher derivatives.

Thus, by (27) we get

THEOREM 7. If AB is of class C''' , then $\omega'(1)$ in Theorem 6 exists. Furthermore, if $\omega'(1) = 0$, then the free and fixed boundary have the same curvature at the separation point and the acceleration vanishes on both sides¹⁸.

A similar discussion can be carried out for separation points which at the same time are dividing points. One finds that there must be a cusp at the separation point and that expansions (31)–(35) hold with $\alpha_1 = 0$. Thus, unless $\omega'(1) = \omega''(1) = 0$, the curvature of the free streamline is infinite. This result holds true, a fortiori, for cusps on free streamlines. In such cases, $\omega'(1) = 0$ (since ω is a regular function of T), and it is necessary that $\omega''(1) \geq 0$ to avoid local overlapping near the cusp.

8. Inflections of free boundaries. Much qualitative information about the geometry of free streamlines can be obtained from the following theorem.

THEOREM 8. In the infinite cavity flow of an unbounded stream past a fixed analytic barrier¹⁹, the number of inflections of the free boundary is at most equal to the number of inflections on the wetted barrier, including its ends²⁰. This bound can be reduced by two if the barrier is convex away from the fluid at the dividing point.

Proof. The function κ/q , as the real part of an analytic function, is harmonic by (27). The locus $\kappa = 0$ of streamline inflections consists of level curves of κ/q , which, since κ/q is harmonic, must begin and end on the boundary. Further, the “inflection lines” (lines of inflection points) starting on the free boundary cannot end on the free boundary (separation points excluded) nor at infinity. For, if this were not the case, a domain bounded by free streamlines and inflection lines would be formed, and either κ/q or its normal derivative $d(aq^{-3})/ds$ would be zero on its boundary; by Green’s identity, this would imply that κ/q is constant, which is impossible²¹. The same argument proves that no two inflection lines can end at the same inflection point on the wetted barrier or its endpoints²².

Now from the asymptotic formulas (8) and (9) of §3, with $d = 0$, we get

¹⁸ One can easily check that the hodograph has a continuous tangent in this case.

¹⁹ As in the flow described in Ch. II, §§2–4, with a general barrier in place of the plate. See also Ch. VI, §5. The proof can be extended to non-analytic barriers with angular points.

²⁰ We say that the barrier has an inflection at one end if the fixed and free boundary have curvatures of opposite signs there.

²¹ From the asymptotic developments of §3, it follows that the reasoning applies to inflection lines starting on the free boundary and ending at infinity.

²² At such points κ/q may be singular; in such a case, formula (35) shows that there is no more than one inflection line leading there.

$d\xi^{-1}/dz = d \log \xi^{-1}/dW = i(\alpha/2t^3 + \beta/t^4 + \dots)$, showing that there are three or (if $\alpha = 0$) more inflection lines leading from the interior of the fluid to infinity.

At the dividing point, since the barrier is analytic, we have $\xi^{-1} = a/z + b + cz + dz^2 + \dots$, $d\xi^{-1}/dz = -a/z^2 + c + 2dz + \dots$. If we take the inner normal as the positive imaginary axis and assume that the x -axis points in the direction of the fluid motion, then $a > 0$, and, setting $z = re^{i\phi}$, $\kappa/q = r^{-2}(a \sin 2\phi + \dots)$, by (27). Thus, locally, κ/q is positive in the first quadrant and negative in the second, and an inflection line detaches perpendicularly from the barrier. Now if the barrier is convex in the immediate right vicinity of the stagnation point, κ/q is negative there, and a further change in the sign of κ/q occurs producing an inflection line tangent to the obstacle. Similarly on the left. In conclusion, there are 1, 2 or 3 inflection lines leading to the stagnation point, according as the stagnation point is in a concave, inflected, or convex point of the obstacle, respectively. Therefore, on the barrier, the number of terminals for inflection lines is equal to the number of inflection points plus the number of inflections at the points of separation plus 3 or 1, according as the stagnation point is convex or not. Three of these terminals must lead to infinity, leaving the number indicated in the theorem to be joined, in the most favorable case, with the inflection points on the free boundary.

COROLLARY 1. Each free streamline bounding an infinite cavity behind a convex obstacle (cavities of zero drag excluded) has one inflection or none according as the corresponding separation point is a point of inflection or not.

The above method can be applied to other flows, and only requires the determination of the number of inflection lines leading to the characteristic singularities. One obtains in this way such results as the following

COROLLARY 2. The symmetric cusped cavities²³ of a convex or doubly inflected symmetric obstacle are concave.

The number of inflection points of the free boundary can also be related to the number of points in the barrier where the acceleration vanishes, that is, to the number of maxima and minima of the velocity.

THEOREM 9. In infinity cavity flow, the free boundary inflects at most as often as the acceleration vanishes along the barrier.

Proof. The lines of zero tangential acceleration are by (27) level lines of the harmonic function dq^{-1}/ds , and as such start and end on the boundary. The only singularities of dq^{-1}/ds are the stagnation points and possibly the separation points. The free boundaries are themselves lines of zero acceleration and hence they are met by other such lines at points where the

²³ See Ch. V, §14 and Ch. VI, §10. Also, U. Cisotti, *Ann. sc. norm. sup. Pisa* 1 (1932), 101-12.

normal derivative of dq^{-1}/ds is zero, that is, where the tangential derivative of κ/q vanishes. Now, since κ/q vanishes at the points of inflection and at infinity on the free boundary, there must be, between any two such points, a point where $d(\kappa/q)/ds$ is zero. Thus there are at least as many lines of zero acceleration starting on the free boundary as inflections. Such lines obviously cannot end on the free boundary nor at infinity, and must end on the obstacle. A local expansion, as in the proof of Theorem 8, shows that there are exactly two lines of zero acceleration leading to the dividing point. At the separation points, it follows from (35) that the velocity is stationary if and only if the free and fixed boundary have the same curvature there, and that in this case only there is an interior line of zero acceleration detaching from the separation points. Furthermore, as in the case of inflection lines, one sees from the asymptotic expansions that there are two interior lines of zero acceleration leading to infinity. Consequently, all lines of zero acceleration starting on the free boundary, and the two at infinity, must end at points of zero acceleration on the obstacle, except for two ending at the dividing point, and the theorem is proved.

9. Free stream surfaces. In §2, we saw that any free streamline was analytic. This result has the following partial converse, due to Volterra²⁴.

THEOREM 10. Locally, any analytic surface S can be a free stream surface, and any analytic curve C can be a free streamline.

Proof. On S , choose an analytic curve A ; the geodesics in S cutting A orthogonally will then be an analytic family covering S locally, and the orthogonals to these curves will intercept equal lengths. Let $U = s$ be the directed distance from A .

Extend the resulting coordinate net to a (u, v, w) system in space. Then the boundary conditions $U = s$ and $\partial U/\partial w = \partial U/\partial n = 0$ on S are analytic initial data for $\nabla^2 U = 0$ ²⁵; hence there is an analytic U satisfying them and $\nabla^2 U = 0$ in an open region containing S . For this U , the gradient curves (streamlines) will be the given geodesics, and $\nabla U \cdot \nabla U = 1$; hence S will be a free stream surface.—The proof for the plane is similar, but simpler.

We shall now characterize the geometry of streamlines on free stream surfaces in space. Since the pressure is constant on a free surface S , the pressure gradient is normal to S . Hence the fluid acceleration is normal to S . It follows²⁶ that the free streamlines are geodesics. Thus

THEOREM 11. On any free stream surface, the free streamlines are geodesics.

²⁴ V. Volterra, *J. de math.* 11 (1932), 1–35. In the plane, any free streamline is analytic (Theorem 2, Corollary 1, above).

²⁵ J. Hadamard, *Lectures on Cauchy's problem*, New Haven, 1923, Ch. I.

²⁶ W. Blaschke, *Vorlesungen über Differentialgeometrie*, vol. 1, Berlin, Springer, 3d ed., 1930, p. 150.

Using this fact, Hamel²⁷ has shown that the only irrotational space flows in which all streamlines are "free" are helical flows (vortex line plus uniform flow parallel to this line).

The sense of the curvature is indicated by Brillouin's Principle (Ch. I, §13), which we now sharpen. We appeal to the following

*Strict Maximum Principle*²⁸. Let ψ satisfy $L[\psi] \leq 0$ in a region R with (smooth) boundary S , where

$$L = \sum a_{ik}(\mathbf{x}) \partial^2 / \partial x_i \partial x_k + \sum b_i(\mathbf{x}) \partial / \partial x_i,$$

with $a_{ik}(\mathbf{x})$ positive definite. Then either ψ is constant, or ψ assumes its maximum only on the boundary, and satisfies $\partial\psi/\partial n > 0$ at all its maxima occurring at regular points²⁹.

As in Ch. I, §12, this principle applies to the (subharmonic) pressure function, to give the following result.

THEOREM 12. If a barrier (or orifice) is nowhere strictly convex away from a plane or axially symmetric flow, then the cavity behind it (jet issuing from it) is everywhere strictly convex away from the flow.

*Proof*³⁰. The fluid velocity, being bounded and continuous, must assume a maximum somewhere. By the Strict Maximum Principle, this maximum cannot be assumed on the fixed boundary, but is assumed somewhere on the boundary; hence it is assumed (constantly) on the free boundary. The proof is completed by using the preceding lemma.—Three typical special cases of Theorem 12 are sketched in Figs. 9a-9c.

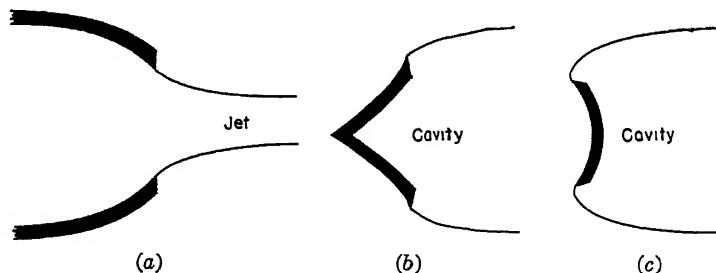


FIG. 9.

²⁷ G. Hamel, Preuss. Akad. Wiss. Sitzungsber. (1937), 5-20; see also L. Castoldi, Rend. Accad. Lincei 3 (1947), 333-7; also P. Nemenyi and R. Prim, J. math. phys. MIT 27 (1948), 130-5; J. Weingarten, Gött. Nachr. (1890), 313-35; W. C. Graustein, Trans. Am. math. soc. 47 (1940), 173-206.

²⁸ See E. Hopf, Proc. Am. math. soc. 3 (1952), 791-3, for a precise formulation and proof. (Alternatively, see L. Lichtenstein, Enzykl. Math. Wiss. 2 (II C 12), pp. 1290, 1310).

²⁹ A point on the boundary is regular if there is a circle through it totally contained in the domain.

³⁰ For plane jets, this result is due to T. Boggio, Atti accad. sci. Torino 46 (1911), p. 1043.

We shall now prove a dual principle of the *flattening of equipotentials* near free streamlines³¹. In three dimensions, let the x -axis be tangent at the origin to a free streamline with velocity $v \neq 0$. Then the (y, z) -plane will be tangent to the equipotential surface $U = U(0, 0, 0)$, while $U_x = v$, $U_y = U_z = 0$, where subscripts denote partial derivatives. Also

$$0 = \frac{\partial}{\partial x} (\nabla U \cdot \nabla U) = U_x U_{xx} + U_y U_{xy} + U_z U_{xz} = v U_{xx}.$$

Hence $U_{xx} = 0$; but since $\nabla^2 U = 0$, this implies $U_{yy} + U_{zz} = 0$. Thus the equipotential surface $U = U(0)$ has, near the origin 0, the expansion

$$x = \frac{1}{2v} [U_{yy}(y^2 - z^2) + 2U_{yz}yz] + \dots$$

The mean curvature of $x = \frac{1}{2}[Ly^2 + 2Myz + Nz^2]$ is however $L + N$; hence we have proved

THEOREM 13. On a free streamline, every equipotential surface has mean curvature zero.

COROLLARY 1. In plane flow, equipotential curves have curvature zero on a free streamline.

COROLLARY 2. In axially symmetric flow, equipotential surfaces curve on a free streamline towards the axis of symmetry with curvature $r^{-1} \sin \phi$, where ϕ is the angle between the axis of symmetry and the flow direction, and r is the distance from the axis.

10. Variational principle. We shall now show that, under certain conditions, free streamlines give stationary values to the kinetic energy³².

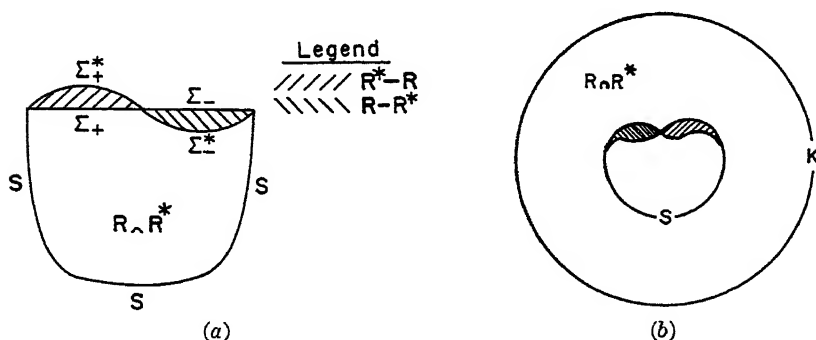


FIG. 10.

³¹ Due to P. Molenbroek, Verh. Kon. Akad. Wet. (Amsterdam) (1893), p. 31; Ann. der Phys. u. Chem. 52 (1894), 207-8; Verh. Ges. Deutsch. Nat. u. Ärzte 65 (1894), 9-12.

³² This result is due to Riabouchinsky [71]. A fuller discussion of the literature will be given in Chap. VII, §1 and §§10-12.

To show this, we suppose the flux given across a portion S of the boundary $S \cup \Sigma$ of a *finite* regular region R , where Σ is a stream surface. If U is the associated velocity potential, we will thus have $\partial U/\partial n$ given on S , and zero on Σ .

Now let Σ be displaced to a new surface Σ^* , a part Σ_+ being moved outward to Σ_+^* and the rest Σ_- inwards to Σ_-^* , as in Fig. 10a. Let R^* denote the interior of $S \cup \Sigma^*$.

LEMMA. If U and U^* denote the velocity potentials of the ideal flows inside R resp. R^* , having a given flux across S , then the difference $T^* - T$ between their kinetic energies satisfies

$$(36) \quad \begin{aligned} T^* - T = & -\frac{\rho}{2} \left\{ \iiint_{R^*-R} |\nabla U^*|^2 dR - \iiint_{R-R^*} |\nabla U|^2 dR \right. \\ & + \iint_{\Sigma_+^*} (U^* - U) \frac{\partial(U^* - U)}{\partial n} dS \\ & \left. - \iint_{\Sigma_-^*} (U^* - U) \frac{\partial(U^* - U)}{\partial n} dS \right\}. \end{aligned}$$

Proof. Almost by definition,

$$\begin{aligned} T^* - T = & \frac{\rho}{2} \left\{ \iiint_{R \cap R^*} \nabla(U^* + U) \cdot \nabla(U^* - U) dR \right. \\ & \left. + \iiint_{R^*-R} |\nabla U^*|^2 dR - \iiint_{R-R^*} |\nabla U|^2 dR \right\}. \end{aligned}$$

We now apply Green's First Identity [44, p. 212] systematically, together with the relations $\partial U/\partial n = 0$ on Σ , $\partial U^*/\partial n = 0$ on Σ^* , and

$$\partial(U - U^*)/\partial n = 0 \quad \text{on} \quad S.$$

Applied to the first term of the preceding display, it gives

$$\iint_{\Sigma_+^*} (U^* + U)(\partial U^*/\partial n) dS - \iint_{\Sigma_-^*} (U^* + U)(\partial U/\partial n) dS,$$

where positive normal derivatives are out from $R \cap R^*$. Applied to the other terms, it gives two relations like

$$\begin{aligned} \iiint_{R^*-R} |\nabla U^*|^2 dR &= -\iint_{\Sigma_+^*} U^* \frac{\partial U^*}{\partial n} dS - \iiint_{R-R^*} |\nabla U|^2 dR \\ &= \iint_{\Sigma_-^*} U \frac{\partial U}{\partial n} dS. \end{aligned}$$

Summing all three terms, we get the simple formula

$$(37) \quad T^* - T = \frac{\rho}{2} \left\{ \iint_{\Sigma} U \frac{\partial U^*}{\partial n} dS - \iint_{\Sigma} U^* \frac{\partial U}{\partial n} dS \right\}.$$

Obviously, this is equivalent to

$$T^* - T = \frac{\rho}{2} \left\{ \iint_{\Sigma} U^* \frac{\partial U^*}{\partial n} dS + \iint_{\Sigma} (U - U^*) \frac{\partial U^*}{\partial n} dS \right. \\ \left. - \iint_{\Sigma} U \frac{\partial U}{\partial n} dS + \iint_{\Sigma} (U - U^*) \frac{\partial U}{\partial n} dS \right\}.$$

Substituting from the identities above (37), and using $\partial U / \partial n = 0$ on Σ , $\partial U^* / \partial n = 0$ on Σ^* , we get (36).

THEOREM 14. If the boundary Σ is varied, while the flux through S is held constant, then

$$(38) \quad \delta T = -\frac{1}{2}\rho \iint_{\Sigma} (\nabla U \cdot \nabla U) \delta R \quad [\delta R = \delta n dS],$$

provided $S + \Sigma$ is piecewise analytic and bounds a *finite* region.

Proof. In formula (36), the last terms are second-order infinitesimals. Passing to the limit as the normal displacement tends to zero, we get (38). (The rigorous proof requires further assumptions, which are certainly fulfilled if Σ is piecewise analytic; we omit the details.)

COROLLARY 1. For a given flux through S , the sum $T + \frac{1}{2}\rho q^2 \text{vol}(R)$ has an extremal if and only if Σ is a free stream surface with constant velocity q .

COROLLARY 2. Any free stream surface Σ extremalizes the kinetic energy, subject to variations which leave the volume enclosed by Σ invariant.

Related to Cors. 1-2 is the following Minimax Principle of Garabedian and Spencer [28]. For a given flux through S , a free streamline Σ minimizes the maximum velocity on Σ , and maximizes the minimum velocity on Σ . If Σ is analytic, the converse is also true. We refer to [28] for details.

11. Extension to infinite stream. Now consider a finite obstacle B with boundary $S \cup \Sigma$, held in an infinite stream moving with free stream velocity c parallel to the x -axis. Formula (38) is meaningless because the total kinetic energy involved is infinite. One can, however, replace (38) by another variational principle (41), as follows.

Letting ϕ denote the velocity potential relative to the fluid, we can write

$$(39) \quad U = cx + \phi = c(x + \mu_1 x/r^3 + \mu_2 y/r^3 + \mu_3 z/r^3) + \phi',$$

where ϕ is regular at infinity, the μ_i are the *dipole moment* coefficients, and the remainder ϕ' dies out like $1/r^3$ at infinity, and its gradient like $1/r^4$. All terms of (39) are harmonic.

Relative to the fluid, the total kinetic energy is finite, being

$$(40) \quad T = \frac{1}{2}\rho \iiint_R \nabla\phi \cdot \nabla\phi \, dR = \frac{1}{2}\rho k c^2.$$

Here k is, by definition [4, Ch. V], the *induced mass* coefficient for translation parallel to the x -axis; thus ρk is the inertia of the fluid against acceleration of B parallel to the x -axis.

THEOREM 15. If one varies a part Σ of the boundary of B , past which an unbounded stream is moving with velocity $(c, 0, 0)$, then

$$(41) \quad c^2 \delta[k + \text{vol}(B)] = 4\pi c^2 \delta\mu_1 = - \iint_{\Sigma} (\nabla U \cdot \nabla U) \, dR,$$

where $\delta R = \delta n \, d\Sigma$ as in (38).

Proof. The first equality follows from G. I. Taylor's identity

$$(42) \quad 4\pi\mu_1 = k + \text{vol}(B);$$

we omit the proof [4, p. 161].

To prove the second equality, we proceed as in the Lemma of §10, but enclosing R in a large sphere K of radius a , replacing S by $S \cup K$ (see Fig. 10b), and replacing U and U^* by ϕ and ϕ^* . The difference of the kinetic energies is

$$\begin{aligned} T^* - T = \frac{1}{2}\rho \left\{ \lim_{a \rightarrow \infty} \iiint_{R \cap K^*} \nabla(\phi^* + \phi) \cdot \nabla(\phi^* - \phi) \, dR \right. \\ \left. + \iint_{R^* - R} |\nabla\phi^*|^2 \, dR - \iint_{R - R^*} |\nabla\phi|^2 \, dR \right\}. \end{aligned}$$

By application of Green's Identity to each term, and by noting that $\partial U/\partial n = 0$ on Σ , $\partial U^*/\partial n = 0$ on Σ^* and $\partial(U^* - U)/\partial n = 0$ on S , this becomes

$$\begin{aligned} (43) \quad T^* - T = \frac{1}{2}\rho \left\{ \iint_{\Sigma} (\phi^* + \phi) \frac{\partial U^*}{\partial n} \, dS - \iint_{\Sigma} (\phi^* + \phi) \frac{\partial U}{\partial n} \, dS \right. \\ - \iint_{\Sigma} \phi^* \frac{\partial \phi^*}{\partial n} - \iint_{\Sigma} \phi^* \frac{\partial \phi}{\partial n} \, dS + \iint_{\Sigma} \phi \frac{\partial \phi}{\partial n} + \iint_{\Sigma} \phi \frac{\partial \phi}{\partial n} \, dS \\ \left. + \lim_{a \rightarrow \infty} \iint_K (\phi^* + \phi) \frac{\partial}{\partial n} (\phi^* - \phi) \, dS \right\}. \end{aligned}$$

By (40), the integrand in the last term is $O(a^{-3})$, so the integral tends to

zero as $a \uparrow \infty$. Moreover, in (43), the integrals over Σ_+ and Σ_+^* add up to

$$\iint_{\Sigma} U \frac{\partial U^*}{\partial n} dS + \iint_{\Sigma} \left(U^* \frac{\partial cx}{\partial n} - cx \frac{\partial U^*}{\partial n} \right) dS - \iint_{\Sigma} \left(U^* \frac{\partial cx}{\partial n} - cx \frac{\partial U^*}{\partial n} \right) dS \\ + c^2 \left[\iint_{\Sigma} x \frac{\partial x}{\partial n} dS - \iint_{\Sigma} x \frac{\partial x}{\partial n} dS \right].$$

The second and third terms cancel because U^* and cx are harmonic functions in $R^* - R$; the term in brackets is equal to the volume of $R^* - R$. Proceeding similarly with the integrals over Σ_- and Σ_-^* , and adding the results, we get

$$T^* - T = \frac{1}{2}\rho \left[\iint_{\Sigma} U \frac{\partial U^*}{\partial n} dS - \iint_{\Sigma} U^* \frac{\partial U}{\partial n} dS + c^2 \text{vol}(R^* - R) \right. \\ \left. - c^2 \text{vol}(R - R^*) \right].$$

That is, since $\text{vol } B^* - \text{vol } B = \text{vol}(R - R^*) - \text{vol}(R^* - R)$,

$$(43') \quad 2\pi\rho c^2(\mu_1^* - \mu_1) = \frac{1}{2}\rho \left[\iint_{\Sigma} U \frac{\partial U^*}{\partial n} dS - \iint_{\Sigma} U^* \frac{\partial U}{\partial n} dS \right].$$

The right sides of (43') and (37) are identical. We now repeat the argument of §10, showing that the right sides of (37) and (36) are equal, getting

$$2\pi\rho c^2(\mu_1^* - \mu_1) = \text{Right side of (36)}.$$

We then argue as in the proof of (38), that the last terms of (36) are second-order infinitesimals. Passing to the limit as $\delta n \rightarrow 0$, we get the second equation of (41).

COROLLARY 1. If the volume is fixed, then the kinetic energy, the induced mass, and the dipole moment are extremalized by the free stream surface.

The converse is true for extremalizing surfaces to which (41) is applicable. In particular, analytic extremalizing surfaces are free stream surfaces (cf. Ch. VII, §11).

In terms of the cavity underpressure coefficient $Q = (q^2 - c^2)/c^2$ defined as in Ch. I, (3a), we infer also

COROLLARY 2. A cavity flow, uniform at infinity, extremalizes $k(B) - Q \text{vol}(B)$, in the sense that

$$(44) \quad \delta[k(B) - Q \text{vol}(B)] = 0$$

for all variations of the free stream surface Σ .

Proof. In (41), $-\iint_{\Sigma} (\nabla U \cdot \nabla U) dR = q^2 \delta[\text{vol}(B)]$. Substituting, and dividing by c^2 , we get (44).

Unfortunately, our proof of (41) breaks down in the case $Q = 0$ of infinite cavity volume.

12. Lavrentieff's theorem. The comparison method of hydrodynamics, recently developed³³ for plane and axially symmetric flows, has greatly simplified the theory of the uniqueness and qualitative behavior of free streamlines. The method consists in comparing the stream functions of two flows with different boundaries, using as a basic tool the fact that the stream functions satisfy the equation

$$(45) \quad V_{xx} + V_{yy} - py^{-1}V_y = 0$$

(in $p + 2$ dimensions (cf. Ch. X, §1)), and hence satisfy the Strict Maximum Principle. In this section we present two comparison theorems of importance for the free boundary problem.

THEOREM 16 (Lavrentieff). Let two plane or axially symmetric ideal flows having the same free stream velocity be defined in regions D and \bar{D} , bounded respectively by streamlines S and \bar{S} extending to $\pm\infty$ (Fig. 11). If $D \leq \bar{D}$ and if the bounding streamlines have a point P in common, then the respective flow speeds q and \bar{q} satisfy at P the inequality

$$(46) \quad q(P) \leq \bar{q}(P),$$

the equality holding only when the flows are identical or $\bar{q}(P) = 0$.



FIG. 11.

Proof. Let V and \bar{V} be the stream functions for the two flows. We may assume without loss of generality that the free stream velocities are in the positive x -direction, and that

$$(47) \quad \begin{aligned} V &= 0 \text{ on } S, & \bar{V} &= 0 \text{ on } \bar{S}, \\ V &> 0 \text{ in } D, & \bar{V} &> 0 \text{ in } \bar{D}, \end{aligned}$$

the regions D , \bar{D} being open. It may also be assumed that $D \neq \bar{D}$, for otherwise the theorem is trivial.

If we put $w_a = \bar{V} - aV$, where a is any constant less than unity, then w_a satisfies (45), and hence obeys the Strict Maximum Principle (§9).

³³ The method was originated by Lavrentieff [51]; his ideas have been extended and simplified in a series of papers by Gilbarg [29] and Serrin [75, 76] and J. rat. mech. anal. 3 (1953), 563-75. Dr. Serrin helped us draft §§12-14.

Since at any point in D

$$\partial w_a / \partial y = y^p (\bar{u} - au),$$

where u, \bar{u} are the horizontal velocity components, it follows that

$$(48) \quad \lim_{x, y \rightarrow \infty} \partial w_a / \partial y > 0.$$

Also, $w_a \geq 0$ on S , and so

$$(49) \quad w_a \geq 0$$

outside any suitably large circle. These two inequalities, together with the Strict Maximum Principle, imply $w_a > 0$ in D . By letting a approach 1 we derive for $w = w_1$

$$(50) \quad w(x, y) = \bar{V} - V \geq 0 \quad \text{in } D.$$

Since w also obeys a strict maximum principle, equality cannot hold; that is, $w > 0$ in D .

Choose points A and B on S such that P is between A and B and neither $w(A)$ nor $w(B)$ is zero; this construction fails only when $S = \bar{S}$ on one side of P . Now connect A and B by a line C lying inside D . Evidently $w > 0$ on C so that, for some $b > 1$,

$$w_b = \bar{V} - bV = w - (b - 1)V > 0 \text{ on } C.$$

Since $w_b \geq 0$ on APB it follows that $w_b > 0$ in the (open) region bounded by the arcs APB and C . Thus the inward normal derivative of w_b satisfies at P the inequality³⁴ $\partial w_b / \partial n(P) \geq 0$. From this we derive

$$\bar{q}(P) - q(P) = \frac{1}{y^p} \frac{\partial w}{\partial n}(P) \geq \frac{b - 1}{y^p} \frac{\partial V}{\partial n}(P) = (b - 1)q(P).$$

It follows that

$$\bar{q}(P) \geq q(P),$$

equality holding if and only if $\bar{q}(P) = 0$.

If $S = \bar{S}$ on one side of P , we choose a regular point B on this side, so

³⁴ In axial symmetry, when P is on the axis, this is replaced by

$$\partial w_b / \partial y(P) = 0, \quad \partial^2 w_b / \partial y^2(P) \geq 0.$$

The inequality is then obtained as follows:

$$\bar{q}(P) - q(P) = \lim_{y \rightarrow 0} \frac{1}{y} \frac{\partial w}{\partial y} = \frac{\partial^2 w}{\partial y^2}(P) \geq (b - 1) \frac{\partial^2 V}{\partial y^2}(P) \geq (b - 1)q(P).$$

that by the Strict Maximum Principle $\partial w / \partial n(B) > 0^{35}$. Defining C and w_b as before, we have $w_b(B) = 0$; moreover

$$(51) \quad \frac{\partial w_b}{\partial n}(B) > 0$$

provided that $b - 1$ is sufficiently small. Thus $w_b \geq 0$ on some arc BB_1 of C . Since $w > 0$ on the arc B_1A of C we see that, for sufficiently small $\epsilon > 0$, $w_b \geq 0$ on C , and the desired conclusion follows as before.

13. Under-over theorem. A more subtle comparison theorem is the following under-over theorem.

THEOREM 17. Let two ideal flows having well-defined velocities at infinity (not necessarily in the same direction) be defined in regions D and \bar{D} , bounded respectively by streamlines S and \bar{S} extending to ∞ . Suppose that S and \bar{S} have a common arc MN , and a common point J outside MN such that arcs JM of S and NJ on \bar{S} together with MN bound a simply connected region $MNJ \equiv D'$ interior to D and \bar{D} . The possibility that J is the point at infinity is not excluded. Then

$$(52) \quad \frac{q(M)}{q(N)} \leq \frac{\bar{q}(M)}{\bar{q}(N)},$$

provided the ratios are well defined. Equality holds only when the flows are geometrically similar or $\bar{q}(M) = 0$.

Proof. Since the theorem is obvious when the flows are geometrically similar, we need not consider this case further. Also, in order to avoid repetitious discussion of particular cases, we shall present the proof only in case the speeds at infinity are both in the x -direction and J is the point at infinity (Fig. 12).

Suppose for the moment that there is a point P on MN where

$$(53) \quad q(P) = \bar{q}(P) \neq 0,$$

and that the velocities at infinity, q_∞ and \bar{q}_∞ , are different. Let V and \bar{V} be the stream functions, defined so that relations (47) hold. Setting

³⁵ The above argument breaks down in the axially symmetric case when B is on the axis. In this case we choose B so that

$$w(B) = \partial w / \partial y(B) = 0, \quad \partial^2 w / \partial y^2(B) > 0.$$

Equation (51) is then replaced by

$$(51a) \quad \partial w_b / \partial y(B) = 0, \quad \partial^2 w_b / \partial y^2 > 0,$$

but the rest of the proof is unchanged.

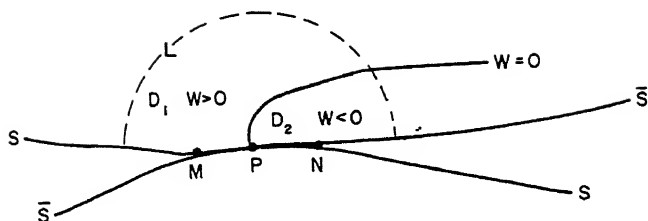


FIG. 12.

$w = \bar{V} - V$ we have

$$(54) \quad \begin{cases} w > 0 \text{ on the arc } JM \text{ of } S, \\ w = 0 \text{ on the arc } MN, \\ w < 0 \text{ on the arc } NJ \text{ of } \bar{S}. \end{cases}$$

By the Strict Maximum Principle, since $\partial w / \partial n(P) = 0$, P is neither a point of local maximum nor a point of local minimum and a level line $C: w = 0$, runs in the interior of D' in the vicinity of P . Its endpoints are both on the boundary of D' , and since obviously not both are on MN , one at least is at infinity (by (54) w does not vanish on JM and JN). We shall now see that not both endpoints are at infinity.

Consider the arc L of a circle of large radius, joining a point on the arc JM of S to a point on the arc NJ of \bar{S} and lying entirely in D' . It is apparent from the condition

$$\lim_{x, y \rightarrow \infty} \frac{1}{y^p} \frac{\partial w}{\partial y} \neq 0,$$

and the inequalities (54), that there is exactly one point R on L where $w = 0$.

We can thus define two (open) subregions of D' , say D_1 and D_2 (see Fig. 12). From the Strict Maximum Principle,

$$w > 0 \text{ in } D_1, \quad w < 0 \text{ in } D_2,$$

and hence, as in Theorem 16

$$\bar{q}(M) - q(M) \geq \alpha q(M),$$

$$q(N) - \bar{q}(N) \geq \beta \bar{q}(N).$$

In order that the ratios in (52) be defined, it is necessary that $\bar{q}(N) > 0$; hence

$$(55) \quad q(N) > \bar{q}(N) > 0.$$

If $\bar{q}(M) = 0$ we derive $q(M) = 0$ and (52) holds trivially. Otherwise we get

$$(56) \quad q(M) < \bar{q}(M),$$

and from (55) and (56) follows

$$\frac{q(M)}{\bar{q}(M)} < 1 < \frac{q(N)}{\bar{q}(N)}.$$

Therefore

$$\frac{q(M)}{q(N)} < \frac{\bar{q}(M)}{\bar{q}(N)},$$

proving the theorem in the special case that (53) holds.

If there is no point on MN where $\bar{q} = q$, we choose P^* on MN such that $q(P^*) \neq 0$ and $\bar{q}(P^*)/q(P^*) \neq \bar{u}/u$. This is possible as long as the flows are not similar. Define a new flow by the stream function

$$V^* = (\bar{q}(P^*)/q(P^*))V.$$

Then $q^*(P^*) = \bar{q}(P^*)$ and $q_\infty^* \neq \bar{q}_\infty$. From the special case proved above we obtain

$$\frac{q(M)}{q(N)} = \frac{q^*(M)}{q^*(N)} \leq \frac{\bar{q}(M)}{\bar{q}(N)},$$

the equality holding if and only if $\bar{q}(M) = 0$, q.e.d.

14. Uniqueness theorem. The two theorems of the preceding section have far-reaching application to the free boundary problem; they are instrumental in reducing the previously complicated (see Ch. VII, §1) uniqueness problem to comparatively simple geometric considerations, and they provide a powerful tool for the discovery of geometrical properties of the free streamlines.

In the following demonstration of the uniqueness of an infinite cavity set up by a fixed obstacle in an infinite stream (with given points of separation) we assume that the flow is plane symmetric or axially symmetric and has uniform free stream speed v in the positive x -direction. We may confine all consideration to the "upper half" of the flow, which will constitute the basic flow region D . The letter T denotes the streamline consisting of the negative x -axis and the "upper half" wetted wall; the free streamline detaching from T is denoted by Σ , and we put $S \equiv T + \Sigma$. The proof of Theorem 18 will be confined to the plane case for greater simplicity: a more refined version of the argument suffices for axial symmetry (see [29]). We shall make the further assumption that the flow is simply covered, thus avoiding some difficulties which only obscure the main ideas.

THEOREM 18. No infinite straight line which fails to cut T can intersect the free streamline Σ in more than one point.

Proof. Suppose for contradiction that a line l intersects Σ in more than one point. We can assume that l is not horizontal, for a line making a small angle with l would also intersect Σ in more than one point. Since Σ is horizontal at infinity we can find a line m in D parallel to l and tangent to Σ such that all lines parallel to m and to the right of m intersect Σ in just one point. Let M denote the point of tangency: consider the two rays of m determined by M . Two cases arise according to whether one of the half-rays is in D or outside D .

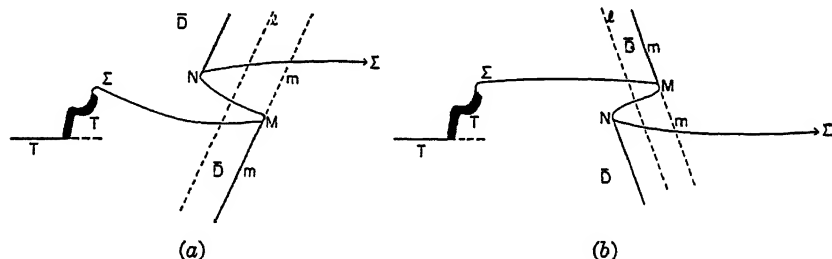


FIG. 13.

In the former case (see Fig. 13a), consider the points of the arc (M, ∞) of Σ which are on the left of m , and let N be one at a maximal distance from M . Finally let \bar{D} be the region bounded by MN and the parallels to l indicated in Fig. 13a by heavy lines. Its construction is apparent. Clearly there exists a flow in \bar{D} with uniform velocity at infinity. By translating a replica of \bar{D} along the vector \overrightarrow{MN} we obtain a configuration of the type envisaged in Theorem 16, and thus derive

$$\bar{q}(M) < \bar{q}(N);$$

but from Theorem 17

$$\frac{q(M)}{q(N)} < \frac{\bar{q}(M)}{\bar{q}(N)},$$

and these inequalities imply $q(M) < q(N)$. This result, however, contradicts the assumption of constant speed on Σ . In the remaining case (Fig. 13b) a similar contradiction is obtained and the proof is complete.

A curve is called *starlike* if there exists a point O having the property that every straight line through O intersects the curve in at most one point or along a segment. Let us call an obstacle *starlike* if the corresponding curve T is starlike, and, in the case of axial symmetry, O is on the axis. Then it is an easy consequence of Theorem 18 that, if an obstacle is starlike with respect to a point O , the whole streamline S is starlike with respect to O .

In proving the following uniqueness theorem, we shall again restrict attention to the plane case, although it will be seen that the proof need be changed only in one place to account for the axially symmetric case.

THEOREM 19. There can be at most one symmetric cavity flow with given separation points past a given starlike obstacle.

Proof. Consider two flows of the required type, with corresponding free streamlines Σ and Σ^* (Fig. 14). If the origin is taken at O , then these curves may be represented by

$$r = r(\theta), \quad r = r^*(\theta),$$

in polar coordinates, and by Theorem 18, $r(\theta)$ and $r^*(\theta)$ are *single valued* functions. From the asymptotic expansion for a free streamline

$$y \approx cx^{\frac{1}{2}},$$

derived in (11d) we find³⁶

$$(57) \quad \lim_{\theta \rightarrow 0} \frac{r^*(\theta)}{r(\theta)} = \left(\frac{c^*}{c} \right) \leq 1.$$

In view of (57) the ratio r^*/r is bounded from above; moreover $r^*/r = 1$ at the separation point. Therefore r^*/r has a maximum value $\rho \geq 1$ at some value θ , say θ_P , corresponding to a *finite* point P on Σ . Let a region \bar{D} be obtained by a similarity transformation (expansion about Q) of D^* in the ratio ρ^{-1} ; in \bar{D} we take a flow similar to the original flow in D^* and with velocity unchanged at corresponding points, defined by the stream function $\bar{V}(P) = \rho^{-1}V(\rho P)$. Evidently $D \leq \bar{D}$ and S and \bar{S} have the common point P , so that Theorem 16 applies. But since $q(P) = \bar{q}(P) = v$ the equality must hold in (46) and the two flows are identical. So that $D = \bar{D} = D^*$, q.e.d.

D. Gilbarg³⁷ has shown that some of these results carry over to the compressible case.



FIG. 14.

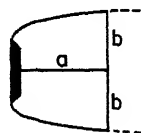


FIG. 15.

³⁶ This result can be obtained alternately in the axially symmetric case by using Levinson's formula (Ch. X, §5),

$$y = cx^{1/2}(\log x)^{-1/4}$$

for the asymptotic shape of the free streamline.

³⁷ Cf. J. rat. mech. anal. 2 (1953), 233-51; 3 (1954), 201-30; see also J. Serrin, J. math. phys. MIT 33 (1954), 27-45.

15. Minimum cavity drag. Using comparison methods, one can determine the symmetric³⁸ obstacles of given length a and diameter $2b$, having least cavity drag. The correct formulation of this problem is, however, rather subtle.

If not restriction is made on separation, the minimum is zero attained by the "cavity of zero drag" behind any such obstacle. Hence we assume *Brillouin's separation condition* (Ch. I, §14): the velocity is a maximum on the free streamline. Next, we define a *Kirchhoff profile* K to consist of a flat plate or disc L , followed by a symmetric cavity having a diameter $2b$ at a distance a behind (see Fig. 15), as in Ch. II, §2.

THEOREM 20. Any Kirchhoff profile K minimizes cavity drag, relative to any other symmetric barrier of the same length and diameter which satisfies the Brillouin separation condition.

Proof. As the flow is assumed symmetric, we need consider only the flow in a half-plane bounded by the axis of symmetry. Let us consider, for any other obstacle C of length a and half-diameter c , the corresponding flow satisfying Brillouin's condition. There is a flat plate or disk L^* whose free streamline Σ^* is tangent to C , say at Q , and which lies entirely above C ³⁹. Clearly the plate L^* is at least as wide as L . We assert that the free streamline Σ associated with C is above Σ^* at infinity. If this were not the case, then we would have

$$\lim_{\theta \rightarrow 0} r(\theta)/r^*(\theta) \leq 1.$$

From this and the fact that the ratio r/r^* is greater than or equal to one at Q , we see that r/r^* attains a maximum value $\rho \geq 1$ at some value of θ , say θ_P , corresponding to a *finite* point P . As in the proof of Theorem 19, using Lavrentieff's theorem, we thus obtain a contradiction of the Brillouin condition stated above. Now, of two obstacles, the one setting up the larger drag will be the one whose free streamline separates the most from the x -axis at infinity (cf. (17a), (17b)). Hence

$$\begin{aligned} \text{Drag of } C &\geq \text{Drag of } L^* \\ &\geq \text{Drag of } K, \end{aligned}$$

and equality holds if and only if $C + \Sigma = L^* + \Sigma^* = K$, that is, if and only if the flow profile set up by C is the same as the Kirchhoff profile K .

³⁸ Cf. J. Serrin, *J. rat. mech. anal.* 2 (1953), 572-3. Presumably, these obstacles also minimize cavity drag relative to asymmetric obstacles satisfying the same restrictions.

³⁹ If P is (a, b) , then C may not be tangent to Σ^* but in this case it is immediately evident that $C + \Sigma$ does not remain below $L^* + \Sigma^*$, so that the following conclusions remain valid.

CHAPTER V

MULTIPLE PLATES

1. Parametric rectangle. This chapter will be largely devoted to "simple" flows (i.e., to simply connected, smoothly bounded ideal plane flows as defined in Ch. III, §2), whose boundary consists of two straight streamlines ("plates") separated by two free streamlines, in cyclic alternation.¹

The case of a plate held in a nozzle (Fig. 1a) is typical. Since the flow is simply connected, it can be mapped conformally onto the upper half T -plane (Ch. II, §1). By Theorem 2 of Ch. III, the complex potential W will satisfy

$$(1) \quad \frac{dW}{dT} = R(T) = C \prod (T - A_i)(T - A_i^*) \prod (T - B_j) / \prod (T - T_k),$$

where $R(T)$ is a real rational function.

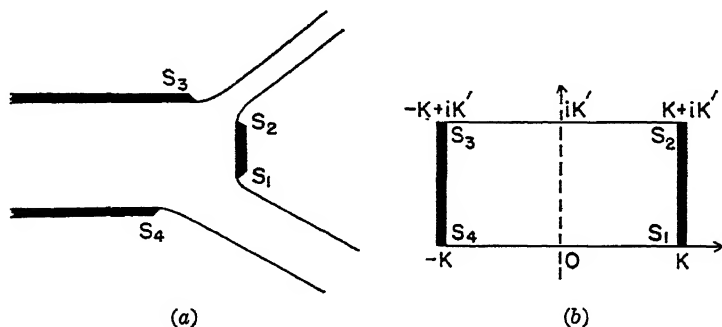


FIG. 1

By a suitable real linear fractional transformation and suitable choice of $k < 1$, we can even make the four "separation points" S_1, S_2, S_3, S_4 fall on $T = 1, k^{-1}, -k^{-1}, -1$. If we define t as the elliptic integral $t = \int dT / \sqrt{(1 - T^2)(1 - k^2 T^2)}$ the flow is then mapped onto a *parametric rectangle*

$$(2) \quad R: \quad -K \leq \operatorname{Re}\{t\} \leq K, \quad 0 \leq \operatorname{Im}\{t\} \leq K'$$

¹ As in Chs. II-III, the boundary is regarded as continuous around any branch of the flow extending to infinity. In §§14-15, we shall even regard the point at infinity as an interior point, since $\zeta(\infty)$ has a well-defined value.

in the auxiliary t -plane. The plates are mapped onto the vertical sides, the free boundaries onto the horizontal sides, and the four separation points S_1, S_2, S_3, S_4 onto the corners, as in Figs. 1a-1b. Here K and K' denote as usual² the complete elliptic integrals associated with a suitable "modulus" k , determined by $\tau = iK'/K$. By definition,

$$(3) \quad t = \int_0^T \frac{dT}{\sqrt{(1-T^2)(1-k^2T^2)}}, \quad T = \operatorname{sn}(t, k), \quad 0 < k < 1,$$

whence $\operatorname{sn}(\pm K) = \pm 1$, $\operatorname{sn}(0) = 0$, and $\operatorname{sn}(iK') = \infty$.

THEOREM 1. If $\zeta = f(t)$ is known, then the flow is completely determined by formulas (1)-(3) and the identity

$$(4) \quad z = \int \zeta^{-1} dW = \int \frac{1}{f(t)} R(\operatorname{sn} t) \operatorname{cn} t \operatorname{dn} t dt.$$

The proof is by direct substitution of $(dW/dT)dT$ for dW , using (1) and the formula $d(\operatorname{sn} t) = \operatorname{cn} t \operatorname{dn} t dt$.

Our analysis will be based on Theorem 1. Usually, $f(t)$ will be determined by "reflecting" the flow in the parametric rectangle R , so as to obtain an analog of Theorem 3 of Ch. III. This method will be described in detail in §4; we shall first digress to outline a more general (but less conclusive) approach, which contains (2)-(3) as special cases.

2. Case of m plates. Formally, flows bounded by m plates separated by m free streamlines, in cyclic alternation, can be treated similarly. Although the determination of parameters becomes extremely involved when $m > 2$, we shall outline the analysis.

Formula (1) is still valid. The upper half T -plane (and hence the flow) can be mapped into a *rectangular polygon* R_m with $2m$ sides, by a Schwarz-Christoffel transformation ([44, p. 370] or [62a, p. 189]) of the form

$$(5) \quad t = \int \sqrt{Q(T)} dT, \quad Q(T) = \prod_{h=1}^m (T - T_h') / \prod_{i=1}^m (T - T_i'').$$

Here the T_h' and T_i'' correspond to the $2m$ separation points S_1, \dots, S_{2m} separating free from fixed boundaries, one of which may be at $T = \infty$. That is, t is a *hyperelliptic integral* in the general case.

We have discussed the case $m = 2$ in §1. The case $m = 1$ corresponds to the case of "simple" flows past straight "wedges" treated in Chs. II-III, with $n = 1$ in the notation of Ch. III, §1. When $m = 1$, R_1 reduces to a quadrant with $Q(T) = T$, $2T = t^2$, if we set $T_1' = 0$ and $T_1'' = \infty$. The variable $u = (1 + it)/(1 - it)$ proves to be more convenient than u , how-

² See [62a, pp. 280-96] or [89, Ch. XXII], for the theory of elliptic functions. The present chapter requires some familiarity with this theory.

ever, when $m = 1$. It maps R_1 onto a unit semicircle Γ , and often makes $\zeta = u$.

We now consider the variable³ $\omega = i \ln \zeta$, as a complex analytic function of t . The derivative $d\omega/dt = i d\zeta/\zeta dt$ is clearly *real on the entire boundary* of R_m (except at isolated singularities), since $\omega = i \ln q - \phi$ has piecewise constant real part on polygonal boundaries. Hence, excluding essential singularities, $d\omega/dT$ must be a real *rational* function of T , and so

$$(6) \quad d\omega/dt = R_1(T), \quad \text{a real rational function.}$$

Substituting from (1)–(3) in $dz = \zeta^{-1} dW$, we get the following very general result [19, pp. 56–64].

THEOREM 2. Simply connected flows, whose boundaries are alternately free and straight, satisfy

$$(7) \quad dz = \left[\exp \left(\int i R_1(T) \sqrt{Q(T)} dT \right) \right] R(T) dT,$$

where $Q(T)$, $R(T)$ and $R_1(T)$ are real rational functions.

Bent plates. Theorem 2 applies also to bent plates (e.g., wedges). Near a vertex, where the flow direction turns through π/n radians, we have $\zeta = A(t - t_0)^{1/n} + \dots$, whence an easy calculation gives

$$d\omega/dt = i d\zeta/\zeta dt = i/n(t - t_0) + \dots$$

Hence (6) still holds near such points, which are poles of $R_1(t)$.

3. Annular sector hodograph. In the special case of flows whose hodograph is an *annular sector*, centered at the origin, $\zeta(t)$ can be guessed by inspection. By a change of units and rotation of coordinates, we can normalize to the case

$$(8) \quad 0 \leq \arg \zeta \leq \beta, \quad v \leq |\zeta| \leq 1,$$

as in Fig. 2a.

Since $\omega = i \ln |\zeta| - \phi$, the ω -diagram is a rectangle bounded by $Re\{\omega\} = -\beta$ on $\overline{S_1 S_2}$, $Im\{\omega\} = \ln v$ on $\overline{S_2 S_3}$, $Re\{\omega\} = 0$ on $\overline{S_3 S_4}$, and $Im\{\omega\} = 0$ on $\overline{S_4 S_1}$. (See Figs. 1b–2a). Hence, if k is so chosen that, in (2),

$$(9a) \quad K'/K = (-2 \ln v)/\beta,$$

the ω -diagram can be mapped onto the parameter rectangle R of (2) by horizontal translation and change of scale. Thus

$$(9b) \quad \omega + \frac{\beta}{2} = -\frac{\beta}{2K} t$$

³ The utility of ω was first pointed out by Max Planck, *Ann. Phys. Chem.* 21 (1884), 499–509.

$$(9c) \quad \zeta = e^{-i\omega} = e^{i\beta(t+\kappa)/2\kappa}.$$

Thus the $R_1(T)$ of (6) reduces in the present case to the real constant $-\beta/2K$.

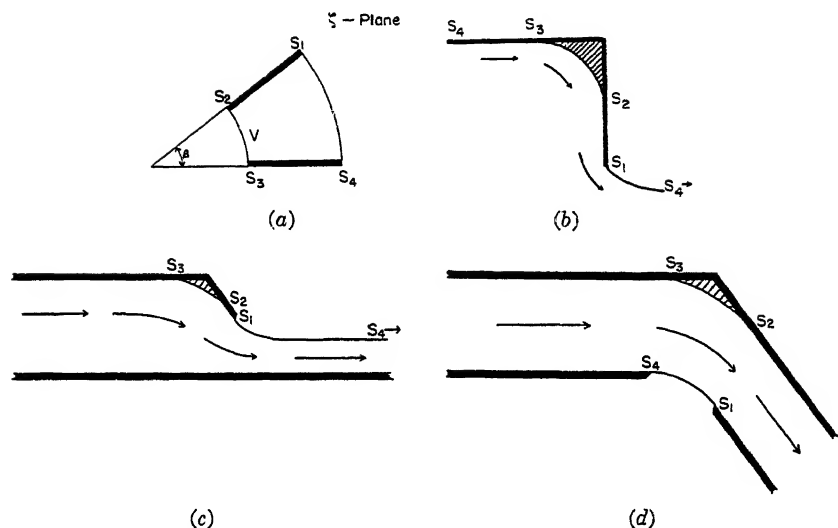


FIG. 2.

The flow of Fig. 2b is interesting, because it shows the *mathematical indeterminacy*⁴ of the symmetric Bobyleff flows discussed in Ch. II, §§2-4. The same indeterminacy applies to the Réthy flow past a wedge in a channel⁵ (Fig. 2c). Physically, the shaded deadwater region is unstable. Finally, Fig. 2d sketches a pipe elbow with constant (theoretical) velocity in both bends; this generalizes the Réthy flow discussed on p. 61 (see Fig. 10b).

In all cases, $dW/dT = R(T)$ in (1) has a simple expression, which can be read off from Theorem 2 of Ch. III. In the case of Fig. 2b,

$$(10a) \quad dW/dT = C/(T - T_1)^2, \quad \text{where } T_1 = 1/k,$$

since the pole of $W(T)$ occurs at S_1 . For given β , there is just one essential parameter $v < 1$; it corresponds to the over-pressure in the hypothetical deadwater region. In the cases of Figs. 2c-2d, we may say

$$(10b) \quad dW/dT = C/(T - T_1)(T - T_2).$$

⁴ This was first pointed out by H. Villat [83, 84]; see also R. Thiry, Ann. sci. ec. norm. sup. 38 (1921), 229-239. For a wedge, other possibilities were pointed out by Villat, Ann. fac. sci. Toulouse (1913), 357-404.

⁵ See F. K. G. Odqvist, Arkiv Mat. Astr. Fys. 19 (1926), No. 13. The flow of Fig. 2d has been discussed by G. Caldonazzo, Annali di mat. pura appl. Milano 25 (1916), p. 40.

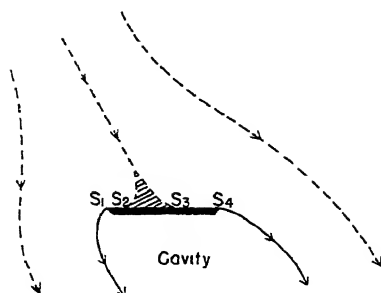


FIG. 3.

In Fig. 2c, one singularity is at S_4 , where $T_2 = 1/k$; in Fig. 2d, there is one singularity on each of the two "plates", so that $-1/k < T_1 < -1$, $1 < T_2 < 1/k$.

In all these cases there are exactly two jets: $n_1 = 2$ and $n_o = n_2 = n_d = n_s = 0$ in Ch. III, (3). To permit a cusp on the free boundary, $2 + n_d \geq 3$: more jets are needed. This is the case for the model represented in Fig. 3, which illustrates the indeterminacy of *asymmetric* Kirchhoff-Rayleigh flows.⁶

We know no flow with annular sector hodograph for which $z = \int \zeta^{-1} dW$ can be expressed in closed form.

4. Method of reflection. In the general case $m = 2$, the determination of $\zeta(t)$ is best accomplished by extending the method of reflection of Ch. III, §2 to the parameter rectangle R of formula (2). We shall now describe this extension.

Let Φ be any "simple flow" (cf. §1) bounded by two plates and two free streamlines. Formulas (1)–(4) are then applicable, and so (Theorem 1) it remains to determine $\zeta = f(t)$.

The conjugate velocity ζ , as a function of t , is analytic and regular in R . It has a finite number of zeros, corresponding to the stagnation points of the flow. It has a constant modulus on each horizontal side of R , and a constant argument on each of the vertical sides. Without loss of generality we can assume $|\zeta| = 1$, $|\zeta| = v < 1$, $\arg \zeta = 0 \pmod{\pi}$ and $\arg \zeta = \beta \pmod{\pi}$ on the lower, upper, left and right side of R , respectively. This amounts to choosing axes and units so that the boundary is in turn (i) horizontal, (ii) free, with constant velocity v , (iii) at an angle $-\beta$ with the horizontal, and (iv) free, with $|\zeta| = 1$. Reflecting in these boundaries, one

⁶ Cf. E. G. C. Poole, Proc. London Math. Soc. 26 (1927), 148–50. A careful discussion by one of us, J. de math. (1954), 29–80, shows that there is no other alternative to Kirchhoff-Rayleigh flow past a plate.

obtains

$$\begin{aligned}
 (11a) \quad & \zeta(t^*) = \zeta^{*-1}(t) && \text{on the lower side,} \\
 (11b) \quad & \zeta(t^* + 2iK') = v^2 \zeta^{*-1}(t) && \text{on the upper side,} \\
 (11c) \quad & \zeta(-2K - t^*) = \zeta^*(t) && \text{on the left side,} \\
 (11d) \quad & \zeta(2K - t^*) = e^{2i\beta} \zeta^*(t) && \text{on the right side.}
 \end{aligned}$$

On the boundaries of the reflected rectangles, ζ behaves as in R . Hence the process can be repeated indefinitely so as to extend $\zeta = f(t)$, as a meromorphic^{6a} function, to the whole t -plane. Since (11a) and (11b) change zeros into poles and poles into zeros, while (11c) and (11d) preserve both poles and zeros, ζ has no singularities except poles; moreover it is meromorphic, even at the corners. By repeated application of (11a)–(11b) and of (11c)–(11d), we derive

$$\begin{aligned}
 (12a) \quad & \zeta(t + 2iK') = v^2 \zeta(t) \\
 (12b) \quad & \zeta(t + 4K) = e^{2i\beta} \zeta(t).
 \end{aligned}$$

This shows that the function $\zeta(t)$ is a *doubly quasiperiodic meromorphic*^{6a} function, with quasi-periods $4K$, $2iK'$, in the following sense.

DEFINITION. A number ω is said to be a quasi-period of a function $f(t)$ if there is an α such that $f(t + \omega) = \alpha f(t)$. A function with two such factors α_1 , α_2 and linearly independent quasi-periods ω_1 , ω_2 is called a doubly quasiperiodic function. If $\alpha_1 = \alpha_2 = 1$, the function is called *doubly periodic*, with “periods” ω_1 , ω_2 .

By a *cell* of a doubly quasiperiodic function $f(t)$ is meant any parallelogram with sides ω_1 , ω_2 equal to the quasi-periods. In the present case, the quasi-periods $\omega_1 = 4K$ and $\omega_2 = 2iK'$ are orthogonal. Hence the “cells” involved are rectangles, similar to R , but with sides twice as long.

LEMMA. Two doubly quasiperiodic meromorphic functions having the same quasi-periods, poles and zeros, coincide up to an exponential factor Ae^{Ct} .

Proof. Let $f(t) = g_1(t)/g_2(t)$ be the quotient of two such functions. Then $f(t)$ will be quasiperiodic and without poles or zeros. Hence the logarithmic derivative $f'(t)/f(t)$ is bounded; it is also doubly periodic. By Liouville's Theorem, it is therefore a constant C . The relation $f(t) = Ae^{Ct}$ follows by elementary calculus.

COROLLARY. Two doubly quasiperiodic meromorphic functions with the same quasiperiods, factors, poles and zeros coincide up to a multiplicative constant.

^{6a} A meromorphic function is one whose only singularities in the finite t -plane are poles.

For, the exponential factor Ae^{Ct} must be doubly periodic, hence a constant.—Applying the preceding corollary to flows satisfying (11a)–(11d), we reach the following conclusion.

THEOREM 3. The conjugate velocity $\zeta = f(t)$ of any “simple” flow satisfying (i)–(iv) is doubly quasiperiodic and meromorphic, with quasi-periods $4K$ and $2iK'$ and factors $e^{2i\beta}$ and v^2 , respectively. It is determined, up to a factor ± 1 , by v , β , k , and the location of the stagnation points in R .

In Thm. 4, §10, we shall extend Thm. 3, showing that the location of the stagnation points in R is not arbitrary.

Elliptic functions. But first, in §§5–9, we shall apply Thm. 3 to some special cases when $v = 1$ and $e^{2i\beta} = \pm 1$, whose stagnation points can be located in R by symmetry. In such cases, $\zeta = f(t)$ is an *elliptic* function, that is, a doubly periodic meromorphic function. In fact, the periods are clearly $4K$ or $8K$, and $2iK'$. More generally, the following result is obvious.

COROLLARY 1. The function $\zeta(t)$ is elliptic if and only if $v = 1$ (i.e., the pressure is the same on both free streamlines), and $\beta = r\pi/s$ is a rational multiple of π .

For, in this case, $\zeta(t)$ is doubly periodic with periods $4sK$ and $2iK'$. Since any elliptic function with periods $4K^*$ and $2iK'^*$ can be represented as a rational function^{6b} of $\operatorname{sn} t = T$ and $\operatorname{cn} t \operatorname{dn} t = \sqrt{(1 - T^2)(1 - k^{*2}T^2)}$, we see that $\zeta = R^*(\operatorname{sn} t, \operatorname{cn} t \operatorname{dn} t)$ for some new modulus k^* . Substituting in Theorem 1 (with k replaced by k^*), we get $z = \int R_2(\operatorname{sn} t, \operatorname{cn} t \operatorname{dn} t) dt$, for some rational function $R_2(u, v)$. But it is classic^{6b} that any such integral can be expressed in terms of elliptic integrals of the first, second, and third kinds. This proves

COROLLARY 2. Under the hypotheses of Corollary 1, $z(t)$ can be expressed in closed form, in terms of elliptic integrals of $T = \operatorname{sn}(t, k^*)$.

This result is analogous to the main result of Ch. II, §9 (see also Ch. III, (1)). Unfortunately, its straightforward application to specific cases gives extremely complicated formulas, unless r and s are both very small. In the following, we shall work out the position integral in a few of the simplest cases, for which $r/s = 0, \frac{1}{2}$ or 1 . We have tried to simplify these formulas using Glaisher's notation

$$\begin{array}{lll} \operatorname{sc} u = \operatorname{sn} u / \operatorname{cn} u, & \operatorname{sd} u = \operatorname{sn} u / \operatorname{dn} u, & \operatorname{cd} u = \operatorname{cn} u / \operatorname{dn} u \\ \operatorname{cs} u = \operatorname{cn} u / \operatorname{sn} u, & \operatorname{ds} u = \operatorname{dn} u / \operatorname{sn} u, & \operatorname{dc} u = \operatorname{dn} u / \operatorname{cn} u. \end{array}$$

The resulting formulas are still complicated.

^{6b} W. F. Osgood, “Lehrbuch der Funktionentheorie”, p. 487, Satz 7. For $\int R_2(\operatorname{sn} t, \operatorname{cn} t \operatorname{dn} t) dt$, see [89, p. 515], or A. Erdelyi *et al.*, “Higher Transcendental Functions,” vol. 2, §13.3.

5. Impinging jets from nozzles I. First, consider two impinging jets from parallel nozzles, *symmetric* about a fixed center of symmetry O , under rotation through 180° , as in Fig. 4a. (The general case will be treated in §10). In the notation of §4, $\beta = \pi$ and $\nu = 1$; hence $\zeta = f(t)$ is an elliptic function with modulus k , if the flow is mapped on the R defined by (2). Further, by reflection of $\zeta(t)$ in the fixed walls, we see that its maximum modulus occurs on the free boundaries. Hence $|\zeta| \leq 1$, and the free streamlines are *convex*, by the Brillouin Principle (Ch. I, §13).

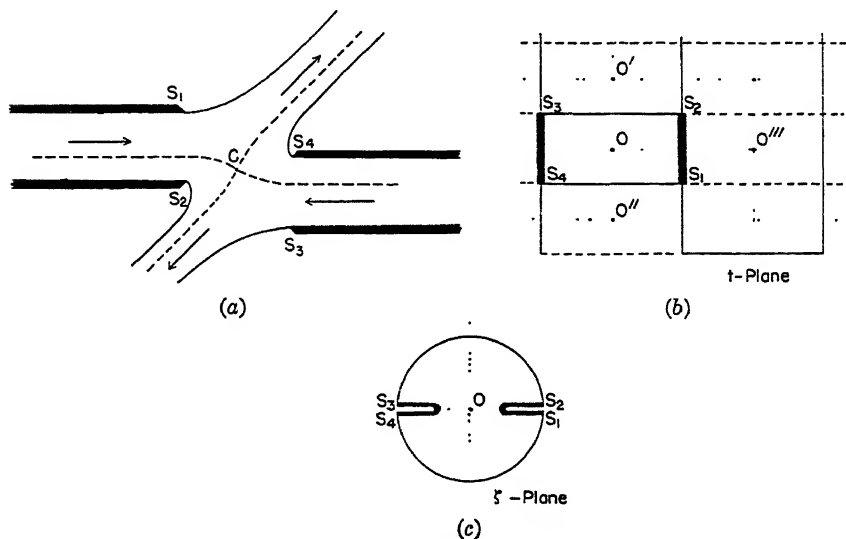


FIG. 4.

Again, from physical intuition^{6a}, we see that there is just one stagnation point, which must be at O by symmetry. Hence $f(t)$ has just one zero in R , at $t = iK/2$. By repeated reflections in the fixed and free boundaries (see Fig. 4b), we get all zeros and poles of $f(t)$ as in §4,

$$(13a) \quad \text{zeros at} \quad t = iK'/2 + 2mK + 2nK'i,$$

$$(13b) \quad \text{poles at} \quad t = -iK'/2 + 2mK + 2nK'i.$$

But it is well known⁷ that the zeros and poles of $\text{sn } t$, being at $2mK + 2niK'$, resp. $2mK + (2n + 1)iK'$, have the same spacing. Hence, by Theorem 3,

^{6a} More rigorously, by Ch. III, (30). Dividing points cannot be on a junction of free streamlines, the latter being convex, nor on a nozzle wall, by definition; hence $n_d = 0$.

⁷ [89, p. 504]; [62a, p. 284]. The fact follows from the method of reflection, noting that $T = \text{sn } t$ has a single zero in R , at $t = 0$, and a pole at $t = iK'$, and is real on the boundary of R .

$\zeta = c \operatorname{sn}(t - iK'/2)$ for some constant c . Since $\zeta = 1$ when $t = iK'$, $c \operatorname{sn}(iK'/2) = 1$, and so⁸ $c = -i\sqrt{k}$. Therefore

$$(14a) \quad \zeta = -i\sqrt{k} \operatorname{sn}(t - iK'/2) = -i\sqrt{k} \operatorname{sn} x, \quad x = t - iK'/2.$$

Hodograph method. Alternatively, the hodograph of such a flow (if simply covered) is obviously a notched circle Γ^* , with two symmetric horizontal notches as in Fig. 4c. Comparing with (14a), we see that $\operatorname{sn} x$ maps the rectangle

$$R^*: \quad -K \leq \operatorname{Re}\{x\} \leq K, \quad -K'/2 \leq \operatorname{Im}\{x\} \leq K'/2$$

into Γ^* , and each quarter of R^* onto a quadrant of Γ^* . Conversely, if one happens to know that the conformal transformation $X = \operatorname{sn} x$ maps the rectangle R^* onto a notched circle like Γ^* , one can deduce (14a) from the hodograph by inspection. (This property of $X = \operatorname{sn} x$ can be deduced analytically somewhat as follows. Substituting $-1/kX$ into

$$x = \int dX / [(1 - X^2)(1 - k^2 X^2)]^{\frac{1}{2}},$$

we get $\operatorname{sn}(iK' - x) = (-1/k)\operatorname{sn} x$. Also, on $\operatorname{Im}\{x\} = K'/2$, $|\operatorname{sn}(iK' - x)| = |\operatorname{sn} x|$. Hence, $|\operatorname{sn} x| = 1/\sqrt{k}$ on $\operatorname{Im}\{x\} = K'/2$.)

Position integral. However, the simplest evaluation of z in closed form is obtained by another parametrization, in which the flow is mapped onto the rectangle^{8a}

$$R_1: \quad -K_1 \leq \operatorname{Re}\{u\} \leq K_1, \quad -K'_1 \leq \operatorname{Im}\{u\} \leq K'_1,$$

with the stagnation point at the center $u = 0$. Then ζ is doubly periodic, with periods $4K_1$, $4iK'_1$. These are the least common periods of the functions $\operatorname{sn} u$, $\operatorname{cn} u$, $\operatorname{dn} u$, which is why R_1 is so convenient.

By symmetry, the points u_1 , u_2 , u_3 , u_4 , which represent the jets and nozzles, go into symmetric pairs on the boundary of R_1 . Thus $u_3 = -u_1$, $u_4 = -u_2$. Now noticing that $\operatorname{cn} u$ is an even function purely imaginary on the boundary, the complex potential is readily found to be (up to a constant real factor)

$$(15) \quad W = \ln \frac{\operatorname{cn} u - \operatorname{cn} u_1}{\operatorname{cn} u - \operatorname{cn} u_2}.$$

To obtain the velocity, one notices that $\frac{1}{2}(\zeta + \zeta^{-1})$ is the unique function real on the boundary with a simple pole at the origin and taking the values

⁸ For the formula $\operatorname{sn}(iK'/2) = i/\sqrt{k}$, see F. Tricomi, "Funzioni ellittiche," 2d ed., p. 147, or the discussion of the hodograph method below.

^{8a} Clearly, the modulus k_1 associated with R_1 is related to the k associated with R by a Landen transformation [89, p. 507].

± 1 at the corners. Such a function is $(k \operatorname{sn} u)^{-1}$, and so solving the equation $\frac{1}{2}(\zeta + \zeta^{-1}) = (k \operatorname{sn} u)^{-1}$, one gets

$$(14b) \quad \zeta = \frac{k \operatorname{sn} u}{1 + \operatorname{dn} u}.$$

From (15) and (14b), there follows

$$(16) \quad \begin{aligned} dz &= \zeta^{-1} dW \\ &= \frac{1}{k} \left[\frac{1}{\operatorname{cn} u - \operatorname{cn} u_2} - \frac{1}{\operatorname{cn} u - \operatorname{cn} u_1} \right] \operatorname{dn} u (1 + \operatorname{dn} u) du. \end{aligned}$$

This can be integrated in closed form, giving $z = G_2(u) - G_1(u)$, where

$$(16') \quad \begin{aligned} G_1(u) = & \frac{1}{k \operatorname{sn} u_i} \ln \frac{\phi(u_i) + \phi(u)}{\phi(u_i) - \phi(u)} + \frac{\operatorname{dn} u_i}{2k \operatorname{sn} u_i} \ln \frac{\operatorname{sd}(u_i) + \operatorname{sd}(u)}{\operatorname{sd}(u_i) - \operatorname{sd}(u)} \\ & - \frac{1}{k \operatorname{sd}(u_i)} \Pi(u, u_i - iK') + u \frac{\operatorname{cn} u_i}{\operatorname{sn}^2 u_i}, \end{aligned}$$

with $\phi(u) = \operatorname{sn} u / (1 + \operatorname{cn} u)$, $\operatorname{sd}(u) = \operatorname{sn} u / \operatorname{dn} u$. In the preceding formula

$$\Pi(u, a) = k^2 \operatorname{sn} a \operatorname{cn} a \operatorname{dn} a \int_0^u \frac{\operatorname{sn}^2 u \, du}{1 - k^2 \operatorname{sn}^2 a \operatorname{sn}^2 u}$$

is the elliptic integral of the third kind [89, p. 522].

6. Perpendicular plates. One can also express $\zeta(t)$ very simply in the case of ideal plane flows about a plate held perpendicularly in the jet from a nozzle (Fig. 1a). Assuming that there is a single stagnation point on the plate, the hodograph is evidently a symmetrically notched semicircle (Fig. 5a), and the logarithmic hodograph is a symmetrically notched semi-infinite rectangle. Comparing Fig. 5a with Figs. 4b–4c, one sees that if the flow is mapped onto the new parametric rectangle (Fig. 5b)

$$R_2: \quad -K \leq \operatorname{Re}\{u\} \leq 0, \quad -K'/2 \leq \operatorname{Im}\{u\} \leq K'/2,$$

then ζ is given by formula (14a), $\zeta = -i\sqrt{k} \operatorname{sn} u$. This formula can also be checked by noting that, when ζ is extended by reflection (§4) to the entire complex u -plane, its zeros are at $u = 2mK + 2inK'$, and its poles at $u = 2mK + (2n+1)iK'$, like those of $\operatorname{sn} v$.

Again, the function $U = \operatorname{sn}(u + iK'/2)$ clearly maps the flow onto the second quadrant of the U -plane. Hence, $T = -\operatorname{sn}^2(u + iK'/2)$ maps the flow onto the upper half T -plane. By Theorem 1 (§1), the flow is completely

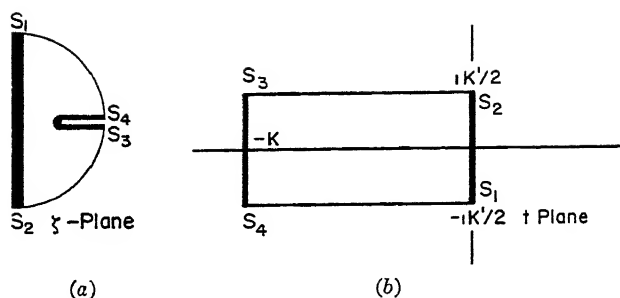


FIG. 5.

determined by these formulas, and a knowledge of

$$(17) \quad \frac{dW}{dT} = \frac{C(T - A)}{\prod_{k=1}^3 (T - T_k)} = \sum_{k=1}^3 \frac{h_k}{(T - T_k)}, \quad h_1 + h_2 + h_3 = 0,$$

where T_1 is on $\overline{S_3 S_4}$, T_2 on $\overline{S_4 S_1}$, T_3 on $\overline{S_2 S_3}$. The constant C determines the scale of the flow, T_1 determines the asymptotic nozzle velocity, while T_2, T_3 determine the directions of the outgoing jets.

Various limiting cases of the flow of Fig. 1a have special interest⁹. Among these may be mentioned: (i) the flow generated by a vertical plate "planing" in a stream of finite depth (Fig. 6a), and (ii) the cavitating flow at $Q = 0$ past a plate held perpendicularly but off-center in an infinite channel (Fig. 6b). In Case (i), $T_3 = -1$ and $T_1 = 1$; in Case (ii), $T_2 = -1$ and $T_1 = 1$. By reflecting the flows of Figs. 6a-6b in one wall, we get (iii) the impact of a symmetric jet from a nozzle on a perpendicular wall with symmetrically placed slot (Fig. 6c), and (iv) two perpendicular plates held symmetrically in a channel.

7. Position integral. We shall now discuss the formal integration of $z = \int \zeta^{-1} dW$, and various related integration formulas. To obtain these in simplest form, we rotate the parametric representation through 90° , mapping the flow onto the rectangle

$$R_3: \quad 0 \leq \operatorname{Re} \{x\} \leq K_3, \quad -K_3' \leq \operatorname{Im} \{x\} \leq 0,$$

where $K_3'/K_3 = K/K'$. Then

$$(18) \quad \zeta^{-1} = \frac{1}{\sqrt{k_3'}} \operatorname{dn}(x - K_3/2) = (1 + k_3') \frac{\operatorname{dn} x + (1 - k_3') \operatorname{sn} x \operatorname{cn} x}{\operatorname{dn}^2 x + k_3'}.$$

⁹ The symmetric case was treated in Ch. II, §§7-8. Case (i) has been treated by A. E. Green, Proc. Camb. Phil. Soc. 32 (1936), 67-85, and 34 (1938), 167-83; Case (ii) by J. Bonder, Ann. Acad. Sci. Techn. Warsaw 3 (1936), 155-93. See §12 for further references.

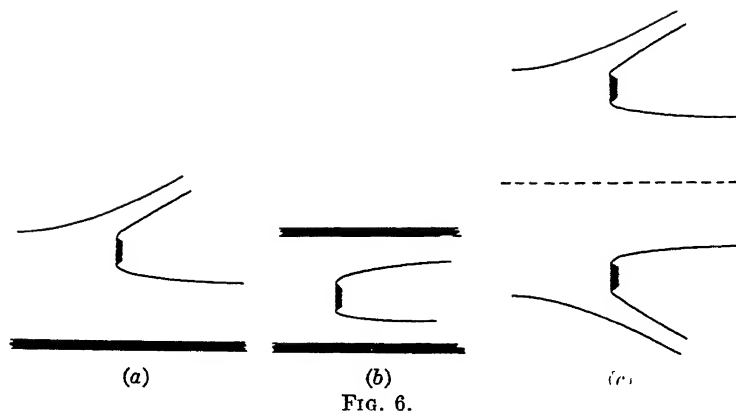


FIG. 6.

Formula (18) can either be derived from $\zeta = -i\sqrt{k} \operatorname{sn} u$ by rotation and translation or (more easily) by comparing the locations of the zeros and poles of ζ^{-1} with those⁷ of $\operatorname{dn} t$.

As to the complex potential, one simply notices that, since the function $\operatorname{sn}^2 x$ maps R_3 onto a half plane, it must be given by (17) with $T = \operatorname{sn}^2 x$ and $T_j = \operatorname{sn}^2 x_j$, where the x_j are three points on the boundary of R_3 . Since the stagnation point is mapped on $x = K_3/2 - iK_3'$, we have⁸

$$(19) \quad A = \operatorname{sn}^2(K_3/2 - iK_3', k_3) = 1/k_3.$$

Substituting in (17), we get

$$(20) \quad W = \sum_{j=1}^3 h_j \ln (\operatorname{sn}^2 x - \operatorname{sn}^2 x_j), \quad \text{where}$$

$$(20)' \quad \sum_{j=1}^3 h_j = 0, \quad \sum_{j=1}^3 h_j/(k_3^{-1} - \operatorname{sn}^2 x_j) = 0.$$

Physically, the $\pi h_j = d_j$ are the jet thicknesses; the first identity of (20') corresponds to conservation of mass, and the second to the condition (19) that $dW/dx = 0$ at the dividing point (i.e., that the stagnation point is in the finite plane.)

The position can now be computed from (18) and (20), as

$$z = 2 \sum_{j=1}^3 h_j (1 + k_3') \left[\int \frac{\operatorname{sn} x \operatorname{cn} x \operatorname{dn}^2 x \, dx}{(\operatorname{dn}^2 x + k_3')(\operatorname{sn}^2 x - \operatorname{sn}^2 x_j)} + (1 - k_3') \int \frac{\operatorname{sn}^2 x \operatorname{cn}^2 x \operatorname{dn} x \, dx}{(\operatorname{dn}^2 x + k_3')(\operatorname{sn}^2 x - \operatorname{sn}^2 x_j)} \right].$$

These two integrals can be evaluated in closed form by the substitutions $u = \operatorname{dn} x$ and $v = \operatorname{dn}(x - iK_3') = i(\operatorname{cn} x)/(\operatorname{dn} x)$ respectively, and using (20') wherever possible. Letting $\operatorname{cs} x = (\operatorname{cn} x)/(\operatorname{sn} x)$, the result is

$$(21) \quad z = \frac{1}{2} \sum_{j=1}^3 h_j \left[(\xi_j^{-1} + \xi_j) \ln \frac{\operatorname{dn} x - \operatorname{dn} x_j}{\operatorname{dn} x + \operatorname{dn} x_j} + (\xi_j^{-1} - \xi_j) \ln \frac{\operatorname{cs} x - \operatorname{cs} x_j}{\operatorname{cs} x + \operatorname{cs} x_j} \right],$$

where the $\xi_j = \sqrt{k_3'} \operatorname{dn} (x_j + K_3/2)$ are the velocities at infinity.

Applications. The length of the plate can be computed directly from (21); it is

$$(22) \quad l = \frac{1}{2} \sum_{j=1}^3 d_j \left[(\xi_j + \xi_j^{-1}) - i(\xi_j^{-1} - \xi_j) \ln \frac{2 + i(\xi_j^{-1} - \xi_j)}{2 - i(\xi_j^{-1} - \xi_j)} \right].$$

By Ch. IV, §4, the force F on the plate is

$$(23) \quad F = \frac{i\rho}{2} [z(2K_3 - iK_3') - z(iK_3')] = \frac{i\rho}{2} \sum_{j=1}^3 [(d_j/2)(\xi_j + \xi_j^{-1})].$$

In the limiting case (ii) of a plate in an infinite channel (Fig. 6b),

$$0 = x_2 < x_1 < x_3 = K_3 \quad \text{and} \quad \xi_1 = v < 1, \quad \xi_2 = \xi_3 = 1.$$

The drag coefficient $C_D = 2F/\rho v^2$ is

$$(24) \quad C_D = 2(1-v) \left/ \left[1 - v + \frac{2}{\pi} (1+v) \arctan \frac{1-v^2}{2v} \right] \right.$$

which shows the surprising fact that C_D does not depend on the position of the plate. For a plate planing in a stream of finite depth (Fig. 6a), $x_2 = 0$, $x_1 = K_3$, and x_3 is on the left side. Correspondingly, $\xi_1 = \xi_2 = 1$, $\xi_3 = e^{i\alpha}$. The drag coefficient is

$$(25) \quad C_D = 2 \left/ \left[1 + \frac{2}{\pi} \cot \frac{\alpha}{2} \ln \cot \frac{1}{2} \left(\frac{\pi}{2} - \alpha \right) \right] \right.$$

If the oncoming jet is allowed to thicken to ∞ , one obtains as a limiting case, half the flow of an infinite stream impinging perpendicularly onto two equal and symmetrically placed plates. An inspection of the above formula shows that C_D then becomes $2\pi/(\pi+4)$, the drag coefficient for a single plate¹⁰.

In the interesting case of a jet impinging perpendicularly and symmetrically on a perforated wall (Fig. 6c), half the flow is obtained by setting $x_1 = K_3$, $x_2 = 0$ and $x_3 = K_3 - iK_3'$. Naturally $\xi_1 = 1$, $\xi_2 = 1$, $\xi_3 = -i$. The aperture of the hole is

$$\pi h = i[z(iK_3') - z(-iK_3')] = -2\pi h_2 - 2h_3 \ln \frac{1+k_3'}{1-k_3'}.$$

¹⁰ This fact has been observed by J. Bonder, op. cit., in footnote 9.

From (20) and (20') follow

$$h_2 = -k_3' h_1 \quad \text{and} \quad h_3 = -(1 - k_3') h_1.$$

Thus, the ratio r of the impinging jet to the hole and the contraction coefficient c of the outcoming jet are

$$r = \frac{2h_1}{h} = 1 / \left[k_3' + \frac{(1 - k_3')}{\pi} \ln \frac{1 + k_3'}{1 - k_3'} \right]$$

$$c = \frac{2h_2}{h} = 1 / \left[1 + \frac{(1 - k_3')}{\pi k_3'} \ln \frac{1 + k_3'}{1 - k_3'} \right]$$

For k_3' sufficiently near 1, $r < 1$. Hence the flow may be in equilibrium even though the diameter of the impinging jet is smaller than the aperture of the hole. It would be interesting to study the stability of this equilibrium, experimentally.

8. U-shaped obstacles. We consider next flows having one free boundary, a "U-shaped" fixed boundary composed of two vertical plates connected by a horizontal one, and no stagnation points except at the corners. Typical are the flows sketched in Figs. 7a-7b, and first¹¹ discussed by Michell [60]. Other variants are sketched in Figs. 8a-8e and 10a-10c. Reflecting such a flow in the horizontal side, we get a flow with two free boundaries separated by two parallel vertical plates (cf. Fig. 7a).

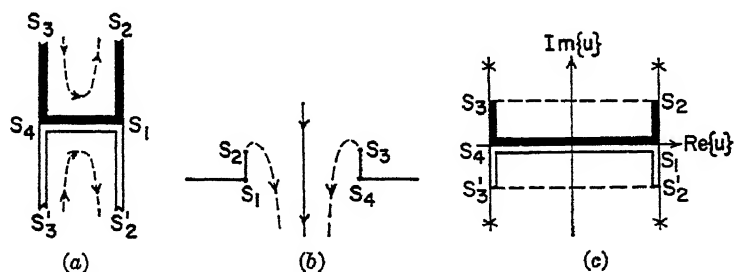


FIG. 7.

It would be natural to map the doubled flow obtained by reflection onto the rectangle R of §1 (formula (2) and Fig. 1b), so that S_2', S_2, S_3, S_3' fall on $K_1, K_1 + iK_1', -K_1 + iK_1', -K_1$, respectively. The zeros and poles of ζ would then fall on $(K_1 + iK_1'/2) + 2mK_1 + 2nK_1$ and $(K_1 - iK_1'/2) + 2mK_1 + 2nK_1$. Comparing with those of $\operatorname{sn} t$, this would give $\zeta = c \operatorname{sn}(t - K_1 - iK_1'/2)$ by Thm. 3, determining the flow by Thm. 1.

¹¹ See also C. W. Witozynski, *Vorträge über Hydro- und Aerodynamik*, Berlin, Springer, 1924, 250-1.

However¹², the formulas are simpler if, instead, we map the original flow onto the rectangle R of an auxiliary u -plane, as in Fig. 7c, so that the vertical plates go into the vertical sides of R , the horizontal plate into the lower side, and the free boundary into the top side. In R , $\zeta = f(u)$ is real and positive on the real axis, imaginary on the vertical sides, of modulus one on the top side, and with no zeros except at S_1, S_4 . By Theorem 3, these properties determine $f(t)$ uniquely. They are however shared by

$$\sqrt{(k' - \operatorname{dn} u)/(k' + \operatorname{dn} u)},$$

since $k' \leq \operatorname{dn} u \leq 1$ on the lower side, $0 \leq \operatorname{dn} u \leq k'$ on the vertical sides, and $\operatorname{dn} u$ is imaginary on the upper side. Therefore

$$(26) \quad \zeta = \sqrt{(k' - \operatorname{dn} u)/(k' + \operatorname{dn} u)} = -k \operatorname{cn} u / (k' + \operatorname{dn} u).$$

Again, the number of jets is two, and so by Ch. III, (4),

$$(27) \quad dW/dT = 1/(T - T_1) - 1/(T - T_2), \quad T = \operatorname{sn} u, \quad T_j = \operatorname{sn} u_j,$$

if the jet thickness is normalized to π . Hence the position

$$z = \int \zeta^{-1} dW = k^{-1} \int \left[\frac{-1}{\operatorname{sn} u - \operatorname{sn} u_1} + \frac{1}{\operatorname{sn} u - \operatorname{sn} u_2} \right] (k' + \operatorname{dn} u) \operatorname{dn} u \, du$$

is the difference of two similar integrals. To integrate, the integrand is developed in the form

$$\begin{aligned} \frac{(k' + \operatorname{dn} u) \operatorname{dn} u}{\operatorname{sn} u - \operatorname{sn} u_1} &= \frac{k' \operatorname{dn} u}{\operatorname{sn} u - \operatorname{sn} u_1} + \frac{\operatorname{dn}^2 u_1 \operatorname{sn} u}{\operatorname{sn}^2 u - \operatorname{sn}^2 u_1} - k^2 \operatorname{sn} u \\ &\quad - \frac{1}{\operatorname{sn} u_1} + \frac{\operatorname{dn}^2 u_1}{\operatorname{sn} u_1} \frac{\operatorname{sn}^2 u}{\operatorname{sn}^2 u - \operatorname{sn}^2 u_1}. \end{aligned}$$

The first four terms are easily integrated by taking $\operatorname{sn} u$, $(\operatorname{dn} u / \operatorname{cn} u)$, $\operatorname{cn} u$ and u as independent variables, and the last, after replacing $\operatorname{sn} u_1$ by $[k \operatorname{sn}(u_1 - ik')]^{-1}$, can be seen to have the canonical form of an elliptic integral of the third kind. Noticing

$$\frac{1}{2}(\zeta_1^{-1} - \zeta_1) = -\frac{k'}{k \operatorname{cn} u_1}, \quad \frac{1}{2}(\zeta_1^{-1} + \zeta_1) = -\frac{\operatorname{dn} u_1}{k \operatorname{cn} u_1}$$

the final result can be written

$$(28) \quad z = z_1 - z_2,$$

where

¹² The modulus k for this map is related to the modulus k_1 for the map just described by a Landen transformation.

$$\begin{aligned}
z_j = & \frac{1}{2}(\zeta_j^{-1} - \zeta_j)[\ln(\operatorname{cg} u - \operatorname{cg} u_j) - \ln(\operatorname{cg} u + \operatorname{cg} u_j)] \\
& + \frac{1}{4}(\zeta_j^{-1} + \zeta_j)[\ln(\operatorname{dc} u - \operatorname{dc} u_j) - \ln(\operatorname{dc} u + \operatorname{dc} u_j)] \\
& + u/(k \operatorname{sn} u_j) + \frac{1}{2}(\zeta_j + \zeta_j^{-1}) \prod(u, u_j - iK', k),
\end{aligned}$$

where $\operatorname{cg} u = (\operatorname{cn} u)/(1 + \operatorname{sn} u)$, $\operatorname{dc} u = (\operatorname{dn} u)/(\operatorname{cn} u)$, and $\prod(u, a, k)$ is the elliptic integral of the third kind (end of §5).

In the special case represented in Fig. 7a, the sink u_1 and source u_2 are at $\pm K + iK'$, hence $\zeta_1 = -i$, $\zeta_2 = i$. Most of the terms drop out, and (28) reduces to

$$(28a) \quad z = 2u + i \ln(k' - ik \operatorname{cn} u) - i \ln(k' + ik \operatorname{cn} u).$$

Figs. 8a-8e depict some other special cases of interest obtained by locating the source and sink (singularities) at different place on the boundary¹³.

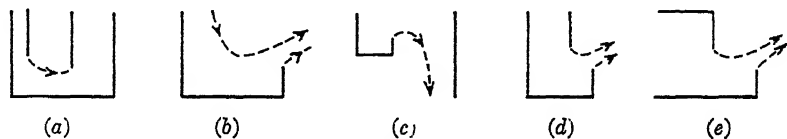


FIG. 8.

Special interest attaches to the flow of Fig. 8b, which represents half the flow of a jet impinging symmetrically on a U-shaped obstacle (plate with "spoiler",¹⁴ or stagnation cup). In this case, u_1 is on the upper side, $u_2 = -K + iK'$ and $\zeta_1 = e^{i\phi}$, $\zeta_2 = i$ correspondingly. The half length

$$b = z(K) - z(-K)$$

of the transversal plate is

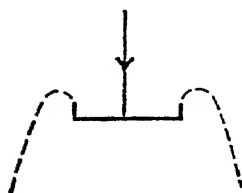
$$b = \pi(1 + \sin \phi) + 2K \frac{1 + k \operatorname{sn} u_1}{k \operatorname{sn} u_1} + 2 \cos \phi Z(u_1 - iK'),$$

where $Z(u) = \int_0^u \operatorname{dn}^2 u \, du - \frac{E}{K} u$ is the Jacobi Zeta function [89, p. 518].

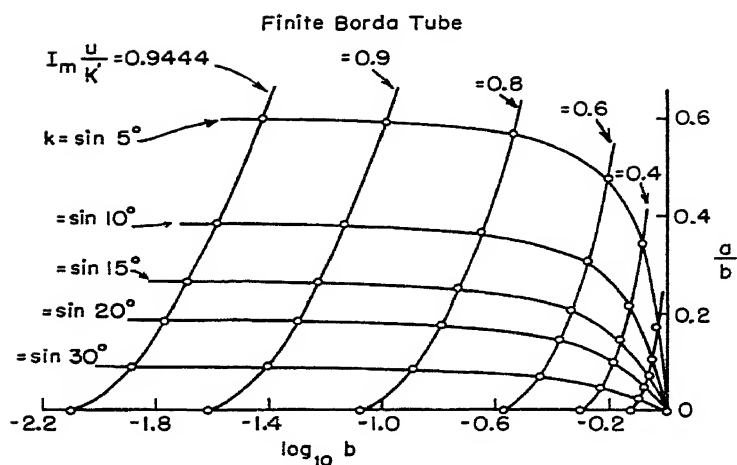
The length $a = |z(K + iK') - z(K)|$ of the spoiler is

¹³ Some of these flows have been considered by G. Greenhill, [32, pp. 39-46], and Michell [60]. U. Cisotti treated the jet from a rectangular vessel (Figs. 8d-8e) and its limiting form of the jet from an infinitesimal orifice, *Rend. Circ. Mat. Palermo* 25 (1908) 145-179; *Rend. Accad. Lincei* 23 (1914) 73-79. Other U-obstacles were considered by Cisotti, *Rend. Accad. Lincei* 22 (1913) 417-22, 580-84; see also [62] Part IV.

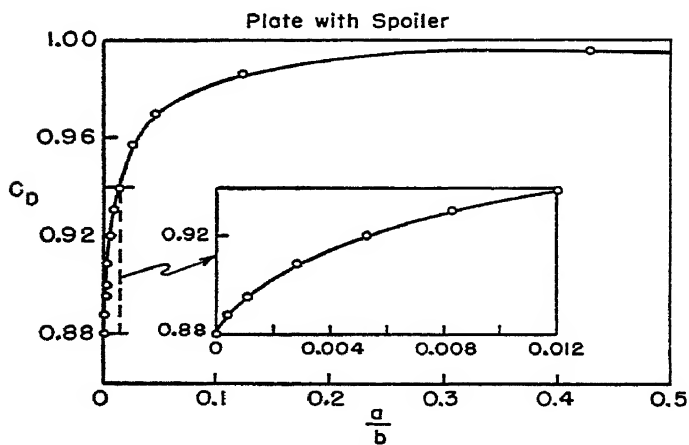
¹⁴ See Love [58] and Greenhill, *op. cit.* Also, [59a, pp. 45-53], where experimental data are given for the axially symmetric analog of Fig. 8b.



(a)



(b)



(c)

FIG. 9.

$$a = \sin \phi \left[\ln \left(\frac{\operatorname{cn} u_1}{1 + \operatorname{sn} u_1} - \frac{ik'}{1 + k} \right) - \ln \left(\frac{\operatorname{cn} u_1}{1 + \operatorname{sn} u_1} + \frac{ik'}{1 + k} \right) \right] \\ + \cos \phi \left[\frac{\pi (K + u_1 - iK')}{2K} + K'Z(u_1 - iK') \right] \\ - \ln k + K'(1 + k \operatorname{sn} u_1)/k \operatorname{sn} u_1.$$

The force on the obstacle is $F = 2d\rho(1 + \sin \phi)$, acting vertically, by Ch. IV, Thm. 7. From these relations, the ratio a/b of the spoiler to the plate and the drag coefficient $C_D = 2F/\rho b$ can be immediately computed. If $u_1 \rightarrow -K + iK'$, the limiting case of a plate with spoiler in an unbounded stream (Figure 9a) is attained. The corresponding limiting values of a, b and C_D are

$$(29a) \quad a/b = \frac{2(K' - E') + \ln k^{-1} - k'^2 K' - k'^2/2}{\pi + 4E - 2k'^2 K}$$

$$(29b) \quad C_D = 2\pi/[\pi + 4E - 2k'^2 K],$$

which show that C_D increases with a/b from $2\pi/(\pi + 4)$ to 1, the variation of C_D being very fast at the beginning ($dC_D/d(a/b) = \infty$), as in Fig. 9c.

Similar formulas hold for the model represented in Fig. 8c, which can be viewed as half the flow either of the Borda's mouthpiece in a finite container or of a plate with "spoiler" in a finite channel¹⁵. In this case

$$u_1 = -K + i(K' - u), \quad u_2 = -K + iK', \quad \zeta_1 = v, \quad \zeta_2 = i.$$

The transformation from the analytic parameters k and u_1 to the geometric ones a and b (taking the width of the channel as unity) is graphed in Fig. 9b.

Half the flow of Fig. 9a is a special case when the source and sink have "coalesced", producing an "ocean" (Ch. III, §3) for which $dW/dT = 1/(T - T_1)^2$, when the flow is suitably normalized. The limiting cases so obtained are sketched¹⁶ in Figs. 10a-10c.

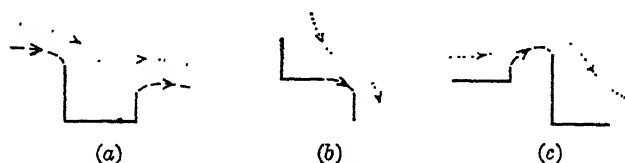


FIG. 10.

9. Riabouchinsky flows. Fig. 11a represents the case of a source and

¹⁵ cf. U. Cisotti, Rend. cir. mat. Palermo, 25 (1908) 145-79; for the limiting case of a jet from a raised slot, see J. H. Michell [60].

¹⁶ Fig. 10a represents a particular case of a class of flows considered by T. Boggio, Atti r. accad. sci. Torino, 46 (1911) 1024-1051. For bibliography on flows of the type of Fig. 10c, see §9.

sink symmetrically placed on the lower side $\overline{S_4 S_1}$ of a flow past a U-shaped obstacle. If the flow is reflected in the lower wall, one gets a flow past a two-dimensional Venturi meter, first considered by Colonetti¹⁷. If the flow is reflected in the upper wall, as in Fig. 11b, one gets a flow past a flat plate in a channel, having a positive wake (cavity) underpressure coefficient

$$(30) \quad Q = (p_\infty - p_c)/\frac{1}{2}\rho v_\infty^2 > 0,$$

as in physical reality. This was first recognized by D. Riabouchinsky¹⁷, in the limiting case of Fig. 11c, when the channel wall recedes to infinity. Because of the great importance of his observation, the name *Riabouchinsky flows* is now give to flows of the type just described.

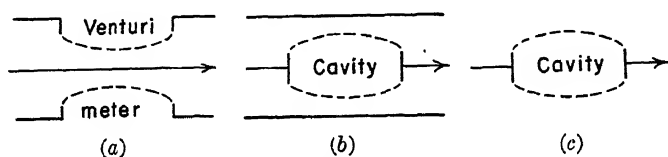


FIG. 11.

The mathematical formulas can be calculated as special cases of those of §8; this we now do. From (27) and (28), setting $u_2 = -u_1$, $\zeta_2 = \zeta_1$, we get

$$(31) \quad dW/dT = 2T_1/(T^2 - T_1^2) = 1/(T - T_1) - 1/(T + T_1),$$

$$(32) \quad z = \frac{1}{2}(\zeta_1^{-1} - \zeta_1) \ln \frac{\operatorname{sc} u - \operatorname{sc} u_1}{\operatorname{sc} u + \operatorname{sc} u_1} + \frac{2u}{k \operatorname{sn} u_1} + \frac{1}{2}(\zeta_1^{-1} + \zeta_1)[\Pi(u, u_1 - iK', k) - \Pi(u, -u_1 - iK_1', k)]$$

Again, the velocity at infinity is

$$(33a) \quad v_\infty = k \operatorname{cn} u_1/(k' + \operatorname{dn} u_1),$$

and the cavitation number Q satisfies (since $v = 1$)

$$(33b) \quad Q = v_\infty^2 - 1 = 2k'/(k' + \operatorname{dn} u_1),$$

The width $b = 2a = -i[z(K + iK') - z(K - iK')]$ of the plate is, with our normalization to a discharge $d = \pi$,

¹⁷ G. Colonetti, Rend. accad. Lincei 20 (1911), 649-55 and 789-96; the dual interpretation is given in [6, Part II]. For Riabouchinsky's work, see Proc. Lond. math. soc. 18 (1920), 206-15, and 25 (1926), 185-94, where other references are given; also [19, Ch. V]. The relation to cavities (as contrasted with wakes) seems to have been first remarked by F. Weinig [46, pp. 294-300].

$$(34) \quad b = \pm \left[-\frac{k'}{k \operatorname{cn} u_1} \arctan k \frac{\operatorname{sn} u_1}{\operatorname{cn} u_1} + K' k \operatorname{sn} u_1 + \frac{\pi}{2kK} \frac{\operatorname{dn} u_1}{\operatorname{cn} u_1} u_1 - \frac{K'}{k \operatorname{cn} u_1} Z(u_1) \right]$$

and the length l of the cavity

$$(35) \quad l = z(-K + iK') - z(K + iK') = 4K \left[-k^2 \operatorname{sn} u_1 + \frac{\operatorname{dn} u_1}{\operatorname{cn} u_1} Z(u_1) \right]$$

The force on a plate computed from Ch. IV, §4, is

$$\begin{aligned} F &= \frac{1}{2} \rho i [z(K) - z(K + 2iK')] \\ &= 2\rho \left[kK' \operatorname{sn} u_1 - \frac{\operatorname{dn} u_1}{k \operatorname{cn} u_1} K' Z(u_1) + \frac{\pi}{2K} u_1 \right]. \end{aligned}$$

From these formulas, the drag coefficient C_D can easily be computed as a function of the dimensionless cavitation number Q and ratio a/b of plate-width $2a$ to channel diameter $2b = 2\pi/v_\infty$.

The most interesting special case is Riabouchinsky's limiting case $u_1 = 0$ of an infinite stream, depicted in Fig. 11c. Then half the flow represents an ocean, with $W = T^{-1}$ and

$$(36a) \quad z = k^{-1} \left[k' \frac{\operatorname{cn} u}{\operatorname{sn} u} + \frac{\operatorname{cn} u \operatorname{dn} u}{\operatorname{sn} u} + E(u) - k'^2 u \right],$$

where $E(u) = E(u, k) = \int_0^u \operatorname{dn}^2 t \, dt$ is the elliptic integral of the second kind [89, p. 517]. Correspondingly, if $E = E(1, k)$ and $E' = E(1, k')$

$$(36b) \quad v_\infty = k/(1 + k'), \quad Q = 2k'/(1 - k'),$$

$$(36c) \quad b = 2k^{-1}[E' - k^2 K' + k'^2], \quad l = 2k^{-1}[E - k'^2 K],$$

$$(36d) \quad C_D = 2F/\rho v_\infty^2 b = 2(1 + Q)(E' - k^2 K')/(E' - k^2 K' + k'^2).$$

It is interesting to compare the Riabouchinsky model for a cavity with the reentrant jet model. (Ch. III, §8). Plate 11 reveals a striking coincidence in many aspects, for cavitation numbers¹⁸ as big as $Q = 0.4$. This coincidence applies to the forward halves of the cavity profiles, to the drag coefficients $C_D \cong 0.88(1 + Q)$, and to various other geometrical quantities graphed in Plate 11 and described verbally in Ch. III, §8. Thus, the two models give nearly identical predictions for the "blocking constant" of a flat plate (Ch. I, §11).

¹⁸ This agreement was observed by D. Gilbarg and H. H. Rock, Nav. Ord. Lab. Memo. 8718 (1946) and M. I. Gurevich, Izv. Akad. Nauk (1947), 143-50 (DTMB Translation 224).

Various generalizations of the Riabouchinsky flow have been treated in the literature. These include: flows past inclined plates, which will be treated in §12; flows past parallel plates held perpendicularly in the middle of an infinite jet¹⁹, and Riabouchinsky flows past symmetric pairs of wedges subtending an angle 2β .

These last can be treated by the hodograph method. If $\eta = \zeta^{2\beta/\pi}$ and $u = (i\eta^{-1} - i\eta)/2$, then (in normalized variables) $W = u/\sqrt{u^2 + \tan^2\alpha}$, where α is determined by the cavitation number Q . In the case $\beta = \pi/4$, $z(u)$ can be expressed quite simply in terms of elliptic integrals.

10. Impinging jets from nozzles, II. We now consider the general case of two impinging jets from two nozzles, whose directions differ by an angle β (Fig. 12a). We assume constant external pressure, so that $|\zeta| = 1$ on all free streamlines, if suitable units are used. For a suitable modulus k , we can map the flow on a parametric rectangle R , as in §1 (see Fig. 12b) so that $\text{sn } t$ maps the flow on the upper half T -plane.

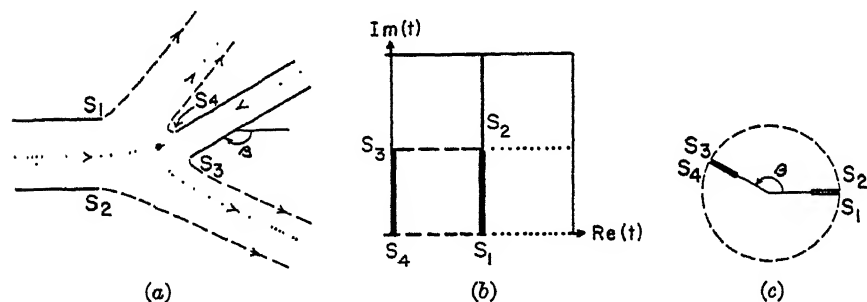


FIG. 12.

Assuming two outgoing jets, the complex potential must satisfy

$$(37) \quad dW/dT = c(T - A)(T - A^*) / \prod_{j=1}^4 (T - T_j) = \sum_{j=1}^4 h_j / (T - T_j),$$

just as in Ch. III, §4. Here the scale factor c is real, A corresponds to the interior dividing point, A^* is the complex conjugate of A , and the T_j correspond to the incoming and outgoing jets (points at infinity of the flow). The rate of influx from T_j is $\pi h_j = d_j$, and $\sum h_j = 0$; thus $W(T)$ involves seven arbitrary real parameters.

¹⁹ For plates in a jet, see [6, Part II]; the limiting case of coalescing plates was treated by U. Cisotti, *Rend. Accad. Lincei* 21 (1912), 583-93 and 22 (1913), 417-22 and 580-4. For Riabouchinsky flows past wedges, see G. Colonetti, *refs. of footnote 17*; M. S. Plesset and P. A. Schaffer, *J. Appl. Phys.* 19 (1948), 934-9; E. L. Aronoff, *Navord Rep.* 1298 (1951); Byrne Perry, *Cal. Tech. Hydro. Lab. Rept.* 21-11; [82, pp. 125-35].

Again, our hypotheses clearly imply that $\zeta = e(t)$ has the following properties: (i) $e(t)$ is regular in R , (ii) $|e(t)| = 1$ on the horizontal sides of R , (iii) $e(t)$ is real on the right side $\overline{S_1 S_2}$ of R , (iv) its argument is constant on the left side $\overline{S_3 S_4}$ of R , (v) it vanishes at $t = a$ (where $\operatorname{sn} a = 1$) and nowhere else in R .

It is also plausible that the hodograph is a unit circle with two notches at an angle β with each other, as in Fig. 12c. Since this configuration involves three parameters, it is plausible that $e(t) = e(t, a, k)$ is determined by the modulus k of R and the complex number a . We shall now establish this conjecture as a special case of the following extension of Theorem 3.

THEOREM 4. Under the hypotheses of Thm. 3, if the stagnation points of $\zeta = f(t)$ are located at a_k in the interior and b_k on the boundary of R , then

$$(38) \quad \beta \equiv \frac{2K}{K'} \ln v^{-1} - \frac{\pi}{K'} [2 \sum \operatorname{Im}\{a_k\} + \sum \operatorname{Im}\{b_k\}] \pmod{\pi}$$

In the case of an annular sector hodograph (§3), the expression in brackets vanishes, and (38) reduces to (9a). In the cases of §§5–9, formula (38) was tacitly assumed from symmetry considerations; thus, in §5, $e(t, iK'/2, k) = c \operatorname{sn}(t - iK'/2)$. In the present case of impinging jets from nozzles, (38) reduces to

$$(38a) \quad \beta = -2\pi \operatorname{Im}\{a\}/K' \pmod{\pi},$$

or

$$(38b) \quad \operatorname{Im}\{a\} = -\beta K'/2\pi \pmod{2K'},$$

which shows how a determines β . In the general case, (38) is a corollary of the following

LEMMA. In any "cell" of a doubly quasi-periodic function, the number of zeros equals the number of poles. Moreover, if ω_1 and ω_2 are quasi-periods, α_1 and α_2 the corresponding factors, z_k the zeros and p_k the poles, then

$$(39) \quad \sum z_k - \sum p_k \equiv \left(\omega_1 \frac{\ln \alpha_2}{2\pi i} - \omega_2 \frac{\ln \alpha_1}{2\pi i} \right) \pmod{(\omega_1, \omega_2)}.$$

Proof. The difference between the number of zeros and poles is the total residue of the logarithmic derivative which, since the logarithmic derivative is elliptic, is zero [89, p. 431]. To prove the last assertion we start from [89, p. 119]

$$\sum z_k - \sum p_k = \frac{1}{2\pi i} \int_C t \frac{f'(t)}{f(t)} dt,$$

where C is the boundary of the cell. Decomposing C in its sides and taking account of the quasi-periodicity of $f(t)$,

$$\begin{aligned}
\int t \frac{f'(t)}{f(t)} dt &= \left[\int_{t_0}^{t_0+\omega_1} - \int_{t_0+\omega_2}^{t_0+\omega_1+\omega_2} - \int_{t_0}^{t_0+\omega_2} + \int_{t_0+\omega_1}^{t_0+\omega_1+\omega_2} \right] t \frac{f'(t)}{f(t)} dt \\
&= \left[\omega_1 \int_{t_0}^{t_0+\omega_2} - \omega_2 \int_{t_0}^{t_0+\omega_1} \right] \frac{f'(t)}{f(t)} dt \\
&= \omega_1 (\ln \alpha_2 + k_1 2\pi i) + \omega_2 (\ln \alpha_1 + k_2 2\pi i),
\end{aligned}$$

which gives (39).

To apply these results to ζ , we let $\omega_1 = 4K$, $\omega_2 = 2iK'$, $\ln \alpha_1 = 2i\beta$ and $\alpha_2 = v^2$. We let the "cell" be $-K \leq \operatorname{Re}\{t\} < 3K$, $-K' \leq \operatorname{Im}\{t\} < K'$, and observe that a zero a inside R generates by reflection a new zero at $a' = 2K - a^*$, and two poles at a^* and a'^* , while a zero b on the boundary produces no new zeros and one pole at b^* . Substituting in (39), we get (38).

THEOREM 5. Properties (i)–(v) above define $e(t) = e(t, a, k)$ up to sign (i.e., a multiplicative factor ± 1).

Proof. By Thm. 3, $e(t)$ is doubly quasi-periodic, with quasi-periods $4K$ and $2iK'$, and corresponding factors $e^{2i\beta}$ and v^2 . By (ii), $v = 1$, and so $4K$ is a period. By (38), since $v = 1$, $\beta \equiv 2\pi \operatorname{Im}\{a\}/K' \pmod{\pi}$, which determines the multiplicative factor $e^{2i\beta}$. Hence, by the Lemma of §4, properties (i)–(v) determine $e(t)$ up to a constant factor c . By (ii), $|c| = 1$, and by (iii), c is real, completing the proof.

From the discussion of (37)–(38), it is now clear that the general case of impinging jets with unit velocity on all free streamlines involves $7 + 1 = 8$ parameters (A determines a , but not k). But the nozzle configuration involves 7 parameters (β and the relative locations of the nozzle edges). Hence, as in the case of freely impinging jets (Ch. III, §4), the flow is not determined by the natural physical assumptions.

11. General formulas. We shall now show that the functions $e(t, a, k)$ defined in §10 can be used to deduce an expression for $\zeta(t)$, in the general case described in §4 (and in Thm. 4 of §10).

THEOREM 6. The complex velocity of any flow satisfying conditions (i)–(v) of §4 is given by

$$(40) \quad \zeta = \pm v^{i(K-\theta)/K'} \prod e(t, a_j, k) \prod e(t, b_n, k),$$

where a_j are the interior zeros of ζ and b_n those on the boundary of R .

Proof. From the properties of the functions e , it follows that the right side has simple zeros at the points a_j, b_n ; has modulus one and modulus v on the lower and upper side of R respectively; is real on right side of R and has constant argument modulo π on the left. But by (38), this constant is β , and so by Theorem 3 the right side of (40) must coincide with ζ .

Theorem 6 shows clearly the importance of the functions $e(t, a, k)$ for the theory of flows bounded by two plates and two streamlines. In view of

this importance, it seems worthwhile to deduce an expression for them in terms of Jacobi theta functions [89, Ch. XXI]. This will, incidentally, prove the existence of $e(t, a, k)$ for any complex $a \in \mathbb{R}$, and any modulus k , $0 < k < 1$. The details follow.

LEMMA. If z_0 is any point of the cell with vertices at $-\frac{\pi\tau}{4}$, $-\frac{\pi\tau}{4} + \frac{\pi}{2}$, $\frac{\pi\tau}{4} + \frac{\pi}{2}$, $\frac{\pi\tau}{4}$, then the function

$$(41) \quad h(z, z_0; \tau) = \begin{cases} \frac{\theta_1(z - z_0 | \tau) \theta_4(z - z_0^* | \tau)}{\theta_1(z + z_0^* | \tau) \theta_4(z + z_0 | \tau)} & \text{if } \operatorname{Im}\{z_0\} \neq \pm \frac{\pi\tau}{4} \\ \frac{\theta_4(z - z_0^* | \tau)}{\theta_4(z + z_0 | \tau)} & \text{if } \operatorname{Im}\{z_0\} = \pm \frac{\pi\tau}{4} \end{cases}$$

is regular in the cell, has a simple zero at z_0 (and no other), it has modulus one on the vertical sides and its argument remains constant (modulo π) on the horizontal ones.

Proof. The proof is a simple verification. We give it for $\operatorname{Im} z_0 \neq \pm \frac{\pi\tau}{4}$, the other case is even simpler. According to the locations of zeros of the theta functions it is immediately seen that h is regular and that it has no other zero than $z_0 = x_0 + iy_0$. On the right side $z = \pi/2 + is$, for some real s . But [89, p. 464],

$$\theta_2(t | \tau) = \theta_1\left(t + \frac{\pi}{2} | \tau\right), \quad \theta_3(t | \tau) = \theta_4\left(t + \frac{\pi}{2} | \tau\right),$$

and so

$$\begin{aligned} h &= \frac{\theta_1\left(-x_0 + i(s - y_0) + \frac{\pi}{2}\right) \theta_4\left(-x_0 + i(s + y_0) + \frac{\pi}{2}\right)}{\theta_1\left(x_0 + i(s - y_0) + \frac{\pi}{2}\right) \theta_4\left(x_0 + i(s + y_0) + \frac{\pi}{2}\right)} \\ &= \frac{\theta_3(-x_0 + i(s - y_0)) \theta_2(-x_0 + i(s + y_0))}{\theta_3(x_0 + i(s - y_0)) \theta_2(x_0 + i(s + y_0))}. \end{aligned}$$

Since θ_2 and θ_3 are even functions taking conjugate values at conjugate points, this shows that $|h| = 1$. Same proof for the left side. Now, on the lower side, $z = -\frac{\pi\tau}{4} + s$ (s real) and

$$h = \frac{\theta_1\left(s - z_0 - \frac{\pi\tau}{4}\right) \theta_4\left(s - z_0^* - \frac{\pi\tau}{4}\right)}{\theta_1\left(s + z_0^* - \frac{\pi\tau}{4}\right) \theta_4\left(s + z_0 - \frac{\pi\tau}{4}\right)}.$$

We now use the identity $\theta_1(t) = -iq^{\frac{1}{2}}e^{it}\theta_4(t + \pi\tau/2)$, whence $\theta_1(t - \pi\tau/4) = -iq^{\frac{1}{2}}e^{it}\theta_4(t + \pi\tau/4)$. Substituting in the last expression for h gives

$$h = e^{-i(z_0 + z_0^*)} \frac{\theta_4\left(s - z_0 + \frac{\pi\tau}{4}\right)\theta_4\left(s - z_0^* - \frac{\pi\tau}{4}\right)}{\theta_4\left(s + z_0^* + \frac{\pi\tau}{4}\right)\theta_4\left(s + z_0 - \frac{\pi\tau}{4}\right)} \\ = e^{-i(z_0 + z_0^*)} \left| \frac{\theta_4\left(s - z_0 + \frac{\pi\tau}{4}\right)}{\theta_4\left(s + z_0 - \frac{\pi\tau}{4}\right)} \right|^2.$$

Thus, the argument of h is constantly equal to $-2Re\{z_0\}$. A similar proof goes for the upper side.

Let us now consider the function $h(z, z_0, 2\tau')$ connected with the parameter $2\tau' = 2iK'/K'$. The transformation $t = \frac{2iK'}{\pi}z$ carries the cell into the rectangle R : $-K \leq Re\{t\} \leq K$, $0 \leq Im\{t\} \leq K'$. Hence

THEOREM 7. For any $a \in R$, the function

$$(42) \quad e(t, a, k) = e^{i\pi Im\{a\}/K'} h\left(\frac{\pi t}{2iK'}, \frac{\pi a}{2iK'}; 2\tau'\right),$$

where $\tau' = iK'/K'$ and $h(z, z_0, t)$ is defined by (41), has properties (i)-(v) listed at the beginning of this section.

By Thm. 5, $\pm e(t, a, k)$ are the only such functions. By (38a) and (12b), they are elliptic if and only if $Im\{a\}/K' = \beta/2\pi$ is a rational fraction p/q . In this case, the periods are $2iK'$ and $2qK$ if q is even; $2iK'$ and $4qK$ if q is odd.

12. Plate in jet from nozzle. As an application of the general formulas of §§10-11, we consider the case²⁰ of a plate held obliquely in the jet from a nozzle (Fig. 13a), and having equal pressure on all free streamlines. As usual, we can normalize to the case $|\zeta| = 1$ on all free streamlines.

Just as in §6 (which dealt with the case $\beta = \pi/2$), we can write

$$(43) \quad dW/dT = c(T - B)/(T - T_1)(T - T_2)(T - T_3),$$

where the $T_j = \operatorname{sn} t_j$ have the same interpretation, and $B = \operatorname{sn} b$ corresponds to the dividing point on the plate. Further $\zeta = e(t)$ evidently has properties (i)-(v) of §10. Hence the hodograph is a notched semicircle (Fig. 13b), and we can write, by Theorem 7, (38), and (41),

$$(44) \quad \zeta = e(t, b, k) = e^{i\beta} \frac{\theta_4(\pi(t + b^*)/2iK' | 2\tau')}{\theta_4(\pi(t - b)/2iK' | 2\tau')},$$

²⁰ See [32, §§10, 11].

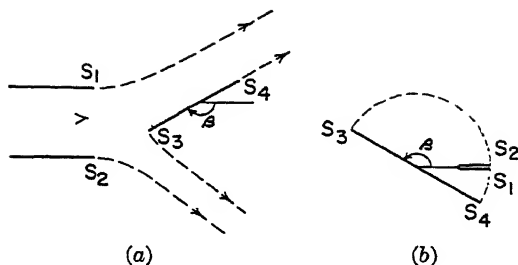


FIG. 13.

where $\tau' = iK/K'$ and $\text{Im}\{b\} \equiv \beta K'/\pi \pmod{K'}$. In the special case $\beta = \pi/2$ of §6, $\text{Im}\{b\} = K'/2$ by symmetry and $e(t, K - iK'/2, k)$ is elliptic.

The limiting cases having special interest when $\beta = \pi/2$, and enumerated in §6, also have special interest here. We mention also the case $t_3 = t_1 = K$, $t_2 = K + iK'$, of a plate in the presence of an infinite wall, treated by Villat²¹, and the case $t_1 = K$, $t_2 = K + iK'$, $\text{Im}\{t_3\} = K$ of a plane jet from a nozzle impinging on an infinite wall. Also, the preceding formulas give a solution to the problem of designing bends which will divide a channel into parallel branches, having constant pressure on the bends (to avoid separation).

Related flows. Closely related to the flows just defined, are analogous flows with *unequal* pressures in the different regions separated by the branches of the flow.

If we modify further by continuity, we get the case of Villat-Morton²², sketched in Fig. 14a. The hodograph includes a reentrant circular arc, which corresponds to the free streamline with a point of inflection.

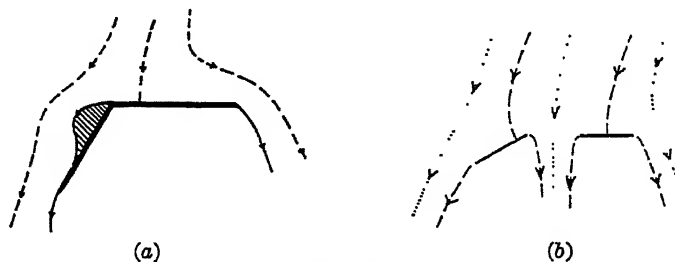


FIG. 14.

By allowing two stagnation points, we get many possible configurations

²¹ H. Villat, Ann. sci. ec. norm. sup. 35 (1918), 251-312; Tomotika and Hasimoto, Appl. mech. revs. 2371 (1950).

²² H. Villat, Ann. fac. sci. Toulouse 5 (1913), 375-404, and [84], [86]; see also W. B. Morton, Phil. Mag. 41 (1921), 301-8 and 48 (1924), 464-76.

involving two plates in a finite or infinite stream, of which a sample is shown in Fig. 14b. We refer the reader to the very considerable literature dealing with this case²³; some results concern the case $m > 2$ (see §2) of multiple plates; others concern flows with circulation and multiply connected flows.

13. Interior sources and vortices. A simple extension of the preceding ideas covers flows bounded by two plates and two free streamlines and having interior point-sources and point-vortices²⁴. As regards the complex potential, $W(T)$ has a logarithmic singularity $W = m \ln(T - T_0) + \dots$ at a point-source, and one of the form $W = im \ln(T - T_0) + \dots$ at a point-vortex [61, p. 324]. By reflection in the real T -axis, we can obtain the contribution to $W(T)$ from any number of interior sources and vortices. As regards $\zeta(t)$, it has a simple pole $a/(t - t_0) + \dots$ at an interior source (sink) or vortex. Such poles introduce factors $e(t, t_0, k)$ into the denominator of (40), which is otherwise unchanged.

We shall treat in detail only two *symmetric* cases; just as in §§5–9, we can then get simple expressions for $\zeta(t)$ and $z(t)$, using elliptic integrals. We consider first the case of a point-vortex between two plates²⁵ (Fig. 15a).

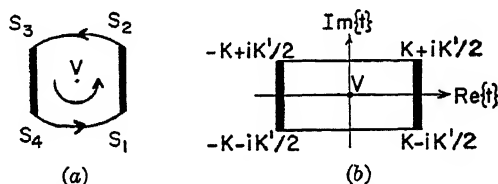


FIG. 15.

The plates are equal and parallel with their ends forming a rectangle and the vortex is placed at the center of this configuration. The plates are joined by two free streamlines and the resulting flow is assumed symmetric about the vortex. We take the rectangle $R: -K \leq \text{Re}\{t\} \leq K, -K'/2 \leq \text{Im}\{t\} \leq K'/2$ as the parameter domain (Fig. 15b), and map the flow onto it so that the plates go onto the vertical sides and the free boundaries onto the horizontal ones. The mapping of this rectangle into the half plane is given by

²³ See E. G. C. Poole, Proc. Lond. math. soc. 22 (1923), 425–53, 25 (1926), 195–212, and 26 (1927), 148–58. Also, R. Thiry, Ann. sci. ec. norm. sup. 38 (1921), 229–329, and [19, Ch. V].

²⁴ The technique is due to B. Hopkinson [38], who made pioneer use of the method of reflection in the hodograph plane.

²⁵ If the plates are allowed to become infinitely long, one obtains the limiting case treated by Greenhill [32]. The interesting case of a vortex in a jet from a nozzle (deviating vortex) has been considered by N. Simmons, Quar. J. math. 10 (1939) 283–311. See also, Phil. Mag. 31 (1941) 81–102. For other cases, see [19, Ch. VII].

the function $T = \operatorname{sn} \left(t + \frac{iK'}{2} \right)$, the vortex being located at the point $T_0 = \operatorname{sn} \frac{iK'}{2} = ik^{-1}$. The complex potential has logarithmic singularities at $T = T_0$, $T = T_0^* = -T_0$ with purely imaginary and opposite coefficients, so (after normalization)

$$(45) \quad W = \frac{i}{2} \ln \frac{T - T_0}{T + T_0}.$$

As to ζ , it has a simple pole at $t = 0$, $|\zeta| = 1$ on the horizontal sides, and is purely imaginary on the vertical sides. By Thm. 3, $\zeta(t)$ is uniquely determined (up to sign) as an elliptic function of periods $4K$ and $2iK'$, having these properties. But (cf. §5) the same properties are shared by $i/\sqrt{k} \operatorname{sn} t$; hence

$$(46) \quad \zeta = i/(\sqrt{k} \operatorname{sn} t).$$

Integrating (45)–(46), we get

$$(47) \quad z = \frac{1}{2}k^{-1}[E(t) - (1 - k)t],$$

where $E(t) = \int_0^t \operatorname{dn}^2 u \, du$ is the elliptic integral of second kind. It follows that the distance d between the plates, and the plate-length l , are given by

$$(48) \quad d = k^{-1}[E - (1 - k)K], \quad l = \frac{1}{2}k^{-1}[kK' - E' + 1 - k].$$

The force separating the plates is, by Ch. IV, §5,

$$(49) \quad F = \rho k^{-1}[E' - kK'].$$

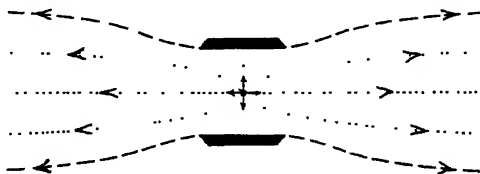


FIG. 16.

The case of a symmetrically placed source between two plates (Fig. 16) can be effectively treated, using the same parametrization. Since the jets, of thickness π , go into $t = \pm iK'/2$, $T = \pm i/\sqrt{k}$, the complex potential can be written

$$(50) \quad W = \frac{1}{2} \ln (T + k^{-1}/T), \quad T = \operatorname{sn}(t + iK'/2).$$

Comparing locations of zeros and poles, we get

$$(51) \quad \zeta = \operatorname{sn}(t - K)/\operatorname{sn} t = -\operatorname{cn} t/\operatorname{sn} t \operatorname{dn} t.$$

Upon integrating $z = \int \zeta^{-1} dW$, one obtains

$$(52) \quad z = \frac{1}{2}[i \ln(i\sqrt{k} \operatorname{sn}(t - iK'/2)) + E(t) - (1 - k)t].$$

From formula (52), one gets the analog of (48),

$$(53) \quad d = \frac{\pi}{2} - E + (1 - k)K, \quad l = \frac{1}{2}[\ln k^{-1} + E' - kK'].$$

The force tending to separate the plates is (Ch. IV, §5) $F = \rho(E' - kK')$.

14. Cusped cavities. Cavities of finite length, ending in a cusp, have frequently been considered, and their existence has been the subject of some controversy. They were introduced in 1876 by M. Brillouin, who later (1911) rejected them [10, p. 170], because they contradicted his principle that cavity pressure²⁶ had to be a minimum, hence (Ch. I, Thm. 2) cavities convex. In 1913, Villat showed that a symmetric cusped cavity behind a wedge was impossible, and conjectured that cusped cavities were mathematically impossible in general.

Although some examples with singularities and some approximate solutions were given earlier, the first explicit construction of a symmetric cusped cavity (behind a curved obstacle) was given by Lighthill²⁷. Here we shall exhibit some cusped cavities behind fish-like bodies. The technique used can be applied more generally to the case of two *bent plates* (wedges) separated by two free streamlines, mentioned at the end of §2.

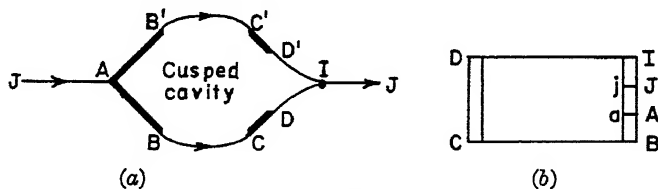


FIG. 17.

Let us consider the flow tentatively drawn in Fig. 17a. It can be viewed

²⁶ Brillouin referred to wakes, for which the principle is not always true [31, p. 422]. However, cusped cavities have never been produced experimentally. Villat's work is in *Ann. fac. sci. Toulouse* 5 (1913), 375-404; see esp. p. 402.

²⁷ ARC RM 2328 (1945). For simple examples with infinite velocities, see U. Cisotti, *Ann. scu. norm. Pisa* 1 (1932), 101-12; C. Schmieden, *Luft. Forschg.* 17 (1940), p. 37. For approximate solutions behind circular obstacles, see M. Kolscher, *Luft. Forschg.* 17 (1940), 154-60; and Southwell and Vaisey [78, p. 159]. See also D. N. de C. Allen, *QJMAM* 2 (1949), 64-71.

a Riabouchinsky model with a "tail" added. BC and DE are free streamlines with velocities which can be 1 and v respectively. Let us map half the flow onto the rectangle R of §1, with BAJE going into the right side (Fig. 17b), CD into the left side and BC and DE into the lower and upper side respectively. The complex potential is clearly

$$(54) \quad W = m'(\operatorname{sn} t - \operatorname{sn} j),$$

where j is the value of t at $z = \infty$.

As to the velocity, we observe that:

$$\arg \zeta = 0 \text{ on } \overline{EA}, \quad \arg \zeta = \alpha_1 \text{ on } \overline{AB}, \quad \arg \zeta = -\alpha_2 \text{ on } \overline{CD};$$

$$|\zeta| = 1 \text{ on } \overline{BC} \quad \text{and} \quad |\zeta| = v \text{ on } \overline{DE}$$

Hence ζ^{π/α_1} satisfies the conditions of Thm. 3 and is a quasi-periodic function. Thus, if $\omega = i \ln \zeta$ as in §3, then $(-i\pi/\alpha_1) d\omega/dt$ is elliptic, takes imaginary values on the boundary and has a pole with residue 1 at $t = a$. Up to an additive constant such a function must coincide with

$$\operatorname{cn} a \operatorname{dn} a / (\operatorname{sn} t - \operatorname{sn} a)$$

and consequently

$$\frac{-id\omega}{dt} = \frac{\alpha_1}{\pi} \frac{\operatorname{cn} a \operatorname{dn} a}{\operatorname{sn} t - \operatorname{sn} a} + C.$$

The constant C can be determined by the condition that the points A and E are of the same level. The jump from A to E can only occur at infinity due to the residue of

$$\frac{dz}{dt} = \zeta^{-1} \frac{dW}{dt} \quad \text{at} \quad t = j,$$

which, therefore, must be zero. In view of the behavior of W at $t = j$, this simply implies $d\omega/dt = 0$ at $t = j$.

Thus C is uniquely determined and

$$(55) \quad \begin{aligned} \frac{-id\omega}{dt} &= \frac{\alpha_1}{\pi} \left[\frac{\operatorname{cn} a \operatorname{dn} a}{\operatorname{sn} t - \operatorname{sn} a} - \frac{\operatorname{cn} a \operatorname{dn} a}{\operatorname{sn} j - \operatorname{sn} a} \right] \\ &= -\frac{\alpha_1}{\pi} \frac{\operatorname{cn} a \operatorname{dn} a (\operatorname{sn} t - \operatorname{sn} j)}{(\operatorname{sn} j - \operatorname{sn} a)(\operatorname{sn} t - \operatorname{sn} a)}. \end{aligned}$$

Recalling that at B , $\zeta = e^{i\alpha_1}$,

$$\zeta = e^{i\alpha_1} \exp \left\{ -\frac{\alpha_1}{\pi} \frac{\operatorname{cn} a \operatorname{dn} a}{\operatorname{sn} j - \operatorname{sn} a} \int_K^t \frac{\operatorname{sn} t - \operatorname{sn} j}{\operatorname{sn} t - \operatorname{sn} a} dt \right\}.$$

Upon integration, this gives

$$(56) \quad \zeta = e^{i\alpha_1} \left(\frac{dc \, t - dc \, a}{dc \, t + dc \, a} \right)^{\alpha_1/2\pi} e^{(\alpha_1/\pi)F(t)}, \quad \text{with}$$

$$F(t) = \prod (t - iK', a, k) - \prod (K - iK', a, k) - (t - k) \frac{cn \, a \, dn \, a}{sn \, j - sn \, a}$$

where $dc = dn/cn$ and $\prod(t, a, k)$ denotes as usual the elliptic integral of the 3rd kind. It is now a matter of inspection to check that the flow defined by (54) and (56) has the qualitative features sketched in Fig. 17a. The details are left to the reader.

If BC is no longer considered free but fixed, one has a cusped cavity flow past a solid bounded by two wedges and two convex curves BC and $B'C'$. This model, however, gives one cusped cavity for each obstacle, because any change of the cavity produces a simultaneous change of the curves BC and $B'C'$, and so of the obstacle. No analytic formula for $\zeta(t, a)$ is known, which gives a one-parameter family of cusped cavities behind a fixed obstacle.

15. Hollow vortices. The case of a hollow vortex in a channel²⁸ (Fig. 18a) can also be treated by the Lemma of §4. We shall assume that the fluid is stagnant at ∞ , that the velocity is one on the vortex boundary and that the flow pattern has a center of symmetry. To parametrize it, we map half the flow (below the dotted line) onto the rectangle $-2K \leq \text{Re}\{t\} \leq 2K$, $0 \leq \text{Im}\{t\} \leq K'$ (Fig. 18b) so that the free boundary goes into the upper

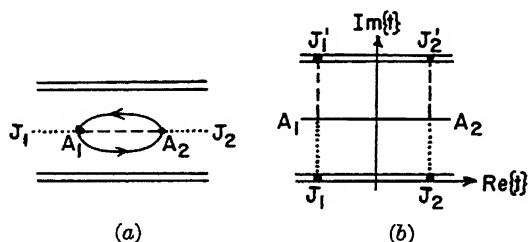


FIG. 18.

side of the rectangle, the lower wall of the channel onto the lower side and the two halves of the line of symmetry onto the vertical sides. Under this mapping, the points at infinity go into $\pm K$. It is clear that the line of symmetry is an equipotential and that the velocity is purely imaginary there. The function $W(t)$ is thus regular, and has constant real part on the vertical sides and constant imaginary part on the horizontal ones. Thus, $W(t)$ must be of the form

$$(57) \quad W = \gamma t/4K + \text{const.},$$

²⁸ Cf. [60] and H. C. Pocklington, Proc. Camb. Phil. Soc. 8 (1894), 173-187.

where the multiplicative constant γ represents the total circulation around the vortex. Again, $\zeta(t)$ is real on J_1J_2 , imaginary on A_1J_1 and A_2J_2 , with modulus 1 on A_1A_2 , and zero at $t = \pm K$. By Thm. 3, these properties uniquely determine $\zeta(t)$ up to sign as an elliptic function with periods $4K$ and $2iK'$. Such a function is however

$$(58) \quad \zeta = \sqrt{k} \operatorname{sn}(t - K) = -\sqrt{k}(\operatorname{cn} t)/(\operatorname{dn} t) = -\sqrt{k} \operatorname{cd} t.$$

We get

$$(59) \quad \begin{aligned} dz &= \zeta^{-1} dW = -\frac{\gamma}{4\sqrt{k}K} \frac{\operatorname{dn} t}{\operatorname{cn} t} dt. \\ z &= \frac{\gamma}{8\sqrt{k}K} \ln \frac{1 - \operatorname{sn} t}{1 + \operatorname{sn} t}. \end{aligned} \quad \text{with}$$

The same method can be applied to a hollow vortex in a regular polygon²³ with n sides, of which the case $n = 4$ of a square is depicted in Fig. 2b, Ch. IV. If a sector of the flow is mapped onto the above rectangle, one gets (57) again, with

$$(60) \quad W = (\gamma t/2nK) + C$$

$$(61) \quad \zeta = [\sqrt{k} \operatorname{sn}(t - K)]^{2/n}$$

where n is the number of sides of the polygon. The integration of z cannot be done in finite terms.

²³ Cf. [60] and G. Greenhill [32, §38 and §45-7]. If the flow is reflected in the vortex, as in Ch. IV, §3, we get the flow between two concentric, similar, regular polygons.

CHAPTER VI

CURVED OBSTACLES

1. Semicircular parametrization. In the present chapter, we shall discuss stationary ideal plane flows with free boundaries past *curved* obstacles. The problem of determining such flows will be reduced, in various cases, to the solution of non-linear integral equations with side conditions. Flows obtained by solving such equations numerically will be described and interpreted physically. The existence of solutions will be proved in Ch. VII and the technique for solving the integral equations will be explained in Ch. IX, §8.

In §§1-6, we shall treat the case of a *divided jet*, and shall assume the flow to satisfy conditions (i)-(iii) of Ch. IV, §1.

Let a jet of width¹ d be divided by a curved obstacle P into two branches J_1, J_2 , as in Fig. 1a. Let C denote the dividing point of the flow, and A, B the points where the flow separates from P . Further, we shall assume that P has finite length and finite curvature², except perhaps at C , where an angle of $\beta\pi$ radians may occur.

We shall assume that the flow is bounded by fixed walls (the wetted portion ACB of P) and by free streamlines of constant pressure. As usual, we shall choose units making $|\zeta| = 1$ on the free boundary. We shall also translate coordinates so that the bisector of $\angle ABC$ is parallel to the positive real axis.

Let ϕ denote (as in Ch. IV, §7) the angle made with the positive real axis by the tangent to P , in the (positive) sense which leaves the flow on the left. Then

$$(1) \quad \phi(C^+) = \phi(C^-) - (1 - \beta)\pi.$$

Further, if l measures arc-length along P from C , the intrinsic equation

$$(2) \quad \phi = \phi(l)$$

will locate P in the physical plane (up to translations).

¹ We include, as limiting cases (d infinite or semi-infinite), a cavity in an infinite stream, and a curved obstacle "planing" near the surface of an ocean. These flows were first described by U. Cisotti, *Rend. Accad. Lincei* (5) 30 (1911), 314-22, 494-502, and H. Villat, *Comptes rendus* 152 (1911), 1081-4.

² In §§1-3, it is enough to assume that the tangential direction ϕ satisfies the Lipschitz condition $|\phi(l_1) - \phi(l_2)| < k |l_1 - l_2|$, where l denotes arc length along the obstacle. In the discussion of separation, stronger conditions are needed (cf. Ch. IV, §7).

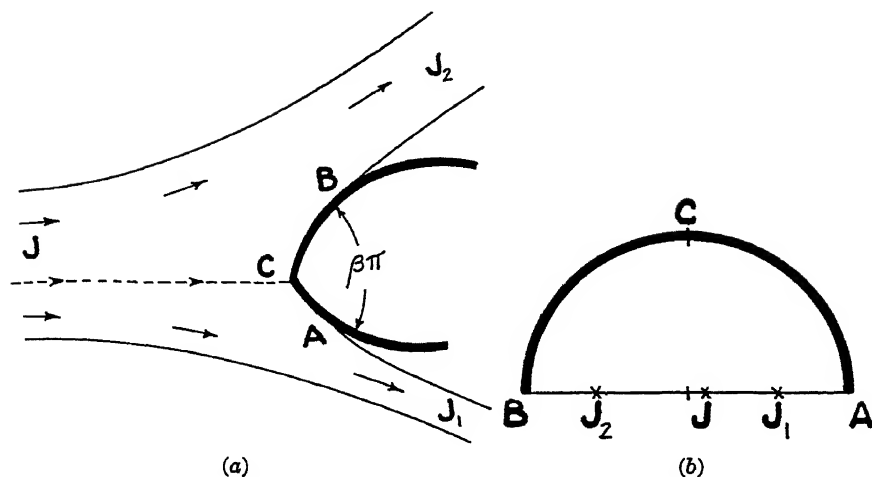


FIG. 1

Following Levi-Civita [54], we shall map the simply connected interior of the flow conformally and one-to-one onto the interior of the semicircle

$$(3) \quad \Gamma: \quad |t| < 1, \quad \text{Im} \{t\} > 0$$

(Fig. 1b). By the Fundamental Theorem of Conformal Mapping, there is exactly one univalent transformation $t = f(z)$ of the domain occupied by the flow onto Γ , which maps A, B, C respectively onto $1, -1$, and i . This transformation $f(z)$ will map the *free* streamlines onto the *real diameter*, and the wetted portion of the *barrier* P onto the *circumference* $t = e^{i\sigma}$ of Γ , as indicated in Figs. 1a-1b. (In this respect, it is the opposite of the parametrization used in Chs. II-III.)

To express the complex potential, it is convenient to map Γ on the upper half-plane by the conformal transformation

$$(4) \quad T = -(t + t^{-1})/2, \quad \text{so that} \quad dT/dt = -(1 - t^{-2})/2.$$

By Theorem 2 and Remark 5 of Ch. III, the complex potential then satisfies, for some $M^* > 0$

$$\frac{dW}{dT} = \frac{M^* T}{(T - T_0)(T - T_1)(T - T_2)},$$

since there are no interior stagnation points, and the dividing point $t = i$ occurs when $T = 0$. In order to include the limiting cases when one or more $T_k = \infty$, and because $|T_k| > 1$ in any case, we write this equation in the alternative form

$$(5) \quad \frac{dW}{dT} = \frac{MT}{\prod_{k=0}^2 (1 - \alpha_k T)} \quad [M > 0, \quad -1 < \alpha_k < 1],$$

where $\alpha_k = T_k^{-1}$.

2. The function $\Omega(t)$. By relation (30) of Ch. III, there are no interior stagnation points. Thus $\zeta(t)$, which is analytic and regular, does not vanish in Γ . We shall now prove that ζ cannot vanish at any point other than C in the closure $\bar{\Gamma}$ of Γ . These facts are also intuitively plausible.

Indeed, since $\zeta = (dW/dz) = (dW/dT)/(dT/dz)$ is nowhere zero on the free streamline, we need not consider $T = \infty$. Elsewhere in $\bar{\Gamma}$, $dW/dT \neq 0$ by (5) except at C , where $T = 0$ and dW/dT has a simple zero. The facts that $dT/dz \neq 0, \infty$ for $T \neq 0$, and $dT/dz \sim T^{1-\beta}$ near $T = 0$, are however classic results³ about conformal mapping which complete the proof. In particular, in the vicinity of $T = 0$, $\zeta \sim T^\beta$, showing that, unless C is a cusp ($\beta = 0$) ζ vanishes at C .

Now consider the function $(i - t)/(i + t) = (1 + it)/(1 - it)$. It has modulus one when t is real, and its argument is by elementary geometry, $\pi/2$ on \widehat{AC} and $-\pi/2$ on \widehat{CB} , with a jump of $-\pi$ at C . Hence the new function $\Omega(t) = \theta + i\tau$, defined by the equations

$$(6) \quad \zeta = \left(\frac{1 + it}{1 - it} \right)^\beta e^{-i\Omega(t)}, \quad \zeta^{-1} = \left(\frac{1 - it}{1 + it} \right)^\beta e^{i\Omega(t)},$$

is still analytic and regular in the interior of Γ . On the free boundary, when t is real, $|1 + it| = |1 - it|$, and so

$$(7) \quad 1 = |\zeta| = \left| \frac{1 + it}{1 - it} \right|^\beta e^{\tau(t)} = e^{\tau(t)}.$$

Hence $\tau(t)$ vanishes on the real diameter of Γ . That is, $\Omega(t)$ is *real on the real diameter of Γ* .

It follows, by Schwarz's Principle of reflection (Ch. III, §2), that $\Omega(t)$ can be extended to an analytic function, regular inside the unit circle and, as we shall see, bounded on its perimeter. We can therefore write

$$(8) \quad \Omega(t) = a_0 + a_1 t + a_2 t^2 + \cdots, \quad \text{all } a_i \text{ real,}$$

where the radius of convergence of the series (8) is at least one. On the fixed boundary $|t| = 1$, the boundedness of $\Omega(t)$ is equivalent by (6) to that of $\zeta(t)$ for $t \neq i$, and to that of ζ/T^β for $t = i$. A more refined argument permits one to prove that $\Omega(t)$ is even continuous in the closed unit circle (Cf. Remark at the end of §3).

³ W. Seidel, Math. Annalen 104 (1930), p. 222; C. Carathéodory, "Conformal representation", Cambridge Univ. Press, 1932, pp. 91, 94.

Conversely, given a function $\Omega(t)$ with expansion (8) and continuous on $|t| = 1$, and given constants β , M , α_0 , α_1 , and α_2 , equations (6), (5), (4) and

$$(9) \quad z = \int_i^t \zeta^{-1} \left(\frac{dW}{dT} \right) \left(\frac{dT}{dt} \right) dt$$

define a "divided" jet flow past a barrier P , having an angle β at the dividing point $z = 0$, and a continuously turning tangent elsewhere. This gives Levi-Civita's classical result⁴.

THEOREM 1. The divided jets past barriers with vertex angle $\beta\pi$ correspond to choices of functions $\Omega(t)$, regular for $|t| < 1$ and continuous on $|t| = 1$, and of constants M , α_0 , α_1 , α_2 . The correspondence is through equations (4), (5), (7), and (9).

Using Theorem 1, it is easy to construct a large class of divided jets and cavities behind curved obstacles⁵. Thus, in the symmetric case (see §5), a large and typical family is given by the *trinomials*

$$\Omega(t) = a_1 t + a_3 t^3 + a_5 t^5$$

(see Ch. IX, §8). The case $\Omega(t) = 0$ gives a wedge (Ch. II, §4).

3. Geometrical interpretations. By Theorem 1, Levi-Civita may be said to have solved the *inverse* problem of describing the class of *all* jets divided by curved barriers⁶. We shall now turn to the direct problem: Given a particular curved obstacle P held in a particular jet, what is $\Omega(t)$?

To solve this problem, it is convenient first to express various geometrical quantities in terms of the unknown function $\Omega(t)$.

Along the fixed boundary $t = e^{i\sigma}$, we get from (8), for $\Omega = \theta + i\tau$

$$(8a) \quad \theta = a_0 + a_1 \cos \sigma + a_2 \cos 2\sigma + \dots$$

$$(8b) \quad \tau = a_1 \sin \sigma + a_2 \sin 2\sigma + \dots \quad \left. \vphantom{\begin{matrix} (8a) \\ (8b) \end{matrix}} \right\} \text{ on } t = e^{i\sigma}.$$

It is convenient to consider also the derivative

$$(8c) \quad \lambda(\sigma) = -d\theta/d\sigma = a_1 \sin \sigma + 2a_2 \sin 2\sigma + \dots$$

⁴ [54]; see also [49]. Levi-Civita treated only the case $\alpha_0 = \alpha_1 = \alpha_2 = 0$ of an infinite stream, but his argument needs only minor modifications.

⁵ Many examples are given in [32, Appendix]. The first cavity flow past a curved obstacle, having a crescent for hodograph, was obtained by G. Kirchhoff, *Vorlesungen über Mechanik*, Leipzig, 1874, p. 293, using conformal mapping. Recently, Lighthill has used this hodograph method effectively to illustrate the bending of jets around obstacles ("Coanda effect") in ARC RM 8943, and to exhibit a flow with a cusped cavity (Ch. V, §14).

⁶ As remarked by M. Brillouin [10], some of these flows are self-overlapping in the large.

We do not assume that the series on the right of (8a)–(8c) converge; the equal signs mean only that they are the formal Fourier expansions of the functions on the left.

We shall first show that $\theta(\sigma)$ is simply related to the obstacle tangential direction. Since $\arg dz/dT = \arg \zeta^{-1} + \arg dW/dT$ and $\arg dz/dT = \phi$ (except at C), evidently

$$\arg \zeta^{-1} = \begin{cases} \phi - \pi & \text{on } \widehat{AC} \\ \phi & \text{on } \widehat{CB}. \end{cases}$$

(See also Fig. 1a, and the Remark below.)

On the other hand, by our discussion of $\arg (i - t)/(i - t)$

$$\arg \zeta^{-1} = \begin{cases} \theta - \beta\pi/2, & \text{on } \widehat{AC}. \\ \theta + \beta\pi/2, & \text{on } \widehat{CB}, \end{cases}$$

whence by comparison with the previous evaluation of $\arg \zeta^{-1}$, one gets

$$(10) \quad \theta = \begin{cases} \phi - \pi + \frac{\beta\pi}{2} = \phi - (1 - \beta) \frac{\pi}{2} - \frac{\pi}{2} & \text{on } \widehat{AC}, \\ \phi - \frac{\beta\pi}{2} = \phi + (1 - \beta) \frac{\pi}{2} - \frac{\pi}{2} & \text{on } \widehat{CB}. \end{cases}$$

Clearly, θ is then equal to the angle with the y -axis of the tangent to the “straightened barrier” P_1 , obtained from P by rotating \widehat{AC} and \widehat{CB} until they become vertical. Unlike ϕ , θ is a continuous function of l even at C . The condition that $\theta = 0$ when $\sigma = \pi/2$ and $t = i$ amounts, by (8a), to

$$(10') \quad a_0 = a_2 - a_4 + a_6 - \dots$$

In the most interesting case of a smooth obstacle, $\beta = 1$ and $\theta = \phi - \pi/2$ all along \widehat{ACB} .

From equation (10), we see by inspection the interesting fact that the case of a *wedge* with straight sides (Ch. II, §4 and Ch. III, §7) is simply the case $\theta = 0$, whence $\tau = 0$ and $\Omega(t) = 0$, by (8a)–(8b).

Arc-length along P can be found by evaluating (9), which gives⁷

$$dl = |\zeta^{-1}| \cdot |dW/dT| \cdot |dT/dt| \cdot d\sigma.$$

By (7), on $t = e^{i\sigma}$,

$$\begin{aligned} |\zeta^{-1}| &= \left| \frac{1 - it}{1 + it} \right|^\beta \cdot |e^{i\theta - \tau}| \\ &= \left| \frac{2 + 2 \sin \sigma}{2 - 2 \sin \sigma} \right|^{\beta/2} e^{-\tau} = \left| \frac{1 + \sin \sigma}{\cos \sigma} \right|^\beta e^{-\tau}, \end{aligned}$$

⁷ The existence of $dl/d\sigma$ follows from known theorems on conformal mapping (cf. V. Smirnov, *Math. Annalen* 107 (1932), 313–32). For a careful discussion, see [49, p. 163].

using the identity $it = -\sin \sigma + i \cos \sigma$ to evaluate $|(1 - it)/(1 + it)|$. Similarly, by (4) and (5), since $T = -\cos \sigma$,

$$\left| \frac{dW}{dt} \right| = \frac{M |\cos \sigma \sin \sigma|}{\prod_{k=0}^2 (1 + \alpha_k \cos \sigma)} \quad \text{on} \quad t = e^{i\sigma}.$$

For given $\beta, \alpha_0, \alpha_1, \alpha_2$ we may define $\nu(\sigma)$ as the particular function

$$(11) \quad \nu(\sigma) = \frac{\sin \sigma (1 + \sin \sigma)^\beta |\cos \sigma|^{1-\beta}}{\prod_{k=0}^2 (1 + \alpha_k \cos \sigma)}.$$

In terms of $\nu(\sigma)$, we then get by direct substitution in the preceding equations,

$$(12) \quad dl = M\nu(\sigma) e^{-\tau(\sigma)} d\sigma.$$

Using this relation, we can express the curvature κ along P . Defining κ as $-d\phi/dl$, we have by (9), (8c) and (11)

$$(13) \quad \kappa = \lambda(\sigma) e^{\tau(\sigma)} / M\nu(\sigma)$$

Remark. We now prove that $\Omega(t)$ is continuous in $|t| \leq 1$. Let $\theta = \theta(l)$ denote the angle between the y -axis and the straightened obstacle, as a function of l . By hypothesis², $\theta(l)$ satisfies a Lipschitz condition all along ACB . Since also ACB has a continuous tangent (except for an angle $\beta\pi$ at C), the correspondence $l = l(\sigma)$ between ACB and the circumference $t = e^{i\sigma}$ satisfies a Lipschitz condition of order arbitrarily close⁸ to $\min(2 - \beta, 1)$ on the interval $0 \leq \sigma \leq \pi$. Therefore, $\theta(\sigma) = \theta(l(\sigma))$ is itself Lipschitzian on $0 \leq \sigma \leq \pi$. Since $\theta(\sigma)$ is even, it is also Lipschitzian on $-\pi \leq \sigma \leq 0$. By the Fatou-Privaloff Theorem (Ch. IV, §7), it follows that $\Omega(t)$ also satisfies a Lipschitz condition on $t = e^{i\sigma}$ —and hence is continuous on the closed disc $|t| \leq 1$. As a corollary, $\zeta(t)$ is also continuous and vanishes at C only.

Thus, we have shown that the divided jets under consideration are “simple flows” in the sense of Ch. III, §2. Conversely, we have shown that, when all free boundaries are at the same pressure, conditions (iii)–(iv) of Ch. III, §2, can be replaced by the weaker conditions (iii') the fixed boundaries have Lipschitzian tangents, and (iv') the velocity is everywhere bounded.

4. Basic integral equations. It is evident from formulas (8a)–(8c) and (10') that any one of the three real functions on $0 < \sigma < \pi$ determines the other two, if (10') is used. The relation is given either through the

² M. Lavrentieff, *Rec. Math. Moscou* 36 (1929), 112–15.

Fourier coefficients of these formulas, or by the three integral operators⁹ C, J, D defined by

$$(14a) \quad C\theta(\sigma) = \tau(\sigma) = \frac{\sin \sigma}{\pi} \int_0^\pi \frac{\theta(\sigma) - \theta(\sigma')}{\cos \sigma - \cos \sigma'} d\sigma'$$

$$(14b) \quad J\lambda(\sigma) = \theta(\sigma) = \int_\sigma^{\pi/2} \lambda(\sigma') d\sigma'$$

$$(14c) \quad D\lambda(\sigma) = \tau(\sigma) = \int_0^\pi D(\sigma, \sigma') \lambda(\sigma') d\sigma', \quad \text{where}$$

$$(14d) \quad D(\sigma, \sigma') = \frac{2}{\pi} \sum_{j=1}^{\infty} \frac{\sin j\sigma \sin j\sigma'}{j} = \frac{1}{\pi} \ln \left| \frac{\tan \frac{1}{2}\sigma + \tan \frac{1}{2}\sigma'}{\tan \frac{1}{2}\sigma - \tan \frac{1}{2}\sigma'} \right|.$$

In (14a)–(14c), the pairs of letters $C\theta$, $J\lambda$, $D\lambda$ do *not* represent composite functions; thus $C\theta(\sigma) = C[\theta(\sigma)]$ is not, for any individual $\sigma = \sigma_1$, a function of the number $\theta(\sigma_1)$; it is the value at σ_1 of the conjugate of the entire function $\theta(\sigma)$. The integral operators J and D will be discussed in Ch. VII, §5.

Taking advantage of these relations, one can easily reformulate the direct problem of finding $\Omega(t)$ for a given barrier P in terms of a system of *integral equations* with one or more unknown parameters.

Thus, for given P , if l is measured from the dividing point C , the quantity θ is easily expressed by (10) as a function $\theta = \Theta(l)$ of l . The flows past P are then characterized, in virtue of (12) and (14a), by the fact that

$$(15) \quad l(\sigma) = M \int_{\pi/2}^\sigma \nu(\sigma) e^{-C\Theta(l(\sigma))} d\sigma.$$

This formulation of the direct problem is due to Villat [83].

We have developed¹⁰ an alternative formulation, which seems well adapted to computation in the case of barriers having *curvature of constant sign* (i.e., no points of inflection). For given P , using (10), one can easily express the curvature κ as a function $\kappa = K(\theta)$ of the pseudo-tangent angle θ . Using (13) and (14b)–(14c), the divided jet flows past a given barrier P are then characterized by the fact that $\lambda(\sigma)$ in (8c) satisfies the functional equation

$$(16) \quad \lambda = M\nu K(J\lambda) e^{-D\lambda}.$$

where $\nu = \nu(\sigma)$ is given by (11). Thus we have proved

⁹ The integral form of the conjugation operator C can be deduced from the limiting form of the Poisson integral; see also A. Zygmund, "Trigonometric series", p. 146. The expression for the conjugate integral D is due to Dini, *Annali di mat.* 5 (1871), 305–45.

¹⁰ The curvature function was previously used by Brodetsky [11, 12], Nekrassoff [63], and others to find τ .

THEOREM 2. For a flow given by Theorem 1 to involve a barrier P having the intrinsic equation $\theta = \Theta(l)$, it is necessary and sufficient that (15) hold; if P has curvature $\kappa = K(\theta)$ of constant sign, it is necessary and sufficient that (16) hold.

5. Symmetric cavities. Apart from other difficulties, the solution of the direct problem by (15) or (16) is complicated, in the general case, by the fact that one does not know M , α_0 , α_1 , or α_2 . Thus *there are four free parameters in the general case.*

In the important special case of a *symmetric cavity in an infinite stream*, however, every parameter except M is known a priori. Thus $\alpha_0 = 0$ since C is on the axis of symmetry of P ; and $\alpha_0 = \alpha_1 = \alpha_2 = 0$ since, in (5), $W = MT^2/2$ as in Ch. II, §2. This greatly simplifies (11); in the most important case $\beta = 1$ of a smooth obstacle, $\nu(\sigma)$ reduces to the function

$$\nu(\sigma) = \sin \sigma(1 + \sin \sigma).$$

Again, in the symmetric case, $\theta(\pi - \sigma) = -\theta(\sigma)$, so that by (8a) $a_0 = a_2 = a_4 = \dots = 0$, and $\Omega(t)$ is an *odd* function

$$\Omega(t) = a_1 t + a_3 t^3 + a_5 t^5 + \dots \quad (\text{symmetric case}).$$

The curvature function is also easily expressed in such simple cases as that of an *ellipse*, when we can take $K(\theta) = [\cos^2 \theta + C^2 \sin^2 \theta]^{3/2}$, a *parabola*, when $K(\theta) = \cos^3 \theta$, or a *cycloid*, when $K(\theta) = \sec \theta$. Note that the absence or presence of a constant factor in $K(\theta)$ does not affect $\Omega(t)$; such a factor simply corresponds to a reciprocal factor in M .

Since the angular extent of the wetted portion of a barrier (or solid cylindrical obstacle) having the intrinsic equation $\kappa = K(\theta)$ is nowhere reflected in the integral equations (15) and (16), one easily surmises that this extent is determined by the choice of M . Theorems bearing on this surmise are discussed in Ch. VII, §4-6; they are quite deep. Using (8a), (8c) and (10), one can however show very easily that the angular extent $2\theta_*$ of the wetted portion of the "straightened barrier"¹¹ is given by

$$(17) \quad \theta_* = a_1 + a_3 + a_5 + \dots = \frac{1}{2} \int_0^\pi \lambda(\sigma) d\sigma.$$

Again, by formula (17) of Ch. IV, the drag D is given by

$$(18) \quad D = \rho \pi M (2 - a_1^2) / 4.$$

From this, the drag coefficient C_D based on the wetted cross-section is easily computed. Moreover, the condition for a *cavity of zero drag* is clearly $a_1 = 2$. In Table I, we have tabulated the separation angle ϕ_* , M , C_D , and the

¹¹ By this, we mean $\int_0^\pi \kappa dl$, which is simply $\phi(\pi) - \phi(0)$ if $\beta = 1$.

TABLE I

	ϕ_a	C_D	M	a_1	a_3	a_5	a_7	a_9	a_{11}	a_{13}	a_{15}	a_{17}	a_{19}	a_{21}	a_{23}
Convex circular arcs	15°	.81912	.18196	.26704	-.00433	-.00065	-.00016	-.00006							
	30°	.76988	.44723	.52928	-.00149	-.00079	-.00023	-.00009							
	45°	.67766	.81727	.77811	.00746	.00003	-.00010	-.00005							
	60°	.57024	1.31730	1.02394	.02165	.00205	.00037	.00011							
Concave circular arcs	120°	.00766	5.26837	1.93914	.11679	.02420	.00767	.00308	.00146	.00078	.00046	.00020	.00021	.00010	.00013
	-22.5°	.93330	.15579	-.41618	.02263	.00045	.00025	.00008	.00004	.00002	.00001	.00001			
	-45°	.96694	.21367	-.86256	.09912	-.00296	.00076	.00010	.00007	.00003	.00002	.00001			
	45°	.66478	1.24304	.83302	-.05185	.00504	-.00080	.00005							
Parabolic arcs	60°	.52856	3.27640	1.15648	-.13087	.03616	-.00636	.00164	-.00046	.00012	-.00004	.00001	-.00007	.00032	
	75°	.32358	14.22544	1.55506	-.31076	.10667	-.04463	.02069	-.00992	.00466	.00253	.00128	-.00007		
Zero drag	Circle 124.21°	0.0	5.71464	2.00000	.12518	.02681	.00858	.00349	.00167	.00089	.00053	.00035	.00024	.00018	.00016
	1:2 ellipse 110.44°	0.0	18.03004	2.00000	-.17274	.10831	-.02371	.01655	-.00448	.00330	-.00089	.00078	-.00014	.00022	
	2:1 ellipse 140.58°	0.0	2.03067	2.00000	.46700	.01776	-.03348	-.00075	.00480	.00320	.00065	.00003	.00017	.00024	

coefficients a_1, a_2, a_3, a_7, a_9 , for cavity flows past several symmetric barriers¹². The method of computation is explained in Ch. IX, §8.

6. Brillouin-Villat separation condition. The prediction of the separation angle, in the case of a smooth solid obstacle, is not touched by the preceding discussion.

In the case of wakes, the actual location of the separation points depends on several physical parameters (see Ch. I, §5). However, in the case of a vapor-filled cavity, and more generally (approximately) in the case of the air-filled cavity behind a high-speed missile¹³, one can use any of four rather simple conditions, first noted by M. Brillouin [10, p. 180].

In these cases (cf. Ch. I, §13), we can argue that the *pressure must be a minimum in the cavity*. For otherwise, even small reductions in the pressure coefficient $C_p = p/\frac{1}{2}\rho v^2$ would induce cavitation elsewhere. This implies that the free streamlines must be *convex* towards the cavity, in the direction of the negative pressure gradient (Ch. I, Thm. 2). By Bernoulli's Theorem, it is also equivalent to the condition that the *velocity is a maximum on the free streamlines*.

Assuming convexity, for the flow not to penetrate the solid obstacle (assumed in §1 to have finite curvature), the *free streamlines must have finite curvature at the separation points A, B*. In fact, the local curvature of the obstacle cannot be exceeded. Villat [85] has given a neat mathematical criterion for this last of Brillouin's four conditions to be satisfied.

THEOREM 3. The curvature at the separation points A, B , where $t = \pm 1$, is infinite towards the cavity, infinite away from the cavity, or equal to the curvature of the obstacle, according as

$$(19a) \quad \tau'(\pi) > -\beta, \quad \tau'(\pi) < -\beta, \quad \text{or} \quad \tau'(\pi) = -\beta \quad \text{for } A,$$

$$(19b) \quad \tau'(0) < \beta, \quad \tau'(0) > \beta, \quad \text{or} \quad \tau'(0) = \beta \quad \text{for } B.$$

Proof. The conclusion is simply a restatement of Theorem 6, Ch. IV, in terms of $\Omega(t)$. To see this, note that the function $\omega = i \ln \zeta$ of Ch. IV, §7, equals $\Omega(t) + i\beta \ln [(1+it)/(1-it)]$ by (6). The result is now obvious.

Since $\tau' = -\sum k a_k \cos k\sigma$, the first equality in the following corollary is also obvious (cf. (14a)). The limiting form of the Poisson integral permits us to express $\tau'(\sigma)$ in terms of its conjugate function $-\lambda(\sigma)$, and gives the second equality.

COROLLARY. The curvature of a symmetric divided jet is finite at the

¹² Our results for the cavity of zero drag behind a circle are in a fair agreement with those of C. Schmieden, Ing. Archiv 3 (1933), 356-70, and 5 (1934), 373-5.

¹³ By a "high-speed" missile, we mean one travelling at 300 f/s or more, so that the Thoma cavitation number is small.

TABLE II

1:2 ellipse	64.54°	.49656	2.86016	1.19982	-.08574	.01438	-.00262	.00055
1:1 ellipse (circle)	55.04°	.60838	1.13593	.94277	.01643	.00123	.00017	.00004
3:2 ellipse	49.06°	.66520	.66949	.79162	.05838	.00544	.00063	.00011
2:1 ellipse	44.78°	.53426	.46336	.68893	.07902	.01140	.00180	.00033
Cycloid	51.42°	.64328	.86336	.85378	.03769	.00488	.00088	.00019

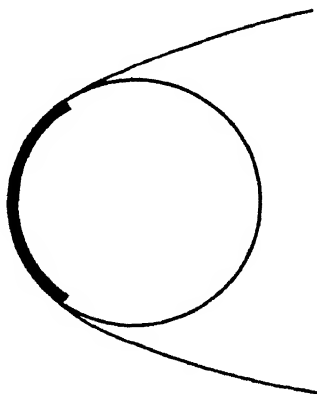


FIG. 2.

separation points if and only if

$$(19c) \quad \beta = a_1 + 3a_3 + 5a_5 + \cdots = \pi^{-1} \int_0^\pi \lambda(\sigma) \csc \sigma \, d\sigma.$$

Of these two forms, the integral form is more general.

We shall refer to conditions (19a)–(19c) as conditions for *smooth separation*, and to cavities satisfying them as *cavities behind solid obstacles*. In Table II, we list ϕ_s , C_D , M , a_1 , ..., a_5 for the symmetric cavities behind various solid obstacles, together with the appropriate wetted angles and drag coefficients¹⁴. Fig. 2 shows the free streamlines in the case of a solid circular obstacle.

7. Asymmetric case: parameter problem. In the asymmetric case, the parameter problem is a good deal more complicated. If the barrier has a sharp vertex, then the dividing point must be at the vertex to avoid infinite velocities. The procedure of §§1–4 is still applicable, but the problem is overdetermined, as in the case of a wedge (Ch. II, §4). There are only

¹⁴ In this tabulation, the drag coefficient C_D is based on the obstacle diameter. The case of the circle was first treated by Brodetsky [11, 12]. C. Schmieden, *Ann. der Physik* 2 (1929), 350–6, gives a comparison with experiment.

four parameters to meet the five conditions fixing separation at the ends of the barrier, the width and direction of the impinging jet, and the distance from the vertex to the jet midline.

The case $\beta = 1$ of a smooth obstacle is better discussed in terms of the original parametrization of Levi-Civita [54]. This also maps the flow conformally onto the semicircle Γ of (3), so that ACB is mapped onto the circumference, and the free boundary onto the real diameter. However, the flow is rotated so that the impinging jet is parallel to the positive real axis, and the point J at infinity on the impinging jet is mapped onto $t = 0$. In the symmetric case, the dividing point C is still mapped on $t = i$, and §§1-6 apply. But in general, the image $t_0 = e^{i\sigma_0}$ of C is *unknown*, as are those t_1, t_2 of the outgoing jets. Corresponding to (5), one has

$$(5') \quad \frac{dW}{dT} = \frac{M(T - T_0)}{(1 - \alpha_1 T)(1 - \alpha_2 T)}$$

where $T_0 = -(t_0 + t_0^{-1})/2$, $\alpha_i = -2/(t_i + t_i^{-1})$.

In place of (6), one writes

$$(6') \quad \zeta^{-1} = ((tt_0 - 1)/(tt_0^{-1} - 1))e^{i\Omega_1(t)}, \quad \Omega_1(t) = \theta_1(t) + i\tau_1(t).$$

Like $\Omega(t)$, $\Omega_1(t)$ is regular in $|t| < 1$, real on the real axis, and continuous on the boundary. Theorem 1 holds with σ_0 in place of t_0 . In addition, $\Omega_1(0) = 0$, so that $\alpha_0 = 0$ in the analog of (8a).

As to the geometrical interpretation one obtains, as in §3:

$$\theta_1(\sigma) = \psi + \left(\frac{\pi}{2} - \sigma_0\right); \quad dl = M\nu_1(\sigma)e^{-\tau_1(\sigma)}; \quad \kappa = \lambda_1(\sigma)e^{\tau_1(\sigma)}/M\nu_1(\sigma),$$

where ψ is the angle of the positive tangent with the y -axis, and

$$\nu_1(\sigma) = \sin \sigma (1 - \cos(\sigma + \sigma_0))/(1 - \alpha_1 \cos \sigma)(1 - \alpha_2 \cos \sigma).$$

Villat's equation becomes

$$(15') \quad l(\sigma) = M \int_0^\sigma \nu_1(\sigma') e^{-C[\Theta(l(\sigma'))]} d\sigma';$$

similarly, the curvature equation takes the form

$$(16') \quad \lambda_1 = M\nu_1 K(J_1 \lambda_1 - \sigma_0') e^{-D\lambda_1}, \quad \sigma_0' = \frac{\pi}{2} - \sigma_0.$$

Here $\Theta(l)$ indicates the tangential direction as a function of the arc-length measured from the endpoint A , and $K(\psi)$ is the obstacle curvature as a function of the tangential direction. J_1 is the integral operator

$$J_1 \lambda = b_0 + \int_\sigma^\pi \lambda(\sigma) d\sigma, \quad b_0 = -\frac{1}{\pi} \int_0^\pi \sigma \lambda(\sigma) d\sigma.$$

Finally the conditions for smooth separation at A and B become

$$\tau_1'(\pi) = -\tan(\sigma_0/2), \quad \tau_1'(0) = \cot(\sigma_0/2),$$

respectively. In terms of $\lambda_1(\sigma)$ these are simply

$$(19') \quad \frac{1}{\pi} \int_0^\pi \lambda_1(\sigma) \tan \frac{\sigma}{2} d\sigma = \tan \frac{\sigma_0}{2}; \quad \frac{1}{\pi} \int_0^\pi \lambda_1(\sigma) \cot \frac{\sigma}{2} d\sigma = \cot \frac{\sigma_0}{2}.$$

The preceding formulas show how the integral equation (16') depends on four real parameters: M , σ_0 , t_1 , t_2 . In any reasonable mathematical formulation of a physical problem, one would expect the number of parameters to equal the number of natural geometrical or physical conditions.

This requirement of "reasonableness" is fulfilled in the case of a smooth barrier held in a jet, where there are four conditions to fulfill: two separation conditions, one condition fixing the width of the impinging jet, and one condition giving the distance from, (say), A to the jet midline. The case of a smooth solid obstacle involves the same parameters and conditions, the conditions for separation being given by (19').

The limiting case of a barrier in an infinite stream contains only the two parameters M and σ_0 , which presumably are determined by the two separation conditions, as one would expect from physical intuition.

On the other hand, the case of a planing barrier with given orientation involves three parameters. It would be natural to suppose that one of these represented the depth of the cylinder submergence. This is however not true, as already shown in Ch. III, §6.

8. Analogs of Réthy flows. The case of a *symmetrically* divided jet reduces, in the case $K(\theta) = 0$ of a flat plate, to a reflected Réthy flow of the type discussed in Ch. II, §7 (see Figs. 11a–11c there). Corresponding figures for the case of a curved barrier, held symmetrically in a jet from a straight nozzle, are shown in Figs. 3a–3b¹⁵. One can modify the Levi-Civita parametrization, mapping half the flow on the quarter-circle.

By reflection, one gets a single-valued function $\Omega(t) = a_1 t + a_3 t^3 + a_5 t^5 + \dots$ defined in the unit circle, just as in §§2–3; moreover the geometrical interpretation of §§4–6 holds without change, *provided* attention is restricted to the symmetric case, and *provided* the formulas involving dW/dT are changed correctly. To find dW/dT , use the transformation $t \rightarrow (t + t^{-1})^2/4 = T^2$ to map half the flow onto a half-plane. Theorem 2 of Ch. III then applies with T^2 in place of T , giving

$$(21) \quad dW/dT = MT/(1 - T^{-2}T^2)(1 - T^{-2}T^2),$$

¹⁵ Treated by U. Cisotti, Rend. cir. mat. Palermo 23 (1909), 307–52; H. Villat, Bull. Soc. Math. France 40 (1912), p. 266. See also E. B. Schieldrop, Sk. Norske Vidensk. Akad. 1 (1928) No. 2.

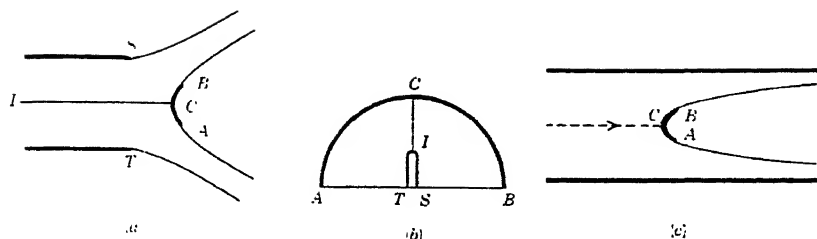


FIG. 3.

where T_I and T_J correspond to the upstream and downstream points at infinity. If v is the upstream velocity and d the channel width, clearly

$$(21a) \quad vd = \pi M / (T_J^{-2} - T_I^{-2}).$$

On the boundary, $T = -\cos \sigma$, and substituting in the expression for dl in §3, one finds

$$(21b) \quad v(\sigma) = \frac{\sin \sigma (1 + \sin \sigma)^\beta |\cos \sigma|^{1-\beta}}{(1 - \alpha^2 \cos^2 \sigma)(1 + \gamma^2 \cos^2 \sigma)}$$

where we have set $\alpha = T_I^{-1}$ and $\gamma = -iT_I^{-1}$. Clearly α and γ are real, and $|\alpha| < 1$. Formula (21b) can be simplified in the case of a symmetrically divided free jet, since $\gamma = 0$, and in the case of a curved barrier symmetrically placed in an infinitely long channel (Fig. 3c), when $\alpha = 0$.

By reflecting the flow of Fig. 3c in the channel wall, we can get symmetric jets from curved nozzles, at the end of infinite straight pipes. Figs. 4a-4b illustrate two cases, with $\beta = 0, 1$, respectively. More general jets from nozzles are considered in §14.

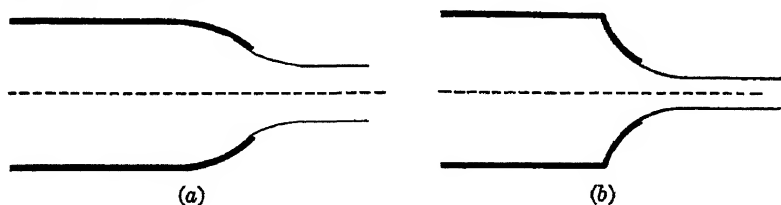


FIG. 4.

9. Physical applications. Most quantities of physical interest have quite simple expressions in terms of our basic parameters. We shall briefly derive some of the more useful formulas, and give some numerical results of possible interest.

If the upstream point at infinity is at $t = is$, then $\gamma = 2s/(1 - s^2)$. The ratio v of the (upstream) channel velocity at infinity to the (downstream) free streamline velocity is, using (7),

$$(22) \quad v = \left(\frac{1-s}{1+s} \right)^{\beta} e^{a_1 s - a_3 s^3 + a_5 s^5 \dots}$$

Similarly, if the ends of the jets correspond to $t = \pm r$, then $\alpha = 2r/(1 + r^2)$. The corresponding velocities $\zeta = e^{\pm i\delta}$ at infinity are given by

$$(23) \quad \delta = 2\beta \arctan r - a_1 r - a_3 r^3 - a_5 r^5 - \dots$$

Knowing v , one can compute the channel width d from the expression for M in (21a)

$$(24) \quad vd = \pi M / (\alpha^2 + \gamma^2).$$

Finally, the drag D is the difference

$$(25) \quad D = vd (\cos \delta - v) = \pi M (\cos \delta - v) / (\alpha^2 + \gamma^2)$$

between the time rates of efflux and influx of horizontal momentum (cf. Ch. I, §10).

Of considerable interest for applications is the case of an obstacle of diameter b in an infinite channel of breadth d . Table III gives, for solid

TABLE III

d/b	ϕ_s	v	Q	C_D	$\frac{C_D}{1+Q}$	s	M	a_1	a_3	a_5
∞	54.988°	1.000	.000	.499	.499	.0	1.134	.941	.017	.002
49.747	55.280°	.899	.236	.621	.503	.1	1.293	.948	.015	.001
14.026	56.159°	.809	.526	.778	.509	.2	1.394	.972	.007	.001
7.076	57.610°	.729	.880	.974	.518	.3	1.428	1.010	-.006	.001
4.522	59.596°	.658	1.306	1.216	.527	.4	1.718	1.063	-.026	.003
3.271	62.198°	.597	1.809	1.495	.532	.5	2.210	1.135	-.056	.006

TABLE IV

Solid circular obstacle in a free jet

d/b	ϕ_s	δ	r	M	a_1	a_3	a_5	a_7	a_9
2.8571	50°39'52"	23°13'33"	.3782	.7965	.8337	.0446	.0049	.0008	.0002

Solid circular obstacle in jet from nozzle

d/b	l/b	ϕ_s°	δ°	v	r	s	M	a_1	a_3	a_5
2.395	1.779	50.408	25.409	.801	.419	.186	.5484	.827	.045	.007
6.904	.888	54.968	11.830	.804	.200	.200	.1129	.940	.017	.002
2.922	.023	57.119	15.709	.639	.289	.400	1.1579	.999	-.006	.004

(nearly) circular cylinders, the variation with the ratio d, b of channel width to obstacle width, in r , $Q = 1 - r^{-2}$, C_D (based on downstream velocity), s , and the separation angle ϕ_s . The changes in the entries C_D give a measure of the *wall effect*.

Table IV gives corresponding results for solid circular cylinders in jets and jets from nozzles. The tabulated results were calculated in almost all cases using a three-point approximation (Ch. IX, §8). However, the results agree pretty well with more accurate^{15a} sample calculations using 24 points.

10. Cusped cavities. Symmetric cusped cavities (Fig. 5) behind convex obstacles in an infinite stream can also be treated by mapping the flow conformally onto the semicircle Γ of Fig. 1b. The complex potential evidently

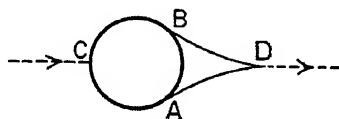


FIG. 5.

corresponds to a vertical dipole at the point at infinity, whose image in the z -plane we denote by $t = is$.

Let Γ be mapped by $T = -\frac{1}{2}(t + t^{-1})$ onto the half-plane, and let $iS = -\frac{1}{2}(is - is^{-1})$, so that $S = \frac{1}{2}(1 - s^2)/s$. Then by the method of reflection (Ch. III, §2) $W(T)$ is given by a vertical dipole at iS , and its image at $-iS$. Hence

$$(26) \quad W = \frac{M^*}{T^2 + S^2}, \quad \text{and} \quad \frac{dW}{dT} = \frac{MT}{(1 + \gamma^2 T^2)^2},$$

where $\gamma = S^{-1} = 2s/(1 - s^2)$. In the case $\beta = 1$ of a smooth obstacle,

$$(27) \quad \nu(\sigma) = \frac{\sin \sigma (1 + \sin \sigma)}{(1 + \gamma^2 \cos^2 \sigma)^2}$$

Conversely, the flow determined by any solution of (27) and (16) has the structure of Fig. 5, except that the two parallels ∞C and $D \infty$ to the x -axis will usually be on different levels. These parallels will coincide so that the correspondence $z \rightleftharpoons t$ is one-one at ∞ , giving a cusped cavity, if and only if the residue of dz/dt at $t = is$ is zero—that is,

$$(28) \quad \Omega'(is) = a_1 - 3a_3s^2 + 5a_5s^4 - \dots = 2(1 - s^2)^{-1}.$$

This can be written in an integral form by expressing $\Omega(t)$ by Schwarz's

^{15a} G. Birkhoff, H. H. Goldstine and E. H. Zarantonello, Rend. Sem. Mat. Torino 13 (1953), Cases 10, 14, 18.

formula [4, p. 77] in terms of its real part on the boundary $-\lambda(\sigma)$. Taking account of $\lambda(\sigma) = -\lambda(-\sigma)$, one gets

$$(28') \quad \Omega'(t) = \frac{2i}{t(t+t^{-1})} \frac{1}{\pi} \int_0^\pi \lambda(\sigma) \frac{\sin \sigma d\sigma}{1 - 2(t+t^{-1})^{-1} \cos \sigma}.$$

In the symmetric case this reduces to

$$(28'') \quad \Omega'(t) = \frac{2i}{t(t+t^{-1})} \frac{1}{\pi} \int_0^\pi \lambda(\sigma) \frac{\sin \sigma}{1 - 4(t+t^{-1})^{-2} \cos^2 \sigma} d\sigma.$$

With this (28) becomes

$$(28''') \quad \frac{1}{\pi} \int_0^\pi \lambda(\sigma) \frac{\sin \sigma}{1 + \gamma^2 \cos^2 \sigma} d\sigma = 1.$$

It can be proved (Ch. VII, §6) that for a given γ (i.e., $0 < s < 1$), a positive M can be found for which (28) holds: that there is one cavity at least for every *negative* number

$$(29) \quad Q = \zeta^{-2}(is) - 1 = \left(\frac{1+s}{1-s} \right)^2 e^{-2(a_1 s - a_3 s^3 + \dots)} - 1.$$

Hence there is a one-parameter family of cusped cavities behind a given convex obstacle.

The cusped cavity behind a circular cylinder for $Q = -.2819$ has the coefficients: $s = .47$, $a_1 = 2.5026$, $a_3 = -.0855$, $a_5 = .02928$, $a_7 = .0065$, $a_9 = .0066$. Cusped cavities behind circular cylinders have been previously computed by M. Kolscher¹⁶ and by Southwell and Vaisey. Cusped cavities behind non-circular cylinders have been exhibited by Lighthill.

11. Reentrant jets¹⁷. Symmetric reentrant jets offer no new difficulties. Such a flow (Fig. 6a) is again mapped into the unit semicircle, with the free boundary going into the real axis, the barrier into the semicircle, and the axis of symmetry into the imaginary axis. Then J and C go into $t = 0$ and $t = i$, respectively, while the point at infinity I and the stagnation point S on the back of the cavity are also represented on the imaginary axis (see Fig. 6b).

Clearly, ζ has a simple zero at $t(S) = t_0$ (cf. Ch. III, §8), so that if we set

$$(30) \quad \zeta^{-1} = \left(\frac{1-it}{1+it} \right)^{\beta} \frac{(t_0 - t_0^{-1}) + (t - t^{-1})}{(t_0 - t_0^{-1}) - (t - t^{-1})} e^{m(t)},$$

¹⁶ Luftfahrtforschung 17 (1940), 154-60; he used the method of Schmieden, loc. cit. in §5. See also R. Eppler, Dissertation, Tech. Hoch. Stuttgart, July, 1951. Southwell and Vaisey [58] used relaxation methods. M. J. Lighthill, ARC RM 2328 (1945), published in 1949, also gave special solutions of the "inverse problem".

¹⁷ See Ch. III, §8, where a bibliography is given.

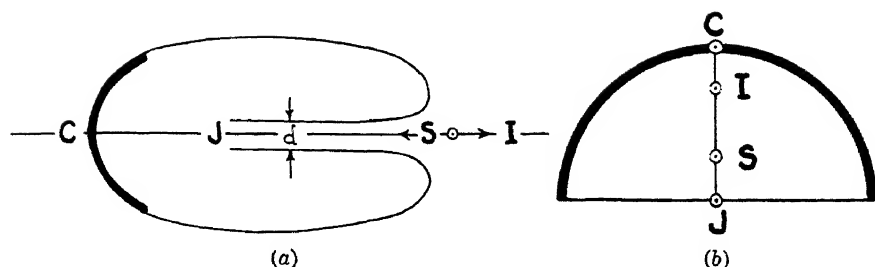


FIG. 6.

then $\Omega(t)$ must be, as in §2, a regular function real on the real axis and vanishing at the origin. The complex potential, having a logarithmic singularity at J and a simple pole at the point at infinity I , must satisfy (cf. Ch. III, (20), whose T is the negative reciprocal of our T)

$$(31) \quad \frac{dW}{dT} = \frac{2d}{\pi} \frac{T(T^2 - T_0^2)}{(T^2 - T_1^2)^2}, \quad \text{where} \quad T = -(t + t^{-1})/2.$$

From (30) and (31) we obtain for $\nu(\sigma)$

$$(32) \quad \nu(\sigma) = \sin \sigma |\cos \sigma|^{1-\beta} (1 + \sin \sigma)^\beta \left(\frac{1 + \gamma \sin \sigma}{1 + \alpha^2 \cos^2 \sigma} \right)^2,$$

where

$$\alpha = iT_r^{-1}, \quad \gamma = iT_0^{-1}, \quad \alpha > \frac{\gamma}{(1 - \gamma^2)^{1/2}}, \quad d = \frac{\pi M}{2} \frac{\gamma^2}{\alpha^4}.$$

Moreover, since $z(t)$ must be single-valued, the residue of $dz/dt = \zeta^{-1} dW/dt$ must be zero at $t = t_r$. By direct computation, this condition is found to be

$$\Omega'(t_r) = [1 + (1 + \alpha^2)^{1/2}] \left[\beta - \frac{2\gamma}{\alpha(\alpha + \gamma(1 + \alpha^2)^{1/2})} \right].$$

By (28''), this can also be written

$$(32') \quad \frac{1}{\pi} \int_0^\pi \lambda(\sigma) \frac{\sin \sigma}{1 + \alpha^2 \cos^2 \sigma} d\sigma = \beta - \frac{2\gamma}{\alpha(\alpha + \gamma(1 + \alpha^2)^{1/2})}.$$

12. Riabouchinsky flows. Symmetric "Riabouchinsky" flows (cf. Ch. V, §9) of the type sketched in Fig. 7a can be treated similarly. One maps half of such a flow (i.e., the part on one side of the axis of symmetry) conformally onto the unit semicircle Γ slit along the imaginary axis, so that the free streamline goes into the real diameter, each half-barrier into a quarter-circle, and the dividing streamline into the slit, as in Fig. 7b. The

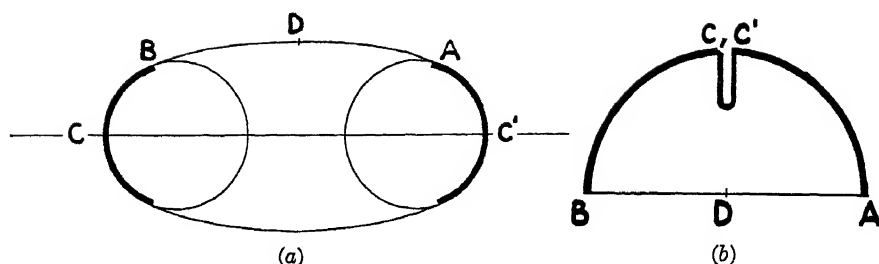


FIG. 7.

TABLE V

$\phi, ^\circ$	Q	C_D	$C_D/(1+Q)$	s	M	a_1	a_3	a_5
54.988	0	.499	.499	0	1.134	.941	.017	.002
55.143	.135	.568	.500	.06	1.150	.945	.016	.002
55.431	.235	.621	.503	.1	1.178	.952	.013	.001

two stagnation points C and C' are mapped in the point $t = i$ at each side of the slit, and the point I at infinity is mapped on the end of the slit. By symmetry, ζ is a single-valued function on the unit semicircle, the slit included, so (6) holds. The complex potential is (note that $(T^2 - T_I^2)^{1/2}$ maps the T -domain onto a half-plane, and apply Thm. 2 of Ch. III),

$$W = M(T^2 - T_I^2)^{-1/2} T_I^3, \quad M > 0.$$

Hence, using (6) and (9), we get (11) with

$$(33) \quad \nu(\sigma) = \frac{\sin \sigma (1 + \sin \sigma)}{(1 + \alpha^2 \cos^2 \sigma)^{3/2}}, \quad \text{if} \quad \beta = 1,$$

where $\alpha = T_I^{-1} = -2t_I/(1 + t_I^2)$.

Table V, computed by a three-point approximation, gives, for the Ria-bouchinsky flows past a solid circular cylinder, several relevant quantities for $Q = .135$ and $Q = .235$. (See also Cases 23a-23c and 24 of the reference of ftnt. 15a.)

13. Cascades of airfoils. Cavitation behind a cascade of flat plates has been treated by Betz and Petersohn [2] and applied to pump impellers by Gongwer¹⁸. The theory can be extended to a periodic array ("cascade") of curved barriers as in Fig. 8a¹⁹. To compute the flow, we use the parametri-

¹⁸ Trans. Am. soc. mech. eng. 63 (1941), 29-40.

¹⁹ The more general case of a cascade of reentrant jets has been described by D. A. Efros, Bull. Acad. Sci. URSS, Class. Tech. (1947), p. 1068.

zation described in §7, and map this periodic array onto the unit semicircle, with a branch point at an interior point $t = t_r$ corresponding to the point at infinity upstream (Fig. 8b), in such a way that the plates go onto the semicircle with the dividing point at $t = t_0 = e^{i\sigma_0}$, and the free boundaries into the real axis. The jets between the cavities correspond at $z = +\infty$

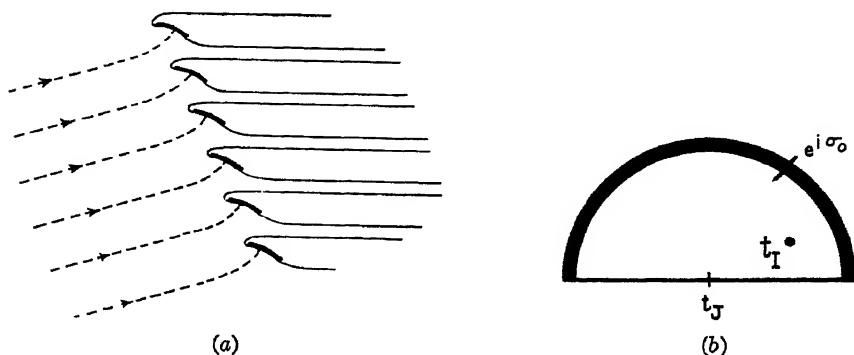


FIG. 8.

to $t = 0$. This mapping can be carried out in two steps: First, by means of $e^{2\pi i z/\delta}$ (δ is the relative displacement of two consecutive plates), the periodic array is mapped onto a simply connected domain, its boundary being in a one-to-one correspondence with the boundary of any of the periodic cavities, and the point at infinity upstream going into the origin: Second, by the (standard) conformal mapping theorem, this domain may be mapped conformally onto the unit semicircle with the indicated correspondences. The complex potential obviously has logarithmic singularities at t_r and 0, the first corresponding to a source-vortex and the second, to a sink of the same strength. Upon differentiation, these become poles of the first order, and, since dW/dt vanishes only at $t = t_0$

$$\frac{dW}{dT} = \frac{M^*(T - T_0)}{(T - T_r)(T - T_r^*)} = \frac{M(T - T_0)}{(1 - 2\gamma T + \alpha^2 T^2)},$$

where

$$T = -\frac{1}{2}(t + t^{-1}), \quad \alpha = |T_r^{-1}|, \quad \gamma = \text{Re}\{T_r^{-1}\}.$$

The conjugate velocity is the same on all sheets of the semicircle, and we can write (6') as in §7. We get for $v_1(\sigma)$

$$(34) \quad v_1(\sigma) = \frac{\sin \sigma (1 - \cos(\sigma + \sigma_0))^\beta |\cos \sigma - \cos \sigma_0|^{1-\beta}}{(1 - 2\gamma \cos \sigma + \alpha^2 \cos^2 \sigma)},$$

The problem thus depends on four parameters, M , α , γ , σ_0 , which pre-

sumably correspond to the orientation of the profile in the stream, the separation points, and the relative distance between adjacent barriers.

14. Other examples. Various other simply connected flows bounded by one fixed wall and one free boundary²⁰ can be treated in the same way. We shall content ourselves with a brief recapitulation of the main formulas in each case.

Jet from curved nozzle. The jet from a curved nozzle with asymptotic angle $\beta\pi$ at infinity can be similarly represented²¹ by (see Figs. 9a, 9b)

$$\zeta^{-1} = \left(\frac{i - it}{i - it} \right)^{\beta} e^{i\Omega(t)}, \quad W = M \ln [T/(T - T_J)]$$

$$(35) \quad v(\sigma) = \frac{\sin \sigma}{\cos \sigma (1 - \alpha \cos \sigma)} \left(\frac{1 + \sin \sigma}{1 - \sin \sigma} \right)^{\beta/2}$$

$$d = \pi M, \quad \alpha = [-\frac{1}{2}(T_J + T_J^{-1})]^{-1},$$

where t_J is the image of the jet in the t -diagram. The symmetric case is obtained by setting $t_J = 0$, $T_J = \infty$, $W = M \ln T$, $\alpha = 0$.



FIG. 9.

For a channel of finite width h , $\beta = 0$. In this case, if v is the velocity upstream and h the asymptotic width of the channel, then $d = vh$, and in the integral equation corresponding to (16), M can be eliminated and, in the case of symmetry, the equation can be transformed to

$$(36) \quad \lambda = \frac{h}{\pi} \tan \sigma K(\theta(\sigma)) e^{-(\tau(\sigma) - \tau(\pi/2))}.$$

This integral equation is clearly *singular*; we do not know how to solve it. It contains no free parameter and yet, to account for separation from a variable point, it must have a one-parameter family of solutions.

²⁰ As usual (Ch. III, §7, etc.) the boundary is allowed to pass through the point at infinity.

²¹ U. Cisotti, Rend. cir. mat. Palermo 26 (1908), 378-82, Comptes rendus 152 (1911), p. 181; H. Villat, Comptes rendus 152 (1911), 1081-4; A. Weinstein [87, 88].

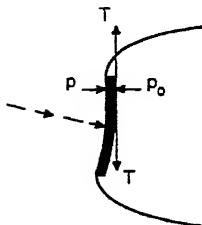


FIG. 10.

Flexible profile. If the rigid barrier is replaced by a flexible one, fixed at its endpoints as in Fig. 10, one gets an interesting problem also treated by Cisotti²².

Analytically, one only has to replace, in the formulation of §§1-4, the equation $\kappa = K(\theta)$, giving the shape of the profile, by the equilibrium condition $\kappa T = p_c - p$ equating the pressure jump across the barrier to the local pressure exerted by the (constant) tension T . By Bernoulli's equation, the above condition becomes $\kappa = -(\rho/2T)(1 - |\xi|^2)$. Equating this to the curvature in formula (13), one obtains an integral equation for $\lambda(\sigma)$ of the form

$$(37) \quad \lambda = M(\nu_1 e^{D\lambda} - \nu_2 e^{-D\lambda}),$$

where ν_1 and ν_2 ($\nu_1 \leq \nu_2$) are positive continuous functions depending on the type of flow under consideration, vanishing at $\sigma = 0, \pi$. For instance, for a symmetric barrier in an unbounded flow: $\nu_1 = \sin \sigma(1 - \sin \sigma)$, $\nu_2 = \sin \sigma(1 + \sin \sigma)$.

Variationally, a flexible barrier minimizes the kinetic energy among barriers of constant length²³.

Further literature. In the literature, still other models of interest have been investigated and their formulas derived. Such are, for instance, the free jet deflected by a curved plate and its limiting forms²⁴, the flow of a stream in a partially uncovered channel²⁵, and different types of planing surfaces²⁶.

Flows with two fixed boundaries and two free boundaries of different

²² Rend. Accad. Lincei 15 (1932), 165-73, 253-7. Using the "dead water" wake interpretation (Ch. I, §12), this may be imagined to correspond to a sail.

²³ An existence proof for flexible barriers based on this variational property has been given by P. R. Garabedian and H. Royden, Proc. nat. acad. sci. 38 (1952), 57-61.

²⁴ T. Boggio, Atti. accad. sci. Torino 46 (1911), 1024-51; A. Broikos, Comment. Pont. Acad. 3 (1939), 627-57; M. J. Lighthill, Ministry of Supply, London, Rep. MO 2105.

²⁵ G. Colonetti, Rend. Accad. Lincei 20 (1911), 649-55 and 789-96; V. Segre, Giorn. di Mat. Battaglini 55 (1917), p. 1.

²⁶ A. Franke, ZaMM 18 (1938), 155-72.

velocities have also been studied. The analytical treatment of such flows requires the change of the semicircular parametrization of Levi-Civita (see §2) to a semi-annular one, and the corresponding change of the different kernels and operators to those corresponding to the annulus²⁷. Thus have been treated flows in interrupted channels²⁸, obstacles in curved channels and curved nozzles²⁹, asymmetrical Riabouchinsky flows³⁰, etc.

²⁷ H. Villat (60).

²⁸ G. Caddonazzo, *Annali di mat. pura appl.* Milano 25 (1916), p. 40.

²⁹ H. Villat, *Comptes rendus* 152 (1911), 1081-4; [60]; *J. de math.* (6) 7 (1911), pp. 353, 408; *Ann. Sci. ec. norm. sup.* 29 (1912), 127-97; *Bull. soc. math. France* 40 (1912), p. 206; §5, 86.; J. Kravtchenko (49); R. Huron, *Comptes rendus* 228 (1949), 290-2, 357-8; A. Oudart, *J. Math. Pures Appl.* 22 (1943), 245-320; 23 (1944), 1-36.

³⁰ B. Demtchenko, *Proc. 3d Intern. Cong. Appl. Mech.*, Stockholm, 1930.

CHAPTER VII

EXISTENCE AND UNIQUENESS

1. Historical introduction. The question of the existence and uniqueness of potential flows past general obstacles, having free boundaries of given type, has intrigued many outstanding mathematicians. Remarkable success has been achieved, especially in the case of *symmetric* flows involving one parameter. The most important methods and results are described in the present chapter. However, the reader should be warned that the proofs are highly technical, and cannot be understood without considerable mathematical background and effort.

It was only after the study by Brillouin [10] and Villat [84] of the indeterminacy of the separation point, that a reasonable existence and uniqueness theorem was even formulated as a conjecture. Gradually, it became clear that a continuum of ideal plane cavity flows past a given solid convex obstacle was possible¹. Hence, to obtain a satisfactory existence and uniqueness theory, one must either specify the separation points ("barrier problem"), or require that the cavity pressure be a minimum ("prow problem"), or specify other side conditions (e.g., the cavitation number for reentrant jets or cusped cavities).

The first positive existence theorems for curved barriers were obtained in 1922 by Nekrassoff [63], for circular arcs of small extent. We shall explain his method (in generalized form) in §2; it corresponds roughly to the observation that, for small M , the integral equations of Ch. VI can be solved by direct iteration.

However, the first general results were obtained by Weinstein [87]², who treated symmetric jets from convex nozzles (Fig. 9a, Ch. VI). Weinstein proved first the impossibility of two infinitely close jets from the same nozzle, by showing that a certain quadratic form (48) was positive definite (see §8). In the case of polygonal nozzles having n sides, and hence involving n parameters (cf. Ch. V, §2), this definiteness implies that the correspondence from physical dimensions to values of the parameters is locally one-one, for any n . Hence, starting with a known convex polygonal nozzle, one can obtain a jet from any other polygonal nozzle by continuous variation of the vertices. Jets from curved boundaries can then be obtained by

¹ See Ch. I, §14; Ch. V, §3; Ch. VI, §6; also, S. Bergman, *ZaMM* 12 (1932), 95-121.

² Also *Rend. Accad. Lincei* 4 (1926), 119-23; *ibid.* 5 (1927), 157-61. Excellent expositions of the method, by Weinstein himself: *Proc. First Canadian Math. Congress* (1945), 355-64; *Proc. 1st Symp. Appl. Math. of Amer. Math. Soc.* (1949), 1-18; [82].

a passage to the limit. The class of nozzles to which this "method of continuity" applies was successively enlarged by Hamel³, Weyl³, and Friedrichs [26], with the final result that one and only one symmetric jet issues from any given symmetric convex nozzle turning through an angle less than π .

The method of continuity pioneered by Weinstein was given much larger scope by Leray [52] in 1935, who extended it to function spaces, using the now classic Leray-Schauder theory [53]. In §§3-4, we present various applications of Leray's methods to cavity flows past general obstacles, using Villat's integral equation (15) of Ch. VI. In §§5-6, we give other applications to cavity flows past convex obstacles, using equation (16) of Ch. VI and a Lemma of Jacob.

In §§7-9, we indicate how Weinstein's method of continuity can be applied in another form to cavity flows, so as to give uniqueness theorems. This form of the method of continuity is applicable in principle to *asymmetric* plane flows, though we treat only the symmetric case here.

The preceding methods, all based on the integral equations for plane cavity flows derived in Ch. VI, provide no basis for existence and uniqueness theorems for *axially symmetric* flows. Techniques for treating such flows, discovered in the past decade, have already been introduced in Ch. IV. For example, we presented there uniqueness theorems based on the comparison methods created by Lavrentieff [51], as simplified by Serrin [75] and Gilbarg [29]. Since these methods seem inapplicable to the asymmetric case, the results of §§7-9 below complement them,

Even more striking are the applications of Riabouchinsky's variational principle (Ch. IV, §§10-11). An important contribution to this variational approach was made by Friedrichs [26], who showed that the second variation was positive in the case of a symmetric jet from a convex nozzle, thus showing that the *kinetic energy* is a local minimum. Very recently [27, 28], Garabedian, Lewy, Spencer and Schiffer have exploited Riabouchinsky's principle and Steiner symmetrization, so as to prove the existence of axially symmetric cavity flows in the plane and in space. We indicate how this may be done in §§10-11.

2. Nearly flat obstacles. The method of Nekrassoff [63] and his followers⁴ can be easily described in terms of the theory of non-linear integral

³ G. Hamel, Proc. sec. int. congr. appl. mech., Zurich (1926), pp. 76 and 489; H. Weyl, Gött. Nachr. (1927), p. 227.

⁴ N. Arjanikoff, Rec. Math. Moscou 35 (1928), 5-17; P. Miasnikoff, S. Kalinin, W. Slioskine, Diss. Inaug. Univ. Moscou (1935). J. Sekerj-Zenkowitch, Publ. CAHI Moscow (1935-41), Y. Berman, Prikl. mat. mekh. 13 (1949), 543-6; S. V. Kalinin, Izv. Akad. Nauk SSSR (1950), 966-84; P. P. Kufarev, Prikl. mat. mekh. 16 (1952), 589-98. The early work dealt mainly with circular barriers.

operators. We shall take as our starting point the integral equation (16) of Ch. VI, rewritten as

$$(1) \quad \lambda = MS[\lambda], \quad S[\lambda] = \nu K(J\lambda)e^{-D\lambda}.$$

Here M is fixed and $\nu = \nu(\sigma)$ a given non-negative function.

We now define the "distance" between two functions $\lambda_1(\sigma)$ and $\lambda_2(\sigma)$ as

$$(2) \quad \|\lambda_1 - \lambda_2\| = \sup |\lambda_1(\sigma) - \lambda_2(\sigma)|.$$

LEMMA. If $K(\theta) > 0$ satisfies a Lipschitz condition

$$(3) \quad |K(\theta) - K(\theta')| \leq L |\theta - \theta'|,$$

then the operator S satisfies, for some finite N ,

$$(4) \quad \|S[\lambda_1] - S[\lambda_2]\| \leq N \|\lambda_1 - \lambda_2\|,$$

identically in the unit sphere $\|\lambda_i\| \leq 1$.

Proof. The function $\nu(\sigma)$ is bounded, in all the cases considered in Ch. VI. Again, by (14b) of Ch. VI, a change of $\Delta\lambda$ in λ changes $J\lambda$ by at most $\pi \|\Delta\lambda\|/2$; hence $K(J\lambda)$ by at most $\pi L \|\Delta\lambda\|/2$, by (3). Similarly,

$$\begin{aligned} \int_0^\pi |D(\sigma, s)| ds &= \int_0^\pi D(\sigma, s) ds = \frac{2}{\pi} \sum_{n=1}^\infty \frac{\sin n\sigma}{n} \int_0^\pi \sin ns ds \\ &\leq \frac{4}{\pi} \left(1 + \frac{1}{9} + \frac{1}{25} + \cdots\right) = \frac{\pi}{2} < 2. \end{aligned}$$

Hence $\|D[\lambda]\| \leq 2 \|\lambda\|$ and, if $\|\lambda_i\| \leq 1$,

$$\|e^{-D\lambda_1} - e^{-D\lambda_2}\| \leq e^2 \|D[\lambda_1] - D[\lambda_2]\| \leq 2e^2 \|\lambda_1 - \lambda_2\|.$$

Combining these results, we get the bound (4); we omit the detailed computation of N .

THEOREM 1. If M is small enough, then the integral equation (1) can be solved by direct iteration. For $\|\lambda\| < 1$, the solution is unique.

Proof. If $M < 1/N$, and all the iterates $\lambda_{n+1} = MS[\lambda_n]$ of $\lambda_0 = 0$ lie in the unit sphere, then it is classic (the Picard iteration process⁵) that the λ_{n+1} converge to a unique solution. In fact, by (4),

$$\|\lambda_{n+1} - \lambda_n\| \leq MN \|\lambda_n - \lambda_{n-1}\|,$$

whence $\|\lambda_{n+1} - \lambda_n\| \leq (MN)^n \|\lambda_1\|$ by induction. Thus, by repeated applications of the triangle inequality, since $MN < 1$,

$$\|\lambda_m - \lambda_n\| \leq \sum_{k=n}^{m-1} \|\lambda_{k+1} - \lambda_k\| \leq \frac{(MN)^n - (MN)^m}{1 - MN} \|\lambda_1\|$$

⁵ É. Picard, *Traité d'analyse*, 2d. ed., vol. 2, p. 301; the abstract version was given around 1930 by Hadamard, and, for Banach spaces, by Cacciopoli and others.

tends to zero as $m, n \rightarrow \infty$. In other words, the sequence $\{\lambda_n\}$ is a Cauchy sequence. Consequently, the sequence of functions $\lambda_n(\sigma)$ converges *uniformly* to a limit function $\lambda(\sigma)$. Clearly

$$MS[\lambda] = \lim MS[\lambda_n] = \lim \lambda_{n+1} = \lambda,$$

and $\lambda(\sigma)$ is a solution of (1). The uniqueness (for $\|\lambda\| < 1$) follows since, if $\lambda_1 = MS[\lambda_1]$ and $\lambda_2 = MS[\lambda_2]$, then

$$\|\lambda_1 - \lambda_2\| = M\|S[\lambda_1] - S[\lambda_2]\| \leq MN\|\lambda_1 - \lambda_2\|,$$

whence $\|\lambda_1 - \lambda_2\| = 0$ and $\lambda_1 = \lambda_2$, since $MN < 1$.

To obtain a sufficient condition that all λ_n lie in the sphere $\|\lambda\| \leq 1$, one need only calculate $\lambda_1(\sigma) = MS[0] = MK(0)\nu(\sigma)$, whence it is easily shown to be sufficient that

$$M < 1/[N + K(0) \sup \nu(\sigma)].$$

Theorem 1 is often called a *fixpoint* theorem, because the solution $\lambda(\sigma)$ of (1) is a fixpoint of the operator S . In §3 ff., we shall apply other (non-constructive) fixpoint theorems to existence proofs. To exploit such fixpoint theorems fully, it is convenient to use other Banach spaces, defined by various distance functions. Thus, Leray [52], in his treatment of Villat's equation, originally used the norm

$$\|\lambda\| = \sup_{\sigma} |l(\sigma)| + \sup_{\sigma', \sigma''} |l(\sigma') - l(\sigma'')| / \|\sigma' - \sigma''\|^p,$$

while Kravtchenko¹⁵ used $\|\lambda\| = \sup |l(\sigma)| + \sup |l'(\sigma)|$. In §5, we shall use the Hilbert space norm $\|\lambda\| = \left[\int_0^\pi |\lambda^2(\sigma)| d\sigma \right]^{1/2}$ to handle the curvature equations. The norms $\|\lambda\| = \left\{ \int |\lambda^p(\sigma)| d\sigma \right\}^{1/p}$ have also been introduced (see [67]) for this purpose.

With the norm $\|\lambda\| = \sup |l(\sigma)|$, one can extend the proof of Theorem 1 to the Villat integral equation (15) of Ch. VI, provided $\Theta(l)$ is smooth enough to make the operator $l(\sigma) \rightarrow C[(\Theta(l(\sigma)))]$ satisfy a Lipschitz condition (§3, Lemma 3).

In either case, for each sufficiently small *fixed* M , our proof guarantees *constructively* the *existence and uniqueness* of symmetric flows past symmetric obstacles of otherwise arbitrary shape. In fact, for symmetric data the solution of (1) must be symmetric, since any nonsymmetric solution would produce by reflection ($\sigma \rightarrow \pi - \sigma$) another solution, contradicting uniqueness. Further, by the general theory of "bounded operators" satisfying (4),

¹⁵ Because continuous functions form, under the "distance" (2), a so-called *Banach space*, or B-space in the sense of S. Banach, "Théorie des opérations linéaires", Warsaw, 1933.

it is easy to show that $\lambda(\sigma)$ and $l(\sigma)$ vary *continuously* with M , if $MN < 1$. Since $\lambda(\sigma)$ and $l(\sigma)$ tend to zero with M , we have the following theorem.

THEOREM 2. There exists a symmetric cavity flow behind any sufficiently small symmetric arc of an arbitrary smooth contour.

Since $\nu(\sigma)$ was unspecified, a similar result holds for Riabouchinsky flows, etc.

COROLLARY. For sufficiently small M , the separation angle ϕ_s behind a *convex* contour varies *monotonely*⁷ with M .

For, by Ch. VI, (17), θ_s and hence ϕ_s uniquely determines M : the correspondence $\phi_s(M)$ is locally one-one. But we have already seen that it is continuous; the corollary now follows since *any* one-one locally continuous function $\phi_s(M)$ must be monotone.

3. Leray's use of fixpoint theory. A very general but non-constructive existence theorem can be based on the Leray-Schauder theory of functional operators, which was developed partly for just this purpose. The theorem we want may be summarized as follows [53, p. 63].

Leray-Schauder Theorem. Let $F_k[x]$ be any one-parameter family of completely continuous⁸ transformations of a Banach space⁹ \mathcal{E} into itself, $0 \leq k \leq 1$. Let \mathcal{D} be a bounded domain of \mathcal{E} on which the F_k are "equi-continuous in k ", in the sense that for any $\epsilon > 0$ there is an $\eta > 0$ with the property that $|k - k'| < \eta$ implies $\|F_k[x] - F_{k'}[x]\| < \epsilon$ for all $x \in \mathcal{D}$. Let $x = F_k[x]$ for no x on the boundary of \mathcal{D} . Under these hypotheses, if

- (i) $x = F_0[x]$ has a unique solution x_0 in \mathcal{D} , and
- (ii) in some neighborhood of x_0 , $G_0[x] = x - F_0[x]$ is one-one (locally)⁹, then

$$(5) \quad x = F_1(x)$$

has at least one solution in \mathcal{D} .

We first apply the preceding theorem to Villat's integral equation (15) of Ch. VI,

$$(6) \quad l(\sigma) = M \int_{\pi/2}^{\sigma} \nu(\sigma) e^{-Cl(\sigma)} d\sigma = F_M[l(\sigma)],$$

letting M play the role of the parameter k . We let \mathcal{E} be the space of all continuous functions $l(\sigma)$ on the interval $0 \leq \theta \leq \pi$ with $l(\pi/2) = 0$,

⁷ J. Sekerj-Zenkowitch has shown that, if the barrier is analytic, then so is $\phi_s(M)$.

⁸ A transformation is called "completely continuous" if it is continuous, and carries bounded sets into compact sets.

⁹ In the language of topology, (i) and (ii) state that the total index of $x = F_0[x]$ in \mathcal{D} is one; F_0 and F_1 are "homotopic".

under the norm

$$(7) \quad \|l\| = \max_{0 \leq \sigma \leq \pi} |l(\sigma)|.$$

We shall assume $\nu(\sigma)$ non-negative and continuous, and shall require $\Theta(l)$ to be continuous and have an oscillation $2\gamma = \max \Theta(l) - \min \Theta(l) < \pi$. Thus, we shall consider only obstacles with continuously turning tangent, and angular extent $2\gamma < \pi$.

Some of the hypotheses of the Leray-Schauder Theorem are obvious. Thus, since $F_0[l(\sigma)] = 0$ for all $l(\sigma)$, $F_0[l] = l$ has the unique solution $l(\sigma) \equiv 0$. Also, $G_0[l] = l - F_0[l] = l$ is obviously one-one. Again, in any domain \mathfrak{D} of \mathcal{E} , evidently

$$\|F_M[l] - F_{M'}[l]\| = \|M - M'\| \cdot \|F_1[l]\|;$$

hence equicontinuity in M will follow if we can show that $\|F_1[l]\|$ is bounded. (The choice of $0 \leq M \leq 1$ as the interval of M is, of course, irrelevant.)

The other hypotheses of the Leray-Schauder Theorem will follow when we have shown that, (α) $F_M[\mathcal{E}]$ is compact, and (β) F_M is continuous in \mathcal{E} . For, from (α) and (β), it follows that F_M is completely continuous. And, from (α) alone, it follows that $F_M[\mathcal{E}]$ is contained in the interior of some sphere \mathfrak{D} : $\|m\| < r$, whence $F_M[l] = l$ for no $l(\sigma)$ on the boundary of \mathfrak{D} . Hence, when we have proved (α) and (β), we will have proved

THEOREM 3. For any $M \geq 0$, bounded $\nu(\sigma) \geq 0$, and continuous $\Theta(l)$ with oscillation less than π , the integral equation (6) has at least one continuous solution $l(\sigma)$.

The proofs of both (α) and (β) depend on the following lemma.¹⁰

LEMMA 1. If $\theta(\sigma)$ has finite oscillation $2\gamma = [\max \theta(\sigma) - \min \theta(\sigma)]$ on $0 \leq \sigma \leq \pi$, then

$$(8) \quad \int_0^\pi \cosh(pC[\theta(\sigma)]) d\sigma \leq \pi \sec p\gamma,$$

for any positive number $p \leq \pi/2\gamma$.

Proof. Let $\tau(\sigma) = C[\theta(\sigma)]$. Then $h(\sigma) = \theta(\sigma) + i\tau(\sigma)$ are the boundary values on $t = e^{i\sigma}$ of an analytic function $\Omega(t)$ regular in $|t| < 1$ and real for t real. Now let $\beta = \frac{1}{2}[\theta_{\max} + \theta_{\min}]$; by the residue theorem,

$$e^{ip(\Omega(0)-\beta)} = \frac{1}{2\pi i} \oint e^{ip(\Omega(t)-\beta)} dt/t = \frac{1}{2\pi} \int_{-\pi}^{\pi} e^{ip(h(\sigma)-\beta)} d\sigma$$

and, since $h(-\sigma) = \theta(\sigma) - i\tau(\sigma)$,

¹⁰ A. Zygmund, Fund. Math. 13 (1929), 284-303. Here and below, we write $\theta(\sigma) = \Theta(l(\sigma))$, thus avoiding ambiguity.

$$e^{i p(\Omega(0) - \beta)} = \frac{1}{\pi} \int_0^\pi e^{i p(\theta(\sigma) - \beta)} \cosh p\tau \, d\sigma.$$

Taking the real parts, since $\cos(\Omega(0) - \beta) \leq 1$,

$$\pi \geq \int_0^\pi \cos p(\theta - \beta) \cosh p\tau \, d\sigma.$$

But, by definition of γ , $|p(\theta - \beta)| < p\gamma$, while $\cos p(\theta - \beta) \geq \cos p\gamma$ if $0 \leq p \leq \pi/2\gamma$. Substituting in the preceding inequality, we get (8).

LEMMA 2. If $0 < s < (\pi - 2\gamma)/\pi$, then there is a positive constant $B = B(s)$ such that

$$(9) \quad |m(\sigma) - m(\sigma')| \leq MB \|\nu\| |\sigma - \sigma'|^s$$

for any transform $m(\sigma) = F_M[l(\sigma)]$ of any $l \in \mathcal{E}$.

Proof. By definition,

$$|m(\sigma) - m(\sigma')| = M \left| \int_\sigma^{\sigma'} \nu(\sigma) e^{-C[\Theta(l(\sigma))]} \, d\sigma \right|.$$

Letting $\|\nu\| = \sup \nu(\sigma)$, we get from Hölder's inequality, for any $p > 0$, $q > 0$ with $p^{-1} + q^{-1} = 1$,

$$\begin{aligned} |m(\sigma) - m(\sigma')| &\leq M \|\nu\| \left\{ \int_\sigma^{\sigma'} d\sigma \right\}^{1/q} \left\{ \int_\sigma^{\sigma'} e^{-p\tau(\sigma)} \, d\sigma \right\}^{1/p} \\ &\leq M \|\nu\| \cdot |\sigma - \sigma'|^{1/q} \left\{ \int_0^\pi e^{-p\tau(\sigma)} \, d\sigma \right\}^{1/p}, \end{aligned}$$

where $\tau(\sigma) = C[\Theta(l(\sigma))]$. Applying Lemma 1 to the last integral, since $e^{-p\tau} \leq 2 \cosh(-p\tau)$,

$$|m(\sigma) - m(\sigma')| \leq M \|\nu\| \cdot |\sigma - \sigma'|^{1/q} (2\pi \sec p\gamma)^{1/p},$$

valid for any p , $1 < p < \pi/2\gamma$. Now set $q^{-1} = s$ and $p^{-1} = 1 - s$; we get (9) with $B = (2\pi \sec p\gamma)^{1/p}$.

Lemma 2 shows that $F_M[\mathcal{E}]$ is a set of equicontinuous functions contained within a sphere of finite radius $MB \|\nu\| \pi^s$. Since any such set is compact [18, vol. 1, p. 49], we have proved hypothesis (α).

LEMMA 3. Each operator F_M is continuous on \mathcal{E} . Namely,

$$(10) \quad \|F_M[l'] - F_M[l]\| \leq MC \|\nu\| \cdot \|\Theta(l') - \Theta(l)\|,$$

for some positive constant $C = C(\gamma)$.

Proof. Clearly,

$$\|F_M[l'] - F_M[l]\| \leq M \int_0^\pi \nu(\sigma) |e^{-C[\Theta(l'(\sigma))]} - e^{-C[\Theta(l(\sigma))]}| \, d\sigma.$$

Replacing ν by its supremum ν^+ , using the inequality $e^{-x} - e^{-x'} \leq x' - x + (e^{-x'})^2 + e^{-x}$, and writing $\delta\theta(\sigma) = \Theta(l(\sigma)) - \Theta(l'(\sigma))$, we get,

$$F_M[l'] - F_M[l] \leq M \nu^+ \int_0^\pi (e^{-C\theta} + e^{-C\theta'}) \cdot C[\delta\theta] d\sigma,$$

where $\theta'(\sigma) = \Theta(l'(\sigma))$, etc. If $p^{-1} + q^{-1} = 1$, we get by Hölder's inequality

$$F_M[l'] - F_M[l] \leq M \nu^+ \left\{ \left(\int_0^\pi e^{-pC\theta} d\sigma \right)^{1/p} + \left(\int_0^\pi e^{-pC\theta'} d\sigma \right)^{1/p} \right\} \left\{ \int_0^\pi |C\delta\theta|^q d\sigma \right\}^{1/q}.$$

The last integral can be majorized by the Riesz Theorem¹¹, while if $1 < p < \pi/2\gamma$, the other two integrals can be majorized by Lemma 1, to give

$$F_M[l'] - F_M[l] \leq 2M \nu^+ (2\pi \sec p\gamma)^{1/p} \pi^{1/q} A_q \|\delta\theta\|.$$

Here A_q is the constant in Riesz' Theorem. If C is properly defined, (10) follows directly. This completes the proof of (β) and hence of Thm. 3.

4. Parameter problem. The preceding argument can be supplemented quite easily, so as to prove existence for problems involving a single geometrical or physical parameter. (The parameter M in (6) has of course no direct physical interpretation¹², although it usually increases with the separation angle ϕ_0 .) We shall illustrate the technique by treating the case of an obstacle of prescribed total length L . That is, we shall assume the side condition

$$(11) \quad L = M \int_0^\pi \nu(\sigma) e^{-C[\Theta(l(\sigma))]} d\sigma, \quad \text{for given } L > 0.$$

In the symmetric case, this amounts to the *barrier problem* with prescribed separation point. We suppose $\nu(\sigma)$ given, non-negative and bounded. Thus for the symmetric infinite cavity $\nu(\sigma) = \sin \sigma + \sin^2 \sigma$; in other cases (e.g., Riabouchinsky flows), $\nu(\sigma)$ involves one or more additional parameters whose physical interpretation may be uncertain.

We first eliminate M from (6) and (11), getting the equivalent functional equation

$$(12) \quad l(\sigma) = F_1[l(\sigma)] = L \int_{\pi/2}^\sigma \nu(\sigma) e^{-C[\Theta(l(\sigma))]} d\sigma \bigg/ \int_0^\pi \nu(\sigma) e^{-C[\Theta(l(\sigma))]} d\sigma,$$

in which L is supposed specified. The function $\Theta(l)$ is also given. Geo-

¹¹ A. Zygmund, "Trigonometrical series", Warsaw, 1935, p. 147.

¹² Also, the solution $l(\sigma) \equiv 0$ corresponding to $M = 0$ does not, strictly speaking, correspond to a free boundary problem.

metrically, it is not defined for $l > L$, or $l < 0$. Yet, in order that the operator $F_1[l]$ be defined on a linear space, it is necessary to have $\Theta(l)$ defined for all l , which can always be achieved by setting $\Theta(p) = \Theta(0)$ for $p < 0$, and $\Theta(p) = \Theta(L)$ for $p > L$. In this way F_1 is defined as a single-valued transformation on the space \mathcal{E} of all continuous functions vanishing at $\sigma = \pi/2$.

The next step is to find a convenient one-parameter family of functional transformations F_k , $0 \leq k \leq 1$, fulfilling all hypotheses of the Leray-Schauder Theorem. For this purpose we shall use the one-parameter family of angular functions: $\Theta_k(l) = k \Theta(l)$, $0 \leq k \leq 1$, and define $F_k[l]$ as the transformation associated with Θ_k in the same way as $F_1[l]$ is associated with Θ . Physically, the change of F_1 into F_0 amounts to a deformation of the obstacle into a straight plate.

The continuity and complete continuity of the F_k 's, as well as the fact that all solutions of $l = F_k[l]$ remain within a fixed sphere, follow from Lemmas 2 and 3, provided the constants $M_k = L \left(\int_0^\pi \nu e^{-C[\Theta_k(l(\sigma))]} d\sigma \right)^{-1}$, which are also continuous with regard to l , remain uniformly bounded for all l and k . Such is the content of the following lemma.

LEMMA 4. For every $l \in \mathcal{E}$ and every k , $0 \leq k \leq 1$,

$$(13) \quad \int_0^\pi \nu e^{-C[\Theta_k(l(\sigma))]} d\sigma \leq 1/A,$$

where A , is a positive constant depending on ν only.

Proof. By Jensen's inequality¹³

$$\int_0^\pi \nu e^{-C\theta_k} d\sigma \geq \left(\int_0^\pi \nu d\sigma \right) \exp \left\{ - \int_0^\pi \nu C\theta_k d\sigma / \int_0^\pi \nu d\sigma \right\}$$

Hence, observing¹⁴ that for any two function $\alpha(\sigma)$ and $\beta(\sigma)$,

$$\int_0^\pi \alpha(\sigma) C\beta(\sigma) d\sigma = - \int_0^\pi \beta(\sigma) C\alpha(\sigma) d\sigma,$$

¹³ G. H. Hardy, D. E. Littlewood, and G. Polya, *Inequalities*, Cambridge University Press, 1934, p. 138. As in Ch. VI, §4, $C\theta_k = C\theta_k(\sigma)$ denotes the function $C[\Theta_k(l(\sigma))]$, $C\beta$ denotes the conjugate of $\beta(\sigma)$, etc.

¹⁴ To prove it, let $A(t)$ and $B(t)$ be functions analytic in $|t| < 1$ and real on the real axis, whose real parts coincide with $\alpha(\sigma)$ and $\beta(\sigma)$ respectively ($0 \leq \sigma \leq \pi$) on $t = e^{i\sigma}$. Then

$$2 \int_0^\pi (\alpha C\beta + \beta C\alpha) d\sigma = -Re \oint A(t)B(t) dt/t,$$

integrated around $|t| = 1$. Since $A(0)B(0)$ is real, this is however zero.

we have

$$\int_0^\pi \nu e^{-C\theta_k} d\sigma \geq \left(\int_0^\pi \nu d\sigma \right) \exp \left\{ -k \int_0^\pi \theta C\nu d\sigma / \int_0^\pi \nu d\sigma \right\}$$

But $-k\Theta C[\nu] \geq -\sup \{ \Theta(l) \mid \cdot \mid C[\nu] \mid \} \geq -2\pi \mid C[\nu] \mid$, because the angular extent of the barrier is at most π , and so

$$\int_0^\pi \nu e^{-C\theta_k} d\sigma \geq \left(\int_0^\pi \nu d\sigma \right) \exp \left\{ -2\pi \int_0^\pi \mid C\nu \mid d\sigma / \int_0^\pi \nu d\sigma \right\}.$$

Since the right member is never zero (unless $\nu \equiv 0$), Lemma 4 is proved. It remains only to check that the F_k are equicontinuous with regard to k , which is obvious, and that conditions (i) and (ii) are satisfied, which is also immediate, because $F_0[l]$ maps all functions onto a fixed function. This, in particular, completes the proof of the following result.

THEOREM 4. For any barrier of angular extent less than π with continuous tangent, placed symmetrically in an unbounded flow, there is a symmetric cavity flow with infinite cavity, and a one-parameter family of Riabouchinsky flows.

The same method applies, with a few modifications, to the asymmetric barrier problem which has one more side condition. Limitations of space forbid the inclusion of the many other applications of Leray's method which may be found in the literature¹⁵.

From Theorem 19 of Ch. IV, it follows further that for some $\nu(\sigma)$ the solution of (12) is *unique*. We have not, however, excluded the possibility that distinct values of L , and hence two functions $l(\sigma)$, may correspond to the same M . (Jacob's Lemma (§5) will show that this is impossible for ogival barriers.)

5. Jacob's Lemma. We shall now show that, at least in the case of a convex¹⁶ ogival obstacle, the separation angle (i.e., the L of §4) and many other quantities increase monotonely with M . To prove this, we shall need some information about the operators J and D defined in Ch. VI, §4. This information is expressed most conveniently in terms of the Hilbert space $H = L_2(0, \pi)$, that is, of the Banach space⁶ defined by the distance

¹⁵ J. Kravtchenko, J. de math. 20 (1941), 35-239; and Ann. sci. ec. norm. sup. 62 (1946), 233-68 and 63 (1947), 161-84; A. Oudart, J. de math. 22 (1943), 245-320 and 23 (1944), 1-36; R. Huron, Ann. fac. sci. Toulouse 15 (1951), 5-78; P. Théron, Comptes rendus 228 (1949), 1922-3; [75]; [76].

¹⁶ The theory of §§5-6 breaks down, for example, in the case $M < 0$ of concave circular arcs. Thus (14) may have zero, one, or two solutions. The methods of §§3-4 show, however, the existence of a unique infinite cavity for any concave circular arc of angular extent less than π .

function

$$\|\lambda\|^2 = \left[\int_0^\pi \lambda^2(\sigma) d\sigma \right]^{\frac{1}{2}} = (\lambda, \lambda).$$

where the "inner product" (λ_1, λ_2) is defined as usual as

$$\int_0^\pi \lambda_1(\sigma) \lambda_2(\sigma) d\sigma.$$

LEMMA 1. (i) \mathbf{J} and \mathbf{D} are linear transformations of the Hilbert space \mathbf{H} of all square integrable functions on the interval $(0, \pi)$, into the space of continuous functions on the same interval. For every λ in \mathbf{H} , $\tau = \mathbf{D}[\lambda] = \mathbf{D}\lambda$ vanishes at the endpoints of the interval $(0, \pi)$.

(ii) For every σ' and σ in the interval $(0, \pi)$,

$$|\theta(\sigma') - \theta(\sigma) + i\tau(\sigma') - i\tau(\sigma)| \leq \sqrt{2} \|\sigma' - \sigma\| \|\lambda\|.$$

(iii) \mathbf{D} is symmetric: $(\mathbf{D}\lambda_1, \lambda_2) = (\lambda_1, \mathbf{D}\lambda_2)$.

(iv) \mathbf{D} is positive definite: $0 \leq (\lambda, \mathbf{D}\lambda)$, and $(\lambda, \mathbf{D}\lambda) = 0$ implies $\lambda = 0$ almost everywhere.

(v) \mathbf{D} is a contraction: $(\mathbf{D}\lambda, \mathbf{D}\lambda) \leq (\lambda, \mathbf{D}\lambda) \leq (\lambda, \lambda)$.

(vi) \mathbf{D} is order preserving: $\lambda_1 > \lambda_2$ implies $\mathbf{D}\lambda_1 > \mathbf{D}\lambda_2$.

Proof. (i) Since $\theta = \mathbf{J}\lambda$ is the indefinite integral of λ , the statement about \mathbf{J} is obvious. The kernel $D(\sigma, s)$ has a logarithmic singularity at $\sigma = s$; thus, for fixed σ , it is a square integrable function of s on $(0, \pi)$. So the transform (scalar product) $\tau(\sigma) = \int_0^\pi D(\sigma, s)\lambda(s) ds$ is defined and finite for every σ in $(0, \pi)$ and any λ in \mathbf{H} . Moreover, since $D(0, s) = D(\pi, s) = 0$, τ vanishes at $\sigma = 0, \pi$.

As to the continuity of τ , we first get, by the Schwarz inequality,

$$\begin{aligned} |\tau(\sigma') - \tau(\sigma)| &\leq \int_0^\pi |D(\sigma', s) - D(\sigma, s)| |\lambda(s)| ds \\ &\leq \left\{ \int_0^\pi |D(\sigma', s) - D(\sigma, s)|^2 ds \right\}^{\frac{1}{2}} \left\{ \int_0^\pi |\lambda(s)|^2 ds \right\}^{\frac{1}{2}}. \end{aligned}$$

Moreover, by Ch. VI, (14d),

$$D(\sigma', s) - D(\sigma, s) = \frac{2}{\pi} \sum \left[(\sin j\sigma' - \sin j\sigma) \frac{\sin js}{j} \right],$$

and by the Plancherel Theorem

$$\int_0^\pi |D(\sigma', s) - D(\sigma, s)|^2 ds = \frac{2}{\pi} \sum_{j=1}^{\infty} \frac{|\sin j\sigma' - \sin j\sigma|^2}{j^2}.$$

The series on the right converges uniformly and tends to zero as $\sigma' \rightarrow \sigma$; hence $\tau(\sigma)$ is continuous.

(ii) Let $\sum a_j \sin j\sigma$ be the Fourier series of λ , and let μ be the function whose Fourier series is $\sum a_j \cos j\sigma$; then $\int_0^\pi |\mu|^2 d\sigma < +\infty$, and $-\int_0^\sigma \mu d\sigma$ is a continuous function having the same Fourier series as $\tau(\sigma)$; hence $\tau(\sigma') = -\int_0^{\sigma'} \mu d\sigma$. Thus, by the Schwarz inequality

$$\begin{aligned} |\theta(\sigma') - \theta(\sigma) + i(\tau(\sigma') - \tau(\sigma))| \\ \leq \int_\sigma^{\sigma'} |\lambda + i\mu| d\sigma \leq |\sigma' - \sigma|^{\frac{1}{2}} \left\{ \int_\sigma^{\sigma'} |\lambda + i\mu|^2 d\sigma \right\}^{\frac{1}{2}}. \end{aligned}$$

But by Plancherel's Theorem,

$$\int_\sigma^{\sigma'} |\lambda + i\mu|^2 d\sigma \leq \int_0^\pi |\lambda + i\mu|^2 d\sigma = \pi \sum a_j^2 = 2 \int_0^\pi |\lambda|^2 d\sigma.$$

(iii) This property follows immediately from the symmetry of $D(\sigma, s)$.

(iv) From the Fourier series' for λ and $D\lambda$, we compute

$$(\lambda, D\lambda) = \sum a_j^2/j \geq 0.$$

Further, if $(\lambda, D\lambda) = 0$, all Fourier coefficients vanish and $\lambda = 0$ almost everywhere.

(v) One readily computes

$$(D\lambda, D\lambda) = \frac{\pi}{2} \sum a_j^2/j^2, \quad (\lambda, \lambda) = \frac{\pi}{2} \sum a_j^2,$$

and (v) follows at once by term-by-term comparison of the series.

(vi) This is an obvious consequence of $D(\sigma, s) > 0$.

Properties (i) and (ii) show that J and D are smoothing operators transforming bounded sets of Hilbert space into bounded families of equicontinuous functions. Such families being compact [18, vol. 1, p. 49], J and D are completely continuous integral operators.

THEOREM 5. Given $M \geq 0$ and $\nu(\sigma) \geq 0$ on $0 \leq \sigma \leq \pi$, the integral equation (cf. (1) or Ch. VI, (16))

$$(14) \quad \lambda(\sigma) = M\nu(\sigma)e^{-D[\lambda(\sigma)]}$$

has one and only one solution $\lambda(\sigma)$. It is continuous, non-negative, and vanishes only where $\nu(\sigma)$ vanishes¹⁷.

¹⁷ Much of Theorem 5 is contained in the general theory of Hammerstein's integral equations (Acta Math. 54 (1930), 117-76). For convergence under iteration, see Ch. IX, §8.

Proof. Clearly, any solution of (14) must be non-negative. Since \mathbf{D} is order-preserving (Lemma 1, (vi)), it follows that $\tau(\sigma) = \mathbf{D}\lambda \geq 0$, and so, by (14), that $0 \leq \lambda(\sigma) \leq M\nu(\sigma)$. Since \mathbf{D} carries bounded functions into continuous ones (Lemma 1, (i)), we conclude that $\tau(\sigma) = \mathbf{D}\lambda$ and so $\lambda = M\nu e^{-\tau}$ are continuous. Finally, τ being bounded, $\lambda(\sigma)$ vanishes only where $\nu(\sigma)$ vanishes, proving the second sentence of the theorem.

Therefore, any solution of (14) lies in the Hilbert space \mathbf{H} of all square integrable functions on $0 \leq \sigma \leq \pi$. Now consider, on \mathbf{H} , the functional

$$(15) \quad \phi(\lambda) = \frac{1}{2} \int_0^\pi \lambda \mathbf{D}\lambda \, d\sigma + \int_0^\pi M\nu(\sigma)e^{-\mathbf{D}\lambda} \, d\sigma.$$

By Lemma 1, $\phi(\lambda)$ is defined and satisfies $\phi(\lambda) \geq 0$ for all $\lambda \in \mathbf{H}$; further, one readily computes

$$(16) \quad \begin{aligned} \phi(\lambda + \delta\lambda) - \phi(\lambda) &= \int_0^\pi (\lambda - M\nu e^{-\mathbf{D}\lambda}) \mathbf{D}[\delta\lambda] \, d\sigma + \frac{1}{2} \int_0^\pi \delta\lambda \mathbf{D}[\delta\lambda] \, d\sigma \\ &\quad + \int_0^\pi M\nu e^{-\mathbf{D}\lambda} (e^{-\mathbf{D}\delta\lambda} - 1 - \mathbf{D}[\delta\lambda]) \, d\sigma. \end{aligned}$$

This shows that $\phi(\lambda + \delta\lambda) - \phi(\lambda)$ is $O(\|\delta\lambda\|)$ if and only if $\lambda(\sigma)$ satisfies (14). That is, the solutions of (14) are the stationary points of (15).

To prove uniqueness, it is therefore sufficient to prove that (15) is strictly convex¹⁸. But this is evident, since $\lambda \neq \lambda'$ implies

$$(17) \quad \begin{aligned} \frac{1}{2}[\phi(\lambda) + \phi(\lambda')] - \phi(\tfrac{1}{2}[\lambda + \lambda']) &= \frac{1}{8} \int_0^\pi (\lambda - \lambda') \mathbf{D}[\lambda - \lambda'] \, d\sigma \\ &\quad + \frac{1}{2} \int_0^\pi M\nu(\sigma)(e^{-\mathbf{D}\lambda/2} - e^{-\mathbf{D}\lambda'/2})^2 \, d\sigma > 0. \end{aligned}$$

To prove existence, we show that the minimum of $\phi(\lambda)$ is attained; this requires some ingenuity.

Let $\mu = \text{g.l.b. } \phi(\lambda)$ for $\lambda \in \mathbf{H}$, and take a minimizing sequence $\{\lambda_n\}$ such that $\phi(\lambda_n) \rightarrow \mu$ as $n \rightarrow \infty$. By (17) and the definition of μ ,

$$\frac{1}{2}[\phi(\lambda_n) + \phi(\lambda_m)] \geq \phi(\tfrac{1}{2}[\lambda_n + \lambda_m]) \geq \mu.$$

Since the left member tends to μ as $m, n \rightarrow \infty$, by (15),

$$(18) \quad \begin{aligned} 0 &= \lim_{m, n \rightarrow \infty} \{ \tfrac{1}{2}[\phi(\lambda_n) + \phi(\lambda_m)] - \phi(\tfrac{1}{2}[\lambda_n + \lambda_m]) \} \\ &= \lim_{m, n \rightarrow \infty} \left\{ \frac{1}{8} \int_0^\pi (\lambda_n - \lambda_m) \mathbf{D}[\lambda_n - \lambda_m] \, d\sigma \right. \\ &\quad \left. + \frac{1}{2} \int_0^\pi M\nu(e^{-\mathbf{D}\lambda_n/2} - e^{-\mathbf{D}\lambda_m/2})^2 \, d\sigma \right\}. \end{aligned}$$

¹⁸ The point is that any stationary point of a strictly convex function on a linear space is a strict minimum, as one easily sees from the one-dimensional case. Hence it is unique.

Both terms on the right, being positive, must tend separately to zero. It follows, since

$$\int_0^\pi (\mathbf{D}[\lambda_n - \lambda_m])^2 d\sigma \leq \int_0^\pi (\lambda_n - \lambda_m) \mathbf{D}[\lambda_n - \lambda_m] d\sigma,$$

that $\tau_n = \mathbf{D}[\lambda_n]$ tends in the mean to a square integrable function τ , and that $\int_0^\pi M\nu e^{-\tau_n} d\sigma$ has the finite limit $\int_0^\pi M\nu e^{-\tau} d\sigma$. It is, however, difficult to show directly that $\{\lambda_n\}$ is convergent in the Hilbert space \mathbf{H} . This difficulty can be circumvented as follows. Let ω be a continuous function; then from $0 \leq \liminf_{n \rightarrow \infty} \{\phi(\lambda_n + \varepsilon\omega) - \phi(\lambda_n)\}$, we see that

$$\varepsilon \int_0^\pi \tau \omega d\sigma + \frac{\varepsilon^2}{2} \int_0^\pi \omega \mathbf{D}\omega d\sigma + \int_0^\pi M\nu e^{-\tau} (e^{-\varepsilon \mathbf{D}\omega} - 1) d\sigma \geq 0.$$

Dividing by ε and letting $\varepsilon \rightarrow 0$,

$$(19) \quad \int_0^\pi \tau \omega d\sigma - \int_0^\pi M\nu e^{-\tau} \mathbf{D}\omega d\sigma = \int_0^\pi (\tau - \mathbf{D}(M\nu e^{-\tau})) \omega d\sigma \geq 0,$$

which is only possible if $\tau = \mathbf{D}(M\nu e^{-\tau})$. The function $\lambda = M\nu e^{-\tau}$ clearly satisfies (14).

THEOREM 6 (Jacob's Lemma [39]). Let λ and $\lambda + \Delta\lambda$ be the solutions of (14) corresponding to two different non-negative values M and $M + \Delta M$ of the parameter M . Then $\Delta\lambda/\Delta M$ is a non-zero function of σ which satisfies

$$(20) \quad 0 \leq \frac{\Delta\lambda}{\Delta M}(\sigma) < \nu(\sigma) \quad \text{on} \quad 0 < \sigma < \pi.$$

Proof. By Theorem 5, $\Delta\lambda$ (hence $\Delta\lambda/\Delta M$) and $\Delta\tau = \mathbf{D}[\Delta\lambda]$ are continuous functions of σ , vanishing at $\sigma = 0, \pi$. Moreover, since M is uniquely determined by the other terms of (14), $\Delta M \neq 0$ implies $\Delta\lambda \neq 0$.

Next, from (14), direct computation gives

$$(21) \quad \frac{\Delta\lambda}{\Delta M} = \lambda e^{-\Delta\tau} \left[\frac{1}{M} - \frac{\Delta\tau}{\Delta M} \frac{e^{\Delta\tau} - 1}{\Delta\tau} \right].$$

Observe that, since $(e^u - 1)/u$ is positive for all u , the right side of (21) is non-negative when $\Delta\tau/\Delta M \leq 0$. But, since $\Delta\tau = \mathbf{D}[\Delta\lambda]$, $\Delta\tau/\Delta M$ represents (as in Ch. VI, §4) the boundary values of a harmonic function $h(re^{i\sigma})$, continuous in the unit semicircle Γ , zero on the real diameter, and having $\Delta\lambda/\Delta M$ as its outer normal derivative $\partial h/\partial n$ on the semicircular part $e^{i\sigma}$ of the boundary. The minimum of $h(re^{i\sigma})$ is therefore reached on the boundary of Γ . If this minimum were not zero, then by the Strict Maxi-

imum Principle (Ch. IV, §9), $\Delta\lambda \cdot \Delta M < 0$ at this point, contradicting (21) since (supra) the right side is positive. The same contradiction holds, if the zero minimum is attained on $0 < \sigma < \pi$. Hence $\Delta\tau \cdot \Delta M > 0$ on $0 < \sigma < \pi$.

By the Strict Maximum Principle again, assuming $\Delta M > 0$, we get $\Delta\lambda > 0$ at the *maximum* of $\Delta\tau$. By (21), this implies $e^{\Delta\tau} - 1 < \Delta M \cdot M$; that is, since $\Delta M > 0$, $(\Delta\tau \cdot \Delta M) < \Delta M^{-1} \ln(1 + \Delta M \cdot M)$. Substituting the two preceding inequalities into (21), one gets

$$(21^*) \quad 0 \leq \Delta\lambda / \Delta M < \lambda e^{-\Delta\tau} / M \leq \nu$$

by (14), completing the proof.

Again, by Ch. VI, (17), the separation angle θ_s increases monotonely with $\lambda(\sigma)$. We infer the

COROLLARY. In the case of ogival obstacles, the separation angle θ_s increases monotonely with M .

Clearly, if $\partial\lambda/\partial M$ exists, it satisfies

$$(21^{**}) \quad \partial\lambda/\partial M = M^{-1} - D[\partial\lambda, \partial M].$$

By a refinement of the above argument one can prove that $\partial\lambda/\partial M$, $\partial\tau/\partial M$, \dots exist, and that $\partial\lambda/\partial M \geq 0$, $M^{-1} \geq \partial\tau/\partial M \geq 0$, $-2M^{-2} \leq \partial^2\tau/\partial M^2 \leq 0$, $\partial^3\tau/\partial M^3 \geq 0$, etc. More generally, one can prove that $\tau(\sigma)$ increases with $\nu(\sigma)$ if $\nu(\sigma)$ is varied.

6. Convex obstacles. When one tries to apply the method of §4 to cases (such as that of smooth separation or of cusped cavities) where existence and uniqueness theorems for straight obstacles are meaningless or unavailable, serious complications result. The case of convex obstacles can, however, be treated by first appealing to Jacob's Lemma to derive an existence and uniqueness theory for *ogival* obstacles. We now follow this procedure.

To unify the discussion, we recall from Ch. VI, formulas (17), (19c), (28'''), and (32'), that various side conditions for such flows can be expressed by integral relations of the form

$$(22) \quad \int_0^\pi \lambda(\sigma) f(\sigma) d\sigma = 1,$$

where $f(\sigma)$ is positive except perhaps at $\sigma = 0, \pi$. For instance, $f(\sigma) = \text{const.}$ corresponds to a fixed separation angle, $f(\sigma) = (\pi \sin \sigma)^{-1}$ to smooth separation, $f(\sigma) = \pi^{-1} \sin \sigma$ to a cavity of zero drag, etc.

THEOREM 7. Let (i) $\nu(\sigma)$ be continuous on $0 \leq \sigma \leq \pi$, and positive on $0 < \sigma < \pi$, (ii) $f(\sigma)$ be positive and continuous on $0 < \sigma < \pi$, (iii) $N =$

$\int_0^\pi f(\sigma, \nu, \sigma) d\sigma < +\infty$, and¹⁹ $(iv) D[f\nu] \leq Cf$. Then the system (14), (22) admits one and only one solution.

Proof. For given $M \geq 0$, (14) has one and only one solution $\lambda_M(\sigma)$. We consider $I(M) = \int_0^\pi f(\sigma) \lambda_M(\sigma) d\sigma$; by (iii) and (14), $I(M) \leq MN$, and so $I(0) = 0$. Again, $I(M)$ is an increasing function of M by (ii) and Theorem 6; unicity follows from this. Further, by (20), $I(M)$ is a continuous function of M . To prove existence, it is therefore sufficient to show that $I(\infty) = \infty$. To show this, we first use (14) and Jensen's inequality¹⁰ that the arithmetic mean exceeds the geometric one, to get

$$(23) \quad \int_0^\pi f \lambda_M d\sigma / \int_0^\pi f \nu d\sigma = M \int_0^\pi f \nu e^{-\tau} d\sigma / \int_0^\pi f \nu d\sigma \\ \geq M \exp \left\{ - \int_0^\pi \tau f \nu d\sigma / \int_0^\pi f \nu d\sigma \right\}.$$

But

$$\int_0^\pi \tau f \nu d\sigma = \int_0^\pi \lambda_M D[f\nu] d\sigma \leq C \int_0^\pi \lambda_M f d\sigma, \quad \text{so by (23)}$$

$$I/N \geq M e^{-C I/N},$$

since $N = \int_0^\pi f \nu d\sigma$, which implies

$$(24) \quad I(M) \geq (N/2C) \ln (CM).$$

Thus, $\lim_{M \rightarrow \infty} I(M) = \infty$.

COROLLARY. There is a unique symmetric cavity flow having "smooth" separation (with finite curvature at the separation point), past any ogival obstacle.

Leray [52, p. 261] has shown that this is true more generally for symmetric obstacles with non-decreasing curvature ("accolades").

We are now ready to prove the existence of various flows with free boundaries satisfying various side conditions, past general convex obstacles. The integral equation (16) of Ch. VI for a convex obstacle is

$$(25) \quad \lambda = M \nu K(J\lambda) e^{-D\lambda};$$

in the ogival case, this simplifies to (14). The parameter M can be elim-

¹⁹ If $D[f\nu]$ is bounded, this condition is certainly verified when f is also positive at the endpoints; if f is zero at the endpoints, it is enough that its derivative be different from zero there. This is the case for the functions f appearing in formulas (18), (20c), (28'), (32') of Ch. VI.

inated, and the system (22), (25) reduced to the single integral equation

$$(25^*) \quad \lambda(\sigma) = \nu(\sigma)K(J\lambda)e^{-D\lambda} \bigg/ \int_0^\pi f(\sigma)\nu(\sigma)K(J\lambda)e^{-D\lambda} d\sigma.$$

To apply the Leray-Schauder Theorem (§3) to (25*) we set $K_\alpha(\theta) = \alpha K(\theta) + (1 - \alpha)$ and identify F_α with the operator on the Hilbert space H of §5,

$$(26) \quad F_\alpha[\lambda] = \nu K_\alpha(J\lambda)e^{-D\lambda} \bigg/ \int_0^\pi f\nu K_\alpha(J\lambda)e^{-D\lambda} d\sigma.$$

As α varies from 1 to 0, the curvature $K_\alpha(\theta)$ changes from $K(\theta)$ to unity, producing a continuous deformation of the obstacle into an ogive.

LEMMA. The operator F_α defined above satisfies all conditions of the Leray-Schauder Theorem, provided ν and f satisfy the conditions of Theorem 7, and provided $K(\theta)$ is a continuous function defined for all θ , and bounded away from both zero and infinity, so that

$$(27) \quad 0 < k \leq K(\theta) \leq k^{-1} < \infty.$$

Proof. We first determine a sphere containing all solutions of $\lambda = F_\alpha[\lambda]$. By (27), $k \leq K_\alpha(\theta) \leq k^{-1}$ for all α , and so

$$(28) \quad \int_0^\pi f\nu K_\alpha(J\lambda)e^{-D\lambda} d\sigma \geq k \int_0^\pi f\nu e^{-D\lambda} d\sigma.$$

As in (23) and below,

$$\int_0^\pi f\nu e^{-D\lambda} d\sigma \geq N \exp \left\{ - (C/N) \int_0^\pi f\lambda d\sigma \right\}.$$

If λ is a solution, then $\int_0^\pi \lambda f d\sigma = 1$ and

$$(29) \quad \int_0^\pi f\nu K_\alpha(J\lambda)e^{-D\lambda} d\sigma \geq kNe^{-C/N}.$$

Taking this into the equation $\lambda = F_\alpha[\lambda]$, one gets

$$\lambda \leq k^{-2}N^{-1}e^{C/N}\nu;$$

and finally, since $\lambda \geq 0$ by (25*),

$$(30) \quad \begin{aligned} \|\lambda\| &\leq k^{-2}N^{-1}e^{C/N} \|\nu\| = R. \\ \|\lambda\| &= \left[\int_0^\pi \lambda^2(\sigma) d\sigma \right]^{\frac{1}{2}}. \end{aligned}$$

This says that the solutions of $\lambda = F_\alpha[\lambda]$ are all in the interior of a sphere of radius $2R$. This sphere we can take as the domain \mathfrak{D} of the Leray-Schauder Theorem.

We prove that the F_α are completely continuous by showing that they transform bounded sets of functions in the Hilbert space $L_2(0, \pi)$ into (bounded sets of equicontinuous functions. By Lemma 1 of §5, this is true for the operator $\nu e^{-D\lambda}$, and, $J\lambda$ being an indefinite integral and K_α continuous, it holds also for $K_\alpha(J\lambda)$. Hence, since by (29) the factor $\left[\int_0^\pi f \nu K_\alpha(J\lambda) e^{-D\lambda} d\sigma \right]^{-1}$ remains bounded, this is also true for the operator F_α .

The equicontinuity of F_α with regard to α is obvious, and the uniqueness of the solution of $\lambda = F_0\lambda$ has already been established in §5. It only remains to prove that the transformation $G_0[\lambda] = \lambda - F_0[\lambda]$ is one-one in the vicinity of a solution λ of $\lambda = F_0\lambda$. Let λ and $\lambda + \Delta\lambda$ be two different functions transformed into the same function by the operator G_0 . The equation

$$(31) \quad \lambda - F_0[\lambda] = \lambda + \Delta\lambda - F_0[\lambda + \Delta\lambda]$$

can be given the form

$$(32) \quad \Delta\lambda = M\nu e^{-(\tau+\Delta\tau)} \left(1 + \frac{\Delta M}{M} - e^{\Delta\tau} \right), \quad \Delta\tau = D[\Delta\lambda].$$

We now argue as in the proof of Thm. 6. If the maximum value $\Delta\tau_{\max}$ of $\Delta\tau$ is positive, then $\Delta\lambda > 0$ at any point where $\Delta\tau = \Delta\tau_{\max}$ by the Strict Maximum Principle (Ch. IV, §9). Hence, by (32), $\Delta\tau_{\max} < \ln(1 + \Delta M/M)$ there, whence $\Delta\tau < \ln(1 + \Delta M/M)$ identically, and $\Delta\lambda > 0$ except at $\sigma = 0, \pi$ by (32). Likewise, if $\Delta\tau_{\min} < 0$, then $\Delta\lambda < 0$ wherever $\Delta\tau = \Delta\tau_{\min}$, whence $\Delta\tau_{\min} > \ln(1 + \Delta M/M)$ by (32). This implies $\Delta\tau > \ln(1 + \Delta M/M)$ identically, and so $\Delta\lambda < 0$ except at $\sigma = 0, \pi$. In either case, $\Delta\lambda$ will have constant sign.

On the other hand, $f(\sigma) > 0$ in (22); hence $f\Delta\lambda$ must also have constant sign. Moreover $\int f\Delta\lambda d\sigma = 0$, as one easily sees by substituting λ and $\lambda + \Delta\lambda$ into (22) and subtracting. Combining these results, we see that $\Delta\lambda = 0$ almost everywhere, which implies that G_0 must be one-one.

Combining the preceding lemma with the Leray-Schauder Theorem, we have the following result.

THEOREM 8. Under hypotheses (i), (ii), (iii), and (iv) of Theorem 7, and (27) on $K(\theta)$, the system (22), (25) has a solution.

COROLLARY. Let C be any symmetric convex obstacle in an unbounded flow. Then there exist

- (a) A symmetric cavity for each angle of separation
- (b) A symmetric cavity with smooth separation
- (c) A symmetric cavity of zero drag

- (d) A one-parameter family of cusped symmetric cavities
- (e) A one-parameter family of symmetric Riabouchinsky flows for each angle of separation
- (f) A one-parameter family of symmetric Riabouchinsky flows with smooth separation
- (g) A two-parameter family of symmetric reentrant jets.

If C is ogival, the solutions are unique in cases (a)–(c).

7. Method of continuity. Earlier proofs ([52], [49]) of uniqueness were based on extensions of Weinstein's method of continuity to functional equations. This method, though lacking the elegance and simplicity of the comparison methods of Ch. IV, §§12–14, has compensating advantages. Thus, it brings out the close connection between existence and uniqueness; it is applicable to asymmetric plane flows, and some of the ideas may even be applicable to asymmetric space flows.

Since the details are quite technical, we shall treat only symmetric plane flows past convex obstacles. However, not only can the argument be greatly generalized, but it yields variational formulas of intrinsic interest. These express the variation in cavity (or jet) shape induced by a given perturbation of the obstacle (or orifice). Expressed in terms of functional equations such as (1) or (6), they involve differentials of operators between Banach spaces, a concept which we shall now define.

Definition. An operator F from one Banach space into another is said to be differentiable at a point λ_0 if there is a continuous linear operator L such that

$$(33) \quad \|F[\lambda_0 + \delta\lambda] - F[\lambda_0] - L[\delta\lambda]\| = o(\|\delta\lambda\|),$$

the norms being taken in the corresponding spaces. In this case, $L[\delta\lambda]$ is called the differential of $F[\lambda]$ at the point λ_0 . We shall denote it $dF[\lambda_0; \delta\lambda]$.

A one-parameter family $F_\alpha[\lambda]$, $0 \leq \alpha \leq 1$, of operators on the Banach space \mathcal{E} , can be conceived as a single operator from the Banach space $\mathcal{E} \times R$ ($R = \text{real line}$)³⁰ into \mathcal{E} , and as such we can speak of its differential $dF[\lambda, \alpha; \delta\lambda, \delta\alpha]$ at a point λ and a value α of the parameter, when it exists. (In the following, and for simplicity, we shall omit indicating the point (λ, α) where the differential is taken, and simply write $dF[\delta\lambda, \delta\alpha]$.) We now appeal to the following general principle ([52], beginning of Part II, and [53]).

Principle of Continuity. Let λ be a solution of $\lambda = F_\alpha[\lambda]$, and assume $F_\alpha[\lambda]$ has a completely continuous differential $dF[\delta\lambda, \delta\alpha]$ at the point λ for the value of α of the parameter. Under these conditions, if the "variation

³⁰ $\mathcal{E} \times R$ is the space of all couples (λ, α) , $\lambda \in \mathcal{E}$, $\alpha \in R$, under the norm $(\|\lambda\|^2 + \alpha^2)^{1/2}$.

equation" $\delta\lambda = dF[\delta\lambda, \delta\alpha]$ admits a unique solution for every $\delta\alpha$, then: a) λ is an isolated solution of $\lambda = F_\alpha[\lambda]$; b) the equation $\lambda + \Delta\lambda = F_{\alpha+\delta\alpha}[\lambda + \Delta\lambda]$ admits a solution $\Delta\lambda$ for sufficiently small $\delta\alpha$; c) $\delta\lambda$ is the principal part of $\Delta\lambda$, that is, $\|\Delta\lambda - \delta\lambda\| = o(\|\delta\alpha\|)$.

With the help of this theorem, the unicity of solutions of $\lambda = F_1[\lambda]$ can be proved from the unicity assumed for $\lambda = F_0[\lambda]$ by observing that if its hypotheses are fulfilled for all α , $0 \leq \alpha \leq 1$, and for all solutions of $\lambda = F_\alpha[\lambda]$, then the number of solutions (these being isolated and varying continuously with α), must be independent of α . Hence it must be equal to the number of solutions of $\lambda = F_0[\lambda]$, that is, to one. Similarly, the existence of a solution of $\lambda = F_1[\lambda]$ follows if existence is assumed for $\lambda = F_0[\lambda]$.

In applications to free boundary problems, we shall apply the Principle of Continuity to the operator family $F_\alpha[\lambda]$ defined by (26). In this case, $K_0(\theta) \equiv 1$, so that existence and uniqueness follow for $\lambda = F_0[\lambda]$ by Thm. 5. For simplicity, we shall consider only infinite symmetric cavity flows past convex barriers, with $W = MT^2/2$ and $\nu(\sigma) = \sin \sigma(1 + \sin \sigma)$. We shall also assume that

$$(34) \quad |K'(\theta) - K'(\theta_1)| \leq L|\theta - \theta_1|, \quad K(\theta) > 0$$

for some finite "Lipschitz constant" L . Finally, we shall let \mathcal{E} be the Hilbert space $L^2(0, \pi)$. Then $\mathcal{E} \times R$ will also be a Hilbert space²⁰.

A simple inspection shows that $F_\alpha[\lambda]$ is differentiable for every α and λ , and that its differential is

$$(35) \quad dF[\delta\lambda, \delta\alpha] = F_\alpha[\lambda] \left(\frac{\delta M}{M} + \frac{\delta K(\theta)}{K_\alpha(\theta)} + \frac{K'_\alpha(\theta)}{K_\alpha(\theta)} J[\delta\lambda] - D[\delta\lambda] \right)$$

where

$$(36) \quad \delta K = \frac{\partial K_\alpha}{\partial \alpha} \delta\alpha = (K(\theta) - 1)\delta\alpha; \quad M = \left(\int_0^\pi f\nu K_\alpha(\theta) e^{-\tau} d\sigma \right)^{-1};$$

$$\frac{\delta M}{M} = - \int_0^\pi f F_\alpha[\lambda] \left(\frac{\delta K(\theta)}{K_\alpha(\theta)} + \frac{K'_\alpha(\theta)}{K_\alpha(\theta)} J[\delta\lambda] - D[\delta\lambda] \right) d\sigma.$$

The smoothing properties of the operators J and D (Lemma 1, §5) make $dF[\delta\lambda, \delta\alpha]$ a completely continuous operator in $\delta\lambda$, for all $\delta\alpha$, transforming bounded sets of \mathcal{E} into uniformly bounded classes of equicontinuous functions. Hence the first hypothesis of the Principle of Continuity holds.

Let now λ be a symmetric solution of $\lambda = F_\alpha[\lambda]$, whose existence was proved in §6. The variational equation $\delta\lambda = dF[\delta\lambda, \delta\alpha]$, when written out, is an integral equation of Fredholm type. For such equations, the *existence* of a solution, and its *unicity*, required by the second hypothesis of the Principle of Continuity, are each equivalent to the non-existence of a non-

zero solution of the corresponding homogeneous equation ($\delta K = 0$). (Cf. [18, vol. 1, p. 99]). Thus all consequences of the Principle of Continuity, uniqueness in particular, will hold provided $\delta\lambda = 0$ is the only solution of the equation

$$(37) \quad \delta\lambda = \lambda \left(\frac{\delta M}{M} + \frac{K'_\alpha(\theta)}{K_\alpha(\theta)} J[\delta\lambda] - D[\delta\lambda] \right),$$

where

$$\frac{\delta M}{M} = - \int_0^\pi f\lambda \left(\frac{K'_\alpha(\theta)}{K_\alpha(\theta)} J[\delta\lambda] - D[\delta\lambda] \right) d\sigma,$$

for each α , $0 \leq \alpha \leq 1$.

8. Weinstein's function. Following an idea of Weinstein^{20a}, we now construct from any $\delta\lambda$ satisfying (37), an analytic function $\Lambda(t)$ satisfying special boundary conditions (see Lemma 1 below.) In §9, we shall show how these properties imply that $\Lambda(t) = 0$, and why this implies, in turn, that the corresponding $\delta\lambda = 0$.

Let us first observe that any solution of (37) must be a continuous function satisfying a Lipschitz condition and vanishing at $\sigma = 0$ and $\sigma = \pi$ (Lemma 1, §5). Let now $\delta\Omega(t)$ be the analytic function regular in the unit circle, real on the real axis and imaginary on the imaginary axis, which assumes the boundary values $\delta\Omega(e^{i\sigma}) = \delta\theta(\sigma) + i\delta\tau(\sigma)$, $0 \leq \sigma \leq \pi$ ($\delta\theta = J[\delta\lambda]$, $\delta\tau = D[\delta\lambda]$). Since $d(\delta\theta)/d\sigma = -\delta\lambda(\sigma)$ is Lipschitzian, the Fatou-Privaloff Theorem (Ch. IV, §7) guarantees that $\delta\Omega(t)$ admits a continuous derivative satisfying a Lipschitz condition in the closed unit circle.

Let us investigate the function²¹

$$(38) \quad \Lambda(t) = \frac{\delta M}{M} W(t) - \zeta(t) \int_i^t \left(\frac{\delta M}{M} + i\delta\Omega \right) \frac{dz}{dt} dt,$$

where ζ , W and z denote as usual the conjugate velocity, complex potential and position of the flow corresponding to λ . $\Lambda(t)$ is regular in the unit circle, except possibly where $W(t)$ is singular; in the case of an infinite cavity ($W = MT^2/2$) the only singularity is at $t = 0$. Near $t = 0$, $\Lambda(t)$ has an ex-

^{20a} A. Weinstein, Math. Zeits. 19 (1924), 265-74.

²¹ $\Lambda(t)$ has an interesting interpretation. For any $\varepsilon > 0$, the functions

$$\zeta_\varepsilon(t) = \zeta(t)e^{-\varepsilon\delta\Omega}, \quad W_\varepsilon(t) = (1 + \varepsilon\delta M/M)W(t),$$

define a flow past an obstacle with curvature $K_\varepsilon = K + o(\varepsilon)$; at a fixed point of the physical plane the complex potential W_ε is a function of ε only, and its derivative $\lim_{\varepsilon \rightarrow 0} (W_\varepsilon - W)/\varepsilon$ is precisely equal to Λ . Using this interpretation, some of the results of this and the next section can be carried over to space.

pansion of the form

$$(39) \quad \Lambda(t) = \zeta(t) \left\{ a(t^{-1}) + b \ln(t^{-1}) + \sum_{k=0}^{\infty} c_k (t^{-1})^k \right\}$$

where, since $\Lambda(t)$ is real on the imaginary axis, all coefficients are real. Outside the origin and including the boundary of the unit circle, $\Lambda(t)$ has a continuous derivative, because of the continuity properties of $\delta\Omega$ obtained above, and those of Ω shown in Ch. VI, §3. On $t = e^{i\sigma}$, $0 \leq \sigma \leq \pi/2$,

$$(40) \quad \Lambda(e^{i\sigma}) = \frac{\delta M}{M} W(e^{i\sigma}) - \zeta(e^{i\sigma}) \int_{\pi/2}^{\sigma} \left(\frac{\delta M}{M} + i\delta\Omega(e^{i\sigma}) \right) \frac{dz}{d\sigma} d\sigma.$$

By Ch. VI, (9), (10) and (12)

$$dz/d\sigma = e^{i\sigma} \{ d/d\sigma \} = M\mu e^{-\tau+i\theta} e^{i\pi(2-\beta)/2} = \frac{\lambda}{K_{\alpha}(\theta)} e^{i\theta} e^{i\pi(2-\beta)/2},$$

and from (37),

$$(41) \quad \frac{\delta M}{M} - \delta\tau = \frac{\delta\lambda}{\lambda} - \frac{K_{\alpha}'}{K_{\alpha}} \delta\theta.$$

With this, the integrand in (40) becomes

$$(42) \quad e^{i\pi(2-\beta)/2} \left[\frac{\delta\lambda}{\lambda} - \frac{K_{\alpha}'}{K_{\alpha}} \delta\theta + i\delta\theta \right] \frac{\lambda e^{i\theta}}{K_{\alpha}}$$

which, since $\lambda = -d\theta/d\sigma$ and $\delta\lambda = -d\delta\theta/d\sigma$, reduces to $e^{i\pi(2-\beta)/2} \frac{d}{d\sigma} (\delta\theta e^{i\theta}/K_{\alpha}(\theta))$. Integrating, and noticing that $\zeta(e^{i\sigma})e^{i\theta+i\pi(2-\beta)/2} = -[\zeta(e^{i\sigma})]^{-1}$, one obtains

$$(43) \quad \Lambda(e^{i\sigma}) = W(e^{i\sigma}) \delta M/M + [\zeta(e^{i\sigma})]^{-1} \delta\theta K_{\alpha}(\theta).$$

In particular, $\text{Im} \{ \Lambda(e^{i\sigma}) \} = 0$.

To study $\Lambda(t)$ on the real axis, we first differentiate (38) with regard to z , obtaining

$$(44) \quad \zeta^{-1} \frac{d\Lambda}{dz} + \left(\Lambda - \frac{\delta M}{M} W \right) \frac{d\zeta^{-1}}{dz} = -i\delta\Omega.$$

Dividing (44) through by $d\zeta^{-1}/dz$ and taking imaginary parts it follows, since W , $\delta\Omega$ and $d\zeta^{-1}/dz$ are real on the real axis (Ch. IV, (27)), that

$$(45) \quad \text{Im} \left[\frac{d\Lambda}{d \ln \zeta^{-1}} + \Lambda \right] = 0, \quad t \text{ real.}$$

The corner $t = 1$ has a special interest. Since $\delta\Omega(t)$ has a Lipschitzian derivative everywhere, it admits the local expansion

$$\delta\Omega(t) = \delta\Omega(1) + \delta\Omega'(1)(t-1) + (t-1)O(|t-1|^{\gamma}),$$

which combined with the local expansions of $\zeta(t)$ and $z(t)$ (cf. Ch. IV, §7) yields

$$(46) \quad \Delta(t) - \Delta(1) = -\frac{iM}{2} \delta\theta(0)(t-1)^2 + (t-1)^2 0(1).$$

Summarizing:

LEMMA 1. The function $\Delta(t)$, defined by (38), is analytic and regular in the first quadrant of the unit circle and, the origin excepted, has a continuous derivative in the closed quadrant. Moreover, it is real on the imaginary axis and on the circular part of the boundary, satisfies (45) along the real axis, and has the local expansions (39) and (46) at the points $t = 0$ and $t = 1$, respectively.

9. Uniqueness. The unicity of flows was shown in §7 to follow when $\delta\lambda = 0$ was the only solution of (37). We shall now obtain sufficient conditions for this to hold, by first obtaining a sufficient condition for $\Delta(t) = 0$ to imply $\delta\lambda = 0$, in Lemma 2, and then (in Lemma 3) getting sufficient conditions to imply $\Delta(t) = 0$. Following this plan, we first prove

LEMMA 2 For $\Delta(t) = 0$ to imply $\delta\lambda = 0$, it is necessary and sufficient that the function $\mu(\sigma) = \frac{d}{d\sigma} (\lambda(\sigma) \cot \sigma)$ fail to satisfy equation (37).

Proof. If $\Delta(t) = 0$ then from (43)

$$(47) \quad \delta\theta(\sigma) = -\frac{\delta M}{M} W(e^{i\sigma}) K_\alpha(\theta(\sigma)) | \zeta^{-1}(e^{i\sigma}) |,$$

and recalling that $dz/d\sigma = | \zeta^{-1}(\sigma) | | dW/d\sigma | = M\nu(\sigma)e^{-\tau(\sigma)}$,

$$\delta\theta(\sigma) = -\frac{\delta M}{M} \frac{W(e^{i\sigma})}{|dW/d\sigma|} M\nu(\sigma) K_\alpha(\theta(\sigma)) e^{-\tau(\sigma)} = -\frac{\delta M}{M} \lambda(\sigma) \cot \sigma.$$

Hence $\delta\lambda = -d(\delta\theta)/d\sigma = (\delta M/M)\mu$. Thus, if $\delta\lambda \neq 0$, then $\delta M/M \neq 0$ and μ satisfies (37). Conversely, if μ satisfies (37), then μ itself is a non-zero solution of (37) whose corresponding $\Delta(t)$ vanishes identically.

It is easy to see that for $f = \text{const.}$ or $f = \pi^{-1} \sin \sigma$, corresponding to a fixed angle of separation and to the cavity of zero drag respectively (Ch. VI, §5), equation (37) cannot be satisfied by μ for any obstacle with positive curvature. In fact, if μ satisfies (37), then $\int_0^\pi f \mu d\sigma = 0$. But

$$\int_0^\pi \mu d\sigma = \int_0^\pi \frac{d}{d\sigma} (\lambda \cot \sigma) d\sigma = -2\lambda'(0) = -2M\nu_2'(0) K_\alpha(\theta(0)) \neq 0$$

$$\int_0^\pi \mu \sin \sigma d\sigma = \int_0^\pi \sin \sigma \frac{d}{d\sigma} (\lambda \cot \sigma) d\sigma = - \int_0^\pi \lambda \frac{\cos^2 \sigma}{\sin \sigma} d\sigma \neq 0.$$

We next investigate when the properties of Lemma 1 imply the vanishing of $\Lambda(t)$. Sufficient conditions have been given by different authors²²; but the following result due to K. Friedrichs [26] is the most general.

LEMMA 3. If there is a harmonic function γ vanishing nowhere in the closed first quadrant of the unit circle, and satisfying $\partial\gamma/\partial n = \gamma \partial(\ln q)/\partial n$ ($\partial/\partial n$ normal derivative, $q = \zeta$) on the real axis, then any $\Lambda(t)$ having the properties of Lemma 1 vanishes identically.

Proof. Let $\beta = \text{Im}\{\Lambda(t)\}$. It will be enough to prove that β vanishes identically. We begin by noticing that β is a harmonic function in the first quadrant, vanishing on both the imaginary axis and the circular part of the boundary. On the real axis, $d\beta/dn = \beta\partial(\ln q)/\partial n$ follows from (45) so that $\partial \ln(\beta/\gamma)/\partial n = 0$.

We shall now see that there is a level line $\beta = 0$ starting at $t = 1$ and continuing into the interior of the first quadrant. From (46),

$$\beta = \text{Im}\{\Lambda(t) - \Lambda(1)\} = -\frac{M}{2}\delta\theta(0)\text{Im}\{(t-1)^2\} + O(|t-1|^3),$$

showing that, if $\delta\theta(0) \neq 0$, such a line exists. If $\delta\theta(0) = 0$, then (46) implies that $(d\Lambda/dT)_{T=-1} = -\lim_{t \rightarrow -1} (\Lambda(t) - \Lambda(1))2t/(t-1)^2$ exists and is zero. Hence β , *qua* function of $T = -(t+t^{-1})/2$, has a zero normal derivative at the point $T = -1$ of the boundary. Therefore, by the Strict Maximum Principle (Ch. IV, §9), β has neither a local maximum nor a local minimum at $T = -1$, ($t = 1$), and again the existence of a level line leading to $t = 1$ is assured. Now, since β is harmonic, such a level line must end somewhere on the boundary. If it ended on the imaginary axis or on the circumference, then β would be zero all along the boundary of one of the domains thus formed and so would vanish identically. If it ends on the real axis, we take that domain B with boundary C composed of the real axis and the level line and consider Weinstein's quadratic form²³

$$(48) \quad \int_C \beta \frac{\partial \beta}{\partial n} - \beta^2 \frac{\partial(\ln q)}{\partial n} ds = \int_C \beta^2 \frac{\partial \ln(\beta/\gamma)}{\partial n} ds.$$

Set $\rho = \beta/\gamma$; then by Green's identity

$$\int_C \beta^2 \frac{\partial(\ln \rho)}{\partial n} ds = \iint_B [\beta^2 \nabla^2 \ln \rho + \nabla \beta^2 \cdot \nabla \ln \rho] d\sigma,$$

and by the identity $\beta^2 \nabla^2 \ln \rho + \nabla \beta^2 \cdot \nabla \ln \rho = \beta^2 |\nabla \rho|^2$ valid for harmonic

²² Cf. A. Weinstein, *Math. Zeits.* 19 (1924), 265-274; G. Hamel, *Proc. 2nd Int. Cong. Appl. Mech.*, Zurich (1926), 76, 489; H. Weyl, *Nach. Ges. Wis., Göttingen* (1927), p. 227; R. Finn, *J. d'analyse math.* 4 (1956), 246-91.

²³ This quadratic form is closely related to the second variation with respect to ε of the flows described in footnote 21. Cf. [26]. The singularity of the integrand on the right, as well as in the formulas below, where $\beta = 0$, is only apparent.

β and γ ($\rho = \beta/\gamma$),

$$\int_C \beta^2 \frac{\partial(\ln \rho)}{\partial n} ds = \iint_B \beta^2 \nabla \rho^2 ds.$$

If the level line ends at the origin, then by (39) β is bounded in B and the same argument applies.

The integral on the left is zero by construction, so that the integrand on the right, being non-negative, must vanish identically. Hence ρ must be a constant, which, since β vanishes at $t = 1$, must be zero. That is, $\beta = 0$, proving Lemma 3.

We now look for a function $\gamma(t)$ satisfying the conditions of Lemma 3. Clearly, $\partial\gamma/\partial n = \gamma\partial(\ln q)/\partial n$ is the same as $\gamma = \text{Im}\{M(t)\}$, with $M(t)$ an analytic function satisfying $\text{Im}\{\xi dM/d\xi - M\} = 0$ along the real axis. (Notice that $\text{Im}\{\xi dM/d\xi\} = \text{Im}\{dM/d \ln \xi\} = \partial\gamma/\partial \ln q$). Such a function is $\gamma = \text{Im}\{e^{-i\alpha}\xi\}$, since then $\gamma = \text{Im}\{M\}$ where $\xi dM/d\xi - M = 0$. Let us now see under which conditions α can be so chosen that γ does not vanish in the first quadrant. Clearly, γ vanishes along the level lines $\arg \xi = \alpha \pmod{\pi}$. Since $\arg \xi$ is harmonic, takes the same values at conjugate points and vanishes on the imaginary axis, these level lines must end on $t = e^{i\sigma}$, $0 \leq \sigma \leq \pi/2$. Moreover, at these points $-\arg \xi$ coincides with the tangential direction, except at $t = i$, where its limit values fill an angle equal to the semiaperture of the vertex. Thus, to assure the existence of an α never attained by $\arg \xi$, and consequently the existence of a γ with the desired properties, it is sufficient that *half the wetted portion of the obstacle have an angular extent less than π* . For convex obstacles this is the case for the cavity of zero drag (Ch. IV, §8), and obviously for a fixed separation angle less than π .

Finally, collecting the results just obtained we can conclude:

THEOREM 9. For each closed symmetric convex obstacle there is:

- only one symmetric cavity flow for each separation angle less than π .
- only one symmetric cavity of zero drag.

10. Variational method; symmetrization. The existence of flows with free boundaries can also be treated as an "isoperimetric problem", using Riabouchinsky's variational principle (Ch. IV, §§10-11). Thus, if B minimizes the induced mass $k(B)$ among all bodies bounded in part by given fixed boundaries S_i , and having given volume, then the remaining boundary of B must consist of free streamlines, by Ch. IV, Thm. 15. This means that, for some "Lagrange multiplier" Q , $k(B) - Q \text{ vol}(B)$ must be extremalized; actually, Q is the cavitation number (Ch. IV, (44)). Hence any body minimizing or extremalizing $k(B) - Q \text{ vol}(B)$ must be bounded by the S_i and free streamlines; this formulation is variational.

Isoperimetric proofs of the existence of plane and axially symmetric flows with free boundaries were first obtained by Garabedian, Spencer, Lewy and Schiffer in 1952-3 [27, 28]. These proofs rely heavily on the technique of "symmetrization". They involve two main steps

- (i) proof that a body exists which minimizes $k(B) - Q \text{vol}(B)$ locally, for given Q .
- (ii) proof that formula (44) of Ch. IV can be applied to this body.

The first question is dealt with in §§10-11, the second is the subject of a separate report^{23a}, where it is proved that the minimizing boundary is analytic.

We first recall the notion of symmetrization, introduced in 1836 by J. Steiner to prove the isoperimetric property of the sphere²⁴.

Definition. The (Steiner) "symmetrization" of a solid B in a plane Π is the body B^* constructed by taking along each line M perpendicular to Π and intersecting B , a segment centered on Π equal in length to the intersection $M \cap B$.

Clearly, B^* is symmetric in Π . Steiner proved²⁵

Steiner's Theorem. Symmetrization preserves volume and reduces area. The area remains unchanged if and only if the body is already symmetrized.

One can define similarly the (Schwarz) "symmetrization" of a plane region in a line L . In this case, symmetrization preserves area and reduces the perimeter.

It is known²⁴ that many physical quantities, such as capacity and torsional rigidity, change monotonically under symmetrization. It may be proved similarly that *induced mass* decreases under symmetrization. This result can be proved in space [27, §4], but we confine our attention to plane flows²⁶.

THEOREM 10. The induced mass of an ideal plane flow with no circulation decreases under successive symmetrizations of an obstacle B , first in a line L parallel to the flow, and then in a line M perpendicular to it.

Proof Assuming the velocity at infinity to be one, and taking the x -axis in the flow direction, the complex potential of the flows admits an expansion about the point at infinity of the form: $W = z + W_1/z + W_2/z^2 + \dots$. The stream function $V = \text{Im}\{W\}$ is then a harmonic function vanishing

^{23a} E. H. Zarantonello, "Proof of analyticity of minimizing profile". A limited number of copies are available on request from the Department of Mathematics, Harvard University.

²⁴ For a full account, see G. Polya and G. Szegő, "Isoperimetric inequalities in mathematical physics", Princeton Univ. Press, 1951.

²⁵ W. Blaschke, "Differentialgeometrie", Berlin, 1930, vol. 1, p. 249. For Schwarz symmetrization, see the ref. of fnnt. 24, p. 190.

²⁶ See [28, §4]; L. E. Payne and A. Weinstein, Pacific J. Math. 2 (1952), 633-8.

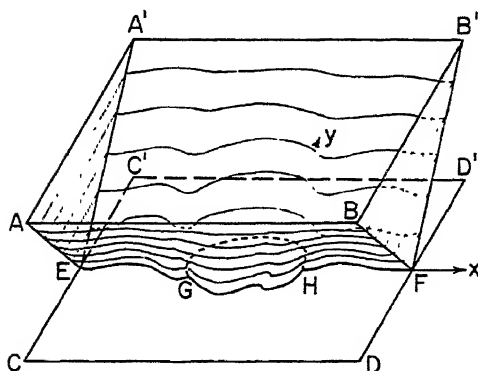


FIG. 1.

on B and approaching y uniformly at infinity. Let $Q = Q(r)$ be the square of side $2r$ centered at the origin, having two sides parallel to the stream and containing the obstacle, and let V_r be the harmonic function inside Q which vanishes on B and coincides with y on the boundary of Q . Clearly, V_r tends uniformly to V as r goes to infinity; the absolute value of V_r never exceeds r . Consider now, in (x, y, z) -space, the body (see Fig. 1) bounded below by the portion of the xy -plane inside B and the surface $z = \varepsilon |V_r(x, y)|$, $\varepsilon > 0$; laterally by the planes $x = \pm r$, and above by the plane $z = \varepsilon r$. We now symmetrize this body with regard to the xy -plane. In this process, the lateral and upper boundaries remain unchanged because they are already symmetrized. As to the lower boundary, the plane part inside B is replaced by the symmetrization B^* of B with regard to the x -axis. The surface $z = \varepsilon |V_r(x, y)|$ is replaced by a new surface $z = \varepsilon |\bar{V}_r(x, y)|$. Here \bar{V}_r is differentiable (except possibly on the x -axis) in Q , is equal to y on the boundary of Q and equal to zero on the boundary of B^* . The decrease of the total area produced by symmetrization implies an area decrease of the surface $z = \varepsilon |V_r|$, since the area of the other parts is unchanged. Therefore, comparing the analytic expressions for the area of the two surfaces,

$$\iint_{Q-B^*} [1 + \varepsilon^2 |\nabla \bar{V}_r|^2]^{\frac{1}{2}} dx dy \leq \iint_{Q-B} [1 + \varepsilon^2 |\nabla V_r|^2]^{\frac{1}{2}} dx dy.$$

Since the areas of $Q - B^*$ and $Q - B$ are the same, letting $\varepsilon \rightarrow 0$ and ignoring terms in ε^4 , we obtain

$$\iint_{Q-B^*} |\nabla \bar{V}_r|^2 dx dy \leq \iint_{Q-B} |\nabla V_r|^2 dx dy.$$

By Dirichlet's Principle, this inequality is strengthened if the function \bar{V}_r on the left is replaced by the harmonic function V_r^* taking the same

boundary values,

$$(49) \quad \iint_{Q-B^*} |\nabla V_r|^2 dx dy \leq \iint_{Q-B} |\nabla V_r|^2 dx dy.$$

Moreover,

$$\begin{aligned} \iint_{Q-B} |\nabla(V_r - y)|^2 dx dy \\ = \iint_{Q-B} |\nabla V_r|^2 dx dy - 2 \iint_{Q-B} \nabla V_r \nabla y dx dy + \iint_{Q-B} dx dy. \end{aligned}$$

By Green's formula, the middle term on the right equals $-2 \int V_r \partial y / \partial n ds$ taken over the boundary of Q , where $V_r = y$. Hence it is -2 times the area of Q , while the last integral equals the area of $Q - B$. Therefore

$$\iint_{Q-B} |\nabla(V_r - y)|^2 dx dy = \iint_{Q-B} |\nabla V_r|^2 dx dy - \text{area } Q - \text{area } B,$$

where $Q = Q(r)$.

From this and the analogous relation for V_r^* , and (49), since B and B^* have the same area, we conclude

$$(50) \quad \iint_{Q^*-B^*} |\nabla(V_r^* - y)|^2 dx dy \leq \iint_{Q-B} |\nabla(V_r - y)|^2 dx dy.$$

As $r \rightarrow \infty$, V_r^* and V_r tend uniformly to the stream functions V^* and V of the Euler flows past B^* and B respectively. It remains to show that the two sides of (50) tend to the corresponding limits, which are the induced masses of B and B^* . By Green's formula [44, p. 212] (letting Q_∞ denote the whole plane),

$$\begin{aligned} \iint_{Q_\infty-B} |\nabla(V - y)|^2 dx dy - \iint_{Q-B} |\nabla(V_r - y)|^2 dx dy \\ = - \oint_C (V - y) \partial(V - y) / \partial n ds + \oint_C (V_r - y) \partial(V_r - y) / \partial n ds \\ = \oint_C y \partial(V - V_r) / \partial n ds = \oint_C [y \partial(V - V_r) / \partial n - (V - V_r) \partial y / \partial n] ds, \end{aligned}$$

where C is the boundary of B . Again, by Green's formula, since y and $V - V_r$ are harmonic, C can be replaced by any closed curve around B without changing the value of the last integral. Thus, taking for C an analytic curve at positive distance from B , $V - V_r$ and $\partial(V - V_r) / \partial n$ both converge uniformly to zero on C (see [44, p. 248]) as $r \rightarrow \infty$, and so the integral itself

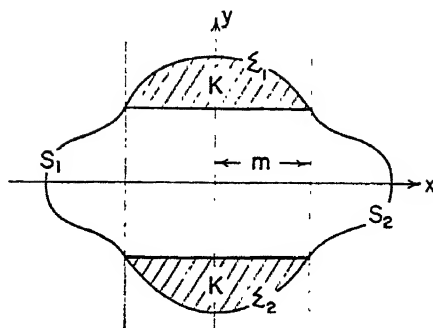


FIG. 2.

tends to zero. Hence, in the limit the right side of (50) tends to $k(B)$, the corresponding induced mass. The left side can be treated in the same way. This proves that induced mass decreases under symmetrization in L .

All steps of the above proof are valid for symmetrization in M , except perhaps for invariance of the lateral surface. But if the obstacle is already symmetrized in L , then obviously $|V_r| \leq |y|$ and the surface $z = \varepsilon |V_r(x, y)|$ bulges out, so that lines parallel to L across the lateral triangles have no intersection with it. This removes the difficulty.

11. The minimizing profile. Theorem 10 will now be applied to prove the existence of plane Riabouchinsky flows past general symmetric profiles (cf. Ch. VI, §12).

Accordingly, let C be a closed curve, symmetric in both axes, consisting of two piecewise analytic^{26a} arcs S_1 and S_2 (jointly called S) lying outside the lines $x = \pm m$, and of two horizontal straight lines, as in Fig. 2. Consider now the regions B bounded by $S = S_1 \cup S_2$ and two variable curves Σ_1 and Σ_2 (jointly called Σ), lying outside C but inside $|x| \leq m$. For all Euler flows having vector velocity $\zeta^* = 1$ at infinity, and given Q , we shall try to minimize the difference

$$(51) \quad k(B) - Q \cdot \text{Area}(B) = F(B).$$

First notice that successive symmetrizations in the x - and y -axes reduce $F(B)$ by Thm. 10, and leave C and the strip $|x| \leq m$ invariant. Hence we need only consider doubly symmetrized B 's, which, by virtue of this property, are bounded by curves monotonic in each quadrant.

Next, we show that the set of $F(B)$ is bounded below²⁷, and that the

^{26a} There is some obscurity about the precise conditions which should be imposed, as well as about some other details of the proof.

²⁷ Without the restriction of Σ to the strip $|x| \leq m$, this would not be true for $Q > 0$. To see this, let B approximate a large prolate spheroid with $k(B)/\text{vol}(B) < Q$; see [50, p. 155].

widths $h(B_n)$ of any "minimizing sequence" with $F(B_n) \downarrow I = \inf F(B)$ are bounded above. For, by Ch. IV, (42), $k(B) + \text{Area}(B)$ increases with B , and so exceeds its value for the Euler flow past a transverse plate of diameter h , which is $\pi h^2/4$ (see [50, p. 85]). On the other hand, $\text{Area}(B) \leq 2mh$, and so $F(B) \geq (\pi h^2/4) - (1+Q)2mh$. For any fixed m, Q , this is bounded below, and for $F(B)$ bounded, h is bounded above.

Since the $\{B_n\}$ are doubly symmetrized, they are defined by functions $y_n(x)$ of uniformly bounded variation. Hence, by Helly's Theorem²⁵, there is a convergent subsequence of curves $\{B_{n(k)}\}$, such that $F(B_{n(k)}) \downarrow I$ also. Since the $B_{n(k)}$ are doubly symmetric, $0 = V_n \leq y$ on the boundary in the upper half plane, and so $V_n \leq y$ identically. Hence the $V_{n(k)}$ form a compact family, from which a convergent sub-sequence can be picked [44, p. 267]. Passing to the limit, we get a doubly symmetric B minimizing $F(B)$, for any given Q and m . The boundary of B will therefore be *rectifiable*. We have thus proved

THEOREM 11. There exists a doubly symmetric domain B with rectifiable boundary, which minimizes $F(B)$ within the class of obstacles considered.

The boundary of $B = B(Q, m)$ may consist in part of the lines $x = \pm m$, or of the portion of \mathcal{C} lying in $|x| \leq m$. However, the remainder Σ_f is a *free boundary*.

To prove this, it suffices by Thm. 15 of Ch. IV to prove that Σ_f is analytic. This crucial result is derived in a separate report^{23a}, using the methods of Garabedian and Spencer [28, §§5-6], but in our notation and explaining some obscure points. Assuming it, we can deduce the existence of Riabouchinsky flow by considering the dependence of the minimizing profile $B = B(Q)$ on the cavitation number Q . In this deduction, the following lemma is crucial.

LEMMA. For each $Q > 0$, there is a unique minimizing body, which increases continuously with Q . For Q positive but small, Σ_f is a part of \mathcal{C} , while for large Q it lies entirely outside \mathcal{C} .

Proof. Let F_1 and F_2 be the upper halves of two different minimizing flows with cavitation numbers Q_1 and Q_2 , and let D_1 and D_2 be the corresponding half domains. Let F_1 be translated vertically until D_1 is entirely contained in D_2 ; the boundaries of D_1 and D_2 will then be tangent at some point P . Applying Lavrentieff's Comparison Theorem (Ch. IV, §12), the velocities at P satisfy $q_1(P) < q_2(P)$. Similarly, displacing F_2 and comparing with F_1 , a point R is found with $q_2(R) < q_1(R)$. The points P and R correspond to the maximum and minimum vertical distance between the two profiles. Since the free boundaries are strictly monotonic in each quadrant, these extremal distances cannot be attained on a vertical line cutting one profile on a free streamline and the other on the horizontal part

²⁵ M. H. Stone, "Linear transformations in Hilbert space", New York, 1932, p. 165.

of \mathcal{C} . The only exceptions occur when the extremal distance is zero, or when P or R is on the imaginary axis, in which case one flow profile must coincide with \mathcal{C} .

Hence, if neither flow domain originally contained the other, both P and R would be on free streamlines and

$$q_1(P) = q_1(R) = (1 + Q_1)^{\frac{1}{2}}, \quad q_2(P) = q_2(R) = (1 + Q_2)^{\frac{1}{2}},$$

contradicting the inequalities obtained above. Therefore either D_1 contains D_2 or conversely; to fix ideas assume $D_2 \subset D_1$, so that by the first inequality

$$q_1(P) < q_2(P) = (1 + Q_2)^{\frac{1}{2}}.$$

Unless the minimizing profile for F_1 is identical with \mathcal{C} , then

$$q_1(P) = (1 + Q_1)^{\frac{1}{2}}, \quad \text{and} \quad Q_1 < Q_2.$$

If the minimizing profile for F_1 is \mathcal{C} , then the variational formula (41) of Ch. IV (applied to a straight piece of boundary) implies $(1 + Q_1)^{\frac{1}{2}} < q_1(P)$, and again $Q_1 < Q_2$. Hence, if the minimizing flows are different their cavitation numbers are different, proving *unicity*. Furthermore, since the smaller flow domain corresponds to the larger Q , the minimizing obstacle *increases* with the cavitation number.

To show the continuous dependence of the minimizing profile on Q , consider a sequence of Q_n converging to a positive Q_0 . Then, as in the proof of Theorem 11, the corresponding profiles and stream functions form compact sequences, whose limits must coincide respectively with the minimizing profile and stream function corresponding to Q_0 . In other words, as Q tends to a positive value the minimizing flow tends to the corresponding limit. We have thus proved *continuity*.

We pass now to the last part of the lemma. Let us compare (half) the flow past a minimizing profile different from \mathcal{C} with cavitation number Q , with (half) the flow past \mathcal{C} . By displacing the latter vertically until the minimizing profile touches the horizontal part of \mathcal{C} at the point P_0 on the imaginary axis, and using Lavrentieff's Comparison Theorem again, we have

$$q(P_0) = (1 + Q)^{\frac{1}{2}} > q_0(P_0), \quad \text{or} \quad Q > q_0(P_0)^2 - 1,$$

where $q_0(P_0)$ denotes the velocity at P_0 of the flow past \mathcal{C} . Thus, if $Q < q_0(P_0)^2 - 1$ the minimizing profile must be \mathcal{C} .

Finally, we compare (half) the minimizing flow to the flow past a smooth symmetrized curve \mathcal{C}' , containing \mathcal{C} and coinciding with it along S_1 and S_2 only. Unless the minimizing profile lies entirely outside \mathcal{C}' , half the minimizing flow can be raised above \mathcal{C}' by an appropriate vertical translation, so that the minimizing profile is tangent to \mathcal{C}' at a point P (necessarily on

the free boundary). Comparing velocities at P , $(1 + Q)^{\frac{1}{2}} < q_0'(P)$, where $q_0'(P)$ is the velocity at P of the flow past \mathcal{C}' . Therefore, for all $Q > M^2 - 1$, where M is the maximum velocity for the flow past \mathcal{C}' , the minimizing profile must lie entirely outside \mathcal{C}' , and hence outside \mathcal{C} . This completes the proof of the lemma.

It follows that the length of the portion of Σ_f along $|x| = m$ is a continuous and increasing function of Q , which vanishes for Q small but not for Q large. Therefore, there is a largest $Q = Q_0$ for which it vanishes. The free boundary corresponding to Q_0 joins the endpoints of S and lies outside \mathcal{C} . Thus, the associated flow is a Riabouchinsky flow. By the lemma above this flow is unique. This proves

THEOREM 12. There is a unique Riabouchinsky flow past any doubly symmetric barrier, separating at the endpoints.

CHAPTER VIII

COMPRESSIBILITY AND GRAVITY

1. Hodograph equations. Many of the methods of Chs. II–VII can be applied to *subsonic* flows of compressible non-viscous fluids. This will be shown in §§1–7 below; supersonic flows (which involve shock waves and other complications) will be treated in §§8–9. Some of the methods of Chs. II–VII can also be applied to the free fall of incompressible, non-viscous fluids under gravity; this extension will be sketched in §§10–11.

Throughout, we shall be concerned with steady, irrotational plane flows of a non-viscous fluid. We shall continue to let ρ denote density, and shall let u, v , denote the x - and y -components of velocity. In this notation, irrotationality and mass-conservation are equivalent locally to

$$(1) \quad u_y = v_x; \quad (\rho u)_x + (\rho v)_y = 0;$$

subscripts denote differentiation. They are also equivalent to the existence of a velocity potential \mathcal{U} and stream function \mathcal{V} , satisfying

$$(2a) \quad u = \partial \mathcal{U} / \partial x = (\rho_0 / \rho) \partial \mathcal{V} / \partial y,$$

$$(2b) \quad v = \partial \mathcal{U} / \partial y = -(\rho_0 / \rho) \partial \mathcal{V} / \partial x.$$

Here ρ_0 denotes the stagnation density. On cross-differentiation, we get from (2a)–(2b)

$$(3) \quad (\rho \mathcal{U}_x)_x + (\rho \mathcal{U}_y)_y = 0.$$

Such a flow satisfies Euler's equations of motion for a *compressible* non-viscous fluid, if and only if the pressure satisfies the Bernoulli equation $q dq + dp/\rho = 0$, where $q = \sqrt{u^2 + v^2}$ is the local speed of the flow. It is *isentropic* (which usually means adiabatic), if and only if p and ρ are related by an *equation of state*¹ of the form $p = f(\rho)$, where $f(\rho)$ is an increasing function of ρ . The derivative $f'(\rho) = dp/d\rho = c^2$ of $f(\rho)$ is the *square* of the local speed of sound c , so that $M = q/c$ is the local *Mach number*. By a subsonic flow, is meant one for which $M < 1$ everywhere; §§1–7 will be concerned with such flows.

In integrated form, Bernoulli's equation in isentropic compressible flow

¹ Strictly, for "barotropic" flows. The reader who wishes to derive the formulas of §1 may consult H. W. Liepmann and A. E. Puckett, *Aerodynamics of a compressible fluid*. The final hodograph equations (7) are derived on pp. 170–1.

is clearly

$$(4) \quad q^2/2 - \int \rho^{-1} f'(\rho) d\rho = A, \quad [p = f(\rho)]$$

where A is a "reservoir constant" depending on the flow. It follows that q , p , ρ and M are all single-valued monotone functions of each other; see (11)–(11') and (26), (27). Substituting in (3), with $q^2 = U_x^2 + U_y^2$, we get a nonlinear differential equation for U , which is of elliptic type in the subsonic case.

It is well-known that the preceding equations become linear if the velocity components are taken as independent variables. Writing

$$(5) \quad \zeta = u - iv = qe^{-i\phi},$$

as in Chs. II–VII, one gets from (2a)–(2b)

$$\zeta dz = (u - iv) dx + (v + iu) dy = dU + (i\rho_0/\rho) dV.$$

This gives directly the relation

$$(6) \quad dz = dx + i dy = \zeta^{-1} [dU + (i\rho_0/\rho) dV].$$

From this, the identity $z_{q\phi} = z_{\phi q}$ leads immediately to the "hodograph" equations

$$(7) \quad \frac{\partial U}{\partial q} = - \frac{\rho_0(1 - M^2)}{\rho q} \frac{\partial V}{\partial \phi}, \quad \frac{\partial U}{\partial \phi} = \frac{\rho_0 q}{\rho} \frac{\partial V}{\partial q},$$

which are reminiscent of the Cauchy-Riemann equations. Indeed, in the incompressible case, $M = 0$ and $\rho_0/\rho = 1$, so that they become precisely the Cauchy-Riemann equations in the conjugate independent variables $\ln q$ and ϕ .

Although the preceding derivation is strictly local, and may involve even local complications when $\partial(q, \phi)/\partial(x, y)$ is zero or infinite, we shall avoid cases where such difficulties are serious², by applying (7) only to subsonic flows.

Eliminating U from (7), we get

$$(8) \quad \frac{\partial}{\partial q} \left(\frac{\rho_0 q}{\rho} \frac{\partial V}{\partial q} \right) + \frac{\rho_0(1 - M^2)}{\rho q} \frac{\partial^2 V}{\partial \phi^2} = 0.$$

A few solutions of (8) can be obtained by inspection. For example, radial flow is expressed by $V = k\phi$, which clearly satisfies (8) for any k . Again, locally irrotational *vortex flow*, with concentric circular (free) streamlines,

² As in the case of "limiting lines", Prandtl-Meyer flows, interior stagnation points, etc. The restriction to subsonic flows rules out the first two possibilities; see Liepmann-Puckett, Ch. XII, for details.

can be obtained (knowing $\rho = \rho(q)$) by integrating the ordinary differential equation $\rho_0 q dV = \rho dq$, or

$$(9) \quad V = \int (\rho/\rho_0 q) dq = \psi(q).$$

More generally, any linear combination

$$V = k\phi + k_1\psi(q)$$

represents a flow with *spiral* streamlines, all of which are congruent to each other under rotation about a fixed center.

2. Chaplygin equation of state. In the hypothetical case of an ideal fluid³ whose equation of state has the special form of Chaplygin [13],

$$(10) \quad p = p_0 - k^2/\rho,$$

the preceding equations simplify enormously. In fact, the mathematical difficulties are only slightly greater than in the incompressible case, as we shall now show.

Clearly $c^2 = f'(\rho) = k^2/\rho^2$, whence $M = q\rho/k$. Also, the Bernoulli equation (4) reduces to

$$(11) \quad q^2/2 - k^2/2\rho^2 = A.$$

Hence, writing $C = -2A$,

$$(11') \quad M^2 = 1 - C\rho^2/k^2, \quad \text{and} \quad 1 - M^2 = (C/k^2)\rho^2.$$

Thus, depending on the choice of sign for the "reservoir constant" C , the flow is always subsonic, always sonic, or always supersonic; we consider in §§1-7 only the first case, $C > 0$.

By (11'), with $M = 0$, C/k^2 is $1/\rho_0^2$. Consequently, equations (7) reduce (using 11') to

$$\frac{\partial U}{\partial q} = -\frac{\rho}{\rho_0 q} \frac{\partial V}{\partial \phi}, \quad \frac{\partial U}{\partial \phi} = \frac{\rho_0 q}{\rho} \frac{\partial V}{\partial q}.$$

Introducing the new variable $h = \int (\rho/\rho_0) dq/q$, which is determined by q or ρ , these equations reduce to

$$(12) \quad \partial U/\partial h = -\partial V/\partial \phi, \quad \partial U/\partial \phi = \partial V/\partial h;$$

³ Note that, as $M \uparrow 1$, $q \uparrow \infty$ and $\rho \downarrow 0$ if (10) is assumed. Thus equation (10) gives a good quantitative approximation to compressible flows of known real fluids, when M is confined within narrow limits (say, $M < 0.3$ or $0.6 < M < 0.8$). In this range it is the basis of the Karman-Tsien and related methods.

these are the *Cauchy-Riemann* equations. Introducing the "distorted hodograph" variable

$$(13) \quad \omega = \phi + ih,$$

we have thus shown that $W(\omega)$ is a *complex analytic function*, just as in the incompressible case.

We now normalize, by choosing units so that $\rho_0 = k = 1$, whence (11) reduces to $q^2 = \rho^{-2} - 1$ since $-2A = C = k^2/\rho_0^2$. Then clearly

$$(14) \quad \begin{aligned} h &= \int \rho \, d(q^2)/2q^2 = -\int \rho^2 \, d\rho/(\rho^{-2} - 1) \\ &= -\int d\rho/(1 - \rho^2) = \frac{1}{2} \ln \left(\frac{1 - \rho}{1 + \rho} \right). \end{aligned}$$

Conversely, we have for ρ in terms of h ,

$$(15) \quad \rho = \frac{1 - e^{2h}}{1 + e^{2h}} = -\tanh h, \quad \text{whence } q = -\operatorname{csch} h.$$

Here $h < 0$, corresponding to $q > 0$, $M = \operatorname{sech} h < 1$.

Referring to (6), since $q^{-1} = -\sinh h$ and $\rho_0/q\rho = \cosh h$, we get

$$(16a) \quad dx = -\sinh h \cos \phi \, dU - \cosh h \sin \phi \, dV = -\operatorname{Im}\{\sin \omega \, dW\}$$

$$(16b) \quad dy = -\sinh h \sin \phi \, dU + \cosh h \cos \phi \, dV = \operatorname{Im}\{\cos \omega \, dW\}.$$

Note that since $[\partial x/\partial U] \neq [\partial y/\partial V]$ in general, $z(W)$ is *not* a complex analytic function. The normalization to $k = 1$ makes it so that the incompressible case is not a limiting case.

THEOREM 1. Let $W = f(\zeta)$ define an incompressible flow Φ , whose maximum velocity $|\zeta| = 1$ is attained along a free streamline. Then, at each free streamline Mach number $M = \operatorname{sech} H < 1$, there exists a compressible flow of the ideal fluid (10) with $k = 1$, defined by $W = f(e^{H-i\omega}\zeta)$. This has the same W -diagram, geometrically similar free streamlines, and the same velocity directions at infinity as Φ .

Proof. By (12) and (13), $W = f(e^{H-i\omega}\zeta)$ defines for $W = i \ln(e^{-H}\zeta)$ a compressible flow Φ' of the ideal fluid (10). Moreover W and ϕ will be the same at corresponding points of Φ and Φ' —including points at infinity. When $|\zeta| = 1$, $h = \operatorname{Im}\{\omega\} = -H$, giving a free streamline of Φ' with $M = -\operatorname{sech} H$ and

$$(16c) \quad x = \sinh H \int \cos \phi \, dU, \quad y = \sinh H \int \sin \phi \, dU,$$

where $\phi(U)$ is the same as in the given incompressible flow. Hence free streamlines are geometrically similar, expanded in the ratio $1:\sinh H$. Further, jet thicknesses (measured across equipotentials) are expanded in the ratio $1:\cosh H$, whence length/thickness is multiplied by ρ/ρ_0 .

In particular, if the hodograph lies on one side of a straight line through the origin, the corresponding compressible flow will be non-overlapping in the physical plane.

3. Flows past wedges. Most of the results in Chs. II-III, concerning ideal plane flows with free boundaries past wedges, can be extended by Theorem 1 to any "Chaplygin" fluid satisfying an equation of state of the form (10). (To simplify the formulas, we continue to assume that units have been chosen making $\rho_0 = C = k = 1$.) Even effective numerical calculation is not substantially more difficult. We shall now sketch this extension.

Circular sector hodograph. First, consider any flow having a circular sector hodograph, which subtends an angle π/n . By a rotation, we can assume that the angle is $0 < \phi < \pi/n$, and that the value of h on the free streamline is $-H < 0$. The variable $n(\omega + iH)$ then occupies the same half-strip,

$$(17) \quad \operatorname{Im} \{n(\omega + iH)\} < 0, \quad 0 < \operatorname{Re} \{n(\omega + iH)\} < \pi,$$

as the analogous variable $\omega = i \ln \zeta$ does in the incompressible case. Thus $T = -\cos n(\omega + iH)$ occupies the upper half-plane. Consequently, flows with a circular sector hodograph will satisfy, as in Theorem 5 of Ch. III, an equation of the form

$$(18) \quad dW/dT = 1 / \prod_{i=1}^m (T - T_i) \quad [m = 1, 2, \text{ or } 3].$$

If a square grid is used in $n(\omega + iH)$, values of T can be computed by iterative formulas as in Ch. IX, §6. The position coordinates x, y are then obtained using (16a)-(16b), by numerical quadrature of the harmonic functions

$$(19a) \quad x = -\operatorname{Im} \left\{ \int \sin \omega \, dW \right\} = -\operatorname{Im} \left\{ \int \frac{\sin \omega \sin n(\omega + iH)}{\prod_{i=1}^m (T - T_i)} d(n\omega) \right\}$$

$$(19b) \quad y = \operatorname{Im} \left\{ \int \cos \omega \, dW \right\} = \operatorname{Im} \left\{ \int \frac{\cos \omega \sin n(\omega + iH)}{\prod_{i=1}^m (T - T_i)} d(n\omega) \right\}.$$

Thus x and y are harmonic functions of ω , although *not conjugate* harmonic functions. It follows that the quadrature formulas of Ch. IX, §6, can be used without loss of accuracy.

Furthermore, if $\sin \omega$ and $\cos \omega$ are replaced by their linear expressions in terms of the exponentials $e^{\pi - i\omega}$, $e^{i\omega - \pi}$, x and y can be expressed in (16a)-(16b) by integrals of the type used in the incompressible case (Ch. II, §9), so that an analog of von Mises' closed form and expressions in terms of incomplete beta functions are again possible.

Reflection principle. When the hodograph is not simply covered, it is possible to adapt the Reflection Principle of Ch. III, §§2-3. We consider simply connected flows bounded (in the extended sense, counting points at infinity as ordinary points) by a wedge (or plate) and a single free streamline. We use again t , a complex parameter ranging over the unit semi-circle. The origin in the t -plane corresponds to the vertex of the wedge (or the stagnation point on a plate), and the points ± 1 to the separation points, so that the bounding diameter $-1 \leq t \leq 1$ corresponds to the wedge, and the circumference $|t| = 1$ to the free streamline. Then $T = \frac{1}{2}(t + t^{-1})$ occupies the lower half-plane, and V is piecewise constant on the real T -axis. From this fact, dW/dT can be determined as in Ch. III, Theorem 2, by studying its zeros (stagnation points) in the lower half-plane, and its singularities (jumps, sources and sinks) on the real axis.

Similarly $e^{\pi(H-i\omega)}$ is a rational function of t , whose zeros and poles can be determined using the Reflection Principle, as in Ch. III, §7. From this, x and y can be obtained by numerical quadrature, using (19a)-(19b).

4. Curved obstacles. Compressible flows of "Chaplygin" fluids past curved obstacles can also be constructed, by a similar generalization of the methods described in Ch. VI.

We use again the Levi-Civita parameter t , and note trivially that $W(t)$ and $\Omega(t)$ have unchanged meanings. In place of the conjugate velocity, we use its analog

$$(20) \quad \zeta = e^{-i\omega} = e^{\lambda - i\phi} = e^{-H} \left(\frac{1 + it}{1 - it} \right)^{\beta} e^{-i\Omega(t)}, \quad [\Omega = \theta + i\tau],$$

where H depends on the Mach number $M = \text{sech } H$. On the free boundary, where t is real, $\tau = 0$. Hence, applying the Reflection Principle to τ , w^e have much as in Ch. VI, (8a)-(8b)

$$(21a) \quad \theta = a_0 + a_1 \cos \sigma + a_2 \cos 2\sigma + \dots,$$

$$(21b) \quad \tau = a_1 \sin \sigma + a_2 \sin 2\sigma + \dots$$

On the fixed boundary, $h \neq -H$, and in fact,

$$(22) \quad e^{\lambda+H} = e^{\tau} \left| \frac{1 + it}{1 - it} \right|^{\beta} = e^{\tau} \left| \frac{\cos \sigma}{1 + \sin \sigma} \right|^{\beta},$$

whence $q^{-1} = \sinh(-h) = \frac{1}{2}(e^{-h} - e^h)$ can be calculated. Arc-length along the fixed boundary can then be obtained by integrating

$$(23) \quad \begin{aligned} l &= \int q^{-1} dU = \int_{\pi/2}^{\sigma} \frac{1}{2}(e^{-h} - e^h) \frac{L |\cos \sigma \sin \sigma|}{\Pi(1 - \alpha_k \cos \sigma)} d\sigma \\ &= L \int_{\pi/2}^{\sigma} \frac{e^{-\tau(\sigma)} F_1(\sigma) - e^{\tau(\sigma)} F_2(\sigma)}{\Pi(1 - \alpha_k \cos \sigma)} d\sigma. \end{aligned}$$

In (23), L refers to the parameter denoted by M in Chs. VI and VII; the functions $F_1(\sigma)$ and $F_2(\sigma)$ are

$$F_i(\sigma) = e^{\pm H} \sin \sigma \cos \sigma^{1-\beta} (1 \pm \sin \sigma)^\beta$$

and are independent of $W(t)$. Note that the functions $F_i(\sigma)$ have no singularity in the interval $0 \leq \sigma \leq \pi$, if $\beta \leq 1$. Thus, in the case $\beta = 1$ of a smooth barrier,

$$F_1(\sigma) = e^H \sin \sigma (1 + \sin \sigma),$$

$$F_2(\sigma) = e^{-H} \sin \sigma (1 - \sin \sigma).$$

Finally, using the curvature equation $d\theta/d\sigma = -K(\theta) dl/d\sigma$, and the argument leading to formula (16) of Ch. VI, we get the integral equation

$$(24) \quad \lambda = LK(J\lambda) \cdot [\nu_1(\sigma)e^{-D\lambda} - \nu_2(\sigma)e^{D\lambda}].$$

Here $\lambda = -d\theta/d\sigma$ and $\nu_i(\sigma) = F_i(\sigma)/\Pi(1 - \alpha_k \cos \sigma)$; $J\lambda = \theta$ and $D\lambda = \tau$ are computed just as in Ch. VI, (14a)-(14d). Also, solving $M = \operatorname{sech} H$ (Theorem 1), we have

$$(24^*) \quad e^H = M^{-1}(1 + \sqrt{1 - M^2}), \quad e^{-H} = M^{-1}(1 - \sqrt{1 - M^2}).$$

In summary, we have proved

THEOREM 2. Subsonic "Chaplygin" flows past a barrier P having curvature $\kappa = K(\theta)$ of constant sign correspond one-one to functions $\lambda(\sigma)$ satisfying integral equations of the form (24), under the preceding formulas.

5. Polytopic equation of state. Chaplygin [13] also invented a way to calculate subsonic "simple" flows with circular sector hodographs from the corresponding incompressible flows (Chs. II-III), for any fluid satisfying a "polytopic" equation of state⁴

$$(25) \quad p - p_0 = k\rho^\gamma.$$

Chaplygin's method, which has since been carried further by other authors^{4a}, will now be described briefly.

With a polytopic equation of state, Bernoulli's equation takes the form

$$(26) \quad \rho = \rho_0(1 - \tau)^\beta,$$

⁴ In a "perfect gas", $p = k\rho^\gamma$; see Liepmann-Puckett, op. cit. For gases, (25) gives an adequate approximation over the entire range of subsonic flow.

^{4a} C. Jacob, *Mathematica (Cluj)* 7 (1934), 205-11, and *Bull. Acad. Roum.* 28 (1946), 637-41. A. Busemann, *ZaMM* 17 (1937), p. 73; B. Demtchenko, *Publ. sci. tech. min. air* 144 (1938); D. F. Ferguson and M. J. Lighthill, *Proc. roy. soc. A* 192 (1947), 135-42; N. A. Slezkin, *Prikl. mat. mekh.* 16 (1952), 227-30; A. Shapiro, "Compressible flow", New York, 1953, pp. 358-9; L. C. Woods, *QJMAM* 7 (1954), 262-82, and *Proc. roy. soc. A* 227 (1955), 367-86. For experimental data for jets from slots, see J. A. Perry, *Trans. Am. soc. mech. eng.* 71 (1949), 757-64; the agreement with theory is good.

where

$$(27) \quad \tau = \frac{(\gamma - 1)}{2k\gamma\rho_0^{\gamma-1}} q^2, \quad \beta = 1/(\gamma - 1).$$

The hodograph equations (7) become

$$(28) \quad \begin{aligned} U_\tau &= -\frac{(1 - (2\beta + 1)\tau)}{2\tau(1 - \tau)^{\beta+1}} V_\phi \\ U_\phi &= 2\tau(1 - \tau)^\beta V_\tau. \end{aligned}$$

Eliminating U , we obtain for V the differential equation (cf. (8))

$$(29) \quad \frac{\partial}{\partial \tau} [2\tau(1 - \tau)^\beta V_\tau] + \frac{1 - (2\beta + 1)\tau}{2\tau(1 - \tau)^{\beta+1}} V_\phi = 0.$$

Solutions of this equation can be obtained by the simple device of separating variables. Setting $V = B_m \tau^m {}_2F_m(\tau) \sin(m\theta + \epsilon_m)$, where B_m and ϵ_m are constants, one obtains for F_m the differential equation

$$\begin{aligned} \tau(1 - \tau)F_m''(\tau) + [(m + 1) - (m + 1 - \beta)\tau]F_m'(\tau) \\ + \frac{1}{2} m(m + 1)\beta F_m(\tau) = 0, \end{aligned}$$

which is satisfied by the hypergeometric function

$$(30) \quad F_n(\tau) = F(a, b, c; \tau) = 1 + a \cdot b \tau + \frac{a(a + 1)b(b + 1)}{1 \cdot 2c(c + 1)} \tau^2 + \dots,$$

where $a + b = m - \beta$, $c = m + 1$ and $ab = -(\frac{1}{2})\beta m(m + 1)$. Since (29) is linear, any convergent series of the form

$$(31) \quad V = \sum B_m \tau^m {}_2F_m(\tau) \sin(m\phi + \epsilon_m),$$

with convergent derivatives, is a solution of (29).

Now consider a compressible flow bounded by a straight wall and a free streamline of constant subsonic velocity q_0 . Thus θ and τ are alternately constant on the boundary. We compare this flow with the incompressible flow having the same fixed wall and having a free boundary of the same velocity q_0 . The complex potential $W_1 = U_1 + iV_1$ of the incompressible flow is an analytic function of $i\omega_1 = \ln(\xi/q_0)$. Assume that W_1 has an expansion of the form

$$(32) \quad W_1 = k + iB\omega_1 + \sum k_n(e^{i\omega_1})^{2n}, \quad k_n = B_n e^{i\alpha_n},$$

so that the stream function is

$$(33) \quad V_1 = A + B\phi + \sum B_n(q^2/q_0^2)^n \sin(2n\phi + \alpha_n).$$

Chaplygin's Theorem asserts

THEOREM 3. If (33) is the stream function for an incompressible flow bounded by a straight line and a free boundary, then

$$(34) \quad V = A + B\phi + \sum B_n(\tau/\tau_0)^n (F_{2n}(\tau)/F_{2n}(\tau_0)) \sin(2n\phi + \alpha_n)$$

is the stream function for a compressible flow having the same fixed boundary and a free boundary of the same velocity.

Proof. We first verify that V satisfies the proper boundary conditions. For $\tau = \tau_0$, the right side of (34) coincides with the right side of (33) and so V is constant along the free streamline. Moreover, since V_1 is constant along the straight part $\phi = \phi_0$ of the boundary, evidently $\sin(2n\phi_0 + \alpha_n) = 0$ for all n . Therefore V is also constant for $\phi = \phi_0$.

Secondly, we observe that (34) formally satisfies the differential equation (29) for stream functions of polytropic flows. The proof that the series (34) is not merely formal requires delicate arguments of convergence, which cannot find space here⁵.

For applications to jets from slots and funnels, to jets impinging on plates, etc., we refer to the literature^{4a}.

Theoretically, the transformation $V_1 \rightarrow V$ of (33)-(34) also enables one to construct compressible cavity flows past curved barriers from incompressible ones. However, as the boundary shape changes in a complicated way, the method does not seem promising in such cases.

6. General equation of state. Quite recently, P. W. Berg⁶ has obtained existence and uniqueness theorems for subsonic compressible flows having a general equation of state, thus partly extending Chs. VI-VII.

We shall now present this extension. For simplicity, we consider only symmetric cavity flows past (symmetric) barriers with vertex angle $\beta\pi$ in an infinite stream. The first step is to obtain an appropriate system of integral equations.

In this treatment, it is convenient to use the "symmetrized hodograph", defined by⁷ $h = \int (1 - M^2)^{\frac{1}{2}} dq/q$ and ϕ . This gives the "symmetrized hodograph" equations

$$(35a) \quad \frac{\partial U}{\partial h} = -\frac{\rho_0}{\rho} \sqrt{1 - M^2} \frac{\partial V}{\partial \phi}$$

⁵ See [13, Part II]. Also, "Modern developments in fluid dynamics. High speed flow", Oxford, 1953, Ch. VII, §4; R. von Mises and M. Schiffer, *Advances in Applied Mechanics*, vol. 1 (1948), 249-85. On p. 277 of the last article, a flow with cusped cavities is given.

⁶ Ph.D. Dissertation, New York University, April, 1953. We assume that $p = p(\rho)$ and $M = M(q)$ are increasing functions, in the equation of state. For the underlying theory of pseudo-conformal maps, see [82, p. 120] and M. Lavrentieff, *Mat. Sbornik* 21 (1947), 285-325 and *Izv. Akad. Nauk* 12 (1948), 513-34.

⁷ See Liepmann-Puckett, *op. cit.* in *fnnt.* 1, §11.2.

$$(35b) \quad \frac{\partial U}{\partial \phi} = \frac{\rho_0}{\rho} \sqrt{1 - M^2} \frac{\partial V}{\partial h};$$

in the special case of Chaplygin fluids, this simplifies to (12). We further define $\xi = \exp(-i\omega) = \exp(h - i\phi)$ as in (20). Along the free boundary (cavity wall), clearly h is constant; and as in §4, we denote this constant $-H$.

The first step consists in mapping the flow symmetrically, as in Ch. VI, onto the unit semicircle

$$(36) \quad \Gamma: |t| < 1, \quad \text{Im } t > 0,$$

so that the fixed boundary is mapped onto the arc $t = e^{i\sigma}$ [$0 \leq \sigma \leq \pi$], the free streamline is mapped onto the diameter $-1 < t < 1$, and $\tilde{\xi}(t)$ is a complex analytic function. The existence of such a "conformal map" follows from a generalization⁶ of the Fundamental Theorem of Conformal Mapping, which applies in its usual form when the ξ -domain ("distorted hodograph") is simply covered.

By symmetry, the dividing point is mapped onto $t = i$. Hence, as in Ch. VI, §2, if we write

$$(37) \quad \xi^{-1} = e^H \left(\frac{1 - it}{1 + it} \right)^\beta e^{i\Omega(t)}, \quad \Omega(t) = \theta + i\tau,$$

$\Omega(t)$ is a complex analytic function of t , regular in Γ , real on the real axis, and vanishing at $t = 0$. Moreover by the Schwarz Reflection Principle (Ch. III, §2), it can be extended to a function regular in $|t| < 1$. Taking note of the symmetry, we can therefore write

$$(38) \quad \Omega(t) = a_1 t + a_3 t^3 + a_5 t^5 + \dots$$

Again, since $\tilde{\xi}(t)$ and $\omega(t)$ are complex analytic functions, we can infer from (35a)–(35b) the analogous equations for ξ and η ($t = \xi + i\eta$),

$$(39) \quad \alpha \partial U / \partial \xi = \partial V / \partial \eta, \quad \alpha \partial U / \partial \eta = -\partial V / \partial \xi,$$

where $\alpha = \alpha(h, (t))$ can be determined, using (37), if $\Omega(t)$ and the equation of state are given.

We now introduce the complex-valued function

$$(40) \quad r(t) = \partial U / \partial \xi - i \partial U / \partial \eta = \alpha^{-1} \left(\partial V / \partial \eta + i \partial V / \partial \xi \right).$$

Introducing the notation

$$\frac{\partial}{\partial t} = \frac{1}{2} \left(\frac{\partial}{\partial \xi} - i \frac{\partial}{\partial \eta} \right), \quad \frac{\partial}{\partial t^*} = \frac{1}{2} \left(\frac{\partial}{\partial \xi} + i \frac{\partial}{\partial \eta} \right),$$

this can be written $r(t) = [2/(1 + \alpha)]\partial W/\partial t$. In the incompressible case, $r(t)$ reduces to the derivative dW/dt . In the compressible case, one can show that $r(t)$ satisfies a differential equation, as follows. Let

$$\mu = -\frac{h}{4} \frac{\alpha'}{\alpha} \left(\frac{d\xi}{\xi dt} \right)^* = -\frac{ih}{4} \frac{\alpha'}{\alpha} \left\{ \Omega'(t) - \frac{2\beta}{1 + \beta} \right\}^*.$$

Like α , $\mu = \mu(h, t)$ is determined by $\Omega(t)$ and the equation of state.

From (39), we get directly

$$\alpha r(t) = i\partial V/\partial t, \quad \alpha r^*(t) = -i\partial V^*/\partial t^*.$$

Differentiating with respect to t^* and t , respectively, and adding, one gets

$$\partial(\alpha r)/\partial t^* + \partial(\alpha r^*)/\partial t = 0,$$

and, carrying through the differentiations

$$(41) \quad \frac{\partial r}{\partial t^*} = \mu r + \mu^* r^*.$$

The vanishing of V along the boundary implies by (40) that $r(t)$ is real along the real axis and that $tr(t)$ is imaginary along the semicircle $t = e^{i\sigma}$, $0 \leq \sigma \leq \pi$. At $t = i$ (corresponding to the dividing point) $r(t)$ should vanish and at $t = 0$ it should go to infinity. At these points, we assume that $r(t)$ behaves as in the incompressible case. With the help of an unknown function $\Lambda(t)$, we also let

$$(42) \quad r(t) = r_1(t)e^{\Lambda(t)},$$

where $r_1(t) = M(t - t^{-3})/4$ is the function r for the incompressible case. Clearly, $\Lambda(t)$ is real on the boundary, and without loss of generality we can assume $\Lambda(0) = 1$. Inserting (8) into (41) and taking account of the analyticity of $r_1(t)$, one gets for $\Lambda(t)$ the differential equation

$$(43) \quad \frac{\partial \Lambda}{\partial t^*}(t) = \mu + \frac{r_1^*(t)}{r_1(t)} \mu^* e^{\Lambda^*(t) - \Lambda(t)}.$$

Finally, writing (7) in terms of t , we get for the position in the physical plane

$$(44) \quad dz = \zeta^{-1} \left[\frac{1}{2} \left(1 + \frac{\rho_0}{\rho} \alpha \right) r(t) dt + \frac{1}{2} \left(1 - \frac{\rho_0}{\rho} \alpha \right) r^*(t) (dt)^* \right],$$

and both the complex velocity and the position are expressed by (37) and (44) in terms of an analytic function $\Omega(t)$ and of a complex-valued function $\Lambda(t)$ satisfying the differential equation (43).

7. Integral equations. The determination of the functions Ω and Λ so that they yield a flow past a prescribed obstacle can be reduced to the solution of a system of integral equations, as we shall see.

Taking the modulus on both sides of (44), we get for the arc-length element dl along the obstacle ($t = e^{i\sigma}$),

$$(45) \quad dl = |\dot{\zeta}^{-1}| |r(t) dt| = Mq^{-1}e^{\Lambda(\sigma)} |\sin \sigma| |\cos \sigma| d\sigma.$$

The conjugate velocity ζ and the distorted velocity ξ have the same argument, and so, as in Ch. VI, §2, $\theta(\sigma)$ coincides on the obstacle with the angle of the tangential direction with the y -axis. We get for the curvature

$$\kappa = -\frac{\partial\theta}{\partial l} = -\theta'(\sigma) |Mq^{-1}e^{\Lambda(\sigma)} \sin \sigma| |\cos \sigma|.$$

Thus if the obstacle is given by the curvature equation $\kappa = K(\theta)$ (cf. Ch. VI, §3) we get for $\lambda = -\partial\theta/\partial\sigma$ the integral equation

$$(46) \quad \lambda = MK(\theta(\sigma))q^{-1}e^{\Lambda(\sigma)} |\sin \sigma| |\cos \sigma|.$$

It is important to make clear the dependence of q upon Ω , and we write $q^{-1} = Q(|\dot{\zeta}^{-1}|)$ where Q is a known increasing function (see footnote 6). From (37), $q^{-1} = Q\left(e^H \left(\frac{1 + \sin \sigma}{|\cos \sigma|}\right)^\beta e^{-\tau(\sigma)}\right)$ and so (46) becomes

$$(47) \quad \lambda(\sigma) = Me^{\Lambda(\sigma)} K(\theta(\sigma)) |\sin \sigma| |\cos \sigma| Q\left(e^H \left(\frac{1 + \sin \sigma}{|\cos \sigma|}\right)^\beta e^{-\tau(\sigma)}\right)$$

where $\tau = D\lambda$, $\theta = \int_{\sigma}^{\pi/2} \lambda d\sigma$ as in Ch. VI. This corresponds to equation (16) of Ch. VI. An analog of the Villat equation (Ch. VI, (15)) can also be derived.

Equation (47) still contains the function Λ . We shall now derive an integral equation for it. For this purpose, we apply to $\Lambda(t)$ the generalized Cauchy formula (for the semicircle)

$$(48) \quad \Lambda(t) = \frac{1}{2\pi i} \oint \frac{\Lambda(t')}{t' - t} dt' - \frac{1}{\pi} \iint \frac{\partial\Lambda(t')/\partial t'^*}{t' - t} d\xi' d\eta'$$

valid for any complex valued function. This formula follows from the classical identities of potential theory,

$$\begin{aligned} f(t) &= \frac{1}{2\pi} \oint f \frac{\partial \ln r}{\partial n} ds - \frac{1}{2\pi} \iint (r_{\xi} f_{\xi} + r_{\eta} f_{\eta}) \frac{d\xi' d\eta'}{r} \\ 0 &= -\frac{1}{2\pi} \oint f \frac{\partial}{\partial s} \ln r ds - \frac{1}{2\pi} \iint (r_{\eta} f_{\xi} - r_{\xi} f_{\eta}) \frac{d\xi' d\eta'}{r}. \end{aligned}$$

These are obtained by applying Green's first identity [44, p. 212] to the pairs of functions $(f(t'), \ln |t - t'|)$ and $(f(t'), \arg(t' - t))$ respectively.

On account of (43), (48) becomes

$$(49) \quad \Lambda(t) = \frac{1}{2\pi i} \int \frac{\Lambda(t')}{t' - t} dt' - \frac{1}{\pi} \iint \frac{\mu + (r_1^*, r_2^*)\mu^* e^{\Delta^*, t - \Delta, t'}}{t' - t} d\xi' d\eta'.$$

This equation involves $\Omega(t)$, and so $\lambda(t)$, through the function μ . Equations (47) and (49) form the systems of integral equations for λ and Λ , to which Berg has reduced the compressible cavity flow problem. The full statement of the problem also involves a side condition (separation condition) permitting one to determine also the parameter M . The existence of a solution for (47) and (49) has been proved by Berg⁶, in the case of the barrier problem, by an application of the Leray-Schauder theory (cf. Ch. VII, §2-3). From his results, it follows that there is one cavity flow for any symmetric curved barrier which is cut at most once by any line parallel to the axis, and for any subsonic maximum of the velocity q .

8. Supersonic jets. The structure of supersonic jets and wakes is very complicated, and their mathematical analysis correspondingly difficult. We shall defer to Ch. XIV the discussion of supersonic wakes, and that of the turbulent "mixing zone" which bounds supersonic jets, presenting here only some properties of supersonic jets which do not involve viscosity or turbulence⁸, and which occur in muzzle blast, the exhaust from rocket motors, and jets used in stream turbines.

Within the limitations of the Chaplygin equation of state (10), the problem of a supersonic jet from a slot has no solution, since mixed subsonic-supersonic flow is then impossible (§2). In the approximation of a polytropic equation of state, the subsonic part of the flow of a supersonic jet from a funnel (which is subsonic upstream) has been worked out by Frankl⁹, following the ideas of Chaplygin [13].

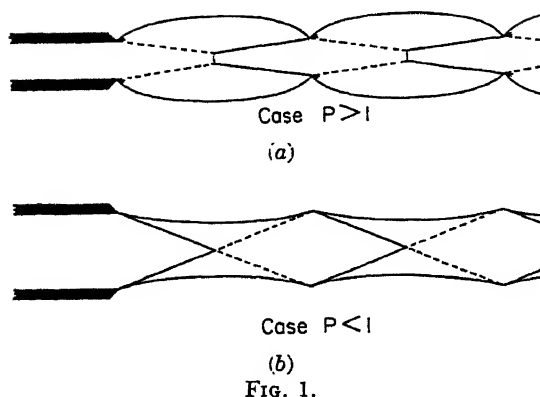
For a realistic understanding of plane and axially symmetric supersonic jets, one must begin with the experimental fact¹⁰ that such jets have an essentially *periodic* structure which involves *discontinuities* in the velocity $u(\mathbf{x})$ as a function of position. This structure was first analyzed by Prandtl¹¹.

⁸ We shall also omit discussing the paradox of Wantzel and St. Venant (1839), which is treated in [50, §25].

⁹ Doklady Akad. Nauk SSSR 58 (1947), 381-4. With $\gamma = 1.4$, Frankl found a maximum discharge coefficient of 0.85. For an interesting theoretical discussion of periodic "jets" satisfying (10), see N. Coburn, J. appl. phys. 22 (1951), 124-30.

¹⁰ R. Emden, Ann. der Physik und Chemie 69 (1899), 264-89 and 426-53. Emden refers to earlier work by L. Mach and Parenty (1897). See also T. Stanton, Proc. roy. soc. A111 (1926), 306-39; J. Hartmann and F. Lazarus, Phil. Mag. 31 (2941), 35-50; M. S. Kisenko, NACA TM 1066.

¹¹ L. Prandtl, Phys. Zeits. 5 (1904), 599-601 and 8 (1907), 23-32. See also Th. von Karman, ibid. 8 (1907), 209-11; Rayleigh, Phil. Mag. 32 (1916), 177-87; Stodola-Loewenstein, "Steam and gas turbines", New York, 1927, §42a ff; Courant-Friedrichs, "Supersonic flow and shock waves", New York, 1948, §148.



In this analysis, the nozzle is assumed parallel, and the ratio $P = p_n/p_e$ of the nozzle pressure p_n to the external pressure p_e plays a basic role¹².

If $P = 1$, the simple parallel flow of Ch. I, Fig. 5a, provides a mathematical solution to the problem.

In the usual case $P > 1$, the jet first *expands* at the nozzle edges through a Prandtl-Meyer expansion fan, as in Fig. 1a, so that the velocity increases discontinuously at the edges. The jet continues to expand until its mean pressure drops well below the pressure of the surrounding gas, assuming extreme values on the axis. It then starts to contract, and goes in this way through several cycles of alternate contraction and expansion, more or less periodically.

The case $P < 1$ can also be realized, using a Laval (convergent-divergent) nozzle. In this case, a compression shock springs from the nozzle edges, as in Fig. 1b; the velocity decreases discontinuously across the shock. Moreover, the cycle of alternate expansions and contractions starts with a contraction.

The wave-length λ of (periodic) supersonic jets can be estimated¹¹ by perturbing the trivial case $P = 1$, so that linearized supersonic flow theory is applicable. As usual [4, p. 113], if $U = vx + \phi$ denotes the perturbed velocity potential of a supersonic jet with velocity v parallel to the x -axis and diameter D , then ϕ satisfies the wave equation

$$(50a) \quad (M^2 - 1)\partial^2\phi/\partial x^2 = (\partial^2\phi/\partial y^2 + \partial^2\phi/\partial z^2),$$

the pressure perturbation being given by

$$(50b) \quad p_0 - p = v(\partial\phi/\partial x).$$

¹² If the reservoir (chamber) pressure is p_r , then the (sonic) pressure in the nozzle throat is $p_r/[(\gamma + 1)/2]^{\gamma/(\gamma-1)}$, which is about 1.9 for air. Hence $p_r/p_e > p_r/p_n > 1.9$ for supersonic air jets.

In Prandtl's original paper, v was taken to be the efflux velocity; when $P > 1$, the mean jet velocity is, however, greater.

For periodic perturbations with period $\lambda = 2\pi/\omega$ one naturally tries

$$\phi = \cos \frac{\omega x}{\sqrt{M^2 - 1}} \begin{cases} \cos \omega y \\ J_0(\omega r) \end{cases}$$

in the plane and axially symmetric case, respectively. (As usual, $M = v/c$ where c denotes the speed of sound.) To satisfy the condition of constant pressure on the jet boundary $y = \pm D/2$ (resp. $r = D/2$), we set $(\omega D/2)\sqrt{M^2 - 1} = \pi/2$ with plane jets, and $(\omega D/2)\sqrt{M^2 - 1} = \beta_1$, the first zero of $J_0(u)$, with axially symmetric jets. This gives

$$(51) \quad \lambda/D = 2\pi/\omega D = \begin{cases} 2\sqrt{M^2 - 1} & (\text{plane jets}) \\ 1.3\sqrt{M^2 - 1} & (\text{ax. symm. jets}), \end{cases}$$

since (π/β_1) is about 1.3. These predictions agree with observation, to a first approximation.

In the plane case, one can derive (51) even more simply [64, p. 87], by assuming that pressure changes are propagated along characteristics. For P near one, characteristics make an angle α with the jet axis which satisfies $M = \sec \alpha$; and they return to their original position after crossing the jet twice. From this, $\lambda/2D = \cot \alpha = \sqrt{M^2 - 1}$ follows by elementary trigonometry.

However, to compute λ for large P , and to compute the detailed streamline configuration, one must use numerical integration (the "method of characteristics"). For the details, we refer the reader to the literature¹³.

9. Ultra-fast jets. Considerable effort has been expended in trying to obtain ultra-fast jets, using the cavity charge principle of Ch. 1, §10. Theory¹⁴ shows that, for detonation waves moving parallel to the axis with detonation velocity v_D , a maximum jet velocity of $2v_D$ can be expected. However, if the detonation can be made to impinge normally on the liner, the jet velocity v_j should increase without limit as the angle β between the liner and the axis of symmetry tends to zero, both for plane (wedge-shaped) and axially symmetric (conical) liners.

We shall now show that the preceding prediction overlooks the possibility of *jetless wedge collapse*, which is to be expected for β sufficiently small

¹³ See [64, Chs. VI-VIII]; D. C. Pack, QJMAM 1 (1948), 1-17 and 3 (1950), 173-81; more refined calculations of λ have recently been made by Z. Hasimoto, J. phys. soc. Japan 8 (1953), 394-9. For jets impinging on obstacles, see M. Holt, QJMAM 3 (1950), 200-16, and 4 (1951), 419-31; D. C. Pack and L. Roberts, Phil. Mag. 44 (1953), 561-3. See also C. C. Lin, J. math. phys. MIT 33 (1954), 126-8.

¹⁴ G. Birkhoff, D. P. MacDougall, E. M. Pugh and Sir Geoffrey Taylor, J. appl. phys. 19 (1948), p. 571. With typical explosives, $v_D = 5,000$ -8,000 meters per second.

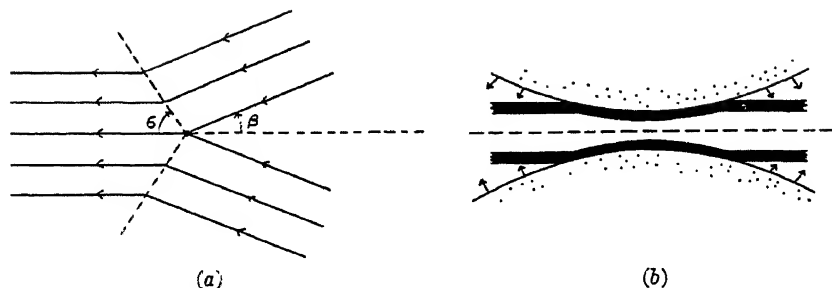


FIG. 2.

in the plane case. Fig. 2a sketches the type of flow, which was discovered in 1929 by A. Busemann¹⁵, and applied to jetless wedge collapse by K. Fuchs. Two symmetric shocks making an angle σ with the axis are propagated from the moving impact point J (cf. Ch. I, §10), and divide the flow into three regions. In each of these regions, the flow is uniform. Relative to J , it is $v_1 = v_0 \sin \beta$ ahead of the shock, and v_2 parallel to the axis behind it. For a given Mach number $M = v_1/c$ (c denotes the speed of sound in the collapsing material), the maximum deflection angle δ can be predicted¹⁵. What is especially remarkable, the predictions so obtained have been confirmed experimentally¹⁶.

However, in the axially symmetric case, the configuration of Fig. 2a is impossible¹⁷. Therefore, the preceding theoretical consideration no longer applies, and the maximum jet velocity must be limited by other factors.

Experimental data have been published¹⁸ for the case of a cylindrical liner collapsed by a toroidal explosion, initiated simultaneously all around a circle whose axis coincides with the liner axis. A meridian section through the axis is sketched in Fig. 2b; since the collapse angle β is initially 0° , increasing gradually as the collapse progresses, the velocity of the jet tip should approach the maximum obtainable. It was found that, in fact, the velocity of the plastic "penetrating jet" considered in Ch. I, §10, never greatly exceeded $2v_D$. However, if the cavity was evacuated, this penetrating jet was preceded by an ultra-fast (ionized) gaseous jet, with velocity as high as 80 km/sec. The maximum velocity apparently was determined by considerations from the kinetic theory of gasses, as it depended systematically on the atomic weight.

10. Potential flows with gravity. It is very well known [50, p. 19] that any solution of Laplace's equation $\nabla^2 U = 0$ can be taken as the

¹⁵ See H. W. Liepmann and A. E. Puckett, "Aerodynamics of a compressible fluid", pp. 51-60; G. Birkhoff and J. M. Walsh, *Quar. appl. math.* 12 (1954), 83-6.

¹⁶ J. M. Walsh, R. G. Shreffler, and F. J. Willig, *J. appl. phys.* 24 (1953), 349-59.

¹⁷ G. Birkhoff and J. M. Walsh, *Riabouchinsky Jubilee Volume* (1954), 1-12.

¹⁸ J. M. Walsh, R. G. Shreffler, and F. J. Willig, *J. appl. phys.* 23 (1952), 1300-5.

velocity potential for steady ideal flow in a gravity field, with gravitational potential G per unit mass, provided the pressure p satisfies

$$(52) \quad (p, \rho) + \frac{1}{2} \nabla U \nabla U + G = \text{const.}$$

This suggests trying to extend the methods of Chs. II-VII so as to obtain steady plane flows with free streamlines in a gravity field.

In the case of practical interest, the gravity field is of course uniform. For suitably chosen axes, the condition that the streamline $\Gamma = \Gamma_0$ be "free" is then

$$(52a) \quad |\xi|^2 = \nabla U \nabla U = 2gy \quad \text{on } \Gamma = \Gamma_0.$$

Writing $\xi = qe^{-i\phi}$, and differentiating (52a) with respect to arc-length, one gets

$$(52b) \quad qdq/ds = g \sin \phi, \quad \text{or} \quad d(q^2)/dU = 3g \sin \phi,$$

since $qds = dU$ on $\Gamma = \Gamma_0$. In such cases of steady plane flow, it has recently been proved by Lewy¹⁹ that the free streamlines are analytic. Using this analyticity, any such ideal plane flow is theoretically determined by the shape of any segment of any free boundary.

Conversely²⁰, any analytic curve $C: -y = f(x)$, $x = g(-y)$, $y < 0$, can be made the free streamline $\Gamma = 0$ of an ideal plane flow under gravity. We assume that axes have been so chosen that (52a) holds. Then U must satisfy

$$(53) \quad \begin{aligned} U &= \sqrt{2g} \int_0^x \sqrt{f(x)[1 + f'^2(x)]} dx = P(x) \\ &= \sqrt{2g} \int_{f(0)}^y \sqrt{y[1 + g'^2(y)]} dy = Q(y). \end{aligned}$$

The real functions $x = p(U)$, $y = q(U)$ inverse to $U = P(x)$ and $U = Q(y)$ will then be *analytic* in some neighborhood of C . Hence the complex power series $z = p(U) + iq(U)$ can be extended to define locally a complex analytic function $z = h(W)$, with $dz/dW \neq 0$.

For example, if C is $3x = 2(ay - 1)^{1/2}$, the preceding method gives the

¹⁹ H. Lewy, Proc. Am. math. soc. 3 (1952), 111-13; the proof does not apply to points of zero velocity.

²⁰ We follow the analytical procedure of C. Sautreaux, Ann. sci. ec. norm. sup. 10 (1893), S.95-S.182, and J. de math. 7 (1901), 125-60. See also H. Blasius, Zeits. math. phys. 58 (1909), 90-110; H. Villat, Ann. sci. ec. norm. sup. 51 (1915), 177-214; A. R. Richardson, Phil. Mag. 40 (1920), 97-110; Fritz John, Comm. pure appl. math. 6 (1953), 497-503; M. J. Vitousek, Tech. rep. 25, Appl. Math. Lab. Stanford Univ., 1954. The trochoidal waves of Gerstner [50, §251] should perhaps be mentioned in this connection, even though these exact solutions of Euler's equations of motion are not irrotational.

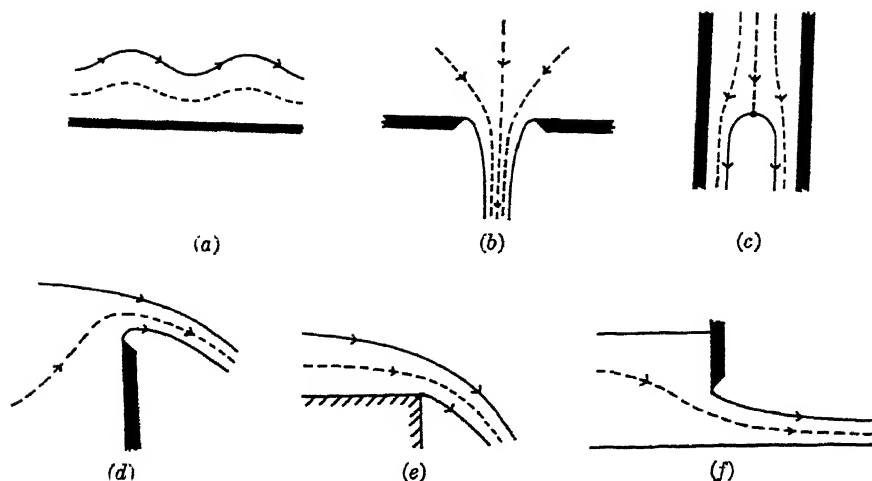


FIG. 3.

function

$$(53a) \quad z = (2/3a)(ab\sqrt{W} - 1)^2 + ib\sqrt{W}, \quad b = \sqrt{2}/ag.$$

However, the preceding "inverse method" gives no indication of how to obtain *in the large* flows past *given fixed boundaries*, in this way. Treatments in the literature are usually by approximate methods.

11. Integral equation method. It is therefore of interest to describe a method for finding ideal steady plane flows in a gravity field, bounded by free streamlines and *polygonal* fixed boundaries, which is very like the method of Ch. VI. This "integral equation" method is applicable to the following classic examples: periodic gravity waves of finite amplitude (Fig. 3a), the jet from a slot (Fig. 3b), rising bubbles (Fig. 3c), flow over a sharp-crested weir (Fig. 3d), flow over a flat sill (Fig. 3e), and flow under a sluiceway (Fig. 3f). All these cases have been treated in the literature by approximate methods²¹, but exact results in the literature seem confined to existence and uniqueness theorems for the case of periodic gravity waves²².

²¹ See [50, §250], and refs. given there; [1a, vol. 5, pp. 241-4]; Richardson, loc. cit.; R. von Mises [62, p. 496]; A. Craya and P. Gariel, *La Houille Blanche* 4 (1949), 45-64; A. M. Binnie, *QJMAM* 5 (1952), 395-407; F. W. Blaisdell, *Proc. Am. soc. civ. eng.* 80 (1954), No. 482; E. Marchi, *Annali di mat.* 35 (1953), 327-41.

²² D. J. Struik, *Math. Annalen* 95 (1926), 595-634, following T. Levi-Civita, *ibid.* 93 (1925), 264-314, and corrected by J. N. Hunt, *QJMAM* 6 (1953), 336-43. See also L. Lichtenstein, "Vorlesungen uber einige Klassen nichtlinearer Integralgleichungen . . .", Berlin, 1931; H. Poncin, *Thèse*, Paris, 1932; M. L. Dubreil-Jacotin, *J. de math.* 13 (1934), 217-91 and 16 (1937), 43-67; R. Gerber, *Thèse*, Grenoble, 1955 (also *Comptes rendus*, vols. 233 and 235).

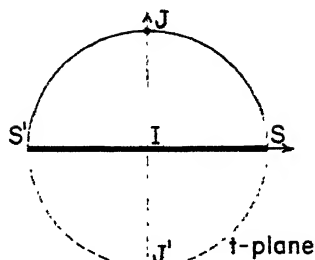


FIG. 4.

In this case, for each wave velocity c (wave length λ), a one-parameter family of solutions exists (one for each amplitude up to a certain limit). In other cases, physical intuition has suggested various plausible conjectures.

Our method will be illustrated by the case of the symmetric jet from a slot²³ (Fig. 3b). The flow considered can be mapped conformally and symmetrically onto the unit semicircle

$$\Gamma: |t| \leq 1, \quad \text{Im}\{t\} \geq 0$$

in an auxiliary t -plane (see Fig. 4), so that the fixed walls go into the real diameter, and the free boundaries onto the circumference. Then $t = 0$ will correspond to the stagnation point I at infinity, and J to the point at infinity on the descending jet.

By Thm. 2 of Ch. III, if $T = -(t + t^{-1})/2$, the stream function W will satisfy $W = C \ln T$ and $dW/dT = C/T$, for some scale factor C . In order to determine the flow, it remains to find $\zeta(t)$; this will give $z = \int \zeta^{-1} dW$.

To get an expression for $\zeta(t)$, we now construct an analog of Levi-Civita's function $\Omega(t)$ (Ch. VI, § 2).

Namely, we observe that ζ vanishes at I like $1/T$, hence like t (cf. Ch. II, §5). Since ζ is real on the real diameter, moreover, the Reflection Principle applies; hence $\zeta(t)$ can be extended to a function analytic in the unit circle $|t| < 1$. Since ζ is imaginary when t is imaginary, we therefore have

$$(54) \quad \zeta = a_1 t + a_3 t^3 + a_5 t^5 + \dots \quad \text{on } |t| < 1.$$

By Lewy's Theorem, $\zeta(t)$ is analytic on the unit circle $t = e^{i\theta}$, except at the separation points $t = \pm 1$, where $\zeta = \pm 1$, and at $t = \pm i$ (i.e., J and J'),

²³ This case was worked out by Mr. Kenneth Wilson, following suggestions by one of us. A similar integral equation for the case of periodic waves has been given by H. Villat, *Ann. sci. éc. norm. sup.* 32 (1915), 177-214.

where $\zeta = \pm \infty$. Near J , $\zeta \sim \sqrt{2igz}$ asymptotically, whence

$$W \sim \int \sqrt{2igz} dz = (\sqrt{8g/3})(iz)^{3/2}, \quad z \sim -i(3W/\sqrt{8g})^{2/3}.$$

Since also $W \sim \ln(1 + it)$ near J , we conclude

$$(55) \quad \zeta \sim \sqrt{2igz} \sim W^{3/2} \sim [\ln(1 + it)]^{3/2},$$

where we now ignore asymptotic constant factors. Near J' , by symmetry, $\zeta \sim [\ln(1 - it)]^{3/2}$.

Consequently, if $0 < C < 0.5$, then the ratio

$$(56) \quad f(t) = \zeta(t)/t[-\ln C(1 + t^2)]^{3/2}$$

is bounded away from zero and infinity throughout $|t| \leq 1$. It follows that we can write

$$(56^*) \quad \zeta = t[-\ln C(1 + t^2)]^{3/2} e^{\Omega(t)} \quad \text{if } 0 < C < 0.5,$$

where $\Omega(t) = \Omega(\bar{t})$, C is bounded and continuous in $|t| \leq 1$, and analytic in the interior. Because of the symmetries of ζ , we can therefore write

$$(56^{**}) \quad \Omega(t) = \tau + i\theta = a_0 + a_2 t^2 + a_4 t^4 + \dots$$

for suitable real coefficients a_{2k} .

The final step consists in substituting back in the free boundary condition (52b), second equation. If this is done, one gets an equation of the form

$$(57) \quad e^{i\tau} \{A(\sigma) + B(\sigma)\tau'(\sigma)\} = g \sin[\theta + P(\sigma)],$$

where $A(\sigma)$, $B(\sigma)$ and $P(\sigma)$ are known real functions. In terms of the single unknown function $\mu(\sigma) = -d\tau/d\sigma$, and the operators D , J of Ch. VI, §4, we can rewrite (57) as the integral equation

$$(57^*) \quad e^{iJ\mu} \{A(\sigma) - B(\sigma)\mu(\sigma)\} = g \sin[P(\sigma) + D\mu].$$

A similar integral equation has been obtained for the case of a rising bubble²⁴. In this case, the factor $(1 + t^2)$ in (55), (56), and (56*) must be changed to $(1 - t^2)$, but the formulas are otherwise very similar. The numerical results for this case are given in Ch. X, §11.

²⁴ G. Birkhoff and D. Carter, Report LA-1927, Los Alamos Sci. Labs. (1956).

CHAPTER IX

EFFECTIVE COMPUTATION

1. General remarks. We described our concern with the problem of effective computation in Ch. I, §15. Actually, this is perhaps the most complex problem of all. It has however been very much slighted in the literature, and so our discussion of it will be based largely on our own experience.

To formulate the computational problem, one must of course have clearly defined objectives, as regards the quantities to be calculated and the precision desired.

Even in the simplest case of Réthy flows (Ch. II, §7), we found it essential to distinguish three levels of computation: (i) the calculation of *constants* (contraction coefficients, drag coefficients, etc.) associated with given configurations, (ii) the calculation of *free boundaries*, and (iii) the calculation of *interior* streamlines and equipotentials, or isobars and isoclines. The calculation of interior streamlines is the subject of §§2-3; §§4-5 are devoted to the computation of constants (and the related *parameter problem*, mentioned in Ch. I, §15); §6 concerns isobars and isoclines. It will appear that the correct strategy differs sharply with the level of computation involved.

The case of curved barriers (Ch. VI) involves two separate stages: the solution of an integral equation $\lambda = M\nu(\sigma)K(J\lambda) \exp(-D\lambda)$ involving an unknown function $\lambda(\sigma)$, and the calculation of the flow from a known $\lambda(\sigma)$. Since the second stage involves relatively little novelty, we consider below (in §§8-9) primarily the first stage.

In all cases, *three significant figures* of precision are sufficient, for two reasons. First, only three figures have any physical significance, because of neglected variables like viscosity, capillarity, etc. Second, they are all that can be represented graphically on a 6" by 9" page. Even when using a drop-point pen on engraved paper, and reading results through a magnifying glass, an accuracy of 0.01" is all that can be obtained.

Economic problem. Once the objectives have been specified, the problem of effective computation becomes largely one of *cost*. We shall therefore make a rough cost analysis of our computing problems.

Since this book was written during a revolution in computing methods, some interpretation of our experience is necessary. In principle, the cost of making a multiplication on a desk machine is about 2.5¢; on an electronic

machine, it may¹ cost only .002¢, or less than $\frac{1}{1000}$ as much. Further, it will take months for a human computer to perform 10^4 – 10^5 multiplications, whereas the fastest electronic computing machines can make 10^8 multiplications in a day or two.

On the other hand, it takes much time to plan and code any new problem for a high-speed machine; this was actually our major cost². Therefore, to utilize the potential efficiency of high-speed machines, it is essential to develop *unified computational schemes*, applicable to large classes of problems, preferably involving many points. For this reason, we concentrated our attention on problems of type (iii). We shall now describe our experiences with various such problems.

2. Cavity behind a plate. We first used the Mark I Calculator at Harvard³ in 1949, to compute the interior streamlines and equipotentials for cavities behind a plate making an angle α with an infinite stream (Ch. II, §2). Our plan was to substitute directly in closed formulas given for $z(W)$, over a rectangular grid in the W -plane. The simplest such formulas for use with the Mark I seemed to be

$$(1a) \quad T = \sqrt{W}, \quad h = T^{-1} + 2C \quad (C = \cos \alpha),$$

$$(1b) \quad \zeta^{\pm 1} = (h \pm \sqrt{h^2 - r})/2, \quad \text{Im } \zeta > 0,$$

$$(1c) \quad z = [W - (CT/2S^2)]\zeta^{-1} + T/2S^2 - z_0 \\ - (i/4S^3) \ln [(\zeta - e^{i\alpha})/(\zeta - e^{-i\alpha})].$$

However, direct substitution in these formulas involves several unexpected complications, as we discovered when we made sample hand calculations.

First, the decimal point in $z(W)$ shifts rapidly as $\alpha \rightarrow 0$, having already moved two places when $\alpha = 15^\circ$. This would, for example, make computations near the stagnation point (which is practically at one end of the plate; see Plate 2) troublesome if $\alpha = 5^\circ$. Second, the computation of a complex square root $R + iS = T = \sqrt{U + iV}$ can best be done algebraically

¹ The first figure would hold if a computer, paid \$1.50 an hour, could make and check two multiplications a minute. The second figure would be true of a computing machine costing \$6 per hour to operate, and having a multiplication time of 10 milliseconds. The primitive machines used by us cost about 0.1¢–0.6¢ per point. See R. F. Clippinger, *Harvard Business Review* 33 (1955), 77–88.

² We also paid about 10¢ per point for plotting, and 10¢ more per point for preparing a plate for publication by photoengraving. Unless 5000 multiplications per point are required, this is more than the cost of making the calculations on an electronic machine.

³ This was made possible by Contract AT(30-1)-497, Code HUX, with the Atomic Energy Commission: The numerical results were printed in *Helmholtz-Rayleigh flow streamlines and equipotentials*, Report No. 1, Computation Laboratory, Harvard University; they are graphed in Plates 1–3.

(not trigonometrically). In this, decimal point trouble is also had unless one uses an *option*, solving always for

$$(1d) \quad Q = \sqrt{\frac{1}{2}[\bar{U} + \sqrt{U^2 + 1^2}]}, \quad \text{where } Q = \begin{cases} R & \text{if } U > 0 \\ S & \text{if } U < 0 \end{cases}$$

and then using $2RS = V$ to solve for the other, by computing $V/2Q$. Otherwise, large loss of significance can be caused by subtraction in the radicand.

Third, the branch of the many-valued function $\ln[(\zeta - e^{i\alpha})/(\zeta - e^{-i\alpha})]$ of Ch. II, (8), must be specified; we used the inequality $\alpha - \pi < \arg[(\zeta - e^{i\alpha})/(\zeta - e^{-i\alpha})] < \alpha$. Fourth, the function $z(W)$ is actually ambivalent (two-valued) on the slit $V = 0$, $U > 0$; this fact made it necessary to compute $z(W)$ on the free streamlines by desk machine. —A similar limitation will presumably apply to *all* attempts to calculate streamlines in divided flow.

The machine calculation took about five minutes (120 multiplication times) per point; it required 1–1.5 hours per point when done by a human computer using desk machines and tables; it would take less than two seconds on the Harvard Mark IV! On the boundary (free streamlines and plate), 30–40 minutes per point were needed by human computers, using the same formulas.

However, a human computer can often take advantage of tables which cannot be easily stored and scanned on a large computing machine. Thus, using the ingenious formulas⁴

$$T = \sqrt{W}, \quad \phi = \frac{1}{2}\alpha + \frac{1}{2} \cos^{-1}(2S^2T - C), \quad \zeta = C + S \tan \phi, \\ z = \{S\phi + 2 \cos(2\phi - \alpha) + \frac{1}{4} \cos(4\phi - \alpha)\}/2S^2,$$

2–3 significant figures can be obtained by a human computer in 5 minutes per point (2 minutes on the boundary).

3. Jet from a slot. Streamlines and equipotentials for jets from slots (Ch. II, §5) were computed in 1950 on IBM machines at the Naval Ordnance Laboratory⁵. As in the calculations described in §2, only rational functions, square roots, logarithms and arc-tangents of real numbers are needed. However, various new points had to be realized to get efficiency.

Thus, there was a serious loss in significant figures in solving

$$\zeta + \zeta^{-1} = 2h; \quad h = (Ae^W + B)/(Ce^W + D)$$

⁴ Suggested by D. M. Young [82, p. 128], who used Kennelly's *Complex circular and hyperbolic functions*, Harvard University Press, 1914.

⁵ S. Kaplan, NOL Memo. 10,818, dated June 20, 1950. Dr. Harry Polachek helped to plan the computations.

near the separation points where $\zeta = \pm 1$, $dh/d\zeta = 0$. Again, except in the neighborhood of the slot, it was essential to use asymptotic series (cf. Ch. IV, §3). We used

$$(2a) \quad z(W) = -e^{-i\alpha} + i\alpha e^{i\alpha} - S\pi - 2iS \ln 2S + e^{-i\alpha}W + \frac{e^{-i\alpha}}{2iS} e^{-W} - \frac{i}{16S^3} e^{-2W} + \dots$$

in the jet, when $\alpha \neq 0$;

$$(2b) \quad z(W) = -1 + W - 2e^{-W/2} - \frac{1}{2}e^{-W} - \frac{1}{12}e^{-3W/2} + \dots$$

in the jet, if $\alpha = 0$; and

$$(3) \quad z(W) = -2(S + S\alpha) - e^{-W} + 2CW - e^W + Ce^{2W} + \dots$$

towards the stagnation point at infinity.

The computation near the slot required about 100 multiplication times per point (7 minutes on the IBM machines then available), to get $z(W)$ and $\zeta(W)$. The asymptotic formulas (2)–(3) are clearly better over the rest of the flow. Actually, because of their superior ability to use tables, human computers would have been more efficient than the older-type IBM machines used in this problem. However, this would not be true with more modern machines.

4. Incomplete beta functions. After having gained experience by working through the cases discussed in §§2–3, we thought it desirable to handle all flows with circular sector hodograph by a *unified* computation scheme. We began by trying to apply the general formulas of Ch. II, §§9–10, and considered⁶ the computational problems involved. This line of attack had been proposed in [6].

Using formulas (29) and (32) of Ch. II, one could easily compute isobars and isoclines with the help of tables of $B_\beta(\tau)$. The computation of tables of the $B_\beta(\tau)$ would itself be straight-forward. One could first write

$$(4) \quad B_\beta(\tau) = \frac{1}{\beta} \tau^\beta C_\beta(\tau) = \frac{1}{\beta} \tau^\beta \left(1 + \frac{\beta}{1+\beta} \tau + \frac{\beta}{2+\beta} \tau^2 + \dots \right).$$

Clearly $C_\beta(\tau) = F(1, \beta, \beta + 1; \tau)$ is a complex *hypergeometric function*. There is no particular difficulty in computing a table of $C_\beta(\tau)$ for any one β , rational or not. For example, this might be done in polar coordinates on

⁶ In collaboration with Professor Douglas Hartree, who suggested (5)–(5'). Partial tables of the *real* incomplete beta functions already exist; see K. Pearson, *Tables of incomplete beta function*, Cambridge Univ. Press, 1934.

radii $\tau = r e^{i\phi}$, using the real differential equations:

$$(5) \quad \frac{d}{dr} (RC_\beta) = \frac{\beta}{r} \left[\frac{1 - r \cos \phi}{1 + r^2 - 2r \cos \phi} - RC_\beta \right],$$

$$(5') \quad \frac{d}{dr} (IC_\beta) = \frac{\beta}{r} \left[\frac{r \sin \phi}{1 + r^2 - 2r \cos \phi} - IC_\beta \right],$$

to compute the real and imaginary parts RC_β and IC_β of $C_\beta(\tau)$. Here the left-hand term of each expression in square brackets is independent of β , and can be computed once and for all. Starting values for $r < 0.2$ can be conveniently computed by (4). Finally, $C_\beta(\tau)$ can be computed in the plane, knowing its values in the semicircle $0 \leq r \leq 1, 0 \leq \phi \leq \pi$, by simple transformation formulas.

For our purposes, a table containing 100,000 five-place entries (5000 for each β) would probably be adequate; using the formulas $C_\beta(\tau) = C_\beta^*(t^*)$, and

$$C_\beta(\tau) = \beta \tau^{-\beta} \left[\frac{\pi}{\sin \pi \beta} e^{-\pi \beta} + \frac{\tau^{1-\beta}}{1-\beta} C_{1-\beta}(\tau^{-1}) \right]$$

in the upper half-plane, tabulation in the unit semicircle would suffice. Modern electronic machines could probably *compute* such tables (using (5)-(5')) in less than one day. However, the *printing* of the tables by such a machine would be much slower; a week might be required with machines available until recently.

It would be most convenient to have available tables of the related functions

$$(6) \quad -I_n(t) = n \int_0^t \frac{t^{n-2}}{1-t^n} dt = B_\beta(t^n), \quad [\beta = (n-1)/n].$$

These could be easily computed while the machine was calculating the $B_\beta(\tau)$. Thus, with Réthy flows (Ch. II, §7), since by Ch. II, (29'),

$$I_n(\xi, \xi_1) = \xi_1^{-1} I_n(\xi/\xi_1) = -\xi_1^{-1} B_\beta(t^n), \quad t = \sqrt[n]{\xi/\xi_1},$$

we would have, by formula (29) of Ch. II,

$$(7) \quad z = -\frac{1}{v} I_n(\xi/v) - v I_n(\xi v) + e^{i\alpha} I_n(e^{i\alpha} \xi) + e^{-i\alpha} I_n(e^{-i\alpha} \xi).$$

If tabulated on a square grid in the $\ln t$ plane, then for *rational* angles α and $\ln v$ one could use the tables *without* complex interpolation. Such tables would provide a very convenient means for determining the *geometrical dimensions* associated with given values of the parameters. They would also solve very simply the problem of computing *constants* associated

with Réthy flows. (We omit the formulas expressing C_D , etc., in terms of beta functions.)

5. Parameter problem. Thus, if available, tables of the $B_\beta(t^n)$ would solve effectively the *parameter problem* for Réthy flows—and more generally, by the Corollary of Theorem 3, Ch. III, the same problem for “simple flows past wedges”.

To illustrate this, consider the problem of determining the symmetric flow past a wedge having slant length l and vertex angle $2\pi\beta$ (see Ch. II, Fig. 11a), held in the jet from a nozzle of diameter $2b$, at a distance d from the orifice. The “solution” (Ch. II, (24)) involves two parameters α and v , without saying how they are to be determined! Hence, to solve the flow problem, one must be able to express α and v as functions of the geometrical data l/b and d/b .

The only way to do this is to calculate l/b and d/b as functions of α and v , and then to use inverse interpolation to get the inverse functions. Accordingly, nomograms for these functions are shown in Plates 9–10. We know of no practical way to calculate similar nomograms in the case of curved barriers⁷, because $z(t)$ cannot be expressed simply in closed form.

Because of the unavailability of suitable tables of the incomplete beta functions, recourse was taken to the formula of von Mises [62]. Namely, we substituted into (7) from formula (30) of Ch. II, which reduces when $\xi_1 = 1$ to

$$(8) \quad I_{r/s}(u) = \sum_{k=0}^{r-1} e^{-2\pi i k s/r} \ln(1 - e^{-2\pi i k/r} u).$$

Since $d = Re\{z(1)\}$, and $l = e^{i\pi/n} z(e^{i\pi/n})$, one calculate⁸ the nomograms shown in Plates 9–10.

The labor involved can be considerably reduced by using the Superposition Principle of Ch. II, §8. Specifically, it is convenient to write

$$(9) \quad \begin{aligned} H_n^*(v) &= v^{-1} I_n(1/v) + v I_n(v) \\ H_n(\alpha) &= e^{-i\alpha} I_n(e^{-i\alpha}) + e^{i\alpha} I_n(e^{i\alpha}) \\ H_n^\dagger(v) &= \frac{e^{i\pi n}}{v} I_n\left(\frac{e^{i\pi/n}}{n}\right) + v e^{i\pi/n} I_n(v e^{i\pi/n}), \end{aligned}$$

whence it follows that

$$d = H_n^*(v) - H_n(\alpha); \quad l = H_n^\dagger(v) - H_n\left(\frac{\pi}{n} - \alpha\right).$$

⁷ The parameter problem for curved barriers will be discussed further in §8.

⁸ The technique described below, and the calculations, are due to Mrs. Eleanor Lawry and Dr. Richard Varga.

The effective calculation of $I_{r/s}(u)$ in (8) is troubled by the necessity of specifying the branch of $\ln(1 - cu)$ referred to. To illustrate the pains that must be taken with this apparently innocuous formula, we display the formula which was actually used to calculate $H_n^*(v)$, namely,

$$\begin{aligned}
 H_{r/s}^*(v) = & \frac{\pi}{v} \cot \pi/n + (v + v^{-1}) \ln(1 - v^{1/s}) \\
 & + \sum_{k=1}^{m(r)} \left\{ \cos \frac{2\pi ks}{r} \cdot \left(v + \frac{1}{v}\right) \cdot \ln \left(1 - 2v^{1/s} \cos \frac{2\pi k}{r} + v^{2/s}\right) \right. \\
 (10) \quad & \left. - 2 \left(\frac{1}{v} - v\right) \sin \frac{2\pi ks}{r} \cdot \arctan \frac{v^{1/s} \sin \frac{2\pi k}{r}}{1 - v^{1/s} \cos \frac{2\pi k}{r}} \right\} \\
 & + \left(v + \frac{1}{v}\right) \cos \pi s \cos^2 \frac{1}{2} r\pi \cdot \ln(1 + v^{1/s}).
 \end{aligned}$$

In (10), $m(r) = (r - 2)/2$ or $(r - 1)/2$, according as r is even or odd; while $\arctan y = \theta$ is selected to satisfy $-\pi/2 < \theta \leq \pi/2$. The formulas for $H_n(\alpha)$ and $H_n^\dagger(v)$ in real form are just as complicated. Moreover these formulas hold only for $r > 2$; the case $r = 2$ should be based directly on (8).

Clearly, about $10r$ multiplication times are needed to calculate one $I_{r/s}(u)$ in this way, and four times as much to calculate d . The Superposition Principle, however, greatly reduces the total time when a nomogram is calculated. Much greater efficiency could be achieved with tables of the $B_\beta(i^n)$.

6. Isobars and isoclines. Even if tables of the incomplete beta function were available, the methods of §§4-5 would not be very efficient ways to calculate flow boundaries or flow interiors—i.e., to solve problems (ii) and (iii) of §1. This is partly because the number of points involved makes the use of high-speed automatic machines advisable, and such machines cannot efficiently store and scan a large table of functions. It is also because *numerical quadrature* based on formula (1) of Ch. II is very efficient, if simple formulas for dW and ζ are available.

In the case of flows with circular sector hodograph, such is the case. If the hodograph angle is π/n , then Planck's variable

$$(11) \quad \omega = n \operatorname{Ln} \zeta$$

maps the flow onto the semi-infinite strip

$$(11a) \quad R\omega \leq 0, \quad 0 \leq I\omega \leq \pi$$

in the ω -plane, and makes coordinate lines correspond to *isobars* and *isoclines*. Here $R\omega$ and $I\omega$ denote $Rc\{\omega\}$ and $Im\{\omega\}$, respectively.

From ω , one gets $T = \frac{1}{2}(\xi^n + \xi^{-n})$ by

$$(11b) \quad T = \cosh R\omega \cos I\omega + i \sinh R\omega \sin I\omega,$$

which covers the *lower* half-plane. By Theorem 5 of Ch. III,

$$(12) \quad z = \int \frac{e^{-\omega'n} \sinh \omega}{\prod_{j=1}^N (T - T_j)} d\omega = \int F(\omega) d\omega, \quad [N \leq 3].$$

We used formulas (11b) and (12) to compute isobars and isoclines for about twenty flows having circular sector hodographs⁹, on the Mark II Computing Machine at Dahlgren, Virginia. Some of the results are plotted in Plates 5-7. We shall now describe some of the most important features of the method used.

First, a *unified coding* was used, which permitted all twenty cases to be calculated from a single coding tape. To achieve this, we used a basic mesh unit of $\pi/144$, and tabulated $\cosh \xi$, $\cos \eta$, $\sinh \xi$, $\sin \eta$ over this mesh. This made it easy to calculate T and $\sinh \omega$ at all mesh-points, although it somewhat restricted the choice of mesh-length h . (Alternatively, recurrence relations could have been used.)

The path of integration in each case was chosen with care¹⁰, and consisted of a series of "ribs" leading from a central "spine" $I\omega = \text{const.}$ This "spine" was chosen to avoid the singularities T_i (where $z = \infty$), so as to avoid the accumulation of large *absolute* errors. Integrating along ribs, we used the formula

$$(13) \quad \Delta z = \frac{ih}{15} [24F_0 + 4(F_1 + F_3) - (F_2 + F_4)]$$

for complex numerical quadrature¹¹. The error was estimated from the empirical rule that this formula should give at most 0.1% *relative* error, if the nearest singularity was at a distance $5h$ or more¹². —Alternatively, we could have taken care of our simple singularities (case of distinct T_j) by

⁹ The project was made possible by the collaboration of Lt. J. C. Aller, who made up the tapes and kept us informed regarding the limitations of the Mark II, and by Professor Douglas Hartree, who suggested various simplifications and alternative numerical procedures.

¹⁰ The approximate integral is *not* independent of the path, though the exact integral is!

¹¹ G. Birkhoff and D. M. Young, Jr., J. math. phys. MIT 29 (1950), 217-21. A special "column-changing tape" was used to pass from one rib to the next.

¹² A numerical check on the error was made, by calculating the "residual" of the harmonic function $F(\omega)$, and the effect of integrating around each unit square.

formulas like

$$z = e^{-\omega_{1/n}} \sum C_j \ln (T - T_j) + \int \frac{e^{-\omega_{1/n}} - e^{-\omega_{1/n}}}{\Pi(T - T_j)} dT.$$

But this would have complicated the coding, by requiring special formulas when $T_1 = T_2$ or $T_1 = T_2 = T_3$.

The procedure followed clearly requires about five complex multiplication times, or twenty real multiplication times, to calculate each $F(\omega)$. This is about 80% of the total work, and took about 45 seconds per integrand point¹³. We estimate that if the problem were done by human computers it would take 30-40 minutes per point. Thus the Mark II proved about *five* times as economical as a human computer for the problem considered, if the effort of preparing the problem is neglected or charged to experience.

Had we wished to determine only the location of the free boundaries, and the pressure distribution on the fixed boundaries, desk machines would have been adequate. Such computations were actually performed, and supplemented by crude graphical conformal mapping (see §10) in the interior, to predict which choice of mesh points would give the most interesting results¹⁴. However, our study of the *interior* of the flow multiplied the complexity of each algebraic operation by about four, the number of points to be computed by about ten, and made it more economical to use a large-scale computing machine.

7. Related methods. The methods described in §§2-6 solve effectively several flow problems involving circular sector hodographs; thus they parallel the analysis of Ch. II and part of that of Ch. III. The methods have other analogs which seem worth mentioning, because we considered them carefully, even though we did not actually calculate with them.

We considered carefully the problem of calculating, on a high-speed machine, *streamlines and equipotentials* of flows having circular sector hodographs. Because of the irregular distribution of $W(\zeta)$, it seems advisable to use W as an independent variable, instead of trying to use inverse interpolation in $W(\zeta)$ or $W(\omega)$. One can compute $T(W)$ by integrating an ordinary differential equation of the form

$$(14) \quad dT/dW = \Pi(T - T_k)/\Pi(T - A_i)(T - A_i^*)(T - B_j),$$

using formula (5) of Ch. III. In the case of flows with circular sector hodographs, the denominator disappears; hence (14) becomes everywhere regu-

¹³ As in the case of the Mark I, the original estimate (though intended conservatively) was only 50-70% as much.

¹⁴ The work was done by Dr. Samuel Kneale and Mrs. Lawry.

lar. Otherwise, care must be taken to avoid stagnation points, and to refine the mesh when near them.

For any T , one can find $\zeta(T)$ by the sequence of formulas

$$(15) \quad t + t^{-1} = -2T,$$

$$(15') \quad \zeta = t^{1/n} r(t),$$

using formula (18) of Ch. III. Thus one might solve (15) by the method of §2, and use Newton's series for $(1 + u)^{1/n}$ to obtain successive solutions of (15'). One could then get z by the complex numerical quadrature formula (13), using $z = \int \zeta^{-1} dW$. Although some accuracy would be lost near separation points, refinement of the mesh there should give all the accuracy required.

Two plates. We also considered the construction of a unified coding for calculating the interior of flows past two plates, such as were considered in Ch. V.

The formulas of Ch. V, §1, suggest a general procedure, in which W is chosen as the independent variable; this choice would give a net of *streamlines and equipotentials*. One could calculate $T(W)$ by (14). One could then calculate $t(T)$ by formula (3) of Ch. V,

$$(16) \quad t = \int dT / \sqrt{(1 - T^2)(1 - k^2 T^2)},$$

which could also be replaced by the formula

$$(16') \quad d^2 T / dt^2 + (1 + k^2 - 2k^2 T^2) T = 0.$$

Formula (16') could be integrated very accurately¹⁵; it would however have the disadvantage, as compared with (16), of not giving a net of streamlines and equipotentials.

Using formula (6) of Ch. V, one could then calculate $\omega = \int R_1(T) dt$, and $\zeta^{-1} = e^{i\omega}$. Alternatively, one could calculate ζ^{-1} from

$$(17) \quad d(\zeta^{-1})/dt = i\zeta^{-1} R_1(T).$$

Finally, one could get $z = \int \zeta^{-1} dW$, using (13).

We did not, however, actually carry through the procedure just sketched. This was partly because equations (14), (16) and (17) involved so many parameters in all, that we thought the *parameter problem* should be solved first. For the parameter problem, the closed analytical formulas of Ch. V appear more efficient than the numerical method outlined above.

¹⁵ D. Hartree, *Numerical analysis*, Oxford, 1952, §7.2.

Also, we thought that the case of curved barriers was more challenging than that of polygonal barriers, and concentrated our attention on it.

8. Curved barriers. In Ch. VII, we have discussed the existence and uniqueness of ideal plane flows past curved barriers, and of solutions to the corresponding integral equations (15)–(16) of Ch. VI. We shall now discuss the effective approximate solution of these integral equations, from both theoretical and practical points of view.

Following Brodetsky, we used *polynomial* approximations to the Levi-Civita function $\Omega(t)$, of the form

$$(18) \quad \Omega(t) = a_0 + a_1 t + \cdots + a_n t^n \quad [\text{all } a_i \text{ real}]$$

(cf. Ch. VI, (8)). For any such approximation, we replaced the integral equation (16) of Ch. VI with *discrete* equations of the form

$$(19) \quad \lambda(\sigma_k) = M\nu(\sigma_k)K(\theta(\sigma_k))e^{-\tau(\sigma_k)} \quad [k = 1, \dots, n];$$

where

$$(19') \quad \lambda = \sum h a_h \sin h\sigma, \quad \theta = J\lambda = \sum a_h \cos h\sigma, \quad \text{and} \\ \tau = D\lambda = \sum a_h \sin h\sigma.$$

(Cf. (14b)–(14c) of Ch. VI.) Equations (19) are satisfied if and only if the flow defined by $\Omega(t)$ (cf. Theorem 1 of Ch. VI) satisfies $\kappa = K(\theta)$ at the points $z(\sigma_k)$; thus our approximate solutions correspond to *polynomial interpolation*. Specifically, we let

$$(20a) \quad \sigma_k = (2k - 1)\pi/2n$$

or

$$(20b) \quad \sigma_k = k\pi/n,$$

so that we used equally spaced interpolation,

One of us has proved elsewhere [91] that, if (16) has a unique solution, then the solutions of the sequence of “discretized” equations (19) converge to this exact solution as $n \rightarrow \infty$; space does not permit including a proof here¹⁶. This leaves us with the problem of solving systems of the form (19).

¹⁶ The corresponding result for trigonometric interpolation is classic (D. Jackson, “Theory of approximation”, New York, 1930, p. 123). The use of trigonometric interpolation, and the idea of using (19) are due to S. Brodetsky. See [8, 9], Proc. Edinburgh math. soc. 41 (1923), 58–62, and Proc. sec. int. congr. appl. mech. Zurich (1926), 527–31. Also, L. Rosenhead, Proc. roy. soc. 117 (1928), 417–33. Iteration was tried in the ogival case, by the authors listed in fnnt. 4, Ch. VII. The Villat integral equation (Ch. VI, (15)) has been treated by S. M. Rapoport, Ukr. mat. zh. 2 (1950), 107–17; see J. Kravtchenko, Ann. de l’Inst. Fourier 3 (1952), 287–99. See also P. P. Kufarev, Prikl. mat. mekh. 16 (1952), 589–98.

We did this by regarding the $\lambda(\sigma_k)$ as unknown constants, from which the $\theta(\sigma_k)$ and $\tau(\sigma_k)$ can be expressed as

$$\theta(\sigma_i) = \sum_{l=1}^n J_{kl}^{(n)} \lambda(\sigma_l), \quad \tau(\sigma_k) = \sum_{l=1}^n D_{kl}^{(n)} \lambda(\sigma_l),$$

where the matrices $J^{(n)}$, $D^{(n)}$ depend on n only.

For small M , this system can be solved by direct iteration. In fact, the argument of Ch. VII, §2, applies, and shows that the convergence is like that of a geometric series.

For larger M , however, direct iteration proves to be no longer convergent. We therefore had to devise a more subtle procedure. Our idea for doing this was suggested by observing that, in the *ogival* case $K \equiv 1$, the operator

$$(21) \quad S[\lambda] = M\nu(\sigma)K(J\lambda)e^{-D\lambda}$$

is *antitone*; more generally, this is true for symmetric flows if $K(\theta)$ is an increasing function. This suggests using *averaged iteration*, with respect to a "weight factor" ϵ ; i.e., it suggests iterating

$$(21') \quad S_\epsilon[\lambda] = (1 - \epsilon)\lambda + \epsilon S[\lambda].$$

This scheme proved successful in almost all cases; a more detailed discussion has appeared elsewhere¹⁷. Typical numerical results have already been presented in Ch. VI.

However, this procedure for solving (19) did not seem adequate to us, because it failed to face squarely the *parameter problem*, which is perhaps the most important problem of all. As a first step towards solving this difficult problem, we therefore tried a scheme which corresponds roughly to Jacob's Lemma (Ch. VII, §5), and is based on the observation that, in many cases, *parameters are monotone functions of M* .

When this is the case, one can "hunt" for the correct value of M while iterating (21) or (21'). The method consists in choosing a small positive constant c , and replacing the simple iterative scheme (21') by the more elaborate recursive scheme

$$(22a) \quad \lambda^{(r+1)} = \epsilon M_r S[\lambda^{(r)}] + (1 - \epsilon)\lambda^{(r)}$$

$$(22b) \quad M_{r+1} = M_{r+1} + c\epsilon(\bar{M}_r - M_r),$$

where $\bar{M}_r = g(S[\lambda^{(r)}])$ is defined so that the pair $(\bar{M}_r, S[\lambda^{(r)}])$ would satisfy some side condition (e.g., any of conditions (17), (19c), (28'') or (32') in Ch. VI).

¹⁷ G. Birkhoff, H. H. Goldstine, and E. H. Zarantonello, *Rend. Sem. Mat. Torino* 13 (1954), 205-23.

As our experience with this scheme, and the scheme itself, have been reported fully elsewhere¹⁷, we will not enter into further details here.

9. Theoretical discussion. Instead, we will *justify* the use of averaged iteration in §8, by proving that it converges for small enough ϵ . This will provide a *constructive* existence theorem for many kinds of flows with free boundaries; hence §9 may be regarded as a continuation of Ch. VII. We are convinced of the importance both of such constructive existence theorems, and of rigorous justifications of numerical methods.

We shall consider convergence of averaged iteration as defined by (21'), for fixed M ; thus we shall not consider the parameter problem. We shall also consider only *ogives*, for which $K \equiv 1$. The discussion will be phrased for the *continuous* case of Ch. VI, (16); however it will apply (in slightly simplified form, because of finite-dimensionality) to the discretized system (19) as well [91].

THEOREM. For every positive ϵ in the interval $0 < \epsilon < 2/(1 + \max \nu)$, the averaged iterates $\lambda_n = S_\epsilon^n[\lambda_0]$ of a continuous function $\lambda_0(\sigma)$, $0 \leq \lambda_0(\sigma) \leq \nu(\sigma)$, converge uniformly to a solution of $\lambda = \nu e^{-D\lambda}$.

The proof will be based on the following lemma:

LEMMA 1. Let ω be a non-negative bounded function. Then, for every square integrable function x and every ϵ , $0 < \epsilon < 1$, we have¹⁸

$$(23) \quad (-\epsilon\omega Dx + (1 - \epsilon)x, \quad D(-\epsilon\omega Dx + (1 - \epsilon)x))^{\frac{1}{2}} \leq \gamma(\omega)(x, Dx)^{\frac{1}{2}}$$

where

$$(24) \quad \gamma(\omega) = \begin{cases} 1 - \epsilon & \text{for } 0 < \epsilon \leq 2/(\max \omega + 2) \\ \epsilon \max \omega + \epsilon - 1 & \text{for } 2/(\max \omega + 2) \leq \epsilon < 1. \end{cases}$$

Proof. Let us consider the operator $D_\omega = \sqrt{\omega}D\sqrt{\omega}$ obtained by first multiplying by the function $\sqrt{\omega}$, then applying the operator D and finally multiplying by $\sqrt{\omega}$ again. It is an integral operator with the non-negative, symmetric and square integrable kernel $D_\omega(s, t) = \sqrt{\omega(s)}D(s, t)\sqrt{\omega(t)}$. Like D , D_ω is non-negative definite, for $(D_\omega x, x) = (D\sqrt{\omega x}, \sqrt{\omega x}) \geq 0$. Hence¹⁹ D_ω has at most a countable sequence of eigenfunctions $\varphi_k(t; \omega)$ and eigenvalues $c_k(\omega)$; the eigenvalues are all non-negative and the largest of them, $c_1(\omega)$, is precisely given by

$$(25) \quad c_1(\omega) = \text{l.u.b.}_{(x, x)=1} \int_0^\pi \int_0^\pi D(s, t) \sqrt{\omega(s)} \sqrt{\omega(t)} x(s) x(t) ds dt.$$

¹⁸ Parentheses indicate scalar products: $(x, y) = \int_0^\pi x(\sigma)y(\sigma) d\sigma$. See [91, Theorem 2], for further details.

¹⁹ Cf. P. Hamel, *Integralgleichungen*, Berlin, Springer, 1937, p. 68.

It is clear that, since $D(s, t)$ is non-negative, the l.u.b. is attained by some $x \geq 0$, and so $c_1(\omega)$ increases with ω . In particular, replacing ω by its maximum and recalling that the largest eigenvalue $c_1(1)$ of D is 1, we get: $c_1(\omega) \leq \max \omega c_1(1) = \max \omega$.

Any square integrable function y can be uniquely developed in a series of eigenfunctions of D_ω as follows

$$(26) \quad y = \sum_{k=1}^{\infty} \alpha_k \phi_k + y_1,$$

where $(y_1, \phi_k) = 0$ for $k = 1, 2, \dots$. An easy computation yields

$$(27) \quad \begin{aligned} &(-\epsilon D_\omega y + (1 - \epsilon)y, D_\omega(-\epsilon D_\omega y + (1 - \epsilon)y)) \\ &= \sum_{k=1}^{\infty} (-\epsilon c_k + 1 - \epsilon)^2 c_k \alpha_k^2, \end{aligned}$$

$$(28) \quad (y, D_\omega y) = \sum_{k=1}^{\infty} c_k \alpha_k^2,$$

and since $c_k \geq 0$, a simple comparison of (27) and (28) gives

$$(29) \quad \begin{aligned} &(-\epsilon D_\omega y + (1 - \epsilon)y, D_\omega(-\epsilon D_\omega y + (1 - \epsilon)y))^{\frac{1}{2}} \\ &\leq \text{l.u.b.}_k | -\epsilon c_k + 1 - \epsilon | (y, D_\omega y)^{\frac{1}{2}}. \end{aligned}$$

Setting $y = \sqrt{\omega}x$ and observing that $\text{l.u.b.}_k | -\epsilon c_k + 1 - \epsilon | \leq \max \{ \epsilon c_1 + \epsilon - 1, 1 - \epsilon \} \leq \gamma(\omega)$, one obtains (23).

Proof of Theorem. Since S transforms non-negative functions into non-negative functions less than or equal to ν , $0 \leq \lambda_k(\sigma) \leq \nu(\sigma)$ for all k . The difference $\delta_{n+1} = \lambda_{n+1} - \lambda_n$ between two consecutive iterates can be written as

$$\delta_{n+1} = -\epsilon \omega_n D \delta_n + (1 - \epsilon) \delta_n,$$

where

$$\omega_n = \nu \frac{e^{-\tau_n} - e^{-\tau_{n-1}}}{-\tau_n + \tau_{n-1}}, \quad \tau_n = D \lambda_n.$$

Hence, by Lemma 1,

$$(30) \quad (\delta_{n+1}, D \delta_{n+1})^{\frac{1}{2}} \leq \gamma(\omega_n) (\delta_n, D \delta_n)^{\frac{1}{2}}.$$

But $0 \leq \omega_n \leq \nu$, and since $\gamma(\omega)$ increases with ω , $\gamma(\omega_n) \leq \gamma(\nu)$. Moreover, if ϵ is restricted to the interval described in the statement of the Theorem, then, according to the definition (24) of γ , $\gamma(\nu) < 1$.

Iterating (30), we get

$$(31) \quad (\delta_n, D \delta_n)^{\frac{1}{2}} \leq \gamma(\omega_1) \gamma(\omega_2) \cdots \gamma(\omega_{n-1}) (\delta_1, D \delta_1)^{\frac{1}{2}} \leq \gamma(\nu)^{n-1} (\delta_1, D \delta_1)^{\frac{1}{2}}.$$

Since \mathbf{D} is positive definite (Ch. VII, §5, Lemma 1), $(x, \mathbf{D}X)^{\frac{1}{2}}$ satisfies the triangle inequality, and if $m < n$

$$(32) \quad (\lambda_n - \lambda_m, \mathbf{D}(\lambda_n - \lambda_m))^{\frac{1}{2}} = \left(\sum_{k=m+1}^n \delta_k, \mathbf{D} \sum_{k=m+1}^n \delta_k \right)^{\frac{1}{2}} \\ \leq \sum_{k=m+1}^n (\delta_k, \mathbf{D}\delta_k)^{\frac{1}{2}} \leq (\delta_1, \mathbf{D}\delta_1)^{\frac{1}{2}} \sum_{k=m+1}^n \gamma^{k-1} = (\delta_1, \mathbf{D}\delta_1)^{\frac{1}{2}} \frac{\gamma^m - \gamma^n}{1 - \gamma},$$

which shows that $\{\lambda_n\}$ is a Cauchy sequence under the metric $(x, \mathbf{D}x)^{\frac{1}{2}}$. From this, we shall derive the uniform convergence of λ_n . By Lemma 1 of Ch. VII, §5, the uniform boundedness of λ_n implies that $\tau_n = \mathbf{D}\lambda_n$, and so $\mu_n = \nu e^{-\tau_n}$, are equicontinuous functions. Therefore, for any $\epsilon > 0$, there is an $\eta(\epsilon) > 0$ such that $|\sigma' - \sigma''| < \eta$ implies $|\mu_n(\sigma') - \mu_n(\sigma'')| < \epsilon$ for all n . If in addition $\eta(\epsilon)$ is chosen so that $|\sigma' - \sigma''| < \eta$ implies $|\lambda_0(\sigma') - \lambda_0(\sigma'')| < \epsilon$, then it also implies $|\lambda_n(\sigma') - \lambda_n(\sigma'')| < \epsilon$ for $n = 0, 1, \dots$. In fact, the last inequality is true for $n = 0$, and from

$$|\lambda_n(\sigma') - \lambda_n(\sigma'')| \leq \epsilon |\mu_n(\sigma') - \mu_n(\sigma'')| + (1 - \epsilon) |\lambda_{n-1}(\sigma') - \lambda_{n-1}(\sigma'')|$$

it follows, by induction, for every n . Hence the λ_n are equicontinuous and, since they are uniformly bounded, a uniformly convergent subsequence can be extracted from every infinite subset [18, vol. 1, p. 49]. But, because of (32), all limit functions thus obtained are at zero distance apart in the metric $(x, \mathbf{D}x)^{\frac{1}{2}}$ and, since they are continuous, they are identical. Having a unique limit function, the sequence λ_n is itself uniformly convergent to a continuous function λ , and $\mathbf{S}\lambda = \epsilon^{-1}(\mathbf{S}_\epsilon\lambda - (1 - \epsilon)\lambda) = \lim_{n \rightarrow \infty} \epsilon^{-1}(\mathbf{S}_\epsilon\lambda_n - (1 - \epsilon)\lambda_n) = \lim_{n \rightarrow \infty} \epsilon^{-1}(\lambda_{n+1} - (1 - \epsilon)\lambda_n) = \lambda$, Q.E.D.

10. Other methods. Other methods have been applied to solve free boundary problems; they are mostly methods for solving the Laplace equation $\nabla^2 U = 0$ approximately in general regions either by analogy in an *electrolytic tank* or *resistance network*, graphically by constructing a *conformal net*, or numerically by *relaxation*.

Since small variations in the velocity $|\nabla U|$ along the free boundary correspond to considerable changes in its position, gradients must be accurate to at least two significant figures if methods such as those mentioned above are to be satisfactory. This requirement of precision seems to limit the role

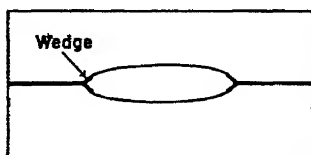


FIG. 1.

of graphical conformal mapping to that of getting a first approximation to the flow.

Again, the fact that curved free boundaries are involved makes it awkward to approximate to the condition $\nabla^2 U = 0$ near the boundary, by resistance networks. The corresponding treatment of irregular stars in relaxation solutions is annoying if one tries to code the problem for a high-speed computing machine, but not a serious problem for a skilled hand computer²¹.

The electrolytic tank method is also quite adequate in skilled hands, at least for problems involving ideal plane flows. However, one should be cautioned against trying to develop this specialized apparatus to the necessary degree of perfection just to solve a few free boundary problems. (Fixed boundary problems are much easier.)

In summary, both relaxation methods and a high-precision electrolytic tank are effective methods for solving free boundary problems. They have the great advantage over analytical methods (Chs. II–VI) that the *parameter problem* is eliminated at the start. They are especially well adapted to flows in narrow channels, but because of the large effect of distant fixed walls on free boundaries, they are not well adapted to the approximate solution of flow problems in infinite space (which, moreover, usually involve fewer parameters, and so are easier to solve analytically).

They can also be applied to problems involving axial symmetry (cf. Ch. X, §§7–9), gravity (cf. Ch. VIII, §10) and surface tension; relaxation methods can even be adapted in principle to flows with free streamlines involving viscosity and compressibility. However, the adjustment of the free boundary so as to satisfy the condition $|\nabla U| = \text{const.}$ must be done by trial and error, squeezing the flow in where $|\nabla U|$ is too small, and letting the boundary out where it is too large. Although this method can be justified qualitatively by using the variational principle of Riabouchinsky (Ch. IV, (38)), it seems hard to find a systematic quantitative procedure.

In Fig. 1, there is shown one free streamline of a flow past a 90° wedge in a channel, computed approximately by these two methods²². The two computations gave results which coincided within a line thickness, on the scale shown. When applied to axially symmetric flows past a disc, however, the agreement was less good (Ch. X, Fig. 8).

²¹ See R. V. Southwell, "Relaxation methods in theoretical physics", Oxford, 1946, for "irregular stars". For applications, see *ibid.*, pp. 212–26, and [78].

²² One by Miss G. Vaisey; the other by P. Marchet, Problème D359A, Institut Blaise Pascal, C.N.R.S. (Paris), 1949. For other flows obtained with an electrolytic tank, see Abdel-Hati Abul-Fetouh, Ph.D. Thesis, Iowa State University, 1949.

CHAPTER X

AXIALLY SYMMETRIC FLOWS

1. Typical problems. The present chapter will be concerned with steady, axially symmetric flows with free boundaries, under conditions where the effects of compressibility, viscosity and turbulence are small. Except in §10, the effects of gravity will be neglected also.

The subject matter may be divided into two roughly equal halves. The first half (§§2-6) will concern mathematical deductions from *potential theory*, whose physical applicability under the conditions specified above has already been discussed in Ch. I, §7. Unfortunately, the complex variable technique which was applied in Chs. II-VII has no effective analog in the axially symmetric case, and exact analytical techniques have so far yielded little information of physical interest¹. Approximate analytical techniques have proved more useful (see §§3, 6).

In fact, the most useful information has come from a *comparison* of approximate theoretical results with experimental data. These comparisons are presented in §§7-10, for the various special types of flow which have received the most attention. We shall now enumerate these types of flow, in order to give a clearer idea of the scope of this chapter.

One of the oldest hydraulic problems is the determination of the discharge rate and contraction coefficient from a conical orifice. The cases of a circular orifice in a flat plate (Fig. 1a) and of a circular Borda tube (Fig. 1b) are of particular interest. Such flows are studied in detail in §7.

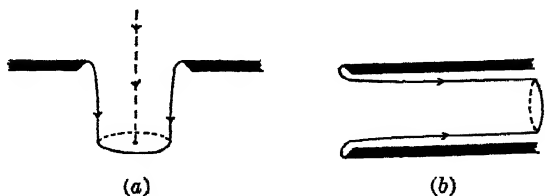


FIG. 1.

Next may be mentioned the normal impact of a circular jet on a flat plate, disc, or cup. The mathematical analysis of flows of this type is im-

¹ For special flows obtained analytically, see the references of fnnt. 27, Ch. IV, §9; also, P. R. Garabedian, von Mises Anniversary Volume, Academic Press, 1954, 149-59.

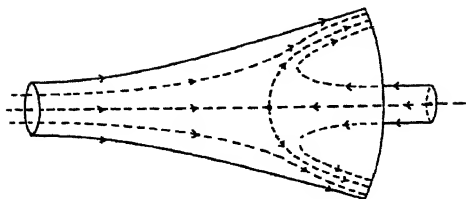


FIG. 2.

portant for the understanding of the action of Pelton wheels², and will be given in §8.

An interesting military application of axially symmetric flows with free boundaries is furnished by shaped charges with conical liners (Ch. I, §10). In a moving reference frame, the liner flow is the reverse of the flow produced by two impinging coaxial circular jets (see Fig. 2), which is also discussed in §8.

Again, the cavity flow past a disc, sphere, or other surface of revolution, is important for the underwater ballistics of air-launched missiles. Axially symmetric cavity flows are treated in §9.

Finally, many important axially symmetric flows swirl about a *hollow vortex* extending along the axis of symmetry. Such hollow vortices occur in the tip cavitation of propellers, in whirlpools, and in other applications; swirling flows about them will be considered in §10.

2. Potential theory. In Ch. I, §9, the concept of an (ideal) steady, swirl-free flow with free boundaries has already been defined mathematically. Such a flow has a velocity potential $U = U(\mathbf{x})$ satisfying $\nabla^2 U = 0$, is tangential to all solid "fixed" boundaries, and satisfies $\nabla U \cdot \nabla U = \text{const.}$ on each "free" boundary.

In the axially symmetric case, using cylindrical coordinates (x, r) , $\nabla^2 U = 0$ is equivalent to [50, p. 126]

$$(1a) \quad \partial^2 U / \partial x^2 + \partial^2 U / \partial r^2 + r^{-1} \partial U / \partial r = 0,$$

or to the existence of a "stream function" $V(x, r)$ satisfying

$$(1b) \quad \partial^2 V / \partial x^2 + \partial^2 V / \partial r^2 - r^{-1} \partial V / \partial r = 0.$$

The axial and radial velocity components satisfy

$$u = \partial U / \partial x = r^{-1} \partial V / \partial r, \quad v = \partial U / \partial r = -r^{-1} \partial V / \partial x,$$

respectively.

Straight circular jets, with $u = c$, $v = 0$, $U = cx$, $V = -cr^2/2$ seem to

² See A. H. Gibson, *Hydraulics*, Arts. 125-28; H. Addison, *Applied hydraulics*, §§105-8, 193.

be about the only interesting swirl-free, axially symmetric flows with free boundaries, whose velocity-field have been explicitly described in the large by known mathematical functions¹. Hence the specific analytical formulas of Chs. II-III and V have no analogs in the axially symmetric case.

However, many of the general theorems of Chs. IV and VII are applicable to axially symmetric flows. Thus, this is true of certain convexity principles (Ch. IV, Thms. 12-13), Riabouchinsky's variational principle (Ch. IV, Thm. 14), the comparison and uniqueness theorems of Gilbarg and Serrin (Ch. IV, §§12-14), and the existence theorems of Garabedian-Lewy-Schiffer (Ch. VII, §§10-11).

In addition, mechanical *conservation laws* of mass, momentum, and energy are of course applicable to axially symmetric as well as to plane flows. Thus we have seen (Ch. I, §10) that the contraction coefficient of a circular Borda tube is $C_c = 0.5$. Also, that the velocities and mass-ratio of the jet and "slug" produced by a collapsing cone (Fig. 2) can be predicted, as can the rate of penetration of one liquid by a jet of another liquid.

Again, a somewhat more refined asymptotic potential-theoretic analysis shows³ that, in the case of an axially symmetric cavity flow with reentrant jet and cavitation number Q , we have

$$(2) \quad C_D = 2[1 + Q + \sqrt{1 + Q}]A^*/A,$$

where A^* is the jet cross-section, and A the obstacle cross-section.

Relaxation methods. Using difference equation approximations to (1a)-(1b), Southwell and Vaisey [78] have determined approximately various important axially symmetric flows with free boundaries, by "relaxation methods" described in Ch. IX, §10. We would like to mention a modification of this approach, worked out in collaboration with David Young and Richard Varga, which avoids "irregular stars".

Namely, if U , V are used as independent variables, and $f = r^2$ as dependent variable, then (1a)-(1b) are equivalent⁴ to the single equation

$$(3) \quad \frac{\partial}{\partial U} \left(\frac{1}{f} \frac{\partial f}{\partial U} \right) + \frac{\partial^2 f}{\partial V^2} = 0,$$

or to the pair of equations

$$(4) \quad 2f/\partial V = 2\partial x/\partial U, \quad 2f\partial x/\partial V = -\partial f/\partial U.$$

If the system (4) is used, then a staggered mesh is recommended, involving f and x at alternate points; moreover, the boundary conditions must satisfy

¹ G. Birkhoff, *Rev. Ciencias Lima* 50 (1948), 105-116.

⁴ L. C. Woods, *QJMAM* 4 (1951), 353-70.

the difference analogs of the compatibility conditions

$$(5) \quad \oint (f dU + 2x dV) = 0, \quad \oint (2x dU - \ln f dV) = 0.$$

The singularity on the axis $f = 0$ is troublesome.

3. Axial source distributions. Various authors⁵ have successfully approximated potential flows about airship forms having given analytical *fixed* boundaries, by superposing axial source-sink distributions on uniform flow parallel to the axis of symmetry. Such flows are called "Rankine flows" [61, §15.27]. The same method has been applied to approximate cavity flows.

Thus Bauer⁶ proposed regarding the flow past a source in a uniform stream—i.e., so-called "half-body" flow [61, §15.23],—as an approximation to the *infinite cavity* flow past a moving sphere (see §10). In view of Levinson's asymptotic theory (§5), a better approximation is however furnished by the flow past a *half-line* of sources with constant density on the positive x -axis. This is known to correspond to a *paraboloidal cavity* [61, §15.58]. From the known formulas for a single source at $(0, 0)$,

$$(6) \quad U = 1/\sqrt{x^2 + r^2}, \quad V = x/\sqrt{x^2 + r^2} = \cos \theta,$$

one calculates, as an improper integral, the stream function

$$(7) \quad V = \frac{1}{2}r^2 - m(x + \sqrt{x^2 + r^2})$$

for a half-line of sources in a uniform stream. Moreover, after transposing $\sqrt{x^2 + r^2}$, squaring both sides, and cancelling, we see that

$$(7') \quad V = 0 \quad \text{on the paraboloid} \quad r^2 = 4m(x + m).$$

From the preceding representation, some idea can be had of the velocity field surrounding a missile in high-speed cavity motion. The axial and radial velocity components are

$$(7'') \quad u = \frac{1}{r} \frac{\partial V}{\partial r} = 1 - \frac{m}{\sqrt{x^2 + r^2}}, \quad v = -\frac{1}{r} \frac{\partial V}{\partial x} = \frac{m}{r} + \frac{mx}{r\sqrt{x^2 + r^2}}.$$

From (7''), the pressure coefficient can be calculated by Bernoulli's equation, using Levinson's equation (12') and (7'), which give $D = 2\pi\rho m^2$ when $v = 1$, to estimate the source intensity from the drag D .

Similarly, the velocity field induced by a moving prolate spheroid is known⁷ to be that of a source distribution between the foci $(\pm f, 0)$ with

⁵ W. J. Rankine, Phil. Trans. A161 (1871), 267-304; G. Fuhrmann, Jahrb. Motorluftschiffahrt Ges. (1911-12); Th. von Karman, NACA TM574 (1930).

⁶ Ann. der Physik 82 (1927), 1014-16; see [72, p. 98].

⁷ M. Munk [20 vol. 1, pp. 284-5].

density $m(\xi) = -a\xi$ varying *linearly*. Since long cavities are nearly spheroidal (see §6), superposition of this distribution on a uniform stream gives an approximate representation of the flow around a long *finite cavity*, as a "Rankine flow".

Unfortunately, axial source-sink distributions cannot be used to give an exact description of *any* complete flow with free boundaries. For, let $V(x, r)$ be the stream function of any Rankine flow, so that⁸

$$(8) \quad V(x, r) = \frac{1}{2}cr^2 + \int \frac{x - \xi}{\sqrt{(x - \xi)^2 + r^2}} dm(\xi).$$

Then [44, p. 139], $\nabla U \cdot \nabla U = r^{-2} \nabla V \cdot \nabla V$ is an analytic function of (x, r) , and hence of (U, V) , except on the axis itself. Suppose also that a section of the bounding streamline $V = 0$ were "free", so that $\nabla U \cdot \nabla U = k^2$ there. Then, by the analyticity of $\nabla U \cdot \nabla U$, we would have

$$(8^*) \quad \nabla U \cdot \nabla U = k^2 + k_1(U)V + k_2(U)V^2 + \dots$$

on this section. By analytical⁹ (harmonic) continuation, (8*) would hold all along the bounding streamline, whence $\nabla U \cdot \nabla U = k^2 > 0$ on the nose of the Rankine body. Therefore *no "Rankine flow" can be a cavity flow*. For instance, a Rankine flow could not have a weak singularity at the separation point (cf. Ch. IV, §7).

4. Source and vortex rings. However, it is classic [44, p. 219] that any harmonic function is the potential of a suitable distribution of sources and dipoles (single and double layer) on the boundary—and even [44, Ch. XI] of either alone. In the plane and axially symmetric case, representations by *vortex layers* (sheets) are also well known.

Further, any axially symmetric source distribution is evidently a superposition of *source rings*. The potential of a single ring of sources on $x = 0$, $r = a$ is clearly¹⁰

$$(9a) \quad \begin{aligned} U(x, r) &= \int_0^{2\pi} d\theta / (x^2 + r^2 + a^2 - 2ar \cos \theta)^{\frac{1}{2}} \\ &= \frac{1}{r_1} \int_0^\pi \frac{2 d\phi}{\sqrt{1 - k^2 \cos^2 \phi}} = \frac{4}{r_1} K(k) \end{aligned}$$

where $r_1^2 = x^2 + (r + a)^2$, $\phi = \theta/2$, $k^2 = 4ar/r_1^2$, and $K(k)$ is the complete

⁸ [50, p. 127]. The integral in (8) is a Stieltjes integral, for a source density $dm/d\xi = n(\xi)$ on the x -axis, in a uniform stream of velocity c .

⁹ For harmonic continuation, see W. J. Sternberg and J. L. Smith, "The theory of potential and spherical harmonics", Toronto, 1944, p. 220.

¹⁰ See [44, p. 59], or M. A. Sadowsky and E. Sternberg, *Quar. appl. math.* 8 (1950) 113-26, esp. §3.

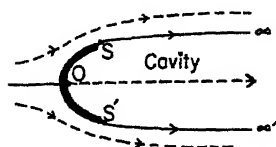


FIG. 3.

elliptic integral of the first kind. The associated velocity components are¹⁰

$$(9b) \quad u = 4xE/r_1r_2^2, \quad v = (2/r_1r)(K + (r^2 - x^2 - a^2)E/r_2^2),$$

where $r_2^2 = x^2 + (r - a)^2$, and E is the complete elliptic integral of the second kind. The potentials of rings of axial and radial dipoles are given by similar formulas. The stream function of a source ring is multiple-valued, and has a more complicated expression¹⁰ involving the Jacobi zeta function.

Similarly, any axially symmetric vortex distribution is a superposition of *vortex rings*. The stream function of a vortex ring is¹¹

$$(10a) \quad V = (r_1^2 + r_2^2)(K/2r_1) - r_1E$$

from which the velocity components can be calculated as

$$(10b) \quad u = \frac{1}{r_1} [K + (a^2 - x^2 - r^2)(E/r_2^2)]$$

$$(10c) \quad v = \frac{-x}{rr_1} [K - (a^2 + x^2 + r^2)(E/r_2^2)]$$

The velocity potential $U = U(x, r)$ is multiple-valued, and the expression for it is very like¹⁰ that for the stream function of a source ring.

5. Integral equation approaches. Using the formulas of §4, one can express axially symmetric free boundary problems as integral equation problems involving functions of one real variable, in several ways. We consider first infinity *cavity* problems, for which $\phi = U - x$ is a convenient function to consider, because $\nabla\phi$ dies out at infinity.

For a given *trial* free boundary $\widehat{S\infty}$ (see Fig. 3), one can take the density $\sigma(\mathbf{x})$ of the source distribution on $\infty'S'OS\infty$ defining ϕ as the unknown function. Then the condition that $\partial U/\partial n = 0$ on $\widehat{OS\infty}$ reduces to a known¹² Fredholm integral equation involving $\sigma(\mathbf{x})$. A similar remark applies if a dipole distribution or vortex distribution on $\infty'S'OS\infty$ is taken as the un-

¹¹ Sadowaky-Sternberg, *op. cit.* in fnnt. 10, or [50, p. 237, (9)]. The formulas are due to Kelvin (1860) and Maxwell. See also A. Weinstein, *Quar. appl. math.* 5 (1948), 429-44, and A. van Tuyl, *ibid.* 7 (1950), 399-409. By the Biot-Savart Theorem, the field is that of a uniform disc of doublets.

¹² See [44, Ch. XI], or L. Landweber, *DTMB rep.* 761, 1951 (second method).

known function. One can then test for the "free boundary" condition $\nabla U \cdot \nabla U = 1$ on $\widehat{S\infty}$, and hope to locate the correct free boundary approximately, after a succession of trials.

A variant would be to hope that a source distribution on $\widehat{S'O'S}$ and the circular cylinder $r = r(S)$ would suffice to generate ϕ . For any such distribution, one could locate the streamline through S , and try to match the conditions $\partial U / \partial n = 0$ on $\widehat{OS\infty}$, and $\nabla U \cdot \nabla U = 1$ on $\widehat{S\infty}$.

A still more reasonable procedure¹³ is to assume trial values $\phi = f(s)$ along $\widehat{S'O'S}$, and a plausible shape $r = \pm g(s)$ for the free boundary. For given $f(s)$ and $g(s)$, ϕ and $\partial\phi/\partial n$ are determined on the entire boundary $\infty'\widehat{S'O'S\infty}$, as follows. Since $\partial U / \partial n = 0$, $\partial\phi/\partial n = -\partial x/\partial n$ on the entire boundary. On \widehat{OS} , $\phi = f(s)$ by hypothesis. On $\widehat{S\infty}$, if s denotes arc-length measured from S , $U = s + \text{const.}$, whence $\phi = (s - x) + \phi(S) + x(S)$. The values of ϕ on $\widehat{OS'\infty}$ are found by symmetry: $\phi(x, r) = \phi(x, -r)$. Substituting the values of $\partial\phi/\partial n$ and ϕ so found in Green's Third Identity [44, p. 219], we get, in the interior of the flow

$$(11) \quad \phi(x, r) = \int \frac{-\partial x}{\partial n} U_1(x, r; x', r') ds' - \int \phi U_2(x, r; x', r') ds',$$

where U_1 is the potential (cf. (9a)) of a source ring at (x', r') , and U_2 that of a dipole ring at (x', r') normal to $\widehat{OS\infty}$, both suitably normalized.

It is plausible that, if (11) converges to the assumed ϕ as the boundary is approached, then $U = \phi + x$ has the properties asked for. In fact, $\nabla U \cdot \nabla U = 1$ is immediate, but $\partial U / \partial n = 0$ is not so obvious. In any case, the condition that (11) converge to the assumed ϕ as the boundary is approached is *necessary*.

Using this fact, Levinson¹⁴ [55] was able to determine the *asymptotic shape* of an axially symmetric cavity with $Q = 0$. Making rather mild "Tauberian" assumptions about the regularity of the asymptotic cavity shape, Levinson showed that, as $x \rightarrow \infty$, we have

$$(12) \quad r(x) = (cx^{\frac{1}{2}}/\ln^{\frac{1}{2}}x)[1 - (\ln(\ln x))/(8 \ln x) + O(1/\ln x)].$$

The drag is, moreover, given by

$$(12') \quad D = \pi \rho v^2 c^4 / 8.$$

More precisely, $xr'(x)/r(x) = k + o(x)$ is only possible for $k = \frac{1}{2}$, which

¹³ First applied by E. Trefftz (Zeits. math. phys. 64 (1916), 34-61) to the jet from a circular orifice.

¹⁴ See also M. I. Gurevich, Prikl. mat. mekh. 11 (1947), 97-104; F. Scheid, Am. J. Math. 72 (1950), 485-501. For the plane analog, see Ch. IV, §3.

gives the exponent $\frac{1}{2}$ in (12). And $xr'(x)/r(x) = k + O(1/\ln x)$ is only possible if (12) holds. Formula (12') can also be derived heuristically from an asymptotic computation of the kinetic energy per unit x for the flow around the paraboloid $r^2 = c^2x$, which is due to a half-line of sources behind the focus.

6. Approximate methods. At the present time, the practical analysis of cavity flows is based on less refined considerations. Some important results follow from conservation laws (see Ch. I, §§10–11); these have been summarized in §2. Others follow from non-rigorous, approximate considerations.

Thus, one can reach the conclusion that finite *axially symmetric cavities are roughly ellipsoidal*, by extending¹⁵ the approximate analysis of Ch. I, §11. One again assumes that the flow and energy transfer are dominantly radial. Taken literally, this assumption would make the (radial) velocity $\dot{r} = a\dot{a}/r$, where $a(x, t)$ is the cavity radius. Hence the kinetic energy per unit length would be infinite: $\pi\rho a^2\dot{a}^2 \int_a^\infty r dr/r^2 = +\infty$. To avoid this paradox

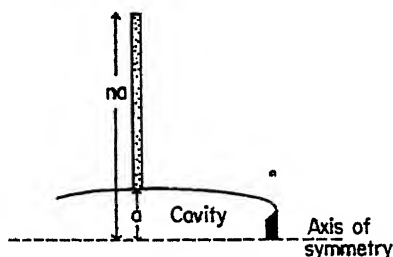


FIG. 4.

we replace \int_a^∞ by \int_a^{na} (see Fig. 4); this makes the energy density $\pi\rho a^2\dot{a}^2 \text{Log } n$. As long as n is assumed to vary in the range (say) 10–20 or 15–30, $\text{Log } n$ can be treated as a constant. (This would not be true in the plane.)

We now make the further assumption that this kinetic energy and the (hydrostatic) potential energy $\pi(p_\infty - p_c)a^2$ both come from the work done by the missile against the drag D . This gives the energy equation

$$\frac{1}{2} \pi\rho a^2\dot{a}^2 \text{Log } n + \pi(p_\infty - p_c)a^2 = D.$$

¹⁵ The argument was concocted in 1945 by L. Loomis and G. Birkhoff, but not published; H. Munzner and H. Reichardt reached the same conclusion empirically in 1944 (UM No. 6616). In this connection, see also M. P. Tulin, DTMB Rep. 834 (1953). It seems likely that Tulin's method can be adapted to treat axially symmetric flows.

Writing $\dot{a} = v da/dx$ and simplifying, we get

$$(13) \quad (da/dx)^2 \text{Log } n + Q = (a_m/a)^2 C_D,$$

where a_m is the missile radius. Or

$$(13') \quad \frac{a da}{\sqrt{C_D a_m^2 - Q a^2}} = \frac{dx}{\sqrt{\text{Log } n}}.$$

Integrating and squaring both sides, we deduce an ellipsoidal cavity whose axes are in the ratio $2A_m/L = (Q/\text{Log } n)^{1/2}$, where A_m is the cavity width and L the length. Experimentally, A_m/L seems to grow more like Q than like \sqrt{Q} , as is shown in the accompanying Fig. 5.¹⁸

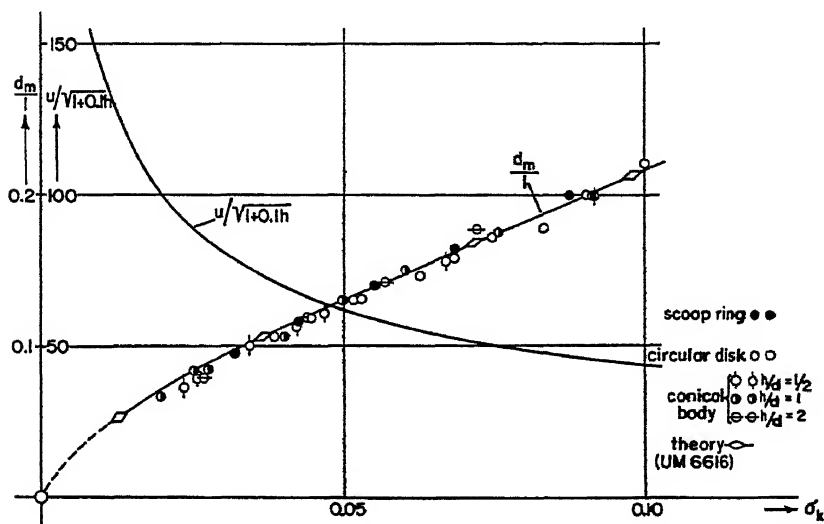


FIG. 5.

To a better approximation, one may suppose that n is proportional to L/A_m . This has a minor effect on the preceding calculations, but completely alters the results obtained by similar methods in *plane* flow.

7. Jets from conical orifices. The most thoroughly studied axially symmetric flow is probably the jet from a sharp-edged circular hole in a flat wall (Fig. 1a, §1). The contraction and discharge coefficients for this flow have been of interest for centuries.

If the effects of viscosity, surface tension and gravity are minimised, and

¹⁸ Copied from Fig. 18 of H. Reichardt [67a]. As $Q \downarrow 0$, the ellipsoidal cavities of fig. 7 approach the paraboloidal cavity of (7).

the hole is sharp-edged, one measures¹⁷ a contraction coefficient C_c of about 0.61, as in the analogous case (Ch. II, §5) of the jet from a slot. The corresponding diameter-ratio is about 0.78.

Numerous authors have made theoretical studies confirming the experimental value $C_c = 0.61$. The work of Trefftz¹⁸, Southwell and Vaisey [78, Example 3] and Rouse and Abul-Fetouh¹⁸ deserves especial mention. The authors used integral equation methods (§4), relaxation methods, and electrolytic tank methods.

The axially symmetric "free" flow from a Borda tube (Ch. I, §10) has also been calculated, by relaxation methods [78, Example 2]. So has the jet from a circular hole in the center of a disc at the end of a circular tube, by Rouse and Abul-Fetouh¹⁸, using relaxation and electrolytic tank methods.

In all cases, the contraction coefficient differs imperceptibly from that of the corresponding plane ("Réthy") flow. This suggests that the same principle holds for jets from conical orifices making any angle β with the axis of symmetry.

Kretzschmer¹⁹ has even suggested that axially symmetric jets can be calculated from known plane jets by the preceding principle of area-correspondence. If $\psi(x, y)$ is the stream function for a plane potential flow, this amounts to defining

$$(14) \quad V(x, r) = \psi(x, kr^2).$$

It is easy to show that, denoting differentiation by subscripts,

$$(14') \quad V_{xx} + V_{rr} - r^{-1}V_r = \psi_{xx} + 2kr^2\psi_{rr}.$$

Hence $\nabla^2\psi = 0$ implies (14) approximately, and for any k , if ψ_{xx} or ψ_{rr} is small. Also, since $r^{-2}(V_r^2 + V_x^2) = 4k^2\psi_r^2 + r^{-2}\psi_x^2$, the free boundary condition is approximately preserved if r is nearly $\frac{1}{2}k$. See the end of §9.

8. Impinging jets. The normal impact of a circular jet against a flat plate (Fig. 6) has also been studied repeatedly²⁰. Elementary considerations show that, in the case of smooth flow, all the momentum is trans-

¹⁷ J. Weisbach, "Experimental-Hydraulik", 1855, p. 116; H. Smith, *Hydraulics*, New York, 1886, p. 59; R. Basin, *Mem. de l'Acad. des Sciences (Paris)* 32 (1902), 31-45; [25, Ch. X], and refs. given there; C. W. Harris, *Hydraulics*, Ch. II; H. Bouasse, *Jets, tubes et canaux*, Paris, 1923, pp. 5, 29, 120; G. de Marchi, *Annali dei lavori pubblici*, Rome, 1925, 45 pp.; A. H. Gibson, *Hydraulics*, 1947, 110-13.

¹⁸ E. Trefftz, *Zeits. math. phys.* 64 (1916), 34-61; H. Rouse and A.-H. Abul-Fetouh, *J. appl. mech.* 17 (1950), 421-6. See also F. Kotter, *Archiv fur Math. Phys.* 5 (1887), 392-417, and T. Levi-Civita, *Rend. Sem. Mat. Fis. Milano* 5 (1931), 1-20.

¹⁹ VDI Forschungsheft 381 (1936). For general confirmation of the applicability of the "area-ratio" concept, see [50a].

²⁰ Fr. Reich, VDI Forschungsheft 290 (1929); A. H. Gibson and F. Haywood, *Phil. Mag.* 45 (1923), 229-38; H. Bouasse, *Ann. fac. sci. Toulouse* 28 (1936), 1-62.

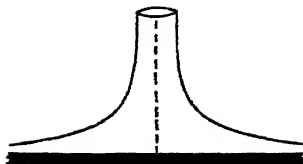


FIG. 6.

mitted to the plate. However the pressure distribution and flow pattern are also of interest; usually, the former is measured and the latter calculated by approximate potential-theoretic methods. Thus, approximate calculations of the flow pattern have been made by Reich²⁰ using expansions, by Schach²¹ using the integral equation method of Trefftz¹⁸, and by Leclerc²¹ using an electrolytic tank.

Various related flows are also of interest. Among these are circular jets impinging normally on cones and hemispherical cups, and obliquely on plates²².

The normal impact of a jet on a plate can be regarded as half of the flow produced by the impact of two equal coaxial circular jets having the same velocity. This case was thoroughly studied by Savart²³, who showed experimentally that the disc-like sheet formed was stable. In the case of unequal jets, a conical sheet is thrown off, and the reverse of this flow corresponds to the collapse of a conical liner, as envisaged in the theory of shaped charge action (Fig. 2 and Ch. I, §10). The limiting case, when one of the jets has infinite diameter, corresponds to the penetration of a target by a jet, and is also of interest. In none of these cases has the flow been calculated theoretically.

9. Underwater cavities. Due to the advent of high-speed underwater missiles, considerable attention has recently been devoted to axially symmetric cavities, and especially to the dependence of cavity drag coefficients on head-shape and the cavitation number Q . Because of the apparent validity of the formula $C_D(Q) = (1 + Q)C_D(0)$ (Ch. I, §11), it suffices to determine $C_D(Q)$ for a single Q , say $Q = 0$.

The earliest results are those of Bauer²⁴ on spheres, which gave $C_D(0) =$

²⁰ W. Schach, *Ing. Archiv* 6 (1935), 51-8; A. Leclerc, *La Houille Blanche* 5 (1950), 816-21. Since there is no separation-point singularity, this is perhaps the easiest case to treat.

²¹ This has been studied by W. Schach, *Ing. Archiv* 5 (1934), 245-65.

²² F. Savart, [73a, 257-310]. Savart's figures, involving 3mm-6mm jets for which surface tension is important, come at the beginning of the issue. See also V. Volterra, *J. de math.* 11 (1932), 1-35.

²⁴ W. Bauer, *Ann. der Physik* 80 (1926), 232-44 and 82 (1927), 1014-16; see [72, p. 98], and especially A. May and J. C. Woodhull, *J. appl. phys.* 19 (1948), 1109-21.

0.30. This result seems reliable to within $\pm 10\%$, although experimental observations are subject to various corrections. For instance, if the concept of induced mass is applicable to cavity motion (cf. Ch. XI, §6), then the drag D will vary with the acceleration a according to the formula $D = ma(1 + \sigma k)$, where m is the missile mass, σ is the ratio of fluid density to missile density, and $k = k(Q)$ is an "induced mass" coefficient depending on the missile shape [4, p. 164]. The term in σk is commonly ignored in measurements of cavity C_D .

For a disc, values near $C_D = 0.81$ have been obtained repeatedly²⁵, and are probably accurate to within $\pm 5\%$. For cones with vertex angle $2\beta = 90^\circ$, $C_D = 0.50$; if $2\beta = 30^\circ$, $C_D = 0.15$. For a "stagnation cup" with profile as in Fig. 7 evidently $C_D = 1.0$ nearly.

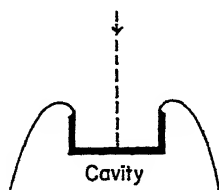


FIG. 7.

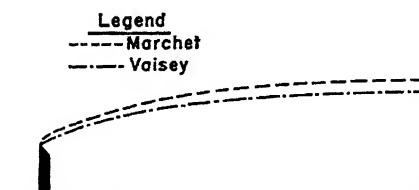


FIG. 8.

Various attempts have been made to calculate the cavity C_D of a sphere, and the flow pattern, by source-sink methods (§3). Thus, if the flow past a "half-body" (§3) is taken as an approximation to that past a sphere having the same vertex curvature, and the pressure excess integrated over the zone of positive pressure, one gets the "theoretical" estimate $C_D = 0.34$. More elaborate axial source distributions can be used to get other approximations, but the method has the defect in principle mentioned in §3: the flow near the separation point cannot be duplicated.

Relaxation and electrolytic tank methods have been applied²⁶ to the

²⁵ See M. S. Plesset and B. Perry, *Riabouchinsky Jubilee Volume*, Paris, 1954, 251-61.

²⁶ Miss Vaisey's and Mr. Brunauer's results are unpublished: those of M. Marchet were mimeographed as *Problème D350A*, Institut Blaise Pascal, C.N.R.S. (Paris), 1949. See also J. S. McNown et al. *Trans. Am. Soc. civ. eng.* 120 (1955), 650-86. For a very thorough study, see NPG Rep. 1413, Dahlgren, U. S. A., by David M. Young.

axially symmetric analog of Riabouchinsky flow past two discs of diameter d , in a channel of diameter $8d$. The cavity profiles in one quadrant are drawn in Fig. 8; the estimated values of Q were 0.23, 0.32; those of $C_D(0) = C_D(Q)/(1 + Q)$ were 0.82, 0.77. Similarly, Mr. Brunauer of the Illinois Institute of Technology has treated the Riabouchinsky flow past a disc (180° cone) in a channel, while Southwell and Vaisey [78, Example 11] have calculated cavity flows past a sphere, both by relaxation methods.

A very simple method for estimating the cavity C_D of discs and cones in cavity flow has been proposed by Reichardt, Fisher, Plesset and Shaffer²⁷. This consists in rotating the known pressure distribution for Bobyleff flow (Ch. II, §4), past wedges with the same vertex angle 2β , about the axis of symmetry. If $2\beta > 60^\circ$, the calculated C_D agrees quite well with observation; this is not too surprising, since the pressure distribution $C_p(r)$ satisfies $C_p(0) = 1$, $C_p'(0) = 0$, $C_p(a) = 0$, $C_p'(a) = \infty$ for any blunt obstacle having "abrupt separation" (Ch. IV, §7), at $r = a$.

However, the predicted pressure distributions are inaccurate²⁸, and the method does not rest on a sound theoretical basis. The same may be said for other formulas purporting to transform plane flow with free boundaries into axially symmetric flows with free boundaries²⁸. In particular, the proposed principle may be contrasted with that used by Kretzschmer (§7).

Garabedian's power series. A more plausible comparison between plane and axially symmetric flows has recently been invented by Garabedian^{28a}. Garabedian considers the $(p + 2)$ -dimensional problem $V_{xx} + V_{yy} = (p/y)V_y$, for variable p . He conjectures that, if $\delta = p/(p + 2)$, power series in δ will converge in $|\delta| < 1$, and tries to calculate values for $\delta = \frac{1}{2}$.

Using this method, he computes $C_c = 0.58$ for the jet from a circular hole, instead of 0.61 (cf. §7). And he calculates $C_D = 0.83$ for a disc, instead of 0.81. A very thorough analysis^{28a} gives him great confidence in these values.

10. Swirling flows. Swirling flows with axial symmetry occur in various contexts: in whirlpools, in tornados, in flow through turbines, and in the flow down a bathtub drain. The mathematical theory has been highly developed in connection with turbine theory²⁹; we shall here be concerned with some simple considerations involving such swirling flows with free boundaries.

The simplest mathematical models represent pure swirl. They have a

²⁷ H. Reichardt, [67a]; J. W. Fisher, UBRC Report 34 (1945); M. Plesset and P. A. Shaffer, J. appl. phys. 19 (1948), 934-9; see also A. H. Armstrong, Arm. res. est. rep. 21/54.

²⁸ See M. I. Gurevich, Doklady SSSR 57 (1947), 763-4, who shows the inexactness of formulas proposed by Vasilescu (Comptes rendus 196 (1933), 896-8 and 1284-6).

^{28a} Bull. Am. math. soc. 62 (1956), 219-35.

²⁹ A classic paper is that by R. von Mises, Zeits. math. phys. 57 (1909), 1-120; see also F. E. Marble and I. Michelson, NACA TN 2614 (1952).

velocity potential $U = \gamma\theta$, where $2\pi\gamma$ is the circulation about the axis of symmetry, assumed constant. For such models, the velocity $v_\theta = \gamma/r$ is wholly angular, and a cylindrical "hollow vortex" $r = R$ can be taken as a free surface if gravity is neglected. The pressure is then given by $p = p_0 - \gamma^2/2r^2 = p_0 - v_\theta^2/2$; such idealized hollow vortices have been studied by various authors, with special reference to their stability theory³⁰ (cf. Ch. XI, §16).

If the positive x -axis is taken as vertically down, then a gravity field of strength g may be superposed on pure swirl, provided the free surface is given the profile

$$(15) \quad r^2 = \gamma/2gx.$$

The case of general axially symmetric potential flows with circulation is hard to treat analytically. If gravity is neglected, one solution is given by a hyperboloid of revolution having one sheet; the rulings are streamlines³¹.

If gravity is taken into account, then Bernoulli's equation gives $r^2 \geq \gamma/2gx$, for the free surface of the vortex core. If the swirl is large, we have near equality, as in (15). One ideal flow of this type has been calculated by Binnie and Davidson^{31a}, using relaxation methods.

From a practical viewpoint, the most striking fact³² is the large reduction in discharge which swirl can cause in trumpet-shaped circular outlet weirs, owing to the development of intense centrifugal forces.

Because of the loss of angular momentum ("swirl") in the boundary layer, which therefore falls most freely, the discharge often consists largely of the boundary layer in convergent, rapidly swirling flows. This was first shown by Sir Geoffrey Taylor³³, in connection with "swirl" atomizers, and later by Binnie and Harris³², in connection with discharges through trumpet-shaped weirs. Similarly, Rankine's classic "combined vortex" [61, §13.13] is inapplicable to the dimple often formed on the surface of a discharge with moderate swirl.³⁴ The "gulping" of air by a weak, partly hollow vortex

³¹ See [50, §166], and refs. given there. Also, J. Ackeret, *Ing. Archiv* 1 (1930), 399-402, and especially A. M. Binnie, *Proc. roy. soc. A* 197 (1949), 545-55, and A205 (1951), 530-40.

³¹ See V. Volterra, *J. de math.* 11 (1932), 1-35, for a mathematical discussion of flows in thin sheets with free boundaries.

^{31a} *Proc. roy. soc. A* 199 (1949), 443-57. See also V. Volterra, *op. cit. supra*.

³² A. H. Gibson, *Mem. Manchester Lit. Phil. Soc.* 55 (1911), no. 7; A. M. Binnie and G. A. Hookings, *Proc. roy. soc. A* 194 (1948), 398-415; A. M. Binnie and D. P. Harris, *QJMAM* 3 (1950), 89-106.

³³ *Proc. seventh int. congr. appl. mech. London* (1948), vol. 2, 280-5. See also Ch. XV, §12.

³⁴ Binnie and Hookings, *op. cit. in fnnt.* 32, p. 413; as remarked there, the contrary assertion is (mistakenly) made on p. 104 of Gibson's "Hydraulics".

tube is also very interesting, but an adequate theoretical account of any of these phenomena would be very lengthy.

Attention should also be called to an interesting paper of H. Reissner³⁵, dealing with the free boundary of a propeller slip-stream, analyzed as a jet with possible vorticity.

II. Rising bubbles in tubes. Air bubbles rising under gravity in a vertical cylindrical tube of diameter $d = 2a$ have been investigated experimentally and theoretically, by various scientists.³⁶ The velocity v of rise satisfies $v = 0.45 \sqrt{ga}$, approximately; the radius of curvature of the bubble tip satisfies $R = 0.7a$; one can also deduce $v = (\frac{2}{3})\sqrt{gR}$ by considering the pressure gradient in ideal flow around a solid sphere.

The preceding formulas are valid over the range $d = 1-10$ cm. For $d < 1$ cm., surface tension becomes very important; the range $d > 10$ cm. has not been explored. It is noteworthy that ripples form on long bubbles, and that bubbles more than $15d-20d$ long are unstable.

The limiting case $d = \infty$ of bubbles in an unlimited fluid is very complicated, physically, and will be discussed in Ch. XV, §7.

The steady rise of bubbles in a vertical $4'' \times 1''$ rectangular tube has also been observed³⁷. Mean values of $v/\sqrt{ga} \simeq 0.41$ and $R/a \simeq 0.70$ were measured, with $a = 4''$. The observed value of v/\sqrt{ga} may be compared with a theoretical value of 0.33 ± 0.01 for ideal plane flow, calculated by the methods of Ch. VIII, §11. The discrepancy is presumably due to the three-dimensionality of the real flow. (In a square, due to flow in the corners, v/\sqrt{ga} should exceed the value 0.45 for a cylinder by about 20 %.)

³⁵ ZaMM 12 (1932), 25-35.

³⁶ Förster, Zeits. math. phys. 62 (1912), 319-27; A. H. Gibson, Phil. Mag. 26 (1913), 952-65; D. T. Dumitrescu, ZaMM 23 (1943), 139-49; R. M. Davies and G. I. Taylor, Proc. roy. soc. A200 (1950), 375-90.

³⁷ The observations, due to Russell Duff, are reported in Rep. LA-1927 of the Los Alamos Scientific Labs. The calculations, also described there, were planned jointly with David Carter.

CHAPTER XI

UNSTEADY POTENTIAL FLOWS

1. Vapor-filled spherical bubbles. The simplest case of an unsteady potential flow with a free boundary is furnished by the collapse of a spherical bubble, in an infinite medium at constant pressure p_∞ . Following ideas of Besant and Rayleigh¹, we give an approximate treatment of this case, neglecting the effects of viscosity, compressibility, gravity, surface tension, and vapor condensation.

Consider a spherical bubble of variable radius $a(t)$, in an incompressible liquid of density ρ . At a distance r from the center, the outward velocity $\dot{r} = dr/dt$ will satisfy $r^2\dot{r} = a^2\dot{a} = A$, where A is a function of time. Hence the total kinetic energy of the liquid will be

$$(1) \quad \mathcal{E} = \frac{1}{2}\rho \int_a^\infty 4\pi r^2 (Ar^{-2})^2 dr = 2\pi\rho\dot{a}^2 a^3.$$

The simplest case is that in which the collapse starts from a bubble with radius $a(0) = R$, initially at rest, and where the pressure p_∞ at a large distance exceeds the vapor pressure p_v in the bubble, by a fixed amount P .

In this case, neglecting surface tension, conservation of energy gives

$$(1') \quad 2\pi\rho\dot{a}^2 a^3 = 4\pi P(R^3 - a^3)/3.$$

This gives the differential equation

$$(2) \quad (\dot{a}/R)^2 = K^2[(a/R)^{-3} - 1], \quad K = \sqrt{\frac{2P}{3\rho R^2}}.$$

This can be integrated in terms of incomplete β -functions or elliptic integrals². Setting $x = a^3/R^3$, and $\tau = Kt$, we have

$$(2a) \quad 3\tau = \int_x^1 x^{-1}(1-x)^{-1} dx = B(\frac{5}{6}, \frac{1}{2}) - B_x(\frac{5}{6}, \frac{1}{2}).$$

In particular, the time of collapse is given by $\tau_1 = \frac{1}{3}B(\frac{5}{6}, \frac{1}{2})$, or

$$(2b) \quad t_1 = .915R\sqrt{\rho/P}.$$

¹ H. Besant, "Hydrostatics and hydrodynamics" (1859), §158; Rayleigh, Phil. Mag. 34 (1917), 94-8 and 45 (1923), 257-65; [50, p. 122].

² For the expression in terms of incomplete β -functions, see [50, p. 122] or [17, p. 275]; that in terms of elliptic integrals seems to be new; it was worked out by Arthur H. Read.

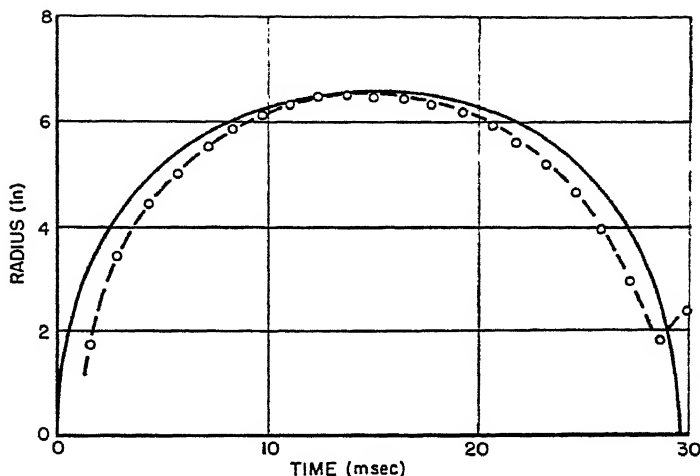


FIG. 1.

For a periodically *oscillating* vapor-filled bubble, rebounding elastically after collapse, the period is thus $2t_1$.

Alternatively, we have

$$(3) \quad \tau = \int_{\alpha}^1 \frac{\alpha^2 d\alpha}{\sqrt{\alpha - \alpha^4}}, \quad \text{where} \quad \tau = Kt, \quad \alpha = \frac{a}{R}.$$

This expression can also be integrated in terms of tabulated elliptic integrals, but the formulas are less simple.

A graph of the solution is shown as Fig. 1; even in the case of underwater explosions (§3), a quite good agreement with the observed radius-time curve is obtained³.

As $a \downarrow 0$, clearly $\dot{a} \propto a^{-1/2}$ by (1'). Thus, in the limit, *infinite* collapse velocities (and hence pressures) are predicted. As we shall see later (Ch. XV, §6), very large pressures do in fact occur; and "cavitation damage" from collapsing vapor-filled cavities is of the greatest practical importance⁴. However, a realistic discussion of the subject involves many physical variables which we have neglected (see also §3, §13 below), and so we shall postpone this discussion.

2. Cavitation in a variable pressure field. Typically, cavitation occurs in a rapidly flowing liquid when it flows through a region of negative

³ [17, p. 277]; D. R. Yennie and A. B. Arons, Navord Report 425 (1949). See also ftnt. 5.

⁴ See, for example, Proc. Am. soc. civ. eng. 71 (1945), No. 7, and the discussion in subsequent issues. Sound radiation from collapsing bubbles is also important; see Ch. XV, §5.

pressure. The local pressure deficiency $-P(t) = p_e - p$ can often be estimated from Bernoulli's equation, knowing the geometry of the solid boundaries involved. A rough prediction of the observed rate of growth can then be obtained⁵ by neglecting surface tension, and writing down the energy equation

$$d\mathcal{E}/dt = -4\pi a^2 \dot{a} P(t).$$

This, in turn, gives by (1) the second-order differential equation $\rho d(a^3 \dot{a}^2)/dt = -2P(t)a^2 \dot{a}$ for a , or

$$(4) \quad \frac{3}{2} \dot{a}^2 + Ca\ddot{a} = -P(t)/\rho,$$

which can be integrated numerically. If this is done, fair agreement with observation is obtained. The special solution

$$(4') \quad a = At^{1/6}, \quad -P(t) = \frac{3}{8} \rho A^2 t,$$

roughly describes the growth of a static bubble in a linearly increasing tension $P(t)$; if the tension is constantly T_0 , then $a = (2T_0/3\rho)^{1/2} t$.

As neither surface tension, compressibility, nor viscosity destroys the spherical shape of vapor-filled cavities (indeed, surface tension tends to make them spherical), it is natural to try to extend the preceding mathematical theory so as to include the effects of these forces.

The effect of surface tension γ in a static field can be easily taken into account, by noting that the internal energy is then

$$4\pi P(R^3 - a^3)/3 + 4\pi\gamma(R^2 - a^2).$$

This replaces (2) by the differential equation

$$(5) \quad 1.5\rho a^4 \dot{a}^2 = (PR^3 + 3\gamma R^2)a - 3\gamma a^3 - Pa^4.$$

In this case also, $t = f(a)$ can be expressed by elliptic integrals.—In case $P < 0$, R^3 may be taken as negative or positive, and various qualitatively different types of solutions are possible. It is easily verified that surface tension does not alter the asymptotic formula $\dot{a} \propto a^{-1.5}$ as $a \downarrow 0$.

The effects of liquid compressibility and viscosity are also important as $a \downarrow 0$, and will be discussed in Ch. XV, §6.

Demtchenko and Poncin⁶ have studied the collapse of ellipsoidal cavities, but without obtaining any simple results.

⁵ [48]; M. S. Plesset, *J. appl. mech.* 16 (1949), 277–338; B. E. Noltingk and E. A. Neppiras, *Proc. phys. soc.* B63 (1950), 674–85, and B64 (1951), 1032–8. See however Ch. XV, §1. Observed collapse times exceed predictions somewhat; see W. B. Chesterman, *Proc. phys. soc. London* B65 (1952), 846–58; M. Harrison, *DTM B Rep.* 815 (1952); A. T. Ellis, *Caltech. hydro. lab. rep.* 21–12 (1952).

⁶ B. Demtchenko, *J. de l'Éc. Polyt.* 27 (1926), 113–24; H. Poncin, *Thèse* (1932); *J. de math.* 18 (1939), 385–404; *Acta Math.* 71 (1939), 1–62; *Publ. sci. tech. min. air*, No. 18 (1933).

3. Gas-filled cavities. In the case of a (nearly) spherical bubble produced by an underwater explosion, account must be taken of the internal potential energy of the explosive gases. This prevents the bubble radius from shrinking to zero, and determines the maximum cavity radius R . Clearly, R is related to the total explosive energy Y by the formula $Y = 4\pi PR^3/3$, where P is the ambient pressure.

The importance of the explosive gases is confined largely to the time when the radius a is relatively small, $a \ll R$. Hence they do not affect much the *period* of the oscillation produced by an underwater explosion. Substituting in (2b) from the formula $Y = 4\pi PR^3/3$, we get

$$(6) \quad 2t_1 = 1.14\rho^{\frac{1}{2}}Y^{\frac{1}{2}}p^{-5/6},$$

a formula which gives quite good results⁷.

One can also apply dimensional analysis, to correct (6) for gas compression effects. Similarity considerations⁸ show the invariance of the oscillations under the substitutions $a \rightarrow \beta a$, $Y \rightarrow \beta^3 Y$, $t \rightarrow \beta t$; hence $2t_1 = Y^{\frac{1}{2}}\tau(\rho, P)$, where ρ is the density of the surrounding water. If the gas bubble is assumed to expand homogeneously and adiabatically, and only its potential energy is considered, then we get the simpler formula $2t_1 = Y^{\frac{1}{2}}\rho^{\frac{1}{2}}\phi(P)$. The determination of the functions $\tau(\rho, P)$ and $\phi(P)$ requires further analysis.

Under the preceding assumption of homogeneous adiabatic expansion, the behavior of an underwater explosion bubble near its *minimum* radius R_1 can be estimated as follows. Assume a perfect gas, with mean pressure $p(t)$ and density $\rho_b(t)$. If p_1 denotes the mean pressure at minimum radius R_1 , then $p = k\rho_b^\gamma = p_1(R_1/a)^{3\gamma}$, for a suitable exponent γ . The total potential energy of gas compression is thus

$$4\pi p_1 R_1^{3\gamma} \int_a^\infty a^{2-3\gamma} da = 4\pi p_1 R_1^{3\gamma} a^{2-3\gamma}/(3-3\gamma).$$

Putting this into the energy equation (1'), and dividing by $2\pi a^3$, we get

$$(7) \quad \rho \dot{a}^2 = \frac{H}{a^3} - \frac{2P}{3} - \frac{2p_1}{3(1-\gamma)} \left(\frac{R_1}{a}\right)^{3\gamma}.$$

Near the minimum radius R_1 , we can⁹ neglect P , and obtain the simplified equation

$$(7a) \quad \dot{a}^2 = \frac{2p_1}{3(\gamma-1)\rho} \left\{ \left(\frac{R_1}{a}\right)^3 - \left(\frac{R_1}{a}\right)^{3\gamma} \right\},$$

where H is evaluated by setting $\dot{a} = 0$ when $R = R_1$.

⁷ [17, pp. 276, 280]. In practical applications, a correction is made for the "percent of explosive energy converted into mechanical energy."

⁸ We are appealing to the so-called Cranz Similarity Law; see also [4, Ch. III, §18].

⁹ See the refs. of footnote 1; also H. Lamb, *Phil. Mag.* 45 (1923), p. 257.

In the special case $\gamma = \frac{4}{3}$, which corresponds roughly to explosive gases, (7a) can be integrated in closed form. Writing $a/R = 1 + \alpha$, we get⁹

$$(7b) \quad \sqrt{\frac{p_1}{\rho}} \frac{t}{R_1} = \sqrt{2\alpha} \left(1 + \frac{2}{3}\alpha + \frac{1}{3}\alpha^2\right).$$

For a numerical case, see [50, p. 123].

In actual underwater explosions, about 30 % of the energy is lost by acoustic radiation during the first collapse and rebound, while as much again is lost through turbulence and bubble asphericity^{9a}. Hence the periodically oscillating bubble assumed above is a considerable idealization. See also §13 and Ch. XV, §§4-6.

The above ideas are also applicable to the collapse of an air-filled cavity; the air content cushions the shock of final collapse. The absolute temperature T will satisfy

$$(8) \quad T_1/T = (R_1/R)^{3\gamma-3},$$

where $3\gamma - 3 = 1.2$ approximately.

Formula (8) shows that a gas-filled bubble in a rapidly compressed medium may be heated to many times its original (absolute) temperature. It has recently been shown that this is an important factor in the initiation of explosions¹⁰.

4. Transient cavities behind missiles. The transient cavity formed when a missile enters the water can be treated approximately, by methods similar to those already used in Ch. X, §6, for treating steady-state underwater cavities¹¹. The approximate predictions agree reasonably well with model experiments involving water entry *in vacuo*; both are invariant under *Froude scaling* (Ch. XV, §8).

To provide a basis for effective approximate calculation, one assumes that the water is constrained to flow between *concentric spheres*, centered at the point of entry. This assumption corresponds fairly well to the observed streamlines¹². This artificial constraint, combined with the assumption that the energy lost by drag over any interval goes into the spherical shell containing that interval, and ideal fluid theory, suffices to determine the motion.

In the case of vertical entry, the maximum angle $\alpha_m(y)$ subtended by the

^{9a} [17, p. 377]; A. B. Arons and D. R. Yennie, *Revs. mod. phys.* 20 (1948), 519-36.

¹⁰ F. P. Bowden and A. D. Yoffe, *The initiation and growth of explosions in liquids and solids*, Cambridge Univ. Press, 1952, Ch. III.

¹¹ The discussion of §4 summarizes part of Navord Report 1490 (1951), by G. Birkhoff and R. Isaacs.

¹² See the photographs in G. Birkhoff and T. E. Caywood, *J. appl. phys.* 20 (1949), 646-59.

TABLE I

Y	10	14	18	22	26	30
$W_m(Y)$	3.78	2.96	2.52	2.26	1.93	1.76
W_m/W_p	.94	.97	1.04	1.15	1.18	1.30

cavity at depth y , satisfies the relation

$$(9a) \quad \cos \alpha_m(y) = 1 - D(y)/2\pi\rho gy^5,$$

where $D(y)$ is the missile drag at depth y . In dimensionless form, setting $Y = y/d =$ depth in missile diameters, and $F(Y) = v^2(Y)/g d$, where $v(Y)$ is the missile velocity after Y diameters of travel, we get the approximate formula

$$(9b) \quad W^2 = C_D F(Y)/2Y,$$

where Wd is the maximum cavity diameter. Table I compares predicted values W_p of W with values W_m measured by Gilbarg and Anderson [31], at $F(0) = 1986$ and $\frac{1}{37}$ atmospheric pressure. The time of collapse was also predicted rather well.

In the case of missiles entering water from the air, the phenomenon of "surface seal" discussed in Chap. XV, §8, may produce much larger disagreements with observation. In the case of oblique entry, the hydrostatic buoyancy of the cavity causes a further discrepancy.

5. Bubble migration; laws of Bjerknes. Actually, underwater explosion bubbles (and other pulsating bubbles) *migrate*, under the influence of gravity, fixed walls, and the free surface. We shall now show that the tendency is to migrate *towards* a *fixed* boundary (ship hull or sea bottom), and *away* from the horizontal *free* surface. For the effect of gravity on bubbles, see Ch. XV, §9.

It is well known [61, §8.41, §13.31] that the effect of a rigid plane wall on a source is exactly the same as that of an equal "image" source (Fig. 2a) symmetrically situated with respect to the plane. That of a plane free boundary is approximately the same as that of an image sink (Fig. 2b). For, an image sink makes $U = 0$ on the plane boundary; since $\partial U/\partial t = 0$ and $\nabla U \nabla U = O(1/R^4)$ there, this implies small variations in the pressure.

But now, it was shown long ago^{12a}, by C. A. Bjerknes, that spheres pulsating in phase attract each other, while spheres pulsating 180° out of phase repel each other. This fact proves the laws stated above; we shall now derive them in another way.

^{12a} In 1868; a full publication was made by V. Bjerknes, "Hydrodynamische Fernkräfte", Leipzig, 1900 (2 vols.); see vol. 1 p. 285. For applications to underwater explosions, see [17, pp. 312-52].

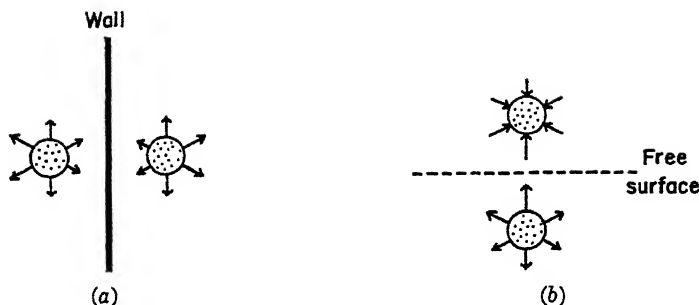


FIG. 2.

In the case of a fixed pulsating source (spherical bubble) whose intensity $E(t)$ varies with time, drawing the x -axis through the source and its image, the velocity potential near the source is thus approximately

$$U = -E(t)/r + \epsilon E(t)r \sin \theta \quad [\epsilon = \pm 1/4R^2],$$

where r is the distance from the source (bubble center), R is the distance to the plane boundary, θ denotes latitude, and the sign of ϵ is plus or minus according as the boundary is fixed or free.

We now suppose that the bubble shape is still constrained to be spherical, but that its center is free to migrate. This amounts to writing

$$(10) \quad U = -\frac{E(t)}{r} + \epsilon E(t)r \sin \theta + \frac{B(t) \sin \theta}{2r^2},$$

where $B(t)$ is the dipole moment corresponding to the translation velocity $b(t)$ of the sphere (we neglect the image dipole). Thus, if $a(t)$ is the bubble radius, $E(t) = a^2 \dot{a}$ and $B(t) = a^3 \dot{b}$.

If the bubble is supposed of negligible weight, then the net pressure thrust on it must vanish. But pressure terms which are independent of θ , or which are proportional to $\sin^2 \theta$ or $\cos^2 \theta$ on the surface, have no net effect. Hence writing

$$p + \frac{\rho}{2} \left[\left(\frac{\partial U}{\partial r} \right)^2 + \left(\frac{1}{r} \frac{\partial U}{\partial \theta} \right)^2 \right] + \rho \frac{\partial U}{\partial t} = \text{const.},$$

and substituting from (10), we obtain for the net pressure thrust, the integral of $-\rho$ times

$$\frac{E(t)}{r^2} \left[\epsilon E(t) - \frac{B(t)}{r^2} \right] \sin \theta + [\epsilon \dot{E}r + \dot{B}/2r^2] \sin \theta.$$

This is zero, if and only if

$$(11) \quad \dot{B} = \frac{2BE}{a^2} - 2\epsilon E^2 - 2\epsilon \dot{E}a^3.$$

Over a complete cycle, the integrated effect of E and \dot{E} is zero. Therefore the sign of \dot{B} (and hence B) is the opposite of that of ϵE^2 (and hence ϵ), proving the statements made earlier. Since $b(t) = B(t)/a$, we see moreover that *most of the migration takes place when the radius is small*. If $E(t)$ is known (§3), of course quantitative estimates can be given, but departures from spherical shape and turbulence effects make such theoretical predictions of doubtful reliability.

6. Cavity induced mass. In §§6-10, we shall consider the reaction of an incompressible fluid with free boundaries to the sudden acceleration of a solid in contact with it. Thus we shall extend the classic concept of "induced mass" ([4, Ch. V], [50, §93, Ch. VI], [61, pp. 235, 419]), or "apparent inertia" to this case; see also §10.

To fix ideas, let first $\phi(\mathbf{x})$ be the velocity potential of an ideal "cavity flow" past a stationary rigid body, so that $\nabla^2\phi = 0$. The degenerate case $\phi(\mathbf{x}) = 0$ is included. Let the body be given a sudden acceleration a at time $t = 0$, in the direction (say) of the x -axis. Then, by general principles of theoretical fluid mechanics, the velocity potential for small $t > 0$ will have the form

$$(12) \quad U(\mathbf{x}; t) = \phi(\mathbf{x}) + at A(\mathbf{x}) + \dots, \quad \nabla^2 A = 0.$$

We shall refer to A as the "acceleration potential" for unit acceleration; we shall now reduce its determination to a "mixed" boundary value problem in potential theory.

By hypothesis, $\partial U/\partial n = at \partial x/\partial n$ on the rigid body, while $p = \text{const.}$ on the free boundary. Since the displacement of the rigid body is $O(t^2)$, we will have there

$$\partial U/\partial n = \partial\phi/\partial n + at \partial A/\partial n + \dots = 0 + at \partial x/\partial n + \dots.$$

Hence, at $t = 0$,

$$(13a) \quad \partial A/\partial n = \partial x/\partial n \quad \text{on the rigid body.}$$

We now invoke the Bernoulli equation for the pressure p in accelerated ideal flow. This is [50, p. 19] equivalent to

$$(14) \quad C(t) - p/\rho = \frac{1}{2}\nabla U \cdot \nabla U + \partial U/\partial t = \frac{1}{2}\nabla\phi \cdot \nabla\phi + aA$$

at $t = 0$. But on the free boundary, $\nabla\phi \cdot \nabla\phi = \text{const.}$ by hypothesis. Substituting in (14), and subtracting a meaningless constant from A , we get

$$(13b) \quad A = 0 \quad \text{on the free boundary.}$$

It is well known [44, p. 214] that conditions (13a), (13b), and $\nabla^2 A = 0$ uniquely determine A .

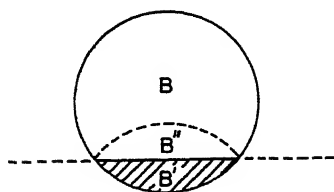


FIG. 3.

It is noteworthy that the conditions determining $A(\mathbf{x})$ are independent of ϕ , and would also be unaffected by the presence of a harmonic gravitational potential $G(\mathbf{x})$. They depend only on the geometry of the free and fixed boundaries, and on the direction of (translational) acceleration.

The simplest and most important case concerns the vertical acceleration of a *floating body* (see Fig. 3) in still water. In this case, S can be taken as $x = 0$, and (13b) gives

$$(15) \quad A(-x, y, z) = -A(x, y, z),$$

by the reflection principle (method of images). Hence A is the velocity potential of steady flow about a new body B^* , consisting of the submerged portion B' of B and its mirror image B'' (see Fig. 3). In the special case of half-submerged spheres and ellipsoids, one thus gets half the ordinary flow about the same body. In the case of a circular cylinder or sphere less than half-submerged, $A(\mathbf{x})$ is the same as for flow around a lens-shaped obstacle; a wedge gives the flow around a rhombus. These cases have been treated in the literature¹³.

Another interesting case is that of a plate in a cavity (Ch. II, §2); this case has been recently treated by M. I. Gurevich¹⁴.

By (14), the net fluid reaction is

$$(16) \quad \mathbf{F} = -\rho a \int A d\mathbf{S},$$

where the vector differential $d\mathbf{S}$ has magnitude equal to the surface area dS , and points along the inward normal to the rigid body. The magnitude m' of $\rho \int A d\mathbf{S}$ may be called the *cavity induced mass*; $\frac{1}{2}m'(at)^2$ is the kinetic energy of acceleration, and it is known¹⁵ that the velocity field induced

¹³ H. Wagner, *ZaMM* 12 (1932), 193–215; W. A. Monaghan, R.A.E. Tech. Note Aero. 1989 (1949); M. Shiffman and D. C. Spencer, *Quar. appl. math.* 5 (1947), 270–88; L. E. Payne, *Quar. appl. math.* 10 (1952), 197–204. The flow around a lens was first determined by Mehler, *J. fur Math.* 68 (1868), 134–50.

¹⁴ *Prikl. mat. mekh.* 16 (1952), 116–118.

¹⁵ G. Birkhoff, *Quar. appl. math.* 10 (1952), 81–6. For the variation of drag coefficients with relative density σ , see [4, p. 164], where σ should be replaced by σ^{-1} to conform to our notation, and A. May, *J. appl. phys.* 21 (1950), 1285–9.

minimizes this. Generally speaking, the cavity induced mass m' defined above seems to be 50%-80% of the ordinary induced mass.

Though $m'v^2/2$ does not express the total kinetic energy of cavity motion (which is infinite), one can use the concept of cavity induced mass (with some caution¹⁵) to explain the observed variation in the apparent C_D of spheres with the ratio $\sigma = (\text{sphere density})/(\text{fluid density})$. May¹⁵ found, approximately, $C_D(\sigma) = 0.28/(1 + .13\sigma^{-1})$, which corresponds to a cavity induced mass equal to about 25% of the ordinary induced mass.

Cavitation zone. In the preceding analysis, it was assumed that the cavitation zone underwent no sudden change. However, in the limiting case of an *impulsive velocity* change, it is well known experimentally that this is not true. If one assumes that the cavitation zone has constant pressure, equal to the pressure at infinity, one gets a more difficult variant to the problem just treated. In general, by (14), the minimum pressure occurs on the boundary¹⁶ in irrotational flow; hence the problem is to determine the extent of the cavitation zone.

This interesting problem was apparently first proposed by Riabouchinsky¹⁷ in 1926-7; it has been solved by Riabouchinsky and Demtchenko¹⁷ for the case of a rigid circular cylinder in a large cylindrical mass of water, and by Sedov¹⁷, for the case of a half-submerged elliptic cylinder.

7. Globule acceleration. Next, consider the initial motion of a liquid globule of density ρ , caused by the sudden acceleration from rest of a surrounding liquid of density ρ' , or by the sudden imposition of a uniform gravity field \mathbf{g} . Letting A and A' denote the acceleration potentials of the two liquids, evidently $\nabla^2 A = \nabla^2 A' = 0$. On the interface S separating the fluids,

$$(17a) \quad \partial A / \partial n = \partial A' / \partial n \quad \text{and} \quad \oint (\partial A / \partial n) dS = 0,$$

by conservation of volume. Also, by (14) with $\phi = 0$

$$(17b) \quad \rho A = \rho' A',$$

because of pressure continuity across S . If \mathbf{g} is the sudden acceleration, we also have $\lim_{x \rightarrow \infty} \nabla A(\mathbf{x}) = \mathbf{g}$.

The limiting cases $\rho = \infty$ (rigid immovable globule) and $\rho = 0$ are espe-

¹⁶ G. Kirchhoff, "Vorlesungen über Mechanik", 1876, p. 186; G. Bouligand, J. de math. 6 (1927), p. 427; [4, p. 61].

¹⁷ D. Riabouchinsky, Comptes rendus 182 (1926), p. 1327, and 184 (1927), p. 584. See B. Demtchenko [19, Ch. IV], and L. I. Sedov, CAHI Rep. 187 (1954), translated by L. Trilling; E. L. Bloh, Prikl. mat. mekh. 17 (1953), 579-92.

cially interesting; the latter corresponds to a conductor in a uniform field. In general, conditions (17a)–(17b) define a boundary value problem in potential theory which arose first in Poisson's theory of magnetic polarization (induced magnetism), in Faraday's theory of electrostatic induction, in electrical and thermal conduction, and in seepage theory¹⁸. Clearly, the combined "polarization potential" $A - \sum g_k x_k$, $A' - \sum g_k x_k$ is defined over all space, is harmonic except on S , where $\partial A / \partial n = \partial A' / \partial n$, and is regular at infinity. Hence [44, p. 286] it is the potential of a double layer of density $\psi(y)$ on S . Further, if $\lambda = (\rho - \rho') / (\rho + \rho')$, then $\psi(y)$ is the solution of the Fredholm integral equation,

$$(18) \quad \psi(y) - \lambda \int_S K(y; n) \psi(n) dS = \sum g_k y_k$$

on S . Here g is the acceleration at infinity, and $K(y; n)$ is the integral kernel $\partial(|y - n|) / \partial n$ of potential theory.

However, very few specific cases have been treated. Poisson¹⁹ proved in 1828 that $\nabla A = c$ was constant for ellipsoids. This is equivalent to the statement that the initial acceleration of any sphere or ellipsoid was rigid. Thus, for a spherical globule, we have

$$(19) \quad A' = kx + k'' x/r^3, \quad A = k'x.$$

In 1931–2, Dive and Niklibore¹⁹ proved that no non-ellipsoidal globules had this "rigidity property".

An interesting related "free boundary" problem, also involving (17a)–(17b), concerns the impulsive acceleration of a vapor-filled cavity in a liquid otherwise at rest. In this case, it is no longer assumed that the globule volume is constant, and the problem is equivalent mathematically to the "conductor problem" of electrostatics.

Finally, one can consider cases involving both a free and a fixed boundary. For example, the cases of a hemisphere and a cylinder, resting on a fixed horizontal plane, have been treated by Penney and Thornhill²⁰.

8. Impact forces. Although initial acceleration fields and impulsive velocity fields, like those studied in §§6–7, are more tractable mathematically, practical applications usually involve flows changing over an appreciable interval of time. Cases in point concern the *impact forces* acting on seaplane floats and air-launched torpedoes as they strike the water, and

¹⁸ See É. Picard, *Rend. cir. mat. Palermo* 22 (1906), 241–59; G. Birkhoff, "Induced potentials", *Studies in Mathematics and Mechanics Presented to Richard von Mises*, Academic Press, (1954), 88–96, where various general results are given.

¹⁹ S. D. Poisson, *Mem. de l'Institut* (1824); Dive, *Comptes rendus* 192 (1931), 1443–1446 and 193 (1931), 141–2; Niklibore, *Math. Zeits.* 35 (1932), 625–31.

²⁰ *Phil. Trans. A244* (1952), 231–334.

the so-called "slamming" of ships. Useful estimates of these impact forces, as functions of time, can be made by applying the ideas of §6.

For instance, following von Karman²¹, one can assume that, for *vertical* impact, the flow is nearly that induced (as in §6) by a flat plate having the same vertical velocity v and instantaneous waterline cross-section S . From this, the total momentum²² transmitted to the water can be calculated. Since the tangential stress components are finite, the impulse transmitted by stresses across any vertical surface is horizontal. The convection (at impact) is negligible. Hence the momentum transmitted equals the momentum of any vertical cylinder of water containing the wetted cross-section. In the two-dimensional case, this is [50, p. 85, (11)]

$$(19a) \quad \pi \rho b^2 v / 2,$$

where $2b$ is the waterline diameter. In the axially symmetric case, S is a disc of radius $a = a(t)$, and the momentum is [50, p. 139]

$$(19b) \quad 4\rho a^3 v / 3.$$

Differentiating, we see that the force is nearly $4\rho v a^2 \dot{a}$, and roughly proportional to \sqrt{t} initially in the case $a \propto t^{1/2}$ of a missile of finite vertex curvature.

H. Wagner²³ studied vertical impact further, estimating the "surface rise" correction which must be made because the wetted area exceeds the waterline cross-section. By considering the acceleration potential A , he also obtained the surprising result that the *pressure is a minimum at the center*, where the stagnation point is located.

The oblique impact of blunt objects has been studied by Sedov¹⁷ and Trilling²⁴. The mathematical approximations involved are much more doubtful in this case.

In all cases, the preceding theoretical analysis neglects compressibility (which limits the peak pressure to ρcv , where c is the velocity of sound in the liquid), and the non-rigidity of the impinging object, which may be important. However, available experimental data²⁵ confirm the theoretical predictions to within $\pm 20\%$ for most of the first quarter-diameter of entry.

²¹ NACA TR321 (1929). See also M. Shiffman and D. C. Spencer, AMP-NYU Repts. 1-2; and V. G. Szebehely, DTMB Rep. 823 (1952), which includes a bibliography of 34 items.

²² A comparison with energy calculations indicates that, in the case of a horizontal plate, about half the energy goes into sound (the impact slap). For the convergence of the momentum integral, see [4, p. 158].

²³ ZAMM 12 (1932), 193-215; (NACA Translation 1366); see also C. Schmieden, ZAMM 33 (1953), 147-51. There is also a "penetration correction", given by the methods of §6.

²⁴ J. appl. phys. 21 (1950), 161-170.

²⁵ S. Watanabe, Sci. Papers Inst. Phys. Chem. Res. Tokyo 12 (1930), 251-67; E. G. Richardson, Proc. phys. soc. 61 (1948), 352-67; E. V. Hobbs, H. I. Breakstone, and J. B. Woodson, Nat. bur. stand. rep. 2788 (1954).

9. Impact of cones and wedges. The vertical impact of a cone on a horizontal free surface gives an especially elegant boundary value problem in potential theory, if viscosity, gravity, compressibility, and surface tension are neglected. Owing to the similitude involved [4, Ch. IV, §8], one looks for a velocity potential of the form

$$(20) \quad U(\mathbf{x}, t) = t\phi(\mathbf{x}/t) = t\phi(\mathbf{y}),$$

yielding a flow *similar to itself at all times* $t > 0$, where 0 is the instant of impact.

This self-similarity was first introduced by Wagner²⁵ who showed that (for right circular cones and wedges) arc-length along the water surface from the cone to any given particle is constant in time²⁶. To get the complete flow, an integral equation of the form

$$(20^*) \quad \phi(y) = \int [\phi(\eta) dK(y; \eta) + L(y, \eta)(\partial\phi/\partial n) ds]$$

must be solved on an unknown boundary. An approximate numerical solution has been given by Shiffman, Spencer and Hillman²⁶.

The oblique impact of a plate or wedge also leads to a velocity potential of the form (20), and to integral equations for $\phi(\mathbf{y})$ involving the location of an unknown free surface²⁷.

The variation of the impact force F with time is especially important. Simple dimensional arguments show that $F = kt^2$ in the case of cones (and $F = kt$ for wedges). Due to instrumental and other difficulties, early experiments²⁸ did not verify this law, and should not be relied on.

10. Constant acceleration coefficient. Another class of unsteady, self-similar ideal flows with free boundaries was discovered by von Kármán²⁹. These flows are defined by potentials of the form

$$(21) \quad U = \phi(\mathbf{x})/ht, \quad V = \psi(\mathbf{x})/ht.$$

²⁵ See M. Shiffman and D. C. Spencer, *Comm. pure appl. math.* 4 (1951), 379-418, formulas (1.1.3), (1.1.10) and (1.2.25).

²⁶ E. P. Cooper, *Navord Report* 1154 (N.O.T.S.); P. R. Garabedian, *Comm. pure appl. math.* 6 (1953), 157-165.

²⁷ S. Watanabe, *Sci. Papers Inst. Phys. Chem. Research Tokyo* 12 (1930), 251-267, and 14 (1930), 157-68; R. L. Kreps (wedge impact), *CAHI Rep.* 438 (1939), translated as *NACA Tech. Mem.* 1046 (1933). For recent measurements, see A. E. McPherson, H. L. Byers, and E. V. Hobbs, *Bu. Standards Ref. PR2, Lab. No. 6.4/1-196*, *NAONR* 8-48.

²⁹ *Annali di mat.* 29 (1949), 247-49; D. Gilbarg, *Zeits. ang. math. phys.* 3 (1952), 34-42. In [4, §14], it is shown that $U = f(t)\phi(x)$ implies (21); see also Gilbarg's formula (12). See further H. S. Tan, *Quar. appl. math.* 12 (1954), 78-80; L. C. Woods, *Appl. mech. revs.* 1041 (1955).

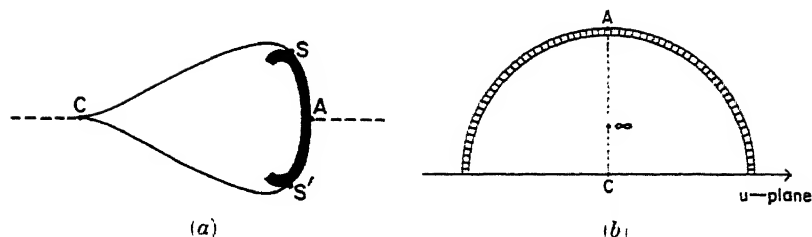


FIG. 4.

Thus the acceleration $a(t) = dv'/dt$ is proportional to $1/t^2$, and the dimensionless *acceleration coefficient* al/v^2 (or deceleration coefficient $-al/v^2$) is constant. Substituting in the Bernoulli equation (14) for unsteady flow, we get

$$(22) \quad \nabla\phi \cdot \nabla\phi - 2h\phi = \text{const.}, \quad \text{on the free boundary.}$$

The limiting case $h \rightarrow 0$ corresponds to steady flow.

We shall treat analytically the case of a symmetric plane flow with cusped cavity (Fig. 4a). Any such flow can be mapped conformally onto the interior of the unit semicircle Γ in an auxiliary u -plane (Fig. 4b), so that the wetted barrier SAS' falls on the semicircle $u = e^{i\sigma}$, and the free boundary SCS' on the diameter. By symmetry, the point $z = \infty$ will fall on $u = i\beta$, where $0 < \beta < 1$.

Setting $W = U + iV = w(z)/ht$, then as in Ch. VI, §10, (26), the reduced complex potential $w(z)$ will be given by

$$(23) \quad w = m/(T^2 + B^2),$$

where

$$(23') \quad B = (\beta^{-1} - \beta)/2 \quad \text{and} \quad T = -(u + u^{-1})/2.$$

On the free boundary, $S'CS$, $w = \phi$ is real, and so by (22), letting $\zeta = dw/dz$ be the reduced velocity,

$$(24) \quad |\zeta|^2 = |\zeta^2| = \frac{2mh}{T^2 + B^2} + \text{const.} = c^2 \frac{T^2 + K^2}{T^2 + B^2}.$$

In (24), all terms are real; $c = |\zeta|$ at C since $T = \infty$ there; and $K^2 > -1$ since $S'CS$ contains no stagnation point. Now write $iK = T_1 = -(u_1 + u_1^{-1})/2$; clearly $u_1 = i\gamma$ with $0 < \gamma < 1$ if $K^2 < 0$, while $u_1 = e^{i\sigma}$ with $0 < \sigma < \pi$ if $-1 \leq K^2 \leq 0$. Moreover, since $T \pm T_j = u^{-1}(u \pm u_j)$ ($u \pm u_j^{-1}$) in (23'), formula (24) implies

$$(24^*) \quad |\zeta|^2 = c^2 \left| \frac{(u + u_1)(u - u_1)(u + u_1^{-1})(u - u_1^{-1})}{(u + i\beta)(u - i\beta)(u - i\beta^{-1})(u + i\beta^{-1})} \right|.$$

Hence, since $(u + u_j)(u - u_j^{-1})$ and $(u - u_j)(u + u_j^{-1})$ are conjugate complex numbers for u real (either when $u_j = i\beta$, $u_j = i\gamma$, or $u_j = e^{i\sigma}$) having the same absolute value, we conclude

$$(24^{**}) \quad |\zeta| = c \left| \frac{(u + u_1)(u - u_1^{-1})}{(u + i\beta)(u + i\beta^{-1})} \right| \quad \text{on} \quad S'CS.$$

In the case of a *flat plate* treated by von Karman and Gilbarg²⁹, ζ is imaginary on $SA'S'$. In this case, the function

$$f(u) = \frac{\zeta(u + i\beta)(u + i\beta^{-1})}{c(u + u_1)(u - u_1^{-1})} = \frac{\zeta[(u - u^{-1}) + i(\beta + \beta^{-1})]}{c[(u - u^{-1}) + (u_1 - u_1^{-1})]}$$

is regular in Γ , has its only zero at $u = i$, is purely imaginary on $u = e^{i\sigma}$, and has modulus one on the real axis. Such a function is $(u - i)/(u + i)$; hence

$$(25) \quad \zeta = c \frac{(u - i)(u + u_1)(u - u_1^{-1})}{(u + i)(u + i\beta)(u + i\beta^{-1})}$$

determines, with (23), an accelerated flow past a flat plate, for any β and γ satisfying the inequalities prescribed above.

Conversely, by analytic reflection in the unit circle (making $\zeta(u^{*-1}) = -\zeta^*(u)$) and the real axis, any $f(u)$ having the above properties can be extended to a function analytic in the whole u -plane, having a zero at $u = i$ and a pole at $u = -i$, and no other zeros or poles. It follows that $f(u) = \pm(u - i)/(u + i)$, so that (25) and (23) define the *only* flows of the type postulated.

Von Karman has shown²⁹ that there is just one case for which $z(C)$ and $z(A)$ have the same imaginary part. However, in view of the discussion of Ch. V, §14, and Ch. VI, §10, one can anticipate that there will be more free parameters in the case of a solid curved obstacle. Hence the physical significance of von Karman's result is uncertain. Actually, the general case of a curved barrier can be treated by the methods of Ch. VI, using (24*) to reflect in the *free* boundary; we omit the details.

Flows of the type postulated may help explain the peculiarities of the virtual mass of an accelerated plate³⁰. However, it is not clear how to generate them physically, nor whether a cusped wake or cavity can ever be stable.

Actually, it is not clear whether a surface of discontinuity can ever be generated in an ideal fluid, initially at rest; this question has been the subject of a long controversy³¹.

²⁹ J. Luneau, *Comptes rendus* 227 (1948), 823-5, and 229 (1949), 927-8.

³¹ J. Hadamard, "Leçons sur la propagation des ondes", Note II, pp. 355-61; F. Klein, *Zeits. Math. Phys.* 58 (1910), 259-62; G. Jaffé, *Phys. Zeits.* 21 (1920), 541-3; L. Anton, *Ing. Archiv* 10 (1939), 411-27.

11. Stability of plane interface. The instability of surfaces of velocity-discontinuity was mentioned in Ch. I, §7, as the main reason why the theory of Chs. II–X cannot be applied to real wakes. We shall now give a first quantitative analysis of this instability; see also Ch. XV, §§10–12.

The simplest case concerns a single plane interface $y = 0$, in a vertical gravity field³² of intensity g , separating two fluids of densities ρ and ρ' . Suppose these fluids have tangential velocities u, u' , and a constant normal acceleration a towards the fluid of density ρ . Relative to axes moving with horizontal velocity $(\rho u + \rho' u')/(\rho + \rho')$, and vertical velocity at , the velocities u, u' will be parallel to the x -axis and satisfy $\rho u + \rho' u' = 0$. Relative to these axes, consider infinitesimal sinusoidal perturbations

$$(26) \quad y = b(t) \sin kx = \eta(x, t)$$

of the interface. Neglecting viscosity, the pressure p will satisfy the Bernoulli equation for non-stationary motion in a gravity field. This equation is, in an accelerated frame moving down with velocity at ,

$$(27) \quad p + \rho(\frac{1}{2} \nabla U \nabla U + \partial U / \partial t + gy - ay) = C(t),$$

in the domain $y > \eta(x, t)$ occupied by the lower fluid of density ρ , and a similar equation involving p', ρ', U' in the upper fluid.

If the interfacial tension is $\gamma \geq 0$, then the pressure condition across the interface is

$$(27a) \quad p - p' = \gamma \partial^2 \eta / \partial x^2.$$

Under the usual perturbation approximations³³, Euler's equations of motion and the interface condition (27a) are equivalent to the ordinary differential equation

$$(28) \quad d^2 b / dt^2 = S(k)b,$$

where

$$(28') \quad S(k) = \frac{\rho \rho' k^2}{(\rho + \rho')^2} (u' - u)^2 + \frac{\rho - \rho'}{\rho + \rho'} (a - g)k - \frac{\gamma k^3}{(\rho + \rho')}.$$

The case $\rho' = 0, a = 0, g > 0$, so that $S(k) = -gk$ and $b(t) = \text{Re}\{C \exp i\sqrt{gk}t\}$, gives the classic theory of gravity waves in an ocean of infinite depth with no wind. We shall make no attempt to summarize the immense literature dealing with this neutrally *stable* case (cf. [50, Ch. IX]).

Instead, we shall discuss some types of *instability* which are most easily explained using formulas (28)–(28'). Our discussion will rely on the classic

³² Such a field is equivalent to a vertical acceleration $-g$, and causes no extra mathematical complication.

³³ See [50, §§232, 234, 268], and refs. given there; the final formula is [50, p. 462, (2)]. The mathematical theory was developed in 1871 by Kelvin [45, pp. 76–100].

principle—whose proof rests on Fourier analysis³⁴—that the condition for *instability* is

$$(29) \quad S(k) > 0 \quad \text{for some } k > 0.$$

The following conclusions are then immediate.

I. The relative tangential velocity $|u' - u|$ is always a *destabilizing* influence. Instability due primarily to this cause may be called *Helmholtz instability*³⁵.

II. Acceleration from the denser towards the lighter fluid exerts a stabilizing tendency; *acceleration from a light towards a dense fluid is destabilizing*. Instability due primarily to this cause may be called Taylor instability³⁶.

III. Surface tension exerts a stabilizing tendency on the shorter ripples, and stabilizes sufficiently short ripples, thus keeping the interface from getting too irregular³⁷.

In fact, if surface tension is neglected, then $S(k)$ is unbounded for both Helmholtz and Taylor instability. It follows³⁴ that the perturbation problem is not “well set” mathematically, in the classic sense (Hadamard) that the perturbation differential equations simply have no solution for a general initial perturbation.

12. Taylor instability. In the case $u = u'$ of pure Taylor instability, viscosity is really negligible in the initial stages. This makes the theory of real Taylor instability simpler than that of Helmholtz instability. Hence we discuss it first, even though the latter is better known and probably more important.

Taylor's theory was originated to explain the instability of underwater explosion bubbles (§3) when near their minimum radius (see §13). Earlier, Riabouchinsky³⁸ had given the stability criterion that a bubble would be stable if its internal pressure was less than atmospheric pressure, and unstable otherwise. Taylor gave, instead, the related criterion II of §11.

The quantitative analysis goes as follows. By (28)–(28'), we have a continuum of unstable eigenperturbations, each of which has its own rate of

³⁴ G. Birkhoff, J. soc. ind. appl. math. 2 (1954), 57–67.

³⁵ Because its importance was first stressed by Helmholtz [35] in 1868. See also Scott Russell, Trans. Roy. Soc. Edinburgh (1840), ref. in [45, p. 282].

³⁶ Because the first clear formulation of this principle was due to Sir Geoffrey Taylor [80], who also inspired its experimental confirmation by Lewis [56]. See also fnt. 38. An exhaustive study of Taylor instability has been made by G. Birkhoff in Reports LA-1862 and LA-1927 of the Los Alamos Scientific Labs.

³⁷ R. Bellman and R. S. Pennington, Quar. appl. math. 12 (1954), 151–62.

³⁸ Comptes rendus 184 (1927), p. 583, and third int. congr. appl. mech., Stockholm (1930), vol. 1, p. 149. See also B. Demtchenko, Comptes rendus 184 (1927), p. 1314.

exponential growth $\sqrt{S(k)}$. The wave-length $\lambda_m = 2\pi/k_m$ giving the biggest $S(k)$ will clearly have the most rapid growth; we call it the "most unstable" wave-length. With pure Taylor instability, since $u = u'$, $k_m^2 = (\rho - \rho')(a - g)/3\gamma$, by (28'). For example, if $a = 50g$ and $\rho' \ll \rho = 1$ as in Lewis' experiments with air and water, $k_m \simeq 14$ and $\lambda_m \simeq 0.45$ cm. In general, the most rapid rate of growth will be

$$\sqrt{S(k_m)} = \frac{2(\rho - \rho')^{\frac{1}{2}} (a - g)^{\frac{1}{2}}}{3\sqrt{3}(\rho + \rho') \gamma^{\frac{1}{2}}}.$$

After a time long enough to permit random initial perturbations to amplify 1000-fold, the interface may be expected to become irregular, and the approximations used to derive (28)-(28') are no longer valid. If $\rho \ll \rho'$, and the initial perturbation is sinusoidal with wave-length $\lambda = 2\pi/k$, then round-ended bubbles of the lighter fluid penetrate the heavier fluid as in Ch. X, §11, with nearly constant velocity of the order of $\sqrt{g\lambda}$. The heavy fluid in the interstices hardly moves. These predictions of Taylor have been verified by Lewis [56] in the case of an air-water interface. The case of two liquids or gases of comparable density is harder to treat experimentally, as it involves Helmholtz instability sooner; it is more symmetrical between the two fluids.

At the end of §11, we observed that the linearized interface instability problem was not "well set" if surface tension was neglected, for either Helmholtz or Taylor instability. It is an interesting open question whether or not the exact *non*-linear theory gives rise to a well set boundary value problem.

13. Spherical and cylindrical bubbles. Taylor instability of spherical and cylindrical cavities can be investigated by methods similar to those of §11. If $b(t)$ is the radius of a spherical cavity as a function of time, then perturbations of the interface expressed in terms of Legendre polynomials $P_h(\cos \phi)$ have amplitudes $b_h(t)$ which, if the surface tension γ is negligible, satisfy³⁹

$$(30) \quad b \ddot{b}_h + 3\dot{b}\dot{b}_h - (h-1)\dot{b} b_h = 0.$$

In the case of underwater explosions, $b > 0$ near the minimum radius, showing that the spherical form has Taylor instability in the usual sense of II, §11. This leads to a large degradation of bulk energy into turbulent energy.

In the case of small vapor-filled cavities, surface tension is an important stabilizing factor, and $\dot{b} < 0$, so that there is no Taylor instability. Nevertheless, due to negative damping ($\dot{b} < 0$), successive oscillations increase in

³⁹ See [17, p. 311].

amplitude, roughly like b^{-1} . Hence the collapse of cavitation bubbles is also unstable theoretically⁴⁰.

The preceding theoretical discussion ignores many important factors⁴¹, such as the increase in vapor pressure which occurs when $b \ll b_{\max}$, departures from sphericity near walls, viscosity effects, etc. Nevertheless, it seems to give a correct qualitative picture.

Many other problems involving cavity stability can be analyzed similarly. For example, one can analyze the stability of a spherical bubble in a variable pressure field⁴². Or, one can treat the stability of a collapsing cylindrical cavity, by supposing perturbations of the form $r = b(t) + b_h(t) \cos h\theta$, where the $b_h(t)$ are infinitesimal. Instead of (30), one has

$$(30a) \quad b\ddot{b}_h + 2\dot{b}\dot{b}_h - (h-1)\dot{b}b_h = 0.$$

In this case, perturbations grow logarithmically at worst⁴⁰, but of course their *relative* amplitude grows like $1/b$.

Again, one can treat the oscillations of nearly spherical droplets under surface tension by similar methods [50, §275]. And finally, the stability of spheres and ellipsoids under gravity has received very intensive study⁴³, because of astrophysical applications.

14. Helmholtz instability. The instability of the free streamlines of Chs. II–XI can be inferred immediately from (28)–(28'). This can be seen most simply by setting $\rho = \rho'$ (or $a = g$) and $\gamma = 0$. For any fixed wave-number k , in the case $\rho' \ll \rho$ of a gas-liquid interface, the rate of growth will then be proportional to $\sqrt{\rho'/\rho}$. This explains the Betz-Petersohn principle (Ch. I, §4), that free streamline theory is applicable to gas-liquid interfaces. The instability is small, and often overcome by surface tension.

A more sophisticated application is to the generation of ocean waves by wind; this theory was developed in 1871 by Kelvin³³. In this case, $\rho' \ll \rho$. A calculation of the most unstable wave-length shows that [50, §268] the interface should be *stable* for winds whose velocity $u' < 646$ cm/sec. (Both gravity and surface tension are stabilizing influences; if $a = g$, as in a falling

⁴⁰ G. Birkhoff, *Quar. appl. math.* 12 (1954), 306–9; see also A. M. Binnie, *Proc. Camb. phil. soc.* 49 (1953) 151–5. M. S. Plesset and T. P. Mitchell, *Quar. appl. math.* 13 (1956), 419–30; D. Layzer, *Astrophys. J.* 122 (1955), 1–12.

⁴¹ See S. A. Zwick and M. S. Plesset, *J. math. phys. MIT* 33 (1955), 308–30; A. T. Ellis, *Caltech. hydro. lab. rep.*; Ch. XV, §4.

⁴² G. Birkhoff, *Quar. appl. math.* 13 (1955), 451–3; see also M. S. Plesset, *J. appl. phys.* 25 (1954), 96–8.

⁴³ [50, Ch. XII, esp. §376 ff.] The method of Jeans has been challenged by S. Rosse-land, *Norske Vid.-Akad., Oslo, Math-Nat. Klasse*, 1931, No. 7. See also S. Chandrasekhar, *Proc. Camb. phil. soc.* 51 (1955), 52–78, and *QJMAM* 8 (1955), 1–21.

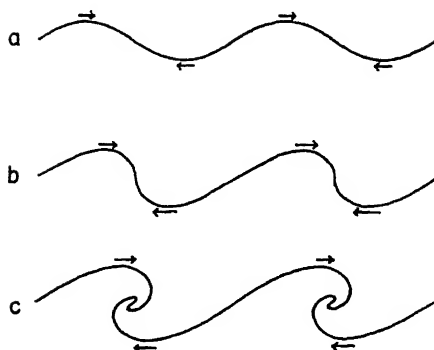


FIG. 5.

elevator, we would always have instability, with $\lambda_m \simeq 3\pi\gamma/\rho'u^2$.) Experimentally⁴⁴, waves form at velocities about 120 cm/sec.

The preceding discrepancy is typical of applications of Helmholtz-Kelvin stability theory to real problems. It has been attributed variously⁴⁴ to viscous effects, to airflow separation near the wave crest (i.e., wake underpressure), and to the turbulence of real winds.

Such applications are also complicated by *non-linear* effects, which occur with steep waves (of "finite amplitude"). Thus, in the case $\rho = \rho'$ of a surface of discontinuity (vortex sheet) separating two fluids of equal density, the vortex sheet tends to "roll up" spirally in a non-symmetric way. Quantitative calculations have been made by Rosenhead⁴⁵, assuming an initially sinusoidal interface; the development of the spirals is sketched in Fig. 5.

15. Stability of capillary jets. Perhaps the most striking application of the technique of §§11–14 is to the stability of capillary jets. This was treated by Rayleigh in a series of classic papers⁴⁶.

Mathematically, Rayleigh idealized such a jet (1 mm.–1 cm. in diameter) as a cylindrical column of radius a . He assumed that the jet disintegration was due to surface tension, and its effect on "varicose" perturbations (i.e., alternate swellings and contractions). Thus, he considered eigenperturbations of the form $r = a + b(t) \sin kx$, as playing the same role as (26)

⁴⁴ See H. Jeffreys, Proc. roy. soc. A107 (1924), 189–205; also [45 p. 85]; W. H. Munk, J. marine research 6 (1947), 203–18. For turbulence effects, see C. Eckart, J. appl. phys. 24 (1953), 1485–94. See also R. Lock, Proc. Camb. phil. soc. 50 (1954), 105–24.

⁴⁵ Proc. roy. soc. A134 (1931), 170–92; [31, p. 30]. New calculations reported in LA-1927 (Los Alamos Scientific Laboratory) suggest modifications in the usual interpretation of Rosenhead's results.

⁴⁶ Proc. Lond. math. soc. 10 (1879), 4–13 and 19 (1887), 67–74; [66, pp. 351–71]. See also Ch. XV, §11.

did in Kelvin's theory. The velocity potentials associated with such perturbations are $U = J_0(kr) \cos kx$ inside the jet, and $U' = K_0(kr) \cos kx$ outside; these replace the $U = e^{ky} \cos kx$ and $U' = e^{-ky} \cos kx$ of Kelvin's calculations.

He showed that such an idealized jet is statically unstable under surface tension γ when its length L exceeds π times its diameter D , and that the "most unstable" wave-length is about $4.5D$. In the case of water, the associated most unstable varicose perturbation will be amplified 1000-fold in time $t = 0.828D^3$. He concluded that the length to break-up should be proportional to the jet velocity. Experimentally, this is observed up to a certain critical speed⁴⁷.

It may be surmised that this is about the speed at which Helmholtz instability becomes more important than surface tension. An exact theoretical prediction of the critical speed would be too much to expect (cf. §14). Thus it is known⁴⁷ that the jet from a *sharp-edged* orifice may have three times the critical speed of one from a hole in a thick plate; other anomalies will be discussed in Ch. XV, §10.

16. Stability of other configurations. Kelvin's technique has been applied to various other configurations involving surfaces of discontinuity.

Thus Rayleigh⁴⁶ applied Kelvin's ideas to explain the flapping of a flag in the wind. A similar technique [50, §232] may be used to analyze the stability of a plane jet of non-viscous fluid, surrounded by a medium of equal density.

Again, Worthington [90] used Rayleigh's model to explain the breakup, into a "crown" of drops, of the splash formed behind a small sphere dropped into water.

The configuration of *non-circular* capillary jets has also been studied by scientists for a long time. The methods are similar to those of §15, and we content ourselves with bibliographical references⁴⁸.

The stability of swirling flow about a cylindrical cavity (of a "hollow columnar vortex") has also been studied by Kelvin⁴⁹. (For the unperturbed flow and its generalizations, see Ch. X, §10.) Kelvin showed that the cavity was neutrally stable, but that corrugations (waves) travelled around it with calculable angular velocity depending on the wave-length. Following

⁴⁷ S. W. J. Smith and H. Moss, Proc. roy. soc. A93 (1917), 373-93; C. Weber, ZAMM 11 (1931), 136-54 [35a, Ch. VI].

⁴⁸ G. Bidone, "Expériences sur la forme . . .", Turin, 1829; [1a]; J. Boussinesq, Mem. acad. sci. Paris 23 (1877), 639-59; Rayleigh, Proc. roy. soc. 29 (1879), 71-97; P. Nemenyi, "Wasserbauliche Strömungslehre", Part VI; Y. Wada, J. phys. soc. Japan 5 (1950), 259-62 and 439-42; J. L. Erickson, J. rat. mech. anal. 1 (1952), 521-38; and J. S. McNown and S. C. Ling, La houille blanche (1955), 775-81.

⁴⁹ Phil. Mag. 10 (1880), 155-68 (or [45, p. 152]); also [50, §§158-9].

Kelvin, Ackeret and Binnie⁵⁰ have proved theoretically the possibility of helical waves, and the possibility of waves having negative group velocity.

Recently, Fox and Morgan⁵¹ have analyzed the stability of various ideal plane flows with free boundaries, under inertial forces alone, with $\rho' = 0$. The following flows were found to be stable: a hollow vortex in a cylinder; the jet from a symmetric funnel (Ch. II, §5), except in the case of a Borda mouthpiece; a jet divided symmetrically by a plate (Ch. III, §5), including Kirchhoff flow in the limit. The case of equal and opposite plane jets, on the other hand, was found to be unstable; this instability may be related to the indeterminacy of impinging jets noted in Ch. III, §4. Experimentally, impinging coaxial *capillary* jets seem to be stable; this was shown by Savart [73a, pp. 257–310].

Impinging coaxial gas jets seem also to be highly stable⁵².

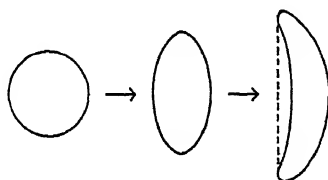


FIG. 6.

The stability of a bubble in an accelerated liquid is more complex; the observed sequence of events is sketched in Fig. 6. Initially, as predicted by (19), the spherical shape is in equilibrium, but the bubble is accelerated 2–3 times as fast as the surrounding liquid. Then, under Helmholtz instability, an equatorial bulge occurs, transverse to the direction of acceleration. Later, the flattened bubble “dishes out” due to unknown causes.

Finally, T. B. Benjamin and F. Ursell⁵³ have made an interesting study of the stability of a horizontal free surface under gravity, when given periodic vertical vibrations.

⁵⁰ J. Ackeret, *Ing. Archiv* 1 (1930), pp. 399–402; A. M. Binnie, *Proc. roy. soc.* A205 (1951), 530–40.

⁵¹ *Quar. appl. math.* 11 (1954), 439–56; this extended a previous analysis by C. M. Ablow and W. D. Hayes, *Tech. rep. on Contract N7onr-35807*, Brown Univ. (1951). Unsteady Kirchhoff “wakes” (cavities) have also been studied by L. C. Woods, *Proc. roy. soc.* A220 (1955), 152–80.

⁵² A. Schaffer and A. B. Cambel, *Jet propulsion* 25 (1955), 284–7.

⁵³ *Proc. roy. soc.* A225 (1954), 505–15. The problem was first considered in 1831 by Faraday (*Phil. trans.*, p. 319).

CHAPTER XII

STEADY VISCOUS WAKES AND JETS

1. Boundary value problem. In Chs. XII–XIV, we shall turn our attention to wakes and jets in *homogeneous* fluids. The theory will be based on the Navier-Stokes equations, and will be almost entirely unrelated to that of Chs. II–XI. In Chs. XII–XIV, a central role will be played by the concepts of viscosity, vorticity, and turbulence, which were ignored in Chs. II–XI. Correspondingly, the concepts of velocity potential and of “free” streamlines (involving discontinuous velocities) will not appear in Chs. XII–XIV.

The reason for this change is, as explained in Ch. I, §7, and in Ch. XI, §§11–14, that Euler’s equations of motion cannot be usefully applied to wakes and jets in homogeneous fluids, but only to cavity flows and liquid jets in gases.

The simplest case, treated in this chapter, is that of steady (i.e., laminar) flow of an incompressible fluid. In this case, the Navier-Stokes equations of motion for the velocity-field $\mathbf{u}(\mathbf{x})$ simplify to¹

$$(1) \quad \rho \sum u_k \partial u_i / \partial x_k = \mu \nabla^2 u_i - \partial p / \partial x_i.$$

In (1), the density ρ and viscosity μ are assumed to be constant—i.e., temperature variations are assumed small. The analysis will be confined to the cases of plane flows and axially symmetric flows. In these cases, the incompressibility condition

$$(2) \quad 0 = \text{Div } \mathbf{u} = \sum \partial u_k / \partial x_k$$

is equivalent to assuming the existence of a *stream function* $V(\mathbf{x})$, satisfying²

$$(2a) \quad \partial V / \partial y = u, \quad \partial V / \partial x = -v \quad \text{in plane flow,}$$

$$(2b) \quad \partial V / \partial r = ru, \quad \partial V / \partial x = -rv \quad \text{with axial symmetry.}$$

In terms of $V(\mathbf{x})$, equations (1)–(2) are equivalent to

$$(3a) \quad \mu \nabla^4 V = \rho \partial(V, \nabla^2 V) / \partial(x, y) \quad \text{in plane flow}$$

[61, p. 536, Ex. 7], and

$$(3b) \quad \mu E^4 V = \rho r \partial(V, r^{-2} E^2 V) / \partial(x, r)$$

¹ [31, p. 96]; [50, p. 577]; [61, p. 509]. The usual equations are simplified since $\partial/\partial t = 0$.

² [50, pp. 63, 126]; [61, pp. 103, 407]. We write $u = u_1$, $v = (u_2^2 + u_3^2)^{1/2}$.

in axially symmetric flow [61, p. 523]. In (2b)–(3b), cylindrical coordinates x, r are used, $\partial(f, g)/\partial(x, r)$ denotes the Jacobian $(\partial f/\partial x)(\partial g/\partial r) - (\partial f/\partial r)(\partial g/\partial x)$, and $E^2 = \partial^2/\partial x^2 + \partial^2/\partial r^2 - r^{-1}\partial/\partial r$.

The differential equations (3a)–(3b) must be supplemented by the boundary conditions

$$(4) \quad V = \text{const.}, \quad \partial V/\partial n = 0 \quad (\text{or } \nabla V = 0),$$

on solid boundaries. Equations (4) clearly express the conditions of impermeability and no slipping, respectively. Combined with the condition $\mathbf{u}(\infty) = (U, 0, 0)$ at infinity, equations (3a)–(4) and (3b)–(4) define two plausible *boundary value problems* for partial differential equations, whose analytical solution might be considered as our ultimate objective.

2. Critical discussion. Unfortunately, the mathematical boundary value problems just defined seem to be very difficult. Although it is known theoretically that solutions exist³, it has never been proved that the solutions are unique. Hence we do not even know that the problem is mathematically “well set”.

Moreover the problem is certainly not well set physically except at low Reynolds numbers. It is known experimentally that real wakes and jets become unstable above some “critical Reynolds number” R_{crit} , usually in the range $25 < R_{\text{crit}} < 1,000$. For $R > R_{\text{crit}}$, the flow becomes time-dependent (periodic or turbulent), and (3a)–(3b) simply do not apply. This time-dependent behavior is illustrated by Figs. 1a–1f, which give sample⁴ time-exposure photographs of wakes behind circular cylinders, at various Reynolds numbers.

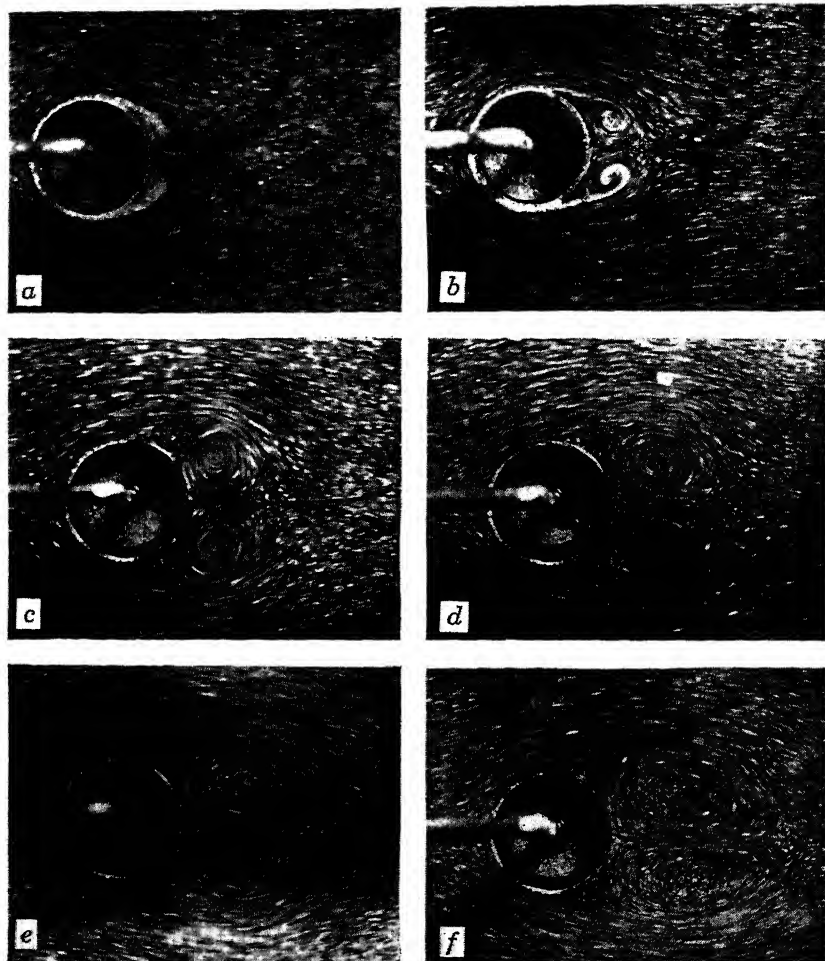
Finally, no special analytical solutions are known of the boundary value problem defined in §1, which describe wakes or jets.⁵ The analytical solutions given below will refer, except to §15, to various *approximations* to the Navier-Stokes equations (1). Among these may be mentioned: the Stokes approximation (§3), the Oseen approximation (§5), and Prandtl’s boundary layer approximation (§8). The first two of these are linear.

In principle, one might hope also to obtain approximate solutions to (3a)–(3b) by numerical methods (cf. Ch. IX). This approach has been ap-

³ J. Leray, J. de math. 12 (1933), 1–82.

⁴ For others, see H. L. Rubach, Gött. Diss. (1914); C. Camichel, Engineering 123 (1927); A. Fage, Proc. roy. soc. A144 (1934), 381–6; F. Homann, Forschung Ingenieur-wensen 7 (1936), 1–10.

⁵ For exact solutions of the Navier-Stokes equations not describing wakes or jets, see A. Rosenblatt, Fasc. 72 Mem. Sci. Math., Gauthier-Villars, 1933; R. Berker, “Sur quelques cas d’intégration . . .”, Paris, 1936; Livre II of H. Villat, “Leçons sur les liquides visqueux”, Paris, 1943.



FIGS. 1a-1f. Wakes behind a circular cylinder, various $R < 50$.
(Courtesy Verein Deutsche Ingenieure)

plied especially to the wake of a circular cylinder⁶. However, it would appear difficult to justify rigorously the methods of computation used, especially as regards flow separation (see §4). Existing calculations also involve somewhat arbitrary assumptions concerning the behavior on nearby walls, which are known (Ch. XIII, §9) to stabilize the flow.

⁶ Bairstow, Cave and Lang, Proc. roy. soc. A100 (1922), 394-413, and Phil. Trans, A223 (1923), 383-42; Southwell and Squire, Phil. Trans. A232 (1933), 27-64; A. Thom, Proc. roy. soc. A141 (1933), 651-69; M. Kawaguti, J. phys. soc. Japan 8 (1953), 747-57. and 9 (1954), p. 303; D. N. de G. Allen and R. V. Southwell, QJMAM 8 (1955), 129-45.

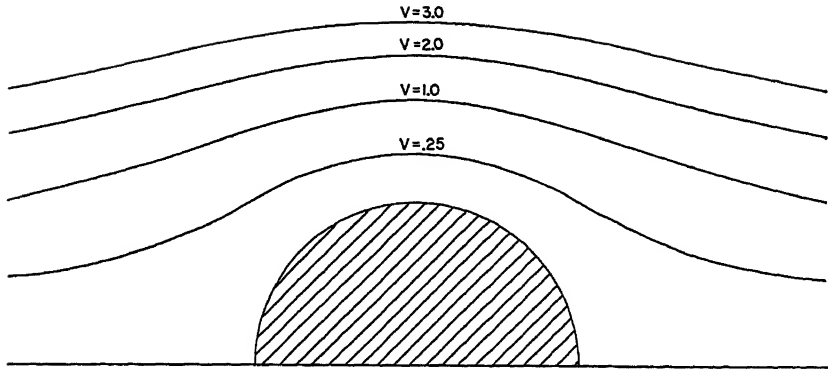


FIG. 2 (a).

3. Wakes in creeping flow. At very low Reynolds numbers⁷ $Re \ll 1$, it is plausible that the right-hand sides of (3a)–(3b) are negligible, because they are quadratic in the velocity. This leads to Stokes' approximate equations for *creeping flow*:

$$(5a) \quad \nabla^4 V = 0,$$

resp.

$$(5b) \quad E^4 V = 0.$$

We first consider the boundary value problems defined by (4), (5a) or (5b), and

$$(6) \quad \lim_{\mathbf{x} \rightarrow \infty} \mathbf{u}(\mathbf{x}) = (U, 0, 0),$$

corresponding to this approximation.

In the *axially symmetric* case, it can be shown⁸ that the problem is "well set". That is, equations (4), (5b) and (6) determine one and only one "creeping flow" past a given axially symmetric obstacle. Further, the flow's theoretical predictions agree extremely well with observation, when $Re \ll 1$.

It is easy to show that the "creeping flow" past any such obstacle having fore-and-aft symmetry, will itself have fore-and-aft symmetry (cf. Fig. 2a and [59, Fig. 3]). This follows because (5b) is invariant under the substitution $V \rightarrow -V$, $p \rightarrow -p$ corresponding to flow reversal. Moreover various

⁷ In the present section, the Reynolds number will be denoted Re , to avoid confusion with the distance R from the origin, in spherical coordinates.

⁸ By analogy with elasticity theory; see K. Schröder, *Math. Zeits.* 48 (1943), 553–675. In Chs. XII–XIV, we use U to denote free stream velocity, instead of a (usually non-existent) velocity potential.

special axially symmetric "creeping flows" can be determined analytically, in closed form.

The most important case is that of a sphere of radius a , solved by Stokes. In spherical coordinates (R, ϕ, θ) , the solution is

$$(7) \quad \Gamma = U(R^2/2 - (3aR/4) + a^3/4R) \sin^2 \phi.$$

(See [50, §§336-8] or [61, §§19.63-4] for derivations.) The radial and angular velocity components are

$$(7a) \quad u_R/U = (1 - (3a/2R) + a^3/2R^3) \cos \phi,$$

$$(7b) \quad u_\phi/U = (3a/4R + a^3/4R^3) \sin \phi.$$

The vorticity $\zeta = (3a/2R^2)U \sin \phi$. The drag D is $6\pi\mu aU$, and drag coefficient $C_D = 24/Re$. The formula for D is accurate to within 5% when $R < 0.3$ [31, pp. 491-3], except that corrections involving the mean free path must be made in a gas.

Exact solutions of Stokes equations have also been given in other cases of physical interest. The case of a liquid sphere falling under gravity [50, p. 600] and of a spheroid [50, §339] should be mentioned. The cases of a sphere in a cylindrical tube⁹, of a sphere in the presence of a plane wall, and of two tandem spheres have also been treated by approximate methods. Thus, it has been shown that a more accurate formula for the drag of a sphere of radius a in a cylindrical tube of radius A is approximately $6\pi\mu a(1 + 2.1(a/A))$, if $Re \ll 1$.

However, Stokes also showed that the analogous boundary value problem for plane "creeping flows", defined by (4), (5a), and (6), has no solution¹⁰. This paradox of Stokes will be resolved in §§5-6, by a more careful consideration of the flow at large radii.

4. Flow separation. But first we shall complete the discussion of wakes near obstacles, by recalling some basic facts about flow separation at low Reynolds numbers.

It has long been known that, in the range^{10a} $5 < R < 30$, the flow separates behind a circular cylinder or other "bluff" (i.e., non-streamlined) obstacle along separating streamlines (see Fig. 1b), which close at a distance behind the obstacle which increases with R . The region bounded by the

⁹ R. Ladenburg, *Ann. der Physik* 23 (1907), 447-58; H. Faxén, *ibid.* 68 (1922), 89-119; J. S. McNown et al., *Proc. seventh int. congr. appl. mech. London* (1948), vol. 2, 17-29.

¹⁰ [50, §343], and H. Lamb, *Phil. Mag.* 21 (1911), 112-21. A very thorough discussion has been given by S. Kneale, *Harvard Doctoral Thesis*, 1952.

^{10a} See Ch. XIII, §9, for a discussion of the various factors influencing the upper limit of this range.

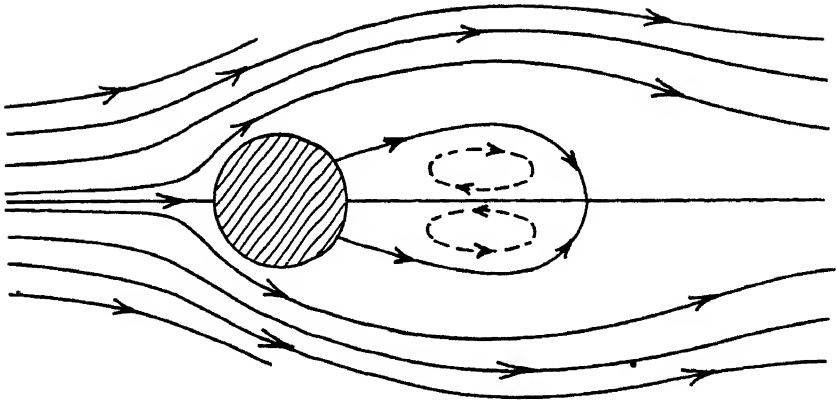


FIG. 2 (b).

separating streamlines is filled with two symmetrically placed eddies, rotating about vortex centers.

By treating these vortex centers as point-vortices, Föppl constructed in 1913 a *potential*-theoretic model for such flows; its streamlines are drawn in Fig. 2b. Because of its mathematical simplicity, its interesting stability theory, and its relation to vortex streets (Ch. XIII), Föppl's model has received considerable attention¹¹. Also, the model gives streamline configurations agreeing well with those observed experimentally.

However, the model is theoretically unsound. In a real fluid, the vorticity at the vortex centers will diffuse outwards, giving a region of slowly varying vorticity instead of point-vortices. Near a vortex center, many velocity fields are compatible with a given streamline configuration, and so agreement between predicted and observed streamlines does not imply agreement between (say) the associated pressure distributions¹¹. (The same remark applies to the vortex streets of Ch. XIII.)

Streamline configurations resembling those due to stable vortex rings have also been observed experimentally behind spheres and discs, at Reynolds numbers as high¹² as $R = 200$.

Finally, recent computations by Tomotika and Aoi¹³, based on the Oseen approximation, indicate that separation may occur behind circular cylinders

¹¹ L. Föppl, S.-B. Bayer. Munich Akad. Wiss., 1913; W. G. Bickley, Proc. roy. soc. A119 (1928), 146-56; W. Müller. Zeits. tech. Physik 8 (1927), 62-8; and Mathematische Strömungslehre, Berlin, 1928, p. 124, where the theoretical base pressure distribution is shown to disagree with observation.

¹² H. Nisi and A. W. Porter, Phil. Mag. 46 (1923), 754-68; T. E. Stanton and D. Marshall, Proc. roy. soc. A130 (1930), 295-301. See Ch. XIII, §11.

¹³ QJMM 3 (1950), 140-61; see also H. Yamada, Math. revs. 15 (1954), p. 837; T. Pearcey and B. McHugh, Phil. Mag. 46 (1955), 783-94.

and spheres even when $R = 0.1$, whereas previous computations had assumed the contrary.

5. Asymptotic wake structure. As observed by Oseen^{13a}, at large distances from an obstacle the "Oseen equation"

$$(8) \quad \rho \mathcal{L} \partial \mathbf{u} / \partial x = \mu \nabla^2 \mathbf{u} - \nabla p$$

will give a better approximation to (1) than (5a)–(5b); the dominant terms of the left side of (1) are included.

The mathematical theory of Oseen's linearized equations is very interesting^{13b}; some applications of it will be made below in §7. Thus, taking the curl of (8), we see that the vorticity $\zeta = \nabla \times \mathbf{u}$ satisfies

$$(8a) \quad \mathcal{L} \partial \zeta / \partial x = \nu \nabla^2 \zeta.$$

Similarly, since $\text{Div } \mathbf{u} = 0$ by (2), (8) implies

$$(8b) \quad \nabla^2 p = \mu \nabla^2 (\text{Div } \mathbf{u}) - \rho U \partial (\text{Div } \mathbf{u}) / \partial x = 0.$$

Since $\nabla U = 0$, equations (8)–(8a)–(8b) will still hold if we change our notation so that $(U + u, v, w) = (U + u_1, u_2, u_3)$ denotes the vector velocity relative to the obstacle, and $\mathbf{u} = (u, v, w)$ the *velocity relative to the free stream*.

The asymptotic wake structure is best inferred by further simplifying (8a) to

$$(8^*) \quad U \partial \zeta / \partial x = \nu [\partial^2 \zeta / \partial y^2 + \partial^2 \zeta / \partial z^2].$$

This simplification can be motivated by observing that $\partial^2 / \partial x^2 \ll \partial / \partial x$ asymptotically, for smoothly decaying quantities; it will be justified in §6 *a posteriori*. Clearly, (8*) is just the *heat equation*, with downstream distance x playing the role of time. We apply the classic Laplace formula¹⁴

$$\zeta(x, y) = \frac{1}{2} \sqrt{\frac{U}{\pi \nu x}} \int_{-\infty}^{\infty} \zeta(0, \eta) e^{-U(y-\eta)^2/4\nu x} d\eta$$

for solutions of (8*). This shows that the vorticity, generated on the surface of the obstacle, is confined to a parabolic or paraboloidal *wake* W behind the obstacle, outside of which the vorticity dies out exponentially. This prediction is confirmed experimentally.

Outside the wake, since the vorticity ζ is negligible, we can set $\partial u_i / \partial x_k = \partial u_k / \partial x_i$ and hence $\nabla^2 u_i = \partial (\text{Div } \mathbf{u}) / \partial x_i = 0$ in (1). From this, the Bernoulli

^{13a} W. Oseen, Arkiv för mat. astr. fys. 6 (1910), No. 29; F. Noether, Zeits. math. phys. 62 (1911), 1–39.

^{13b} W. Oseen "Hydrodynamik", Leipzig, 1927; [50, §§342–343a].

¹⁴ P. Frank and R. von Mises, "Differentialgleichungen der Physik", vol. 2, Ch. XIII, §2.

equation follows (Ch. I, (13)) outside the wake, relative to the obstacle. That is,

$$(9) \quad p \simeq P - \rho U u \quad \text{outside the wake.}$$

Now using (8b), and the asymptotic expansion theory of harmonic functions at infinity [44, p. 269], we deduce

$$(9a) \quad p = P - Cx/r^2 + O(1/r^3) \quad \text{in plane flow,}$$

and

$$(9b) \quad p = P - C'x/r^3 + O(1/r^3) \quad \text{with axial symmetry.}$$

In (9a)–(9b), P is the free stream pressure, and C, C' are appropriate constants. The asymptotic pressure field ("far field") is thus a *dipole* field.

Turning now to $u(\mathbf{x})$, we use (9b) to drop the term $\partial p/\partial x = O(1/r^3)$ in (8), as well as $\partial^2 u/\partial x^2 \ll \partial u/\partial x$. This gives us the heat equation¹⁵ for $u(\mathbf{x})$,

$$(10) \quad U \partial u/\partial x \simeq \nu [\partial^2 u/\partial y^2 + \partial^2 u/\partial z^2].$$

Finally, applying the Laplace formula to (10), one easily deduces

$$(11a) \quad u(x, y) \simeq -Ax^{-1} \exp(-Uy^2/4\nu x),$$

for some constant $-A$. (The sign is for convenience; see (14a).) In space, one can derive from (10) similarly

$$(11b) \quad u(x, r) \simeq -A'x^{-1} \exp(-Ur^2/4\nu x), \quad r^2 = y^2 + z^2.$$

6. Wake momentum. We shall now show that the preceding formulas are self-consistent, and that the paired constants A, C and A', C' in §5 are directly proportional to each other, the wake momentum M , and the drag D . The argument is heuristic (for a more rigorous discussion, see §9).

We first observe that, if V and v are constructed from (11a)–(11b) by equation (2) of continuity, then (1) is satisfied to a first approximation in the wake, in the sense that (10) consists of the dominant terms of (1). Outside the wake, where we have potential flow to a first approximation (§5), the mass-inflow in the wake must be balanced by an equal radial outflow outside the wake.

This conclusion¹⁶ is confirmed by considering the pressure field. In radial outflow, $u = kx/r^2$ in the plane, with mass-outflow $2\pi k\rho$, while $u = kx/r^3$

¹⁵ The idea that (10) dominates asymptotic wake and jet behavior seems due to Rayleigh [66, p. 382]. See also W. Tollmien, *Handb. Exp. Physik*, IV 1 (1931), p. 269. For a discussion based on the complete Oseen equation (8), see [31, §249] and refs. given there.

¹⁶ First exploited by A. Betz, NACA TM 268 (1924) and 337 (1925); see also *Zeits. Flugt. Motorl.* 16 (1925), 42–4.

in space, with mass-outflow $4\pi k\rho$. This agrees with (9a)–(9b), by (9), if and only if the mass-outflow outside the wake is $2\pi C'U$ in the plane, and $4\pi C''U$ in space.

Letting W denote a cross-section of the parabolic or paraboloidal *wake* defined by (11a)–(11b), we now define the *wake momentum per unit length* in the direction of obstacle motion as

$$(12a) \quad M(x) = \rho \int_W -u(x, y) dy \quad \text{in the plane,}$$

$$(12b) \quad M(x) = \rho \iiint_W -u(x, y, z) dy dz \quad \text{in space.}$$

(The integral (12b) corresponds, for example, to the rush of air behind an express train, felt on a station platform.) According to (11a)–(11b), we should have

$$(13a) \quad \lim_{x \rightarrow \infty} M(x) = (4\pi\nu/U)^{\frac{1}{2}} \rho A \quad \text{in the plane,}$$

$$(13b) \quad \lim_{x \rightarrow \infty} M(x) = (4\pi\nu/U) \rho A' \quad \text{in space.}$$

But clearly, (12a)–(12b) also represent the rate of mass-inflow in the wake. Comparing with the preceding paragraph, we deduce

$$(14a) \quad C = \rho(\nu U/\pi)^{\frac{1}{2}} A \quad \text{in the plane,}$$

$$(14b) \quad C' = \mu A' \quad \text{in space.}$$

Finally, we give a heuristic derivation of formulas relating A , C , A' , C' to viscous drag. Relative to an observer stationary with respect to the fluid, forward wake momentum should be created by the obstacle at a rate D per unit time, or at a rate D/U per unit length of wake. Hence we conclude

$$(15a) \quad D = 2\rho A \sqrt{\pi\nu U} = 2\pi C \quad \text{in the plane,}$$

$$(15b) \quad D = 4\pi\mu A' = 4\pi C' \quad \text{in space.}$$

From still another viewpoint, the preceding calculations indicate that streamlines just outside the wake are displaced outwards by a constant distance δ (half the so-called wake “displacement thickness” $2\delta = M/U$) in the plane, and by a constant “displacement area” $A = M/U$ in space.

The preceding relations are fundamental in the theory of real wakes. Their extension to periodic and turbulent wakes will be discussed in Ch. XIII, §6, and Ch. XIV, §7.

7. Oseen equations. Oseen’s equations (8) have been applied in many connections. Thus, using the Oseen approximation and perturbation meth-

ods, higher order corrections to the "creeping" flow (7) past a sphere can be made, giving¹⁷

$$(16) \quad C_D = \frac{25}{R} \left(1 + \frac{3R}{16} - \frac{19R^2}{1280} + \frac{71R^3}{20480} + \dots \right).$$

Of greater interest is the use of the Oseen approximation to resolve Stokes' paradox (§3), and to obtain theoretical estimates of the drag of cylinders for small R . Although measurements are difficult, due to wall effects¹⁸, and not available for $R \ll 1$ [31, p. 15], the formula $D = 4\mu U$ seems approximately correct [50, §343].

Various other calculations of wakes at low R , based on Oseen's "linearized" approximation, have also been made. One can mention the cases of ellipsoids, elliptic cylinders, spheres in tubes, permeable plates, and yawed cylinders¹⁹. These are based on the system (2), (4), (8) and $u(\infty) = 0$, which may be said to determine Oseen's boundary value problem. (Note that, in our new notation, (2) is $u = u_1 = -U$, $v = u_2 = 0$, and $w = u_3 = 0$ on the obstacle surface.)

8. Boundary layer approximation. For flows nearly parallel to the x -axis, one can replace the Navier-Stokes equations by Prandtl's approximate boundary layer equations [31, pp. 118, 130]. Using subscripts to denote differentiation with respect to the variables indicated, these are

$$(17a) \quad (U + u)u_x + vu_y = -\rho^{-1}p_x + \nu u_{yy},$$

in the plane. For axially symmetric flows, they are

$$(17b) \quad (U + u)u_x + vu_r = -\rho^{-1}p_x + \nu r^{-1}(ru_r)_r.$$

Note that, in the boundary layer approximation, the flow in front of an obstacle is supposed undisturbed.

Most theoretical treatments ([31], [74]) of real jets and wakes are based on (17a)–(17b). Therefore, the approximations involved have been analyzed in detail (e.g., in [31, Ch. IV]).

However, we shall avoid this approximation in treating the momentum equation (§9), and have deduced the asymptotic wake velocity profile

¹⁷ [31, §215], and refs. given there. See also H. Villat, *Leçons sur les fluides visqueux*, Paris, 1943, 224–56. For an alternative to Oseen's equations giving a better fit but involving an extra empirical constant, see G. F. Carrier, *Slow viscous flow*, Final Report on Contract Nonr-653(00), Brown University.

¹⁸ C. M. White, *Proc. roy. soc. A*186 (1946), 472–9. See also L. Bairstow et al, *Phil. Trans. A*223 (1923), 383–432; C. Wiesels-berger, *Phys. Zeits.* 22 (1921), 321–8.

¹⁹ See [50, §343], and many refs. given there; R. de Possel and J. Valensi, *Comptes rendus* 236 (1953), 2211–13, and 238 (1954), 1966–8; Tomotika et al., *Proc. roy. soc. A*219 (1953), 233–44, and *QJMAM* 6 (1953), 290–312; S. Sidrak, *Proc. math. phys. soc. Egypt* 4 (1953), 17–27; I. Imai, *Proc. roy. soc. A*224 (1954), 141–60.

THEOREM 1. In an incompressible fluid satisfying the Navier-Stokes equations, we have

$$(19a) \quad D = - \oint p \, dy + \mu \oint \left(\frac{\partial v}{\partial x} - \frac{\partial u}{\partial y} \right) dx - \rho U \oint u \, dy \\ - \rho \oint (u^2 dy - uv \, dx),$$

in two-dimensional flow, and

$$(19b) \quad D = - \iint p \, dS_1 + \mu \iint \sum \left(\frac{\partial u_k}{\partial x_1} + \frac{\partial u_1}{\partial x_k} \right) dS_k \\ - \rho U \iint u \, dy \, dz - \rho \iint \sum u_1 u_k \, dS_k$$

in three-dimensional flow.

(In (19b), we have used the tensor notation $u_1 = u$, $u_2 = v$, $u_3 = w$, $dS_1 = dy \, dz$, $dS_2 = dz \, dx$, $dS_3 = dx \, dy$.) To deduce the preceding equations, one need merely account for all the terms involved in the rate of change of momentum. These are: the pressure thrust D due to the obstacle; the pressure and viscous shear thrust of the fluid; and the rate of x -momentum efflux by convention. Some simplifications can be made by using mass conservation: thus $\oint \sum u_k \, dS_k = 0 = U^2 \oint dy = 0$, etc.

To put (19a)–(19b) in more usable form, we define the *total head* as usual by

$$h = p + \frac{1}{2} \rho [(U + u)^2 + v^2 + w^2],$$

so that the free stream total head will be

$$H = p_0 + \frac{1}{2} \rho U^2.$$

The total head is nearly constant (i.e., nearly equal to H) outside the viscous wake. More exactly, we have in the notation $u_1 = u + u$ of (1),

$$\partial h / \partial x_i = \partial p / \partial x_i + \rho \sum u_k (\partial u_k / \partial x_i) \\ = \partial p / \partial x_i + \rho \sum u_k (\partial u_i / \partial x_k) + \rho \sum u_k \zeta_{ki},$$

where $\zeta_{ki} = (\partial u_k / \partial x_i - \partial u_i / \partial x_k)$ is a component of ζ . By the Navier-Stokes equations (1), therefore,

$$\partial h / \partial x_i = \mu \nabla^2 u_i + \rho \sum u_k \zeta_{ki}.$$

(1926), 7–27, and Phil. Trans. A227 (1928), 93–135; S. Goldstein, Proc. roy. soc. A142 (1933), 563–73; [61, §19.71]. Our (19a) is Taylor's (5), with viscosity included.

Clearly, if the flow is irrotational and incompressible, so that $\mathbf{u} = \nabla\phi$ where $\nabla^2\phi = 0$, then $\nabla h = 0$ and $h = H$ is constant. More generally, in the plane, $\nabla^2 u = \partial\zeta/\partial y$ and $\nabla^2 v = -\partial\zeta/\partial x$; while in space $\nabla^2 u = r^{-1}\partial(r\zeta)/\partial r$ and $\nabla^2 v = -r^{-1}\partial(r\zeta)/\partial x + v/r^2$.

COROLLARY 1. If terms which involve the vorticity (or a derivative of the vorticity) as a factor are ignored outside the wake W , then

$$(20a) \quad D = \int_W (H - h) dy + \rho \oint [uv dx + \frac{1}{2}(v^2 - u^2) dy]$$

in plane flow. In axially symmetric flow,

$$(20b) \quad D = \iint_W (H - h) dS_1 - \rho \iint \sum (u_1 u_k dS_k - \frac{1}{2} u_k^2 dS_1).$$

Proof. By the preceding paragraph, $H - h$ is negligible outside W , since $\partial h/\partial x$ is. Again, the viscous term in (19b) can be rewritten as $2\pi\mu \oint r\zeta dx$, which vanishes if $dx = 0$ across W .

COROLLARY 2. If $|u| = o(X^{-1})$ inside W , if W is of radius $O(X^{-1})$ at a distance X behind the obstacle, if $|u| = o(R^{-1})$ outside W , and if ζ and its derivatives die off exponentially outside W , then asymptotically

$$(21a) \quad D = \int_W (H - h) dy = -\rho U \int_W u dy$$

in the plane, and

$$(21b) \quad D = 2\pi \int_W (H - h)r dr = -2\pi\rho U \int_W ur dr$$

with axial symmetry, as $X \rightarrow \infty$.

For, terms quadratic in u_i can be neglected asymptotically, both inside W and outside. The asymptotic formulas of §6 can be based on Cor. 2, using the considerations of §5 to justify its assumptions.

Connoisseurs of airfoil theory will recognize, in formulas (21a)–(21b), the first terms of expressions of great practical importance. A more refined analysis, due primarily to Betz and Jones²³, enables one to determine quite accurately the drag of an airfoil in flight, from Pitot pressure traverses made a fraction of a chord-length behind the airfoil. However, we shall not give this more refined analysis, partly because it is mathematically less rigorous than the simpler asymptotic formulas derived above.

10. Similarity hypothesis. One can easily verify that the asymptotic velocity profiles (11a)–(11b) in wakes are all *similar* to a single “universal

²³ For references and details, see [31, §115].

TABLE I. *Values of p, q in $n = 2, 3$ dimensions*A. *Jets*. Similarity Hypothesis: $u = x^{-p}f(y/x^q)$.

	Momentum	Laminar Homogeneity $2q = p + 1$	Turbulent $q = 1$
$n = 2$	$2p = q$	$p = \frac{1}{3}, \quad q = \frac{2}{3}$	$p = \frac{1}{2}, \quad q = 1$
$n = 3$	$p = q$	$p = q = 1$	$p = q = 1$

B. *Wakes*. Similarity Hypothesis: $w = x^{-p}f(y/x^q)$

	Momentum	Laminar Homogeneity $2q = 1$	Turbulent $p + q = 1$
$n = 2$	$p = q$	$p = q = \frac{1}{2}$	$p = q = \frac{1}{2}$
$n = 3$	$p = 2q$	$p = 1, \quad q = \frac{1}{2}$	$p = \frac{2}{3}, \quad q = \frac{1}{3}$

C. *Wakes with hydrodynamical self-propulsion*
Same Similarity Hypothesis, hence homogeneity condition

	Momentum	Laminar	Turbulent
$n = 2$	$p = 3q$	$p = \frac{3}{2}, \quad q = \frac{1}{2}$	$p = \frac{3}{4}, \quad q = \frac{1}{4}$
$n = 3$	$p = 4q$	$p = 2, \quad q = \frac{1}{2}$	$p = \frac{4}{3}, \quad q = \frac{1}{3}$

velocity profile", provided the distance and velocity scales are changed appropriately. More precisely, for suitable positive constants p, q , they have the form

$$(22) \quad u(x, y) = x^{-p}f(\eta) \quad [\eta = y/x^q].$$

We shall see that an analogous equation is *assumed* to hold asymptotically in the theory of laminar jets. When so assumed, it may be called the Similarity Hypothesis.

More generally, it forms the basis for the theories of turbulent wakes and jets (Ch. XIV), and of wakes with "hydrodynamic self-propulsion". In all cases, the constants p and q can be determined from approximate forms of the Momentum Conservation Law, and the requirement of being compatible with the assumed approximate Equations of Motion. Table I contains a list²⁴ of the constants p and q determined in this way.

To make clear the method, we note that (21a) implies $p = q$ for plane laminar viscous wakes, while (21b) implies $p = 2q$ in (22). Again, to achieve homogeneity in the simplified equations (10), we must have $2q = 1$. The equation $2q = 1$ is also necessary and sufficient for homogeneity in the

²⁴ Partly in [74, p. 444].

boundary layer equations (17a)–(17b), if we neglect uu_x in comparison with Uu_x . From these two equations, p and q can be computed to have the values listed in Table I.

Thus, in the plane, $p = q = \frac{1}{2}$; the wake breadth is $O(x^{\frac{1}{2}})$; the maximum backflow velocity is $O(x^{-\frac{1}{2}})$; and the Reynolds number is constant along the wake. With axially symmetric laminar viscous wakes, $p = 1$ and $q = \frac{1}{2}$. Hence the wake diameter is $O(x^{\frac{1}{2}})$; the maximum wake velocity $O(x^{-\frac{1}{2}})$; and $R = O(x^{-\frac{1}{2}}) \downarrow 0$. Therefore, an axially symmetric wake should remain laminar if initially laminar.

The critical Reynolds number R_p , above which the wake becomes unsteady (non-laminar), is found empirically to be in the range 30–60 for two-dimensional wakes behind circular cylinders²⁵, about 500 for wakes behind flat plates parallel to the stream [36], and in the range 100–200 for the wakes behind bluff, axially symmetric obstacles (Ch. XIII, §11).

11. Creeping jets. It may be conjectured that, as the Reynolds number R tends to zero, the jet of a very viscous liquid from a conical trumpet will satisfy Stokes equation (5b) for “creeping” flow. Also, that the jet from a slit at the vertex of a wedge will satisfy (5a). Clearly, the cases of a slit in a wall and of a long tube are special cases of such orifices.

It is therefore noteworthy that there exist such flows (see Fig. 3) having (straight) *radial* streamlines—i.e., having stream functions of the form $V = f(\theta)$. These may be supposed to approximate the asymptotic behavior of “creeping jets”, at large distances from the orifice.

First, we take the case of jets from slits. In polar coordinates, (5a) is $0 = \nabla^4 V = \left(\frac{\partial^2}{\partial r^2} + \frac{1}{r} \frac{\partial}{\partial r} + \frac{1}{r^2} \frac{\partial^2}{\partial \theta^2} \right)^2 V$. Substituting $V = f(\theta)$ into (5a) we, get $f^{IV} + 4f'' = 0$. This has the basic solutions 1, θ , $\cos 2\theta$, $\sin 2\theta$. Neglecting additive constants without physical meaning, and assuming symmetry about $\theta = 0$, we get

$$(23) \quad V = a(\sin 2\theta - (2 \cos 2\alpha)\theta).$$

The (radial) velocity is

$$(23') \quad u_r = (2a/r)(\cos 2\theta - \cos 2\alpha),$$

which satisfies the boundary condition $u_r = 0$ on $\theta = \pm \alpha$, since $u_\theta = 0$ everywhere.

For axially symmetric “creeping” jets with radial streamlines, (5b) can

²⁵ [31, pp. 552, 572]; A. Fage, Proc. roy. soc. A142 (1933), 560–2. See also P. Torda, Proc. third midwest conf. fluid mech. (1953), 613–29. For a more thorough discussion, see Ch. XIII, §9.

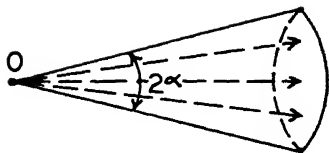


FIG. 3.

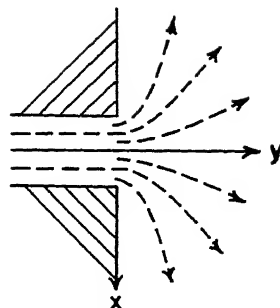


FIG. 4.

be written

$$0 = E^4 V = \left(\frac{\partial^2}{\partial r^2} + \frac{(1 - \mu^2)}{r^2} \frac{\partial^2}{\partial \mu^2} \right)^2 V,$$

using spherical coordinates and $\mu = \cos \theta$. In the case $V = f(\mu)$ of radial streamlines, this reduces to $(1 - \mu^2)f^{IV} - 4\mu f''' + 4f'' = 0$, after multiplication by $r^4/(1 - \mu^2)$. Apart from singular solutions, infinite when $\mu = 1$, this has the regular solutions $1, \mu, \mu^3$. Therefore, the most general creeping flow with radial streamlines having axial symmetry is²⁷ given by

$$(24) \quad V = a(3 \cos^2 \alpha \cos \theta - \cos^2 \theta).$$

The (radial) velocity is accordingly

$$(24') \quad u_r = (3a/r^2)(\cos^2 \theta - \cos^2 \alpha).$$

It is noteworthy that, in the radial jets just described, there is local *inward* flow (i.e., $u_r < 0$) in the interval $\pi - \alpha < \theta < \alpha$, if $\alpha > \pi/2$. This is true in both the plane and axially symmetric cases, by (23')-(24'). Indeed, the net mass-flow is inward if $\alpha > 142.5^\circ$ in space, or if $\tan 2\alpha > 2\alpha$ ($\alpha > \pi$) in the plane.

It is of some interest to try to construct creeping jets representing discharges from orifices of finite diameter. Starting with the elementary solution $V = r(\theta \sin \theta) = x\theta$ of (5a), Dean²⁸ has considered the flow

$$(25) \quad V = (x - a) \arctan \frac{y}{x - a} - (x + a) \arctan \frac{y}{x + a}.$$

This represents a "creeping" jet which is normal to the opening $|x| < a$,

²⁷ Formulas (24)-(24') are taken from M. Beran, "A note on axially symmetric jets", Quar. appl. math. 14 (1956).

²⁸ Phil. Mag. 21 (1936), 727-44. Dean also concludes that an *oblique* plane jet must separate from one wall, for all $R > 0$. Creeping jets have also been studied by W. Wuest, Ing. Archiv. 22 (1954), 357-67.

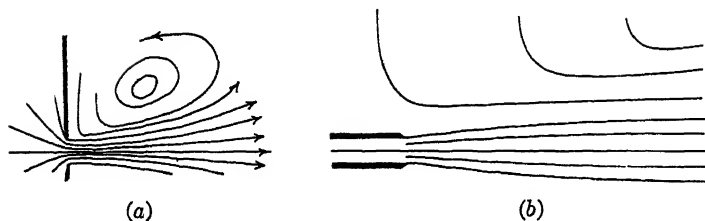


FIG. 5.

$y = 0$, and tangential to the “walls” $|x| > a$, $y = 0$, as in Fig. 4. However, the flow does not adhere to the walls: $\partial V/\partial y \neq 0$ there.

12. Inertial effects. The behavior of laminar viscous jets becomes much more complicated when inertial effects are considered. For purposes of orientation, we first review briefly the rather extensive²⁹ experimental data concerning *circular* laminar viscous jets. These data have not been quantitatively correlated; moreover, the small velocities involved make them especially sensitive to convection currents and other distracting influences. Nevertheless, some general features are evident.

In the case of a circular hole of diameter d in a flat wall, there is separation of flow, and a circular jet forms, when $R = v d/\nu$ exceeds 10 or so (depending on the sharpness of the orifice). This jet generates a toroidal eddy in the surrounding fluid, as sketched in Fig. 5a; hence it can only fulfill the Similarity Hypothesis of §10 near the axis. As R increases beyond 200 or so, the jet becomes more concentrated and less stable [59], finally breaking up and becoming turbulent.

Circular jets from thin tubes, on the other hand, seem to suck in the surrounding fluid radially, as sketched in Fig. 5b. Hence they seem compatible with the Similarity Hypothesis, even far from the axis of the jet.

13. Schlichting's model. Schlichting³⁰ has constructed a mathematical model for circular jets, based on the boundary layer approximation (17a)–(17b). Though propounded for jets from circular holes [74, Figs. 9.12 and 10.3], Andrade's experimental confirmation²⁹ is for jets from a tube. Moreover the fit between theory and experiment involves adjusting two arbitrary parameters: the “angle of spread”, and the distance behind the

²⁹ Oberbeck, Ann. phys. chemie 2 (1877), 1–16; M. Smoluchowski, Bull. Acad. Sci. Cracovie (1904), 371–84; [59, Parts I–II]; E. N. da C. Andrade and L. C. Tsien, Proc. phys. soc. 49 (1937), 381–90, and 51 (1939), 784–93. See also F. J. Bourrieres, Publ. sci. tech. min. air, No. 279 (1953)

³⁰ H. Schlichting, ZaMM 13 (1933), 260–3; cf. [31, §57] and [74, p. 152]. Since $u(\infty) = 0$ for jets, the Oseen approximation would not be appropriate. For the effect of assuming the full Navier-Stokes equations, see §15.

tube orifice at which the origin of coordinates (the "virtual source" or "effective orifice") is placed³¹. In view of these adjustments, and the fact that all differential equations of the diffusion type give rise to bell-shaped velocity profiles, the confirmation can hardly be regarded as decisive.

Schlichting's construction goes as follows. Since $U = 0$ for jets and $p = \text{const.}$ outside the jet, (17a)–(17b) reduce to

$$(26a) \quad u\partial u/\partial x + v\partial u/\partial y = \nu\partial^2 u/\partial y^2$$

for plane jets, and

$$(26b) \quad u\partial u/\partial x + v\partial u/\partial r = \nu[\partial^2 u/\partial r^2 + r^{-1}\partial u/\partial r]$$

in the present axially symmetric case. Originally, Schlichting *guessed* that one should try the Similarity Hypothesis (22) with $p = q = 1$. This amounts to trying

$$(27) \quad V = vxh(\eta), \quad \text{where } \eta = r/x\nu^{\frac{1}{2}},$$

in cylindrical coordinates (x, r, θ) . However, this choice can also be *deduced* (cf. Table I).

In the boundary layer approximation (17a)–(17b), since $U = 0$, the *jet momentum* M_2 is

$$(28a) \quad M_2 = \rho \int_{-\infty}^{\infty} u^2(x, y) dy$$

for plane jets, and³²

$$(28b) \quad M_3 = 2\pi\rho \int_0^{\infty} u^2(x, r)r dr$$

for circular (axially symmetric) jets. For M_3 to be constant in (28b), the condition is clearly $p = q$. Again, $p = q = 1$ is the only choice of $p = q$ compatible with the Similarity Hypothesis (22). Substituting in (26b), we get

$$(29) \quad \frac{d}{d\eta} \left(h'' + \frac{h'}{\eta} + \frac{hh'}{\eta} \right) = 0 \quad \text{if } p = q = 1,$$

The boundary conditions for the ordinary differential equation (29) are: $u = 0$ when $\eta = \infty$, and $v = \partial u/\partial \eta = 0$ when $r = \eta = 0$. Hence the constant of integration in (29) is zero, giving

$$\eta h'' - h' + hh' = (\eta h' - 2h + h^2/2)' = 0.$$

³¹ For the flow near the orifice, see J. Okabe, Reps. Kyushu Univ. 5 (1948), 1–22; Math. revs. 13 (1952), p. 700.

³² Formula (28a) is [31, p. 145, (90)], while (28b) is [31, p. 147, (102)].

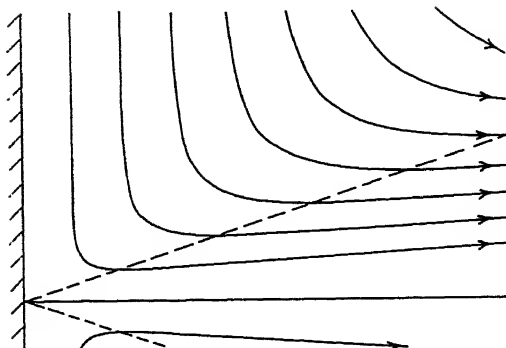


FIG. 6.

Further integration (cf. [31, §57]) gives

$$(30) \quad h(\eta) = a^2 \eta^2 / (1 + a^2 \eta^2 / 4),$$

where a is an arbitrary constant. Correspondingly,

$$(30') \quad v = \frac{\nu a^2 x r^2}{\nu x^2 + \frac{1}{4} a^2 r^2}, \quad u = \frac{2 a^2 \nu^2 x^3}{(\nu x^2 + \frac{1}{4} a^2 r^2)^2}, \quad \frac{v}{u} = \frac{r}{2x} \left(1 - \frac{a^2 r^2}{x^2} \right).$$

A special case is graphed in Fig. 6; clearly, all "Schlichting flows" (30)-(30') are affinely similar.

From (30'), it is clear that the jet cuts all cones inwards in Schlichting's model, and that the "throat" of any streamline is at $r = x/a$. Since a is arbitrary, this means that the "angle of spread" $\alpha = \operatorname{arccot} a$ is theoretically indeterminate. So is the momentum flux.

$$(31) \quad M = 2\pi\rho \int_0^\infty u^2 r \, dr = 16\pi\mu a^2/3.$$

However, the entrainment of the surrounding fluid is determined. Since the flux of volume is

$$(32) \quad Q = 2\pi \int_0^\infty u r \, dr = 8\pi\nu x,$$

the entrainment is $8\pi\nu$ per unit length. Thus the effect of the jet on the surrounding fluid is that of a uniform half-line of sinks.

14. Laminar plane jets. Assuming that boundary layer theory was applicable, and that a "self-similar" flow might be expected, Schlichting³⁰ and Bickley³³ have constructed a model for the flow near the axis of a plane jet issuing from an infinitesimal slit.

³³ W. G. Bickley, *Phil. Mag.* 23 (1937), 727-31. See also [31, §57], [74, p. 137], and P. Y. Chou, *Chinese J. Phys.* 7 (1947), 96-101.

We look again for solutions of the form

$$(22) \quad u = x^{-p}f(y/x^q) = x^{-p}f(\eta) \quad [\eta = y/x^q],$$

which make the jet momentum (28a) constant and satisfy the boundary layer equation (26a). For such a solution to admit separable variables under (22), we must have (as in the axially symmetric case) $2q - p = 1$. Combining with the momentum equation $2p = q$ of (28a), we get $p = \frac{1}{3}$, $q = \frac{2}{3}$, giving

$$(33) \quad V = x^{\frac{1}{3}}\psi(y/x^{\frac{2}{3}}) = x^{\frac{1}{3}}\psi(\eta),$$

and a Reynolds number proportional to $x^{\frac{1}{3}}$, increasing along the jet.

Substituting in (26a), we get

$$(34) \quad \psi'^2 + \psi\psi'' + 3\eta\psi''' = 0.$$

The integration of (34), subject to the boundary conditions

$$(34') \quad \psi(0) = \psi'(0) = \lim_{\eta \rightarrow \infty} \psi(\eta) = 0,$$

gives the general solution

$$(35) \quad \psi(\eta) = 2a \tanh(a\eta), \quad u = \frac{2a^2}{3x^{\frac{1}{3}}} \operatorname{sech}^2(a\eta).$$

As with circular jets, the solution involves an indeterminate "angle of spread", corresponding to a . All flows are again affinely similar, and all streamlines are geometrically similar. One also finds again a bell-shaped velocity profile, and entrainment of the surrounding fluid by the jet, as in Fig. 5b.

Andrade and Tsien²⁹ have realized the preceding model approximately by delicate experimental work. The verification again involves replacing an orifice in a wall by flow from a tube, and putting the origin of coordinates behind the jet-exit, and fitting the "angle of spread" empirically.

Extensions of the theory, intended to describe laminar compressible jets, have also been made³⁴. However, their quantitative experimental realization would seem to be difficult.

Finally, we note that viscosity will affect liquid jets in air. Thus Lelli³⁵ notes that viscosity may reduce the coefficient of contraction of a Borda tube from 0.50 (Ch. I, §10), to 0.45.

³⁴ S. I. Pai, *J. aer. sci.* 16 (1949), 463-9; M. Z. Krzywoblocki, *Quar. appl. math.* 7 (1949), 313-23; C. R. Illingworth, *Proc. roy. soc. A* 199 (1949), 533-48; D. G. Toose, *QJMM* 5 (1952), 155-64; D. C. Pack, *Proc. Camb. phil. soc.* 50 (1954), 98-104. Analogous formulas for wakes have been derived by D. R. Chapman, *NACA Tech. Note* 1800 (1949).

³⁵ M. Lelli, *Rend. Lincei* 10 (1929), 38-44.

15. Exact self-similarity. Yatssev and Squire³⁶ have improved substantially on Schlichting's theory, by obtaining exact solutions of the Navier-Stokes equations under Schlichting's similarity hypothesis (27). Their treatment may be regarded as an extension to the axially symmetric case of the Jeffery-Hamel theory³⁷ of spiral flows ([4, Ch. IV, §6], or [31, §24, and the references on pp. 106, 110]).

Squire's formulas are most conveniently derived in spherical coordinates. In these, assumption (27) becomes

$$(36) \quad V = \nu r f(p), \quad \text{where } p = x/r = \cos \theta.$$

The radial and angular velocity components are

$$(36') \quad u_r = -\nu f'/rq, \quad u_\theta = \nu f/rq,$$

where $q = y/r = \sin \theta$, and a prime denotes differentiation with respect to p , so that $-f' = -df/q d\theta$. The exact Navier-Stokes equations (3b) can be shown³⁶ to be mathematically equivalent to

$$(37) \quad (ff')' = 2f' + [(1 - p^2)f'']' - 2c_1,$$

where c_1 is a pressure constant of integration. This can be integrated by two quadratures, to give

$$(38) \quad f^2 = 4pf + 2(1 - p^2)f' - 2(c_1p^2 + c_2p + c_3),$$

where c_1, c_2, c_3 are arbitrary constants of integration.

On the jet axis, $p = 1, q = 0, u_\theta = 0$, and u_r is bounded. Substituting in (36'), we see that $f' = f = 0$ on the jet axis. Hence, substituting in (38), $c_1 + c_2 + c_3 = 0$. Again, consider the differentiated form of (38), which is twice

$$(38') \quad ff' = 2f + (1 - p^2)f'' - (2c_1p + c_2).$$

On the jet axis, $ff' = 2f = 0$ as before, while

$$(1 - p^2)f'' = q^2f'' = -q(df'/d\theta) = (q/\nu)\partial(rqu_r)/\partial\theta = 0,$$

by (36'). Substituting in (38'), with $p = 1$, we get a second equation, $2c_1 + c_2 = 0$. In summary

$$(39) \quad c_1 + c_2 + c_3 = 2c_1 + c_2 = 0, \quad \text{or} \quad c_1 = c_3, \quad c_2 = -2c_1.$$

Again, in the case of a circular orifice on the plane wall $p = 0$, the condi-

³⁶ V. L. Yatssev, Zh. eksp. teor. fiz. 20 (1950), 1031-4; H. B. Squire, QJMAM 4 (1951), 321-9; and Phil. Mag. 43 (1952), 942-5. See also Y. B. Rumer, Prikl. mat. mekh. 16 (1952), 255-6 (Appl. mech. revs. 3133 (1952) and 17 (1953), 743-4).

³⁷ Both depend basically on the invariance of the exact Navier-Stokes equations, under the group $x \rightarrow cx, u \rightarrow cu$ [4, p. 125].

tion $u_r = u_\theta = 0$ of adherence to the wall gives $f = f' = 0$ there; and a similar condition would hold on any conical wall $p = K$ ($-1 < K < 1$). Substituting in (38), we get $c_1 K^2 + c_2 K + c_3 = 0$, which by (39) implies

$$(40) \quad c_1 = c_2 = c_3 = 0.$$

In the case of a jet from a tube, the condition of differentiability on the tube axis $p = -1$ implies $c_1 - c_2 p + c_3 = -2c_1 + c_2 = 0$, and hence (40), by a repetition of the argument leading to (39). Hence (40) is the only case in which natural physical boundary conditions are satisfied³⁵.

But it is easy to integrate (38)–(38'), in case the constants c_1, c_2, c_3 of integration satisfy (40). The general solution is³⁶

$$(41) \quad f(p) = (2 - 2p^2)/(a + 1 - p) = 2 \sin^2 \theta / (a + 1 - \cos \theta).$$

The only fixed boundary compatible with the flow (41) is a tube of infinitesimal diameter, $\theta = \pi$. This may explain the experimental fact, noted in §12, that only in the case of a jet from a tube does one observe radial streamlines. Even in this case, the condition $f'(-1) = 0$ of adherence to the tube is not satisfied; however, the resulting shear stress acts on "zero" area, and so may be neglected. In other cases, one may surmise that, at very large distance, $R \downarrow 0$ and the "creeping flow" of §11 is approached.

In (41), the case of a jet is the case $a > 0$, where a corresponds to the angle of spread of the jet, and is mathematically indeterminate. As $a \downarrow 0$, we obtain near the axis the Schlichting-Bickley solution of the boundary layer approximation, already described in §13. In the limit, the jet behaves like a half-line of sinks on the jet axis.

If this singular behavior on the jet axis is allowed, then one can fit the boundary conditions $f(K) = f'(K) = 0$ for any conical fixed boundary. Thus, the case $K = 0$ of a circular orifice in a plane wall has already been treated by Squire³⁶.

³⁵ This argument is essentially due to Mark Beran, *Quar. appl. math.* 14 (1956), 213-14.

CHAPTER XIII

PERIODIC WAKES

1. Basic facts. The fact that flows past circular cylinders may be periodic, is often directly audible. Thus it is audible when a thin rod or stalk is swished rapidly through the air, making a whirring sound. It is audible in the whistling and screaming of a high wind (e.g., through a ship's rigging), and it causes the music of an Aeolian harp.

Such audible effects were first studied in the laboratory about 1878 by Strouhal¹, who showed the vibrations causing the sound were transverse to the wind. He also showed that the frequency N of vibration was related to the wind speed U and the cylinder diameter d by the approximate equation

$$(1) \quad N = U/6d.$$

In 1902, Ahlborn² took photographs of periodic wakes, but it was not until 1908 that Bénard correlated the musical notes studied by Strouhal with two (nearly) parallel rows of (nearly) equal spaced vortices behind the cylinder—i.e., with a so-called “vortex street” (see Fig. 1a).

It is interesting to study the periodicity as a function of the Reynolds number $R = Ud/\nu$. The periodicity is most marked over the range $40 < R < 1,000$, above which the wake becomes increasingly turbulent. If the *Strouhal number* is defined as $S = Nd/U$, then a fairly accurate empirical formula is [31, Fig. 149]

$$(1a) \quad S = Nd/U = 0.21 (1 - 20/R), \quad 40 < R < 1,000.$$

Thus, using c.g.s. units, the periodic range in air is roughly $6 < Ud < 150$, corresponding to $6.5/d^2 < N < 30/d^2$; in water, it is $0.4 < Ud < 10$, so that $2.5/d^2 < N < 2/d^2$. This explains why audible notes ($100 < N < 1,000$) are heard in air when $d \simeq 0.5$ –3 mm. and $U \simeq 1$ –10 m/s, and why visible vortex trails ($N \simeq 1$) are seen in water, when $d = 1$ mm. — 1 cm. and $U \simeq 0.5$ –5 m/s.

Even in the dominantly turbulent range, some wake periodicity has been

¹ V. Strouhal, Ann. der Phys. und Chemie 5 (1878); see [66].

² F. Ahlborn, “Mechanismus des hydrodynamischen Widerstandes”, Hamburg, 1902, pp. 26–7 and Fig. 47; H. Bénard, Comptes rendus 147 (1908), 970–2 (see also A. Mallock, Proc. roy. soc. A79 (1907), 262–5); for Leonardo da Vinci, see Handb. Exp. Phys. IV 2, p. 9. Fig. 1a is reproduced from Fig. 16 of G. J. Richards, Phil. Trans. A233 (1934), 279–301.

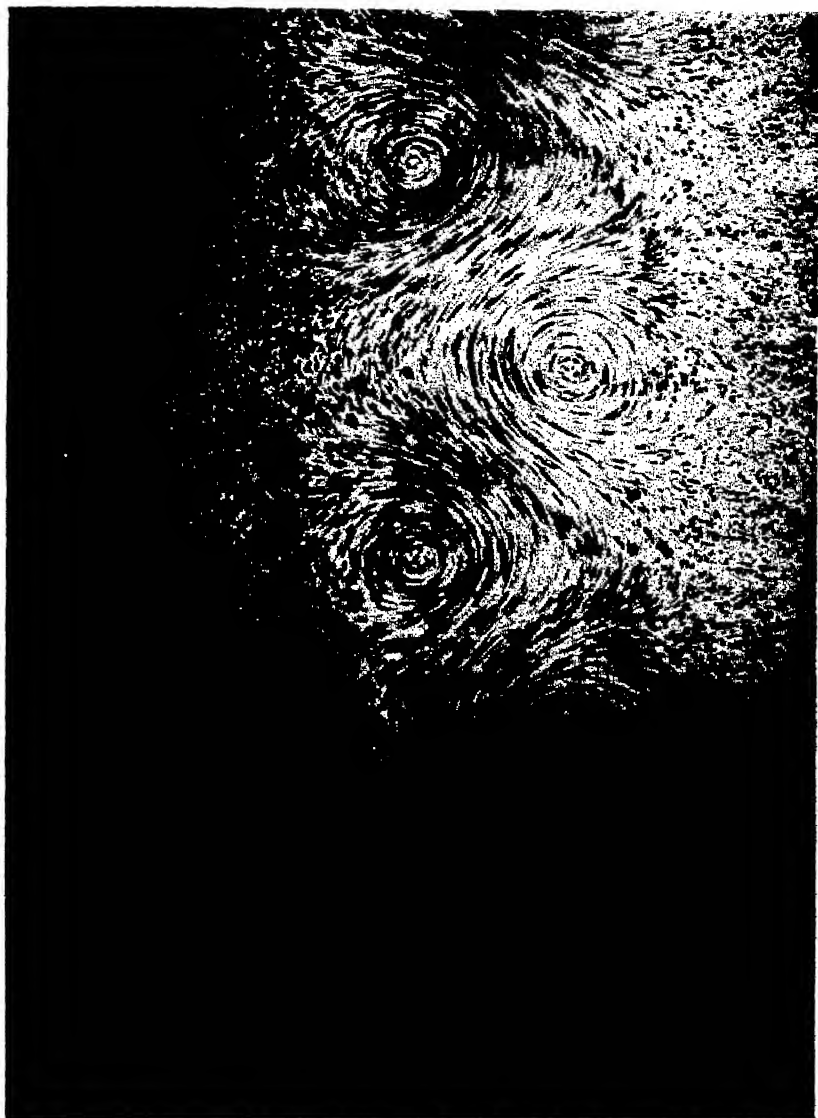


Fig. 1a. Alternating vortices.

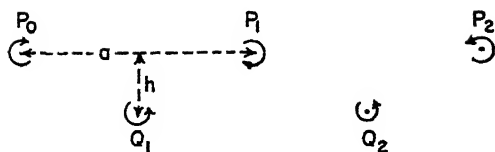


FIG. 1b.

observed³ up to $R = 10^3$ or more. In extreme cases, it may cause serious mechanical vibrations⁴.

2. Karman model. In 1911–12, von Karman⁵ gave a now classic theoretical discussion of periodic wakes in an infinite stream. This discussion centered around a simple mathematical model, in which the flow was imagined to be irrotational except for two parallel rows of equally spaced and staggered *point-vortices* P_i and Q_i , as in Fig. 1b. Such an array may be called an *ideal vortex street*.

It is evident that this model involves *three* arbitrary parameters: the vorticity⁶ κ of each vortex center, the longitudinal spacing a , and the transverse spacing h . In terms of these parameters, the complex potential $W = \phi + i\psi$ is³

$$(2) \quad W = \frac{i\kappa}{2\pi} \left\{ \log \sin \frac{\pi z}{a} - \log \sin \frac{\pi}{a} \left(z - \frac{a}{2} - ih \right) \right\}.$$

In a non-viscous fluid, moreover, an ideal vortex street is in equilibrium, the vortex-configuration moving upstream relative to the fluid at infinity with a velocity u_s , which is easily computed to be

$$(3) \quad u_s = \frac{\kappa}{2a} \tanh \frac{\pi h}{a}.$$

Hence, the rate $K = N\kappa$ at which vorticity is discharged per unit time down-

³ E. F. Relf and L. Simmons, ARC RM rep. 917 (1924); [31, pp. 419–21, 570–1]; [48a]; A. Roshko, NACA TN2913 (1953).

⁴ J. P. den Hartog, "Mechanical vibrations", 2d ed., New York, 1940, pp. 350–1. Other types of periodic wakes are discussed on pp. 343–53, and "galloping transmission lines" explained; see also R. Ruedy, Can. J. Res. 13 (1935), 82–92. Smokestack vibrations at $R = 7,000,000$ are attributed to vortex streets by den Hartog, Proc. nat. acad. sci. 40 (1954), 155–7. The failure of the Tacoma Narrows bridge has also been attributed to periodic vortex shedding; see D. B. Steinman, Univ. Iowa Eng. Bull. 31 (1946), 136–64.

⁵ [41] and [43]. See also [50, §156] and [61, §13.72].

⁶ Defined by $\kappa = \left| \oint d\phi \right|$, where $\phi = \int (u dx + v dy)$ is the velocity potential.

stream from each side of the obstacle, with velocity $U - u_s$ relative to the obstacle, is

$$(4) \quad K = \kappa(U - u_s)/a = 2u_s(U - u_s) \coth(\pi h/a).$$

However, these formulas do not determine κ , a , h as functions of the natural physical parameters U , d . We now consider the approximate determination of $\kappa(U, d)$, $a(U, d)$ and $h(U, d)$, which actually vary somewhat with the Reynolds number and distance downstream.

Using a little algebra, we see that this is essentially equivalent to predicting three of the dimensionless ratios

$$(5) \quad K/U^2 = \lambda, \quad u_s/U = \epsilon, \quad h/a, \quad h/d,$$

and

$$(5') \quad S = Nd/U = (U - u_s) d/av = (1 - \epsilon)(d/h)(h/a).$$

Combining (5) and (4), we also have [34]

$$(5'') \quad \frac{\lambda}{2} \tanh\left(\frac{\pi h}{a}\right) = \frac{K}{2U^2} \tanh\left(\frac{\pi h}{a}\right) = \epsilon(1 - \epsilon).$$

Dimensional analysis suggests that these ratios should be approximately constant, and *empirically* one finds $\lambda \simeq 0.4$, $\epsilon \simeq 0.15$, $h/a \simeq 0.3$, and $h/d \simeq 1.2$ (as well as $S \simeq 0.2$), with considerable experimental scatter.

In §3, we shall treat the approximate prediction of λ . In §8, following a discussion of momentum and stability in §§4–7, we shall discuss the prediction of ϵ , S , h/a , and h/d .

3. Shedding of vorticity. Using boundary layer theory, it is not difficult to predict λ approximately, as was shown by Heisenberg and Prandtl.⁷ Since the vorticity $\zeta = \partial u/\partial y$ in the boundary layer approximation, the rate K_1 of shedding vorticity on each side of an obstacle is roughly

$$K_1 = \int (\partial u/\partial y)u \, dy = 0.5u_1^2$$

where u_1 is the velocity outside the boundary layer near the separation point. (We ignore the fact that boundary layer theory breaks down there, because of flow detachment.)

By the general theory of plane flow, and especially the consequence $d\zeta/dt = \nu \nabla^2 \zeta$ of the Navier-Stokes equations [61, §19.11], this vorticity is carried by convection and diffusion into the wake. Thus, initially, the wake is bounded by two thin vortex layers of equal intensity and opposite sign.

⁷ [34]; see also [31, p. 564], and L. Prandtl and O. Tietjens, "Applied hydro- and aeromechanics", p. 132.

According to the simplest picture of non-viscous plane flow, these vortex layers are "rolled up" by Helmholtz instability (Ch. XI, §14) into periodic point-vortices with conservation of vorticity, so that K_1 equals the K of §2. Making these assumptions, and also assuming that $u_1 = U$ by free streamline theory, Heisenberg [34] deduced $K/U^2 = \lambda = 0.5$ on an *a priori* basis. This value has roughly the correct magnitude.

A better idea of λ can, however, be obtained by supplementing Heisenberg's idea with some remarks of Prandtl⁷. If one applies Bernoulli's theorem to the fluid outside the wake, then $u_1^2 = (1 + Q)U^2$, where

$$Q = 2(p_f - p_w)/\rho U^2$$

is the empirical wake underpressure coefficient of Ch. I, p_f being the free stream pressure and p_w the wake pressure. Hence Prandtl deduced the theoretical formula

$$(6) \quad K_1 = 0.5 u_1^2 = (1 + Q)U^2/2.$$

This agrees with direct measurements of K_1 by Fage and Johansen.⁸

To complete the evaluation of K , one needs an estimate of $\beta = K/K_1$.

In view of the conservation of the total vorticity $\iint_S d\kappa = \iint_S \zeta dx dy$ in viscous plane flow, which follows from the equation $d\zeta/dt = \nu \nabla^2 \zeta$ already mentioned, β is the fraction of the total vorticity of each sign which escapes annihilation by mixing with (diffusing into) an equal amount of vorticity of the opposite sign.

According to the asymptotic theory of Ch. XII, §5, β will ultimately tend to zero far downstream. On the other hand, if there were no mixing of vorticities of opposite sign, we would have $\beta = 1$, as assumed by Heisenberg.

Prandtl asserted that, empirically, β is about one-half for that part of the wake approximating a vortex street. Jeffreys⁹ motivated this by the suggestion that, in the "rolling up" of the boundary layer, half goes into the wake proper, and is mixed there, while the other half goes into the "vortex street". He based this suggestion on the symmetry of perturbations of a single boundary layer. Though this symmetry is quite temporary, as observed by Rosenhead⁹, the figure $\beta = 0.5$ is still usually quoted. It corresponds by (5)-(6) to

$$(7) \quad \lambda = (1 + Q)\beta/2 \simeq (1 + Q)/4;$$

hence to a λ usually somewhat less than one-half.

⁸ Phil. Mag. 5 (1928), 417-441; see [31, p. 555]. The term Q in (6) explains the apparent contradiction referred to in lines 11-15 of [31, p. 555]. For the values of Q , see Chap. XIV, §3.

⁹ H. Jeffreys, Proc. roy. soc. A128 (1930), 376-93, esp. p. 383, foot. For Rosenhead's critique, see *ibid.* A134 (1931), 170-92, esp. p. 171.

4. Vorticity and wake momentum. In §§4-6, we shall apply the considerations of wake momentum and drag, introduced in Ch. XII, to (nearly) periodic wakes. It is convenient to begin by relating (wake) momentum with the distribution of vorticity. It is well known¹⁰ that, if the total vorticity of a plane incompressible flow is zero (i.e., if the positive and negative vorticities cancel), then the vector momentum

$$\mathbf{M} = \rho \left(\iint u \, dx \, dy, \quad \iint v \, dx \, dy \right)$$

converges at infinity, and is related kinematically to the vorticity $\zeta(x, y)$ by the equation

$$(8) \quad \mathbf{M} = \rho \left(\iint y \zeta \, dx \, dy, \quad - \iint x \zeta \, dx \, dy \right).$$

This result suggests that the longitudinal momentum of an ideal vortex street (2) should be $\rho \kappa h$ per vortex pair (i.e., per period), as can also be shown by contour integration [31, §243]. More precisely, let $M(x)$ be defined by

$$(9) \quad M(x) = -\rho \int_{-\infty}^{\infty} u(x, y) \, dy.$$

Then the average wake momentum $\overline{M(x)}$ per unit length of wake satisfies

$$(10) \quad \overline{M(x)} = \rho \kappa h / a,$$

in an ideal vortex street.

In comparing the definition (9) with formula (12a) of Ch. XII, it should be noted that the velocity field associated with a periodic vortex street dies off exponentially as $y \rightarrow \pm \infty$. Hence the integration is, in effect, across the wake W . If a *semi*-infinite real wake is considered instead, this is no longer true: the integral over W is nearly *twice* that over $-\infty < y < +\infty$, due to radial source-flow outside W .

Integrating the preceding result with respect to $d\kappa$, we obtain

THEOREM 1. If $\zeta(x, y)$ is any periodic distribution of positive and negative vorticity, of average vorticity zero, then

$$(10^*) \quad \overline{M(x)} = \rho \int \overline{y \, d\kappa},$$

averaged over a period.

It may be presumed that (10*) is nearly true for nearly periodic wakes.

¹⁰ [50, p. 229]; the case of an ideal vortex street is treated in [61, p. 347]. See also H. Poincaré, "Théorie des tourbillons", Paris, 1893.

As a further confirmation, we note that according to boundary layer theory, where $\zeta = u_y = V_{yy}$,

$$\begin{aligned}\int_{-\infty}^{\infty} y\zeta(x, y) dy &= \int_{-\infty}^{\infty} yV_{yy} dy = \int_{-\infty}^{\infty} y dV_y = [yV_y]_{-\infty}^{\infty} - \int_{-\infty}^{\infty} dV \\ &= V(x, -\infty) - V(x, +\infty).\end{aligned}$$

Hence, to this approximation, $M(x) = \rho \int y\zeta dy$.

5. Vorticity and drag. We shall now relate the vorticity of a periodic wake to the drag associated with it. It should be emphasized that the formulas given are not exact, because they involve mathematical hypotheses which are not fulfilled exactly.

The asymptotic formula $UM(\infty) = D$ of Ch. XII, §9, does not apply to periodic wakes, because the velocity does not tend to U at infinity. If it did, we would have $D \simeq \rho\kappa hU/a$. A better estimate is given by the argument that D is the rate at which forward momentum is created in the wake per unit time by the obstacle. This argument gives the estimate

$$(11) \quad D \simeq (U - u_s)\rho\kappa h/a = \rho hK,$$

by (4). Dividing by $\frac{1}{2}\rho v^2 d$ and using (5''), we get the equivalent dimensionless form

$$(11^*) \quad C_D \simeq 2\lambda h/d = 4\epsilon(1 - \epsilon)(h/d) \coth(\pi h/a).$$

However, this calculation neglects the difference between the upstream and downstream mean pressure. In the proof of Cor. 2 of Theorem 1 of Ch. XII, relating the wake momentum to the drag, the difference tended to zero asymptotically; not so in the present case. If this difference is taken into account, one gets the slightly different estimate ([41], [43], [31, §243, (22)]),

$$(12) \quad D = \frac{\rho\kappa h}{a} \left\{ U - 2u_s + \frac{\kappa}{ah} \right\} = \frac{\rho\kappa^2}{2\pi a} + \frac{\rho\kappa h}{a} (U - 2u_s).$$

This agrees with (11) if and only if $\tan(\pi h/a) = a/\pi h$, or $h/a \simeq .39$.

The preceding calculations assume a doubly infinite vortex street; Synge¹² has estimated that if a periodic *semi*-infinite trail of point-vortices is used instead, the C_D is increased by about 5%. This confirms the idea that it is unnecessary to worry about the fact that the vortex street exists only behind the obstacle.

¹² J. L. Synge, Proc. Roy. Irish Acad. 37 (1927), 95-109; see also von Mises, ZAMM 15 (1935), 71-6.

It should be emphasized that none of the preceding estimates is rigorously exact.

6. Invariance theorem. A second application of momentum conservation, and the kinematical connection between momentum and vorticity moment, concerns the mean spacing of an array of vortices of equal strengths $\pm\kappa$ and alternating sign, both in viscous and non-viscous fluids. To make the problem tractable, we shall neglect the influence of an obstacle on the evolution in time of its downstream wake. We shall also assume the wake to consist initially, at time $t = 0$, of an infinite array of vortex-patches of strengths $\pm\kappa$ and alternating sign, lying in a belt around the x -axis, and having mean longitudinal spacing¹³ \bar{a} and transverse spacing \bar{h} . These assumptions are also made in von Karman's stability theory (§7); therefore the present more general discussion will apply there also.

We now define the average transverse *vorticity moment* $N_y(t)$ per unit length by

$$(13) \quad N_y(t) = \lim_{L \rightarrow \infty} \frac{1}{2L} \int_{-L}^L dx \int_{-\infty}^{\infty} y \zeta(x, y; t) dy,$$

where $\zeta dx dy = d\kappa$ in the case of point-vortices. Setting $2L = n\bar{a}$, there are initially about n (mathematically, $n + o(n)$) vortex-patches of strength $+\kappa$ and about n of strength $-\kappa$ in the interval $-L \leq x \leq L$. Since the mean transverse spacing is \bar{h} , we have

$$(13') \quad N_y(0) = \lim_{L \rightarrow \infty} [(n\kappa\bar{h})/(na) + o(1)] = \kappa\bar{h}/\bar{a}.$$

We next define the average *longitudinal momentum* $M_x(t)$ per unit length of the velocity-field induced by the vorticity, by

$$(14) \quad M_x(t) = \lim_{L \rightarrow \infty} \frac{1}{2L} \int_{-L}^L dx \int_{-\infty}^{\infty} u(x, y; t) dy.$$

Then it is a kinematical theorem¹⁴, generalizing (10), that

$$(15) \quad M_x(t) = N_y(t).$$

Finally, it is a form of the theorem¹⁴ of the conservation of momentum that

THEOREM 2. In a viscous or non-viscous incompressible fluid, $M_x(t) = M_x(0)$; hence $N_y(t) = N_y(0)$ is also constant in time.

In a non-viscous plane flow, vorticity is conserved [61, p. 101]; hence

¹³ As in Fig. 1b, this refers to the mean spacing of vortices of given sign; that of all vortices would be $\bar{a}/2$.

¹⁴ A rigorous and detailed discussion of (15), and of Thm. 2 and its corollaries, first deduced in [5, §4], will be published elsewhere.

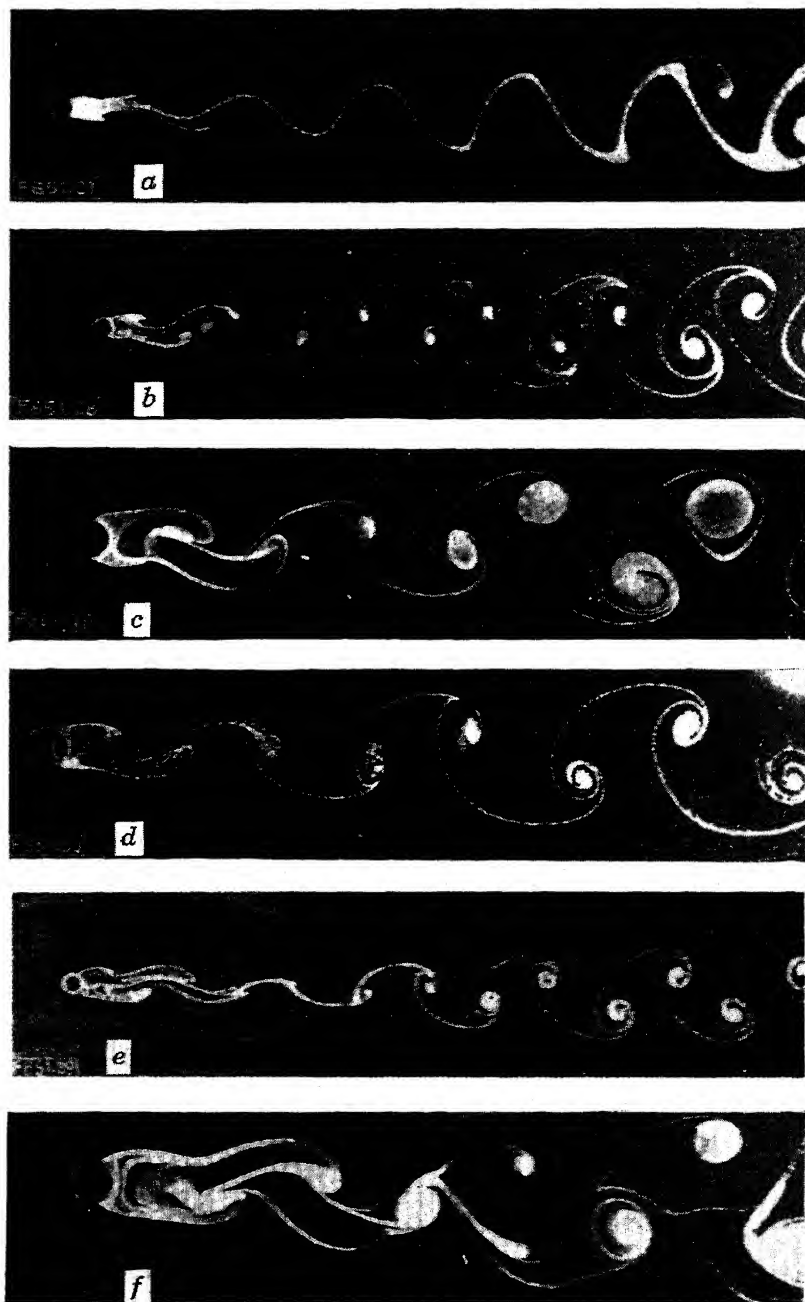


FIG. 2. Spreading of alternating vortices.

vortex-patches move around as time changes, with constant total vorticity $\pm\kappa$. If the velocity is bounded, it is evident that \bar{a} is constant in time; hence

COROLLARY 1. In non-viscous plane flow, κ and \bar{a} are constant in time, and hence so is $\bar{h} = \bar{a}N_y/\kappa$.

In viscous plane flow, there is diffusion [61, p. 578] between patches of positive and negative vorticity. Hence the mean vorticity $\pm\kappa(t)$ per patch decreases in magnitude with time, still totalling zero. Again, $\bar{a} = \bar{a}(t)$ is constant in time. Therefore, by Thm. 2, we see

COROLLARY 2. In viscous plane flow, \bar{a} is constant in time, but $\bar{\kappa}(t)$ decreases and hence $\bar{h}(t) = \bar{a}N_y/\bar{\kappa}(t)$ increases.

The results predicted theoretically by Cor. 2 are in fact observed experimentally¹⁵, as in Fig. 2.

From the approximate constancy of h in a slightly viscous fluid, we also infer that, $h/d_1 \simeq 1.0$, where d_1 is the wake diameter a little behind the obstacle. (For a circular cylinder or flat plate, $d_1/d \simeq 1.0$ – 1.5 , by free streamline theory.)

7. Karman's stability argument. Von Karman [41, 43] has given a classic discussion of the stability of two parallel periodic vortex-rows. He has shown that, in a non-viscous fluid, the equilibrium has *first-order instability* (i.e., that deviations from the array grow exponentially), except if $h/a = 0.281$, corresponding to $\cosh(\pi h/a) = \sqrt{2}$. As his demonstration can be found in many places ([50, §156] and [61, §13.72]), we shall omit it.

Because of von Karman's result, one will find many references in the literature to $h/a = 0.281$ as the "stable spacing-ratio". However, various investigators¹⁶ have shown that the spacing-ratio $h/a = 0.281$ also has higher-order instability. Moreover, since \bar{h} is *invariant* in a non-viscous fluid (Cor. 1 above), it is clear that the ratio h/a is determined by its initial value, and not¹⁷ by the stability of $h/a = 0.281$. (The invariance of \bar{h} and a is also evident in the numerical calculations of Schmieden¹⁶.) Finally, the break up of real vortex-streets does not proceed via irregular wandering of point-vortices, as considered by von Karman. Thus the observed¹⁵ spacing-ratio $0.28 < h/a < 0.50$ must be due to some other cause than a

¹⁵ E. Tyler, Phil. Mag 11 (1931), 849–90; S. G. Hooker, Proc. roy. soc. A154 (1936), 67–89; [31, pp. 568–9] and [24]. Fig. 2. is reproduced from A. Homann, Forschung Geb. Ingenieurwesens 7 (1936), 1–10. For a discussion of the rate of decay of vorticity, in the Oseen approximation, see C. C. Lin, von Mises Memorial Volume, Academic Press, 1954, pp. 170–6.

¹⁶ C. Schmieden, Ing. Archiv. 7 (1936); 215–21 and 337–41; N. Kochin, Doklady URSS 24 (1939), 19–23; see also [5, fnnt. 15].

¹⁷ Thus one does not have "stabile Anordnungen von isolierte Wirbelfäden . . . , die als Endprodukt der aufgelösten Wirbelschicht betrachtet werden können" [43, p. 51].

tendency to a "stable" spacing-ratio, contrary to what was once thought; this question will be discussed further in §8.

From another point of view, it is the *periodicity* of vortex streets which is unstable, not the spacing ratio; all mean spacing ratios are theoretically invariant, in a non-viscous fluid. This raises the question: if vortex streets are theoretically unstable, why do actual vortex streets persist so far downstream, in the range $30 < R < 200$? One answer is, that the velocity induced by vorticity is relatively small (say $0.03U$). Hence, for spacing-ratios reasonably near the slightly unstable ratio $h/a = 0.28$, one can expect the vortices to travel many periods downstream before their relative position becomes greatly disturbed.

In addition, the real vorticity is not concentrated in points (see §9), and there is some viscosity. Both of these factors presumably tend to decrease the real instability.

8. Strouhal number. We now recur to the problem of predicting the dimensionless ratios ϵ , S , h/a , and h/d , already stated at the end of §2. If we accept the approximate prediction $2\lambda = (1 + Q)\beta \simeq 1$ made in (7), then

$$(16) \quad C_D \simeq h/d \quad \text{by} \quad (12^*),$$

and (as remarked before (5)) it remains to predict two of the remaining ratios.

Again, as remarked at the end of §6, the value of h/d can be estimated by applying free streamline theory (Chs. II–VI) a few diameters behind an obstacle, after which h is approximately constant by Thm. 2 and free streamline theory is no longer applicable. This suggests the approximate values

$$(17a) \quad C_D \simeq h/d \simeq 1.25 \quad \text{for a circular cylinder,}$$

$$(17b) \quad C_D \simeq h/d \simeq 2 \cos \alpha \quad \text{for an inclined plate,}$$

inclined at an angle α to the stream.—Of course, h/d can also be measured photographically.

This leaves a single dimensionless ratio to predict. For this, one can accept $h/a = 0.281$ as being necessitated by von Karman's analysis of stability (§7). If one accepts this, one has a complete semi-theoretical prediction of κ , h , a and D from the geometry of the obstacle and the stream, in the range of Reynolds numbers over which vortex streets are formed. In particular, one infers by (5')

$$(18a) \quad S = Nd/U = (1 - \epsilon)(h/a)(d/h) \simeq 0.7 (h/a) \simeq 0.20,$$

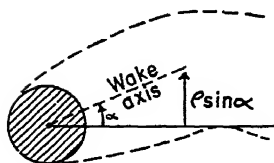


FIG. 3.

for circular cylinders. This is observed experimentally (cf. (1a)). One further predicts, by (5''),

$$(18b) \quad \epsilon(1 - \epsilon) = (\lambda/2) \tanh(\pi h/a) = \frac{1}{4}\sqrt{2},$$

since $\cosh q = \sqrt{2}$ implies $\tanh q = 1/\sqrt{2}$. Taking the smaller root of (18b), we get $\epsilon \simeq 0.175$, also in good agreement with observation, for circular cylinders.

However, for the reasons stated in §7, we do not think that this interpretation is valid. Instead, we believe that the real physical explanation is provided by considering the wake as an oscillator¹⁸. We believe that the frequency is determined by *local* effects, and not by the asymptotic downstream behavior.

Direct visual observation shows that, under the circumstances considered, *the wake swings from side to side*, somewhat like the tail of a swimming fish. The wake *inertia* is clearly about ρh per unit length. We assume a restoring force on the portion of wake extending to the first bend (Fig. 3), equal to the cross-force $\pi \rho U^2 l a$ [31, p. 35] on an airfoil of the same length $2l$ and angle of tilt α . Since the center of mass of the wake has been displaced through the distance $l \sin \alpha$, we get (to a first approximation)

$$(19) \quad m l \ddot{\alpha} = 2 \rho h l^2 \ddot{\alpha} = -\pi \rho U^2 l \alpha.$$

This is related to the frequency N , by $\ddot{\alpha} = -4\pi^2 N^2 \alpha$, or

$$(19^*) \quad N = \frac{U}{\sqrt{8\pi h l}}, \quad \text{whence} \quad S = \frac{N d}{U} \frac{1}{\sqrt{10\pi l/d}},$$

since $h = 1.25d$ as in (17a).

This gives the observed value $S \simeq 0.2$, provided $2l = 1.6d$, which is of the correct order of magnitude. Alternatively, since $Na = U - u_s = (1 - \epsilon)U$, as in (5'), $(1 - \epsilon)(d/a) = Nd/U = (10\pi l/d)^{-\frac{1}{2}}$, by (18*). But, the distance $2l$ to the nearest wake bend oscillates between 0 and $a/2$, with an average value of $2l = a/4$. Substituting $l = a/8$ above, and multiplying both sides by $\sqrt{d/a}/(1 - \epsilon)$, we get

$$(20) \quad \sqrt{d/a} = 1/(1 - \epsilon) \sqrt{10\pi/8}, \quad \text{or} \quad (d/a) = .28.$$

¹⁸ The explanation which follows is condensed from [5, §5], where further details may be found.

Using (17a) again, we get $(h/a) = .35$, which is in good agreement with observation.

In summary, the preceding "oscillator" model also roughly predicts the observed facts.

9. Miscellaneous effects. In §§1-8, we have been discussing the wake behind a circular cylinder in an infinite stream, under the assumption that the wake could be approximated by an ideal vortex street. We shall now consider how the discussion should be altered when non-circular cylinders and walls parallel to the stream are involved, and the effect of varying the Reynolds number, etc.

Changing the cylinder profile has various effects. Elliptic and ogival profiles, and tilted plates, have been studied. As §3 suggests, nearly equal amounts of vorticity are always shed from both sides—thus the vortex trail behind a tilted plate is still approximated by an ideal vortex street. However, the ratio $\epsilon = u_s/U$ is much smaller with slender, nearly streamlined bodies than for wide obstacles¹⁹. Thus, values as low as $\epsilon = 0.03$ have been reported for streamline bodies; whereas²⁰ $\epsilon = 0.22$ for a flat plate normal to the stream. The Strouhal number varies in the range $0.15 < S < 0.21$, if d is taken as the transverse diameter²⁰ of the obstacle—i.e., (approximately) of the wake. This is consistent with the ideas of §8—hence it implies that the Karman ratio h/l should vary within moderate limits.

Even in the case of a circular cylinder, the facts about periodic wakes are much less simple than the "inertial" theories of §§2-8 might suggest. Thus, as is suggested by (1a), the phenomenon depends strongly on the Reynolds number; there is a steady tendency to increasingly rapid vortex-dissipation by turbulence²¹ as R increases. When R exceeds 400, vortex lines (which have three-dimensional instability [73], too) break up within a few cylinder diameters.

Even the Reynolds number does not tell the whole story. For instance, the critical Reynolds number $R_p = (U d/\nu)_p$, above which the wake behind a circular cylinder first becomes periodic, is lowered by external turbulence²². It is also lowered by mounting the cylinder on springs, so that

¹⁹ H. Bénard, Proc. sec. int. congr. appl. mech. Zurich (1932), 502-3; G. J. Richards, Phil. Trans. A233 (1934), 279-301, and ARC RM 1590 (1933).

²⁰ A. Fage and F. C. Johansen, [24] and ARC RM 1143; [31, §247], and refs. given there.

²¹ The turbulence spectrum and wake structure in the intermediate range $300 < R < 10,000$ have been carefully observed by L. S. G. Kovaszny [48a] and A. Roshko, NACA TN 2913.

²² H. L. Dryden, NACA TR231 (1925). For resonance effects, see A. Thom, ARC RM1373 and Proc. roy. soc. A141 (1933), 651-9; C. Camichel et al., Comptes rendus 186 (1927), 203-5 and 200 (1935), 704-7.

the free period resonates with the natural vortex trail period. Thus periodic wakes at $R = 11$ have been obtained in this way²².

On the other hand, confinement between parallel walls increases R_p from its normal value of about 30, to 50 or more. Theoretically, as shown by Rosenhead²³, walls also lower the Karman stability ratio slightly to $h/a = .281 - .09(a^2/H)$, in a channel of diameter $2H$. Other wall effects on an ideal vortex street can also be predicted theoretically.

Finally, even in the absence of viscosity, it may be shown [5, §6] that the vortex sheets behind a cylinder cannot "roll up" into circles of diameter less than about $a/4$, because of energy limitations. A point vortex would have infinite energy.

10. Plate at zero incidence. The limiting case of a flat plate parallel to the stream differs from that of a circular cylinder, because the wake has a diameter 2δ which is much smaller than the length (chord) l of the plate. Also, there is no separation, so that the vorticity is presumably shed at a constant rate into an initially laminar wake (Ch. XII, §4), below $R = Ul/\nu = 10^5$. Slender airfoils at zero incidence angle may be expected to behave similarly, and both cases have been studied²⁴.

However, the laminar wake is unstable if $R = Ul/\nu > 1000$ ([36, pp. 245–250]), and breaks up periodically in the intermediate range of R , especially if there is acoustic stimulation or resonance.—Since $\delta/l = 1.72/\sqrt{R}$ [31, p. 136], it is interesting that the critical Reynolds number $(2U\delta/\nu)_p$ for a periodic wake, based on wake thickness, is about $3.44\sqrt{R} \simeq 110$, which has the same order of magnitude as in the case of a circular cylinder.

The "singing" of propeller and hydrofoil blades in water has been attributed to this periodic break-up of the wake²⁵. Although the field has not been thoroughly explored, it is clear that strong vibrations can be generated in this way. If they are strong enough, cavitation can occur in striae parallel to the trailing edge. In Gongwer's pictures, the associated alternating rectilinear vortices are clearly unstable, as predicted by Kelvin^{25a}.

11. Axially symmetric periodic wakes. At intermediate Reynolds numbers a periodic wake can also be seen behind a sphere, disc, or other axially symmetric obstacle. The periodicity is less regular than in the case

²² L. Rosenhead, *Phil. Trans. A228* (1929), 275–329, *Proc. Camb. Phil. Soc.* 25 (1929), 277–81, and *Proc. roy. soc. A129* (1930), 115–35; H. Villat, *Ann. sci. ec. norm. sup.* 46 (1929), 259–81.

²⁴ [36]; E. Tyler, *Phil. Mag.* 11 (1931), 849–90.

²⁵ F. Gutsche, *Zeits. Deutsche Ing.* 81 (1931), 882–3; C. A. Gongwer, *J. appl. mech.* 19 (1952), 432–8.

^{25a} *Phil. Mag.* 10 (1880), 155–68. This is an interaction instability: as stated in Ch. XI, §15, isolated vortices are stable.

of cylinders; moreover the phenomenon depends on many factors, just as in the two-dimensional case (§9).

Thus, the critical Reynolds number R_p , above which spherical air bubbles wobble as they rise under gravity in water instead of ascending in a straight line, is about $R_p = 50$ (Ch. XV, §7). Whereas, for a rigidly held or falling heavy sphere, R_p seems to be²⁶ about 500. Again, for a stationary disc normal to a non-turbulent stream, Stanton and Marshall²⁷ found $R_p = 200$, whereas Simmons and Dewey found $R_p = 100$ in a turbulent wind-tunnel.

The possibility that the wake behind a sphere or disc might consist of one or two spiral vortex lines has been often suggested^{26, 28}. Thus, one can easily imagine that air bubbles wobbling up rise in a spiral, with pitch about 0.3, and the stability of spiral helices has been considered by Levy and Forsdyke²⁸ with this possibility in mind. However, such is not the case; neither does the vortex sheath bounding the wake roll up into a periodic array of vortex rings (which would moreover be unstable²⁹).

Actually, in the intermediate range of R leading to a non-turbulent periodic wake, one seems to get periodic vortex-loops, oblique to the axis of symmetry. These are especially clearly marked behind a disc in a non-turbulent stream [31, p. 579].

Winny²⁶ quotes a "Strouhal number" $Nd/U = 0.25$ for a sphere, 50 % more than for a cylinder, but his data are not very consistent. He also reports that the diameter of the vortex system is about $4d/5$.

12. Periodic jets; edge tones. Like wakes, homogeneous jets often exhibit periodic behavior at intermediate Reynolds numbers, typically, in the range $100 < R < 6,000$. This periodicity can be stimulated acoustically; if amplified by resonance, it can be made to produce a strong musical note. Various wind instruments utilize the preceding principle³⁰. Because of their musical interest, periodic jets have been extensively studied experi-

²⁶ H. F. Winny, ARC RM 1531 (1952); W. Moller, *Phys. Zeits.* 39 (1938), 57-80; [86a, p. 186].

²⁷ T. E. Stanton and D. Marshall, *Proc. roy. soc.* A130 (1931), 295-301, and ARC RM 1358 (1932); L. F. G. Simmons and N. S. Dewey, ARC RM 1334 (1931). See also J. Schmiedel, *Phys. Zeits.* 29 (1928), 593-610; P. Dupin and M. Teissié-Solier, *Comptes rendus* 195 (1932), 1226-8; [86a, pp. 182-6]; M. Baubiach, *Publ. sci. tech. min. air* No. 98 (1936), p. 20.

²⁸ A. Mallock, *Proc. roy. soc.* A79 (1907), 262-73; Th. von Karman, "Vorträge aus dem Gebiet der . . . Aerodynamik", Th. von Karman and T. Levi-Civita, eds., Berlin, 1924, p. 137; H. Levy and A. G. Forsdyke, *ibid.* A120 (1928), 670-90. For theoretical arguments against spiral vortex lines, see [40] and the appendix by L. Rosenhead to ARC RM 1358 by Stanton and Marshall.

²⁹ H. Levy and A. G. Forsdyke, *Proc. roy. soc.* A114 (1927), 594-604.

³⁰ E. G. Richardson, "Acoustics of instruments and organ", London, 1929; A. B. Wood, "The physics of music", Methuen, 1944.

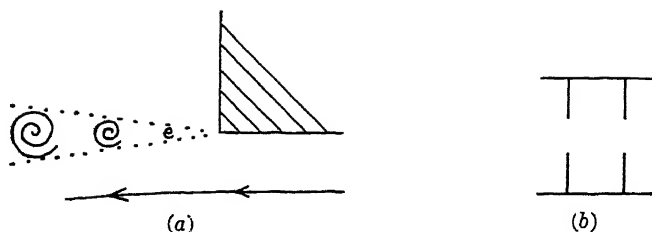


FIG. 5.

and with some *twin* jets flowing into a reservoir from adjacent parallel slots³⁴.

13. Bird tones. The behavior of axially symmetric jets is similar. Thus Marty [59, pp. 52-3] reports that the jet from a circular hole in a plate has a profile resembling a stalk of wheat when $160 < R < 1300$, the vortex sheath rolling up into vortex rings³⁵. This corresponds to varicose Helmholtz instability.

A more definitely periodic behavior is obtained when the circular orifice discharges into a pipe, of equal or larger diameter. Thus Johansen³⁶ reports a mean frequency $N \simeq 0.6 U/d$ (whence $S = Nd/U \simeq 0.6$), in the range $300 < R < 1200$. Walter [86a, p. 158] observes periodic vortex discharge for $2000 < R < 3500$, while Kurzweg records a similar periodicity near sharp-edged pipe inlets. Also, when a fluid starts to move impulsively through a circular orifice, the first few vortices seem to be discharged more or less periodically³⁷.

However, the preceding phenomena are unpredictable, and sensitive to minor changes in the orifice. To obtain a strong musical note, it is most effective to blow air with the right speed through two suitably spaced (and shaped) orifice plates (Fig. 5b). This configuration is called a "bird-call"³⁸; it is involved in some brass instruments³⁰ and in human whistling.

Conversely, air jets can be forced to vibrate by placing them in a strong

³⁴ See [59]; L. Escande, *La technique moderne* 27 (1935), No. 17; A. I. Bellin, et al., NACA TN 2417 (1951).

³⁵ See also L. Oberbeck, *Ann. phys. chemie* 2 (1877), 1-16, H. C. H. Townend, *ARC RM* 1634.

³⁶ F. C. Johansen, *Proc. roy. soc.* A126 (1929), 231-45 and *ARC RM* 1252 (1929). See also [86a, p. 158], R. Curtet, *Comptes rendus* 239 (1954), 387-8 and 452-4; H. von Gierke, *Z. ang. Physik* 2 (1950), 97-106; H. Kurzweg, *Ann. der Physik* 18 (1933), 193-216; A. B. C. Anderson, *J. acoust. soc. Am.* 26 (1954), 21-5 and 27 (1955), 13-21.

³⁷ Johansen, *loc. cit.*; S. G. Bauer, *Proc. roy. soc.* A182 (1944), 347-62; R. Wille, *Jahrb. Schiffbau Ges.* 46 (1952), 181-3.

³⁸ C. Sondhauss and A. Masson, *Comptes rendus* 36 (1853), pp. 257, 1004; [66, §371]; F. Kruger and E. Schmidtke, *Ann. der Physik* 60 (1919), 701-14.

sound field. Moreover the vibration, once started, may continue with a "roaring" noise familiar in gas stoves. This phenomenon of the "sensitive jet" has also received extensive study in the literature³⁹. Apparently, circular jets are more sensitive than plane jets.

³⁹ [66, §370]; W. E. Benton, *Proc. phys. soc.* 38 (1926), 109-25; E. G. Richardson, *ibid.* 43 (1931), 394-404; G. B. Brown, *ibid.* 47 (1935), 703-32; E. N. da C. Andrade, *ibid.* 53 (1941), 329-55.

CHAPTER XIV

TURBULENT WAKES AND JETS

1. General remarks. Most wakes and jets encountered in engineering practice are *turbulent*. That is, the flows involve many small, rapidly fluctuating eddies, distributed at random in space-time. More exactly, real jets and wakes tend to be turbulent if the Reynolds number $R = Ud/\nu$ exceeds 1,000, and this tendency increases with R .

To describe turbulent flow parallel to the x -axis, involving fixed solid boundaries, it is convenient to decompose the vector velocity into three components:

$$(1) \quad \mathbf{u}(\mathbf{x}; t) = (U + u + u', v + v', w + w').$$

Here $(U, 0, 0)$ is the free stream velocity of the main flow, assumed constant; (u, v, w) are time-averaged *mean* velocity components, relative to the main flow; (u', v', w') is the random difference between the instantaneous vector velocity at a point, and the mean velocity at that point.

Using a bar to denote time-averages, clearly $\overline{u'} = \overline{v'} = \overline{w'} = 0$. The average

$$(1*) \quad I = \overline{u'^2} + \overline{v'^2} + \overline{w'^2}$$

is called the *intensity* of turbulence; the ratio I/U^2 measures its relative intensity.

Turbulence involves momentum transfer ("molar diffusion") across surfaces. Thus ([31, p. 192] or [50, p. 674]) the average rate of momentum transfer across the (x, y) -plane is $\tau_{xy} = -\rho \overline{u'v'}$, in incompressible flow. There are similar "Reynolds stresses" across the other coordinate planes.

By analogy with the viscous shear stress caused by molecular diffusion, this momentum transfer (shear force) may be attributed to a fictitious kinematic "eddy viscosity" tensor ϵ_{ij} , defined by the equation $\tau_{ij} = -\rho \overline{u'_i u'_j} = \rho \epsilon_{ij} \partial u_i / \partial x_j$. In most turbulent flows, the molecular viscosity is much less than this eddy viscosity.

Generally speaking, the mean flow in turbulent jets and wakes is quite like that in laminar jets and wakes. Moreover the available asymptotic "theory" is again based on dimensional arguments and approximate conservation principles, so that §§7-11 of the present chapter will closely parallel Ch. XII.

To illustrate this analogy, consider the asymptotic theory of turbulent

wakes. Assuming nearly parallel flow, and neglecting molecular velocity, we are led to the approximate equations

$$(1^{**}) \quad U \frac{\partial u}{\partial x} \simeq \frac{du}{dt} \simeq \frac{\partial}{\partial y} \left(\epsilon_{xy} \frac{\partial u}{\partial y} \right).$$

If ϵ_{xy} were constant, this would give a perfect analog to Ch. XII, (10), and the associated asymptotic wake theory.

Unfortunately, not only is ϵ_{xy} a variable function of position, but there is no known way to predict it theoretically. Until the last two decades, turbulent velocity correlations such as $\overline{u'v'}$, $\overline{u'^2}$, etc. had never been accurately measured, and engineering estimates of the "eddy viscosity" were based on quasi-scientific "transfer" and "mixing length" concepts (see §6).

In the absence of a sound scientific theory, it seems advisable to approach the analysis of turbulent jets and wakes from a semi-empirical standpoint, and this is done below.

2. Flow separation. Wakes occur because, at sufficiently high speeds, the flow *separates* from an obstacle on both sides. Helmholtz [35, p. 219] suggested that, at least in the case of a flat plate, this was necessary to avoid infinite velocities at the edges, and hence infinite underpressures—i.e., that the explanation was to be sought in phenomena associated with cavitation. However, this explanation is wide of the mark. Actually, the Reynolds number $R = Ud/\nu$ is the decisive factor in determining separation, and hence any correct explanation must involve *viscosity* considerations.

The generally accepted explanation of separation is in terms of Prandtl's classic *boundary layer* concept. In the case of flows with *laminar* boundary layers, the velocity profile in the boundary layer may be approximately calculated if the pressure along the surface is known, using the "boundary layer approximation" to the Navier-Stokes equations already mentioned in Ch. XII, §8. However, the calculations are delicate and elaborate, and have only been carried out in a few cases. Since the results do not agree too closely with observation, we shall refer the reader to the literature¹ for details. We recall only the general qualitative picture: separation occurs where the pressure is rising, usually somewhat behind the maximum obstacle cross-section. The location of the separation point is theoretically independent of the Reynolds number R , for obstacles of a given shape, so long as the boundary layer stays laminar (for $R < 10^5$ say). However, the relative thickness of the boundary layer is proportional to \sqrt{R} . By proper

¹ An excellent discussion is in [31, Ch. IV]. For more recent results, see [74], and H. L. Dryden, *Recent advances in the mechanics of boundary layer flow*, *Advances in Applied Mechanics*, vol. 1, 1948, 1-40.

"streamlining" (rounding the nose, tapering the base, etc.), separation can be greatly delayed², and the wake correspondingly narrowed giving, a reduction in the total drag.

Above a "critical Reynolds number" R_{crit} , usually in the range $R = 100,000-500,000$, the boundary layer becomes turbulent; the separation points jump well back; and the drag coefficient is greatly reduced [31, p. 73]. Thus, with circular cylinders, the C_D drops from 1.0-1.2 to .3-.35; with spheres, it drops from .4-.45 to .1-.15 [31, pp. 15-16]. The value of R_{crit} for a given obstacle depends, not only on its shape and surface finish, but also on the turbulence of the impinging airstream [31, pp. 431, 495]. The theory of separation with turbulent boundary layers is in a very rudimentary state [31, pp. 438, 478], but the qualitative facts are similar to those stated above.

3. Base underpressure. In turbulent flow, the wake pressure is less the free stream pressure p_f by an appreciable fraction of the (incompressible) dynamic head $\frac{1}{2}\rho U^2$, U being the free stream velocity. As stated in Ch. II, §2, this causes real free streamlines to lie inside those predicted by ideal fluid theory [4, p. 53]. We shall now summarize some empirical facts about this wake underpressure.

Although the underpressure coefficient

$$(2) \quad -C_p = (p_f - p)/\frac{1}{2}\rho U^2$$

varies considerably over the wake, it is nearly constant along the base of most obstacles between the separation points; hence we define the "base underpressure coefficient" as

$$(2a) \quad Q = (p_f - p_B)/\frac{1}{2}\rho U^2,$$

where p_B is the "base pressure" (cf. Ch. I, (3b)).

For Reynolds numbers $R \gg 1$, in nearly incompressible flow (when the Mach number $M < 0.3$, say), Q is largely determined by the *shape* of the obstacle, except for a rapid jump near the "critical Reynolds number" $R_{crit} = 10^5 - 5 \times 10^5$. We shall give some useful numerical values.

For broadside flat plates, $Q \simeq 1.2-1.4$ [31, p. 37], giving $C_D \simeq 2$. For circular cylinders, $Q \simeq 1.0-1.2$ if $R < R_{crit}$, while $Q \simeq 0.2-0.5$ if $R > R_{crit}$ [31, pp. 24, 422], with wide scatter near $R = R_{crit}$ [31, Fig. 162]. For spheres, $Q \simeq 0.4$ if $R < R_{crit}$, while $Q \simeq -0.0-0.1$ if $R > R_{crit}$ [31, p. 497]. For discs, $Q \simeq 0.4$, giving $C_D \simeq 1.12$.

For long-range artillery applications, the base pressure on a flat-ended obstacle preceded by a long, cylindrical mid-section (see Fig. 1a) is of especial importance. In this case, the base underpressure coefficient de-

² The technique of delaying separation on airfoils is discussed in [20, vol. 3, p. 112].

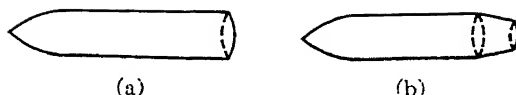


FIG. 1.

depends largely on the Mach number M , but also somewhat on the Reynolds number R , the surface temperature, and the length/diameter ratio.

As a function of M , in the range $1.2 < M < 3.7$, the relative base underpressure satisfies³ approximately

$$(3) \quad (p_f - p_w)/p_w = .176 - .26(M - 1) + .024(M - 1)^2.$$

Assuming this to be unaffected, one easily surmises that the drag can be significantly reduced by "boat-tailing", as in Fig. 1b, if the angle of boat-tailing is kept so small that separation is avoided—for then the wake cross-section is reduced.

However, the base underpressure also depends significantly⁴ on the Reynolds number R , and this effect is naturally much more pronounced with rounded and tapered (e.g., airfoil) shapes. The dependence on the length-diameter ratio is often said to be small if the latter exceeds one or two calibers⁵, but this is not certain.

4. Wake structure. In the original theory of Kirchhoff [47], the wake behind a plate was thought of as a "dead-water" region, consisting of fluid at rest. Actually, as pointed out in Ch. I, §5, this model is very inaccurate; it becomes especially unrealistic when generalized to streamlined obstacles. We shall now state some empirical facts about the complicated structure of real wakes.

Consider first the wake behind a flat disc (see Fig. 2). The wake just behind the disc is surrounded by a thin "vortex layer", which wavers and thickens under turbulence (especially if $R > R_{crit}$), becoming a turbulent "mixing zone" (§9). It is also sucked in towards the axis by the wake underpressure. As a result, it breaks up within a few diameters of the base if $R > 10^4$, while the wake underpressure is largely recovered^{5a}. The wake

³ A. C. Charters and R. A. Turetsky, BRL Rep. 623 (1948) Aberdeen, USA; see also F. K. Hill and R. A. Alpher, *J. aer. sci.* 16 (1949), 153-60; J. O. Reller and F. M. Hamaker NACA TN 3393 (1955).

⁴ See D. R. Chapman and E. W. Perkins, NACA Rep. 1036 (1951); D. R. Chapman, NACA TN 2137 (1950), *J. aer. sci.* 17 (1950), 812-13, and NACA TN 2787 (1952). For earlier work, see A. Eula, *L'Aerotechnica* (1940). For theoretical ideas, see H. H. Kurzweg, *J. aer. sci.* 18 (1951), 743-8; L. Crocco and L. Lees, *ibid.* 19 (1952), 649-76.

⁵ A. C. Charters, *J. aer. sci.* 14 (1947), 155-66, esp. p. 162. See however H. Rouse, "Fluid mechanics for hydraulic engineers," p. 228.

^{5a} See [31, pp. 552-6] and [36]. Accurate data seem hard to find.

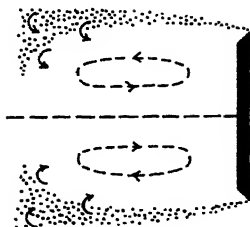


FIG. 2.

proper, inside the vortex layers, is filled with eddies; ordinarily, there is "backflow" in the middle as sketched.

Even at relatively low Reynolds numbers (say $R = 2,000$), the wake becomes turbulent a few diameters behind a bluff obstacle, and its mean velocity is nearly equal to the free stream velocity. The wake behind a flat plate at zero incidence is also turbulent⁶ for $R = 200,000$, a half plate-length behind the trailing edge. Presumably, this is due to the instability of laminar flow.

Spark photographs of supersonic flow past projectiles show an inverted cone of relatively quiet air behind the base, followed by a trail of turbulent fluid, which slowly widens through the medium of puff-like swirls. Outside this puffy "turbulent wake", the flow appears laminar (see Fig. 3). At a given point near the edge of the wake, therefore, one would expect the turbulence to come in intermittent bursts or puffs.

5. Wake turbulence. Townsend [81] has made a fundamental experimental study of incompressible wake turbulence behind a cylinder at $R = 8100$; we shall briefly summarize some of his findings^{6a}.

Just as in the supersonic case (end of §4), the turbulence at a given point comes in intermittent bursts, except in the central third ("core") of the wake; the fraction of time during which the flow is turbulent at a given point may be called the "intermittency factor" γ .

At a given distance x behind the obstacle, the intensity of turbulence in the "turbulent wake" is roughly the same everywhere, variations in γ with distance from the wake axis being much more important. The growth in the diameter of the wake seems to be due primarily to the large-scale eddies or "puffs", and not to the small-scale eddies which carry most of the turbulent energy. The small eddies are responsible for most of the kinematic "eddy viscosity" ϵ , defined by

$$(4) \quad \overline{u'v'} = -\epsilon \partial u / \partial y.$$

⁶ See [31, p. 573]; the data are due to Fage, Proc. roy. soc. A142 (1933), 560-2.

^{6a} See also S. Corrsin and M. S. Uberoi, NACA TN 2124.

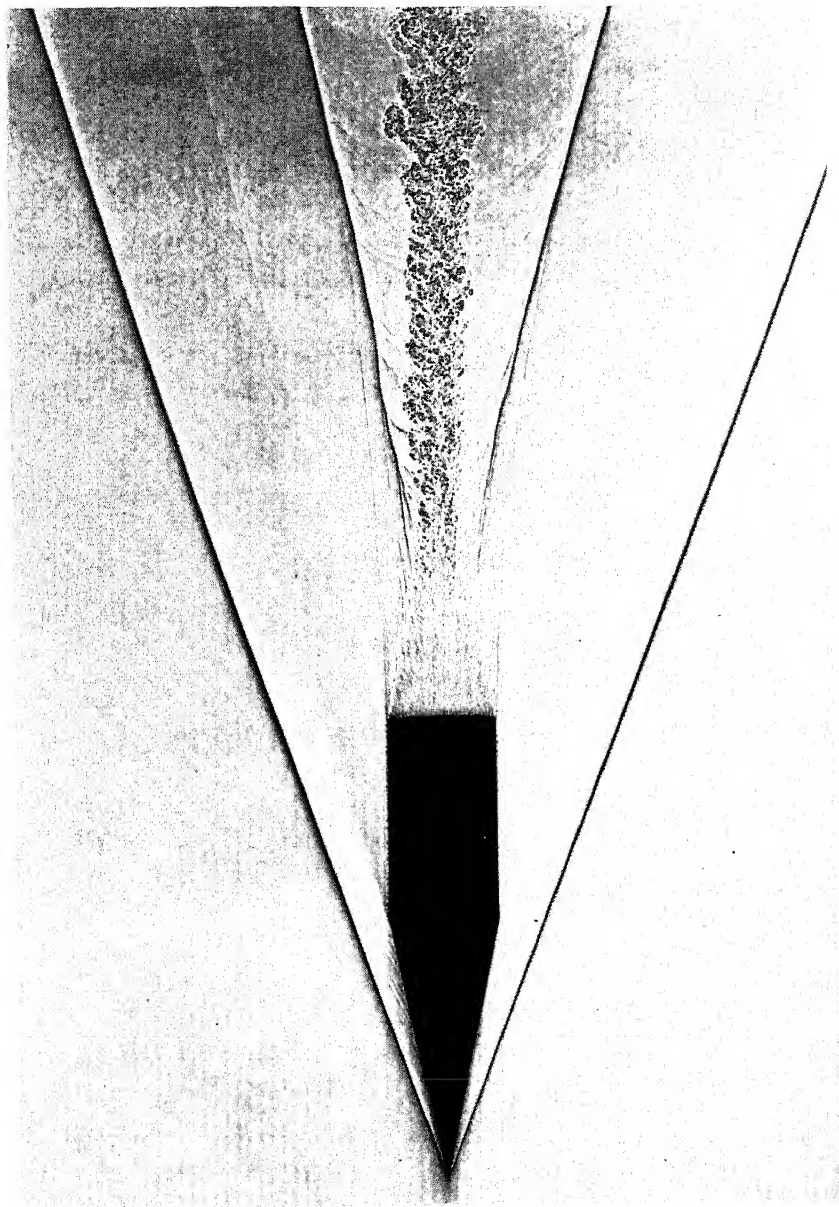


FIG. 3. Wake of supersonic projectile. (Courtesy Naval Ordnance Laboratory)

This eddy viscosity is nearly constant across most of the turbulent wake, if allowance is made for the "intermittency factor"—i.e., ϵ/γ is nearly constant at a fixed distance behind the obstacle.

Experimentally, the relative turbulence $I_r = I/U^2$ (see (1*)) decreases as the relative distance x/d behind the obstacle increases. Thus, $I_r \simeq 0.005$ when $x/d = 80$; $I_r \simeq 0.0026$ when $x/d = 120$; $I_r = 0.0018$ when $x/d = 160$. This corresponds roughly to a decay law $I \propto x^{-1.5}$. Assuming that the wake diameter grows like $x^{.5}$, the total turbulent energy thus decreases like $1/x$.

6. Mixing length concept. Prandtl has analyzed turbulence in nearly parallel flow, using a crude but useful "mixing length" concept, analogous to the concept of mean free path c in the kinetic theory of gases. Namely, Prandtl supposed that fluid masses are carried by turbulence for a "random walk" with mean step-length l perpendicular to the mean flow, with mean velocity \sqrt{l} (say).

By analogy with the classic formula $\nu \simeq kcv$ in kinetic theory, one has $\epsilon = kU^2 l$ in mixing length "theory", where k is a universal dimensionless constant, (say $k = \frac{1}{3}$). Thus, in two-dimensional flow parallel to the x -axis Prandtl deduced $I = l^2(\partial u/\partial y)^2$ and $\epsilon = l^2 |\partial u/\partial y|$, so that the "eddy shear stress" τ was

$$(5) \quad \tau = \rho \epsilon \partial u/\partial y = \rho l^2 |\partial u/\partial y| \cdot (\partial u/\partial y).$$

(For details, see [31, §§80–81] or [74, pp. 345–9].) He further assumed that, in a turbulent wake or jet, l should be proportional to the wake (jet) width $b(x)$, and constant inside the region of turbulence.

The preceding results lead to dimensionally correct formulas for the asymptotic rate of growth and mean velocity profile in wakes and jets, which will be derived in §§7, 11. But first, we shall mention some basic errors in Prandtl's assumptions, which are evident in the light of Townsend's data⁷.

First, the calculations ignore the basic fact of "intermittency". Second, (5) would imply that $\epsilon = 0$ on the wake axis, where $\partial u/\partial y = 0$, whereas Townsend's experiments [81, Figs. 3, 4] show that the eddy viscosity has its maximum on the jet axis! Related to this basic error in (5), is the fact that Prandtl's predicted $\overline{v'^2}$ vanishes on the jet axis, whereas actually $\overline{v'^2}$ is a maximum there.

Again, Prandtl's idea that there is just one "scale" for turbulence is quite incorrect; as already stated in §5, the large eddies are primarily responsible for lateral spreading of the turbulent wake, and the small eddies for momentum transfer. Moreover Prandtl's formulas say nothing about the rate

⁷ See G. Batchelor, *J. aer. sci.* 17 (1950), 441–5. Prandtl himself was aware of some objections to his arguments; see *ZaMM* 5 (1925), p. 136.

of turbulent energy decay, or Reynolds number effects. Finally, to fit experimental data with Prandtl's data, the "mixing length" must be a large fraction of the wake diameter, which is inconsistent with statistical deductions.

From a practical standpoint, Prandtl's original ideas also fail to predict the basic fact, that the turbulent convection of heat and mass exceed that of velocity. This important fact has been rationalized by Sir Geoffrey Taylor⁸, using a "vorticity transport" theory which is an improvement on Prandtl's "momentum transport" theory, but which is still somewhat oversimplified. We shall not try to summarize this interesting theory here.

A corresponding critique of "mixing length" theories, as applied to turbulent jets, will be given in §10.

7. Asymptotic wake behavior. The asymptotic mean velocity profile of turbulent wakes, far downstream, can be treated by considerations analogous to those of Ch. XII, §§5-9. In this analogy, the ν of Ch. XII, (10), must be replaced by a fictitious scalar "eddy viscosity" ϵ (see §1).

We begin by deducing some of the asymptotic dimensional formulas listed in Table I, p. 271. These follow from the momentum equations (21a)-(21b) of Ch. XII, and a Similarity Hypothesis. In this sense, as was first clearly pointed out by Squire [79], they are deduced essentially by *dimensional analysis*.

First we shall justify the asymptotic momentum equations used, which are

$$(6a) \quad D \simeq \int_w (H - h) dy \simeq \rho U \int_w -u(x, y) dy$$

in the plane, and

$$(6b) \quad D \simeq 2\pi \int_w (H - h)r dr \simeq 2\pi\rho U \int_w u(x, r)r dr$$

with axial symmetry. That is^{8a}, we will show that the turbulent velocity component (u', v', w'), described in §1 above, does not affect the final conclusions of Ch. XII, §9. To show this, we begin by noting that equations (19a)-(19b) of Ch. XII, §9, can be applied to turbulent flow if one includes the "Reynolds stress" forces of §1 above. To see the truth of this well-known fact, one need only remark that all quadratic time-averages such as

⁸ G. I. Taylor, Proc. roy. soc. A135 (1932), 685-705 and 697-700; and *ibid.* 151 (1935), 494-7 and 159 (1937), 499-502. See also [31, §§83-5] and [74, pp. 351-3]; H. Reichardt, ZAMM 24 (1944), 268-72 and [67].

^{8a} The argument at the end of Ch. XII, §8, can be generalized more simply; see §11 below. Turbulent wakes behind discs have been similarly studied by R. D. Cooper and M. Lutzky, DTMB Rep. 963 (1955).

$\overline{uu'}$, $\overline{wv'}$ which involve a time-independent factor vanish, and so does $\mu \oint (\partial v' / \partial x - \partial u' / \partial y) dx$.

To finish justifying (6a)–(6b), we observe that the hypotheses made in Cors. 1–2 of Ch. XII, §9, are equally valid for turbulent flow. Experimentally, the turbulence is negligible outside the wake W , while the total head

$$h = p + \frac{1}{2}\rho[(U + u)^2 + v^2 + w^2 + \overline{u'^2} + \overline{v'^2} + \overline{w'^2}]$$

differs negligibly outside W from the free stream total head $H = p_f + \frac{1}{2}\rho U^2$. Therefore, Cor. 1 of Ch. XII, §9, will follow as before, when modified to include terms in $\overline{u' u'}$. These quadratic terms will again drop out asymptotically, under the hypotheses of Cor. 2.

We next make again the Similarity Hypothesis⁹ of Ch. XII, §6, that all wake cross-sections have affinely similar velocity profiles. Thus, we assume

$$(7a) \quad u(x, y) = x^{-p} f(y/x^q) \quad \text{in the plane,}$$

$$(7b) \quad u(x, r) = x^{-p} g(r/x^q) \quad \text{in space.}$$

Substituting back into (6a)–(6b), we get

$$(8a) \quad p = q \quad \text{in plane flow, and}$$

$$(8b) \quad p = 2q \quad \text{with axial symmetry.}$$

The dimensional analysis also involves an assumption about eddy viscosity similarity:

$$(9) \quad \overline{u'v'} = x^{-2p} h(\eta), \quad \text{where } \eta = y/x^q \text{ or } r/x^q.$$

This is equivalent to assuming that $I \propto u^2(x, 0)h(\eta)$, which is plausible, and also agrees dimensionally with Prandtl's mixing length concept. Substituted into the simplified equation of motion, $U \partial u / \partial x = \partial(\overline{u'v'}) / \partial y$, (9) amounts to putting $-p - 1 = -2p - q$ in the exponent of x , or

$$(9') \quad p + q = 1 \quad (\text{homogeneity condition}).$$

From (8a) and (9') we conclude that the turbulent wake breadth $b(x)$ in plane flow satisfies asymptotically

$$(10a) \quad b = Bx^{\frac{1}{2}}, \quad u = x^{-\frac{1}{2}} f(y/Bx^{\frac{1}{2}}).$$

The prediction $b \propto \sqrt{x}$ has been approximately confirmed experimentally

⁹ Prandtl, Proc. sec. int. congr. appl. mech. Zurich (1926), 62–74, made a much more special hypothesis. See [31, §§252, 254] and [74, p. 447]. Curiously, the turbulent case was treated before the laminar one.

[74, p. 450] and [81, Fig. 7]. Again, with *axially symmetric* turbulent wakes, we conclude, similarly,

$$(10b) \quad c = Cx^{\frac{3}{2}}, \quad u = x^{-\frac{1}{2}}g(r/Cx^{\frac{3}{2}});$$

see [31, §254] for details. Thus, turbulent wakes spread more slowly in axially symmetric than in plane flow.

By making specific assumptions about the dimensionless mixing length $\lambda(\eta)$, one can also calculate theoretical universal velocity profiles—i.e., one can determine $f(\eta)$ and $g(\eta)$. Thus, using Prandtl's assumption (5), Schlichting¹⁰ calculated for (10a),

$$(11a) \quad f(\eta) = (1 - \eta^{1.5})^2.$$

In the axially symmetric case, (5) gives likewise, for (10b),

$$(11b) \quad g(\eta) = (1 - \eta^{1.5})^2.$$

These formulas agree quite well with experiment, provided the empirical constant B and the plane $x = 0$ are chosen¹¹ to fit the data.

However, as observed by Reichardt [67] and Squire [79], one should not attach too much significance to this agreement. It is well known that the boundary layer equations used are of parabolic type, like the heat conduction equation [31, p. 127], and that any such "diffusion-type" equation gives asymptotically a bell-shaped distribution from an initially concentrated source. Thus [74, p. 449], the velocity profiles deduced from (11a)–(11b) differ negligibly from the Gaussian error curve obtained from the ordinary heat conduction equation, as in Ch. XII, §5.

Hence we shall not discuss further the large literature on turbulent wakes, based on "mixing length" concepts¹².

8. Wakes with hydrodynamical self-propulsion. The dimensional formulas of Table I, Ch. XII, are not applicable to the wakes behind hydrodynamically self-propelled objects (boats or airplanes). If the propeller thrust is included, $D = 0$ in such cases, and so the momentum equation

¹⁰ Ing. Archiv 1 (1930), 533–71; [74, p. 449], [31, p. 583]. W. Tollmien, Ing. Archiv 4 (1933), 1–15, tried another assumption. For the axially symmetric case, see L. M. Swain, Proc. roy. soc. A125 (1929), 647–59, or [31, §254].

¹¹ See the refs. of fnnt. 10. Also, A. A. Hall and G. S. Hislop, Proc. Camb. Phil. Soc. 34 (1938), 345–50, [67, Fig. 6], and M. Kurihara, Appl. mech. revs. 5 (1952), No. 830.

¹² See [24, §§252–5] and refs. given there, for an account of researches based on such hypotheses. See also S. Tomotika, Proc. roy. soc. 165 (1938), 65–72; P. Y. Chou, Chinese J. Phys. 4 (1940), 1–33; C. C. Lin, Sci. Reps. Natl. Tsing Hua Univ. 4 (1947), 419–50; G. D. Mattioli, *Teoria dinamica de regimi fluidi turbulenti*, Padova, 1937.

$\int_{-\infty}^{\infty} u \, dy = 0$ gives no relation between p and q . We shall now derive alternative formulas for p and q , applicable to this case.

In the *laminar* case, of constant viscosity ν , the facts are suggested by the considerations of Ch. XII, §5. Thus, in plane flow, we assume $U \partial u / \partial x = \nu \partial^2 u / \partial y^2$, and symmetry about the x -axis. In this case, it is readily shown (integrating by parts) that the second moment

$$(12) \quad N = \int_{-\infty}^{\infty} y^2 u(x, y) \, dy$$

must be independent of x . Assuming $N \neq 0$, we have the asymptotic formula

$$(12a) \quad u = A x^{-3/2} H_2(\eta) e^{-\eta^2} = A x^{-3/2} h(\eta),$$

where $H_2(\eta)$ is a Hermite polynomial in $\eta = y/(2\nu x/U)^{1/2}$, and A is proportional to N . In laminar axially symmetric flow, $u \propto x^{-2}$ similarly. Thus, in both cases, *the velocity decay is much more rapid than in ordinary wakes.*

The *turbulent* case is more difficult. The similarity condition (12a) is still valid. The moment condition (12) cannot be strictly justified: integration by parts gives

$$\begin{aligned} \frac{\partial}{\partial x} \int y^2 u \, dy &= \int y^2 \frac{\partial}{\partial y} \left[\epsilon \frac{\partial u}{\partial y} \right] dy && \text{by} && (1**) \\ &= - \int \left(\epsilon \frac{\partial u}{\partial y} \right) y \, dy = - \int \epsilon y \, du = \int u \, d(\epsilon y). \end{aligned}$$

If ϵ were independent of y , this would vanish. We shall assume that the variation in ϵ is negligible. That is, we shall assume that the momentum equations for laminar flow are still valid in turbulent wakes. This assumption amounts to

$$(14a) \quad \int y^2 u \, dy = N \neq 0, \quad \text{or} \quad p = 3q,$$

in plane flow, and

$$(14b) \quad \int r^2 u r \, dr = N^* \neq 0, \quad \text{or} \quad p = 4q,$$

with axial symmetry.

We conclude from (8c) and (14a) that

$$(15a) \quad u = x^{-3/4} f(y/\sqrt[4]{x})$$

in the turbulent wake behind a hydrodynamically self-propelled cylinder, and

$$(15b) \quad u = x^{-4/5} g(y/\sqrt[5]{x})$$

for hydrodynamical self-propulsion in space. This implies $R \propto 1/\sqrt{x}$ in the plane, and $R \propto x^{-3/5}$ in space.

9. Mixing zone. The simplest problem in mixing concerns the turbulent interface between two fluids moving tangentially with relative velocity U , and having an initially plane interface. In the case of equal densities, this can be interpreted as the problem of Helmholtz instability for large t . Helmholtz instability of the same configuration for small t has been discussed in Ch. XI, §14.

The preceding mixing problem was first treated theoretically by Tolmien¹³, using Prandtl's "mixing length" concept. Because this concept is not really valid (see §6), we shall only consider dimensional equations.

The relative velocity U is independent of x ; hence if we make the Similarity Hypothesis of (9), that the "mixing length" is proportional to the breadth $b(x)$ of the "mixing zone", we get $\epsilon \propto b(x)$. This corresponds to the formulas

$$(16) \quad u = f(y/x), \quad v = g(y/x)$$

and to a *wedge-shaped mixing zone*, after turbulence has been initiated.

Empirically, such a mixing zone is found, the breadth $b(x)$ being about $.225x$. The distribution of mean velocity is approximately represented ([67] and [57, Figs. 13-15]) by

$$(16^*) \quad u = \frac{1}{2}U[1 + \operatorname{erf}(11y/x)].$$

However, the theoretical interpretation of the existing experimental data is confused¹⁴.

10. Structure of jets. Above a sufficiently high Reynolds number, say if $R > 1200$ [59, p. 57], free homogeneous jets ordinarily become turbulent. The structure of such a jet from a circular orifice may be pictured roughly as follows.

Near the orifice, the jet boundary is diffused into a highly turbulent, annular "mixing zone" with wedge-shaped profile (Fig. 4), as in §9. This gradually eats into the undisturbed central core of the jet. Though the volumetric discharge can be approximately predicted¹⁵ by potential theory,

¹³ ZaMM 6 (1926), 468-78 (NACA TN 1085 (1945)); see also [31, p. 597], [74, p. 446], and [20, v. 3, pp. 162-78]. Also, work by Pai and Bershader in J. aer. sci. 16 (1949), 463-9, J. appl. phys. 21 (1950), 616, Quar. appl. math. 10 (1952), 141-8, and J. appl. mech. 22 (1955), 41-7.

¹⁴ Relevant refs. include: Forthmann, Ing. Archiv 5 (1934), 42-54; A. M. Kuethe, J. appl. mech. 2 (1935), 87-95; H. Görtler, ZaMM 22 (1942) 244-54; [67]; S. Corrsin, J. aer. sci. 18 (1951), 773-4. The critical discussion of [67] in Appl. mech. revs. 3502 (1952) is quite illuminating; see also [64, Ch. VIII].

¹⁵ Variations of pressure in the mixing zone up to 4% of the total head have been reported by M. Barat, Comptes rendus 238 (1954), 445-7.

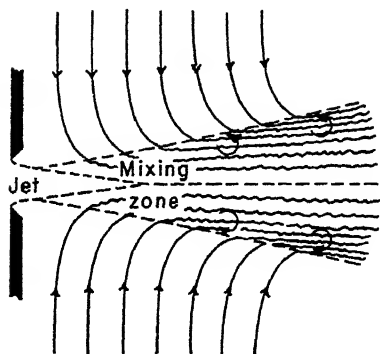


FIG. 4.

as in Ch. X, the angle of spread of the mixing zone causes the non-turbulent conical core (Fig. 4) of the jet to be eaten up after four or five diameters. After about eight orifice diameters [31, p. 596], the asymptotic turbulent jet regime has become pretty well established.

Asymptotically, such round turbulent jets spread *conically* at angles in the range¹⁷ 20° – 25° ; the mean velocity profile $u(r/Bx)$ is bell-shaped, and can be closely fitted by a normal error curve [67]. Earlier data were obtained by Förthmann¹⁸.

The structure of the plane turbulent jet from a slit is quite similar, apart from obvious modifications. The mean velocity profile can again be fitted by a normal error curve [31, Fig. 235]; the jet breadth $b(x)$ is again asymptotically proportional to $x - x_1$, with an angle of spread 25° – 30° .

Although jet behavior is apparent^{18a} little affected by the turbulence levels up to 8%, it may be substantially affected by the jet mean velocity profile as it leaves the orifice.

11. Mixing length “theories”. As in the cases of laminar jets and turbulent wakes, the asymptotic dimensional behavior of turbulent jets can be deduced from momentum and similarity considerations.

¹⁷ P. Ruden, *Naturwiss.* 21 (1933), 375–8; A. M. Kuethe, *J. appl. mech.* 2 (1935), 87–95; [59, p. 57]. See also H. B. Squire, *Aircraft Engineering* 22 (1950), 62–7; M. L. Albertson, Y. B. Dai, R. A. Jensen and Hunter Rouse, *Trans. Am. soc. civ. eng.* 74 (1948), 1571–96; “Some aspects of fluid flow” (Inst. of phys. conference, London, 1953), p. 10; H. G. Elrod, *Appl. mech. revs.* 7 (1954), No. 3941.

¹⁸ E. Förthmann, *Ing. Archiv* 5 (1934), 42–54; the data are reproduced in [31, Fig. 236], and other refs. given. See also D. Citrini, three papers in *L’energia elettrica*, 1946–7.

^{18a} J. F. Taylor and E. W. Comings, *Proc. Midwest conf. fluid dyn.*, Ann Arbor, 1951, 204–15.

Thus, neglecting the pressure variation along the jet, and shear stresses outside the jet, the boundary layer approximation gives

$$(17a) \quad \int u^2 dy = \text{const.} \quad \text{for plane jets}$$

$$(17b) \quad \int u^2 dy dz = \text{const.} \quad \text{for round jets,}$$

just as in formulas (28a)–(28b) of Ch. XII. We make also the Similarity Hypothesis (Ch. XII, (22)),

$$(18a) \quad u = x^{-2} f(y/x^q) \quad \text{for plane jets}$$

$$(18b) \quad u = x^{-2} g(r/x^q) \quad \text{for round jets.}$$

(Empirically, by §10, $q = 1$ in both cases.) In general, (17a)–(18a) imply

$$(19a) \quad q = 2p \quad \text{with plane jets,}$$

while (17b)–(18b) imply

$$(19b) \quad q = p \quad \text{with round jets.}$$

This is just as in Ch. XII, §14 and §13, respectively.

To complete our dimensional analysis, we make the Turbulence Similarity Hypothesis $\overline{u'v'} \propto x^{-2p}$ already made in (9), and for the same reason. (More generally, $I \propto x^{-2p}$ is plausible.)

The boundary layer equations are

$$(20a) \quad u \frac{\partial u}{\partial x} + v \frac{\partial u}{\partial y} + u' \frac{\partial u'}{\partial x} = \frac{\partial}{\partial y} \left(\epsilon \frac{\partial u}{\partial y} \right) = \frac{\partial}{\partial y} \overline{u'v'}$$

in plane flow, and a similar equation involving a factor r in axially symmetric flow. These are compatible with our similarity hypothesis if and only if $q - p - 1 = -p$, or

$$(20^*) \quad q = 1 \quad \text{and} \quad v = x^{-p} k(y/x^q).$$

Combining, we get the similarity rules

$$(21a) \quad u = x^{-\frac{1}{2}} f(y/x) \quad \text{for plane turbulent jets,}$$

$$(21b) \quad u = x^{-1} g(r/x) \quad \text{for round turbulent jets.}$$

These agree with observation¹⁷; as in the laminar case, the angle of spread is theoretically indeterminate.

Note that the total jet flux $\int u dy \propto x^{\frac{1}{2}}$ for plane jets from slits, while

$\iint u \, dy \, dz \propto x$ for round jets. Thus, the fluid around a homogeneous turbulent jet is entrained into the jet as if by a uniform half-line of sinks.

The observed mean jet velocity profile, given by a normal (i.e., Gaussian) error curve is consistent with the hypothesis of turbulent diffusion. If ϵ is calculated using some transfer or mixing length hypothesis, then (21a)–(21b) reduce the boundary layer equations to ordinary differential equations, determining $u(x, y)$ up to the angle of spread.

Such calculations were made by Tollmien^{18b} for the axially symmetric case of round jets, and by Schlichting^{18b} for plane jets. Writing $\eta = y/Bx$, the calculated velocity profiles are given by

$$(22a) \quad u = c(1 - \tan^2 \eta) \quad \text{for plane jets,}$$

$$(22b) \quad u = c/(1 + \eta^2) \quad \text{for round jets;}$$

they are more peaked than the actual profiles.

Similar calculations, based on Taylor's vorticity transfer theory, have been made by Howarth and Tomotika¹⁹. Taylor's qualitative ideas are supported by the observations of Hinze and van der Hegge-Zijnen, which show that as in the case of wakes, heat and mass diffuse about 20 % more rapidly than momentum in turbulent jets.

However, it has been shown by Liepmann and Laufer [57], through hot wire measurements of turbulence²⁰, that the effective "mixing length" (which averages about 4 %) of the total jet width [31, p. 594] is variable across the jet, contrary to the assumptions of Prandtl-Görtler and Tollmien, and that their calculated shear-stress distribution is quite incorrect.

12. Further literature. The known facts about turbulent jets are not limited to the preceding topics.

Thus, because of their importance for aircraft jet propulsion, compound and coaxial jets have been studied by various authors²¹.

Another interesting study concerns the diffusion of smoke from a chimney. When carried by wind, the initial region of diffusion is *conical*, with

^{18b} W. Tollmien, *ZaMM* 6 (1926), 468–78; see also W. Szablewski, NACA TM 1311 (Ing. Archiv 20 (1952), 67–72). H. Schlichting, *Ing. Archiv* 1 (1930), 533–71; [74, pp. 452–4].

¹⁹ L. Howarth, *Proc. Camb. phil. soc.* 34 (1938), 185–94; S. Tomotika, *Proc. roy. soc. A* 165 (1938), 53–72; J. O. Hinze and B. G. van der Hegge-Zijnen, *Appl. sci. res. A* 1 (1949), 435–61, and *Proc. seventh int. congr. appl. mech.* London (1948), 286–99.

²⁰ See also B. H. Little and S. W. Wilbur, NACA TN 2361 (1951).

²¹ F. Landis and A. H. Shapiro, *Heat transfer inst.* Stanford (1951), 130–46; W. R. Keagy and A. E. Weller, *Appl. mech. revs.* 1534 (1950); I. Tani and Y. Kobashi, *ibid.* 1741 (1955); Y. V. G. Acharya, *ibid.* 2150 (1955).

an angle of spread which depends on the turbulence of the atmosphere. However, when the width of the jet exceeds the scale of atmospheric turbulence, the tendency towards the more familiar parabolic diffusion law $r^2 = cx = cUt$ will become dominant.—In still air, the mean rate of rise under thermal convection is roughly proportional to the cube root of the distance above the chimney²².

Finally, the important subject of the noise of turbulent jets has recently been studied, especially by Lighthill²³. It has been deduced theoretically, and roughly confirmed experimentally²⁴, that the maximum intensity is at 45° to the jet axis (corresponding to acoustic quadruples), and that the ratio of sound energy to jet energy is proportional to $M^5 = U^5/c^5$, the fifth power of the Mach number, independent of $R = Ud/\nu$. (Thus, for a given jet, the noise power is proportional to U^8 .)

²² O. G. Sutton, "Micrometeorology", New York, 1953, pp. 295-300. See also W. Schmidt, *ZaMM* 21 (1941), 265-78 and 351-63.

²³ *Proc. roy. soc. A* 211 (1952), 564-82.

²⁴ W. L. Nyborg et al., *J. acoust. soc. Am.* 24 (1952), 293-304; H. M. Fitzpatrick and R. Lee, *DTMB Reps.* 835 (1952) and 868 (1953); E. J. Richards, *J. roy. aer. soc.* 57 (1953), 318-42; E. G. Richardson, *Nature* 172 (1953), 54-8.

CHAPTER XV

MISCELLANEOUS EXPERIMENTAL FACTS

1. General discussion. In Chs. II–XI, it was generally assumed that cavitation occurred spontaneously in liquids as soon as the local pressure dropped below the vapor pressure (see Ch. I, §6),—i.e., as soon as $(C_p)_{\max} > Q$. Assuming the Bernoulli equation, this implies that cavitation should occur when $Q < Q_i = (u_m/u_f)^2 - 1$, where u_m is the maximum velocity and $u_f = U$ is the free stream velocity. It was also assumed that liquid jets in air had smooth boundaries, whose location was determined by the “free boundary” condition of constant boundary pressure.

Actually, the situation is much more complex. Especially, *surface tension* plays a dominant role in many phenomena, to such an extent that the deductions of Chs. II–XI may not even give a first approximation to the true facts. In other cases, traces of dissolved impurities may exercise a decisive influence. In still other cases, such apparently extraneous physical variables as noise level, acoustic stimulation, surface electrification, surface contamination, and turbulence level may play an essential role. Even the interaction of two or more such variables may be involved—e.g., of surface tension and viscosity. Finally, hysteresis effects may be very important.

Because of this complexity, it has seemed desirable to devote a final chapter to the discussion of various experimental phenomena, which cannot be deduced mathematically from the assumptions used in Chs. II–XI, or even from the Navier-Stokes equations. In this chapter, the quantitative deductions will be fragmentary, and the subject matter arranged according to the physical variables involved, rather than the mathematical methods.

2. Bubbling and boiling. When a teakettle is slowly heated, it is easily verified that air bubbles form on the bottom and rise to the surface, long before true boiling (steam formation) occurs. If, however, boiled water is reheated, this no longer occurs. Again, if one shakes a ginger ale bottle, a tremendous volume of gas is released internally.

These are simple illustrations of the fact that cavitation is strongly influenced by the *gas content* of a liquid. It is essential to distinguish between the bubbling or *effervescence* of dissolved gases, and true cavitation in a pure liquid.

Thus, ordinary tap water is not pure or homogeneous. It ordinarily contains dissolved air and other gases, and also undissolved gas “nuclei”

attached to minute solid particles. The gas will gradually come out of solution when the ratio

$$\alpha_1 = (\text{dissolved gas volume})/(\text{volume of water})$$

exceeds a certain "saturation ratio" $\alpha_s = \alpha_s(p, T)$. Ordinarily, α_s is roughly proportional to the pressure p (Henry's Law), and is a decreasing function of the temperature T . Hence we write

$$(1) \quad \alpha_s = (p/p_{at})\alpha_s(p_{at}, T).$$

Thus, under normal atmospheric conditions, α_s is about 2% for air in water, about one for CO_2 in water, and several hundred for NH_3 in water¹. (In the latter cases, chemical affinity plays an obvious and important role.)

When the pressure is reduced, or if heat is applied, we will ultimately have $\alpha_s < \alpha_1$. When this happens, effervescence (bubbling) may be expected, even though the pressure is still far above the vapor pressure of water. This gives a first rough criterion for effervescence, when the pressure alone is varied:

$$(2a) \quad p_{eff}/p_{at} = \alpha_1/\alpha_s(p_{at}, T).$$

Thus, a nearly saturated liquid will effervesce gradually when the pressure is reduced only slightly below atmospheric pressure.

However, once water has been thoroughly boiled, the critical pressure for effervescence has been lowered *ipso facto* to the vapor pressure of water, and the water may be said to be "degassed". If the water is then cooled and boiled again, no effervescent bubbling will be observed, and vapor bubbles rising into cooler water will collapse with a sharp click.

3. Tensile strength of liquids. If filtered water is degassed inside a clean container, it can actually sustain very large tensions. Thus, just as effervescence (bubbling cavitation) can occur when $p > p_v$, so cavitation-free flow is possible when $p \ll p_v$. The criterion (1b) of Ch. I may therefore fail in either direction!

The ability of liquids to sustain large tensions is easily explained by a consideration of the effects of *surface tension*. We recall that the pressure p_e inside a small bubble of radius r is related to the pressure p outside it by the formula

$$(3) \quad p_e = p + 2\gamma/r, \quad \text{or} \quad p = p_e - 2\gamma/r,$$

¹ See Smithsonian Physical Tables, 8th ed., p. 221. For a general discussion, see M. D. Gernez, Comptes rendus 63 (1866), 883-8. Also, P. H. Schweitzer and V. G. Szebehely, J. appl. phys. 21 (1950), 1218-24.

where γ is the surface tension. Neglecting the slight difference between $p_e - p_v$ and zero, we should expect the tensile strength to be about

$$(3') \quad -P = (2\gamma/r)_{\min} = 2\gamma/r_{\max},$$

where r_{\max} is the radius of the largest bubble present. For pure water, $\gamma = 75$ dynes/cm. Hence we have the following rough table

$-P$	0.1 atm.	1 atm.	10 atm.	100 atm.	1000 atm.
r_{\max}	0.015 mm	0.0015 mm	0.15 μ	150 \AA	15 \AA

This suggests that, if *all* bubbles could be eliminated down to molecular dimensions (about 1 \AA), tensions of the order of 10,000 atmospheres could be sustained.

For many years, this simple theoretical picture was generally accepted. It seemed especially plausible, because the order of magnitude of the predicted tensile strength agreed with that obtained from the a/V^2 term in the van der Waals equation of state $(p + a/V^2)(V - b) = RT$. However very different ideas are accepted today.

It seems most realistic to postulate the presence in all real liquids of minute gas *nuclei*, adhering to minute wall crevices or to suspended solid (dust) particles². Gas-filled and vapor bubbles alike form by evaporation into these nuclei. (This explains the formation of successive bubbles from the same point on the surface of a ginger ale bottle, and why gas does not come out of solution from the interior of a dust-free liquid.)

It may be that, even if no such nuclei are present initially, they will form spontaneously at a predictable statistical rate. At a tension $-P$, the free "nucleation energy" required would be

$$(4) \quad W_{\max} = (4\pi r^2 \gamma - \frac{4}{3} r^3 (-P))_{\max} = 16\pi \gamma^3 / 3(-P)^2.$$

This leads to a predicted tensile strength of the order of 1000 atm. for pure water³.

However, observed tensile strengths of pure water have not exceeded 30–50 atm.⁴, although figures as high as 250 atm. have been quoted in the

² F. C. Henrici, Ann. der Physik 147 (1872), 555–69; C. Tomlinson, Phil. Mag. 45 (1873), 276–83. Also, E. N. Harvey et al., J. cell. comp. phys. 24 (1944), 1–22; J. appl. phys. 18 (1947), 162–72; J. Am. chem. soc. 67 (1945), 156–7 and 68 (1946), 2119–20. It also makes a difference whether the container surface is "hydrophilic" or "hydrophobic". The subject is reviewed by A. Weyl and E. C. Marboe, Research 2 (1949), 19–28.

³ L. Bernath, Ind. Eng. Chem. 44 (1952), 1310–13. The ideas are due to M. Volmer, "Kinetik der Phasenbildung", 1939.

⁴ H. N. V. Temperley and L. G. Chambers, Proc. phys. soc. 58 (1946), 420–43, and 59 (1947), 199–208. See also [8], and Scott et al., J. chem. phys. 16 (1948), 495–502.

literature, following the pioneer work of Berthelot⁵. Other pure liquids also have substantial tensile strength, usually amounting to tens of atmospheres⁶.

The preceding ideas apply to effervescence, causing formula (2a) of §2 to be replaced by

$$(2b) \quad p_{\text{eff}} = -(2\gamma/r_{\text{max}}) + p_{\text{at}}\alpha_1/\alpha_s(p_{\text{at}}, T).$$

Thus bubbles below a certain critical size will not grow, but will shrink to a point. This explains qualitatively why pressurized water can be "super-charged": all interior nuclei are eliminated.

Since sea and tap water normally contain bubbles whose diameter exceeds 0.01 mm, it is also easy to see why cavitation normally occurs when $p < p_v$,—i.e., why the simple criterion of Ch. I, §3, is applicable under many practical circumstances. It should however also be easy to see why, in steam boilers, precautions must be taken to avoid superheating⁷ and resultant cavitation "bumping" on the walls.

Finally, it should be remembered that the surface tension γ may be reduced by half, through dissolved impurities having a concentration as low as 0.003 per cent⁸. This illustrates the extreme difficulty of making accurate theoretical predictions.

4. Bubble dynamics. In §§2-3, gradual cavitation has been discussed, and the rate of bubble growth largely ignored. The rate of bubble growth may be influenced by the time required for diffusion, and other factors.

In the case of gas bubbles, growing to and above visible size, good predictions may be made on the basis of relatively simple calculations⁹. However, in the case of steam bubbles in slightly superheated water, heat transfer by vaporization plays an important part, and the calculations are much

⁵ J. Berthelot, *Ann. de chimie phys.* 30 (1857), 232-7. See also M. Gernez, *Comptes Rendus* 63 (1866), 883-8, and J. C. Maxwell, "Theory of heat", London, 1899, pp. 291-2; N. E. Dorsey, "Properties of ordinary water substance", New York, 1940, pp. 179-81 and 620-3; R. S. Vincent, *Proc. phys. soc.* 53 (1941), 126-40, and 55 (1943), 41-8 and 376-82; L. S. Briggs, *J. appl. phys.* 26 (1955), 1001-4.

⁶ Values ranging from 3.5 atm. for liquid nitrogen (A. D. Misener and F. T. Hedgcock, *Nature* 171 (1953), 835-6) to 419 atm. for mercury (L. J. Briggs, *J. appl. phys.* 24 (1953), 488-90), have been reported.

⁷ In 1846, Donny heated water to 135°C without boiling; somewhat later, Dufour obtained 180°C; Kenrich, Gilbert and Wismer have obtained 270°C (*J. phys. chem.* 28 (1924), 1297-1307); see Dorsey, *op. cit. supra*, pp. 579-82.

⁸ N. K. Adam, "The physics and chemistry of surfaces", 3d ed. (1948), Oxford Univ. Press, p. 129.

⁹ P. S. Epstein and M. S. Plesset, *J. chem. phys.* 18 (1950), 1505-9.

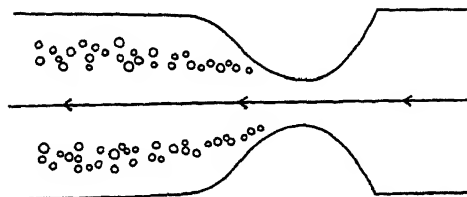


FIG. 1.

more complicated¹⁰. The simple theory of Ch. XI, §2 is grossly inapplicable to either case. To a smaller extent, diffusion effects influence *incipient cavitation*, which we shall now discuss.

In Ch. I, §6, incipient cavitation was defined as the rapid formation and collapse of minute bubbles, in local regions of negative pressure in high-speed flow. For regions 1 cm.-50 cm. in length at flow speeds of 15 meters/sec., corresponding by Bernoulli's equation to a reduction in pressure of one atmosphere in water, the total elapsed time will thus be in the range 0.6-30 milliseconds. We can thus regard this as the normal *time scale for incipient cavitation*.

Following Reynolds¹¹, one can produce incipient cavitation in a "Reynolds tube" (Venturi nozzle) having a narrow constriction (see Fig. 1). Alternatively, incipient cavitation occurs at certain speeds around torpedo models placed in high-speed water tunnels, and near marine propellers.

In all cases, the physical principles involved are the same. As in ordinary boiling, microscopic gas nuclei seem to be required to initiate the growth of cavities. Due to the short time-scale, there is insufficient time for effervescence to be appreciable (i.e., for dissolved gases to diffuse to the bubble surface and come out of solution), unless the initiating gas nuclei are plentiful and fairly large. Thus, effervescence is not ordinarily visible until the pressure has fallen to 0.1 atmospheres or less¹².

There is considerable scatter in the data. This scatter may be due partly to the fact that the critical pressure p_c for cavitation depends on the statistical distribution of gas nuclei, and not merely on the percentage of air content by volume usually measured. It may also depend on the presence of "vortex cavitation", or cavitation near vortex cores having a pressure

¹⁰ M. S. Plesset and S. A. Zwick, J. appl. phys. 23 (1952), 95-8, and J. math. phys. MIT 33 (1955), 308-30; P. Dergarabedian, J. appl. mech. 20 (1953), 537-45; H. K. Forster and N. Zuber, *ibid.* 25 (1954), 474-8.

¹¹ O. Reynolds, "Papers on mechanical and physical subjects", vol. 2, pp. 578-87.

¹² See J. C. Hunsaker, Mech. Eng. 57 (1935), 211-16. The first accurate quantitative data were provided by F. Numachi, Ing. Archiv 7 (1936), 396-409, and Tech. Reps. Tohoku Imp. Univ. 12 (1938), 422-61, 529-42, 591-625; see also S. F. Crump, DTMB Reps. 575 (1949) and 770 (1951).

well below the average local pressure. Such vortex cores commonly accompany flow separation.

As soon as bubbles are so large that $2\gamma/r < 0.1$ atm.—e.g., when $r > 0.15$ mm. in water,—surface tension effects become relatively small, and the approximation $p_e = p_v$ already analyzed in Ch. XI, §2, gives a fairly reliable picture of the radius-time curve (i.e., of bubble growth and collapse). However, the laws of microscopic bubble growth are still not clearly understood.

Temperature gradients. In the opposite extreme case, variations in surface tension due to temperature gradients may dominate the dynamic behavior of small bubbles in highly viscous liquids. This curious effect may, for example, make liquid films creep up walls, cause bubbles to descend against gravity, or deform the free surface of an otherwise static liquid so as to produce a flow.

Thus, it has been noted by A. V. Hershey^{12a} that a layer of liquid of thickness δ , with surface tension $\gamma = a + bT$, can be in dynamic equilibrium on a plate making an angle α with the horizontal. The condition for parallel mass-flow equilibrium is that the tangential velocity profile $u = U[3(y/\delta) - 2](y/\delta)$ be parabolic; the viscous and gravity forces will then be in equilibrium provided $\rho g \delta^2 \sin \alpha = 6\mu U$, or $6\nu U/\delta^2 = g \sin \alpha$. The associated tangential viscous stress on the free surface is $4\mu U/\delta$; this will be balanced by traction due to the effect of the tangential temperature gradient ∇T on the surface tension, provided $4\mu U/\delta = b\nabla T$. Thus, in equilibrium, $b\nabla T = (2\rho g \delta/3) \sin \alpha$ (not $b\nabla T = \rho g \delta \sin \alpha$, as superficial consideration might suggest).

The equations for the static equilibrium of a spherical bubble of radius R in a vertical temperature gradient ∇T is similarly^{12b} $b\nabla T = 2\rho g R/3$. This equation may be deduced by considering the Stokes-like flow past a fluid sphere (cf. Ch. XII, §3), as derived by Rybczynski and Hadamard [50, p. 599], and allowing for the additional tangential stress and normal pressure due to the variation of superficial tension on the surface of the bubble. The distortion of the temperature field due to the presence of the bubble has been considered in this equation.

Finally, it may be shown that, under certain conditions, the convective flow in Bénard cells is similarly determined by thermally produced variations in superficial tension on the free surface^{12b}.

^{12a} Phys. rev. 56 (1939), 203–205.

^{12b} Unpublished result of M. J. Block of Baird Associates and his collaborators N. O. Young and J. S. Goldstein. Mr. Block has communicated his analysis and observations on Bénard cells to *Nature*, and has called our attention to the curious phenomena under discussion.

5. Acoustic cavitation. When an intense sound (or ultrasonic) beam is focussed on the interior of a liquid, minute bubbles are also produced, but the time scale is different.

Though the frequency may be high, the total time duration is long enough for dissolved gas to come out of solution, if the "average" pressure in a minute bubble is low enough to permit gradual effervescence. For a minute bubble oscillating in a sound field, the surface pressure is low during the phase when the surface area is largest. Due to this fact, the evaporation of dissolved gas into the bubble is much larger, relative to the reabsorption of gas into the liquid, than a crude consideration of the average pressure over the liquid as a whole would suggest. This may explain the striking fact that acoustic effervescence can be produced in unsaturated water¹³.

True acoustic cavitation is different in nature. Blake⁹ has studied its dependence on temperature and pressure in degassed water. He has shown that there are also significant "hysteresis" effects involving time-scales of minutes and, in other liquids, viscosity effects as well. In his experiments, the cavitation threshold for a 60 kilocycle beam was found to correspond to peak tensions of several atmospheres. However, in his and other¹⁴ experiments, the peak tensions may have been determined by the extent to which the nuclei clinging to dust particles and walls had not been eliminated. This variable was not controlled in the experiments.

6. Cavitation damage. Cavitation "pitting" is well known as a dangerous source of erosion in marine propellers, and in hydraulic turbines and spillways. It is even more important practically than the vibration and loss of thrust due to cavitation, first observed in the trials of the torpedo boat *Daring*¹⁵.

Extensive research has led to the conclusion that this cavitation pitting is due to the collapse of vapor-filled cavities against solid boundaries, when they return to a region of positive pressure after passing through a "cavitation zone" of negative pressure. Indeed, under the simple Rayleigh theory of a perfectly spherical bubble collapsing in an incompressible fluid

¹³ C. Eckart, *Phys. rev.* 73 (1948), 68-76; F. G. Blake, *Tech. Mem.* 12, Acoustics res. lab., Harvard (1949); M. D. Rosenberg, *Tech. Mem.* 26 *ibid.* (1953); L. Pode, *DTMB Rep.* 854 (1953); G. W. Willard, *J. acoust. soc. Am.* 25 (1953), 669-86; B. Derouet, *Comptes rendus* 234 (1952), 71-3.

¹⁴ H. B. Briggs, J. B. Johnson, and W. P. Mason, *J. acoust. soc. Am.* 19 (1947), 664-77.

¹⁵ For the original discussion of these trials, see the articles by J. W. Barnaby and C. W. Parsons in the *Trans. Inst. Nav. Arch.* 38 (1897), 232-42, and 39 (1898), 139-44. For damage to turbines, see the Symposium *Cavitation in hydraulic structures*, *Proc. Am. soc. civ. eng.* 71 (1945), 1000-13, and comments thereto in vol. 72, p. 715.

(Ch. XI, §§1-2), the peak pressure would be infinite. I.e., a finite total energy would be focussed on a point.

Because of this fact, and visible "pitting" in materials having static yield strengths of 10^5 - 10^6 psi, it was at first concluded that peak collapse pressures were in this range¹⁶. However, Ackeret [46, pp. 227-40] has pointed out that water drops impinging with impact speeds in the range 50-500 f/s , and consequent impact pressures ρcv (here c is the speed of sound in water) in the range 10^3 - 10^4 psi, can also produce pitting. He and his collaborators¹⁷ conclude that peak pressures in collapsing cavities have this much smaller order of magnitude. Other workers incline to the intermediate range 10^4 - 10^5 psi¹⁸.

Such smaller pressures could easily be rationalized, by noting the effects of spherical instability (Ch. XI, §13), compressibility¹⁸, and other physical factors which are often ignored. For instance (cf. §2), it is well known that air-filled bubbles collapse less violently (with a thud instead of a snap¹⁹) in water having high air content. (In this connection, it may be noted that luminescence, which would be expected under adiabatic compression at 10^3 - 10^4 psi, has also been observed²⁰).

Again, simple dimensional calculations of viscous deformation stresses, near a spherical bubble of radius $a(t)$, show that the rate of viscous deformation is proportional to $\partial \dot{r}/\partial r \propto \dot{a}^2 a/r^3$, whence the viscous pressure drop from $r = \infty$ to $r = a$ is proportional to $\dot{a}^2 \int_a^\infty dr/r^3 \propto \dot{a}$. If the Rayleigh theory (Ch. XI, §2) were valid, so that $\dot{a} \propto a^{-1.5}$, infinite viscous work would be done, which is impossible²¹.

¹⁶ See C. A. Parsons and S. S. Cook, *Engineering* 107 (1919), 515-19; F. K. T. van Itersen, *Proc. Kon. Akad. Wet. Amsterdam* 39 (1936), 138-49 and 330-9; W. Mantel, *Zeit. VDI* (1936), 863-7; J. K. Vennard and C. C. Lomax, *Final Rep. under Contract N6-onr-25118*, Stanford Univ. (1950).

¹⁷ J. Ackeret and P. de Haller, *Schweiz. Bauzeitung* 98 (1931), 101 (1933), pp. 243, 260, and 108 (1936), p. 105; I. Vuskovic, *Escher Wyss News* 13 (1940), 83-90; S. Kyropoulos, *Zeits. ang. math. phys.* 2(1951), 406-10. For other theoretical ideas, see W. T. Bottomley, *Proc. inst. mech. eng.* 69 (1947), 253-66; T. C. Poulter, *J. appl. mech.* 64 (1942), A31-A37; R. S. Silver, *Engineering* 154 (1942), 501-2.

¹⁸ For an excellent summary, see M. Kornfeld and J. Suvorov, *J. appl. phys.* 15 (1944), 495-506. See also M. S. Plesset and A. T. Ellis, *Caltech. hydro. lab. rep.* 21-15 (1954). For compressibility effects, see C. Herring, *OSRD Repr.* 236 (1941); [17, pp. 305-7]; E. H. Kennard, *Phys. Rev.* 63 (1943), 172-81; L. Trilling, *J. appl. phys.* 23 (1952), 14-17.

¹⁹ M. F. M. Osborne, *Trans. Am. soc. mech. eng.* 69 (1947), 253-66; M. Harrison, *DTMB Rep.* 815 (1952).

²⁰ L. A. Chambers, *J. chem. phys.* 5 (1937), 290-2.

²¹ H. Poritsky, *Proc. first U. S. congr. appl. mech.* (1951), 813-21; S. S. Shu, *ibid.* 823-5.

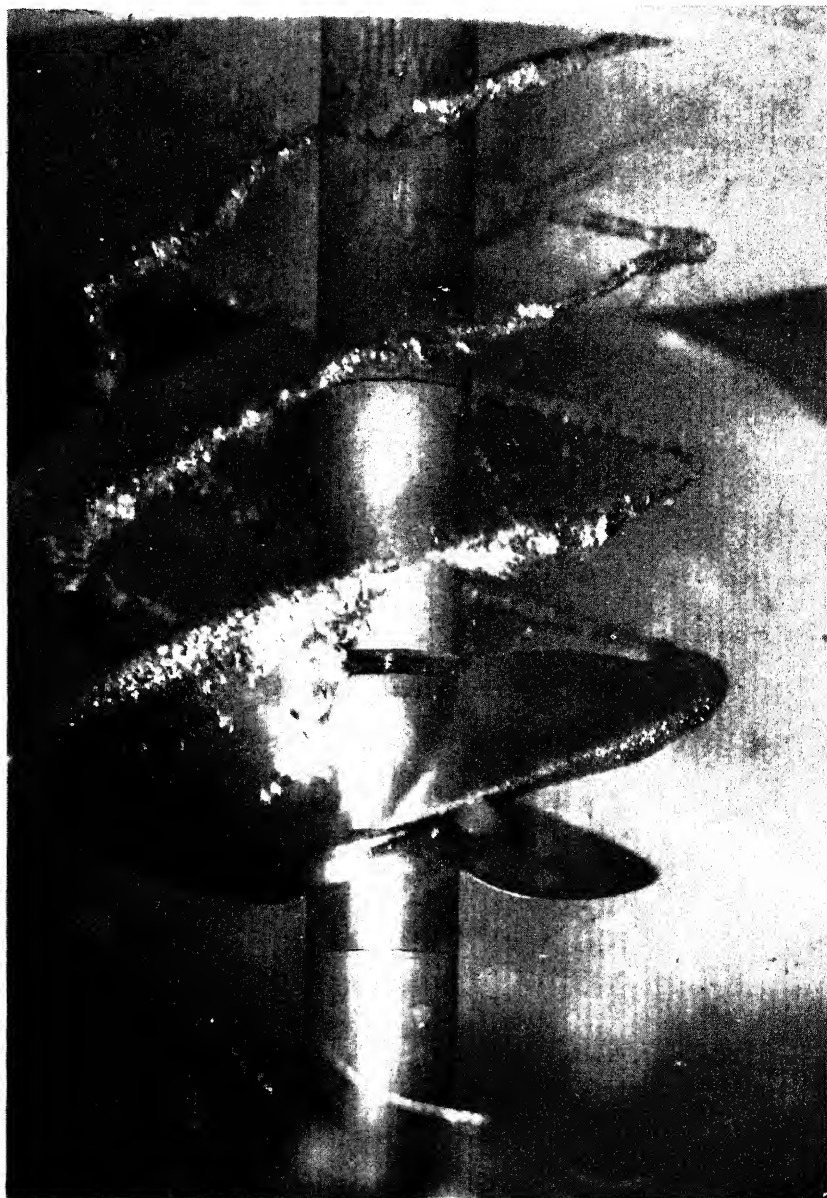


Fig. 2. Tip cavitation. (Official United States Navy Photograph)

Finally, the growth and collapse of cavities is not always determined by the ambient mean pressure. Damage-producing bubbles can also be caused by high local vorticity²² which is not associated with the Bernoulli equation used in deriving the cavitation parameter Q of Ch. I, §4. Thus, in the case of a drowned jet, vortex cavitation begins at the orifice edge when $Q < 0.5$.

7. Propeller cavitation. The complex nature of real cavitation is well illustrated by the various different types of cavitation which have been observed in marine propellers; we shall now describe four such types.

Stroboscopic photographs of propeller cavitation often show cavitation on the *front* face of the propeller, near a sharp leading edge. This is related to the cavitation originally imagined by Helmholtz (Ch. XIV, §2), in connection with flow separation and discontinuous wakes.

Such photographs also reveal cavitation on the *back* face, if the thrust (speed of rotation) is too great. Thus in the original trials of the *Daring*¹⁵, cavitation began when the average propeller thrust was 11 psi. Improved propeller design has enabled much higher thrusts to be obtained²³, up to 22.4 psi. This back cavitation usually begins with intermittent bubbles ("bubbling"), but is followed by "sheet cavitation", which presumably occurs when the mean pressure falls below vapor pressure. At extremely high speeds, the entire rear face is enveloped in an air cavity; this may be called "supercavitation", and has been discussed in the literature²⁴.

Finally, there is the striking phenomenon of *tip cavitation* (see Fig. 2), due to the shedding of vorticity at the propeller tip. According to the Kutta-Joukowski theorem [61, p. 191], the circulation Γ around a propeller of length l should be related to the thrust T by the formula $T = \rho l U \Gamma$. On the other hand, for the pressure inside a hollow vortex of radius r to fall to vapor pressure p_* , if the flow outside the vortex is irrotational, we should have (since the local velocity is $\Gamma/2\pi r$, using Bernoulli's equation)

$$(5) \quad p_0 \simeq p_0 - p_* = \frac{1}{2} \rho (\Gamma^2 / 4\pi^2 r^3) = T^2 / 8\pi^2 \rho l^2 U^2 r^2.$$

It is possible that the radii of tip vortices can be roughly estimated from (5), though boundary layer effects make this doubtful.

²² See H. Föttinger, [46, p. 243]; K. K. Shalnev, Zh. tekhn. fiz. 21 (1951), 206–20, and Doklady SSSR 78 (1951), 33–6, where the role of the Strouhal number (Ch. XIII) is shown. For the occurrence of vortex cavitation in drowned jets, see H. Rouse, La Houille Blanche (1953), 1–19.

²³ The data are taken from D. W. Taylor, *The speed and power of ships*, U. S. Govt. Printing Office, 1943, Ch. 26.3; see also H. E. Rossell and L. B. Chapman, *Principles of naval architecture*, vol. 2, Ch. III, Sec. 11. Dr. F. H. Todd has informed us that 13.5 psi based on *developed* area is now considered a practical maximum.

²⁴ V. L. Posdunine, Doklady URSS 39 (1943), 306–10. The development of mathematical formulas, based on "free boundary" theory, would seem a very worthwhile achievement.

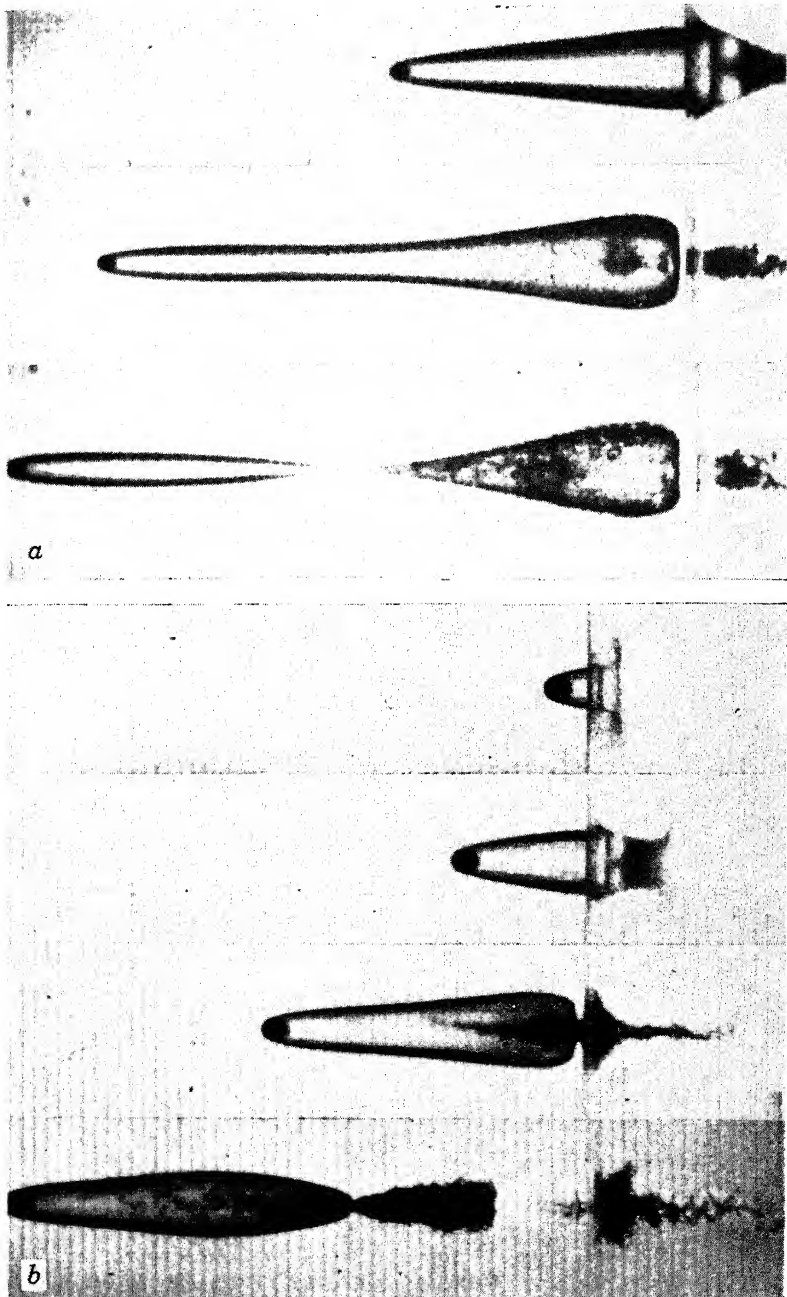


FIG. 3. Deep seal and surface seal. (Courtesy Naval Ordnance Laboratory)

Limitations of space forbid our giving the many interesting facts about propeller cavitation which have been discovered over the past 50 years²⁵. In view of the scale effects mentioned above, the photographs of full-scale cavitation recently obtained by J. W. Fisher²⁶ are very noteworthy; they show at least a qualitative similarity between model and full-scale cavitation.

The analogous problem of cavitation on *hydrofoils* also deserves mention. However, at shallow submergence depth d , it appears that the wave speed $\sqrt{g d}$ is as important a limiting factor as cavitation²⁷.

8. Scale effects in water entry. The entry of a solid into water or another liquid gives rise to a sequence of events of surprising physical complexity. This situation was first studied qualitatively by Worthington [90], for the case of spheres dropped into water from small heights $h = 6$ in.–20 ft.—i.e., having vertical entry velocities of 4–25 feet per second (f/s), and Froude numbers

$$(6) \quad F = h/d = v^2/gd \quad \text{of } 5\text{--}250 \text{ (roughly).}$$

The most important physical variables are (i) the *inertia* of the water, and (ii) *gravity*, which causes water to fill the cavity created by the passage of the solid. An approximate theory of cavity behavior, as determined by these variables, has already been outlined in Ch. XI, §4. The point which we wish to stress here is that an exact treatment of the problem must not only be more sophisticated mathematically, but must also take into account the inertia and viscosity of the *air*, which were ignored in the earlier treatment.

The role of air density was first clearly demonstrated by R. M. Davies²⁸. The most striking observation involves the distinction between “surface seal” and “deep seal”, which we will now define.

When a sphere is dropped into water with $20 < F < 70$ (say), the collapsing walls of the cavity collide audibly, roughly midway between the sphere and the surface, as in Fig. 3a. The sound is a “plop”, and after the collision (which is often accompanied by upjets and downjets [23]), the cavity behind the missile is separated from the surface by a “deep seal”.

At higher speeds, when $F > 150$ (say), this event is preceded by a “sur-

²⁵ See H. Lerbs, Rep. 131, Hamburg, Schiffbau-Vers. (1936), L. P. Smith, Trans. Am. soc. mech. eng. 59 (1937), 409–31.

²⁶ N. E. Coast, Inst. Eng. Shipbuild. Trans. 68 (1951), 19–30.

²⁷ E. V. Laitone, J. appl. phys. 25 (1954), 623–6, and 26 (1955), 1519–20. See also B. R. Parkin et al., J. appl. phys. 27 (1956), 232–9.

²⁸ *The influence of atmospheric pressure on the phenomena accompanying the fall of small scale projectiles into a liquid*, Engineering Lab., Cambridge, England, 1944. See also [23] and [59b].

face seal" as in Fig. 3b. Thus the sound of deep seal resonates in a cavity covered by a thin membrane, and is a "plunk". This variation in sound was first explained by Mallock²⁹. However, it remained for Davies²⁸ to show that surface seal was caused by atmospheric pressure (density). With variable density, surface seal occurs first when

$$(7) \quad F > F_{\text{crit}} = (\rho/80\rho')^2,$$

very roughly [4, Ch. III, §16]. This surface seal creates an underpressure below hydrostatic pressure of uncertain magnitude³⁰, thus introducing a further scale effect. In summary, the criterion $\rho'/\rho \ll 1$ of Betz (Ch. I, §4) is *not* sufficient to guarantee that free boundary theory is applicable, in this case.

Air viscosity causes another scale effect, which is preponderant at shallow entry angles when $v < 100$ f/s and $d = 1$ in. In 1944, L. Slichter showed that a smooth 2-inch diameter dural sphere, entering the water at 50 f/s and an entry angle of 20° with the horizontal, might be refracted downward 5° or more on entry. It is difficult to summarize briefly Professor Slichter's (unpublished) arguments that this is due to air viscosity, but they seem conclusive.

In a somewhat similar vein, Wayland³¹ has shown that, at low speeds, a turbulent boundary layer can inhibit separation and hence reduce the cavity size, much as in ordinary flow.

Finally, as first demonstrated by Worthington [90], the critical entry speed for cavity formation, which is about 12 f/s for 1" spheres under ordinary conditions, can be increased to 20 f/s or more by using carefully cleaned spheres³². The scale effect due to the use of a hydrophilic surface is negligible, however, when $v > 45$ f/s; air viscosity is more important.

9. Bubble entrainment. The size and shape of *vapor*-filled cavities behind discs with $Q < 0.4$ do seem [23, Fig. 23] to be determined quite well by the cavitation number

$$(8) \quad Q = (p_f - p_c)/\frac{1}{2}\rho v^2, \quad \text{where } p_c = p_v.$$

²⁹ A. Mallock, Proc. roy. soc. A95 (1918), 138-43. See E. N. Harvey and J. H. McMillen, J. appl. phys. 17 (1946), 541-55, for pictures of surface seal with F around 10'.

³⁰ E. G. Richardson, Proc. phys. soc. 61 (1948), 352-66, estimated a maximum underpressure of .06 atm. with $v = 20$ f/s when $\rho'/\rho = .0012$; May (op. cit., Fig. 17) estimated .25 atm. with $v = 77$ f/s, when $\rho'/\rho = .0004$, $p_{\text{atm}} = 2.5$ psi (roughly).

³¹ H. Wayland and F. G. White, Proc. 1949 Symposium Heat Transfer, pp. 51-64. See also G. G. Mosteller, Navord Rep. 1012 (1948), N.O.T.S.

³² The best data are given by A. May, J. appl. phys. 22 (1951), 1219-22. See also G. E. Bell, Phil. Mag. 48 (1924), 753-64, for the effect of liquid films.

When the cavity contains air, however, the cavity pressure³³ p_c may differ only slightly from p_f , and so the cavity volume is determined more by the amount of this air than by the velocity v . This is the case with solids dropped into water, as we have seen.

In such cases, therefore, the cavity volume is decreased primarily by the *air entrainment* into the surrounding liquid at the rear of the cavity³⁴, which is caused by the entrapment of bubbles or foam.

The mechanism of air entrainment is not well understood, although the occurrence of "white water" in rapids, on spillways, and beneath waterfalls, is familiar. In these familiar cases, the fluctuating velocities of turbulent eddies must clearly exceed the average speed of undisturbed bubble rise by a considerable factor. In the "pumping" of air out of the cavity behind a missile, the rate-determining factor is less obvious, but turbulence is also a factor.

In the familiar case of "white water", air entrainment is sometimes said to be dual to sediment entrainment, with the direction of buoyancy reversed. This view seems reasonable for air bubbles in water whose diameter is less than 2 mm, since surface tension makes such bubbles behave like nearly rigid spheres under accelerations of less than (say) 10 g. The approximate formula for the drag coefficient of rigid spheres, which is³⁵

$$(9) \quad C_D = 0.4 + 24/R, \quad 0 < R < 1,000,$$

is roughly applicable to such bubbles. From this formula, and the equation

$$(9') \quad v^2/gr = 8/3C_D, \quad (\text{or } D = 4\pi\rho r^3g/3),$$

one can easily estimate the rate of buoyant rise of such bubbles.

However, even such spherical bubbles exhibit surprising behavior to the uninitiated³⁵. When $R > 100$ (roughly), they wobble upwards, instead of rising in a straight line. (This effect is associated with the periodic wake of a sphere, discussed in Ch. XIII, §11.) In a pure liquid, the $24/R$ in (9) would be $16/R$ [50, p. 599].

The theory of larger bubbles is still more complicated. Empirically, they

³³ In foam-filled cavities, p_c may also vary appreciably; thus values of $Q_c = (p_c - p_a)/\frac{1}{2}\rho v^2$ in the range 0.15–0.30 were observed by Eisenberg and Pond (DTMB Rep. 668).

³⁴ See W. M. Swanson and J. P. O'Neill, Caltech hydro. lab. rep. M-24.3. The intermittent jet formed at the back of the cavity is an important factor in air entrainment.

³⁵ There is an immense literature on the rise of air bubbles; thus the bibliography of W. L. Haberman and R. K. Morton, DTMB Rep. 802 (1953), lists fifty items. See also G. Benfratello, *Energia Elettrica* 30 (1953), 80–97. For early work, see H. S. Allen, *Phil. Mag.* 50 (1900), 323–38 and 519–34; the air content of the water is again a factor!

are observed to be lens-shaped³⁶ for $r > 5$ mm ($d > 1$ cm). The rate of rise is 20–30 cm/sec throughout the range $1 \text{ mm} < d < 2 \text{ cm}$, and the water underneath the bubble is presumably turbulent.

Consequently, air entrainment involves a complicated interplay of the forces of gravity, viscosity, and surface tension—as well as effects of impurities (which can form “suds”) and perhaps gas content. It is not surprising that its quantitative prediction should be difficult!

10. Jet persistence. In Ch. XI, §15, we described Rayleigh’s theory of the disintegration of capillary jets, and its agreement with observation at moderate jet speeds. Unfortunately, this theory is inadequate for thicker jets and at higher speeds.

As predicted by the formulas of Ch. XI, §11 (with $a = g$), small local surface wavelets on thick jets get amplified more rapidly by Helmholtz instability than large varicose nodules. When these wavelets get steep enough, the linear perturbation theory of Ch. XI ceases to be applicable. As in the homogeneous case (Ch. XIII, §13), the steepest wavelets billow out and are retarded by the surrounding air, giving a profile like a blade of wheat. Soon after, also as in the homogeneous case (Ch. XIV, §§9–10, esp. Fig. 4), a turbulent “mixing zone” develops, which gradually erodes the jet. After the mixing zone has reached the jet center, the jet spreads as a cone, but with a smaller angle of spread than in the homogeneous case.

The angles of erosion and spread depend greatly on the nozzle design, and especially on the initial *turbulence*. The mean velocity profile may also have a significant effect.

This has been shown repeatedly in tests of jets used in fire-fighting³⁷. Typically, these are 1”–3” diameter water jets, under heads of 50–200 psi, so that R is of the order of 10^6 . In favorable (non-turbulent) cases, the unaerated jet core can persist for 30 or more diameters, and the retarding action of the air is only important after 200 or more diameters, when the inertia of the entrained air becomes appreciable. It is interesting that the factor $\sqrt{\rho/\rho'}$, which expresses relative jet persistence for small perturbations, seems inapplicable to turbulent erosion. Since $\sqrt{\rho/\rho'} \simeq 27$ for water jets in air, the jet core would persist for 100 diameters if the same factor applied (cf. Ch. XIV, §10).

³⁶ R. M. Davies and G. I. Taylor, Proc. roy. soc. A200 (1950), 379–90. For bubbles in tubes, see Ch. X, §11.

³⁷ J. R. Freeman, Trans. Am. soc. civ. eng. 21 (1889), 303–482; H. Rouse et al., ibid. 77 (1951), 147–88, and discussion thereto. The behavior of jets from a garden hose is similar; see also P. Oguey, Bull. tech. Suisse rom. (1944, 1951). The effect in question is illustrated by the upper left corner of Fig. 1, Ch. I; the jet of the left panel had more initial turbulence.

At high speeds, even thin liquid jets of .01" diameter exhibit complicated behavior. Thus, jet disintegration is often *sinuous* or *helical* rather than varicose³⁸. Under other circumstances (cf. §11), ultra-thin ligaments of very short life are pulled off by viscous action; these ligaments then contract into droplets under surface tension³⁹. The theory is supposed to be that of the disintegration of viscous jets, as in emulsions [35a]. Again, Hypospray jets⁴⁰ at 1400 f/s break up when widely spaced nodules, slowed up by air drag, swell under the impact of the jet behind, forming vortex rings of liquid which are blown into a thin mist by the surrounding air (cf. §11).

If the air density is reduced, one gets very interesting effects⁴¹. The distance to break-up is roughly proportional to $\sqrt{\rho/\rho'}$, provided the turbulence is suppressed. Otherwise, internal turbulence is the determining factor.

At the opposite extreme, "creeping" viscous jets (as of honey or molasses), falling under gravity, have a very different mode of disintegration⁴². The tendency to stretch is greatest where the jet is thinnest, and failure occurs by "necking off" at the thinnest point, as with ductile metals.

In view of all these different modes of jet disintegration, it seems too much to hope that the general case will be soon amenable to a straightforward theoretical treatment.

II. Atomization of jets. The behavior of drops from disintegrated liquid jets is very complicated. Though capillary forces are most important, forces in the liquid and surrounding gas due to inertia (Helmholtz instability), acceleration, viscosity, and turbulence, may also be influential. Thus, various behavior patterns can arise.

The simplest case is that of capillary jets. In this case, one can achieve uniform varicose disintegration by monochromatic acoustic stimulation of the right frequency, into uniform drops whose diameter is about twice the jet diameter, separated by much smaller droplets. Because of the uniform drop size, the drop trajectories are uniform.

³⁸ A. Haenlein, *Forsch. Geb. Ing.* 2 (1931), 139-49 (NACA TM 659), C. Weber, *ZaMM* 11 (1931), 355-8; W. Ohnesorge, *ibid.* 16 (1936), 355-8 and *Zeits. VDI* 81 (1937), 465-6; M. Mahrous, *Brit. J. appl. phys.* 3 (1952), 329-31.

³⁹ R. A. Castleman, *J. res. bur. stand.* 6 (1931), 369-76. For the theory, see Rayleigh, *Phil. Mag.* 34 (1892), 145-54; G. I. Taylor, *Proc. roy. soc.* A146 (1934), 501-22; S. Tomotika, *ibid.* A150 (1935), 322-37; V. A. Borodin and Y. F. Dityakin, *NACA TM* 1281 (1951).

⁴⁰ B. Dunne and B. Cassen, *J. appl. phys.* 25 (1954), 569-72, and 27 (1956), 577-82.

⁴¹ D. W. Lee and R. C. Spencer, *NACA Rept.* 454; P. H. Schweitzer, *J. appl. phys.* 8 (1937), 513-21.

⁴² Rayleigh, *Phil. Mag.* 34 (1892), 145-54.

However, even in this case, jet disintegration and subsequent drop behavior are affected by many physical variables. Besides sound (random noise causes non-uniform break-up), impurities like soap in solution affect surface tension and hence distance to break-up. Also, dust in the air, the chemistry of the surrounding gas, and electrification may affect the final behavior decisively, by determining whether colliding drops amalgamate or rebound.

These phenomena fascinated the nineteenth century physicists⁴³ who discovered them. They may still have useful applications⁴⁴.

More recently, the mechanical factors influencing droplet size (and droplet distribution in space) have been studied in relation to fuel injection problems. In such cases, the liquid is commonly atomized by a high speed air jet.

It is easy to estimate roughly the maximum diameter d of a liquid drop moving through air of density ρ' with constant velocity U , compatible with Helmholtz stability. The dynamic pressure differences will be of the order of $\rho'U^2$; the stabilizing force of surface tension, about $4\gamma/d$. Hence, if $W = \rho' dU^2/\gamma$ exceeds a suitable constant⁴⁵, say about 10, such a drop will first be sucked out near the equator, then dished in and broken up.

The maximum size of falling raindrops may be predicted in this way⁴⁶. The velocity of fall corresponds to a mean pressure difference of about $2\rho g d/3$; for this to be stabilized by surface tension, we must have $(2\rho g d/3) < (4\gamma/d)$, or $B = \rho g d^2/\gamma < 6$. Actually⁴⁶, break-up occurs when $B > 10$.

However, the shattering of a jet by an air blast is not always due to Helmholtz instability. In some cases, viscosity is a more important variable⁴⁷, and the condition for break-up is complicated accordingly. In other cases, the mechanism of Castleman⁴⁸ is important. In still other cases, internal jet turbulence is decisive.

12. Other jet configurations. For the sake of completeness, we mention various other jet configurations which have been analyzed scientifically.

⁴³ [73a], 337-386; Magnus, Pogg. Ann. 106 (1859), 1-32; J. Tyndall, Phil. Mag. 33 (1867), 375-91; Rayleigh, Proc. roy. soc. A29 (1879), 71-97; [66, 351-71]. See also G. Littaye, Comptes rendus A212 (1941), 1077-9, and Publ. sci. tech. min. air No. 181 (1942).

⁴⁴ Thus O. Yadoff, Comptes rendus 218 (1944), 104-5, has proposed electrification to improve the behavior of jets striking Pelton wheels.

⁴⁵ H. Triebnigg, "Die Einblase und Einspritzvorgang bei Dieselmotoren", Berlin, 1925; G. Littaye, Comptes rendus 217 (1943), 99-100; [35a, p. 310].

⁴⁶ W. N. Bond and D. A. Newton, Phil. Mag. 5 (1928), 794-800; [35a, p. 286].

⁴⁷ S. Nukiyama and Y. Tanasawa, Trans. soc. mech. eng. Japan 6 (1940), 18-26, and refs. given there; A. C. Merrington and E. G. Richardson, Proc. phys. soc. 59 (1947), 1-13; J. O. Hinze, Appl. sci. res. A1 (1949), 263-88; M. D. Bitron, Ind. eng. chem. 47 (1955), 23-8; N. S. Panasenkov, Zh. tekhn. fiz. 21 (1951), 160-6.

In Ch. X, §10, "swirl atomizers" were briefly described, and their gross mechanics analyzed. It should be mentioned now that the very fine atomization which they induce has also been studied⁴⁸.

Again, emulsions formed by injecting a jet of one liquid into another have been investigated⁴⁹.

Another interesting phenomenon is the stable equilibrium of a ball on a vertical jet. This interested Reynolds⁵⁰, who observed that the equilibrium position was to one side of the jet axis, and that equilibrium was destroyed if greasy water was used.

Still other studies concern a circular jet impinging normally on a flat plate under gravity. One cannot always expect the ideal flow described in Ch. X, §8. In fact, at least three regimes of hydraulic jump have been observed: "turbulent jump", "undulatory jump", and "capillary jump"⁵¹. The first occurs at large flow rates; the second at intermediate flow rates, and is characterized by standing circular capillary waves ("ripples"); the third is characterized by eddy "back-roll" on the interface above the hydraulic jump, and by the absence of waves.

⁴⁸ H. L. Green, "Some aspects of fluid flow", London, 1951, 75-86, and [35a, p. 307]; E. Giffen, *Engineering* 174 (1952), 6-10.

⁴⁹ E. Tyler and F. Watkin, *Phil. Mag.* 14 (1932), 849-81; E. G. Richardson, *J. coll. sci.* 5 (1950), 404-413, and [35a, p. 42].

⁵⁰ O. Reynolds, *Collected Sci. Papers*, vol. 1, pp. 1-16.

⁵¹ I. Tani, *J. phys. soc. Japan* 4 (1949), 212-215; M. I. Leviant, *Rev. gen. hydro.* 16 (1950), 74-82; H. M. Cassel, *Proc. sec. Midwest conf. fluid mech.* (1952), 99-104.

BIBLIOGRAPHY

- [1] J. Ackeret, *Experimentelle und theoretische Untersuchungen über Höhlraumbildung (Kavitation im Wasser)*, Tech. Mech. u. Therm. 1 (1930), 1-22 and 63-70.
- [1a] F. Auerbach, Handb. Phys. Tech. Mech., vol. 5, Johann Ambrosius Barth, Leipzig (1931).
- [2] A. Betz and E. Petersohn, *Anwendung der Theorie der freien Strahlen*, Ing. Archiv 2 (1931), 190-211.
- [3] L. Bieberbach, *Lehrbuch der Funktionentheorie*, Leipzig, Teubner, vol. 1, 1923; vol. 2, 1927.
- [4] G. Birkhoff, *Hydrodynamics, a study in logic, fact and similitude*, Princeton University Press, 1950.
- [5] G. Birkhoff, *Formation of vortex streets*, J. appl. phys. 24 (1953), 98-103.
- [6] G. Birkhoff, M. Plesset and N. Simmons, *Wall effects in cavity flow*, I, Quar. appl. math. 8 (1950), 151-168; II, ibid. 9 (1952), 413-21.
- [7] G. Birkhoff, D. Young and E. H. Zarantonello, *Numerical methods in conformal mapping*, Proc. fourth symp. appl. math., New York, McGraw-Hill, 1953, 117-140.
- [8] F. G. Blake, *The tensile strength of liquids*, Tech. Mem. 9, Contract N5ori-76, Proj. Order X, Harvard acoustic lab., 1949.
- [9] M. Brillouin, *Questions d'hydrodynamique*, Ann. fac. sci. Toulouse 1 (2) (1887), 1-80.
- [10] M. Brillouin, *Les surfaces de glissement de Helmholtz et la résistance des fluides*, Ann. de chim. phys. 23 (1911), 145-230.
- [11] S. Brodetsky, *Discontinuous fluid motion past circular and elliptic cylinders*, Proc. roy. soc. A102 (1923), 542-553.
- [12] S. Brodetsky, *Fluid motion past circular barriers*, Scripta Univ. Bibl. Hierosolymitanarum 1 (1923), 1-14.
- [13] S. Chaplygin, *Gas jets*, Scientific Memoirs Moscow Univ. (1902), 1-121, translated as NACA TM 1063 (1944).
- [14] U. Cisotti, *Vena fluenti*, Rend. cir. mat. Palermo 25 (1908), 145-179.
- [15] U. Cisotti, *Sulla biforcazione di una vena liquida*, Rend. accad. Lincei (5) 20 (1911), 314-322, 494-502.
- [16] U. Cisotti, *Idrodinamica piana*, Milan, Tamburini, 1921.
- [17] R. H. Cole, *Underwater explosions*, Princeton Univ. Press, 1950.
- [18] R. Courant and D. Hilbert, *Methoden der mathematischen Physik*, vol. 2, Berlin, Springer, 1937.
- [19] B. Demtchenko, *Problemes mixtes harmoniques en hydrodynamique des fluides parfaits*, Paris, Gauthier Villars, 1933.
- [20] W. Durand, *Aerodynamic theory*, Berlin, Springer, 1934-6, 6 vols.
- [21] H. B. Dwight, *Tables of integrals and other mathematical data*, rev. ed., New York, Macmillan, 1947.
- [22] F. F. Ehrlich, *The hydrodynamics of flow regulation*, M.I.T. D. Sc. Thesis, Cambridge, 1951. See also J. aer. sci. 20 (1953), 99-104.
- [23] P. Eisenberg, *On the mechanism and prevention of cavitation*, DTMB Rep. 712, 1950; Addendum, 1953.
- [23a] R. Eppler, *Beiträge zur Theorie und Anwendung der unsteady Strömungen*, J. rat. mech. anal. 3 (1954), 591-644.

- [24] A. Fage and F. C. Johansen, *On the flow of air behind an inclined flat plate of infinite space*, Proc. roy. soc. 116 (1927), 170-97.
- [25] P. Forchheimer, *Hydraulik*, 3rd ed., Leipzig, Teubner, 1930.
- [26] K. Friedrichs, *Über ein minimum Problem für Potentialströmungen mit freien Rande*, Math. Annalen 109 (1933), 60-82.
- [27] P. R. Garabedian, H. Lewy and M. Schiffer, *Axially symmetric cavitation flow*, Ann. of math. 56 (1952), 560-602.
- [28] P. R. Garabedian and D. C. Spencer, *Extremal methods in cavitation flow*, J. rat. mech. anal. 1 (1952), 359-409.
- [29] D. Gilbarg, *Uniqueness of axially symmetric flows with free boundaries*, J. rat. mech. anal. 1 (1952), 309-20.
- [30] D. Gilbarg and R. A. Anderson, *Influences of atmospheric pressure on the phenomena accompanying the entry of spheres into water*, J. appl. phys. 19 (1948), 127-39.
- [31] S. Goldstein, *Modern developments in fluid dynamics*, Oxford, Clarendon Press, 1938.
- [32] G. Greenhill, *Theory of a streamline past a plane barrier*, ARC RM 19, 1910.
- [33] G. Greenhill, *Theory of a streamline past a curved wing*, Appendix to ARC RM 19, 1916.
- [34] W. Heisenberg, *Die absoluten Dimensionen der Karmanschen Wirbelbewegung*, Phys. Zeit. 23 (1922), 363-366, and comments by L. Prandtl on page 366.
- [35] H. Helmholtz, *Über discontinuierliche Flüssigkeitsbewegungen*, Monatsber. Berlin. Akad. (1868), 215-28. Reprinted in Phil. Mag. 36 (1868), 337-46 and in Wiss. Abh. 1 (1882).
- [35a] J. J. Hermans, *Flow properties of disperse systems*, Interscience, 1953.
- [36] S. B. Hollingdale, *Stability and configuration of wakes*, Phil. Mag. 29 (1940), 209-57.
- [37] E. Hopf, *Elementare Bemerkungen über die Lösungen partiellen Differentialgleichungen zweiter Ordnung von elliptischen Typus*, Sitzber. Berlin. Akad. Wiss. [Math.-Phys. Kl.] (1927), 147-52.
- [38] B. Hopkinson, *Free streamline flows with singularities*, Proc. Lond. math. soc. 29 (1898), 142-64.
- [39] C. Jacob, *Sur la détermination des fonctions harmoniques par certaines conditions aux limites* (Thèse), Mathematica 11 (1935), 149-75.
- [40] H. Jeffreys, *The wake in fluid flow past a solid*, Proc. roy. soc. 128 (1930), 376-93.
- [41] Th. von Karman, *Über den Mechanismus des Widerstandes den ein bewegter Körper in einer Flüssigkeit erfährt*, Gött. Nachr. [Math.-Phys. Kl.] (1912), 547-56.
- [42] Th. von Karman, *The engineer grapples with nonlinear problems*, Bull. Am. math. soc. 46 (1940), 613-83.
- [43] Th. von Karman and H. Rubach, *Über den Mechanismus des Flüssigkeits- und Luftwiderstandes*, Phys. Zeit. 13 (1912), 49-59.
- [44] O. D. Kellogg, *Foundations of potential theory*, Berlin, Springer, 1930.
- [45] Lord Kelvin (Sir William Thomson), *Mathematical and physical papers*, vol. IV, Cambridge Univ. Press, 1910.
- [46] H. Kempf and E. Foerster, ed., *Hydrodynamische Probleme des Schiffsantriebs*, Hamburg, Springer, 1932, 227-342.
- [47] G. Kirchhoff, *Zur Theorie freier Flüssigkeitsstrahlen*, J. reine angew. Math. 70 (1869), 289-98.
- [48] R. T. Knapp and A. Hollander, *Laboratory investigations of the mechanisms of cavitation*, Trans. Am. soc. mech. eng. 70 (1948), 419-35.

- [48a] A. Kovasznay, *Hot-wire investigation of the wake behind cylinders*. . . , Proc. roy. soc. A198 (1949), 174-90.
- [49] J. Kravtchenko, *Sur le probleme de representation conforme de Helmholtz: Theorie des sillages et des poutes*, J. de math. 20 (1941), 35-239.
- [50] H. Lamb, *Hydrodynamics*, 6th ed., Cambridge Univ. Press, 1932.
- [51] M. Lavrentieff, *Sur certaines proprietes des fonctions univalentes et leurs applications à la theorie des sillages*, Rec. math. (Mat. Sbornik) 46 (1938), 391-458.
- [52] J. Leray, *Les problemes de representation conforme d'Helmholz, theories des sillages et des poutes*, I, II, Comment. Math. Helv. 8 (1935), 149-80, 250-63.
- [53] J. Leray and J. Schauder, *Topologie et equations fonctionnelles*, Ann. sci. ec. norm. sup. 51 (1934), 45-78.
- [54] T. Levi-Civita, *Scie e leggi di resistenza*, Rend. cir. mat. Palermo 23 (1907), 1-37.
- [55] N. Levinson, *On asymptotic shape of cavity behind an axially symmetric nose moving through an ideal fluid*, Ann. of math. 47 (1946), 704-30.
- [56] D. J. Lewis, *The instability of liquid surfaces when accelerated in a direction perpendicular to their planes*, II, Proc. roy. soc. A202 (1950), 81-96.
- [57] H. W. Liepmann and J. Laufer, *Investigations of free turbulent mixing*, NACA TN 1257, 1947, 38 pp.
- [58] A. E. H. Love, *On the theory of discontinuous fluid motion in two dimensions*, Proc. Camb. phil. soc. 7 (1891), 175-201. (Also Enzycl. d. Math. Wiss. IV (3), 97-101.
- [59] L. Marty, *L'écoulement des fluides*, Ann. fac. sci. Toulouse 22 (1930), 41-146.
- [59a] S. S. McNown and C.-S. Yih, editors, *Free-streamline analyses of transition flow and jet deflection*, State Univ. Iowa Studies in Eng., Bull. 35 (1953).
- [59b] A. May, *Vertical entry of missiles into water*, J. appl. phys. 23 (1952), 1362-72.
- [60] J. H. Michell, *On the theory of the streamline*, Phil. Trans. 81 (1890), 389-431.
- [61] L. M. Milne-Thomson, *Theoretical hydrodynamics*, 1st ed., New York, Macmillan, 1950.
- [62] R. von Mises, *Berechnung von Ausfluss und Überfallzahlen*, Zeits. VDI 61 (1917), 447-452, 467-473, 493-497.
- [62a] Zeev Nehari, *Conformal mapping*, McGraw-Hill, 1953.
- [63] N. A. Nekrassoff, *Sur le mouvement discontinu a deux dimensions du fluide autour d'un obstacle en forme d'arc de cercle*, Pub. Inst. Polytech., Ivanovo-Voszniesensk, 1922.
- [64] A. Oudart, *L'étude des jets et le mecanique theorique des fluides*, Publ. sci. tech. min. air 234, Paris, 1948.
- [64a] S. I. Pai, *Fluid dynamics of jets*, van Nostrand, 1954.
- [65] Lord Rayleigh (J. W. Strutt), *Scientific papers*, Cambridge Univ. Press., 1899.
- [65] Lord Rayleigh (J. W. Strutt), *Theory of sound*, London, Macmillan, 2nd ed., 1896, vol. 2, Chs. XX-XXI.
- [67] H. Reichardt, *Gesetzmässigkeiten der freien Turbulenz*, VDI-Forsch. 414, 1951, 30 pp. (revision of paper published in 1942).
- [67a] H. Reichardt, *The laws of cavitation bubbles at axially symmetric bodies*, Min. Aircraft Prod. Reps. and Translations 766. (Original dated Goettingen, 1945).
- [68] M. Réthy, *Strahlenformen incompressibler reibungsloser Flüssigkeiten*, Math. Annalen 46 (1895), 249-272.
- [69] D. Riabouchinsky, *On steady fluid motion with free surfaces*, Proc. Lond. math. soc. 19 (1920), 206-15.
- [70] D. Riabouchinsky, *On some cases of two-dimensional fluid motions*, ibid. 25 (1926), 185-94.

- [71] D. Riabouchinsky, *Sur un problème de variation*, Comptes rendus 185 (1927), 840-41.
- [72] E. G. Richardson, *Dynamics of real fluids*, London, Arnold, 1950.
- [73] L. Rosenhead, *Vortex systems in wakes*, Advances in appl. mech., vol. 3, New York, Academic Press, 1953, 185-95.
- [73a] F. Savart, *Chocs de veines liquides* Ann. chimie phys. 54 (1833), 55-87 and 113-45, and 55 (1833), 257-310.
- [74] H. Schlichting, *Grenzschichttheorie*, Karlsruhe, G. Braun, 1951.
- [75] J. B. Serrin, *Existence theorems for some hydrodynamical free boundary problems*, J. rat. mech. anal. 1 (1952), 1-48.
- [76] J. B. Serrin, *Uniqueness theorems for two free boundary problems*, Am. J. math. 74 (1952), 492-506.
- [77] M. Shiffman, *On free boundaries of an ideal fluid*, Comm. pure appl. math. 1 (1948), 89-99, and 2 (1949), 1-11.
- [78] R. V. Southwell and G. Vaisey, *Fluid motions characterized by "free" streamlines*, Phil. Trans. 240 (1946), 117-161. See also R. V. Southwell, *Relaxation methods in theoretical physics*, Oxford, 1946, pp. 212-26.
- [79] H. B. Squire, *Reconsideration of the theory of free turbulence*, Phil. Mag. 39 (1948), 1-20.
- [80] Sir Geoffrey Taylor, *The instability of liquid surfaces when accelerated in a direction perpendicular to their planes*, I, Proc. roy. soc. 201 (1950), 192-6.
- [81] A. A. Townsend, *Momentum and energy diffusion in the turbulent wake of a cylinder*, Proc. roy. soc. A197 (1949), 124-40.
- [82] U. S. Nat. Bur. of Standards, *Proc. of Symposium on Construction and Application of Conformal Maps*, 1949.
- [83] H. Villat, *Sur la résistance des fluides*, Ann. sci. ec. norm. sup. 28 (1911), 203-240.
- [84] H. Villat, *Sur la détermination des problèmes de l'hydrodynamique relatifs à la résistance des fluides*, *ibid.* 31 (1914), 455-91.
- [85] H. Villat, *Sur la validité des solutions de certains problèmes d'hydrodynamique*, J. de math. (6) 10 (1914), 231-90.
- [86] H. Villat, *Aperçus théoriques sur la résistance des fluides*, Collection Scientia, Paris, Gauthier Villars, 1920.
- [86a] F. Walter, *Experimentelle und theoretische Untersuchungen über die Strömungsformen. . .*, Ber. Sachs. Akad. Wiss., Math.-phys. Klasse, 29 (1940).
- [87] A. Weinstein, *Ein hydrodynamischer Unitätssatz*, Math. Zeit. 19 (1924), 265-274.
- [88] A. Weinstein, *Zur Theorie der Flüssigkeitsstrahlen*, Math. Zeit. 31 (1929), 424-33.
- [89] E. T. Whittaker and G. N. Watson, *Modern analysis*, Cambridge Univ. Press, 4th ed., 1940.
- [90] A. M. Worthington, *A study of splashes*, New York, Longmans, Green, 1908. See also Phil. Trans. 194 (1900), 175-99 and plates.
- [91] E. H. Zarantonello, *A constructive theory for the equations of flows with free boundaries*, Collectanea Mathematica, Barcelona, 5 (1952), 175-225.

PLATES 1-11

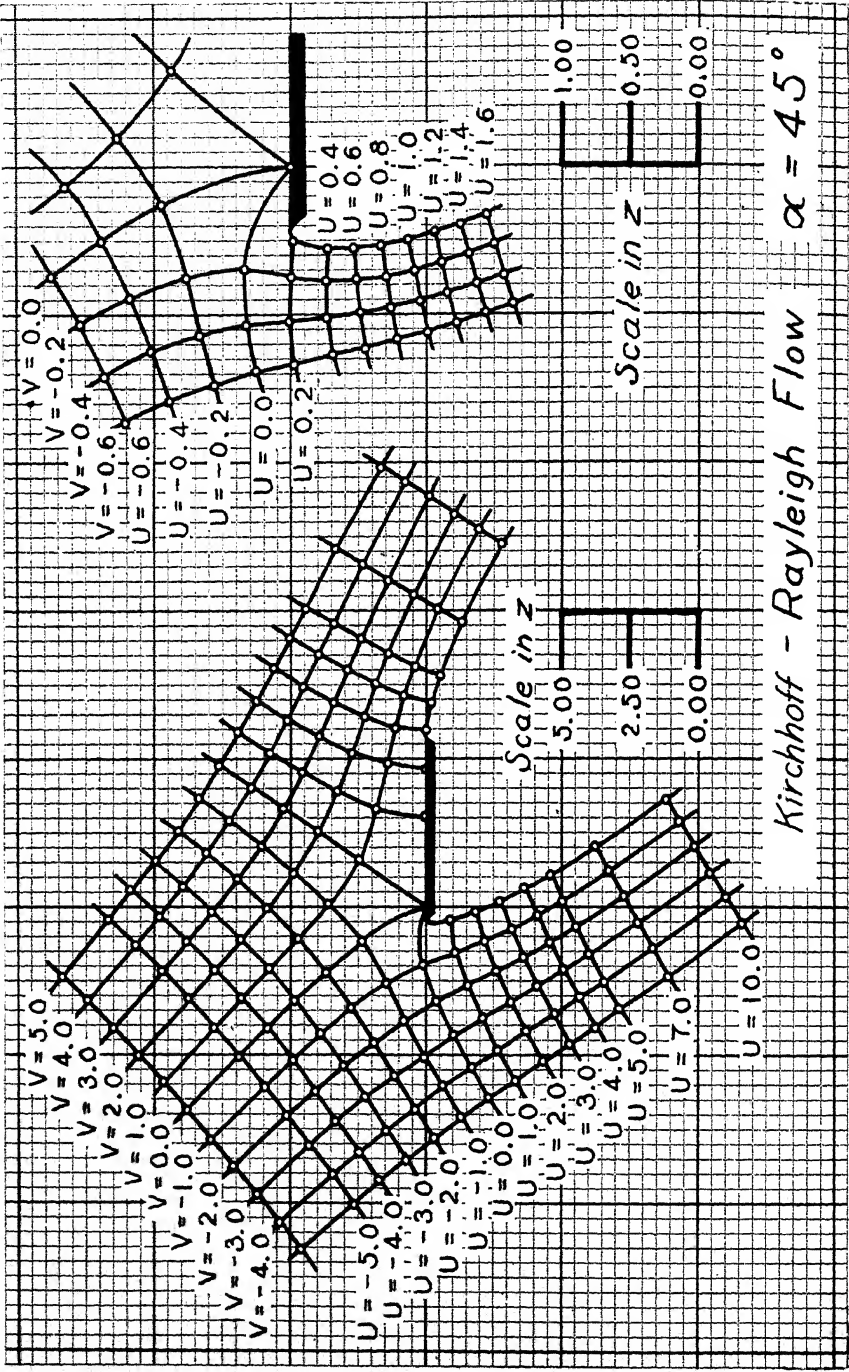
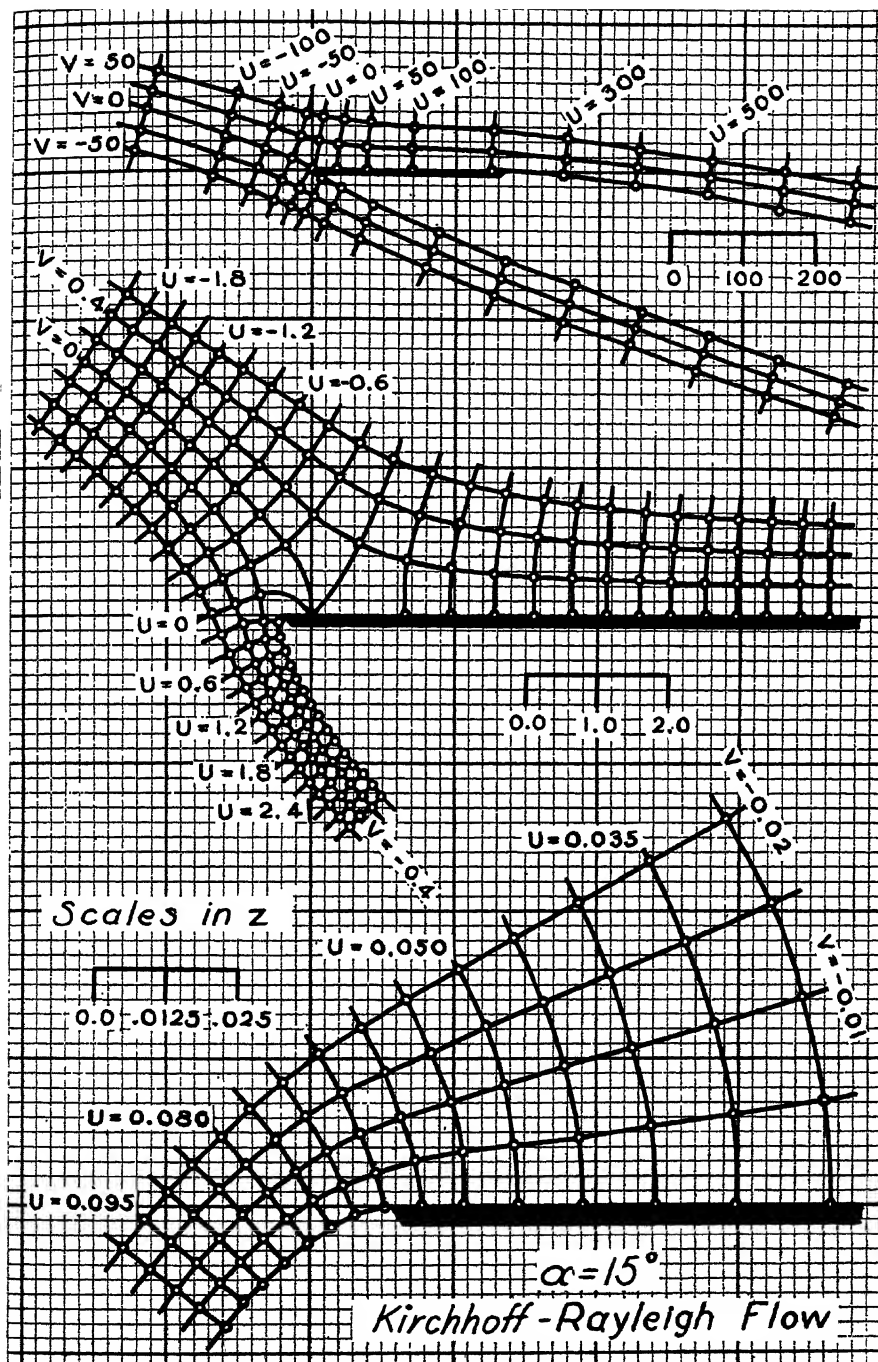


Plate 2



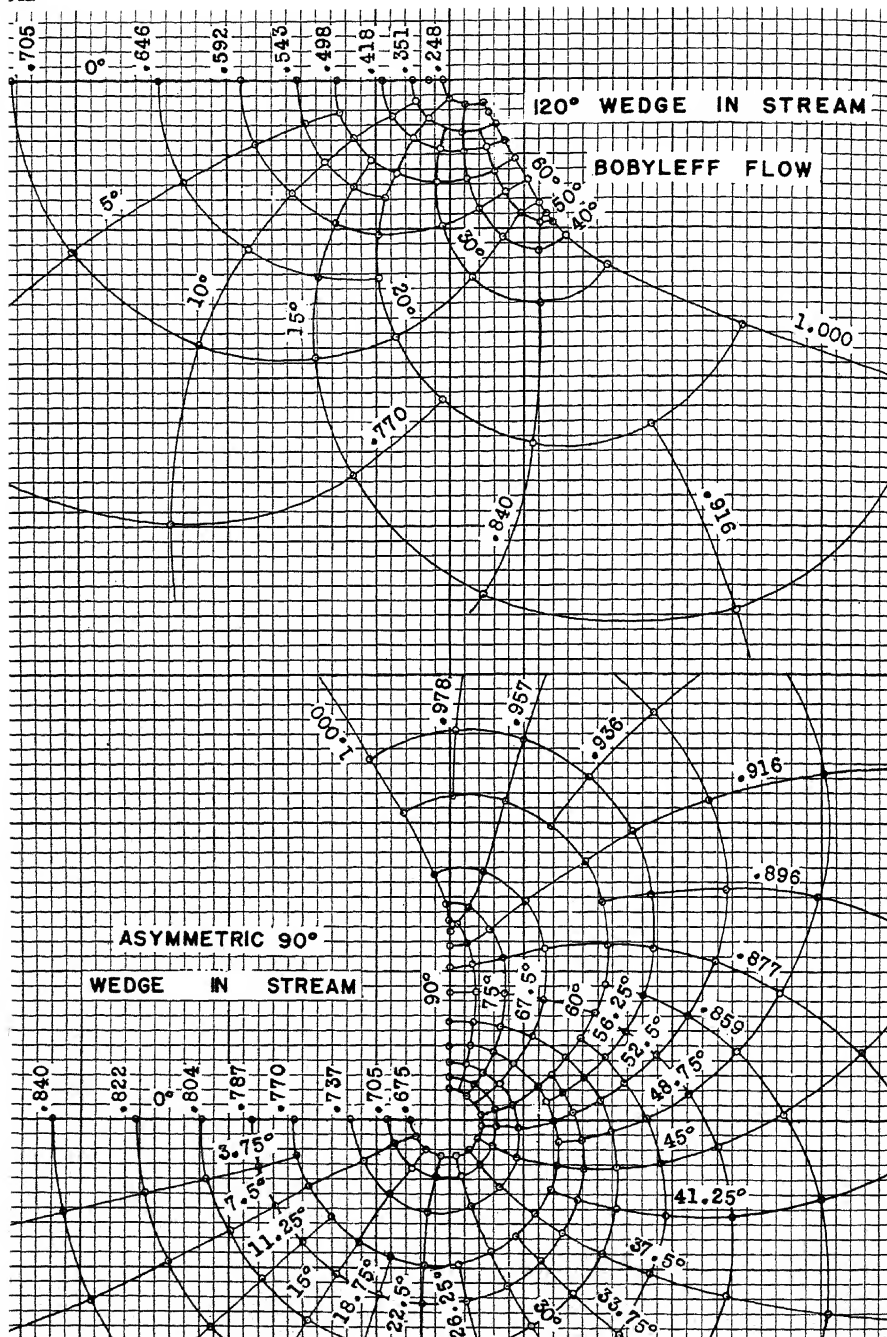


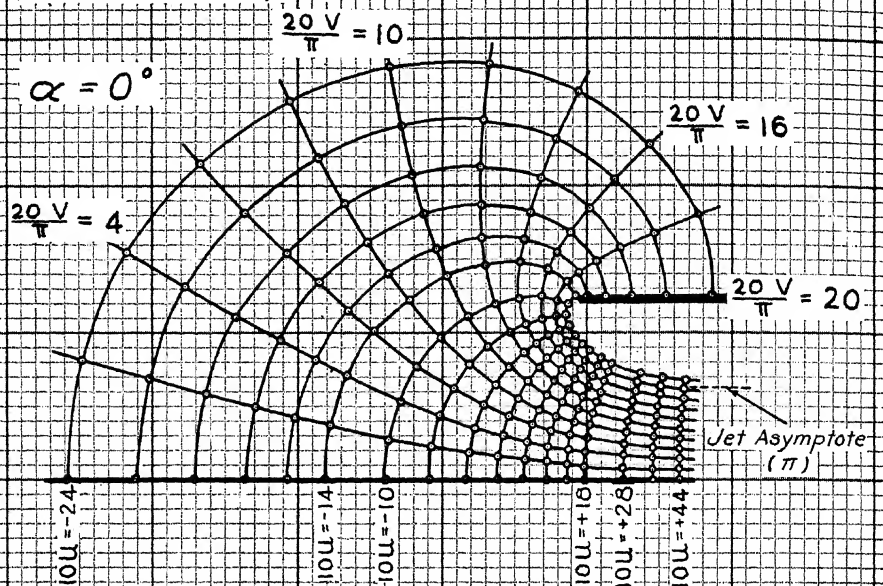
Plate 4

JET FROM 120° NOZZLE
HALF OF FLOW

JET FROM 60° NOZZLE
HALF OF FLOW

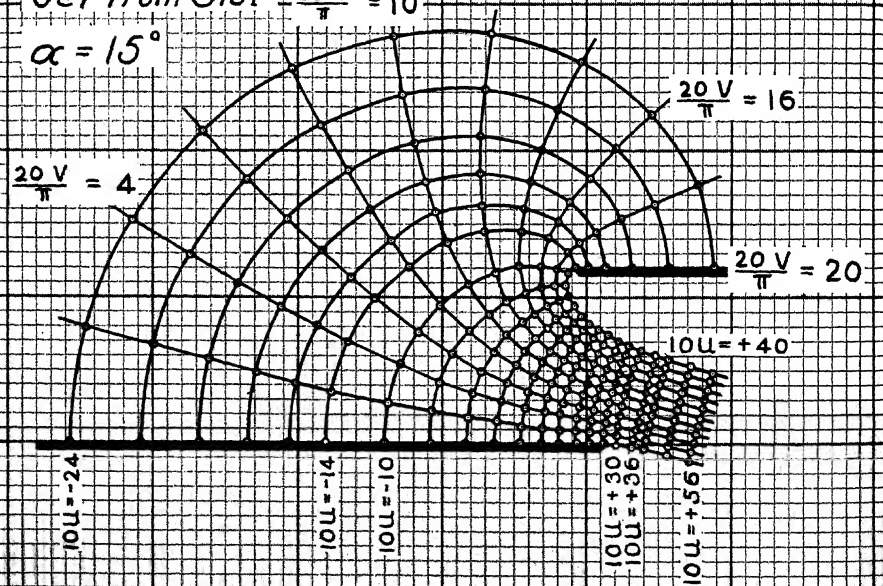
Borda Mouthpiece (Jet from Slot)

Scales in Z
0.00 2.50 5.00



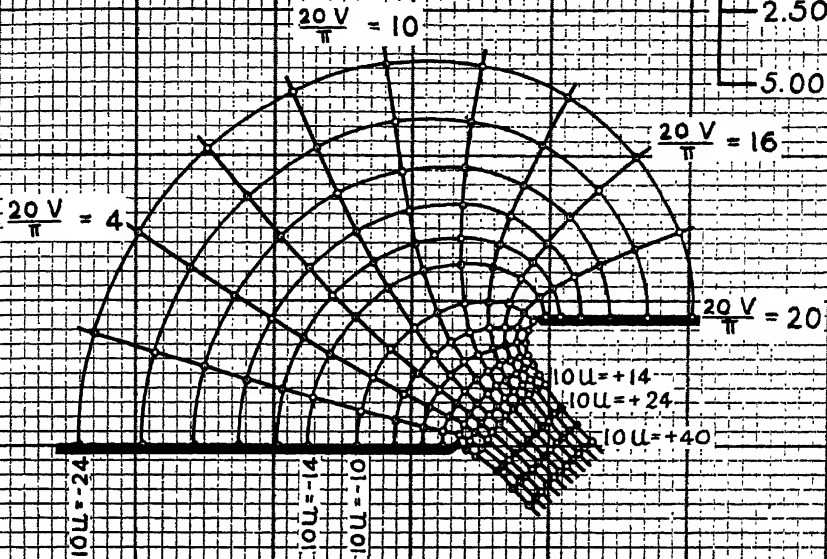
Jet from Slot $\frac{20V}{\pi} = 10$

$\alpha = 15^\circ$



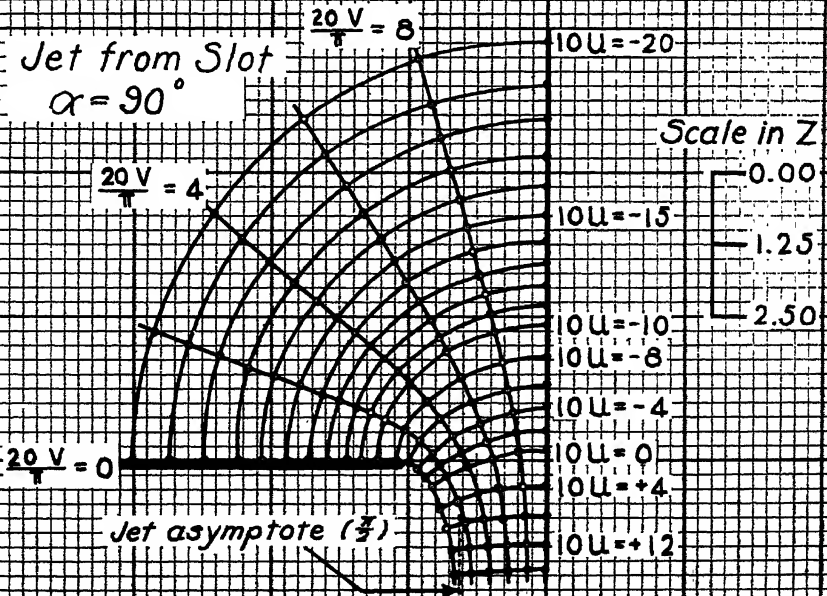
Jet from Slot

$$\alpha = 45^\circ$$



Jet from Slot

$$\alpha = 90^\circ$$



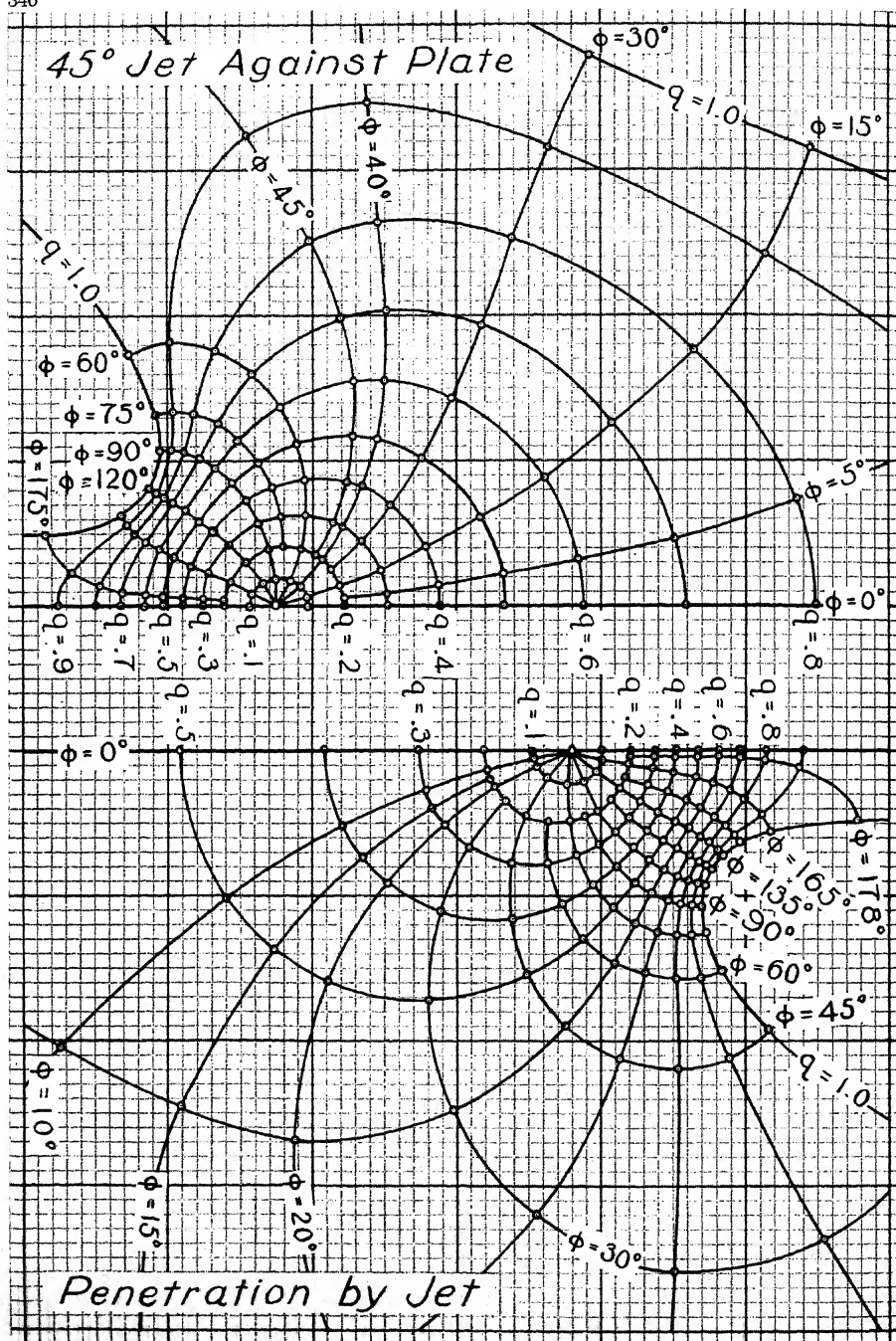


Plate 8

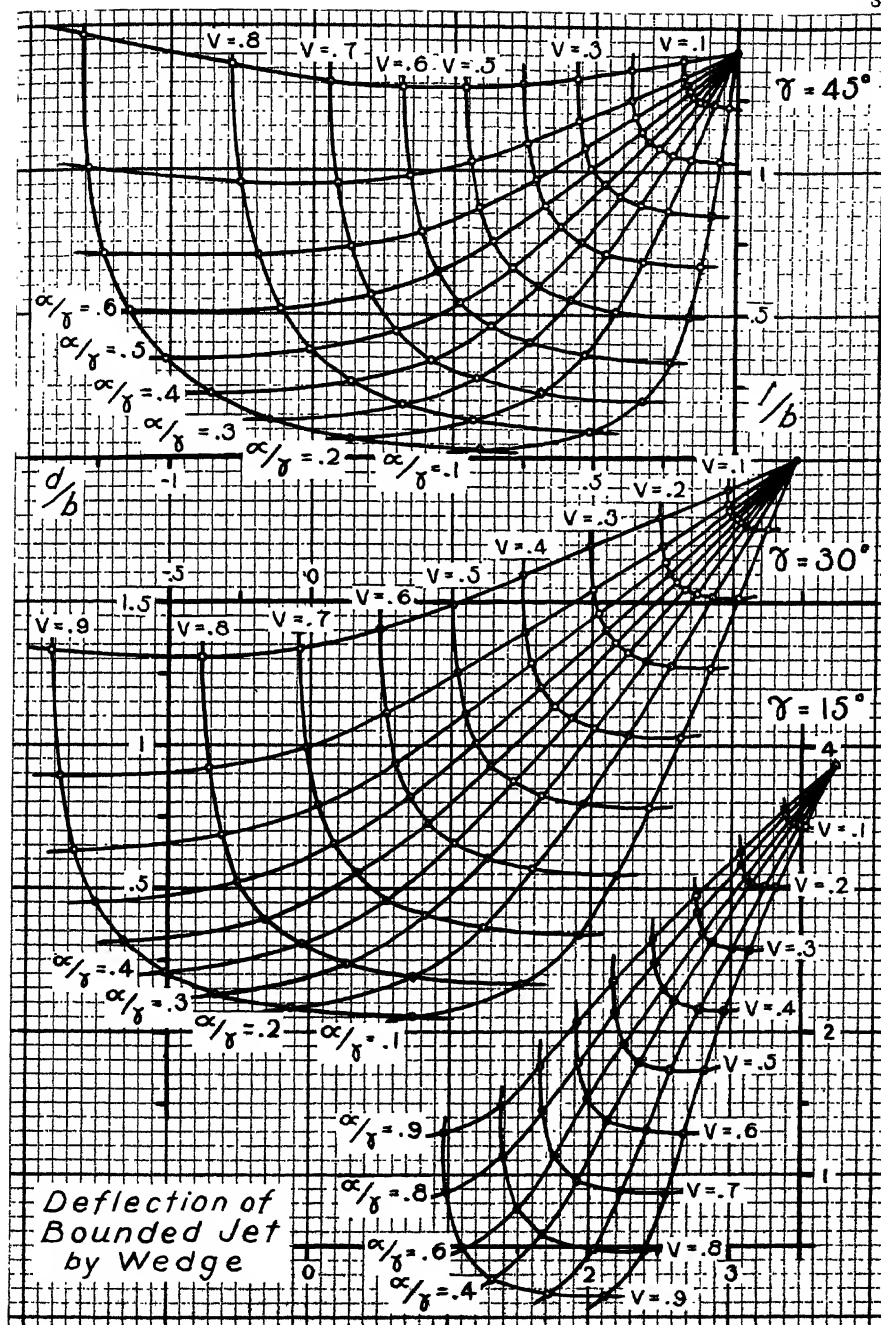


Plate 9a

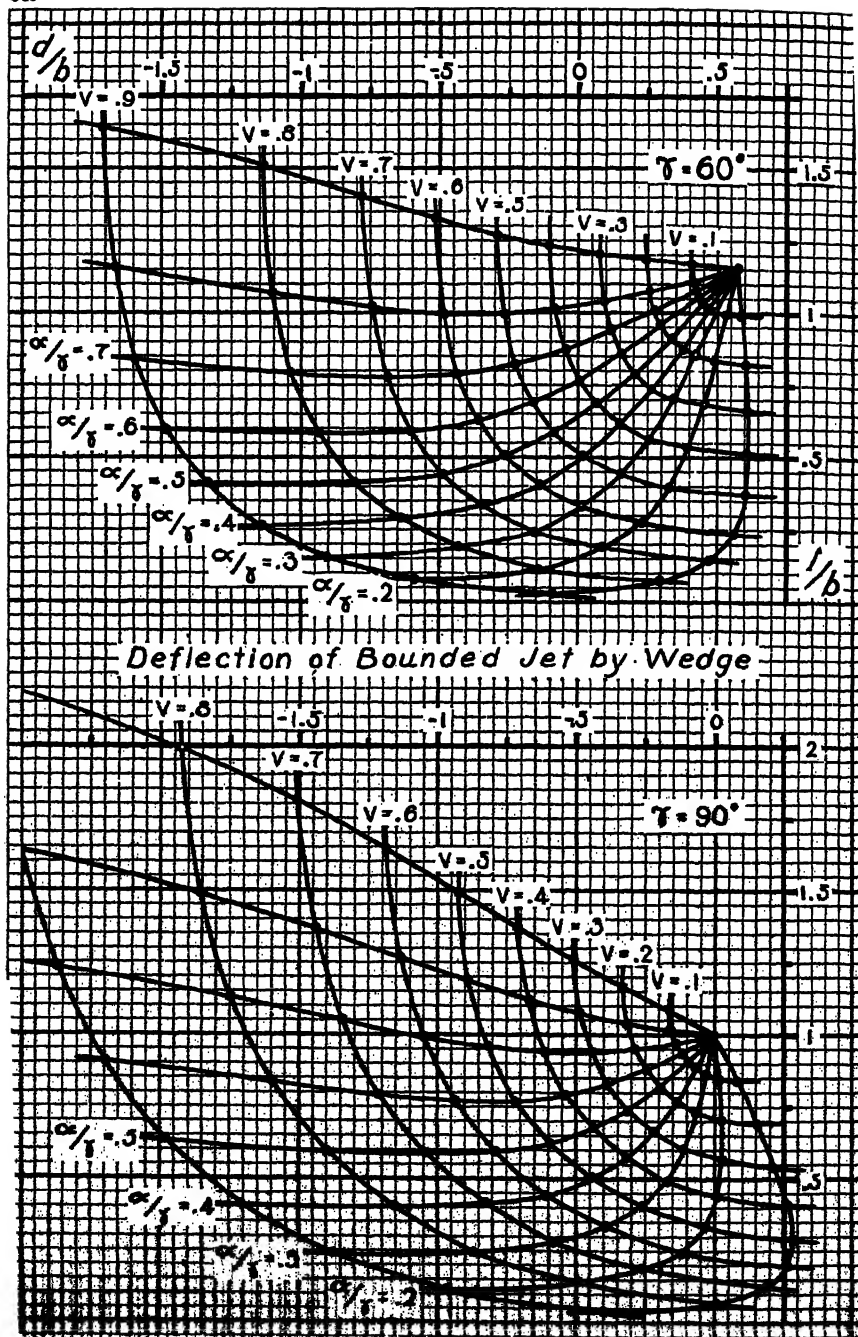
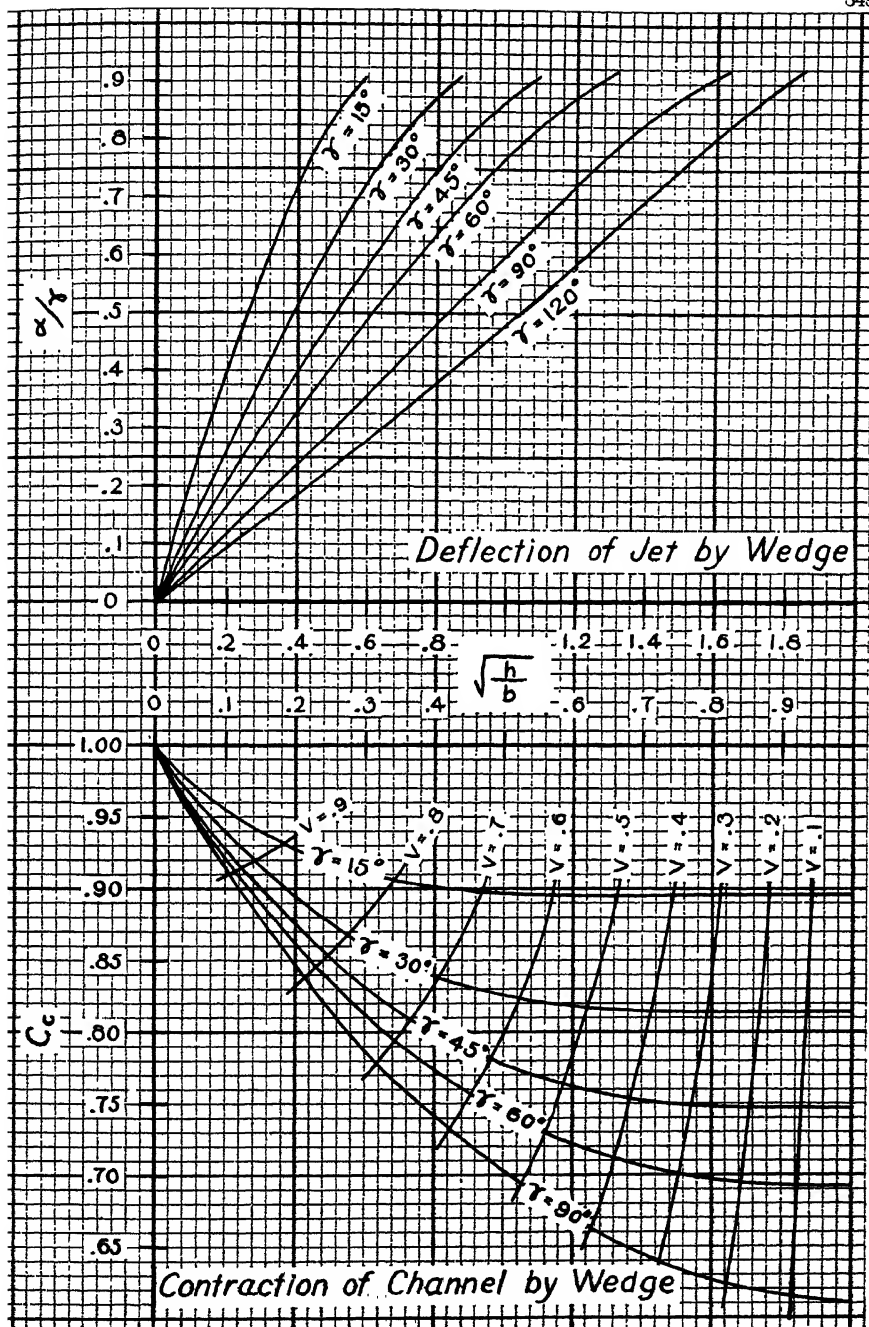


Plate Q5



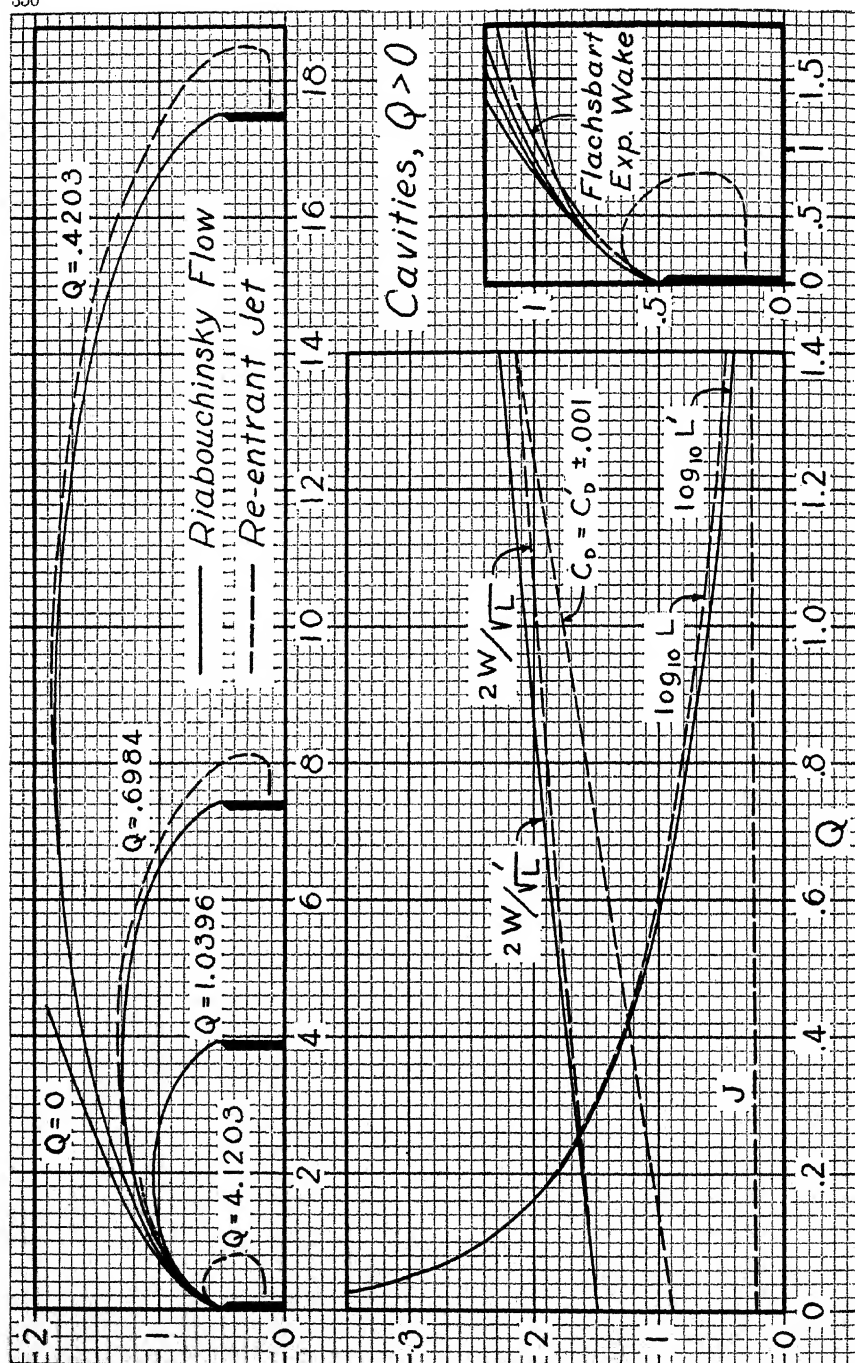


Plate 11

INDEX

A

Asymptotic wake, 264, 305
 Atomization of jets, 329
 Averaged iteration, 216
 Axially symmetric cavity, 228
 Axially symmetric flow, 221

B

Banach space, 156
 Base pressure, 8, 300
 Bernoulli equation, 13
 Bird tones, 296
 Bjerknes, laws of, 241
 Blocking constant, 17
 Bobyleff flow, 31
 Boiling, 314
 Borda tube, 14
 Boundary layer, 267
 equations, 267
 Brillouin's Principle, 20
 Brillouin-Villat separation condition, 139
 Bubbles, 236ff, 314, 327
 rising, 235

C

Cascades of airfoils, 148
 Cavitation, 237, 245
 acoustic, 320
 incipient, 10, 318
 number, 8
 pitting, 320
 propeller, 323
 Cavity, 4
 behind missile, 240
 behind plate, 27, 206
 behind wedge, 30
 of zero drag, 170, 177
 with underpressure, 40, 57, 116
 Chaplygin equation, 187
 Circular jets, 274
 Coaxial jets, 312
 Coefficient of contraction, 14
 Collapsing cavity, 36
 Complex potential, 19

Creeping flow, 261, 272
 Critical Reynolds number, 300
 Curved obstacles, 130, 215
 Cusped cavities, 126, 145, 171

D

Deviating vortex, 62
 Displacement thickness, 266
 Divided jet, 50, 130, 142

E

Edge tones, 294
 Effective computation, 22, 205ff
 Electrolytic tank, 219, 232
 Elliptic functions, 104
 Equation of state, 185
 Euler flows, 12
 Existence theorem, 170

F

Fatou-Privaloff theorem, 79
 Flattening of equipotentials, 85
 Flexible profile, 151
 Flows past wedges, 55, 189
 Free boundary, 7, 13
 inflections of, 81
 Free streamline, 13
 asymptotic geometry of, 68
 Froude number, 8

G

Gas nuclei, 316
 Globule acceleration, 245
 Gravity, 201ff.

H

Helmholtz instability, 252ff
 Hodograph, 25
 annular sector, 100
 equations, 185, 192
 Hollow charges, 16
 Hollow vortices, 128
 Hydrodynamical self-propulsion, 307

I
 Impinging jets, 105, 118, 230
 Incomplete beta functions, 208
 Infinite stream, 46
 Instability, 12, 251
 Intermittency factor, 302

J
 Jacob's Lemma, 162
 Jet, 1, 46
 against plate, 35, 231
 from funnel, 32, 197
 from nozzle, 123, 150
 from slot, 33, 197, 203, 207
 noise, 313
 penetration, 15, 36
 persistence, 328
 pumps, 1
 sensitive, 297
 Jetless wedge collapse, 199

L
 Lavrentieff's theorem, 90
 Leray-Schauder theorem, 157

M
 Mach number, 185
 Meromorphic function, 103
 Method of continuity, 171
 Minimum cavity drag, 97
 Mixing length, 304
 Mixing zone, 309
 Momentum theorem, 268
 Multiple plates, 98

N
 Navier-Stokes equations, 258

O
 Ocean, 46
 Oseen equation, 264, 266

P
 Parallel jets, 49
 Parameter problem, 160
 Periodic jets, 294ff

Periodic wakes, 280ff
 axially symmetric, 293
 Perpendicular plates, 107
 Plane jets, 276
 Plate in jet, 39
 from nozzle, 122
 Point-vortex between plates, 124
 Polytropic equation, 191
 Principle of continuity, 171
 Propeller cavitation, 323

R
 Rankine flows, 224
 Rectifiable curve, 44
 Reentrant jet, 56, 146, 171
 Reflection principle, 44, 65, 244
 Relaxation methods, 220, 223, 232, 233
 Réthy flows, 37
 Reynolds number, 8
 Riabouchinsky flows, 115, 147, 171, 184

S
 Schlicht map, 26
 Sensitive jet, 297
 Separation, 262, 299
 abrupt, 78
 conditions, 139
 curvature, 76
 points, 139
 smooth, 78
 Shaped charge, 231
 Similarity hypothesis, 270
 Simple flow, 44, 55, 59, 64
 Slipstream, 11
 Source
 between plates, 125
 distributions, 224
 interior, 124
 Spacing-ratio, stable, 289
 Stagnation cup, 232
 Stalling angle, 27
 Stream function, 19, 258
 Strict maximum principle, 84
 Strouhal number, 280
 Superposition principle, 40
 Supersonic jets, 197
 Swirl, 233
 Symmetrization, 178
 Symmetrized hodograph, 193

T

Taylor instability, 252ff
Tensile strength (liquids), 315
Torricelli's theorem, 14
Tube, 46
Turbulent jets, 309
Turbulent wakes, 298

U

Ultra-fast jets, 199
Under-over theorem, 92
Underpressure coefficient, 8
Underwater explosion, 239
Uniqueness, 94, 175
U-shaped obstacles, 111

V

Variational method, 177ff
Variational principle, 85ff
Venturi meter, 116
Vortex street, 282ff

W

Wake, 4
 behind plate, 293
 momentum, 265ff, 285
 structure, 301
 turbulence, 302
Wall correction, 39
Water entry, 325
Weinstein's function, 173

43

2152